Visible Light Photocatalyzed Oxidative Functionalization of Alkenes and Cyclic Thioacetals

विद्या वाचस्पति की उपाधि की
अपेक्षाओं की आंशिक पूर्ति में प्रस्तुत शोध प्रबंध

A thesis submitted in partial fulfillment of the requirements of the degree of Doctor of Philosophy

द्वारा / By

मौसुमी बेहेरा / Mousumi Behera

पंजीकरण सं. / ID: 20193710

प्रो. रामकृष्ण जी. भट्ट / Prof. Ramakrishna G. Bhat

भारतीय विज्ञान शिक्षा एवं अनुसंधान संस्थान पुणे

Indian Institute of Science Education and Research Pune

2025

"This thesis is dedicated to…
my family and my navodaya"

भारतीय विज्ञान
INDIAN INSTITUTE OF SCIENCE EDUCATION AND RESEARCH PUNE
IISER PUNE An Autonomous Institution of the Ministry of Education. Govt. of India

Dr. Ramakrishna G. Bhat
Professor
Department of Chemistry
IISER Pune

CERTIFICATE

This is to certify that the research work incorporated in this thesis entitled *"**Visible Light Photocatalyzed Oxidative Functionalization of Alkenes and Cyclic Thioacetals**"* submitted by **Mousumi Behera** and the research was carried out by the candidate at Indian Institute of Science Education and Research (IISER), Pune, under my supervision. The work presented here or any part of it has not been included in any other thesis submitted previously for the award of any degree or diploma from any other University or Institution.

Date: 24/06/2025
Place: Pune (Maharashtra)

Prof. Ramakrishna G. Bhat

(Research supervisor)

rgb@iiserpune.ac.in • Ph: +91-20-25908092 • Fax: +91-20-25898022

DECLARATION

Name of Student: **Mousumi Behera**

Reg. No.: **20193710**

Thesis Supervisor(s): **Prof. Ramakrishna G. Bhat**

Department: **Chemistry**

Date of joining program: **1st August 2019**

Date of Pre-Synopsis Seminar: **18th November 2024**

Title of Thesis: ***Visible Light Photocatalyzed Oxidative Functionalization of Alkenes and Cyclic Thioacetals***

I declare that this written submission represents my idea in my own words and where others' ideas have been included; I have adequately cited and referenced the original sources. I declare that I have acknowledged collaborative work and discussions wherever such work has been included. I also declare that I have adhered to all principles of academic honesty and integrity and have not misrepresented or fabricated or falsified any idea/data/fact/source in my submission. I understand that violation of the above will be cause for disciplinary action by the Institute and can also evoke penal action from the sources which have thus not been properly cited or from whom proper permission has not been taken when needed.

The work reported in this thesis is the original work done by me under the guidance of **Prof. Dr. Ramakrishna G. Bhat**

Date:24/06/2025

Mousumi Behera

Signature of the student

Acknowledgments

I would like to take this opportunity to sincerely thank all the individuals and institutions whose support, guidance, and contributions have been instrumental in the successful completion of this research thesis.

First and foremost, I would like to express my heartfelt gratitude to my thesis supervisor, *Prof. Ramakrishna G. Bhat*, for his exceptional mentorship throughout my Ph.D. journey at IISER Pune. His unwavering support, insightful guidance, and constant encouragement have been invaluable over the years. I deeply admire his thoughtful approach to research and his ability to tackle scientific problems with clarity and depth. His vast knowledge and experience in chemistry have profoundly shaped my scientific thinking and helped refine my research. Prof. Bhat's constructive feedback consistently challenged me to think critically and pushed me to grow, both as a researcher and as an individual. I am especially grateful for his emphasis on maintaining a balance between research and life beyond the lab, reminding us of the importance of health, family, friendships, and spirituality. Beyond academics, his kindness, patience, humility, and positivity have left a lasting impression. It has been a privilege to work under someone so approachable and generous in spirit, and I am truly thankful for the opportunity to be his student.

I sincerely thank my RAC members, *Prof. Benudhar Punji* and *Prof. Muhammed Musthafa*, for their valuable suggestions and insightful discussions. Their constructive feedback during RAC meetings played a significant role in shaping the direction and outcomes of my research. I would also like to extend my heartfelt gratitude to all the faculty members of IISER Pune for their support and academic environment. My sincere thanks to the former Directors of IISER Pune, *Prof. K. N. Ganesh* and *Prof. Jayant B. Udgaonkar*, as well as the current Director, *Prof. Sunil S. Bhagwat*, for providing world-class research facilities and fostering a vibrant research culture.

Words fall short in expressing my heartfelt thanks to my former labmates—Dr. Pankaj, Dr. Vikas, Dr. Prakash, Dr. Debasish, Dr. Javed, Dr. Anindita, Ms. Archana, Mr. Nitin, Mr. Ajit, and Mr. Shaheen. I am equally grateful to my current labmates—Abhijeet, Kajal, Onkar, Sachin ji, Sidharth, Saswata, Chhabi, Ganesh, Shubham, Mohit, Hrishik, Omkar, Snehal, Abhinav, and Bhavya—with whom I have shared not only instruments and experiments but also countless memories, engaging discussions, lab meetings, trips, and celebrations that brought us together as a team.

I especially thank Shubham, Ajit, and Shaheen for their generous support with experimental

work and for the stimulating conversations, debates, and constant encouragement. A very special note of gratitude goes to Dr. Pankaj for being an early mentor in my Ph.D. journey. His hands-on guidance in photoredox catalysis and insightful suggestions were instrumental in helping me troubleshoot research challenges and shaped my understanding during the foundational stages of my work.

I sincerely thank *Dr. Udaya* from Prof. V. G. Anand's lab for his valuable assistance with the cyclic voltammetry experiments. I am also deeply grateful to *Dr. Nirmala* from Prof. G. Boopathy's lab for her warmth and kindness, which made my initial days at IISER Pune feel welcoming and homelike. A heartfelt thank you to my friends *Dr. Shandhya* from Prof. Partha Hazra's lab and *Saswata* for bringing joy, support, and positivity to my journey at IISER. I would also like to acknowledge the efforts of those who work quietly behind the scenes—the instrument operators, administrative team, and non-teaching staff whose dedication plays a vital role in enabling research at the institute.

I am deeply thankful to my school, *JNV Mayurbhanj*, and the teachers who helped shape me as an individual and instilled confidence in me. A special note of gratitude goes to my chemistry teacher, *Mr. Niranjan Dalei*, whose guidance sparked my passion for the subject. I also extend my heartfelt thanks to all my teachers, seniors, and friends from school to throughout my Ph.D. for shaping my knowledge, character, and values.

Words cannot fully express the depth of my gratitude for the unwavering love, blessings, and encouragement of my parents, *Mrs. Subasini Behera* and *Mr. Muchiram Behera*, and my family—my late grandmother *Mrs. Jatrimani Behera*, my grandfather *Mr. Prabhakar Behera*, and my siblings *Nibedita*, *Aparna*, and *Subrat*. Their belief in me at every stage of life has been my greatest strength. This journey would not have been possible without their unconditional emotional support, trust, patience, and countless sacrifices. They are the foundation and inspiration behind all that I have achieved and all that I aspire to accomplish.

Above all, I thank the Almighty (*Lord Jagannath*) for this life filled with opportunities and grace.

Mousumi Behera

Contents

Contents vii

Abbreviations x

Synopsis xv

List of Publications xxxii

Chapter 1: ***Introduction to Photocatalysis in Organic Synthesis: Reactions of Alkenes & Cyclic Thioacetals under Visible Light***

1.1. Introduction 2

1.2. Types of activation modes of photocatalysis 7

1.3. Notable early contributions to organic photoredox catalysis 9

1.4. Alkene difunctionalization reactions under photoredox catalysis 14

1.5. Reactions of cyclic thioacetals under photoredox catalysis 19

1.6. Conclusion 23

1.7. References 24

Chapter 2: ***β-Hydroxytrifluoromethylation of Unactivated Alkenes via Visible Light-Induced Organophotoredox-Catalysis***

2.1. Introduction 29

2.2. Results and Discussions 35

2.3. Conclusion 51

2.4. Experimental section 52

2.4.1. General Details 52

2.4.2. Preparation of Starting Materials 53

2.4.2.A. General procedure A for the synthesis of alkenyl benzoates 54

2.4.2.B. General Procedure B for the synthesis of alkenyl benzoates 54

2.4.3. General Procedure C for the synthesis of *β*-trifluoromethylated alcohols 54

2.4.4. Product Characterization Data 54

2.4.5. Appendix II 72

2.4.6 Copies of ^{1}H, $^{13}C\{^{1}H\}$ and $^{19}F\{^{1}H\}$ NMR Spectra 73

2.4.7 Crystal Data of Compound **3ai** 88

2.5 References 90

Chapter 3: ***Visible Light Driven Organophotoredox Catalyzed Oxidative Functionalization of Styrenes: Synthesis of α-Alkoxylated Ketones***

3.1 Introduction 94
3.2 Results and Discussions 102
3.3 Conclusion 109
3.4 Experimental Section 110
3.4.1 General Details 110
3.4.2 General Experimental Procedure 111
3.4.2A General procedure A for the synthesis of α-alkoxylated ketones 111
3.4.2B General Procedure B for the synthesis of **2a** under sunlight 111
3.4.2C General Procedure C for the scale up synthesis of **2a** 112
3.4.3 Product Characterization Data 112
3.4.4 Appendix III 118
3.4.5 Copies of ^{1}H and $^{13}C\{^{1}H\}$ NMR Spectra 119
3.5 References 129

Chapter 4: ***Visible Light Driven Organophotoredox Catalyzed Oxidative Functionalization of Styrenes: Synthesis of 1,4-Diketones***

4.1 Introduction 133
4.2 Results and Discussions 139
4.3 Conclusion 150
4.4 Experimental Section 151
4.4.1 General Details 151
4.4.2 General Experimental Procedure 152
4.4.2A General Procedure A for synthesis of 1,4-diketones 152
4.4.2B General Procedure B for synthesis of **2a** under sunlight 152
4.4.2C General Procedure C for scale-up synthesis of **2a** 153
4.4.3 Product Characterization Data 153
4.4.4 Appendix IV 160
4.4.5 Copies of ^{1}H and$^{13}C\{^{1}H\}$ NMR Spectra 161
4.5 References 171

Chapter 5: ***Harnessing Aryl Thiocyanate: A Circular Chemical Approach to Thiocyano-Thioesters from Cyclic Thioacetals***

5.1 Introduction 174
5.2 Results and Discussions 181

5.3 Conclusion 200
5.4 Experimental Section 201
5.4.1 General Details 201
5.4.2 Experimental Procedures 201
5.4.2A General Procedure A for the synthesis of cyclic thioacetals 201
5.4.2B General Procedure B for the synthesis of aryl thiocyanates 202
5.4.2C General procedure C for the synthesis of diaryl disulfide **4j** 202
5.4.2D General procedure D for synthesis of thiocyano-thioesters **3** 202
5.4.2E General procedure E for synthesis of aryl thiocyanates under visible light 203
5.4.2F General procedure F for scale-up synthesis of thiocyano-thioester **3a** 204
5.4.3 Product Characterization Data 205
5.4.4 Appendix V 218
5.4.5 Copies of ^{1}H and $^{13}C\{^{1}H\}$ NMR Spectra 219
5.5 References 229
Summary 232

*****

List of Abbreviations

µ	micro
Å	angstrom
Ac	Acetyl
AcOH	Acetic acid
aq	aqueous
Ar	Aryl
AR	Analytical Research Grade
atm	atmosphere
BIOAc	1-acetoxy-1,2-benziodoxol-3(1*H*)-one
BHT	dibutylhydroxytoluene
Boc	*tert*-butoxycarbonyl
Bn	benzyl ($C_6H_5CH_2$)
Bz	benzoyl (C_6H_5CO)
BQ	benzoquinone
bs	broad singlet
°C	degrees Celsius
Calcd.	Calculated
Cbz	benzyloxycarbonyl
CCDC	Cambridge Crystallographic Data Centre
$CDCl_3$	Deuterated chloroform
CFL	Compact Fluorescent Lamp
cm^{-1}	Wavenumber(s)
conc.	Concentrated
CT	Charge Transfer
CV	Cyclic voltammetry
δ	Chemical shift
d	doublet (NMR)
DBU	1,8-diazabicyclo[5.4.0]undec-7-ene
DCE	Dichloroethane
DCM	Dichloromethane
dd	doublet of doublet

DIPEA	*N,N*-diisopropyl methyl amine
DMAP	*N*,*N*-dimethylamino pyridine
DMF	*N*,*N*-dimethyl formamide
DMSO	Dimethylsulfoxide
DMSO-d_6	Duterated dimethyl sulfoxide
DTBP	Di-tert-butyl peroxide
d.r.	Diastereomeric ratio
EDG	Electron donating group
ee	Enantiomeric excess
EnT	Energy transfer
EPR	Electron paramagnetic resonance
equiv.	Equivalents
ESR	Electron spin resonance
ET	Electron Transfer
ESI TOF	Electrospray ionisation time-of-flight
ESMS	Electrospray mass spectrometry
Et	Ethyl (CH_3CH_2)
EtOAc	Ethyl acetate
EWG	Electron withdrawing group
eV	Electron volt
EY	Eosin Y
FTIR	Fourier-transform infrared spectroscopy
g	gram (s)
h	hour (s)
HAT	Hydrogen atom transfer
h	Planck's constant ($6.62607015 \times 10^{-34}$ joule second)
HRMS	High Resolution Mass Spectroscopy
Hz	Hertz
IBX	2-Iodoxybenzoic acid
Imd	Imidazole
^{i}Pr	Isopropyl
ISC	Intersystem crossing
K	Kelvin
kcal	kilocalories

J	*Spin coupling constant (in NMR spectroscopy)*
KOAc	Potassium acetate
L	Ligand
LEDs	Light emitting diode
M	Molar (mol L-1)
mM	Milli molar
m	multiplet (in NMR)
m-	meta
m/z	mass to charge ratio
m-CPBA	*m*-chloroperbenzoic acid
Me	Methyl (CH_3)
MeCN	Acetonitrile
MeOH	Methanol
mg	milligram
MHz	Mega hertz
min	minute(s)
mL	millilitres
mmol	millimoles
mol	mole(s)
mol%	mole percent
mp	melting point
MS	Molecular Sieves
MTBE	Methyl *tert*-butyl ether
µM	Micro molar
NBS	*N*-bromosuccinimide
NHPI	*N*-hydroxyphthalimide
nm	nanometer
NMR	Nuclear Magnetic Resonance
ND	Not detected
NR	No reaction
Nu	Nucleophile
*n*BuLi	*n*-butyllithium
o-	*ortho*
ORTEP	Oak Ridge Thermal-Ellipsoid Plot Program

OAc	Acetate
OTf	trifluoromethanesulfonate
p-	*para*
PC	Photocatalyst
PC*	Excited state photocatalyst
Ph	Phenyl (C_6H_5)
ppm	parts per million
PT	proton transfer
PCET	Proton couple electron transfer
PET	Photoinduced electron trasnfer
Py	pyridine
q	quartet (NMR)
quin.	quintet
RB	Round bottom flask
rr	Regioisomeric ratio
rt	room temperature
R_f	retention factor (in chromatography)
Rh6G	Rhodamine 6G
s	singlet (NMR)
S_1	Singlet ground state
SCXRD	Single Crystal X-ray diffraction
SET	Single electron transfer
t	triplet (NMR)
t	*tert- Tertiary (branched alkyl chain)*
T_1	Triplet ground state
TBHP	*tert*-Butyl hydroperoxide
^{t}Bu	*tert-butyl*
td	triplet of doublet
TEMPO	2,2,6,6-Tetramethylpiperidin-1-yl)oxyl
Tf	triflate (trifluoromethanesulphonyl)
TFA	Trifluoroacetic acid
THF	Tetrahydrofuran
TLC	Thin Layer Chromatography
TMS	Trimethylsilyl

TOF	Turn-over frequency
TS	transition state
Ts	tosyl
UV	ultraviolet
vis	visible
V	Volt
W	Watt
X	Heteroatom
ν	frequency of light
λ	Wavelength
λ_{max}	Wavelength of maximum absorption
*	Excited state

SYNOPSIS

The thesis entitled "***Visible Light Photocatalyzed Oxidative Functionalization of Alkenes and Cyclic Thioacetals***" comprises five main chapters.

Aim of this Thesis

The revival of radical chemistry in organic synthesis has fueled a renaissance in visible-light photoredox catalysis. Researchers across fields, ranging from biomedicine to materials science, are rapidly embracing photoredox catalysis for its mild, sustainable, and unique reactivity. Precious metal photocatalysts, such as iridium and ruthenium, are frequently used, however, they suffer due to some limitations such as less abundance, cost, and toxicity. This underscores the importance of developing organic photoredox catalysis, which offers more than a "metal-free" alternative. Organic photocatalysts enable potent reactivity, allowing access to unique transformations and a broader range of substrates that often drive the reactions beyond the capabilities of traditional synthetic approaches.

Alkenes are among the most abundant classes of organic molecules, available in bulk quantities from petrochemical feedstocks and renewable resources. The widespread availability of alkenes combined with their unique reactivity profile has made alkene functionalization reactions essential in organic synthesis. Their reactivity can be varied depending upon the substituents attached to the double bonds. Difunctionalization of alkenes to synthesize high valued organic compounds have also been expanded the synthetic organic chemists' tool box. In this context, as we have been working in the area of organophotoredox catalysis, we hypothesized to work on the visible light mediated organophotoredox catalyzed oxidative difunctionalization reactions of alkenes to construct various α-hydroxy/α-oxo functionalized products.

Similarly, the cyclic thioacetals are well-known protecting groups for the carbonyl compounds and have also been widely utilized for the umpolung reactivity. However, the selective cleavage of single C–S bond under visible light photoredox catalysis keeping the other C–S bond intact for the synthesis of rearranged and functionalized product has not been explored. Therefore, we propose to explore this new reactivity pattern of the cyclic thioacetals under visible light organophotoredox condition to synthesized functionalized thioester derivatives. The thesis mainly focused on the design and development of visible light organophotocatalyzed transformations of alkenes and cyclic thioacetals to access useful compounds.

Chapter 1: *Introduction to Photocatalysis in Organic Synthesis: Reactions of Alkenes & Cyclic Thioacetals under Visible Light*

This introductory chapter briefly presents the evolutionary development of visible light mediated photoredox catalysis in organic synthesis. The chapter gives an overview about the historical development on the exploration of visible light medicated organic transformations, basic working principles of photocatalysis, its classification and mode of operations. A few selected transformations have been discussed that are representative of the milestones in the field of visible light mediated photoredox catalysis. Undoubtedly, the photoredox catalysis has emerged as a transformative tool in organic synthesis owing to the environmentally benign, sustainable, mild nature, and high functional group compatibility, as well as the unique mechanistic approaches. It has witnessed a modern resurgence of radical chemistry through the streamlined formation of new chemical bonds.

The visible light mediated photocatalytic methodologies have notably advanced the field of alkene 1,2-difunctionalization by providing a sustainable and versatile platform for the regio- and chemo-selective installation of two distinct functional groups across olefinic scaffolds in a single, efficient transformation. In this regard, we have thought to work on the visible light mediated oxidative difunctionalization reactions of alkenes with different reagents or nucleophiles for the synthesis of high valued functionalized alkenes.

The cyclic thioacetals particularly 1,3-dithianes and 1,3-dithiolanes, serve as robust carbonyl protecting groups due to their ease of formation and stability. These are widely used in total synthesis and the Corey–Seebach umpolung strategy. The deprotection of thioacetals leading to unmasked the carbonyl group has been well explored under the operationally simple and mild photoredox catalysis condition under visible light irradiation. Due to the low electronegativity of sulfur atom and the weak polarization of C–S bond, thioethers exhibit remarkable stability toward soft Brønsted acids and bases. Recent developments on the photoredox catalyzed C–S bond cleavage reactions have been discussed for constructing diverse organic motifs. However, the selective cleavage of single C–S bond keeping the other one intact leading to formation of rearranged product using various reagent has not been explored systematically. Hence, highly chemo-selective transformations could be achieved by selective cleavage of C–S bonds.

Chapter 2: *β-Hydroxytrifluoromethylation of Unactivated Alkenes via Visible Light-Induced Organophotoredox-Catalysis*

This chapter presents the exploration of organophotoredox-catalyzed approach for the direct *β*-hydroxytrifluoromethylation of unactivated alkenes using CF_3SO_2Na and acridinium salt. The installation of a trifluoromethyl group into an organic molecule dramatically influences its various properties such as electronegativity, polarizability, and various pharmacokinetic properties including lipophilicity, metabolic stability, and bioavailability. Alkenes are indispensable carbon feedstocks in the realm of chemical synthesis and widely recognized for easily accessible, abundant, and stable nature. The earlier development on the trifluromethylation of alkenes required transition metal catalysts of Cu, V, Mn, Fe, Co, Pd, Ag, and elevated temperature. The revival of visible light photoredox catalysis has revolutionized the synthetic organic chemistry for its mild, sustainable, and unique reactivity. In this regard, there are a very few reports on the metallaphotoredox catalyzed approach towards the *β*-hydroxytrifluoromethylation of activated alkenes. Although the transition metal photocatalysts offer notable synthetic utility, organophotoredox catalysts are favoured for their environmental sustainability, unique reactivity (strong oxidizing nature) and broader applicability. Interestingly, to the best of our knowledge, there are no reported examples on the organophotoredox-catalyzed *β*-hydroxytrifluoromethylation of unactivated alkenes which include both terminal as well as internal alkenes.

Based on the systematic and exhaustive screening of photocatalysts, solvents, oxidants, and visible light sources, allyl benzoate **1a** (0.2mmol), sodium trifluoromethanesulfinate **2** (3 equiv.), $(NH_4)_2S_2O_8$ (2 equiv.), Mes-Acr-Me·BF_4 (5 mol %), 1,4-Dioxane:MeCN (2:1, 3 mL), and blue LEDs (467 nm, 20 W) under open air atmosphere at room temperature for 12 h proved to be the optimum reaction condition to obtain the desired *β*-hydroxy trifluoromethylated product **3a** (Scheme 2.1).

Having obtained the optimum reaction conditions, we explored the substrate scope to assess the practicality and generality of the protocol. The alkenes containing electron-neutral, electron donating, electron withdrawing and electron deactivating substituents on the phenyl ring of allyl benzoates underwent smooth conversion, affording the corresponding *β*-hydroxy trifluoromethylated products (**3a**–**3r**) in good yields (up to 78%, Table 2.1). The homoallylic alkene, the alkene attached to aliphatic substrate, the internal double bond containing alkene, alkenes pendant with various functional groups such as sulfinate, isoindolidinone and ether with varying chain length of alkenes were compatible under the reaction conditions to furnish

the corresponding desired trifluoromethylated products (**3s**–**3z**, **3aa** and **3ab**) in good to very good yields (up to 86%, Table 2.1)

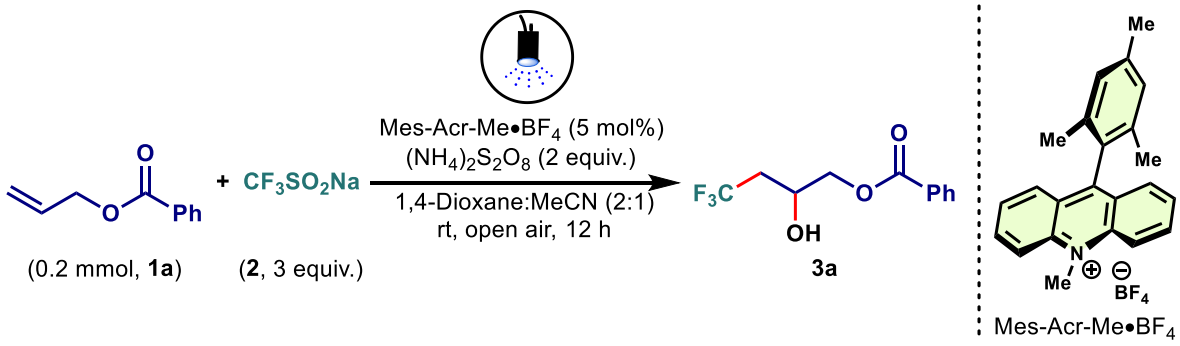

Scheme 2.1 *β*-hydroxy trifluoromethylation of unactivated alkenes via organophotoredox catalysis.

Table 2.1. Diverse substrate scope of *β*-trifluoromethyl alcohols[a]

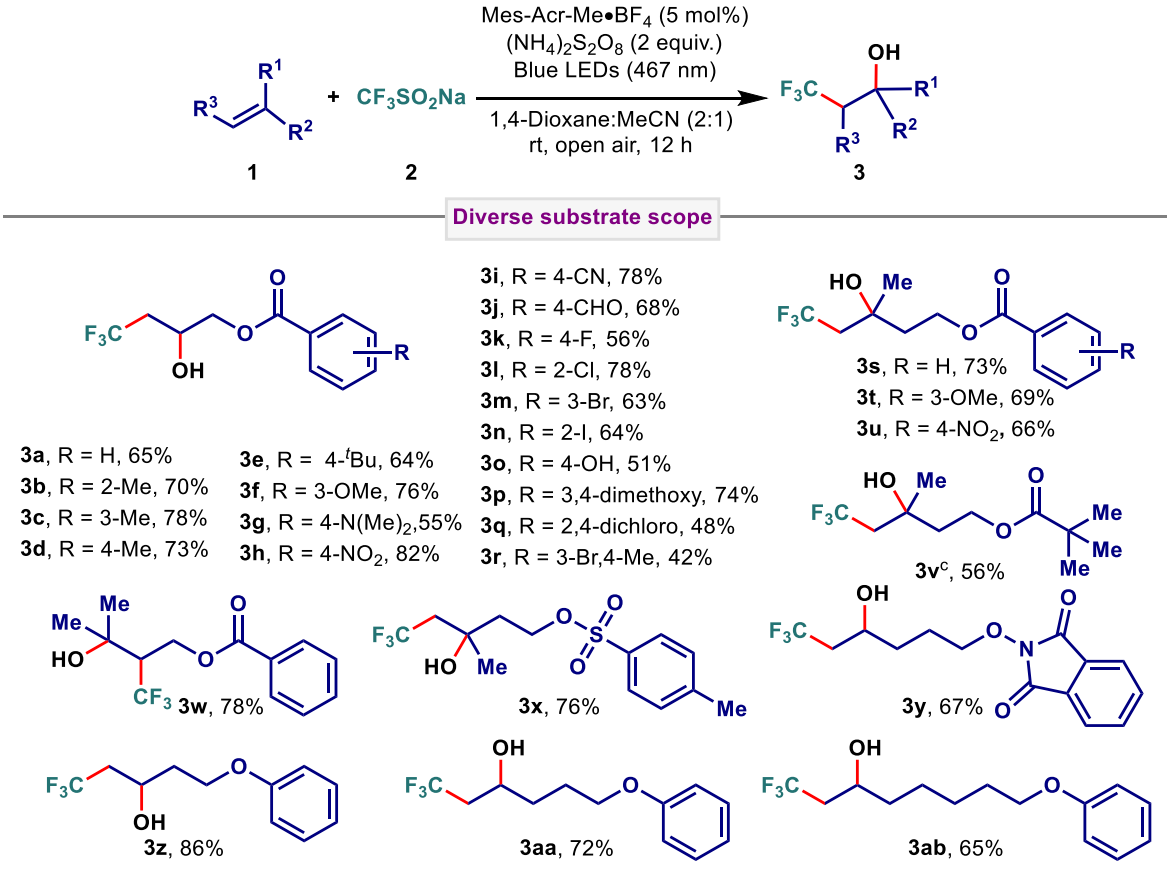

Reaction conditions: [a]**1** (0.2 mmol), CF_3SO_2Na **2** (3 equiv.), $(NH_4)_2S_2O_8$ (2 equiv.), Mes-Acr-Me•BF_4 (5 mol%), 1,4-Dioxane:MeCN (2:1, 3 mL), blue LEDs (467 nm, 20 W), rt, open air, 12 h. [b]1,4-Dioxane (3 mL), 36 h.

Further, alkenes bearing various heterocyclic moieties such as thiophene, furan, benzothiazole and pyrrole were well tolerated to afford the corresponding products (**3ac**–**3ag**) in moderate to

good yields (up to 74%, Table 2.2). Additionally, as a proof of concept, an example of difluoromethylation of allyl benzoate was conducted with sodium difluoromethane sulfinate to obtain the corresponding difluoromethylated product **3ah** in moderate yield (Table 2.2).

Table 2.2. Diverse substrate scope of *β*-trifluoromethyl alcohols[a]

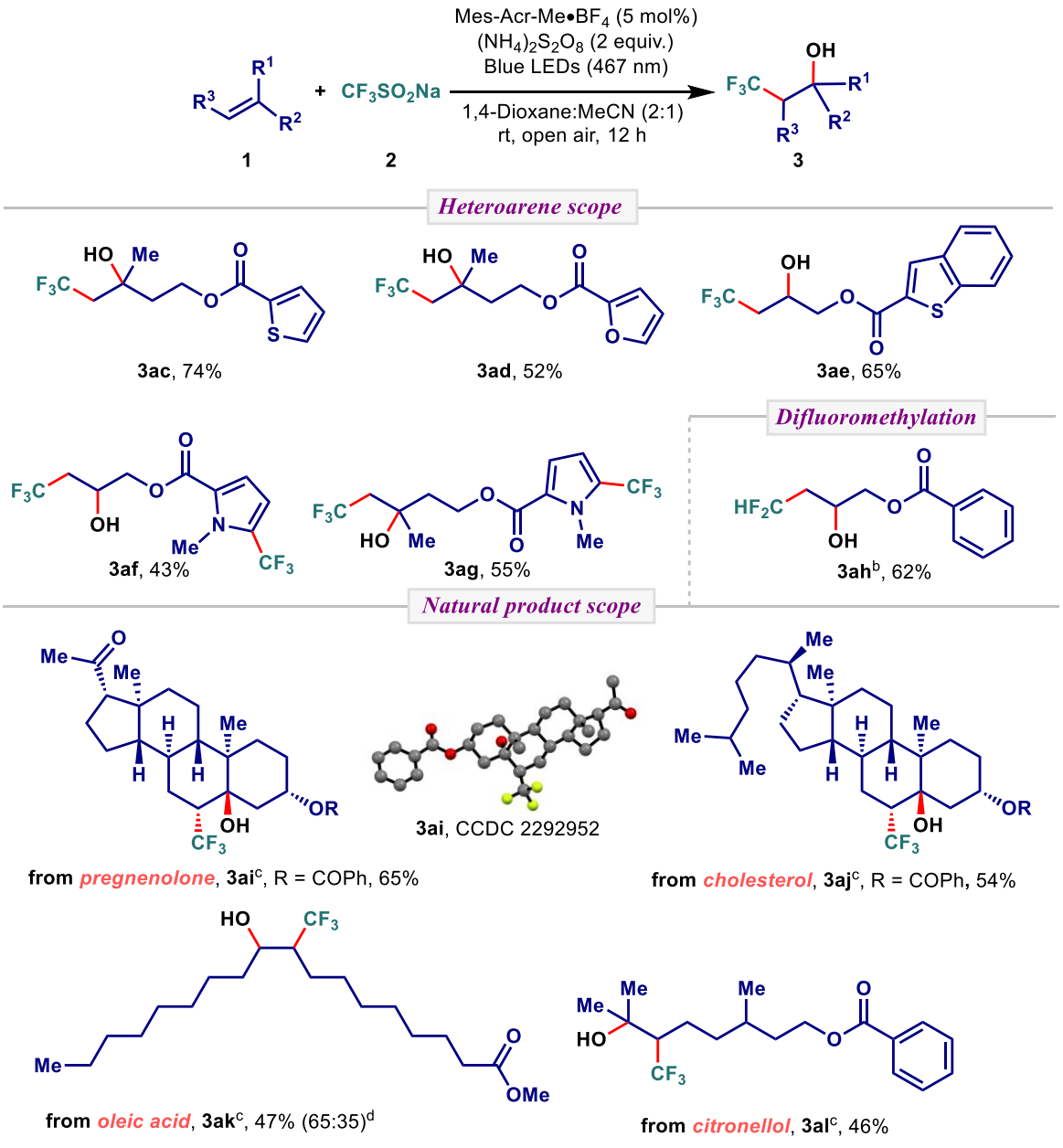

Reaction conditions: [a]**1** (0.2 mmol), CF_3SO_2Na **2** (3 equiv.), $(NH_4)_2S_2O_8$ (2 equiv.), Mes-Acr-Me•BF_4 (5 mol%), 1,4-Dioxane:MeCN (2:1, 3 mL), blue LEDs (467 nm, 20 W), rt, open air, 12 h. [b]CF_2HSO_2Na **2a** (3 equiv.) instead of **2**, 36 h. [c]1,4-Dioxane (3 mL), 36 h. [d]NMR analysis did not allow to conclusively distinguish between *r.r.* or *d.r.*

Moreover, various natural product containing alkenes such as pregnenolone, cholesterol, oleic acid and citronellol upon treatment with CF_3SO_2Na under the optimum reaction conditions

afforded the corresponding *β*-trifluoromethylated alcohol products (**3ai**–**3al**) in moderate yields (Table 2.2).

Later, the synthesized *β*-hydroxy trifluoromethylated products were subjected to various post synthetic modifications such as Suzuki coupling reaction, Fischer esterification reaction and functional group inter conversion reactions to synthesize the corresponding functionalized products (**5a**–**5d**) (Scheme 2.2a–c). Further, a scale up reaction and the reaction under the direct exposure of natural sunlight afforded the desired product **3a** in moderate yield (Scheme 2.2d, e).

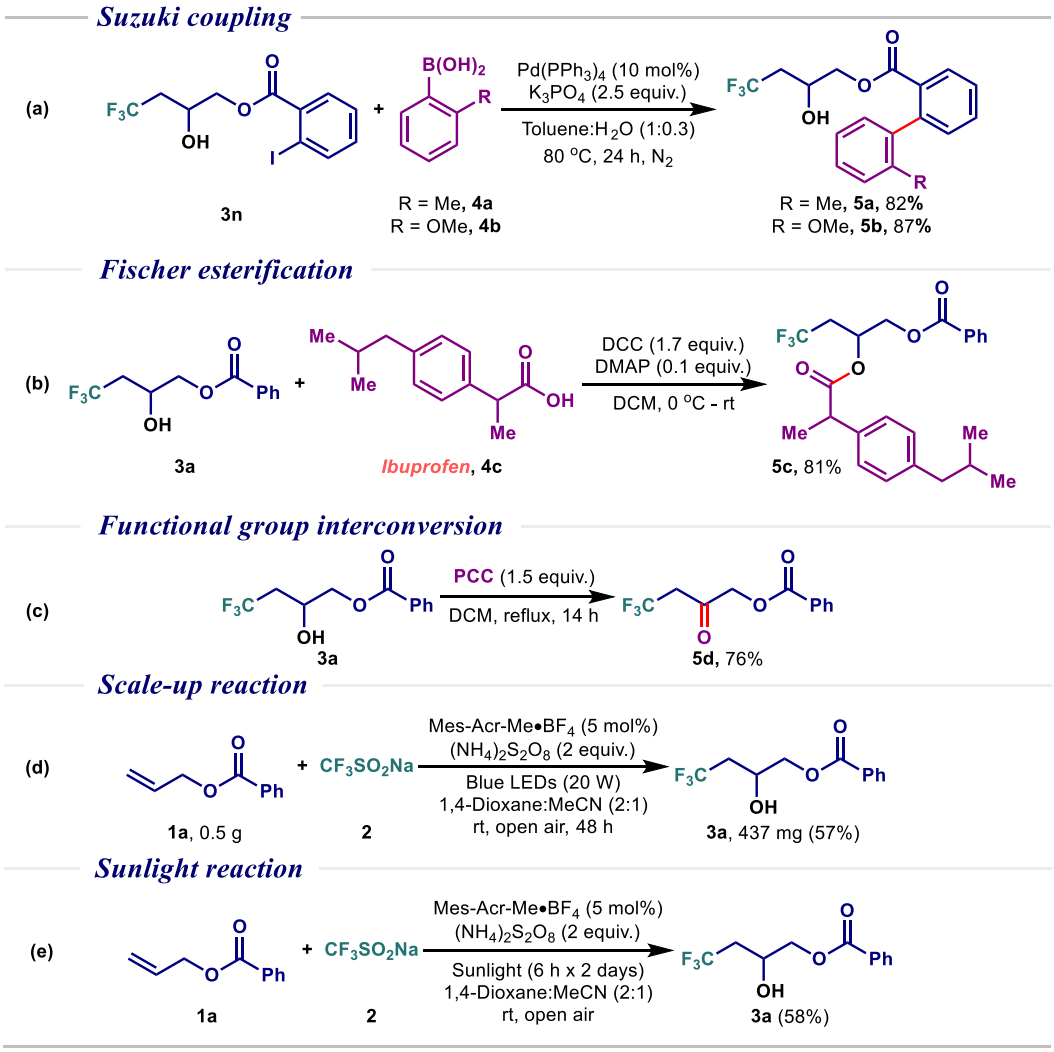

Scheme 2.2 Post synthetic applications, scale-up and sunlight reaction.

Later, we carried out a series of control experiments, fluorescence quenching experiment and cyclic voltammetric analysis to proposed a plausible reaction mechanism for the *β*-hydroxytrifluoromethylation of alkene.

In summary, we have developed a transition metal-free, visible light-induced *β*-

hydroxytrifluoromethylation of terminal and internal unactivated alkenes using the Langlois reagent at room temperature. This mild and operationally simple method employs a non-toxic, cost-effective organic dye as the photoredox catalyst. The protocol shows broad substrate scope and good functional group tolerance. Its synthetic utility was demonstrated through the late-stage modification of natural product-derived substrates and further product derivatization. The reaction is scalable and proceeds efficiently under the exposure of sunlight. The mechanistic studies support a reductive quenching pathway in the photoredox catalysis.

Chapter 3: *Visible Light Driven Organophotoredox Catalyzed Oxidative Functionalization of Styrenes: Synthesis of α-Alkoxylated Ketones*

This chapter discloses a new mild, transition metal-free approach for the synthesis of *α*-alkoxylated ketones, employing an organophotoredox catalyst and readily available, inexpensive styrene derivatives for the first time. The reaction proceeds via the oxidative functionalization of styrenes using molecular oxygen (O_2) as the oxidant. While previous methods have primarily relied on activated substrates such as ketones, enols, or enolates. α-Alkoxylated carbonyl compounds serve as versatile synthetic building blocks, playing a crucial role in the design of bioactive molecules, including adrenergic blockers and HIV-1 integrase inhibitors. In addition, these compounds also act as key precursors in the synthesis of chiral alcohols, making them indispensable in asymmetric synthesis. Consequently, a diverse array of synthetic methodologies has been developed to efficiently access these valuable compounds. The traditional approaches utilize the umpolung strategy with ketones employing excess quantity of oxidizing agents for the synthesis of *α*-alkoxylated carbonyl compounds, with alcohols serving as solvents. However, this approach necessitated the use of an excess oxidant, which in turn resulted in limited functional group compatibility, posing challenges in substrate scope and selectivity.

Photoredox chemistry has recently emerged as a viable alternative to conventional techniques, enabling transformations which are usually inaccessible from the traditional pathways. Additionally, this approach has also been effectively employed to synthesize *α*-alkoxylated carbonyl compounds. However, it relied on the use of pre-functionalized (activated) substates such as enolates, radical precursors (*N*-alkoxypyridinium salt) and relied on precious metallophotocatalyst $[Ru(bpy)_3(PF_6)_2]$. Conventional methods of carbonyl/*α*-functionalized carbonyl compound synthesis either rely on harsh conditions, transition metal-based catalysts/regents, toxic reagents along with the formation of side products in some cases.

Based on the literature precedence, there is a need for the sustainable alternative method and also direct functionalization of alkenes would be of great interest. To the best of our knowledge, α-alkoxylated ketones have not been synthesized directly from inexpensive feedstocks like styrene. Therefore, we hypothesized that α-alkoxylated ketones could be accessed from alkenes under transition metal-free conditions via the oxidative functionalization of alkenes using visible light mediated organophotoredox catalysis (Scheme 3.1).

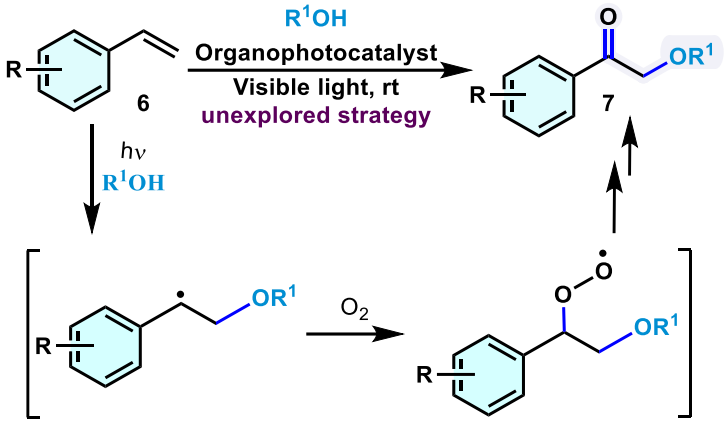

Scheme 3.1 Our hypothesis for oxidative functionalization of alkenes to α-alkoxylated ketones

To evaluate our hypothesis, we commenced the optimization of reaction conditions for the synthesis of α-alkoxylated ketones using styrene as the model substrate. Based on the systematic and detailed screening of various photocatalysts, light sources and co-solvents, styrene **6a** (0.4 mmol) with Mes-Acr-Me·BF_4 (3 mol%) in methanol (serving as both solvent and nucleophile), following O_2 purge (10-min.) and irradiation with Kessil blue LEDs (467 nm, 20 W) at room temperature proved to be the optimum reaction conditions to access the desired α-methoxylated ketone **7** in very good yield (86%).

Having established the optimum reaction condition, we then evaluated the substrate scope to assess the generality of protocol to synthesized various α-alkoxylated ketones (Table 3.2). A series of substituted styrene derivatives bearing electron-neutral, electron- donating, electron-deactivating and electron-withdrawing groups smoothly underwent the transformation, affording the corresponding α-alkoxylated ketones (**7a**–**7q**) in moderate to excellent yields (up to 92%, Table 3.2). Furthermore, the internal alkene β-methyl styrene derivatives also reacted under the optimized conditions to afford the corresponding α-methoxylated ketone products (**7r** and **7s)** in modest yields (Table 3.2). Additionally, heteroaryl substrate 2-vinylthiophene also reacted smoothly under the reaction condition to afford the desired product **7t** in moderate

yield (Table 3.2). Later, various alcohols such as ethanol, *n*-propanol, *i*-propanol, *n*-butanol, and *t*-butanol were successfully reacted with styrene to afford the corresponding *α*-alkoxylated ketone products (**7u**-**7y**) in moderate to good yield (up to 73%, Table 3.2).

Table 3.2 Substrate scope of *α*-alkoxylated ketone products.[a]

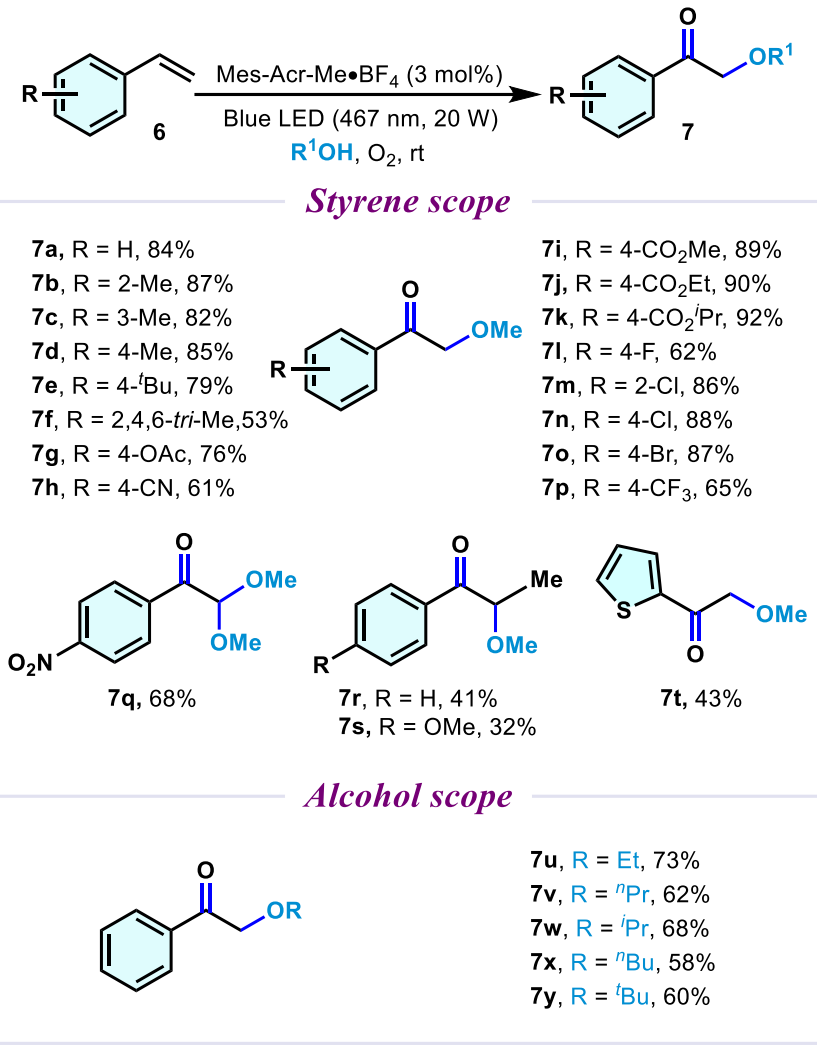

Reaction conditions: : [a]**6** (0.4 mmol), Photocatalyst (3 mol%), **R[1]OH** (3 mL), Kessil blue LEDs (467 nm, 20 W) room temperature (rt), O_2-purging (10 min). [b]Isolated yield after purification by column chromatography.

Having demonstrated the generality of the developed protocol for the synthesis of broad range of *α*-alkoxylated ketone products, we next explored its performance under natural sunlight. This reaction successfully afforded the desired product **7a** in good yield of 76%. To further evaluate the practicality of the method, a scale-up reaction of styrene (1 g) was carried out to obtain the corresponding product **7a** in good yield. Subsequently, the *α*-methoxylated ketone

product **7a** was subjected to post-synthetic modification reaction with secondary amine to obtain the *α*-keto amide **8a** (Scheme 3.2).

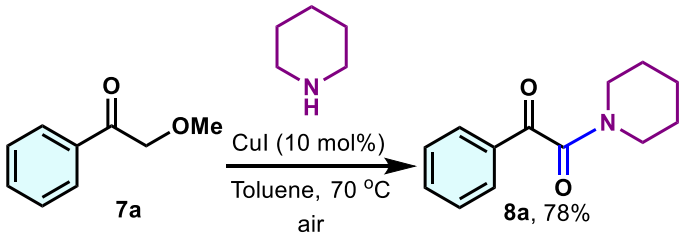

Scheme 3.2 Post synthetic modification of **7a** to synthesize *α*-keto amide **8a**

Later, we carried out a systematic series of control experiments, fluorescence quenching and cyclic voltammetry experiments to have insights into the plausible reaction pathway of the *β*-hydroxytrifluoromethylation of alkene.

In summary, we have successfully demonstrated a transition metal-free, visible light promoted direct synthesis of *α*-alkoxylated ketone from readily available inexpensive styrene derivatives at room temperature. A nontoxic and inexpensive acridinium organophotoredox catalyst has been utilized for the operationally simple and mild protocol. The methodology showed broad substrate scope with respect to styrene and alcohols. The post-synthetic modification of the synthesized product has also been demonstrated for the synthesis of *α*-keto amide. The protocol has been proved to be scalable and it works smoothly under the direct exposure of sunlight. A series of control experiments, fluorescence quenching and cyclic voltammetric studies proved that transformation is driven via reductive quenching mechanistic cycle.

Chapter 4: *Visible Light Driven Organophotoredox Catalyzed Oxidative Functionalization of Styrenes: Synthesis of 1,4-Diketones*

This chapter presents an organophotoredox-catalyzed strategy for the synthesis of 1,4-diketones directly from readily available and cost-effective styrenes. The synthesis of 1,4-diketones presents greater challenges compared to their 1,3- and 1,5-diketone counterparts, primarily due to the inherent polarity mismatch of carbonyl synthetic equivalents, making them less intuitive targets. Recent advances in the construction of 1,4-dicarbonyl frameworks have predominantly focused on umpolung strategies that utilize pre-existing carbonyl-containing

fragments. In contrast, transformations involving non-carbonyl precursors to generate carbonyl functionalities in-situ remain elusive and are relatively underexplored. Therefore, we sought to explore the oxidative functionalization of styrenes followed by dimerization to afford 1,4-diketones.

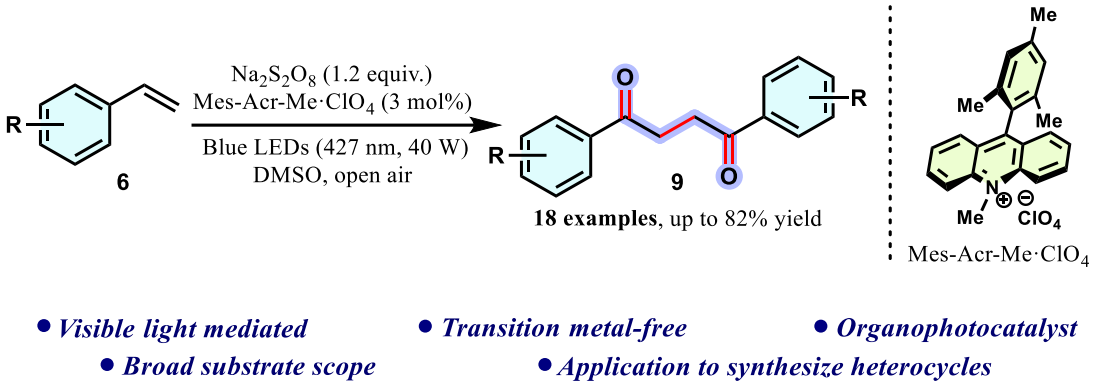

Scheme 4.1 Visible light mediated organophotoredox catalyzed synthesis of 1,4-diketones

To validate our hypothesis, we initiated the optimization of reaction conditions for the synthesis of 1,4-diketones using 4-chlorostyrene as a model substrate. Based on the systematic screening of various photocatalysts, solvents, oxidants and light sources, 4-chlorostyrene (0.2 mmol), $Na_2S_2O_8$ (1.2 equivalents), and Mes-Acr-Me·ClO_4 (3 mol%) in DMSO (3 mL), irradiated with blue LEDs (427 nm, 40 W) under ambient air at room temperature (8 h) proved to be optimized reaction conditions to obtain the desired 1,4-dicarbonyl compound **9** in very good yield.

Having established the optimum reaction conditions, we proceeded to investigate the substrate scope to evaluate the practicality and generality of the developed protocol. Under the optimized reaction conditions, a range of electron-neutral, electron-donating and electron-withdrawing styrenes successfully underwent the transformation, affording the corresponding 1,4-diketone products (**9a**–**9p**) in very good yields (up to 82%, Table 4.1). The heteroaromatic (pyridyl) pendant vinyl derivative as well as polycyclic aromatic substrate vinyl naphthalene found to be susceptible under the reaction condition to afford the corresponding products (**9q** and **9r**) in moderate yields (Table 4.1).

Having demonstrated the broad applicability of the developed protocol for the synthesis of 1,4-diketones, we next explored its performance under the direct exposure of natural sunlight. This reaction successfully afforded the desired 1,4-diketone product **9a** in good yield.

Table 4.1 Substrate scope of 1,4-Diketones[a]

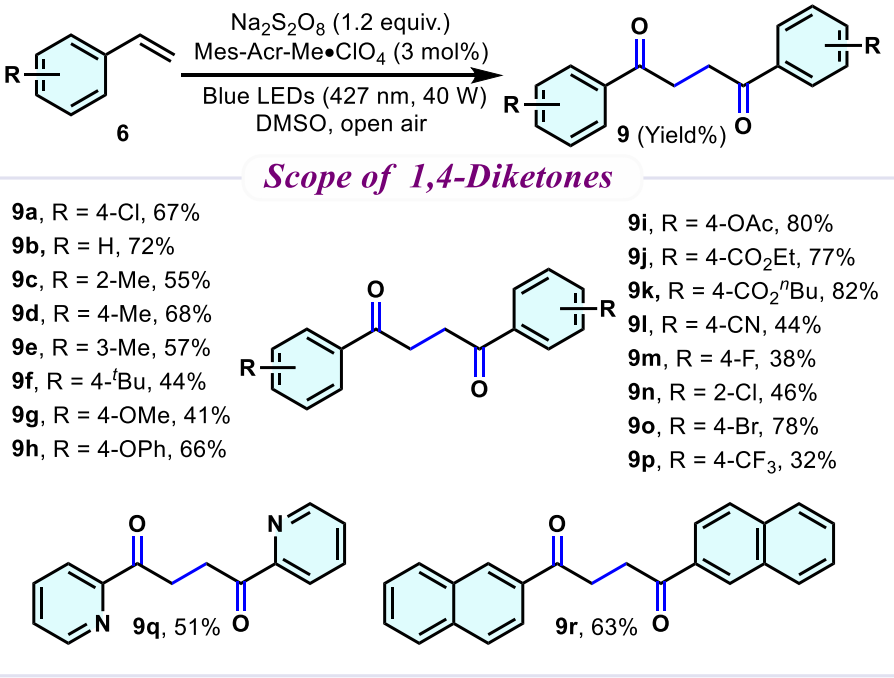

Reaction conditions: [a]**6** (0.4 mmol), $Na_2S_2O_8$ (1.2 equiv.), Mes-Acr-Me·ClO_4 (3 mol%), DMSO (2 mL), blue LEDs (427 nm, 40 W), rt, open air. [b]Isolated yield after column chromatography.

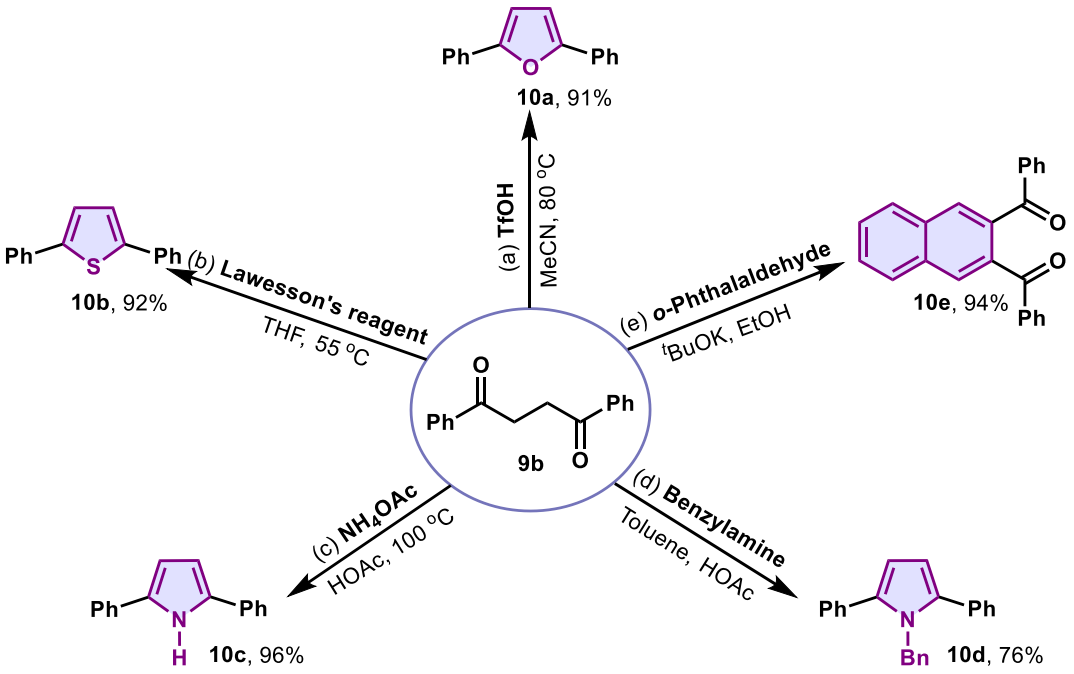

Scheme 4.2 Post-synthetic modification of 1,4-diketone product **9b**

To further evaluate the practicality of the method, we carried out the scale-up reaction using 4-chloro styrene (1 g) to furnish the corresponding product **9a** in a moderate yield (63%).

Subsequently, we turned our attention toward the post-synthetic modification of the 1,4-diketone product **9b** (Scheme 4.2). Leveraging the versatility of product **9b** as a key precursor, we synthesized a variety of synthetically valuable and high-value heterocyclic scaffolds, such as substituted furan, thiophene, and pyrrole derivatives (Scheme 4.2).

To gain a deeper understanding of the reaction mechanism, a series of control experiments, fluorescence quenching, and cyclic voltammetry experiments were performed (Scheme 4.3). Based on these experimental results, a probable reductive quenching mechanism has been proposed for the 1,4-diketone synthesis.

In summary, we have successfully demonstrated synthesis of 1,4-deketones from readily available inexpensive feedstock chemical styrene via organophotoredox catalysis under visible light irradiation at room temperature. The methodology has been generalized with broad substrate scope with respect to styrenes. The post-synthetic modifications of 1,4-diketone product have been demonstrated by synthesizing various heterocycle synthesis such as furan, thiophene, pyrrol and naphthalene. Also, the protocol has been proved to be scalable and it works smoothly under the direct exposure of sunlight. A series of control experiments, fluorescence quenching and cyclic voltammetric studies proved that transformation is driven via reductive quenching mechanistic cycle.

Chapter 5: *Harnessing Aryl Thiocyanate: A Circular Chemical Approach to Thiocyano-Thioesters from Cyclic Thioacetals*

This chapter illustrates a sustainable approach to access thiocyano-thioesters starting from aryl thiocyanate as an organic 'CN' source and leveraging the power of organophotoredox catalysis under visible light. Notably, the process embodies the some of the principles of circular chemistry by repurposing the by-product, diaryl disulfide, into a recyclable and reusable precursor for synthesis of aryl thiocyanates. This strategy boasts broad functional group tolerance, seamlessly accommodating 5- to 8-membered cyclic thioacetals, and is readily scalable to gram quantities. The mechanistic insights have been supported by fluorescence quenching studies, cyclic voltametric data, and control experiments. These studies provided a deeper understanding of the reaction pathway, further underscoring the synthetic utility of this approach.

The cyclic thioacetals such as 1,3-dithianes and 1,3-dithiolanes are stable carbonyl-protecting

groups used in total synthesis. While photoredox-catalyzed C–S bond cleavage is well studied for the formation of new C–C or C–heteroatom bonds. However, the selective single C–S bond cleavage of cyclic thioacetals to synthesize rearranged functionalized thioacetal derivatives remains unexplored. Such transformations could enable novel rearrangements and offer high chemoselectivity under visible light and mild reaction conditions.

Previously, we investigated the reactivity of dithiolanes/dithianes with NaSCN as a cyanating agent to synthesize thiocyano-thioesters. To address some of the issues such as usage of excess reagent and in turn generation of stochiometric water soluble waste during the synthesis of thiocyano-thioester synthesis, we planned to explore the alternative strategy that is more practical. In this regard, we proposed to explore the use of suitable organic cyanating sources so as to enable the reuse of by-products in the subsequent transformations. We hypothesized that aryl thiocyanates (ArSCN) as a radical cyanating source could be ideal for the in photoinduced transformations. We hypothesized that aryl thiocyanates can serve as an ideal source for generating CN radicals under visible light of suitable wavelength and the in turn generated organic by-product, diaryl disulfide, could be recycled for the synthesis of additional aryl thiocyanates, thus aligning with circular economy principles.

Herein, for the very first time we present the use of aryl thiocyanate **12** as an efficient cyanating agent under visible-light organophotoredox catalysis to synthesize thiocyano-thioesters **13** from cyclic thioacetals **11**. The diaryl disulfides **14** formed in the reaction are effectively recycled to produce various aryl thiocyanates **12** efficiently (Scheme 5.1).

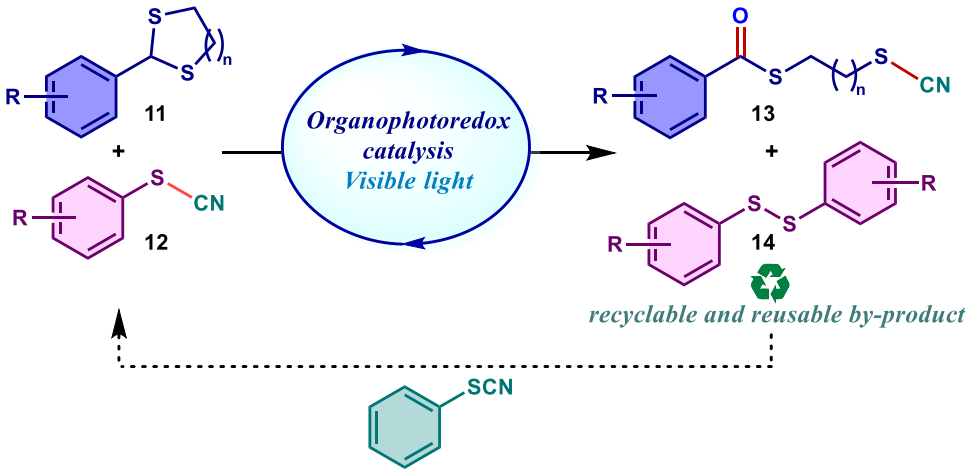

Scheme 5.1 Our hypothesis: Circular chemical economy approach for the synthesis of thiocyano-thioesters using aryl thiocyanates

We commenced with optimization of reaction condition using cyclic thioacetal 2-(*p*-tolyl)-

1,3-dithiolane and phenyl thiocyanate as model substrates.

Table 5.1 Substrate scope of thiocyano-thioester products.[a]

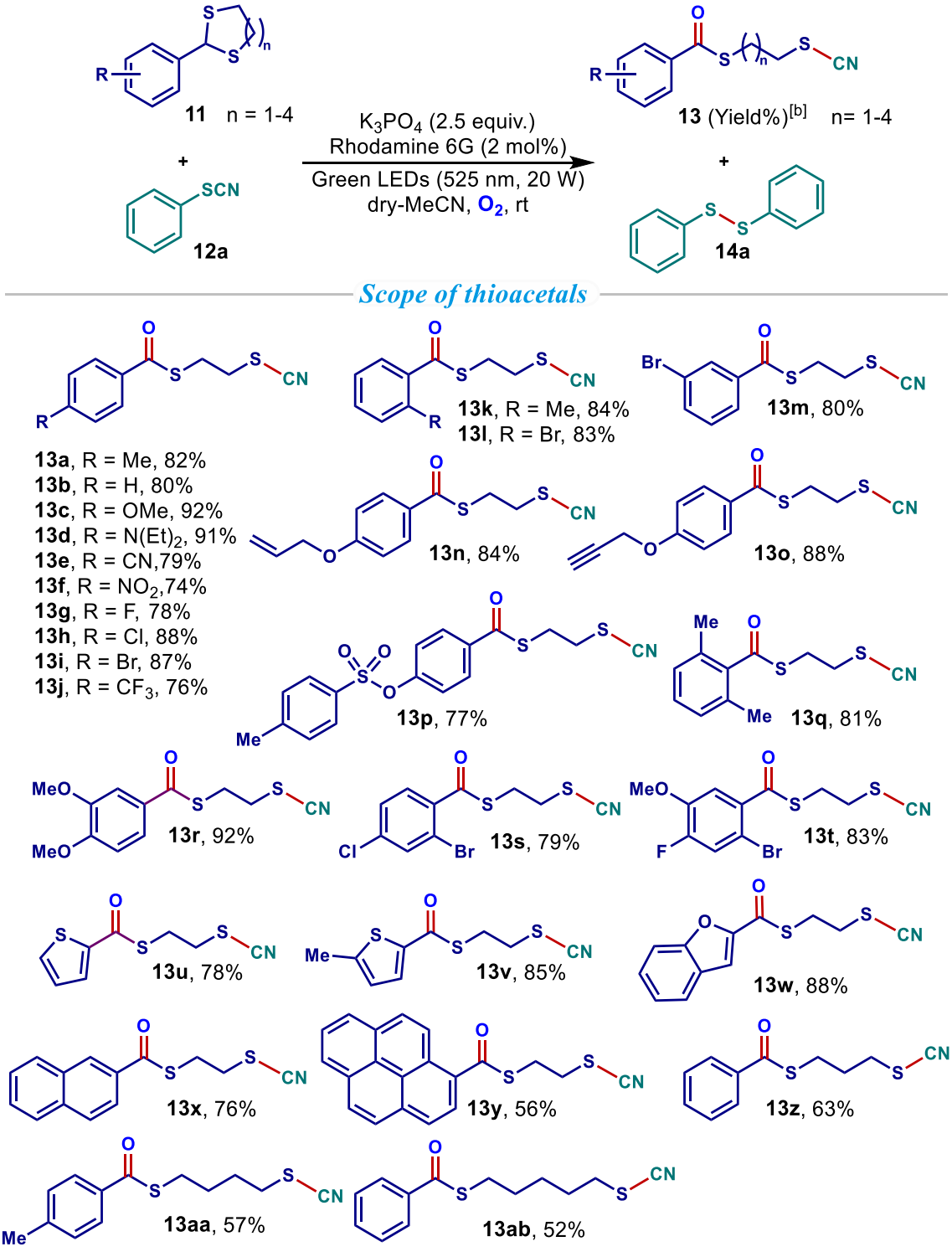

Reaction conditions: [a]**11** (0.2 mmol), PhSCN 1**2a** (1.1 equiv.), K_3PO_4 (2.5 equiv.), Rhodamine 6G (2 mol%), O_2-balloon, dry-MeCN (3 mL), Kessil Green LEDs (525 nm, 20 W) at room temperature (rt). [b]Isolated yield after purification by column chromatography.

After the systematic evaluation of various conditions, such as bases, light sources, photocatalysts, solvents, stoichiometry of reagents and reaction times, we successfully optimized reaction conditions for the synthesis of thiocyano-thioester product from thioacetal. The established optimized reaction conditions comprise of cyclic thioacetal 2-(*p*-tolyl)-1,3-dithiolane (0.2 mmol), phenyl thiocyanate (1.1 equiv.), K_3PO_4 (2.5 equiv.), and Rhodamine 6G (2 mol%) in anhydrous acetonitrile (3 mL), irradiated with green LEDs (525 nm, 20 W) under an O_2 atmosphere at room temperature to access desired products in thiocyano-thioesters **13**.

Following the optimization of reaction conditions, a library of thiocyano-thioester products (**13a-13z**, **13aa** and **13ab**) has been synthesized by varying different substituents such as electron-donating, electron-withdrawing, electron-deactivating and cyclic thioacetals of varying ring sizes from five-eight membered rings (Table 5.1). A scale-up reaction of the protocol has been demonstrated to show the practicality of this transformation.

Table 5.2 Substrate scope of aryl thiocyanate products.[a]

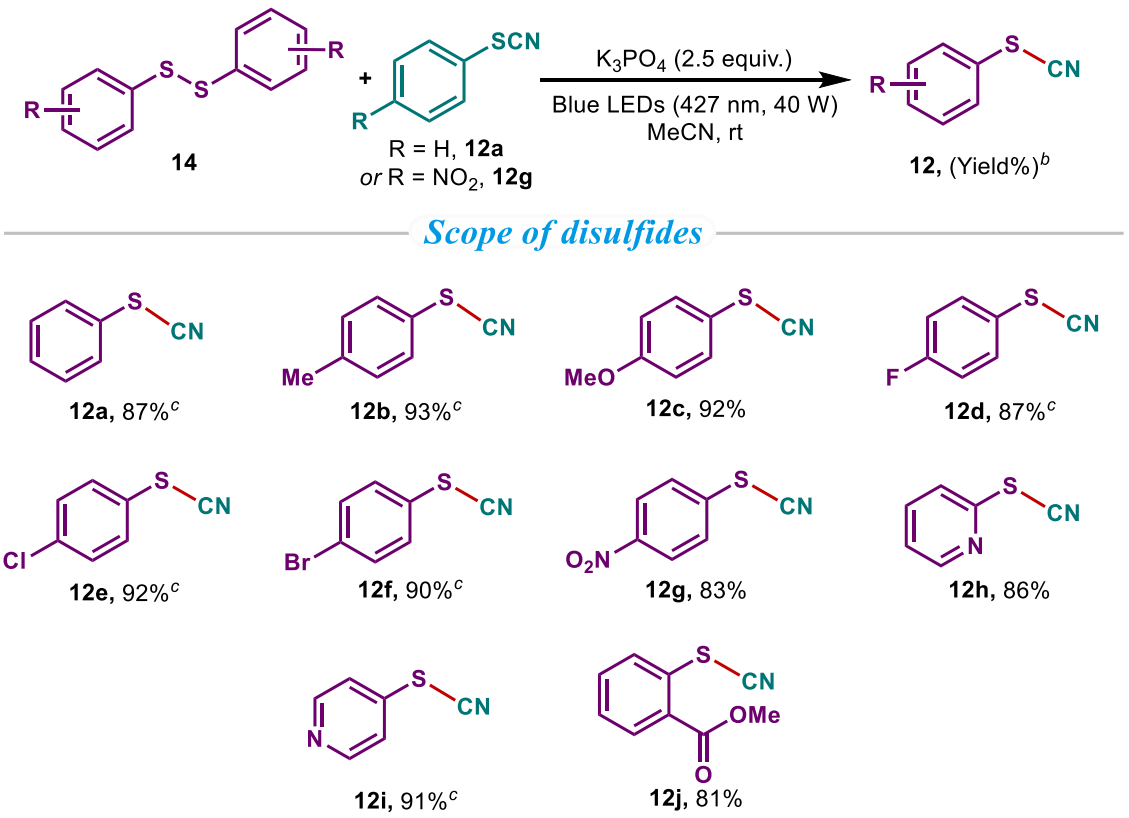

Reaction conditions: [a]**14** (0.2 mmol), PhSCN **12a** (2.1 equiv.), K_3PO_4 (2.5 equiv.), in dry-MeCN (3 mL), Kessil Blue LEDs (427 nm, 40 W) at room temperature (rt). [b]Isolated yield after purification by column chromatography. [c]4-NO_2-PhSCN **12g** (2.1 equiv.) was used instead of **12a**.

To validate our hypothesis of implementing circular economy principle through the reuse of by-products diaryl disulfides **14**, the reaction of diaryl disulfides **14** were conducted with phenyl thiocyanate **12a** or 4-NO_2-PhSCN **12g** under blue LEDs irradiation (427 nm, 40 W) to obtain the corresponding aryl thiocyanates **12** (**12a**–**12j**) (Table 5.2).

To gain insight into the reaction mechanism, we systematically conducted a series of control experiments, UV-Visible absorption studies, fluorescence quenching and cyclic voltametric analysis. The plausible reaction pathways have been proposed for both thiocyano-thioester synthesis and the synthesis of thiocyanates.

In summary, we have successfully demonstrated the effective use of aryl thiocyanates as sustainable 'CN' sources for the direct cyanation of cyclic thioacetals under visible light irradiation. The resulting diaryl disulfide by-products were efficiently recycled to regenerate aryl thiocyanates, promoting a circular economy. This transition metal- and oxidant-free protocol features broad substrate applicability, including both thioacetals and disulfides. The protocol is also scalable to gram quantity. The mechanistic investigations based on UV-visible absorption, fluorescence quenching, and cyclic voltametric studies strongly supported the reductive quenching photoredox cycle, highlighting the practicality and sustainability of this synthetic strategy.

*****

(Numbers of substrates and products in the synopsis are different from those in the thesis chapters. Please note that compound numbers have been assigned in the synopsis and subsequent chapters for the flow and convenience of the readers)

List of Publications

Included in the thesis

1. **Behera**, **M.**; Shukla, S. Y.; Dharpure, P. D.; Bhat, R. G.* Aryl Thiocyanate as an Organic 'CN' Source: Access to Thiocyano-Thioesters from Cyclic Thioacetals. *Chem. Asian J.* **2025**, e00423.

2. **Behera**, **M.**; Dharpure, P. D.; Sahu, A. K.; Bhat, R. G.* Visible Light-Induced Organophotoredox-Catalyzed*β*-Hydroxytrifluoromethylation of Unactivated Alkenes. *J. Org. Chem.* **2024**, *89*, 14695−14709.

3 **Behera**, **M.**; Shukla, S. Y.; Muhammed, S. C.; Pattanaik, S.; Bhat, R. G.* Visible Light Driven Organophotoredox Catalyzed Oxidative Functionalization of Styrenes: Synthesis of α-Alkoxylated Ketones and 1,4-Diketones. (*Manuscript is ready to be communicated*)

Not included in the thesis

4 **Behera**, **M.**; Dharpure, P. D.; Shukla, S. Y.; Bhat, R. G.* Photo Induced Transition Metal-free Synthesis of Disulfide Linked Dithioesters and Amides from Cyclic Thioacetals. (*Manuscript is under preparation*).

5 **Behera**, **M.**; Sahu, A. K.; Shukla, S. Y.; Bhat, R. G.* Electrochemically Promoted Regioselective C3–H Trifluoro/Difluoromethylation of 2*H*-Indazoles at Room Temperature. *Synlett* **2024**, *35*, 2547−2553.

6 Rao, G. N.; **Behera**, **M.**; Kathirvel, K.; Sekar, G.* Stable and Reusable Pd/Cu Bimetallic Nanoparticle Catalysts for the Synthesis of Hydroxy Isoindolones by Domino C–H Activation and Annulation. *Eur. J. Org. Chem.* **2024**, *27*, e202400471.

7 Dharpure, P. D.; **Behera**, **M.**; Khade, V. V.; Thube, A. S.; Bhat, R. G.* Direct Access to Thiocyano-Thioesters from Cyclic Thioacetals via Photoredox Catalysis: An Introduction of Two Functional Groups in One Pot. *Org. Lett.* **2022**, *24*, 6919−6924.

8 Dharpure, P. D.; **Behera**, **M.**; Thube, A. S.; Bhat, R. G.* Base Dependent Rearrangement of Dithiane and Dithiolane under Visible-light Photoredox catalysis. *Chem Asian J.* **2023**, *18*, e202201128.

Book Chapter

9 Book Name: "Handbook of CH-Functionalization (CHF)". Edited by: Dr. Debabrata Maiti Chapter Title: C–H Bond Functionalization by the Confluence of Organocatalysis and/or Transition Metal Catalysis with Photoredox Catalysis. Authors: Bhowmick, A.; **Behera**, **M.**; Bhat, R. G.* Publisher: Wiley-VCH. ISBN: ISBN 9783527834242; **https://doi.org/10.1002/9783527834242.chf0086**

Chapter 1

Introduction to Photocatalysis in Organic Synthesis: Reactions of Alkenes & Cyclic Thioacetals under Visible Light

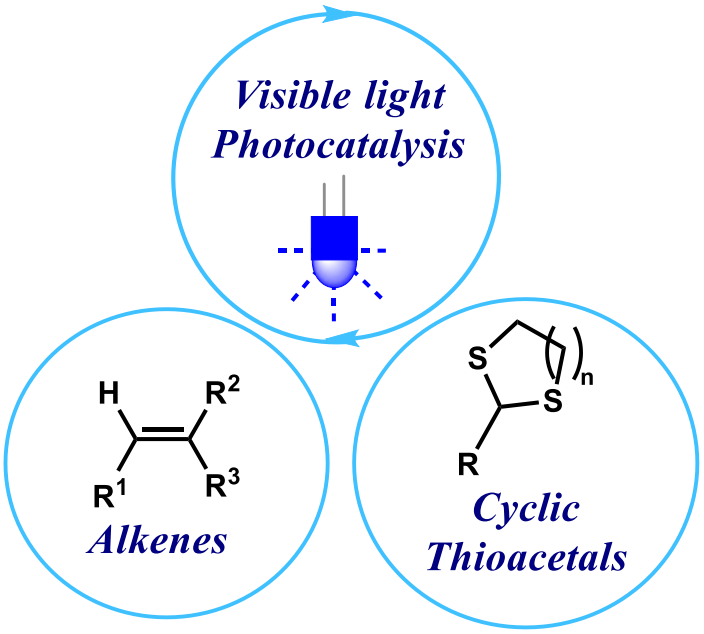

Introduction to Photocatalysis in Organic Synthesis: Reactions of Alkenes & Cyclic Thioacetals under Visible Light

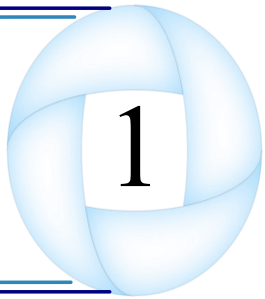

This chapter provides an overview on the fundamental principles of photocatalysis, including its classification, mechanisms of operation, and a concise historical perspective on its development within the field of organic synthesis. Special emphasis is placed on the synthetic relevance of alkenes, with a focus on recent advancements, existing challenges, and emerging opportunities in their difunctionalization through visible-light-driven photoredox catalysis. Additionally, this chapter explores the significance and chemical reactivity of cyclic thioacetals, particularly their transformation via selective C–S bond cleavage under visible-light photoredox conditions, as a strategy for constructing structurally complex organic molecules. The inherent challenges associated with the selective activation of a single C–S bond in these systems, as well as their reactivity with various reagents and substrates to access novel and valuable products, will also be critically reviewed.

1.1 Introduction

Modern organic synthesis has evolved over the years by embracing unconventional mode of activation of reaction pathways by going beyond the conventional methods of heating or chemical catalysis. Over the recent years, visible light photoredox catalysis has rapidly evolved into one of the cornerstones of modern organic synthesis. As a result, the photon is now widely recognized as a quintessential 21st-century reagent.[1] Nevertheless, the first documented study of light-induced chemical change in an isolated organic compound dates back to 1834, when German chemist Johann Bartholomew Trommsdorff observed that Santonin crystals, a sesquiterpene lactone used as an anthelmintic, turned yellow and burst/rupture of the crystal upon exposure to light.[2] To investigate the necessity of light and wavelength dependency of this phenomenon, Trommsdorff employed a prism to disperse sunlight into its constituent colors (Figure 1.1). He discovered that the yellowing of santonin occurred under exposure to unfiltered (white) light, as well as blue and violet light, but not under yellow, green, or red light. This study marked the first documented exploration of wavelength-specific

photochemical reactions in organic compounds. The earliest documented instance of laboratory photodimerization dates to 1867, when Carl Julius Fritzsche (1808–1871) observed the photodimerization of anthracene in St. Petersburg. Fritzsche devoted more than three decades to research in organic chemistry, making notable contributions, including his pioneering discovery in the field of photochemistry.[3] He conducted extensive studies on coal tar, during which he observed its photochemical bleaching and identified the pronounced light sensitivity of anthracene, including crystal formation upon sunlight exposure. His work led to the very first recorded photodimerization of anthracene, although the precise structure of the resulting dimer was elucidated only decades later by Elbs and others through molecular weight determination and X-ray diffraction analysis.[4]

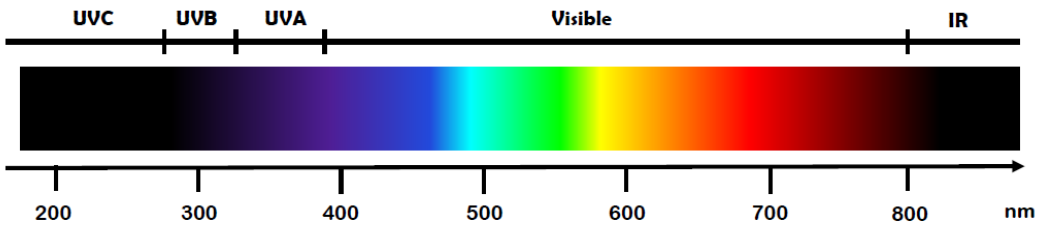

Figure 1.1 The UV-Visible region of the electromagnetic spectrum

Although there were many notable contributions in this field during the 19th century,[5] it was the most remarkable work of Ciamician and Silber in the early 20th century that marked the beginning of systematic investigations into photochemical reactions, particularly emphasizing the use of sunlight as a renewable energy source.[6] They established their photochemical laboratory on the rooftop of their institute to harness natural sunlight. Their research was focused on investigating the reactivity of various carbonyl compounds, aiming to uncover patterns and trends. In 1902, they observed pinacolization upon irradiating alcoholic solutions of certain aldehydes and ketones (Scheme 1.1). They reported that alcohols were oxidized to aldehydes, while aldehydes and ketones underwent transformation into the corresponding pinacol compounds under direct exposure of sunlight for longer reaction times. However, the rationalization of the observed reactivity patterns were often unsuccessful, as numerous "exceptions" were reported by them in the pinacolization studies.

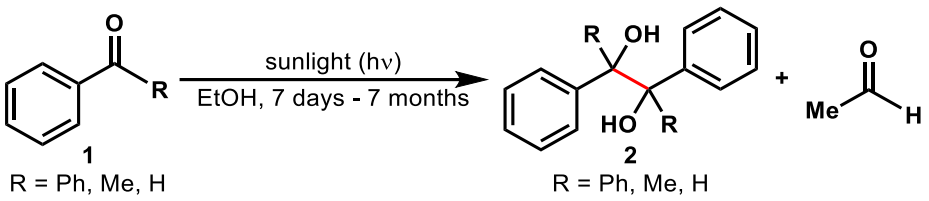

Scheme 1.1 Pinacolization of benzophenone, acetophenone and acetaldehyde under sunlight

The central challenge in photochemistry lied in the involvement of excited-state species, which possess chemical and physical properties that significantly differ from those of their ground-state counterparts. Upon absorbing light, a molecule is promoted to an excited state through the transition of an electron from a lower- to a higher-energy molecular orbital. These photoexcited intermediates often exhibit markedly enhanced and distinct reactivity, enabling transformations that are inaccessible under thermal conditions. As they relax back to the ground state via unimolecular or bimolecular chemical processes, they can facilitate the construction of structurally complex organic molecules.[7] However, until the mid-20th century, photochemistry remained largely an empirical discipline, constrained by the limited understanding of excited-state behavior. Moreover, the advancement of visible-light-driven organic synthesis has historically been hindered by two primary challenges. Firstly, the precise manipulation and control of solar radiation are critical for efficient photochemical transformations. The progress of photochemistry has closely paralleled the development of cost-effective and energy-efficient artificial light sources. Secondly, the inherent limitation lies in the relatively low energy of visible-light photons (λ = 380-700 nm), as described by the equation $E = hc/\lambda$, where h is Planck's constant, c is the speed of light, and λ is the wavelength.[8] For a photochemical reaction to proceed, the organic molecule must be capable of absorbing a photon with enough energy to promote an electron from its ground state to an excited state. However, because many organic compounds exhibit limited absorption in the visible range, higher-energy ultraviolet light is often required to initiate such reactions. This feature poses serious limitations to the widespread use of photochemistry in organic synthesis for three main concerns:

- **Safety considerations:** UV light, especially in the UVB (280–315 nm) and UVC (100–280 nm) regions (see Figure 1.1), is a high-energy radiation which can damage DNA and interact with biological matrices. Special safety measures shall be undertaken when working with UV light.

- **Requirement of special equipment:** Standard borosilicate glassware is not transparent to UV light below 300 nm. As a result, specialized quartz or UV-transparent glassware is required for conducting photochemical reactions in the ultraviolet region.

- **Selectivity issues:** Irradiating a complex reaction mixture with high-energy photons can lead to degradation of the target product or non-selective excitation of multiple components. This often results in unwanted side reactions, reducing overall efficiency and selectivity of the process.

By the 1980s and 1990s, researchers had identified light-absorbing chromophores: namely photosensitizers or photocatalysts (PCs); that effectively addressed the limitations of visible-light energy.[9] These molecules act as intermediaries, bridging the gap between the low energy of visible-light photons and the higher energy requirements of organic substrates. Upon excitation, these photocatalysts reach a higher energy state and can engage in energy transfer or single-electron transfer (SET) processes with organic molecules. This interaction generates highly reactive intermediates, such as radicals and radical ions, which further drive diverse organic transformations and enable the efficient conversion of visible light into chemical energy. Some of the metal based photocatalysts such as ruthenium and iridium polypyridyl complexes have been instrumental in the rapid advancement of photocatalytic methodologies (Figure 1.2).[10] These complexes generate reactive intermediates capable of facilitating the formation of new chemical bonds or inducing structural transformations in organic substrates. Their broad redox windows and accessible excited states enable interactions with a wide range of molecular classes, underscoring their versatility in photoredox catalysis.

The role of metallophotocatalysts in organic synthesis is undeniably significant. However, their broader application is often limited by factors such as high cost, toxicity, and the scarcity of the precious transition metals (Ru, Ir) involved. These challenges have driven the search for more sustainable, cost-effective, and environmentally friendly alternatives. Organic dyes have emerged as a promising solution in this context.[1,11] Known for their light-absorbing and photo-reactive properties since the early days of photochemistry, organic dyes offer an attractive substitute to traditional metal-based photocatalysts (Figure 1.3). These organophotocatalysts are typically inexpensive, readily available, biocompatible, and easily tunable to adjust their photophysical and redox characteristics. Moreover, the organic photoredox catalysis extends well beyond serving as a “metal-free” alternative to traditional transition metal-catalyzed processes. The powerful reactivity exhibited by many organic photocatalysts enables access to

unique transformations and a wide range of otherwise unreactive substrates. Furthermore, the structural diversity of these organic catalysts offers a valuable platform for the development and refinement of innovative synthetic methodologies.[12]

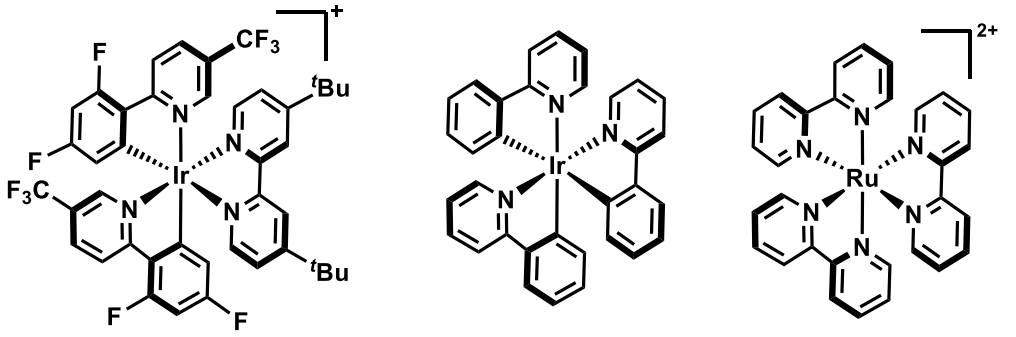

$Ir(dF\text{-}CF_3\text{-}ppy)_2(dtbpy)^{3+}$ = Ir(III)	*fac*-$Ir(ppy)_3^{3+}$ = Ir(III)	$Ru(bpy)_3^{2+}$ = Ru(II)
Ir(III)*/Ir(II) = 1.21 V	Ir(III)*/Ir(II) = 0.31 V	Ru(II)*/ Ru(I) = 0.77 V
Ir(III)*/Ir(IV) = -0.89 V	Ir(III)*/Ir(IV) = -1.73 V	Ru(II)*/ Ru(III) = -0.81 V
Ir(III)/Ir(II) = -1.37 V	Ir(III)/Ir(II) = -2.19 V	Ru(II)/ Ru(I) = -1.33 V
Ir(IV)/Ir(III) = 1.69 V	Ir(IV)/Ir(III) = 0.77 V	Ru(III)/ Ru(II) = 1.29 V
I_{max} 380 nm	I_{max} 375 nm	I_{max} 452 nm

Figure 1.2 Representative examples of metallophotocatalysts

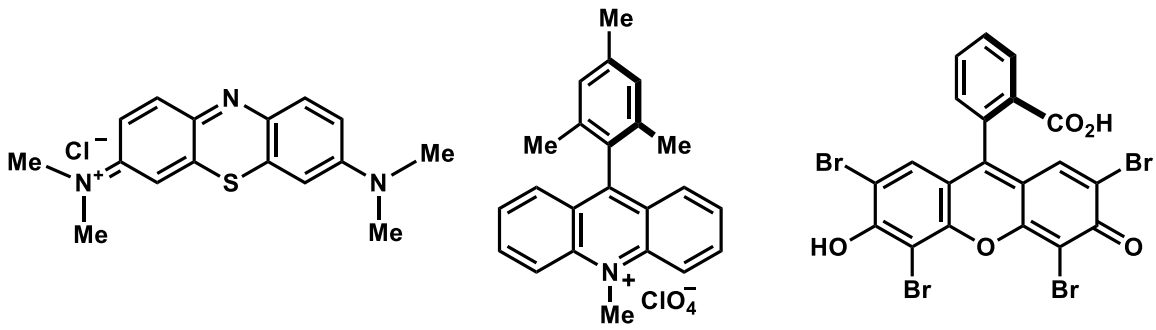

Methylene Blue	Mes-Acr-ClO_4	Eosin Y
E^*_{ox} ($PC^{\bullet+}$/PC*) = -0.33 V	E^*_{ox} ($PC^{\bullet+}$/PC*) = NA	E^*_{ox} ($PC^{\bullet+}$/PC*) = -1.11 V
E^*_{red} (PC*/$PC^{\bullet-}$) = +1.14 V	E^*_{red} (PC*/$PC^{\bullet-}$) = +2.08 V	E^*_{red} (PC*/$PC^{\bullet-}$) = +0.83 V
E_{ox} ($PC^{\bullet+}$/PC) = +1.13 V	E_{ox} ($PC^{\bullet+}$/PC) = NA	E_{ox} ($PC^{\bullet+}$/PC) = +0.78 V
E_{red} (PC/$PC^{\bullet-}$) = -0.30 V	E_{red} (PC/$PC^{\bullet-}$) = -0.57 V	E_{red} (PC/$PC^{\bullet-}$) = -1.06 V
λ_{max} = 650 nm	λ_{max} = 425 nm	λ_{max} = 539 nm

Figure 1.3 Representative examples of organophotocatalysts

1.2 Types of activation modes of photocatalysis

Having identified the types of photocatalysts employed in light-induced reactions, it is also equally important to understand how these electronically excited species interact with organic molecules to achieve the desired transformation. The transformations are driven by molecular interactions predominantly occur through three fundamental pathways: Single Electron Transfer (SET), Energy Transfer (EnT), and Atom Transfer (AT), each enabling a distinct mode of reactivity.[13]

In the case of single electron transfer (Figure 1.4), the photocatalyst (**PC**) upon excitation under visible light attains a higher energy excited state. The excited-state photocatalyst (**PC***) participates in single-electron transfer (**SET**) with either an electron acceptor (**A**) or donor (**D**). In an oxidative quenching cycle, **PC*** donates an electron to **A**, generating the oxidized photocatalyst ($\mathbf{PC}^{\bullet+}$) and the reduced acceptor ($\mathbf{A}^{\bullet-}$). Conversely, in a reductive quenching cycle, **PC*** accepts an electron from **D**, producing the reduced photocatalyst ($\mathbf{PC}^{\bullet-}$) and the oxidized donor ($\mathbf{D}^{\bullet+}$). To complete the catalytic cycle, a second electron transfer is required to regenerate the ground-state photocatalyst.

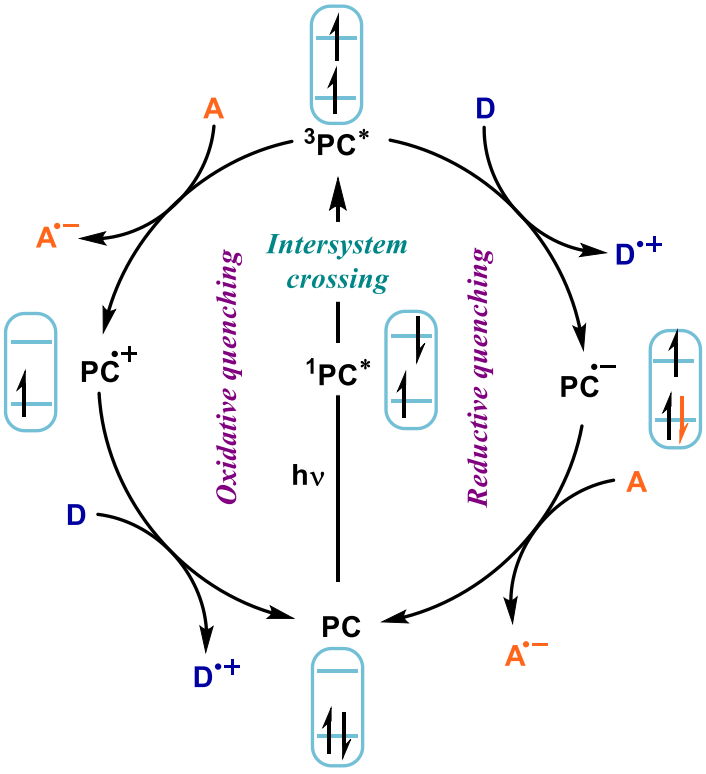

Figure 1.4 SET-mechanism (photoredox catalysis): Oxidative and Reductive quenching

In order to attain ground state PC, the (**PC**$^{\bullet+}$**)** must be reduced by an electron donor, while (**PC**$^{\bullet-}$**)** must be oxidized by an acceptor. These electron donors or acceptors may include the substrate itself, a sacrificial redox agent, or an in situ-generated intermediate. This strategy, commonly referred to as photoredox catalysis, has experienced significant development over the past decade, enabling access to both neutral and charged radical species. The thermodynamic viability of these SET processes is governed by the redox potentials of the interacting species.

In the second scenario (Figure 1.5), the excited photocatalyst operates via an energy transfer (EnT) mechanism, also referred to as photosensitization.

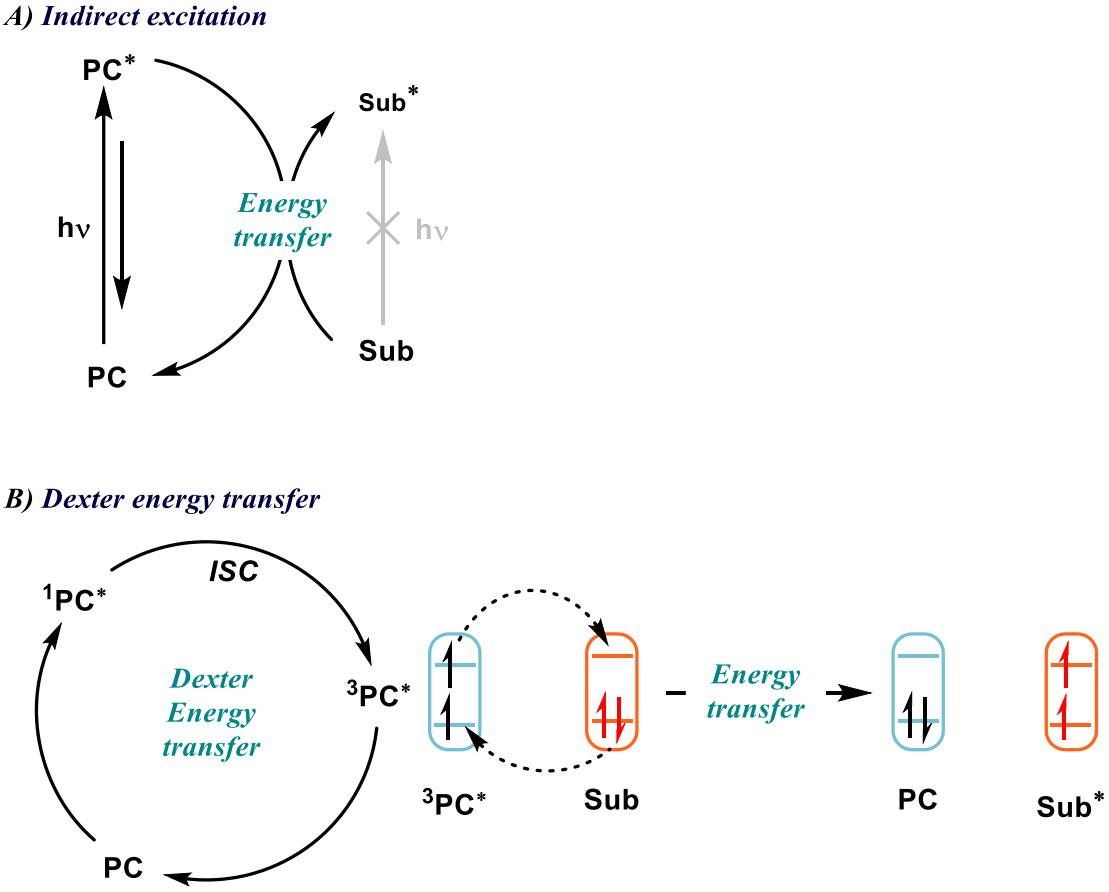

Figure 1.5 EnT-mechanism (photosensitization): Indirect and Dexter energy transfer

This process involves the transfer of excited-state energy from an excited donor, the excited photocatalyst (**PC***) to a ground-state acceptor, the substrate (**Sub**) that is not directly photoactive via a primitive emission-absorption mechanism (indirect excitation, Figure 1.5A). A specific form of this mechanism, known as Dexter energy transfer, proceeds following photoexcitation and intersystem crossing of the photocatalyst (**PC**), which reaches its triplet

excited state (^{3}**PC***) (Figure 1.5B). This triplet state then engages in a two-electron exchange with the acceptor: (^{3}**PC***) donates an electron to the LUMO of the substrate (**Sub**) while simultaneously accepting an electron from the HOMO of the substrate. As a result, the substrate is promoted to its triplet excited state (**Sub***), and the photocatalyst returns to its ground state (**PC**), ready to enter another catalytic cycle.

In the third activation pathway, known as atom transfer (**AT**) mechanism, (Figure 1.6), the excited-state photocatalyst (**PC***) abstracts an atom, typically hydrogen from a suitable substrate (**Sub–X**), resulting in the formation of a reactive radical species (**Sub•**). The photocatalytic cycle is completed when a subsequent atom transfer restores the photocatalyst to its ground state (**PC**), thereby completing the catalytic process.

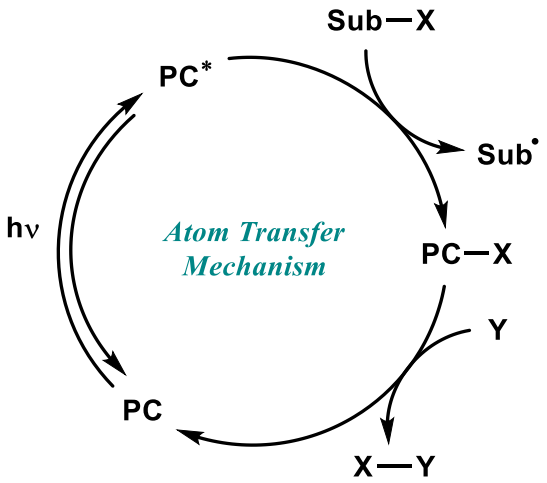

Figure 1.6 AT-type mechanism

1.3 Notable early contributions to organic photoredox catalysis between the 1970s and 1990s

In 1978, Kellogg's group reported the visible-light-induced reduction of phenacyl sulfonium salt **1a** in presence of 1,4-dihydropyridine **2** and photocatalyst $[Ru(bpy)_3]Cl_2$ to access the ketone **3** (Scheme 1.2a). Likewise, the reduction of ammonium as well as phosphonium salts **1b** and **1c** have also been achieved to afford the ketone **3** with $[Ru(bpy)_3]Cl_2$ under the irradiation of light in the subsequent study under the same condition (Scheme 1.2b, c). Control experiments confirmed that neither light nor photocatalyst alone was sufficient to drive the reaction efficiently. When irradiated with organophotocatalyst TPP = meso-tetraphenylporphine or eosin as disodium salt, the reaction reached the completion in longer reaction time. A subsequent mechanistic study, although inconclusive regarding the precise

role of [Ru(bpy)$_3$]Cl$_2$, indeed it still provided a highly insightful discussion on the experimental findings.[14]

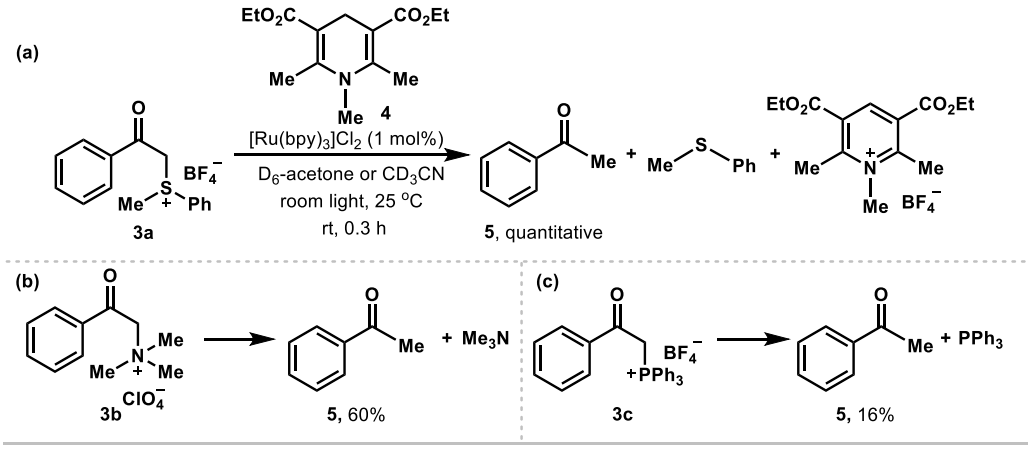

Scheme 1.2 Photoreduction of phenacyl sulfonium salt and related substrates

In 1984, Cano-Yelo and Deronzier reported the first net oxidative photoredox-catalyzed Pschorr cyclization (Scheme 1.3).[15] They studied the photocatalytic conversion of the tetrafluoroborate salt of stilbene diazonium ion **6** to phenanthrene **7** via the Pschorr reaction using Ru(bpy)$_3^{2+}$ (bpy = 2,2'-bipyridine) as the photocatalyst. Their findings revealed that this transformation proceeds quantitatively with a high quantum yield (Φ> 0.4) upon selective photoexcitation of a catalytic amount of Ru(bpy)$_3^{2+}$. Quenching and flash photolysis studies indicated that the excited state of Ru(bpy)$_3^{2+}$ is quenched via an electron-transfer process. In contrast, direct photolysis of compound **6** results in significantly lower yields of phenanthrene (10–20%).

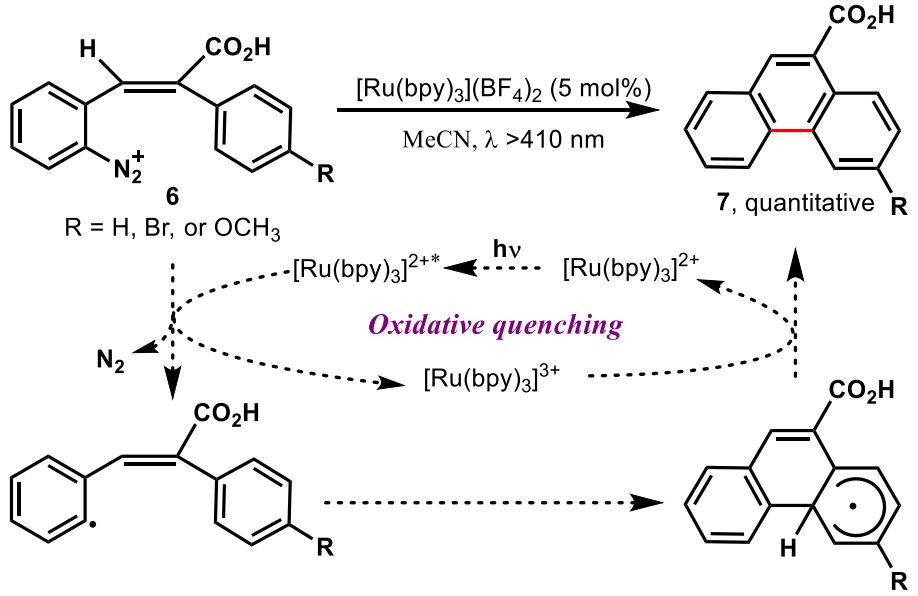

Scheme 1.3 Photocatalysis of the Pschorr reaction by tris-(2,2'-bipyridyl)ruthenium(II)

Pandey and coworkers reported organophotocatalytic cycloadditions using near-visible light (395 nm) (Scheme 1.4).[16]

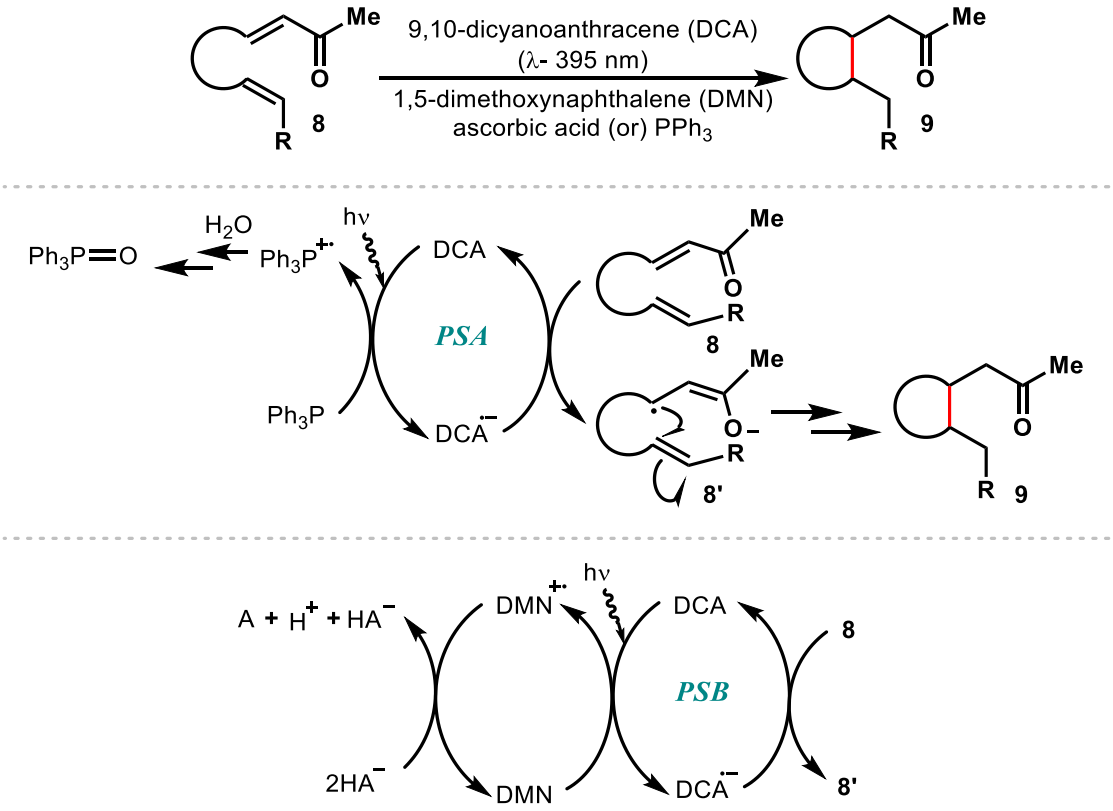

Scheme 1.4 Photocatalytic cycloaddition of dienes using DCA

They developed two photosystems to convert visible-light photons into electrons via sequential electron transfer. In photosystem-A (PS-A), 9,10-dicyanoanthracene (DCA) served as the light-absorbing electron acceptor, while triphenylphosphine (Ph_3P) acted as a sacrificial electron donor. Photosystem-B (PS-B) used DCA as the electron acceptor, 1,5-dimethoxynaphthalene (DMN) as the primary electron donor, and ascorbic acid as a secondary sacrificial donor. *α*, *β*-Unsaturated ketones were employed as secondary electron acceptors. The systems were thermodynamically tailored for the efficient electron transfer, enabling the generation of carbon-centered radicals that cyclized efficiently with activated olefins **8** to access the cyclized product **9**. However, the moderate reactivity was observed in case of non-activated olefins.

Angelo Albini (University of Pavia) and Vincenzo Balzani (University of Bologna) in Italy, Janine Cossy (Paris) in France, and Frederick Lewis (Northwestern University, Illinois, USA) were among the some of the leading researchers who extensively explored the application of

photoinduced electron-transfer processes in organic synthesis.[17] Although the potential of photoredox catalysis in organic synthesis was demonstrated early on, the field remained relatively underrecognized by the broader scientific community until it began to gain significant recognition in the late 2000s.[18]

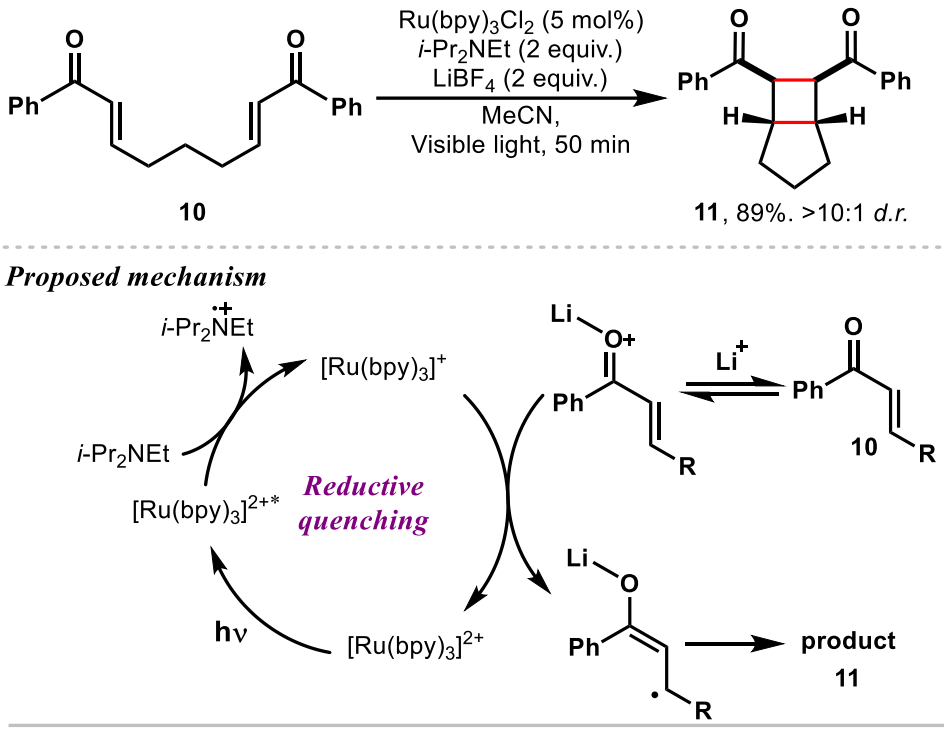

Scheme 1.5 Visible light photocatalysis of [2+2] enone cycloaddition

In 2008, Yoon and co-workers reported a seminal study on the photoredox-catalyzed intramolecular [2+2] cycloaddition of aryl enones, utilizing $Ru(bpy)_3Cl_2$ as a visible-light photocatalyst (Scheme 1.5).[19] Notably, the process effectively utilized sunlight as the sole light source to drive the reaction. In combination with a Lewis acid additive and photoexcitation of $Ru(bpy)_3^{2+}$ generates a strongly reducing $Ru(bpy)_3^{+}$ species that further facilitates one-electron reduction of the enone substrate **10** to afford the bicyclic product **11** via a radical anion cycloaddition pathway.

In the same year, MacMillan and coworkers developed a dual photoredox-organocatalytic strategy for the enantioselective α-alkylation of aldehydes (Scheme 1.6).[20] This approach harnessed the distinctive capabilities of photoredox catalysis to produce electron-deficient radicals, which selectively coupled with catalytically generated enamine. The result was a highly enantioselective transformation, offering a compelling solution to the long-standing challenge of asymmetric α-carbonyl alkylation.

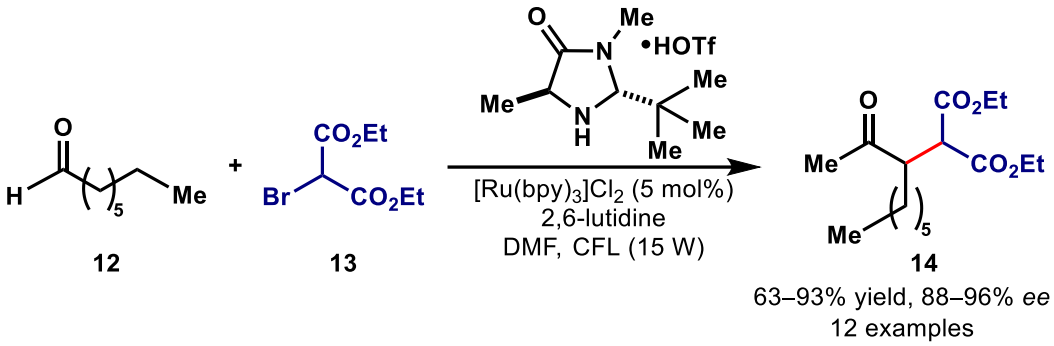

Scheme 1.6 Dual photoredoxcatalyis and organocatalysis for the asymmetric α-alkylation of aldehydes

In 2009, Stephenson and coworkers disclosed a mild method for the reductive dehalogenation of activated benzylic and α-acyl halides, employing the widely used visible-light photoredox catalyst $Ru(bpy)_3Cl_2$ in combination with $^{i}Pr_2NEt$ and either formic acid or a Hantzsch ester as hydrogen atom donor (Scheme 1.7).[21] Notably, this approach avoids the use of toxic tin-based reagents, representing a safer and more environmentally friendly alternative.

These three studies (Scheme 1.4–1.6) collectively highlighted the potential of this activation mode as a powerful catalytic platform for the organic reaction development, sparking a renewed surge in the field of photoredox catalysis. Since these foundational reports, a diverse array of Ru and Ir polypyridyl complexes, along with various organic dyes, have been shown to effectively catalyze the conversion of visible light into chemical energy, enabling transformations across a wide range of substrates.[22]

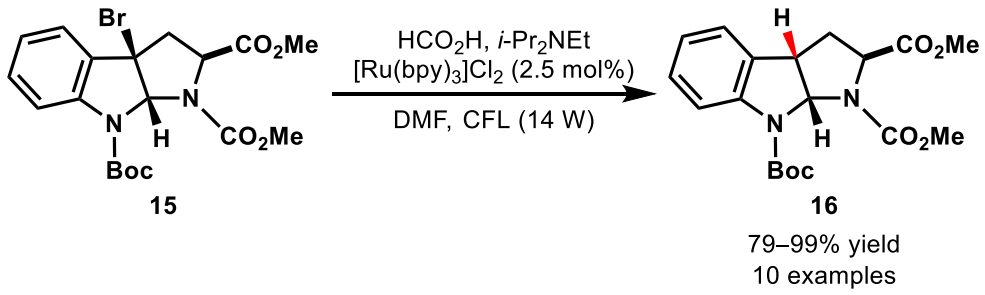

Scheme 1.7 Reductive dehalogenation of activated halides

1.4 Alkene difunctionalization reactions under photoredox catalysis

Alkenes are regarded as essential scaffolds in organic synthesis, owing to their widespread availability, structural simplicity, and diverse reactivity. Among the numerous transformations they undergo, alkene difunctionalization stands out as especially powerful. This strategy allows the simultaneous introduction of two distinct functional groups across the double bond in a single operation, enabling the rapid and efficient construction of densely functionalized molecular architectures.[23] Undoubtedly, the photoredox catalysis has emerged as a transformative tool in organic synthesis owing to the environmentally benign, sustainable, mild nature, and high functional group compatibility, as well as the unique mechanistic approaches. Over the years, it has witnessed a modern resurgence of radical chemistry through the streamlined formation of new chemical bonds.[24] In this context, photocatalytic methodologies have notably advanced the field of alkene 1,2-difunctionalization by providing a sustainable and versatile platform for the regio- and chemo-selective installation of two distinct functional groups across olefinic scaffolds in a single, efficient transformation.[25]

In 2018, Yoon and coworkers reported a photocatalytic method for the intramolecular oxyamination of alkenes **17** using simple nucleophilic nitrogen sources, rather than pre-functionalized electrophilic nitrogen donors to access the corresponding products **18** (Scheme 1.8).[26a] The transformation employed copper (II) salt as terminal oxidant. The methodology has also been successfully generalized to facilitate both diamination and dioxygenation transformations.

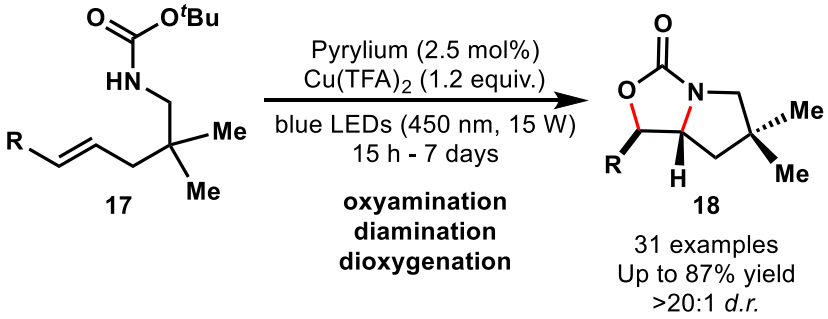

Scheme 1.8 Photocatalytic oxyamination of alkenes

Recently, Chen and coworkers, developed a visible-light photoredox-catalyzed method for intramolecular oxy- and amino-acylation of alkenes **19** using acyl oxime esters **20** (Scheme 1.9).[26b] This cascade acylation/cyclization strategy efficiently furnished diverse acylated

heterocycles **21** from simple unsaturated precursors via acyl radicals, offering a powerful route to tetrahydrofurans, piperidines, and related saturated frameworks.

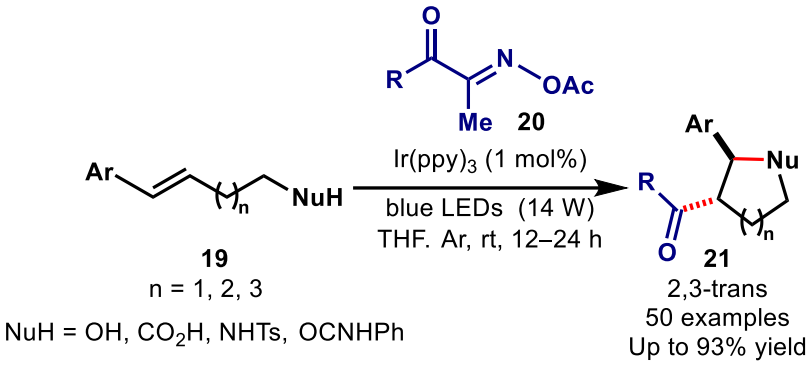

Scheme 1.9 Photoredox-catalyzed oxy- and aminoacylation of alkenes for heterocycle synthesis

In 2024, Zeng and coworkers disclosed a photoredox-catalyzed unsymmetrical diamination of alkenes **22** using *N*-aminopyridinium salts **23** and nitriles as amination reagents to access 1,2 diamino derivatives **24** (Scheme 1.10).[27] The method was successfully applied to the late-stage modification of styrene-derived pharmaceuticals and natural products, including flurbiprofen, l-menthol, piperonyl alcohol, naproxen, estrone, and fluoroquinolonic acid, regioselectively introducing vicinal diamines.

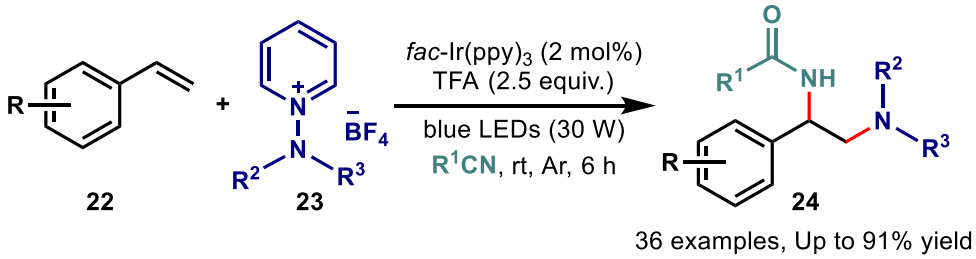

Scheme 1.10 Photoredox-catalyzed unsymmetrical diamination of alkenes

In 2019, Studer and coworkers reported a three-component radical conjugate addition involving unactivated alkenes **26** and Michael acceptors **27**, employing Cbz-protected *N*-radical precursors **25** under iridium-based photoredox catalysis to access functionalized products **28** (Scheme 1.11).[28] The reaction proceeds via oxidative generation of amidyl radicals, which selectively add to unactivated alkenes **26** to form intermediate radical adducts. These adducts subsequently undergo conjugate addition to Michael acceptors, followed by reduction to afford the final carboamination products **28** in a single, efficient transformation.

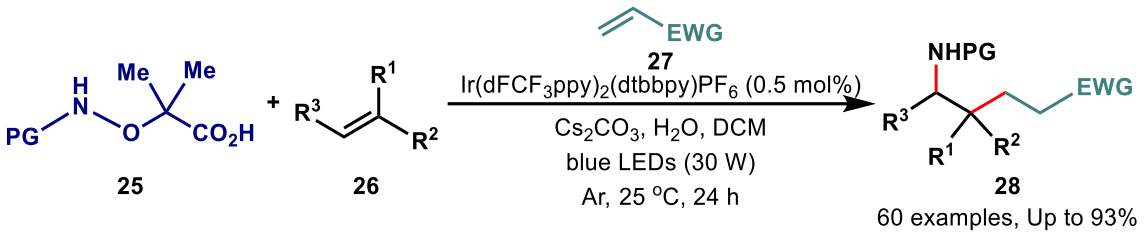

Scheme 1.11 Three component radical conjugate addition of unactivated alkenes

In 2019, Molander and coworkers reported a photocatalytic intermolecular dicarbofunctionalization (DCF) of olefins **30** by integrating Giese-type radical addition with nickel/photoredox dual catalysis (Scheme 1.12).[29a] By leveraging the fast addition of tertiary radicals to alkenes and their limited propensity for single-electron metalation with nickel, the method achieves regioselective alkylation and arylation. The protocol allows for the efficient and chemoselective formation of complex molecular architectures, including quaternary and tertiary centers, from simple and readily available starting materials.

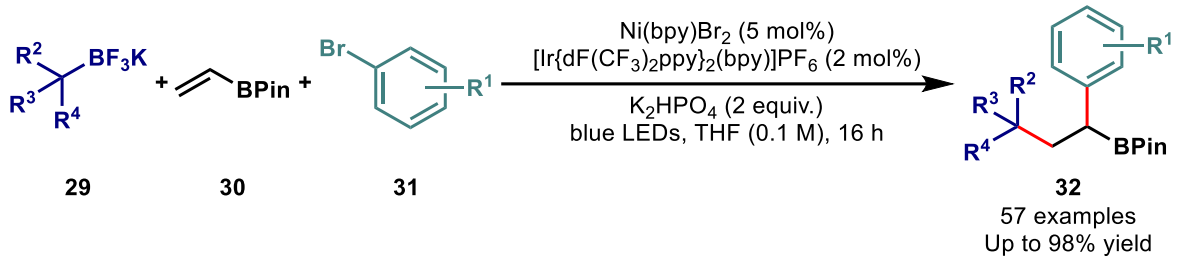

Scheme 1.12 Nickel/photoredox dual catalysis for olefin dicarbofunctionalization

In 2020, Xi and colleagues disclosed a photoredox-catalyzed dicarbofunctionalization of styrenes **22** with amines **33** and CO_2, providing a streamlined approach for the synthesis of *γ*-amino acids **34** (Scheme 1.13).[29b]

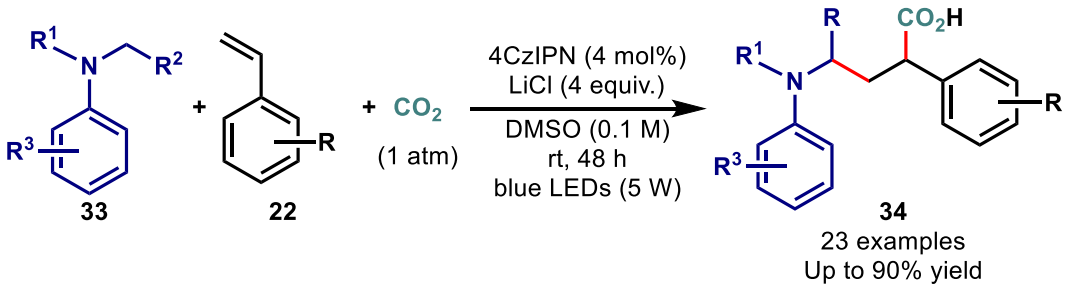

Scheme 1.13 Nickel/photoredox dual catalysis for olefin dicarbofunctionalization

These visible-light-driven methodologies, mediated by either organophotoredox catalysts or transition metal complexes, have unlocked a wide array of synthetic transformations: such as oxyamination, diamination, carboamination, and dicarbofunctionalization.[25-29] These reactions generally proceed via energy transfer or photoredox mechanisms, often engaging radical or radical–polar crossover pathways, all initiated by the photocatalyst in its excited state.[29,30]

Recently, there has been a marked increase in the development of oxo-difunctionalization strategies for alkenes via photoredox catalysis.[31] These methodologies have emerged as powerful tools for the efficient synthesis of *β*-hydroxy and *β*-ketone derivatives, enabling the construction of molecular complexity from simple, readily available precursors—typically redox-active species and olefinic substrates. At the core of these transformations lie single-electron transfer (SET) processes, which govern their reactivity.

In 2014, Akita research group reported the synthesis of *α*-trifluoromethylated ketones **37** from aromatic alkenes **35** using the Togni reagent **36** as an efficient trifluoromethyl radical (•CF_3) source, enabled by iridium-based photoredox catalysis (Scheme 1.14).[32] Dimethyl sulfoxide (DMSO) served as a mild and effective oxidant as a solvent in this transformation.

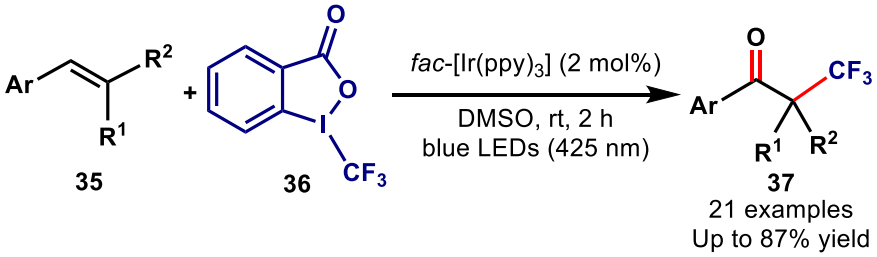

Scheme 1.14 The photocatalytic keto-trifluoromethylation of styrene

More recently, Xiao and coworkers developed a related trifluoromethylation approach by employing trifluoromethylsulfonylpyridinium salt (TFSP) as the •CF_3 precursor under visible-light photocatalytic conditions. [33]

The synthesis of *γ*-keto esters from styrenes **22** under photoredox conditions has been independently reported by Liu and Maity research groups (Scheme 1.15).[34,35] Liu and coworkers first introduced an Ir-based oxidative quenching photoredox method using *α*-bromoesters **38** as convenient radical precursors and DMSO as the oxidant (Scheme 1.14, conditions A).[34] Notably, the electron-withdrawing groups, such as NO_2, CF_3, and CN derivatives were incorporated using the same reaction conditions. Additionally, primary, secondary, and tertiary radicals were successfully introduced into the styrenyl radical acceptor. Later, in 2020, Maity described an organophotoredox approach under aerobic conditions using

α-bromocarbonyls **38** (Scheme 1.15, conditions B).[35] The combination of Eosin Y as a photocatalyst and DIPEA as a base in DMF were crucial for the success of this reaction.

Feng, Wu, and coworkers developed a distinctive oxo-alkoxylation strategy for (gem-difluoro) alkenes, effectively addressing key challenges such as β-fluoride elimination and high redox potentials (Scheme 1.16).[36] Electron-deficient difluorovinyl substrates **40** often resist benzylic radical formation, favouring anionic intermediates that promote side reactions. The optimized protocol employed an Ir-based photocatalyst, TEMPO as an additive, and *o*-dichlorobenzene (*o*-DCB) as the solvent to achieve efficient transformation.

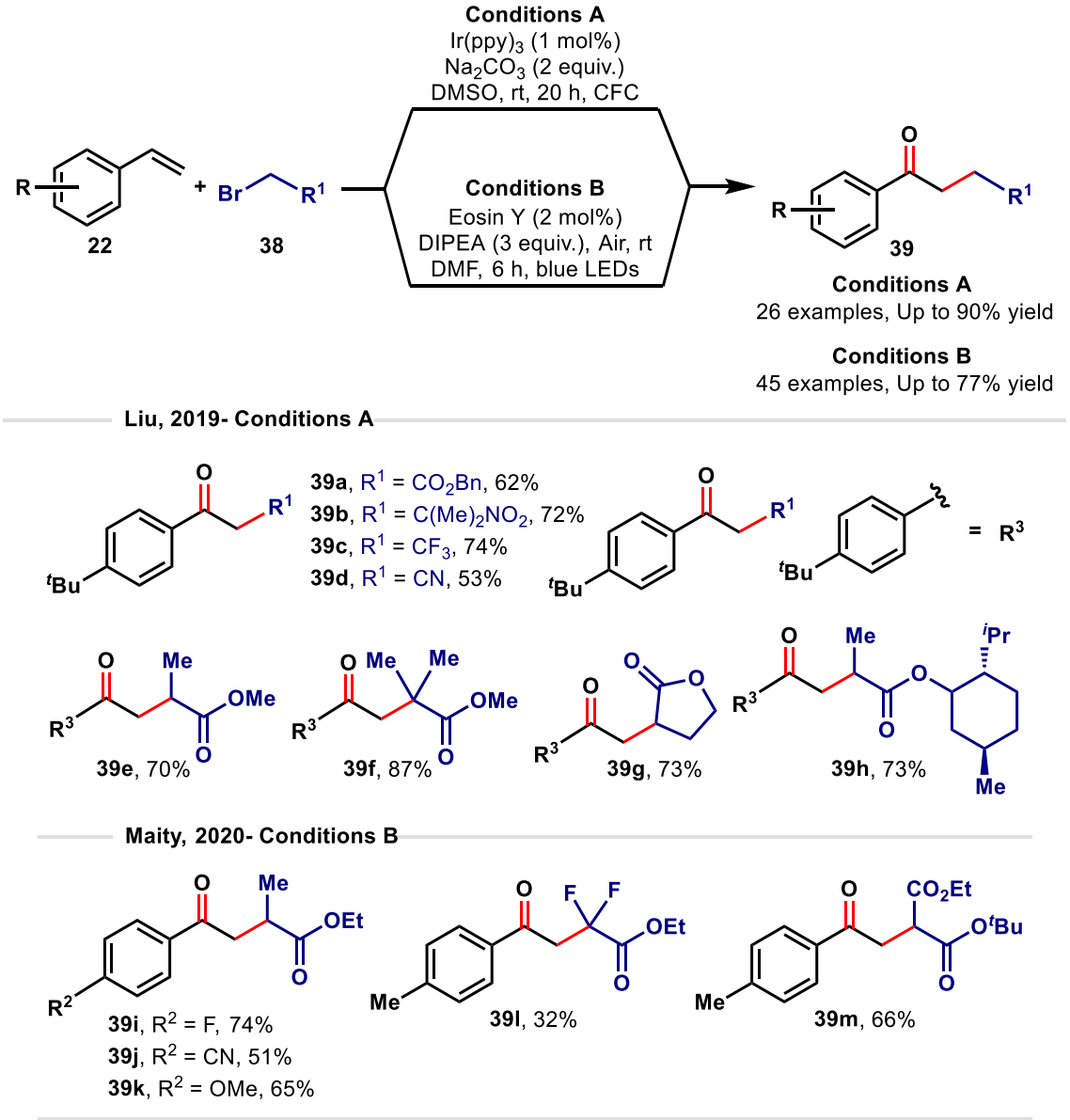

Scheme 1.15 Photoredox strategies for the synthesis of γ-keto esters from alkyl bromides and alkenes

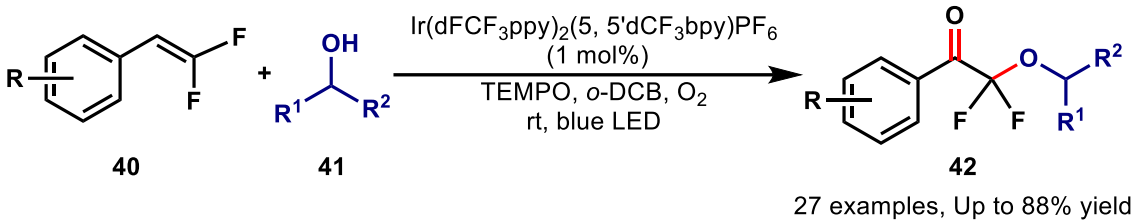

Scheme 1.16 Visible light promoted oxo-alkoxylation of gem-difluoroalkenes

As outlined, alkene difunctionalization reactions have emerged as powerful tools for the synthesis of a wide array of value-added compounds. The advancement of these transformations has largely relied on metallophotocatalysts, likely due to the alkenophilic nature of certain transition metals, which enables effective coordination with alkene substrates to facilitate functionalization. However, concerns regarding the cost, scarcity, and toxicity of metal-based photocatalysts have spurred growing interest in organophotocatalysts, which offer more sustainable and environmentally benign alternatives with unique reactivities. Notably, the oxidative *β*-hydroxy trifluoromethylation of alkenes remains unexplored under organophotoredox catalysis. In this context, we hypothesized that *β*-trifluoromethylated alcohols could be synthesized under mild and sustainable conditions using visible-light-driven organophotoredox catalysis. A detailed discussion of this approach is presented in Chapter 2.

The oxidative functionalization of alkenes to access *β*-alkoxy ketones and 1,4-diketones remains underexplored, likely due to the intrinsic polarity mismatch between the conventional reacting partners. In response to this challenge, we set out to develop a visible-light-driven organophotoredox catalytic strategy utilizing alkenes as they are abundant and cost-effective feedstock starting materials for the synthesis of valuable frameworks. A comprehensive account of the reaction design, optimization studies, substrate scope, and mechanistic insights will be provided in the following chapters.

1.5 Reactions of cyclic thioacetals under photoredox catalysis

Thioacetals and thioketals, particularly 1,3-dithianes and 1,3-dithiolanes, serve as robust carbonyl protecting groups due to their ease of formation and stability.[37] These are widely used in total synthesis and the Corey–Seebach umpolung strategy. Moreover, these are typically synthesized from carbonyl compounds and thiols under acid catalysis.[38] Recent advancements have also improved methods for the efficient deprotection of 1,3-dithiolanes.[39]

Synthetic strategies involving the cleavage of C–S bonds for the formation of new C–C or C–heteroatom bonds are particularly applicable for late-stage functionalization and improving molecular complexity. Due to the low electronegativity of the sulfur atom and the weak polarization of the C–S bond, thioethers exhibit remarkable stability toward soft Brønsted acids and bases. Hence, highly chemoselective transformations could be achieved by selective cleavage of C–S bonds. Significant progress has been made in the catalytic activation of sulfide C–S bonds using transition metal complexes[40] and Lewis acids.[41] However, the scope of these methods often remains limited, as the Lewis basic nature of sulfur can deactivate electron-deficient catalysts.[42]

Recently, photoredox-catalyzed C–S bond cleavage reactions have garnered increasing interest as a valuable strategy for constructing diverse organic motifs.[43] In 2013, Bowers and co-workers disclosed the first demonstration of this concept through a photocatalyzed glycosylation of thioglycosides **43**, initiated by the selective oxidation of a thioether (Scheme 1.17).[44]

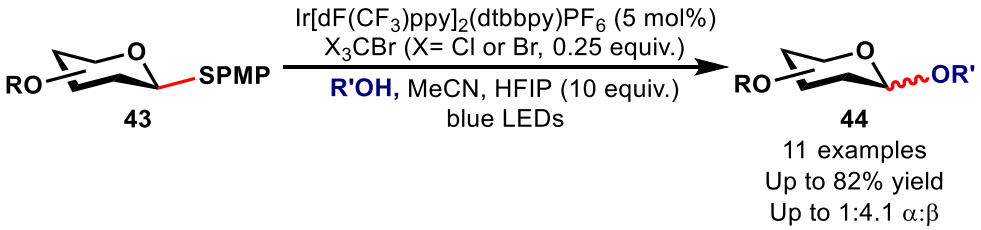

Scheme 1.17 Photoredox-driven activation and *O*-glycosylation of thioglycosides

In 2016, Masson and coworkers developed a visible-light-driven photoredox method for synthesizing *N*-carbamoyl *α*,*α*-disubstituted amines **45** from readily accessible *α*-amidosulfides **46**, employing $Ru(bpy)_3(PF_6)_2$ as a photocatalyst (Scheme 1.18).[45] The same research group also employed the strategy for the synthesis of *N*-substituted azoles via visible-light photoredox-catalyzed coupling reaction of azoles with *α*-carbamoyl sulfides. The heterocyclic units, such as pyrazoles, benzopyrazoles, benzoimidazoles, and purines were efficiently incorporated.[46] The cleavage of thioacetals and thioketals has attracted considerable interest in recent years, particularly under visible-light conditions.

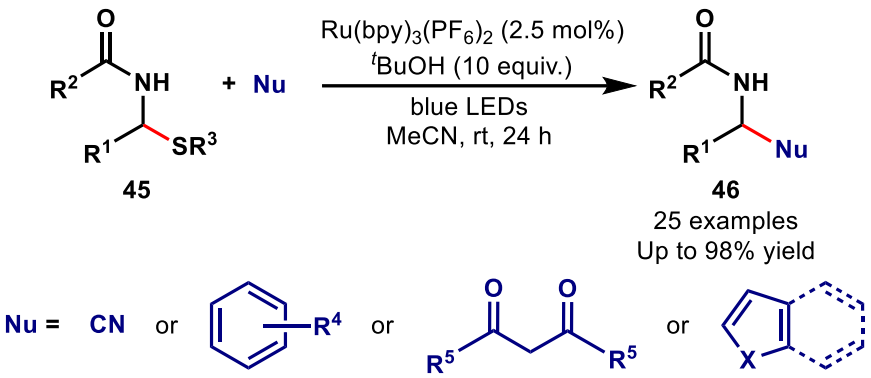

Scheme 1.18 Photoredox-catalyzed synthesis of *N*-carbamoyl *α*,*α*-disubstituted amines

Lamb and coworker demonstrated the selective deprotection of arylthiolanes **47** via singlet oxygen in buffered aqueous-ethanolic media of pH 7.4 (Scheme 1.19).[47] Under white light irradiation (25,000 lumens) and using rose Bengal (RB) *or* methylene blue (MB) *or* methylpyropheophorbide (mPPa) as photosensitizers, various dithianes and oxathiolanes were efficiently converted to the corresponding aldehydes or ketones (Scheme 1.19A).

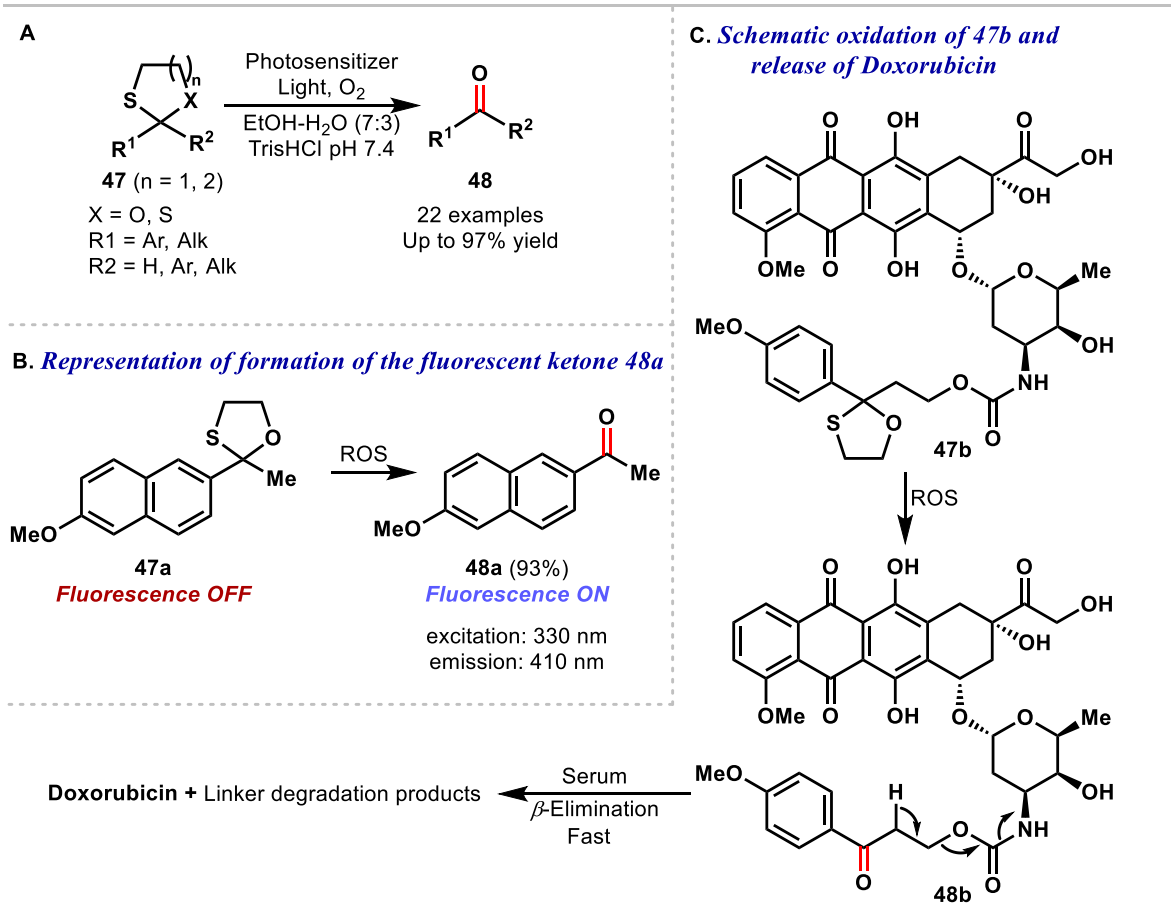

Scheme 1.19 $^1O_2$ enabled thiolane, thioketal, and oxathiolane deprotection

As a fluorescent probe, oxa-thioketal **47a** sensitive to reactive oxygen species (ROS) was degraded by singlet oxygen ($^1O_2$) to furnish the corresponding ketone **48a**, which exhibited fluorescence under UV irradiation (Scheme 1.19B). They synthesized the prodrug **47b**, in which doxorubicin was conjugated to an optimized singlet oxygen–sensitive arylthiolane linker, through a short synthetic sequence. The substrate **47b** was oxidized to **48b** in DMF/ Phosphate Buffered Saline (PBS)/Tris buffer solution (2:1:1), and both the degradation of the arylthiolane moiety and the formation of the corresponding ketone products were detected by HPLC and LCMS (Scheme 1.19C).

In 2020, Opartz and coworkers introduced a visible-light-induced protocol for the efficient cleavage of thioacetals and thioketals, employing molecular iodine as a photocatalyst and oxygen as the terminal oxidant (Scheme 1.20).[48] The methodology demonstrated broad functional group tolerance, including compatibility with common *N*- and *O*-protecting groups. Moreover, the reaction proved effective for the synthesis of unsymmetrical disulfides **53** from thiols **51** and **52**, via formation of unsymmetrical thioacetals **53'** as key intermediates.

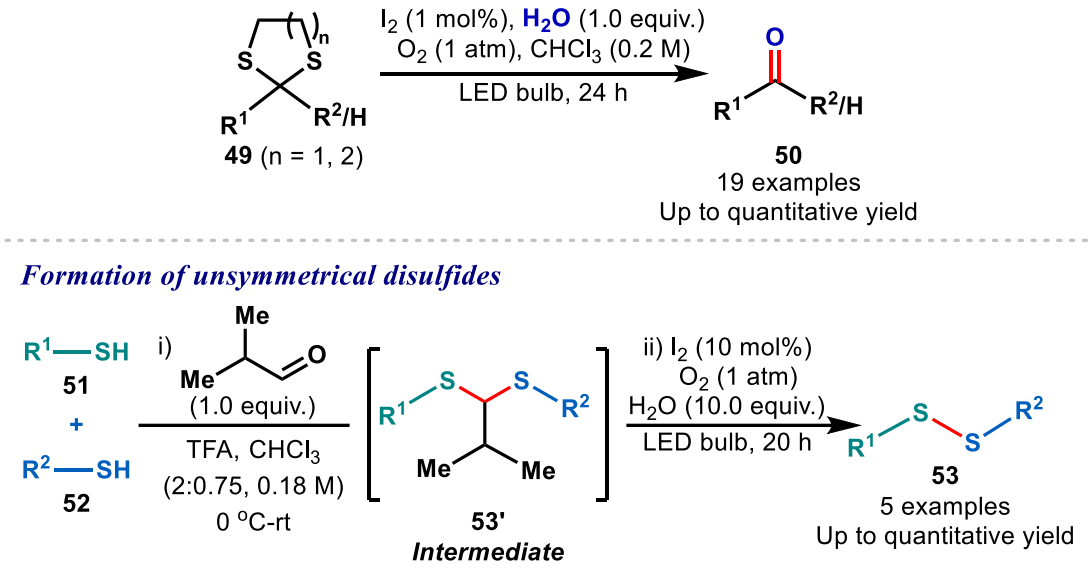

Scheme 1.20 Photocatalytic C−S bond cleavage in thioacetals and thioketals under visible light

In 2020, our research group reported the deprotection of dithianes **54** to the corresponding carbonyl compounds **55** under photoredox catalysis using eosin Y (Scheme 1.21).[49] The reaction proceeded efficiently under open-air conditions with a standard household compact fluorescent lamp (CFL) in aqueous acetonitrile at room temperature. The protocol demonstrated a broad substrate scope, high functional group tolerance, and scalability to gram-

scale synthesis. Additionally, Xie and coworkers also disclosed a general method for the photocatalytic deprotection of 1,3-oxathiolanes, which applies to aromatic and aliphatic aldehyde and ketone derivatives.[50]

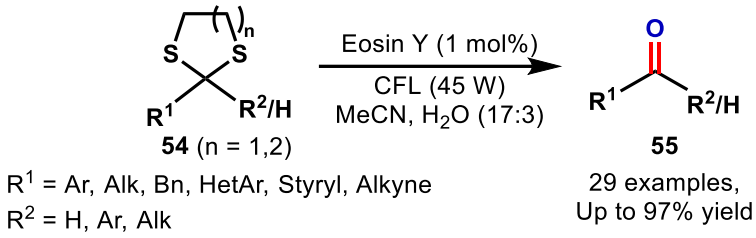

Scheme 1.21 Visible light promoted deprotection of dithianes

Although photoredox catalysis has seen significant advances, the selective cleavage of a single C–S bond within cyclic thioacetals to generate ring-opened, functionalized useful products remains unexplored. To bridge this gap, we proposed a visible-light-mediated strategy that enables the selective activation of one C–S bond while preserving the remaining sulfur functionality. This approach provides a versatile platform for the synthesis of valuable compounds through subsequent reactions with various reagents or substrates. The development, scope, and mechanistic insights of these transformations will be elaborated in the forthcoming chapters.

1.6 Conclusion

This chapter gives a brief account on the history and development of photoredox catalysis over the century. It also summarizes the types of photoredox catalysis, various modes of activation-mechanistic pathways along with the applications of photocatalysis as an effective and sustainable alternative to the conventional approaches. After gleaning through the literature on the importance of alkenes their functionalization, cyclic thioacetals and the opportunities for the useful transformation, we planned to explore some of the visible light photocatalysis as alternative and effective tool to access useful compounds. In the forthcoming chapters designed and developed protocols have been discussed in detail.

1.7 References

1) Bonfield, H. E.; Knauber, T.; Lévesque, F.; Moschetta, E. G.; Susanne, F.; Edwards, L. J. *Nat. Commun.* **2020**, *11*, 804–807.
2) Trommsdorff, H., Über Santonin. *Ann. Pharm.* **1834**, *11*, 190–207.
3) Fritzsche, J. Bull. Acad. St. Petersbourg; reported in *J. Prakt. Chemie* **1867**, *101*, 333–343.
4) (a) Elbs, K. *J. Prakt. Chem. N.F.* **1891**, *44*, 467–469. (b) Linebarger, C. E. *Am. Chem. J.* **1892**, *14*, 597–602. (c) Orndorff, W. R.; Cameron, F. K.; *Am. Chem. J.* **1895**, *17*, 658. (d) Ehrenberg, M. *Acta Crystallogr.* **1966**, *20*, 177–182.
5) Roth, H. D. *Angew. Chem., Int. Ed. Engl.* **1989**, *28*, 1193–1207.
6) (a) Ciamician, G.; Silber, P. *Gazz. Chim. Ital.* **1902**, *32*, 218–245. (b) Ciamician, G., *Science* **1912**, *36*, 385–394.
7) Hoffmann, N. *Chem. Rev.* **2008**, *108*, 1052−1103.
8) Furusawa, A. *Quantum States of Light* Springer, Padova, Italy, **2014**.
9) (a) Tucker, J. W.; Stephenson, C. R. J. *J. Org. Chem.* **2012**, *77*, 1617–1622. (b) Prier, C. K.; Rankic, D. A.; MacMillan, D. W. C. *Chem. Rev.* **2013**, *113*, 5322– 5363. (c) König, B. *Eur. J. Org. Chem.* **2017**, *2017,* 1979−1981.
10) Teplý, F. *Collect. Czech. Chem. Commun.* **2011**, *76*, 859– 917.
11) (a) Hari, D. P.; König, B. *Chem. Commun.* **2014**, *50,* 6688–6699. (b) Joshi-Pangu, A.; Lévesque, F.; Roth, H. G.; Oliver, S. F.; Campeau, L.-C.; Nicewicz, D.; DiRocco, D. A. *J. Org. Chem.* **2016**, *81,* 7244–7249. (c) Shang, T.-Y.; Lu, L.-H.; Cao, Z.; Liu, Y.; He, W.-M.; Yu, B. *Chem. Commun.* **2019**, *55,* 5408–5419. (d) White, A.; Wang, L.; Nicewicz, D. *Synlett* **2019**, *30,* 827–832. (e) Zilate, B.; Fischer, C.; Sparr, C. *Chem. Commun.* **2020**, *56,* 1767–1775. (f) Mandigma, M. J. P.; Kaur, J.; Barham, J. P. *ChemCatChem* **2023**, e202201542.
12) (a) Romero, N. A.; Nicewicz, D. A. *Chem. Rev.* **2016**, *116,* 10075–10166. (b) Ravelli, D.; Fagnoni, M.; Albini, A. *Chem. Soc. Rev.* **2013**, *42,* 97–113. (c) Sideri, I. K.; Voutyritsa, E.; Kokotos, C. G. *Org. Biomol. Chem.* **2018**, *16,* 4596–4614. (d) Bogdos, M. K.; Pinard, E.; Murphy, J. A. *Beilstein J. Org. Chem.* **2018**, *14,* 2035–2064. (e) Bortolato, T.; Cuadros, S.; Simionato, G.; Dell'Amico, L. L. *Chem. Commun.* **2022**, *58*, 1263–1283.
13) Amos, S. G. E.; Garreau, M.; Buzzetti, L.; Waser, J. *Beilstein J. Org. Chem.* **2020**, *16,* 1163–1187.

14) (a) Hedstrand, D. M.; Kruizinga, W. H.; Kellogg, R. M. *Tetrahedron Lett.* **1978**, *19*, 1255–1258. (b) van Bergen, T. J.; Hedstrand, D. M., Kruizinga, W. H., Kellogg, R. M. *J. Org. Chem.* **1979**, *44*, 4953–4962.

15) Cano-Yelo, H. Deronzier, A. *J. Chem. Soc.Perkin Trans. 2*, **1984**, 1093–1098.

16) Pandey, G.; Hajra, S.; Ghorai, M. K.; Kumar, K. R. *J. Am. Chem. Soc.* **1997**, *119*, 8777–8787.

17) (a) Mariano, P. S. (Ed.), *Advances in Electron Transfer Chemistry*, **1996**, JAI Press, London. (b) Mattay, J. (Ed.), *Photoinduced Electron Transfer V, Top. Curr. Chem.* Vol. **1993**, *168*, Springer, Stuttgart.

18) (a) Shaw, M. H.; Twilton, J.; MacMillan, D. W. C. *J. Org. Chem.* **2016**, *81*, 6898– 6926.

19) Ischay, M. A.; Anzovino, M. E.; Du, J.; Yoon, T. P. *J. Am. Chem. Soc.* **2008**, *130*, 12886−12887.

20) Nicewicz, D. A.; MacMillan, D. W. C. *Science* **2008**, *322*, 77−80.

21) Narayanam, J. M. R.; Tucker, J. W.; Stephenson, C. R. J. *J. Am. Chem. Soc.* **2009**, *131*, 8756−8757.

22) Ray, S.; Samanta, P. K.; Biswas, P. *Visible-Light Active Photocatalysts: Nanostructurated Catalysis Design, Mechanisms, and Applications Ghosh, S. Ed.;* Chap. 14, WileyVHC: Verlag, **2018**, pp. 393–419.

23) (a) Yin, G.; Mu, X.; Liu, G. *Acc. Chem. Res.* **2016**, *49*, 2413–2423. (b) Qi, X.; Diao, T. *ACS Catal.* **2020**, *10*, 8542–8556. (c) Li, Y.; Wu, D.; Cheng, H.-G.; Yin, G. *Angew. Chem. Int. Ed.* **2020**, *59*, 7990–8003.

24) Matsui, J. K.; Lang, S. B.; Heitz, D. R.; Molander, G. A. *ACS Catal.* **2017**, *7*, 2563-2575.

25) (a) Cao, M.-Y.; Ren, X.; Lu, Z. *Tetrahedron Lett.* **2015**, *56*, 3732- 3742. (b) Liu, Y.; Liu, H.; Liu, X.; Chen, Z. *Catalysts* **2023**, *13*, 1056-1105.

26) (a) Reed, N. L.; Herman, M. I.; Miltchev, V. P.; Yoon, T. P. *Org. Lett.* **2018**, *20*, 7345–7350. (b) Mou, X.-Q.; Wang, M.; Ren, L.-C.; Jian, Y.-R.; Fu, X.-Y.; Zheng, H.-Y.; Zha, X.; Cui, B.-D.; Zhang, Y.; Chen, Y.-Z. *Org. Chem. Front.* **2024**, *11*, 74–82.

27) (a) Liu, J.; Guo, L.; Chen, Z.; Guo, Y.; Zhang, W.; Peng, X.; Wang, Z.; Zeng, Y.-F. *Chem. Commun.* **2024**, *60*, 3413–3416. (b) Govaerts, S.; Angelini, L.; Hampton, C.; Malet-Sanz, L.; Ruffoni, A.; Leonori, D. *Angew. Chem., Int. Ed.* **2020**, *59*, 15021–15028.

28) (a) Tang, W.; Yan, D.-Y.; Liang, K.-C.; Su, M.; Liu, F. *Org. Chem. Front.* **2022**, *9*, 6535–6539. (b) Jiang, H.; Seidler, G.; Studer, A. *Angew. Chem. Int. Ed.* **2019**, *58*, 16528–16532.

29) (a) Campbell, M. W.; Compton, J. S.; Kelly, C. B.; Molander, G. A. *J. Am. Chem. Soc.* **2019**, *141*, 20069–20078. (b) Zhang, B.; Yi, Y.; Wu, Z.-Q.; Chen, C.; Xi, C. *Green Chem.* **2020**, *22*, 5961–5965.

30) (a) Laskar, R.; Dutta, S.; Spies, J. C.; Mukherjee, P.; Rentería-Gómez, Á.; Thielemann, R. E.; Daniliuc, C. G.; Gutierrez, O.; Glorius, F. *J. Am. Chem. Soc.* **2024**, *146*, 10899–10907. (b) Strieth-Kalthoff, F.; Glorius, F. *Chem* **2020**, *6*, 1888–1903. (c) Wiles, R. J.; Molander, G. A. *Isr. J. Chem.* **2020**, *60*, 281–293.

31) (a) Zhang, T.; Rabeah, J.; Das, S. *Nat. Commun.* **2024**, *15*, 5208–5217. (b) Sarró, P.; Ji, Y.; Gallego-Gamo, A.; Gimbert-Suriñach, C. Vallribera A.; Granados, A. *Org. Chem. Front.*, **2025**, DOI: 10.1039/d5qo00236b.

32) Tomita, R.; Yasu, Y.; Koike, T.; Akita, M. *Angew. Chem. Int. Ed.* **2014**, *53*, 7144–7148.

33) Wang, Z.; Lin, J.-H.; Xiao, J.-C. *Org. Lett.* **2024**, *26*, 1980–1984.

34) Fang, X.-X.; Wang, P.-F.; Yi, W.; Chen, W.; Lou, S.-C.; Liu, G.-Q. *J. Org. Chem.* **2019**, *84*, 15677–15684.

35) Chowdhury, S. R.; Singh, D.; Hoque, I. U.; Maity, S. *J. Org. Chem.* **2020**, *85*, 13939–13950.

36) Liang, Y.; Zhou, N. Ma, G.; Wen, L.; Wu, X.; Feng, P. *Mol.Catal.* **2022**, *528*, 112373–112379.

37) (a) Schelhaas, M.; Waldmann, H. *Angew. Chem. Int. Ed.* **1996**, *35*, 2056–2083. (b) Banerjee, A. K.; Laya, M. S. *Russ. Chem. Rev.* **2000**, *69*, 947–955. (c) Burghardt, T. E. *J. Sulfur Chem.* **2005**, *26*, 411–427. (d) De, S. K. *Tetrahedron Lett.* **2004**, *45*, 2339–2341.

38) (a) Bulman Page, P. C.; van Niel, M. B.; Prodger, J. C. *Tetrahedron* **1989**, *45*, 7643–7677. (b) Gröbel, B.-T.; Seebach, D. *Synthesis* **1977**, *1977*, 357–402. (c) Yus, M.; Nájera, C.; Foubelo, F. *Tetrahedron* **2003**, *59*, 6147–6212. (d) Corey, E. J.; Erickson, B. W. *J. Org. Chem.* **1971**, *36*, 3553–3560.

39) Yan, J.; Pozzo, J.-L.; Hamze, A.; Provot, O. *Eur. J. Org. Chem.* **2022**, *2022*, e202101460.

40) (a) Modha, S. G.; Mehta, V. P.; Van der Eycken, E. V. *Chem. Soc. Rev.* **2013**, *42*, 5042–5055. (b) Pan, F.; Shi, Z.-J. *ACS Catal.* **2014**, *4*, 280–288. (c) Gao, K.; Yorimitsu, H.; Osuka, A. *Angew. Chem. Int. Ed.* **2016**, *55*, 4573–4576. (d) Bhanuchandra, M.; Baralle,

A.; Otsuka, S.; Nogi, K.; Yorimitsu,H.; Osuka, A. *Org. Lett.* **2016**, *18*, 2966–2969. (e) Uetake, Y.; Niwa, T.; Hosoya, T. *Org. Lett.* **2016**, *18*, 2758–2761. (f) Shibata, T.; Mitake, A.;Akiyama, Y.; Kanyiva, K. S. *Chem. Commun.* **2017**, *53*, 9016–9019.

41) George, N.; Bekkaye, M.; Alix, A.; Zhu, J.; Masson, G. *Chem. - Eur. J.* **2014**, *20*, 3621–3625.

42) (a) Zheng, S.; Huang, W.; Gao, N.; Cui, R.; Zhang, M.; Zhao, X. *Chem. Commun.* **2011**, *47*, 6969–6971. (b) Gao, N.; Zheng, S.; Yang, W.; Zhao, X. *Org. Lett.* **2011**, *13*, 1514–1516.

43) (a) Lanzi, M.; Merad, J.; Boyarskaya, D. V.; Maestri, G.; Allain, C.; Masson, G. *Org. Lett.* **2018**, *20*, 5247– 5250. (b) Liang, G.; Wang, S.; Zhou, C.; Ye, C.; Chen, B.; Tung, C.-H.; Wu, L.-Z. *Org. Lett.* **2024**, *26*, 4286–4291.

44) Wever, W. J.; Cinelli, M. A.; Bowers, A. A. *Org. Lett.* **2013**, *15*, 30–33.

45) Lebée, C.; Languet, M.; Allain, C.; Masson, G. *Org. Lett.* **2016**, *18*, 1478–1481.

46) Jarrige, L.; Levitre, G.; Masson, G. *J. Org. Chem.* **2016**, *81*, 7230–7236.

47) Lamb, B. M.; Barbas, C. F. *Chem. Commun.* **2015**, *51*, 3196–3199.

48) Krumb, M.; Kammer, L. M.; Forster, R.; Grundke, C.; Opatz, T. *ChemPhotoChem.* **2019**, *4*, 101–104.

49) Dharpure, P. D.; Bhowmick, A.; Warghude, P. K.; Bhat, R. G. *Tetrahedron Lett.* **2020**, *61*, 151407–151415.

50) Yang, M.; Xing, Z.; Fang, B.; Xie, X.; Sue, X. *Org. Biomol. Chem.* **2020**, *18*, 288–291.

Chapter 2

β-Hydroxytrifluoromethylation of Unactivated Alkenes via Visible Light-Induced Organophotoredox-Catalysis

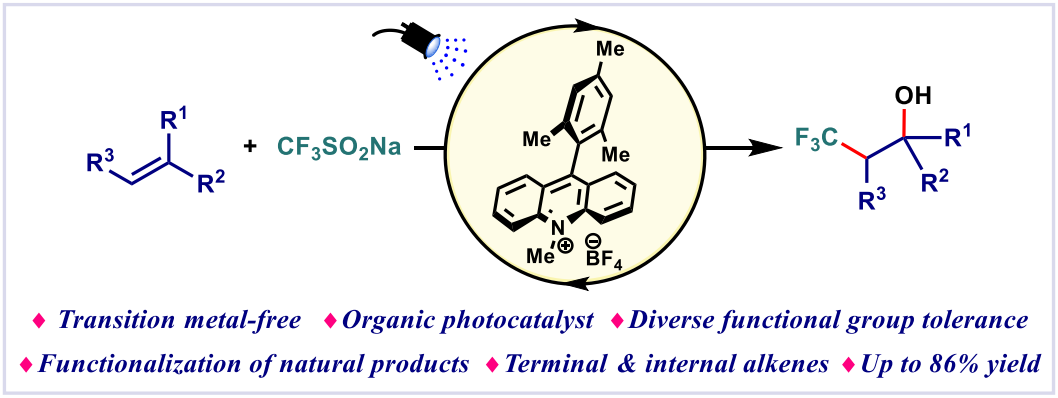

♦ *Transition metal-free* ♦ *Organic photocatalyst* ♦ *Diverse functional group tolerance*
♦ *Functionalization of natural products* ♦ *Terminal & internal alkenes* ♦ *Up to 86% yield*

β-Hydroxytrifluoromethylation of Unactivated Alkenes via Visible Light-Induced Organophotoredox-Catalysis

2

This chapter describes the development of a mild transition metal-free organophotoredox-catalyzed approach for β-hydroxytrifluoromethylation of unactivated alkenes using CF_3SO_2Na and acridinium salt. The protocol is compatible with various mono-, di-, and trisubstituted aliphatic unactivated alkenes containing numerous functional groups and natural product derivatives. Further, the post synthetic modifications of the synthesized β-hydroxytrifluoromethylated products have been demonstrated through cross-coupling and functional group interconversion reactions. The method proved to be scalable and it works smoothly under the direct exposure of sunlight. A plausible mechanism has been proposed based on the fluorescence quenching experiment and cyclic voltammetry analysis.

2.1 Introduction

Trifluoromethylation of an organic molecule dramatically influences its electronegativity, polarizability, and various pharmacokinetic properties such as lipophilicity, metabolic stability, and bioavailability.[1] Thus, making trifluoromethylation a crucial transformation in organic synthesis. Moreover, a myriad of trifluoromethylated organic compounds found applications in pharmaceuticals,[2] agrochemicals,[3] functional materials (liquid crystal displays, LCDs),[4] and useful tracers for positron emission tomography (PET) imaging[5] (Figure 2.1). Consequently, a variety of trifluoromethylating reagents have been utilized by researchers across the globe for exploring trifluoro-methylation of numerous organic molecules.[6] Among the variety of substrates for the functionalization, alkenes are noteworthy as they are indispensable carbon feedstocks in the realm of chemical synthesis and widely recognized for easily accessible, abundant, and stable nature.[7] Their remarkable reactivity in difunctionalization reactions has unlocked boundless possibilities in the construction of structurally diverse and functionally rich molecules.[8] Specifically, the trifluoromethylation of alkenes with concomitant introduction of additional functional groups (radical or nucleophile) across unsaturated moieties is a powerful functionalization tool to attain high valued compounds (Figure 2.2).[9]

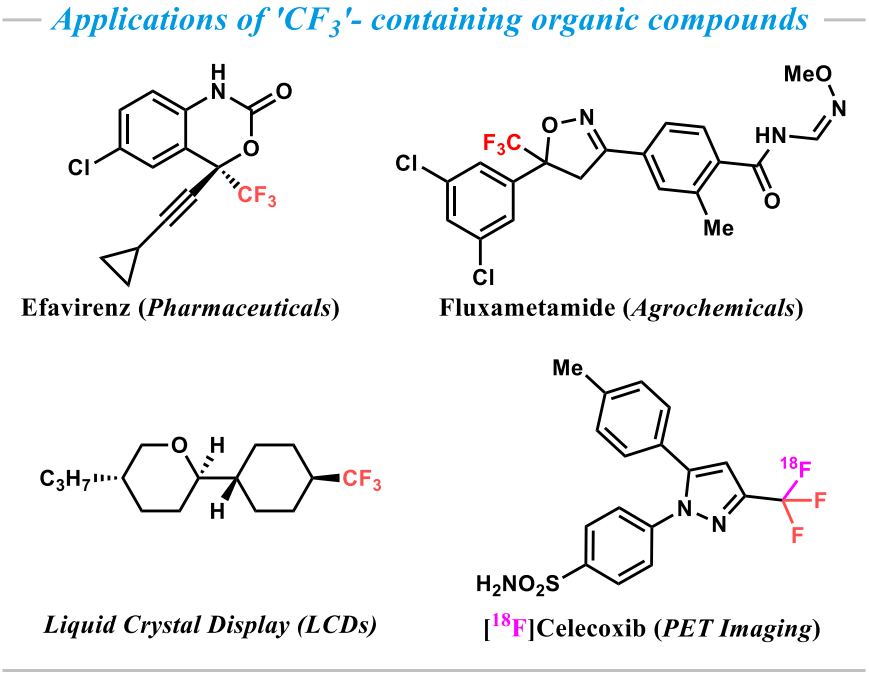

Figure 2.1 Representative trifluoromethylated organic compounds in various applications

In 2015, Yang, Vicic, and coworkers introduced a mild and practical approach for the manganese-catalyzed aerobic oxytrifluoromethylation of olefinic bond in styrene derivatives **1** (Scheme 2.1). This method employs CF_3SO_2Na (Langlois' reagent) as the trifluoromethyl source. A key highlight of this strategy is its ability to generate trifluoromethyl radicals from CF_3SO_2Na using a simple manganese salt and O_2 system under ambient conditions. However, the protocol is somewhat constrained by selectivity challenges, leading to the formation of undesired β-keto side products **3**.[10]

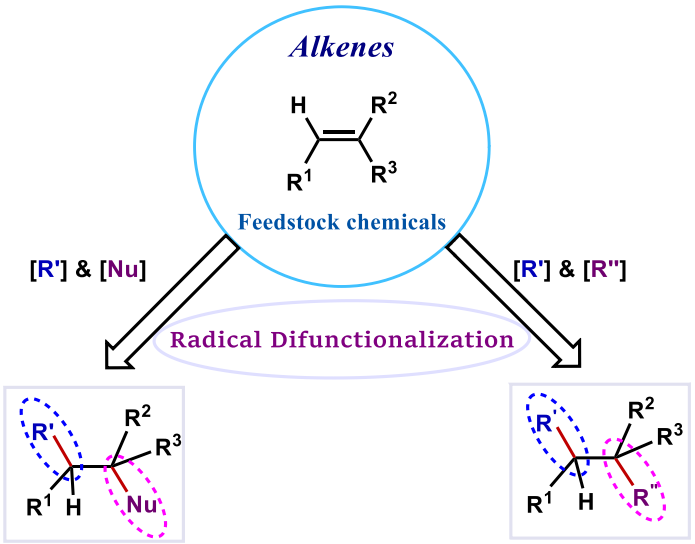

Figure 2.2 Schematic representation of radical difunctionalization of alkenes

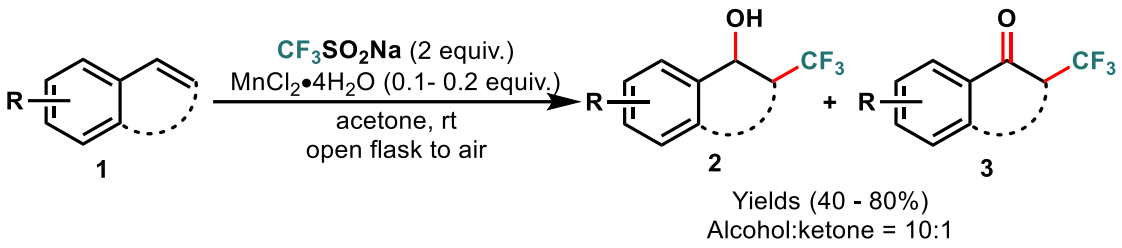

Scheme 2.1 Oxytrifluoromethylation of styrene derivatives using manganese catalysis

In 2017, Tsui and coworkers discovered the hydroxytrifluoromethylation reaction of alkenes reacting the fluoroform-derived [$CuCF_3$] reagent. The [$CuCF_3$] was prepared from CuCl, ^{t}BuOK, and fluoroform according to Grushin's procedure (Scheme 2.2). The protocol employs air as an oxidant and B_2Pin_2 as a key additive. However, it relies on hazardous fluoroform (CF_3H), a stoichiometric amount of the transition metal catalyst CuCl, and is limited to activated alkene substrates such as styrene derivatives.[11]

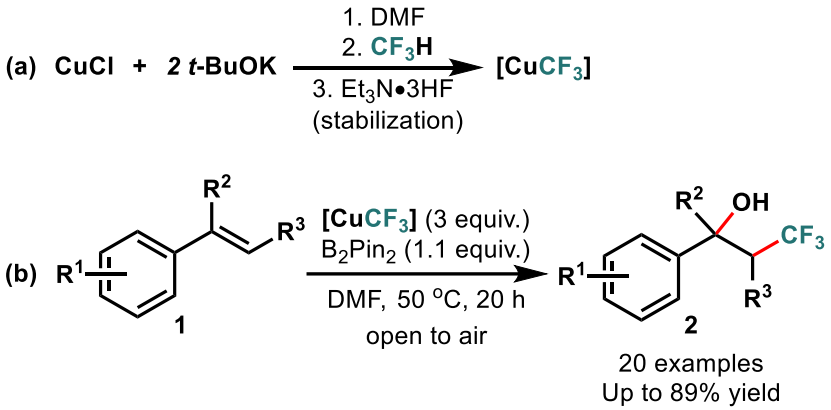

Scheme 2.2 Hydroxytrifluoromethylation of styrenes employing $CuCF_3$ derived from fluoroform

In 2018, Kappe, Cantillo, and their colleagues developed a mild electrochemical method for the oxytrifluoromethylation of alkenes using paired electrolysis in an undivided cell (Scheme 2.3). This catalyst-free protocol employs sodium trifluoromethanesulfinate as the CF_3 source. Notably, water plays a dual role, acting both as the oxidant at the cathode and the nucleophile that introduces the hydroxyl group into the reaction to afford hydroxytrifluoremethylated products **2** in very good yields. However, the applicability of this method remains limited to styrene derivatives.[12]

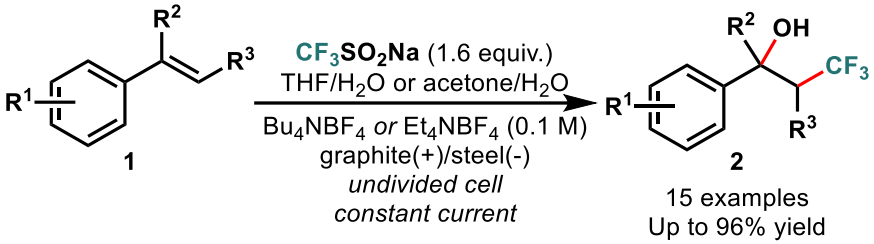

Scheme 2.3 Catalyst-free electrochemical oxytrifluoromethylation of styrene derivatives

As already discussed, the direct *β*-hydroxy trifluoromethylation of activated alkenes such as styrene derivatives has been explored via transition metal catalysis. There are also a few reports available for transition metal-free approaches to access *β*-trifluoromethylated alcohols. Notably, in 2014, Luo's research group introduced a metal-free method utilizing $NaSO_2CF_3$ (Langlois' reagent) in combination with *tert*-butyl hydroperoxide (TBHP) as an oxidant (Scheme 2.4). This approach led to the formation of a mixture of *α*-trifluoromethylated ketones **2** and/or alcohols **3**. However, in addition to challenges with chemoselectivity, the protocol required a super-stoichiometric amount of TBHP (8 equiv.), a stoichiometric quantity of the additive benzoquinone and utilized an elevated temperature of 80 °C.[13]

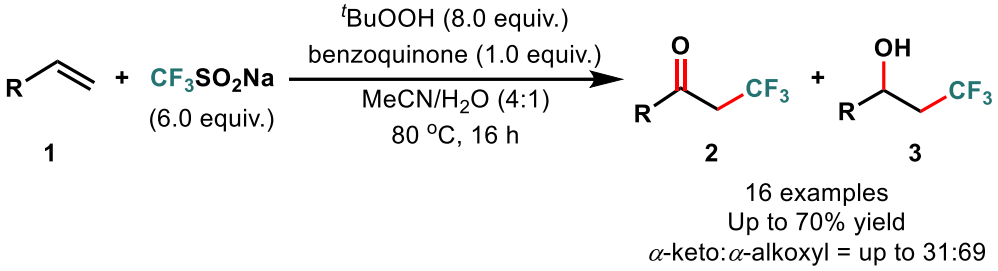

Scheme 2.4 Catalyst-free electrochemical oxytrifluoromethylation of styrene derivatives

It is worth emphasizing that all the aforementioned protocols have been applied exclusively to activated alkenes (i.e., alkenes directly attached to electron-withdrawing groups, aryl rings, or heteroatoms). In contrast, the direct difunctionalization leading to the trifluoromethylation of unactivated alkenes remains largely unexplored in the literature. This is likely due to the inherent inertness of unactivated alkenes, as they lack electron-withdrawing substituents or stabilizing groups in their vicinity. Consequently, the intermediates formed, whether carbocations or radicals, are not effectively stabilized.[14] Additionally, unactivated alkenes possess a higher oxidation potential compared to their activated counterparts, such as styrenes.[15] As a result, only a few studies have reported the direct hydroxytrifluoromethylation

of unactivated alkenes.

In 2019, Liu and coworkers introduced a mild and practical approach for the hydroxytrifluoromethylation of alkenes **1**, utilizing the Langlois reagent as the CF_3 radical source and DMSO as the oxidant, oxygen donor, and solvent (Scheme 2.5). This redox process exhibits a broad substrate scope and excellent functional group tolerance, enabling the efficient synthesis of various *β*-trifluoromethyl alcohols **2** and **3** from both activated and unactivated alkenes. Although, the protocol is applicable to both activated as well as unactivated alkenes, however, the protocol requires elevated temperature and a stoichiometric amount of hazardous trifluoroacetic acid (TFA) for optimal efficiency.[16]

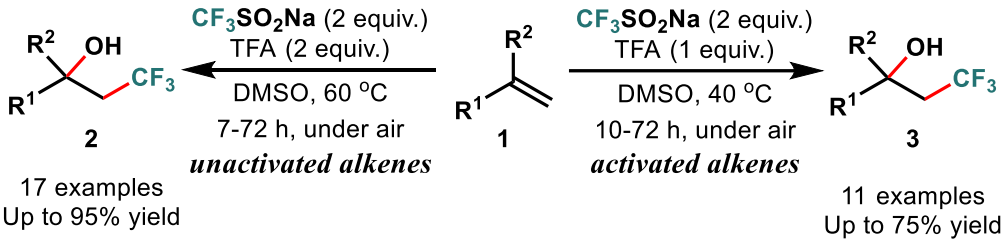

Scheme 2.5 Hydroxytrifluoromethylation of alkenes with Langlois reagent and DMSO

In 2020, Li and coworkers introduced a cobalt-tertiary amine-mediated strategy for the hydroxytrifluoromethylation of alkenes, employing CF_3Br and atmospheric oxygen as essential reagents (Scheme 2.6). This method offered an efficient and practical approach for incorporating trifluoromethyl and hydroxyl groups into alkene substrates to afford the desired products **2**. However, its reliance on a transition metal catalyst and the use of gaseous CF_3Br, which is challenging to handle and limits its practicality.[17]

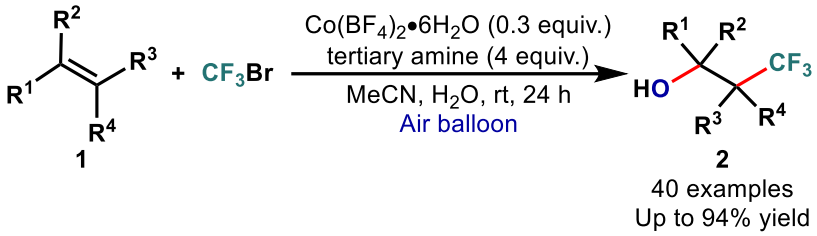

Scheme 2.6 Cobalt-tertiary amine-catalyzed hydroxytrifluoromethylation of alkenes.

Over the past two decades, visible-light photoredox catalysis has experienced a resurgence, offering a versatile approach to synthesizing a wide range of valuable organic compounds under relatively mild, sustainable, and controlled reaction conditions.[18] This process involves

the excitation of a photocatalyst (PC) under visible light, generating an excited-state photocatalyst (PC*) that facilitates productive single-electron transfer (SET) reactions.

Consequently, feedstock alkene substrates have been widely utilized in diverse difunctionalization reactions under visible light mediated photoredox catalysis.[19] Notably, the trifluoromethylative difunctionalization of alkenes has been widely explored for the synthesis of high-value organic compounds.[20] In this context, Koike, Akita, and coworkers reported a visible-light-driven three-component oxytrifluoromethylation of alkenes using the metallophotoredox catalyst [*fac*-Ir(ppy)$_3$] under blue LEDs (425 nm) irradiation at room temperature (Scheme 2.7). While this transformation effectively employs a broad range of oxygen nucleophiles, such as alcohols, carboxylic acids, and water, it relies on a precious transition metal photocatalyst and the expensive trifluoromethylating reagent, Umemoto's reagent.[21]

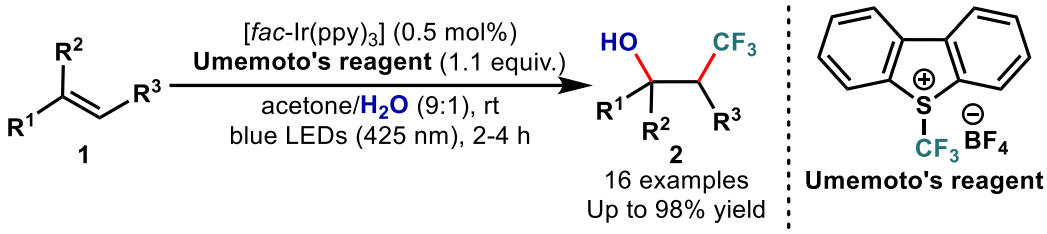

Scheme 2.7. Three-component oxytrifluoromethylation by photoredox catalysis

In 2020, the Wan research group introduced a metallophotocatalyzed Mn(acac)$_3$-mediated approach for the hydroxytrifluoromethylation of unactivated alkenes **1** under blue LEDs (40 W) irradiation (Scheme 2.8). Although effective for unactivated alkene substrates, this method is restricted to terminal alkenes only and relies on a transition metal photocatalyst.[22]

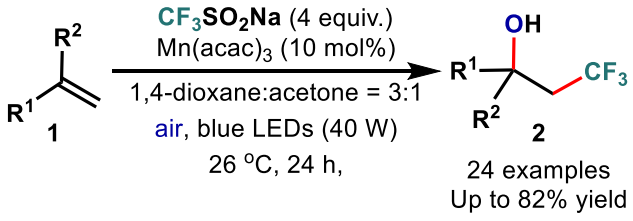

Scheme 2.8 Three-component oxytrifluoromethylation by photoredox catalysis

While transition metal photocatalysts offer notable synthetic utility, organophotoredox catalysts are favoured for their environmental sustainability, unique reactivity (strong oxidizing nature) and broader applicability.[23]

Interestingly, to the best of our knowledge, there are no reported examples of organophotoredox-catalyzed *β*-hydroxytrifluoromethylation of unactivated alkenes applicable for both terminal as well as internal alkenes in the literature. Driven by our enduring research interest with organophotoredox catalysis,[24] we set out to design an elegant, transition-metal-free approach for the synthesis of *β*-trifluoromethylated alcohols from unactivated alkenes, harnessing the power of an organophotoredox catalyst under the illumination of visible light. Herein, we disclose a direct and efficient hydroxytrifluoro-methylation of unactivated alkenes, through organophotoredox catalysis under blue LEDs irradiation at ambient conditions, offering a sustainable avenue for molecular innovation (Scheme 2.9).

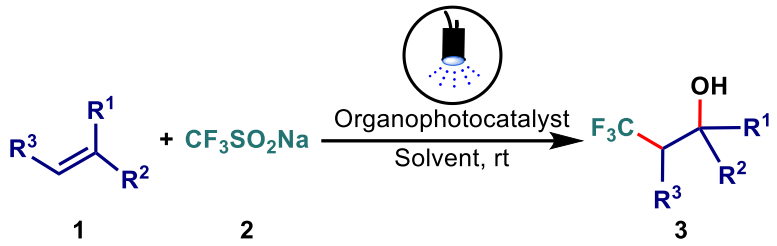

Scheme 2.9 *β*-hydroxy trifluoromethylation of unactivated alkenes via organophotoredox catalysis

2.2 Results and Discussions

We commenced with the optimization studies starting from allylbenzoate **1a** and sodium trifluoromethanesulfinate CF_3SO_2Na **2** as model substrates. The reaction was conducted using $(NH_4)_2S_2O_8$ (2 equiv.) in MeCN (3 mL) under blue LEDs irradiation (20 W) at room temperature for 12 h, while screening various photocatalysts (5 mol%) (Table 2.1). A series of organophotocatalysts, such as Eosin Y, Na_2Eosin Y, Rhodamine 6G (Rh6G), Rhodamine B, Rose Bengal, Riboflavin, Fluorescein, 2,4,6-Triphenylpyrylium·BF_4, and Phenanthrene-9,10-dione, were evaluated (Table 2.1, Entries 1–9). In each case, the desired *β*-trifluoromethyl alcohol product **3a** was obtained, albeit in low yield. However, Mes-Acr-Me·X (ClO_4 or BF_4) emerged as the most effective photocatalyst, providing **3a** in higher yield (Table 2.1, Entries 10 and 11). Notably, the transition metal photocatalyst $Ru(bpy)_3·2PF_6$ did not afford the desired product **3a** (Table 2.1, Entry 12).

Table 2.1 Optimization of photocatalysts[a]

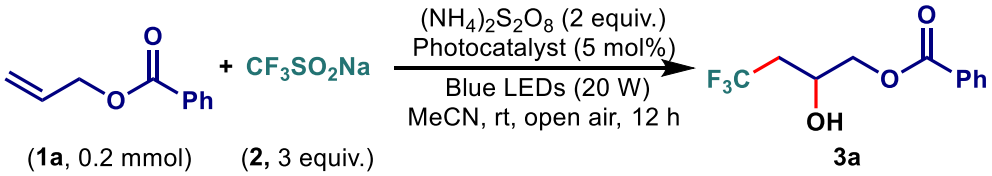

(**1a**, 0.2 mmol) (**2**, 3 equiv.) **3a**

Sr. no.	Photocatalysts	Yield(%)[b]
1	Eosin Y	39
2	Na_2EosinY	Trace
3	Rhodamine 6G	38
4	Rhodamine B	ND
5	Rosebengal	ND
6	Riboflavin	27
7	Fluorescein	46
8	2,4,6-Triphenylpyrylium·BF_4	40
9	Phenanthrene-9,10-dione	38
10	**Mes-Acr-Me·ClO_4**	**55**
11	**Mes-Acr-Me·BF_4**	**55**
12	Ru(bpy)$_3$·$2PF_6$	ND

[a]**Reaction conditions**: **1a** (0.2 mmol), CF_3SO_2Na **2** (3 equiv.), $(NH_4)_2S_2O_8$ (2 equiv.), Photocatalyst (5 mol%) in MeCN (3 mL), Blue LEDs (20 W) for 12 h at room temperature (rt). [b]Determined by ^{1}H NMR analysis of the crude reaction mixtures using 1,3,5-trimethoxybenzene (TMB) as an internal standard.

With Mes-Acr-Me·BF_4 (5 mol%) as the photocatalyst and $(NH_4)_2S_2O_8$ (2 equiv.), we evaluated various solvents, including MeCN, DMF, DMSO, DCM, 1,4-dioxane, acetone, toluene, 1,2-dichloroethane, THF, MeOH, and EtOH (Table 2.2, Entries 1–11). Among these, 1,4-dioxane afforded the desired product **3a** with an improved yield of 60%. Further screening of binary solvent mixtures (Table 2.2, Entries 12–15) revealed that a 1,4-dioxane:MeCN (2:1) combination provided the highest yield of **3a** (66%, Table 2.2, Entry 15). Subsequently, various oxidants, such as $Na_2S_2O_8$, $K_2S_2O_8$, *tert*-butyl hydroperoxide (TBHP), and PhI(OAc)$_2$ were screened for the further optimization of the reaction (Table 2.3, Entries 1–5). Among them, $Na_2S_2O_8$ afforded the highest yield of **3a** (66%, Table 2.3, Entry 1).

Table 2.2 Optimization of solvents[a]

(0.2 mmol, **1a**) (**2**, 3 equiv.) **3a**

Sr. no.	Solvents	Yield(%)[b]
1	MeCN	55
2	DMF	40
3	DMSO	ND
4	DCM	27
5	1,4-Dioxane	60
6	Acetone	18
7	Toluene	ND
8	1,2-Dichloroethane	36
9	THF	ND
10	MeOH	ND
11	EtOH	ND
12	MeCN:DMF (2:1)	43
13	MeCN:1,2-Dichloroethane (2:1)	50
14	MeCN:1,4-Dioxane (2:1)	63
15	**1,4-Dioxane:MeCN (2:1)**	**66**

Reaction conditions: [a]**1a** (0.2 mmol), CF_3SO_2Na **2** (3 equiv.), $(NH_4)_2S_2O_8$ (2 equiv.), Mes-Acr-Me•BF_4 (5 mol%) in solvent (3 mL), Blue LEDs (20 W) for 12 h at room temperature (rt). [b]Determined by ^{1}H NMR analysis of the crude reaction mixtures using 1,3,5-trimethoxybenzene (TMB) as an internal standard.

Table 2.3 Optimization of oxidants[a]

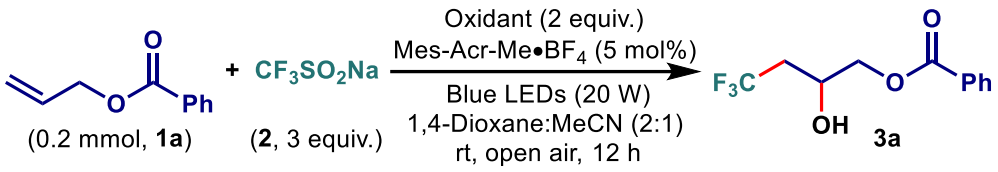

Sr. no.	Oxidants	Yield(%)[b]
1	**$(NH_4)_2S_2O_8$**	**66**
2	$Na_2S_2O_8$	50
3	$K_2S_2O_8$	55
4	TBHP	25
5	$PhI(OAc)_2$	ND

Reaction conditions: [a]**1a** (0.2 mmol), CF_3SO_2Na **2** (3 equiv.), Oxidants (2 equiv.), Mes-Acr-Me•BF_4 (5 mol%) in 1,4-Dioxane:MeCN (2:1, 3 mL), Blue LEDs (20 W) for 12 h at room temperature (rt). [b]Determined by ^{1}H NMR analysis of the crude reaction mixtures using 1,3,5-trimethoxybenzene (TMB) as an internal standard.

Later, we focused on optimizing the light source of different frequencies (Table 2.4, Entries 1–7). Monochromatic LEDs with wavelengths of 427 nm, 440 nm, 456 nm, 467 nm, and 525

nm were evaluated, and among all Blue LEDs - 467 nm (20 W) furnished the desired product in highest yield (Table 2.4, Entry 4). In contrast, broad-range LEDs showed varying efficiencies, with blue LEDs providing a 66% yield, while green LEDs resulted in only a trace amount of **3a** (Table 2.4, Entries 6 and 7).

Table 2.4 Optimization of light sources[a]

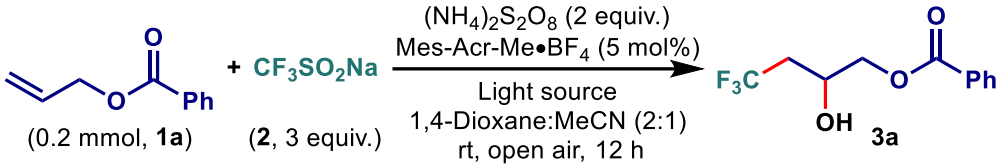

Sr. no.	Light source	Yield(%)[b]
1	427 nm	46
2	440 nm	54
3	456 nm	63
4	**467 nm**	**77(65)**[c]
5	525 nm	51
6	20 W blue LED	66
7	30 W green LED	trace

[a]**Reaction conditions**:**1a** (0.2 mmol), CF_3SO_2Na **2** (3 equiv.), $(NH_4)_2S_2O_8$ (2 equiv.), Mes-Acr-Me•BF_4 (5 mol%) in 1,4-Dioxane:MeCN (2:1, 3 mL), Visible light source for 12 h at room temperature (rt). [b]Determined by ^{1}H NMR analysis of the crude reaction mixtures using 1,3,5-trimethoxybenzene (TMB) as an internal standard. [c]Isolated yield after column chromatography.

Having established the optimum reaction conditions, we explored the substrate scope to assess the practicality and generality of the protocol. Electronically neutral and electron-rich allyl benzoates (**1a**–**1e**) underwent smooth conversion, affording the corresponding products (**3a**–**3e**) in good yields (up to 78%, Table 2.5). Likewise, allyl benzoates featuring electron-donating groups, such as 3-methoxy **1f** and 4-*N*,*N*-dimethylamine **1g**, reacted efficiently to furnish the desired hydroxytrifluoromethylated products (**3f**, **3g**) in yields of up to 76% (Table 2.5). Furthermore, substrates bearing electron-withdrawing substituents (−NO_2, −CN, and −CHO) (**1h**–**1j**) were well tolerated, providing the corresponding products (**3h**–**3j**) in excellent yields (up to 82%, Table 2.5). Notably, allyl benzoates (**1k**–**1n**) containing electron-deactivating halogens, including fluoro, chloro, bromo, and even iodo at the *o/m/p*-positions of the arene ring, were compatible with the reaction conditions, delivering the respective products (**3k**–**3n**) in good yields (up to 78%, Table 2.5). Importantly, these products can serve as

versatile intermediates for further transformations (Scheme 2.9).

Table 2.5 Substrate scope of *β*-trifluoromethyl alcohols[a]

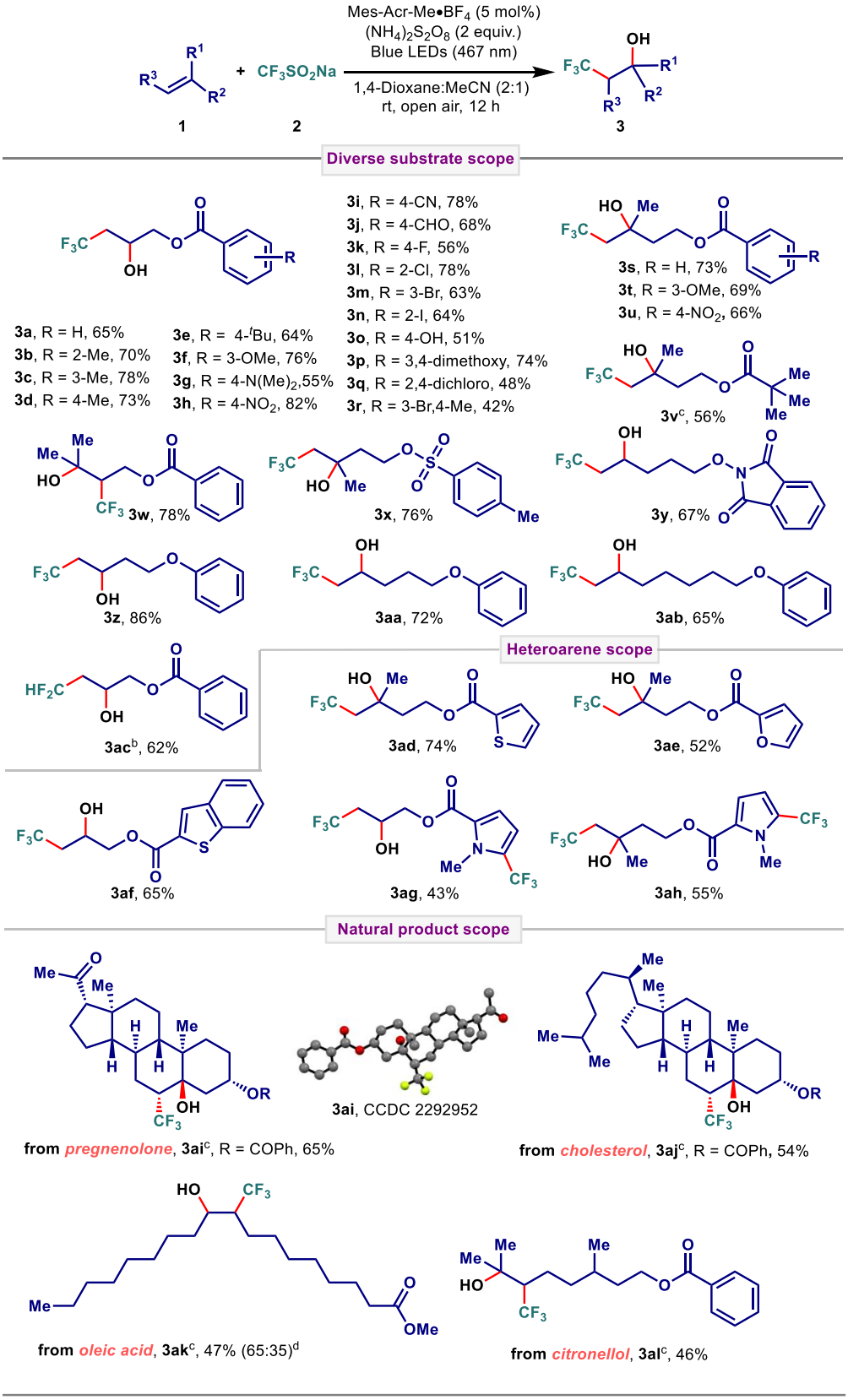

Reaction conditions: [a]**1** (0.2 mmol), CF_3SO_2Na **2** (3 equiv.), $(NH_4)_2S_2O_8$ (2 equiv.), Mes-Acr-Me·BF_4 (5 mol%), 1,4-Dioxane:MeCN (2:1, 3 mL), blue LEDs (467 nm, 20 W), rt, open air, 12 h. [b]CF_2HSO_2Na **2a** (3 equiv.) instead of 2, 36 h. [c]1,4-Dioxane (3 mL), 36 h. [d]NMR analysis did not allow to conclusively distinguish between *r.r.* or *d.r.*

Even an arene with an unprotected hydroxyl group **1o** reacted smoothly under the optimized conditions, offering the trifluoromethylated alcohol **3o** in moderate yield (Table 2.5). Additionally, disubstituted arene derivatives (**1p**–**1r**) furnished the corresponding products (**3p**–**3r**) in moderate to good yields (up to 74%, Table 2.5). Similarly, 1,1-disubstituted terminal alkenes with electron-neutral, electron-rich, and electron-poor substituents (**1s**–**1u**) underwent hydroxytrifluoromethylation to afford the desired alcohols (**3s**–**3u**) in yields of up to 73% (Table 2.5). The aliphatic ester-linked alkene derivative **1v** provided the corresponding product **3v** in 56% yield (Table 2.5). Moreover, the trisubstituted internal alkene **1w** exhibited good reactivity under the optimized conditions to afford the *anti*-Markovnikov adduct **3w** in good yield (78%, Table 2.5). Functionalized alkene substrates, including sulfonate **1x** and oxy-isoindolinedione **1y**, also reacted smoothly, affording the desired products (**3x** and **3y**) in good yields (up to 76%, Table 2.5). Arene ether-linked alkenes with varying chain lengths (**1z**, **1aa** and **1ab**) readily underwent hydroxytrifluoromethylation, furnishing the corresponding products (**3z**, **3aa** and **3ab**).

Furthermore, as a proof of concept, the reaction of CF_2HSO_2Na **2a** with **1a** resulted in the formation of *β*-difluoromethyl alcohol **3ac**. Heterocyclic alkenes, including furan, thiophene, and benzothiophene derivatives (**1ad**–**1af**), efficiently afforded the desired products (**3ad**–**3af**) in moderate to good yields (up to 74%, Table 2.5). Interestingly, *N*-methylated pyrrole-tethered alkenes (**1ag**–**1ah**) underwent exclusive bis-trifluoromethylation to give the corresponding products (**3ag**–**3ah**) in moderate yields (55%, Table 2.5), unlike the furan- and thiophene-based substrates. This selectivity is likely due to the high nucleophilicity of the pyrrole ring, which undergoes photooxidation followed by trifluoromethylation at the heterocyclic ring.

To further highlight the versatility of this protocol, we investigated the reaction of commercially available natural product-derived substrates, including pregnenolone and cholesterol derivatives (**1ai** and **1aj**), under the optimized reaction conditions. This successfully furnished the corresponding trifluoromethylated products (**3ai** and **3aj**) (Table 2.5). The molecular structure of **3ai** was definitively confirmed through single-crystal X-ray diffraction analysis, which established the *anti*-addition of hydroxyl and trifluoromethyl groups across the double bond.[25] Based on this structural analogy, the stereochemistry of **3aj** was assigned.

Notably, a methyl ester derived from natural omega-9 fatty acid, oleic acid (*cis*-9-octadecenoic acid), underwent the reaction to afford the corresponding trifluoromethylated alcohol **3ak**. Additionally, citronellyl benzoate **1al**, derived from natural citronellol commonly used in perfumes and fragrances, reacted to give the desired trifluoromethylated alcohol **3al** in a modest yield (46%, Table 2.5). Furthermore, we attempted the reaction with simple commercially available alkenes, including 1-hexene, *cis*-4-octene, *trans*-4-octene, and *cis*-cyclooctene. However, in all cases, significant degradation of the starting materials was observed, and the formation of the corresponding *β*-hydroxy trifluoromethylated products was not detected.

Cyclic voltammograms

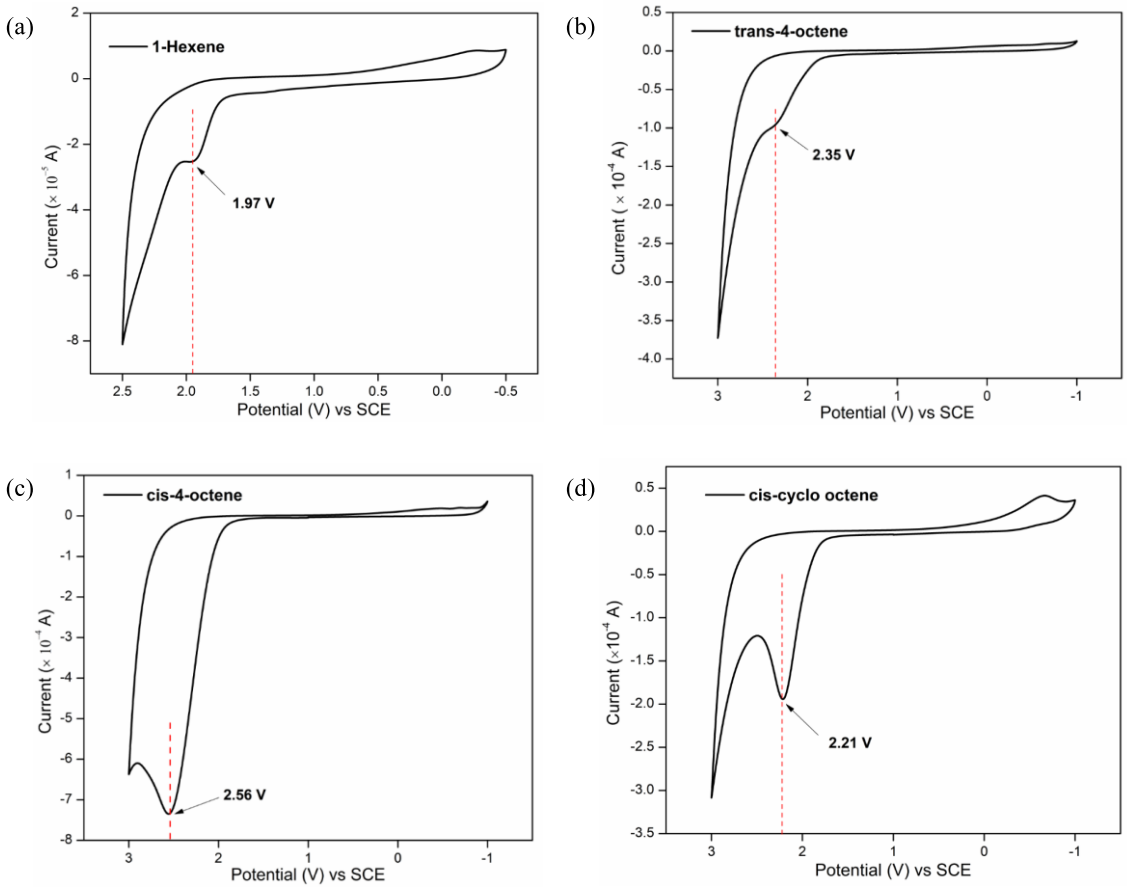

Figure 2.3 Cyclic voltammogram of alkenes. (a) 1-hexene, (b) *trans*-4-octene, (c) *cis*-4-octene, and (d) *cis*-cyclooctene. Samples were prepared with 100 mM analyte and 100 mM $TBAPF_6$ electrolyte solution in MeCN with a scan rate of 100 mV/s. Cyclic voltammetry (CV) was performed using a CHI (model 600E) electrochemical analyzer/workstation. A three-electrode setup was used, consisting of a 3 mm dia. glassy carbon working electrode (Part no- CHI104, CH Instruments), platinum wire counter electrode (CHI115, CH Instruments), and a Calomel

reference electrode (Part no- CHI150, CH Instruments).

To gain insight into these unsuccessful transformations, we recorded the cyclic voltammograms of the starting materials (1-hexene, *trans*-4-octene, *cis*-4-octene, and *cis*-cyclooctene). The analysis revealed that their oxidation potentials are ≥2.0 V (Figure 2.3). We hypothesize that these substrates may undergo electron transfer with either the excited-state or ground-state photocatalyst (Mes-Acr-Me·BF_4* [E_{red*} > 1.8 V vs. SCE] and Mes-Acr-Me·BF_4 [E_{ox} = -0.57 V vs. SCE]), leading to their degradation during the reaction. Despite these, the optimized hydroxytrifluoromethylation conditions demonstrated broad applicability, proving effective for a diverse range of unactivated aliphatic mono-, di-, and trisubstituted alkenes (Table 2.5).

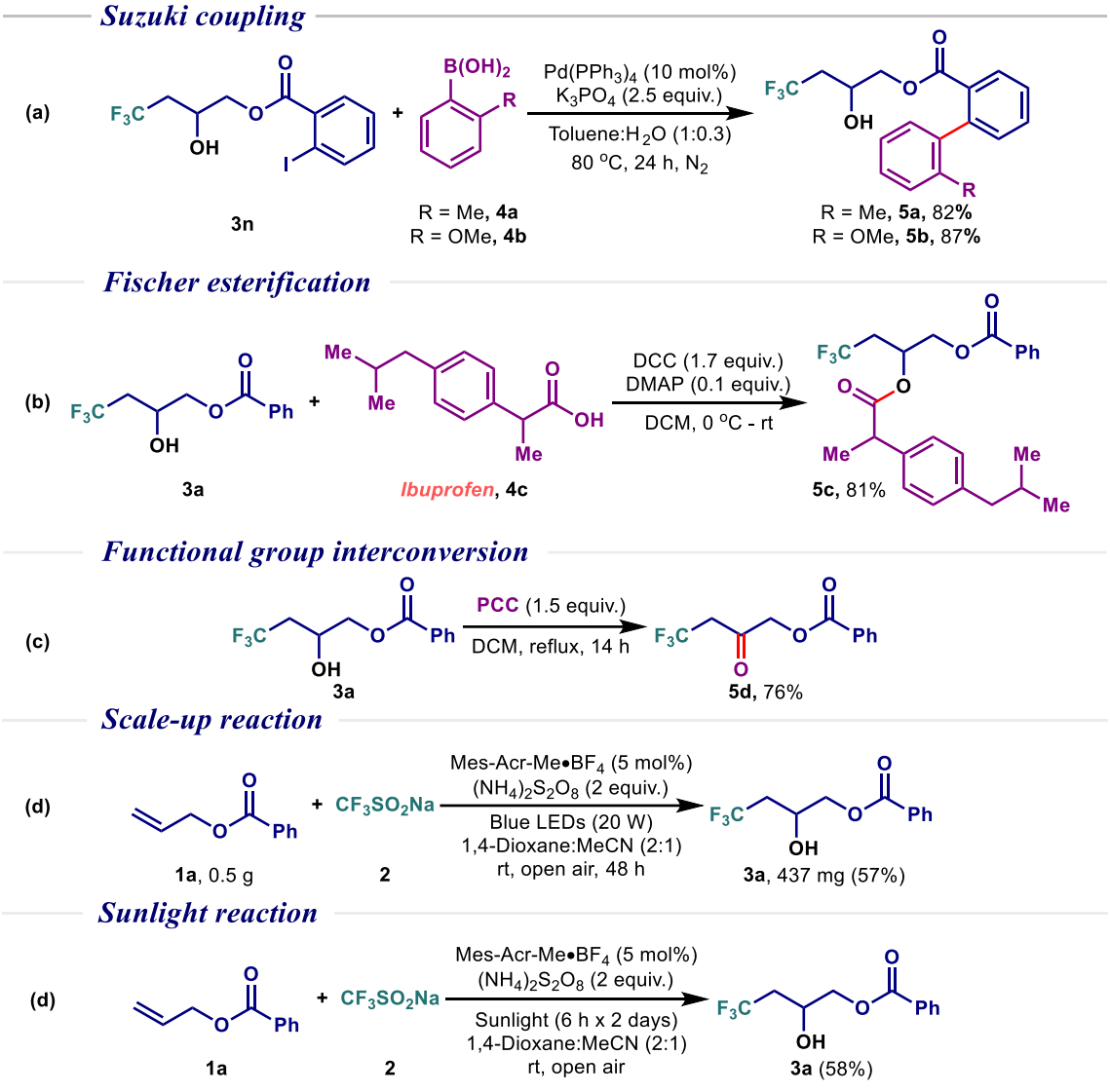

Scheme 2.9 Post synthetic applications, scale-up and sunlight reaction

Having established the broad applicability of this protocol, we next explored its potential for post-synthetic modifications as a practical extension of this strategy (Scheme 2.9).

To demonstrate its versatility, we employed *β*-hydroxy trifluoromethylated products **3a** and **3n** in various synthetic transformations to access valuable organic compounds. Specifically, compound **3n** underwent Suzuki–Miyaura coupling with aryl boronic acids **4a** and **4b**, yielding the corresponding coupling products **5a** and **5b** in excellent yields (up to 87%, Scheme 2.9a). Additionally, esterification of the synthesized compound **3a** with the nonsteroidal *anti*-inflammatory drug (NSAID) ibuprofen **4c** furnished the trifluoromethylated ester derivative **5c** in good yield (81%, Scheme 2.9b). Furthermore, oxidation of **3a** using PCC led to the formation of the synthetically valuable *β*-trifluoromethyl ketone **5d** in 76% yield (Scheme 2.9c). To demonstrate the practicality of this protocol, we successfully carried out the scale-up synthesis of **3a**, (437 mg, 57% yield, Scheme 2.9d). Additionally, the reaction was performed under direct exposure to natural sunlight as an alternative light source, affording **3a** (58%, Scheme 2.9e).

To gain a deeper mechanistic understanding of this transformation, we conducted a series of control experiments (Scheme 2.10). First, reactions were performed under standard conditions while individually omitting light, the photocatalyst, the oxidant, or conducting the reaction under an argon atmosphere. Notably, no product formation was observed in any of these cases, indicating the essential role of light, the photocatalyst, the oxidant, and molecular oxygen (air) in facilitating the reaction.

Control experiments

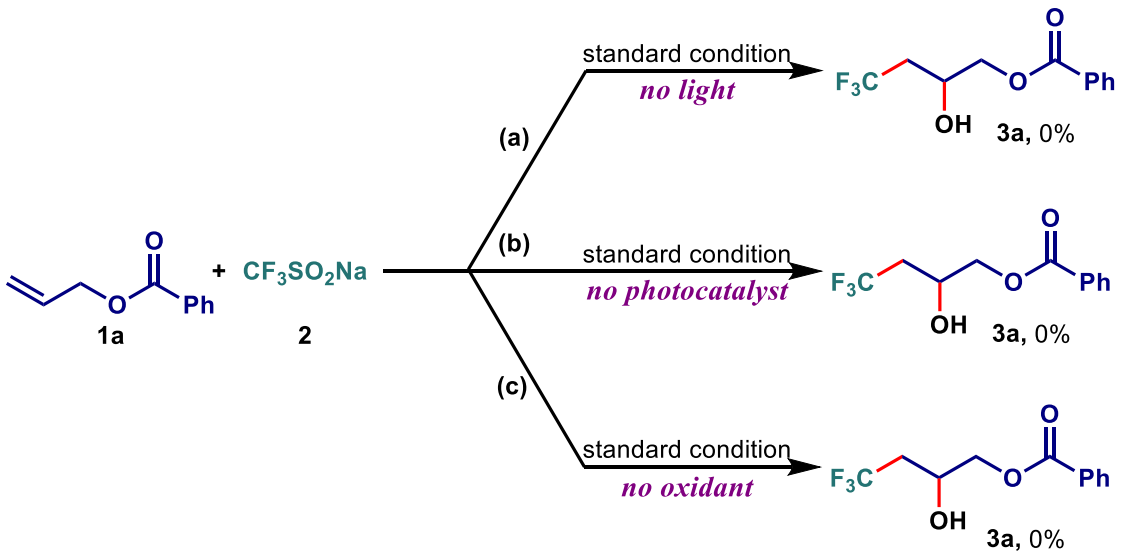

Scheme 2.10 Control experiments

In addition, radical quenching experiments were performed by reacting **1a** with **2** in the presence of radical scavengers such as BHT and TEMPO under the optimized conditions (Scheme 2.11). This resulted in a significantly reduced yield of the desired product **3a**, along with the detection of TEMPO/BHT-trapped radical intermediates, as confirmed by HRMS (Figure 2.4 and 2.5). These findings strongly support the *in-situ* generation of CF_3 radical **A** and trifluoromethylated alkyl radical **B** during the reaction (Scheme 2.11).

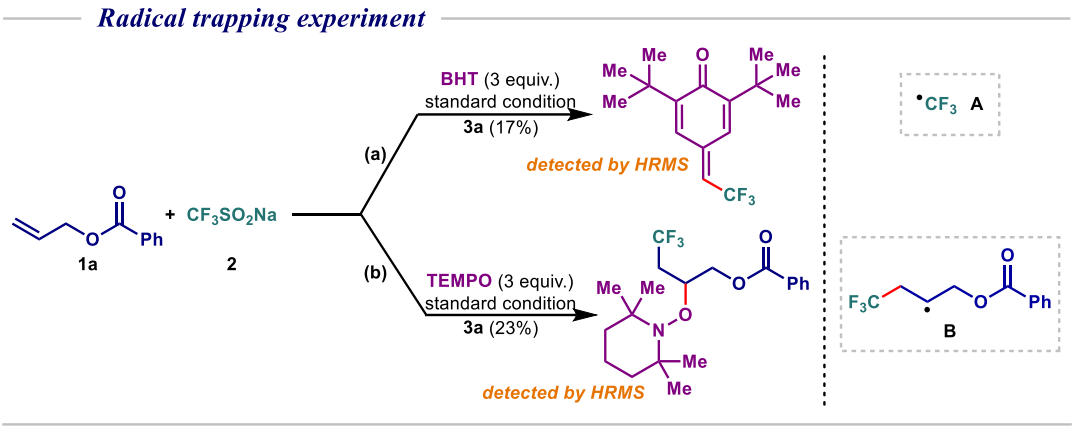

Scheme 2.11 Radical trapping experiments

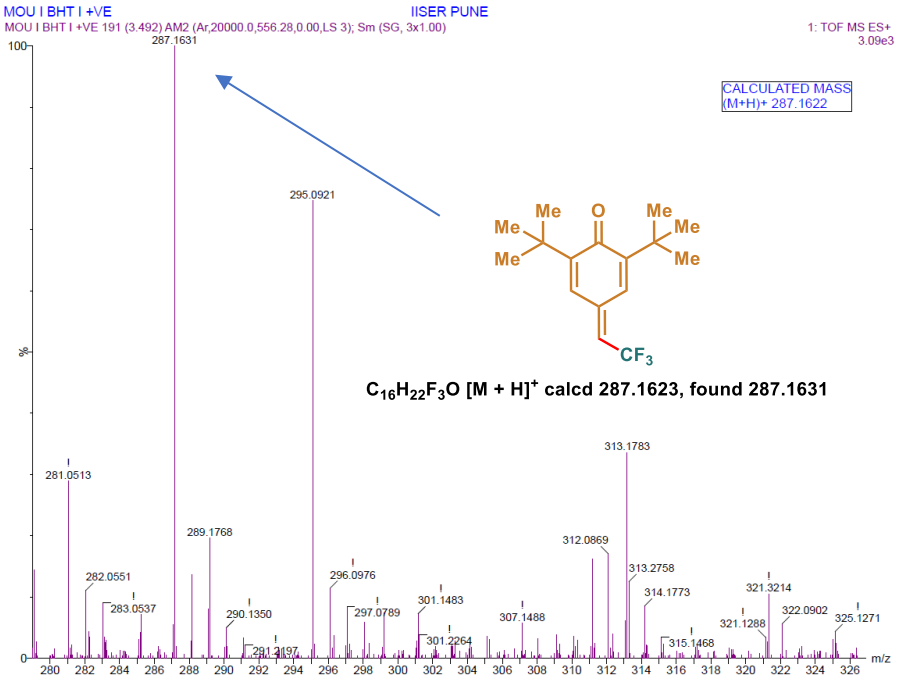

Figure 2.4. HRMS data of BHT trapped radical intermediate

Later, the reaction of **1a** and **2** was conducted under an inert atmosphere in the presence of $H_2{}^{18}O$, but we did not observe the compound **3a** (Scheme 2.12a, Figure 2.6). However, when

the reaction was performed under open-air conditions with $H_2{}^{18}O$, the desired product **3a** was detected without any incorporation of ^{18}O, Scheme 2.12b, Figure 2.7).

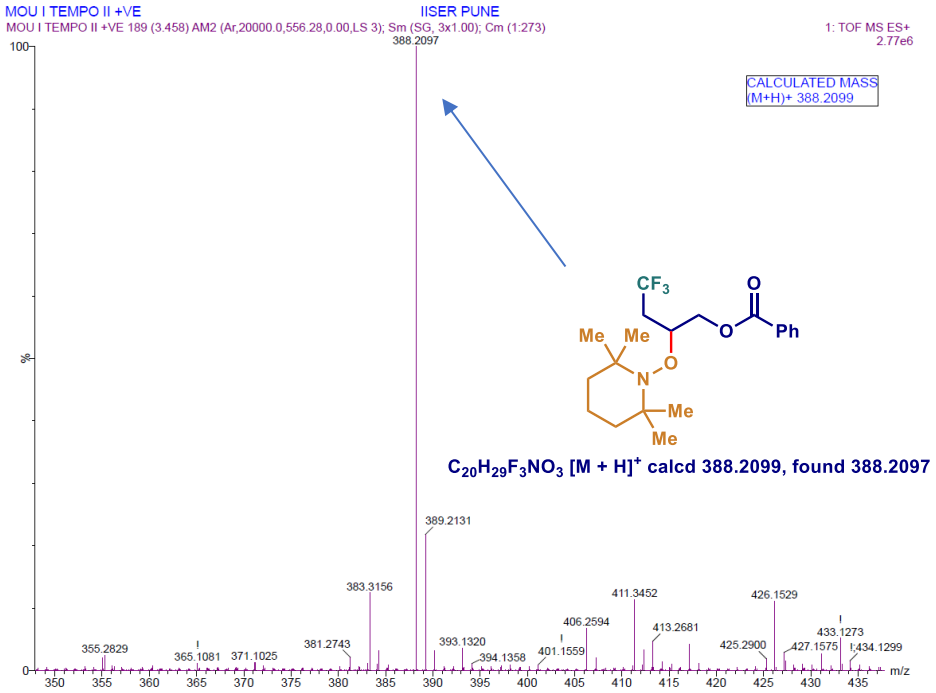

Figure 2.5 HRMS data of TEMPO trapped radical intermediate

This result ruled out the possibility of moisture as the oxygen source. To further confirm the role of oxygen, we conducted the reaction of **1a** in the presence of an $^{18}O_2$ atmosphere while keeping all other conditions unchanged. Gratifyingly, the ^{18}O-incorporated product **3a'** was obtained (confirmed by HRMS) (Scheme 2.12c, Figure 2.8). These results strongly support the crucial role of molecular oxygen (air) in driving the reaction.

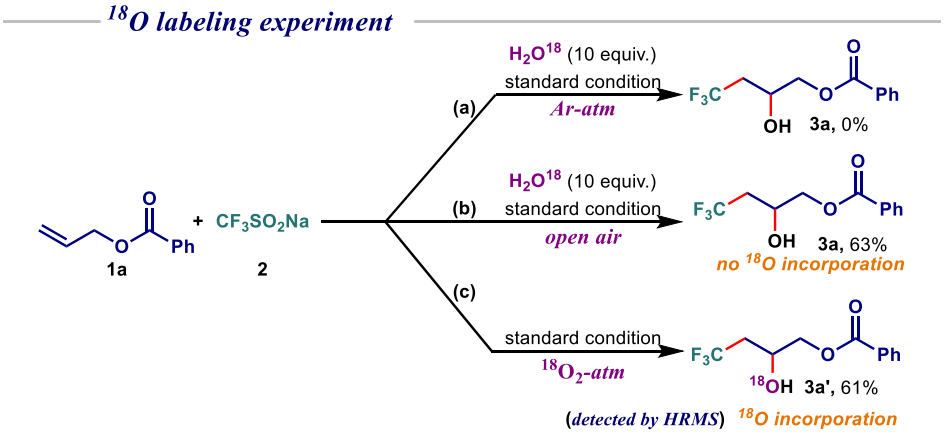

Scheme 2.12 ^{18}O labeling experiment

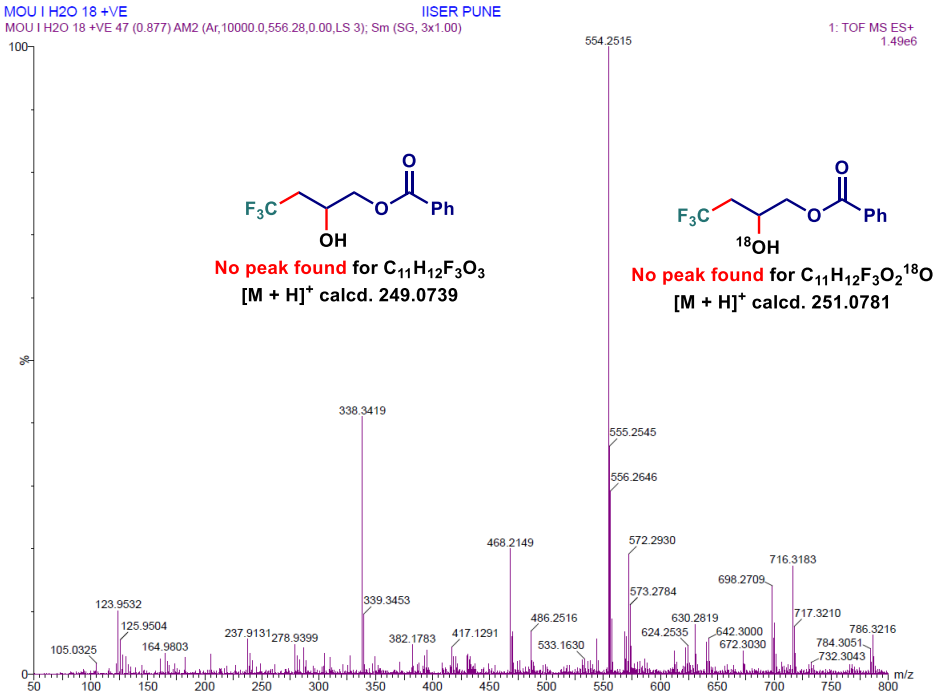

Figure 2.6 HRMS data for ^{18}O labeling experiment with H_2O^{18} under Ar-atm

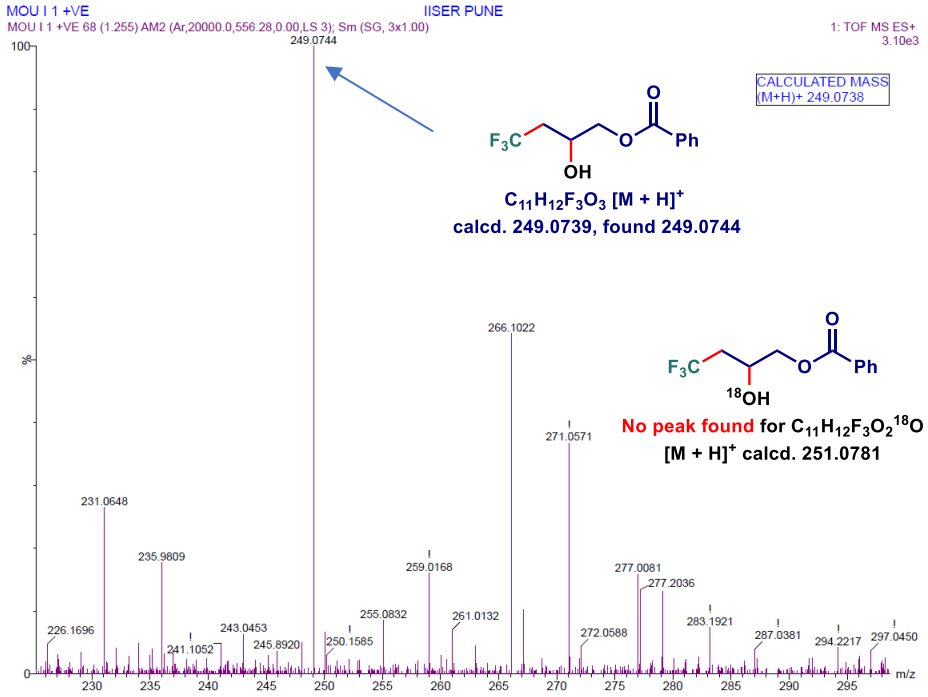

Figure 2.7 HRMS data for ^{18}O labeling experiment with H_2O^{18} under open air

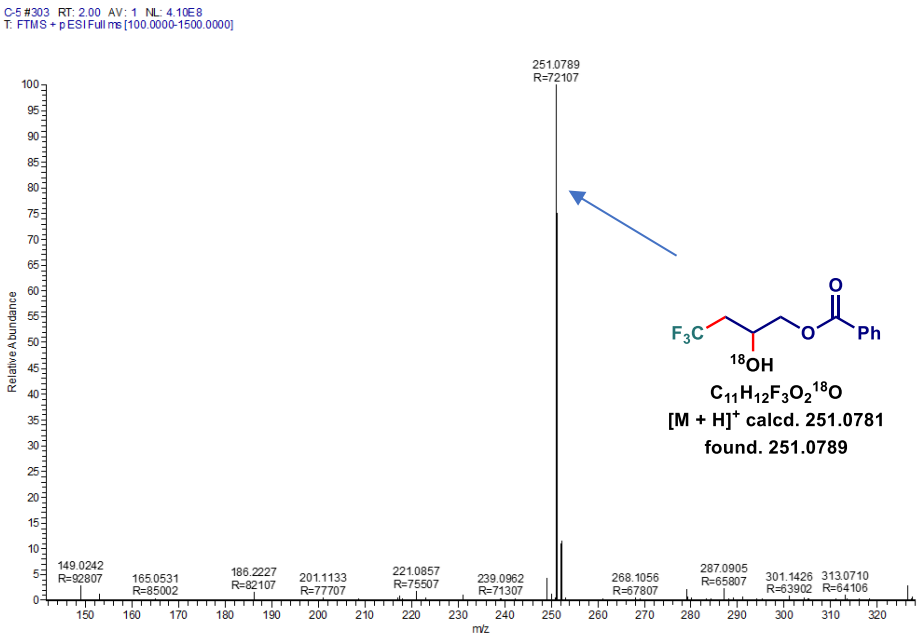

Figure 2.8 HRMS data for ^{18}O labeling experiment under $^{18}O_2$ atmosphere

Furthermore, a deuterium labeling experiment was conducted using MeCN-d_3 as the solvent. The desired product **3a** was obtained without any deuterium incorporation (Scheme 2.13a). However, when the reaction of **1a** and **2** was performed in the presence of D_2O (10 equiv.) under standard conditions, a mixture of deuterium-incorporated product **3aD** and **3a** was observed (Scheme 2.13b, Figure 2.9). These findings suggest that moisture present in the solvent likely serves as the primary proton source.

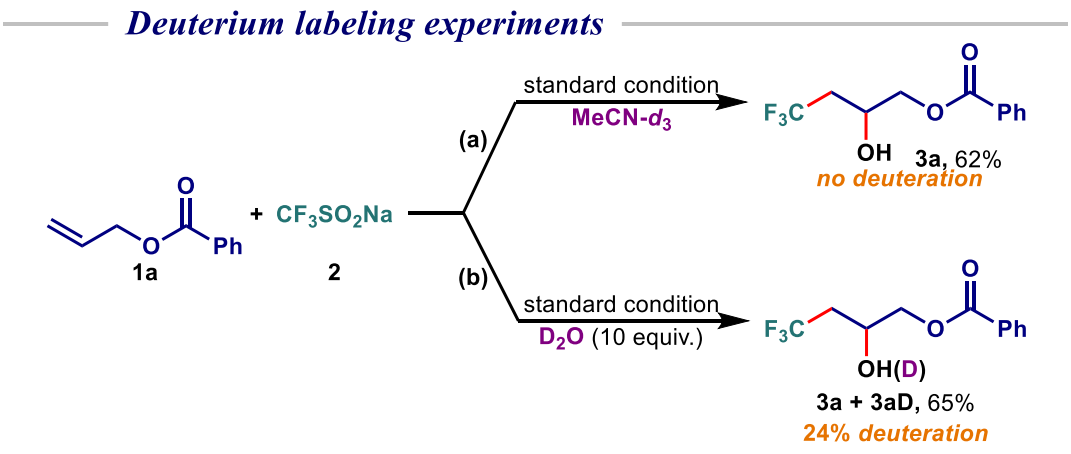

Scheme 2.13 Deuterium labeling experiment

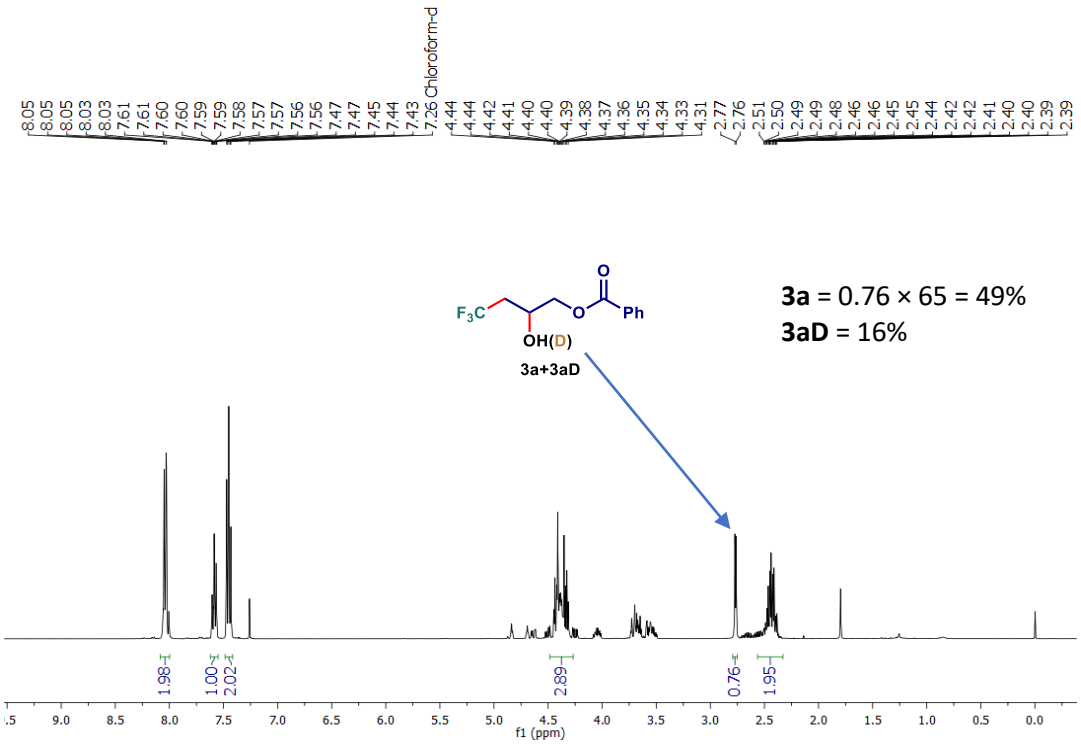

Figure 2.9 ^{1}H NMR spectrum of deuterated product **3a**+**3aD**

To confirm the stereochemical outcome of the protocol, we carried out reactions using a pair of *E/Z* alkenes, **1am** and **1an**, under standard conditions, which exclusively afforded product **3xx** (Scheme 2.14). Based on ^{1}H, ^{13}C{^{1}H}, and ^{19}F{^{1}H} NMR spectral analysis, the products obtained from both **1am** and **1an** were identical (see stacked spectra in Figure 2.10). This suggests that after the addition of the CF_3 radical to the alkene, free rotation of the resulting alkyl radical may occur. Additionally, light exposure could facilitate this rotation, ultimately leading to the formation of product **3xx**.

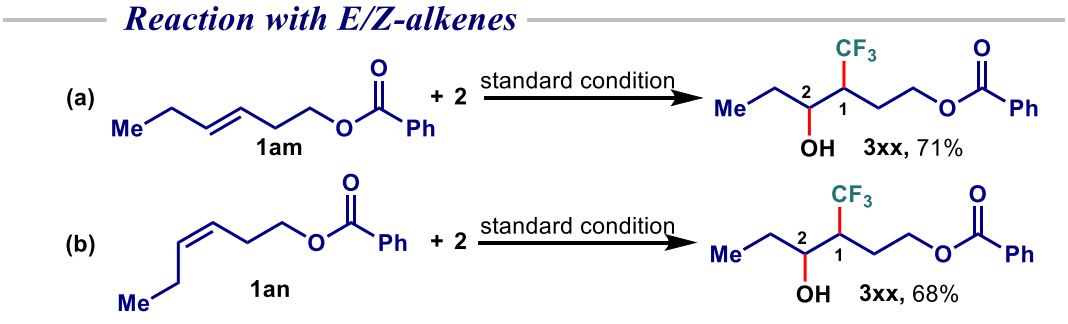

Scheme 2.14 Deuterium labeling experiment

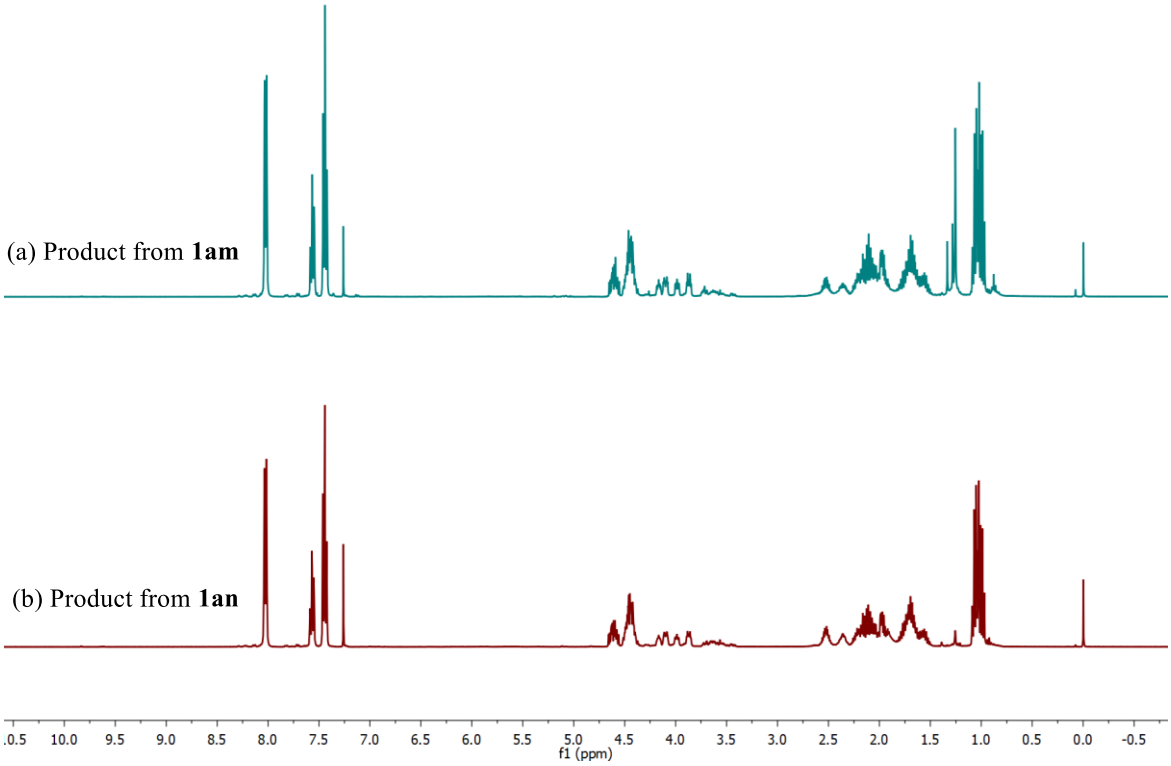

Figure 2.10 Stacked ^{1}H NMR spectrum of product obtained from **1am** and **1an**

Additionally, an intermittent illumination (light ON/OFF) experiment was performed to investigate the correlation between irradiation time and the yield of product **3a** (Figure 2.11). No product formation was observed in the absence of light, while illumination led to an increase in the yield of **3a**, confirming the reaction's dependence on continuous light exposure. These findings rule out the possibility of a light-initiated radical chain mechanism and clearly demonstrate that sustained irradiation is essential for product formation.

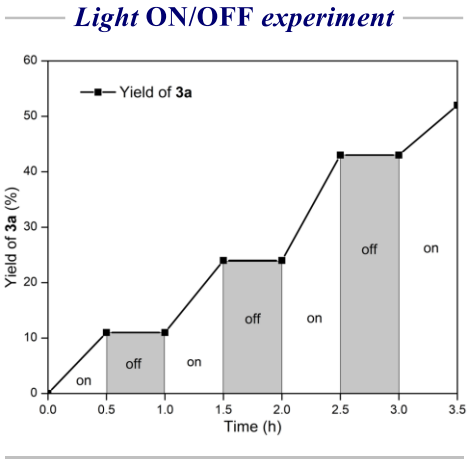

Figure 2.11 Light ON/OFF experiment

Later, we conducted a fluorescence quenching study of the photocatalyst (Mes-Acr-Me·BF_4) with varying concentrations of **1a**, **2**, and $(NH_4)_2S_2O_8$ (Figures 2.12a-c). The Stern-Volmer plot confirmed that CF_3SO_2Na **2** acts as a potent fluorescence quencher of the excited-state Mes-Acr-Me·BF_4* (Figure 2.12d). Furthermore, CF_3SO_2Na efficiently participates in a single-electron transfer (SET) event with Mes-Acr-Me·BF_4*, as supported by its oxidation potential [E_{ox} = 1.05 V vs. SCE], which is lower than the reduction potential of Mes-Acr-Me·BF_4* [E_{red*} > 1.8 V vs. SCE].[26, 27]

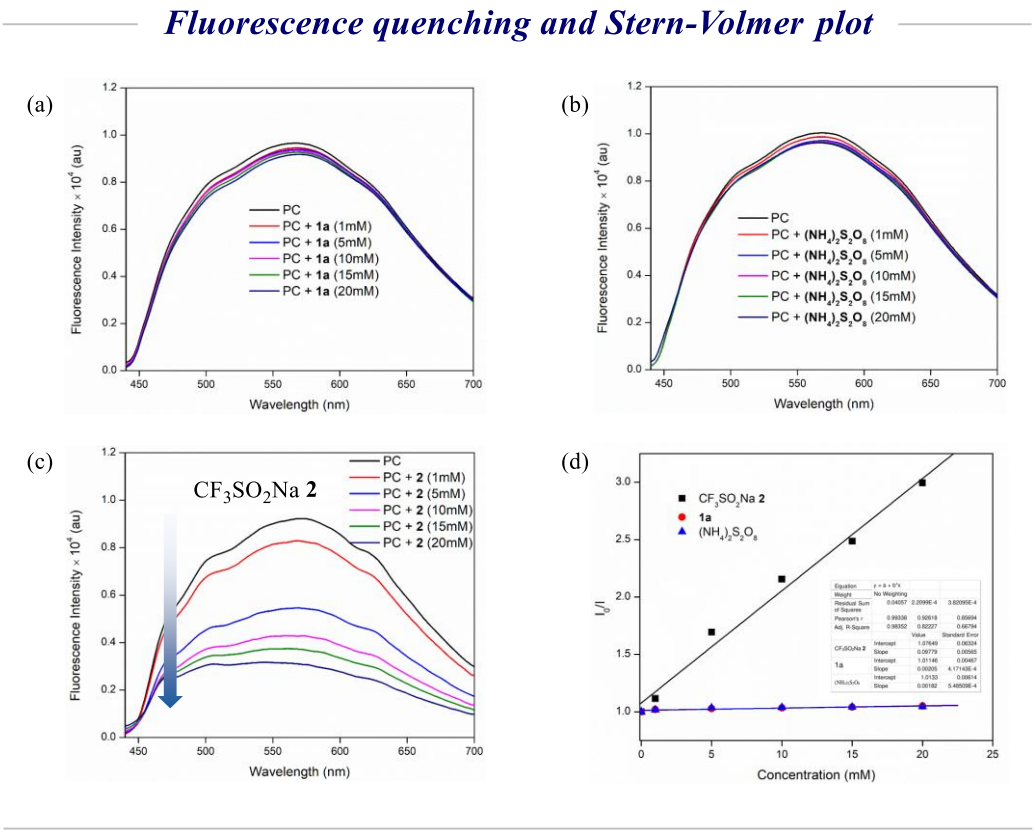

Figure 2.12 Fluorescence quenching of Mes-Acr-Me·BF_4 with increasing in the concentration of (a) allyl benzoate **1a**, (b) $(NH_4)_2S_2O_8$ (c) CF_3SO_2Na **2** (d) Stern-Volmer plot.

Based on the findings from control experiments and relevant literature, a plausible visible-light-mediated radical mechanism for *β*-hydroxytrifluoromethylation has been proposed (Scheme 2.15). Upon blue light irradiation, Mes-Acr-Me·BF_4 (PC) is excited to its high-energy state (PC*), which acts as a strong oxidant [E_{red*} > 1.8 V vs. SCE].[27] The excited photocatalyst (PC*) then undergoes reductive quenching via single-electron transfer (SET) with CF_3SO_2Na **2** [E_{ox} = 1.05 V vs. SCE],[26] leading to the formation of a trifluoromethyl radical

[**A**] (confirmed by HRMS through a BHT-trapped radical adduct) and the reduced form of PC ($PC^{-\bullet}$). The trifluoromethyl radical [**A**] subsequently reacts with **1a**, generating radical intermediate [**B**], which was also detected by HRMS through a TEMPO-trapped radical adduct. This intermediate then reaction with O_2, forming an unstable intermediate [**C**], which subsequently forms the desired product **3a** after proton abstraction. Simultaneously, $(NH_4)_2S_2O_8$ [E_{red} = 1.8–2.7 V][28] oxidizes the reduced photocatalyst [E_{ox} = -0.57 V vs. SCE], restoring it to its ground state, thereby completing the catalytic cycle.

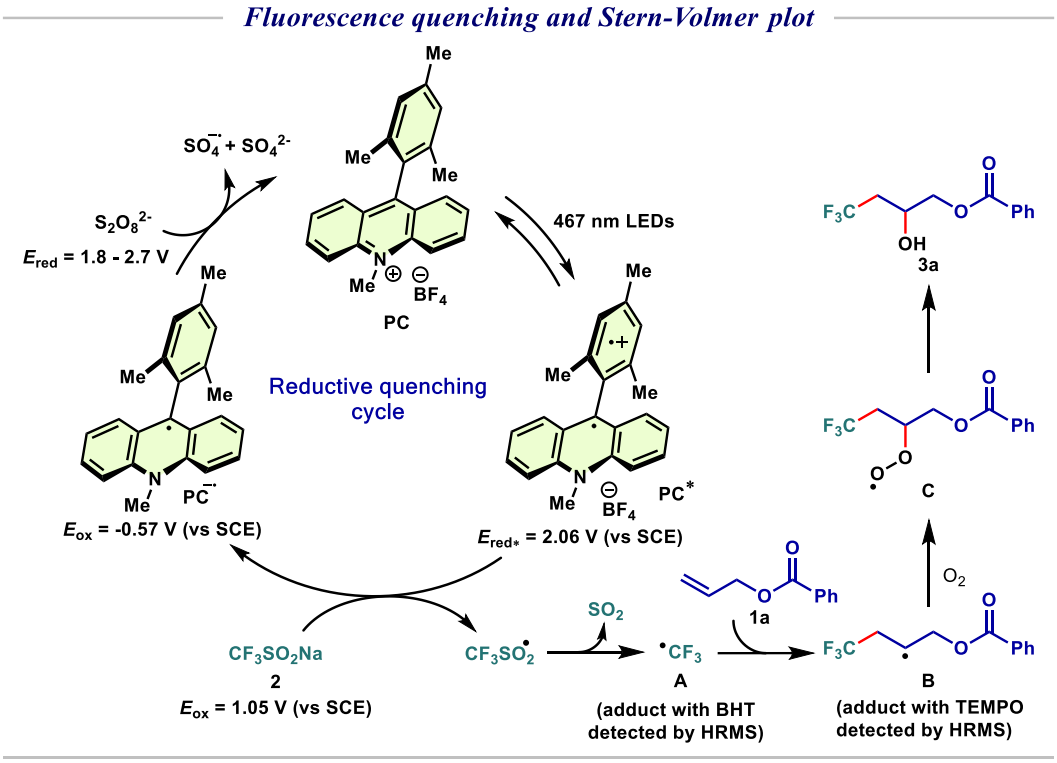

Scheme 2.15 Plausible mechanism for *β*-trifluoromethylated alcohols

2.3 Conclusion

In summary, we have successfully developed a transition metal-free, visible light-induced direct *β*-hydroxytrifluoromethylation of both terminal and internal unactivated alkenes using the Langlois reagent at room temperature. This operationally simple and mild transformation employs a nontoxic, cost-effective organic dye as the photoredox catalyst. The protocol demonstrated excellent practicality, featuring broad substrate scope and good functional group tolerance. Its synthetic utility was further showcased through the functionalization of natural product-derived substrates, functional group transformation, and subsequent derivatization of the synthesized products. Additionally, the reaction was scalable and proceeded efficiently under direct sunlight exposure. A series of control experiments, along with fluorescence

quenching and cyclic voltammetry studies, confirmed that the transformation operates via a reductive quenching mechanistic cycle.

2.4 Experimental Section

2.4.1 General Details

Unless otherwise noted, all the starting materials and reagents were purchased from commercial suppliers (Sigma-Aldrich, TCI, Alfa Aesar, Spectrochem and BLD Pharm) and were used as received. Thin-layer chromatography (TLC) was performed using silica gel 60 GF_{254} precoated aluminum backed plates (2.5 mm). Visualization was accomplished by irradiation with UV light at 254 nm and phosphomolybdic acid (PMA) staining agent. The column chromatography was performed using silica gel (100−200 mesh) eluting with petroleum ether and ethyl acetate. The NMR spectra were recorded using tetramethylsilane as the internal standard. ^{1}H NMR spectra were recorded at 400/600 MHz, $^{19}F\{^{1}H\}$ NMR spectra were recorded at 377/565 MHz and $^{13}C\{^{1}H\}$ spectra were recorded at 100/150 MHz (Bruker and Jeol) using tetramethylsilane as the internal standard, unless otherwise noted. Chemical shifts (δ) are reported in ppm downfield from $CDCl_3$ (δ = 7.26 ppm) for ^{1}H NMR and relative to the central $CDCl_3$ resonance (δ = 77.16 ppm) for $^{13}C\{^{1}H\}$ NMR spectroscopy. For ^{1}H NMR, data are reported as follows: chemical shift, multiplicity (s = singlet, d = doublet, t = triplet, q = quartet, p = pentet, s = sextet, h = heptet, m = multiplet, br = broad), coupling constants (J) are given in Hz and integration. $^{13}C\{^{1}H\}$ NMR spectra were recorded with complete proton decoupling. Mass samples were analyzed by high-resolution mass spectrometry (HRMS)-ESI TOF. Using an open glass capillary, melting points were recorded on a BUCHI M-560 melting point apparatus, and they are not corrected. Fluorescence emission spectra were obtained on a RF-6000 Spectrofluorophotometer from Shimadzu in a 3 mL, Hellma fluorescence cuvette (path length 1.0 cm). All photocatalytic reactions were performed under blue LEDs (Kessil PR160L series Blue LEDs, and IBRA Pure 20 W Blue LED Flood Light, IP Rating: IP66) and reaction mixture was irradiated from 5 cm away from the LEDs.

Note and Caution! 1. Avoid skin contact, eye contact and inhalation of ammonium persulfate and sodium trifluoromethanesulfinate. 2. Avoid inhalation of the reaction mixture as it may contain SO_2 gas (byproduct of the reaction).

List of starting materials used for the *β*-hydroxy trifluoromethylation reaction:

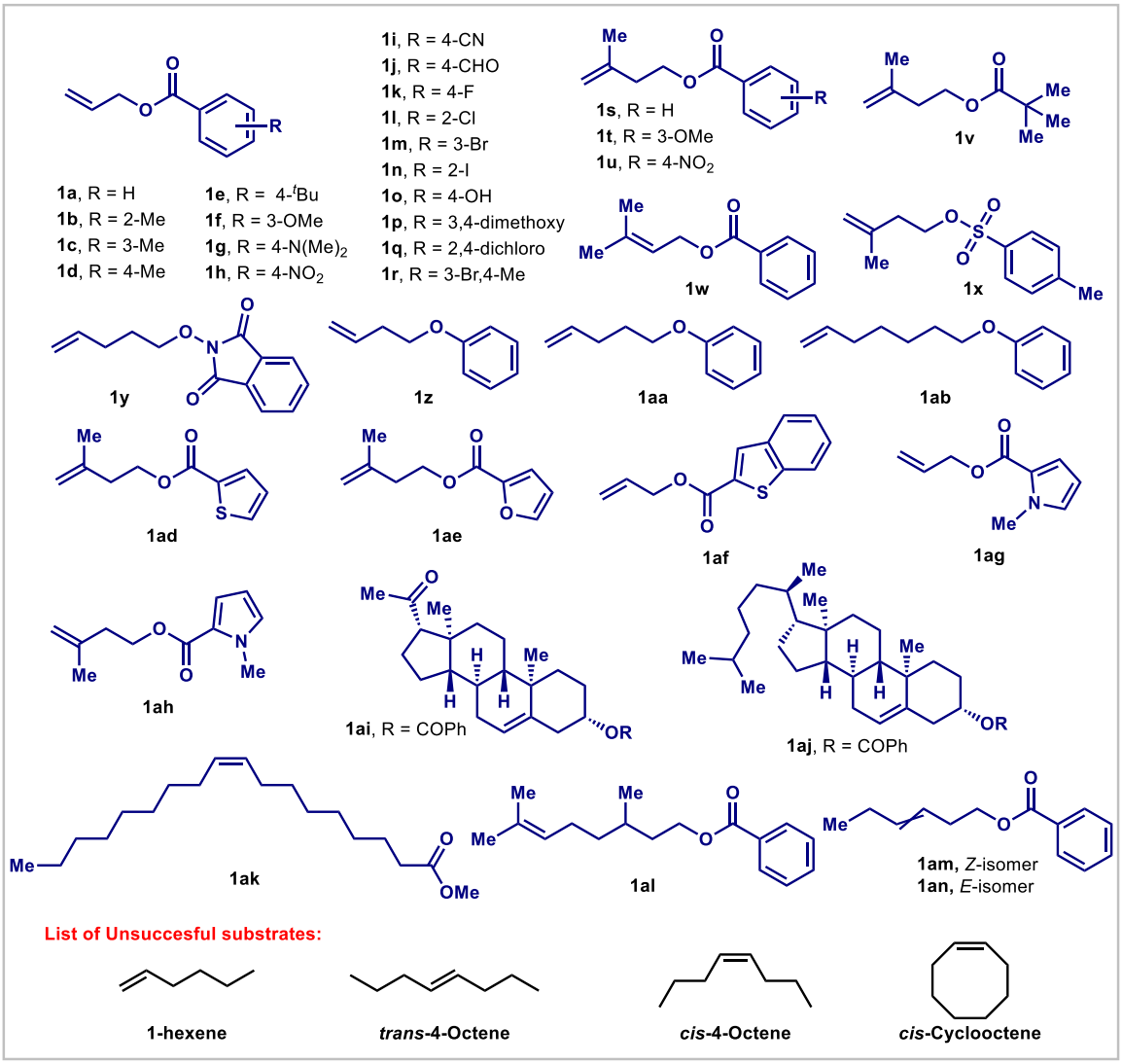

2.4.2 Preparation of Starting Materials

2.4.2A *General procedure A for the synthesis of alkenyl benzoates 1a−1r, 1w, 1y, 1z, 1aa−1ab, and 1af−1ag.* The compounds were synthesized following the previously reported procedure.[29] To an oven-dried reaction tube charged with magnetic stir bar and rubber septum was added DMF (20 mL), benzoic acid or phenol or 2-hydroxyisoindoline-1,3-dione (1 equiv.; 5 mmol), 3-bromoprop-1-ene or 1-bromo-3-methylbut-2-ene or 4-bromobut-1-ene or 5-bromopent-1-ene or 7-bromohept-1-ene (1.5 equiv.) and K_2CO_3 (2 equiv.) and stirred at room temperature for 12−24 h (monitored by TLC). The reaction mixture was then quenched with water and the product was extracted with ethyl acetate (30 mL × 3). The combined organic layers were washed with brine solution and dried over anhydrous Na_2SO_4. The extract was

filtered and evaporated under reduced pressure. The crude products were purified using column chromatography over silica gel to afford **1a**−**1r**, **1w**, **1y**, **1z**, **1aa**−**1ab,** and **1af**−**1ag**.

2.4.2B ***General Procedure B for the Synthesis of Compounds 1s−1v, 1x, 1ad−1ae, 1ah****, and* ***1ai−1al****.* The starting materials **1s**−**1u**, **1ad**−**1ae**, **1ah**, **1ai**−**1al**, **1am** and **1an** were synthesized according to the slightly modified reported procedure.[30] To a stirred solution of alcohol (5 mmol, 1 equiv), carboxylic acid (1.5 equiv.), and dimethylaminopyridine, DMAP (10 mol %) in anhydrous CH_2Cl_2 (20 mL) was added *N,N′*-dicyclohexylcarbodiimide, DCC (1.5 equiv.) at 0 °C, which is then stirred for 5 min at 0 °C and then at room temperature. The progress of the reaction was monitored by TLC. After completion of the reaction, precipitated urea is then filtered off in CH_2Cl_2. The CH_2Cl_2 solution is washed twice with ~ HCl (0.5 N) and with saturated $NaHCO_3$ solution. The combined organic layers were washed with brine solution and dried over anhydrous Na_2SO_4. The crude product was purified using column chromatography over silica gel to afford **1s**−**1u**, **1ad**−**1ae**, **1ah**, **1ai**−**1al**, **1am** and **1an**. The starting materials **1v**, **1x** were synthesized according to the reported literature procedure starting from pivaloyl chloride or 4-methylbenzenesulfonyl chloride and 3-methylbut-3-en-1-ol.[31]

2.4.3 ***General Procedure C for the Synthesis of 3****.* To an oven-dried reaction tube equipped with a stir bar alkene **1** (0.2 mmol, 1 equiv), CF_3SO_2Na, **2** (3 equiv.), $(NH_4)_2S_2O_8$ (2 equiv.), Mes-Acr-Me·BF_4 (5mol %), and 1,4-Dioxane:MeCN (2:1 mL) were added. Then the reaction mixture was irradiated with 467 nm Kessil PR-160L Blue LED (50% intensity), from ~5 cm away under open air and stirred at room temperature (under the continuous flow of fan to maintain the temperature at 25−30 °C) for 12−36 h (monitored by TLC). After completion of the reaction, the reaction mixture was filtered and the solvent was removed under reduced pressure. Then, the crude residue was purified by column chromatography over silica gel (100−200 mesh size) using mixture of petroleum ether/EtOAc as an eluent to afford the corresponding desired β-trifluoromethyl alcohol product **3**.

2.4.4 Product Characterization Data

Allyl 3-bromo-4-methylbenzoate (**1r**). The title compound **1r** was prepared according to the general procedure **A** starting from 3-bromo-4-methylbenzoic acid (5.0 mmol) and 3-bromoprop-1-ene (1.5 equiv.). Colourless liquid (1.17 g, 92% yield), R_f = 0.45 (petroleum ether/EtOAc 95:5). ^{1}H NMR (400

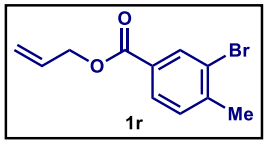

MHz, $CDCl_3$) δ 8.21 (d, *J* = 1.8 Hz, 1H), 7.89 (dd, *J* = 7.9, 1.8 Hz, 1H), 7.30 (dd, *J* = 7.8, 0.8 Hz, 1H), 6.03 (ddt, *J* = 17.2, 10.4, 5.7 Hz, 1H), 5.40 (dq, *J* = 17.2, 1.5 Hz, 1H), 5.30 (dq, *J* = 10.4, 1.3 Hz, 1H), 4.81 (dt, *J* = 5.7, 1.4 Hz, 2H), 2.45 (s, 3H). $^{13}C\{^1H\}$ NMR (100 MHz, $CDCl_3$) δ 165.2 (s), 143.6 (s), 133.6 (s), 132.2 (s), 130.8 (s), 129.6 (s), 128.6 (s), 124.9 (s), 118.7 (s), 65.9 (s), 23.4 (s). HRMS (ESI TOF) *m/z* for $C_{11}H_{12}BrO_2$ $[M + H]^+$ calcd. 255.0021, found 255.0017.

Allyl benzo[b]thiophene-2-carboxylate (**1af**). The title compound **1af** was prepared according to the general procedure **A** starting from benzo[b]thiophene-2-carboxylic acid (5.0 mmol) and 3-bromoprop-1-ene (1.5 equiv.). White solid (1.06 g, 97% yield), R_f = 0.43 (petroleum ether/EtOAc 95:5), mp 43−45 °C. ^1H NMR (400 MHz, $CDCl_3$) δ 8.09 (d, *J* = 0.8 Hz, 1H), 7.97 – 7.80 (m, 2H), 7.61 – 7.31 (m, 2H), 6.05 (ddt, *J* = 17.2, 10.4, 5.6 Hz, 1H), 5.45 (dq, *J* = 17.2, 1.5 Hz, 1H), 5.32 (dq, *J* = 10.4, 1.3 Hz, 1H), 4.86 (dt, *J* = 5.7, 1.4 Hz, 2H). $^{13}C\{^1H\}$ NMR (100 MHz, $CDCl_3$) δ 162.6 (s), 142.4 (s), 138.8 (s), 133.6 (s), 132.0 (s), 130.8 (s), 127.1 (s), 125.7 (s), 125.1 (s), 122.9 (s), 118.8 (s), 66.2 (s). HRMS (ESI TOF) *m/z* for $C_{12}H_{11}O_2S$ $[M + H]^+$ calcd. 219.0480, found 219.0483.

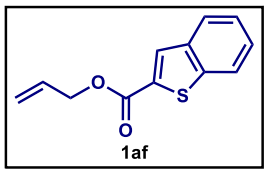

Allyl 1-methyl-1H-pyrrole-2-carboxylate (**1ag**). The title compound **1ag** was prepared according to the general procedure **A** starting from 1-Methyl-1H-pyrrole-2-carboxylic acid (5.0 mmol) and 3-bromoprop-1-ene (1.5 equiv.). Colourless liquid (727 mg, 88% yield), R_f = 0.34 (petroleum ether/EtOAc 95:5). ^1H NMR (400 MHz, $CDCl_3$) δ 6.99 (dd, *J* = 4.0, 1.8 Hz, 1H), 6.79 (t, *J* = 2.2 Hz, 1H), 6.12 (dd, *J* = 4.0, 2.5 Hz, 1H), 6.01 (ddt, *J* = 17.2, 10.7, 5.5 Hz, 1H), 5.38 (dq, *J* = 17.2, 1.6 Hz, 1H), 5.25 (dq, *J* = 10.5, 1.4 Hz, 1H), 4.73 (dt, *J* = 5.5, 1.5 Hz, 2H), 3.93 (s, 3H). $^{13}C\{^1H\}$ NMR (100 MHz, $CDCl_3$) δ 161.1 (s), 132.8 (s), 129.7 (s), 122.4 (s), 118.1 (s), 117.8 (s), 108.0 (s), 64.5 (s), 36.9 (s). HRMS (ESI TOF) *m/z* for $C_9H_{12}NO_2$ $[M + H]^+$ calcd. 166.0868, found 166.0871.

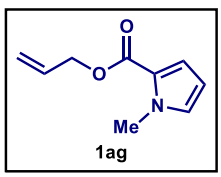

(E)-hex-3-en-1-yl benzoate (**1am**) The title compound **1am** was prepared according to the general procedure **B** starting from benzoic acid (5.0 mmol) and (*E*)-hex-3-en-1-ol (1.5 equiv.). Colourless liquid (980 mg, 96% yield), R_f = 0.32 (petroleum ether/EtOAc 95:5). ^1H NMR (400 MHz, $CDCl_3$) δ 8.08 – 8.01 (m, 2H), 7.61 – 7.52 (m, 1H), 7.48 – 7.40 (m, 2H), 5.62 (dtt, *J* = 15.3, 6.3, 1.3 Hz, 1H), 5.45 (dtt, *J* = 15.2, 6.8, 1.5 Hz, 1H), 4.32 (t, *J* = 6.8 Hz, 2H), 2.46 (qq,

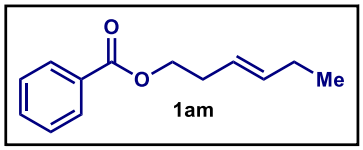

J = 6.8, 1.2 Hz, 2H), 2.03 (dtdd, J = 8.7, 7.4, 6.2, 1.3 Hz, 2H), 0.97 (t, J = 7.5 Hz, 3H). $^{13}C\{^1H\}$ NMR (100 MHz, $CDCl_3$) δ 166.7, 135.4, 133.0, 130.6, 129.7, 128.4, 124.2, 64.7, 32.2, 25.8, 13.9. HRMS (ESI TOF) *m/z* for $C_{13}H_{17}O_2$ $[M + H]^+$ calcd. 205.1229, found 205.1226.

(Z)-hex-3-en-1-yl benzoate (**1an**). The title compound **1an** was prepared according to the general procedure **B** starting from benzoic acid (5.0 mmol) and (*Z*)-hex-3-en-1-ol (1.5 equiv.). Colourless liquid (960 mg, 94% yield), R_f = 0.32 (petroleum ether/EtOAc 95:5). ^1H NMR (400 MHz, $CDCl_3$) δ 8.07 – 8.00 (m, 2H), 7.59 – 7.51 (m, 1H), 7.47 – 7.39 (m, 2H), 5.58 – 5.49 (m, 1H), 5.45 – 5.36 (m, 1H), 4.32 (t, J = 6.9 Hz, 1H), 2.59 – 2.47 (m, 1H), 2.10 (pd, J = 7.6, 1.5 Hz, 1H), 0.97 (t, J = 7.5 Hz, 2H). $^{13}C\{^1H\}$ NMR (100 MHz, $CDCl_3$) δ 166.8, 134.8, 133.0, 130.5, 129.7, 128.5, 123.9, 64.6, 27.0, 20.8, 14.4. HRMS (ESI TOF) *m/z* for $C_{13}H_{17}O_2$ $[M + H]^+$ calcd. 205.1229, found 205.1225.

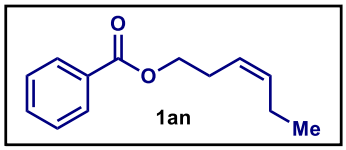

4,4,4-Trifluoro-2-hydroxybutyl benzoate (**3a**). The title compound **3a** was prepared according to the general procedure **C** starting from allyl benzoate **1a** (0.2 mmol) and CF_3SO_2Na **2** (3 equiv.). White solid (32 mg, 65% yield), R_f = 0.28 (petroleum ether/EtOAc 85:15), mp 43−45 °C. ^1H NMR (600 MHz, $CDCl_3$) δ 8.05 – 8.03 (m, 2H), 7.60 (t, J = 7.4 Hz, 1H), 7.46 (t, J = 7.8 Hz, 2H), 4.44 (dd, J = 11.2, 3.6 Hz, 1H), 4.42 – 4.37 (m, 1H), 4.34 (dd, J = 11.1, 5.9 Hz, 1H), 2.60 (d, J = 4.5 Hz, 1H), 2.52 – 2.38 (m, 2H). $^{13}C\{^1H\}$ NMR (150 MHz, $CDCl_3$) δ 166.7 (s), 133.6 (s), 129.9 (s), 129.5 (s), 128.7 (s), 126.1 (q, J = 276.7 Hz), 67.9 (s), 65.0 (d, J = 2.9 Hz), 38.1 (q, J = 27.9 Hz). $^{19}F\{^1H\}$ NMR (565 MHz, $CDCl_3$) δ 64.49 (s). HRMS (ESI TOF) *m/z* for $C_{11}H_{12}F_3O_3$ $[M + H]^+$ calcd. 249.0739, found 249.0741.

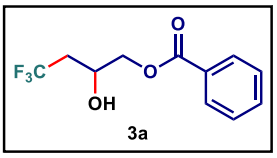

4,4,4-Trifluoro-2-hydroxybutyl 2-methylbenzoate (**3b**). The title compound **3b** was prepared according to the general procedure **C** starting from allyl benzoate **1b** (0.2 mmol) and CF_3SO_2Na **2** (3 equiv.). Colourless oil (37 mg, 70% yield), R_f = 0.26 (petroleum ether/EtOAc 90:10). ^1H NMR (400 MHz, $CDCl_3$) δ 7.92 (dd, J = 8.2, 1.4 Hz, 1H), 7.44 (td, J = 7.5, 1.4 Hz, 1H), 7.26 (dd, J = 7.7, 6.6 Hz, 2H), 4.45 – 4.28 (m, 3H), 2.61 (s, 3H), 2.53 (d, J = 3.3 Hz, 1H), 2.51 – 2.37 (m, 2H). $^{13}C\{^1H\}$ NMR (100 MHz, $CDCl_3$) δ 167.5 (s), 140.7 (s), 132.7 (s), 132.1 (s), 130.8 (s), 128.8 (s), 126.1 (q, J = 276.8 Hz), 126.0 (s), 67.7 (s), 65.0 (q, J = 3.0 Hz), 38.1 (q, J = 27.9 Hz), 21.9 (s). ^{19}F NMR (377 MHz, $CDCl_3$) δ -63.52 (s). HRMS (ESI TOF) *m/z* for $C_{12}H_{14}F_3O_3$ $[M + H]^+$ calcd. 263.0895, found 263.0889.

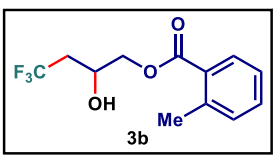

4,4,4-Trifluoro-2-hydroxybutyl 3-methylbenzoate (**3c**). The title compound **3c** was prepared according to the general procedure **C** starting from allyl benzoate **1c** (0.2 mmol) and CF_3SO_2Na **2** (3 equiv.). Colourless oil (41 mg, 78% yield), R_f = 0.26 (petroleum ether/EtOAc 90:10). ^1H NMR (400 MHz, $CDCl_3$) δ 7.85 (m, 2H), 7.40 (d, *J* = 7.8 Hz, 1H), 7.34 (t, *J* = 7.7 Hz, 1H), 4.45 – 4.31 (m, 3H), 2.61 (s, 1H), 2.49 – 2.23 (m, 5H). $^{13}C\{^1H\}$ NMR (100 MHz, $CDCl_3$) δ 166.9 (s), 138.5 (s), 134.4 (s), 130.4 (s), 129.4 (s), 128.6 (s), 127.0 (s), 126.1 (q, *J* = 276.8 Hz), 67.8 (s), 65.0 (d, *J* = 3.1 Hz), 38.1 (q, *J* = 27.9 Hz), 21.4 (s). $^{19}F\{^1H\}$ NMR (377 MHz, $CDCl_3$) δ -63.51 (s). HRMS (ESI TOF) *m/z* for $C_{12}H_{14}F_3O_3$ $[M + H]^+$ calcd. 263.0895, found 263.0894.

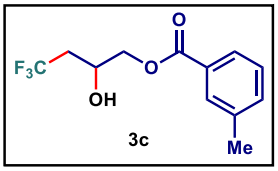

4,4,4-Trifluoro-2-hydroxybutyl 4-methylbenzoate (**3d**). The title compound **3d** was prepared according to the general procedure **C** starting from allyl benzoate **1d** (0.2 mmol) and CF_3SO_2Na **2** (3 equiv.). White solid (38 mg, 73% yield), R_f = 0.21 (petroleum ether/EtOAc 90:10), mp 54−56 °C. ^1H NMR (400 MHz, $CDCl_3$) δ 7.96 – 7.90 (m, 2H), 7.28 – 7.23 (m, 2H), 4.45 – 4.30 (m, 3H), 2.61 (s, 1H), 2.49 – 2.37 (m, 5H). $^{13}C\{^1H\}$ NMR (100 MHz, $CDCl_3$) δ 166.8 (s), 144.5 (s), 129.9 (s), 129.4 (s), 126.7 (s), 126.1 (q, *J* = 276.8 Hz), 67.7 (s), 65.1 (q, *J* = 3.0 Hz), 38.1 (q, *J* = 27.9 Hz), 21.8 (s). $^{19}F\{^1H\}$ NMR (377 MHz, $CDCl_3$) δ -63.52 (s). HRMS (ESI TOF) *m/z* for $C_{12}H_{14}F_3O_3$ $[M + H]^+$ calcd. 263.0895, found 263.0888.

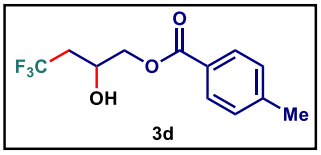

4,4,4-Trifluoro-2-hydroxybutyl 4-(tert-butyl)benzoate (**3e**). The title compound **3e** was prepared according to the general procedure **C** starting from allyl benzoate **1e** (0.2 mmol) and CF_3SO_2Na **2** (3 equiv.). White solid (39 mg, 64% yield), R_f = 0.26 (petroleum ether/EtOAc 90:10), mp 53−55 °C. ^1H NMR (400 MHz, $CDCl_3$) δ 8.00 – 7.94 (m, 2H), 7.50 – 7.46 (m, 2H), 4.46 – 4.30 (m, 3H), 2.60 (d, *J* = 3.9 Hz, 1H), 2.51 – 2.36 (m, 2H), 1.34 (s, 9H). $^{13}C\{^1H\}$ NMR (100 MHz, $CDCl_3$) δ 166.8 (s), 157.5 (s), 129.8 (s), 126.6 (s), 126.1 (q, *J* = 276.8 Hz), 125.7 (s), 67.7 (s), 65.1 (q, *J* = 3.0 Hz), 38.1 (q, *J* = 27.9 Hz), 35.3 (s), 31.2 (s). $^{19}F\{^1H\}$ NMR (377 MHz, $CDCl_3$) δ -63.52 (s). HRMS (ESI TOF) *m/z* for $C_{15}H_{20}F_3O_3$ $[M + H]^+$ calcd. 305.1365, found 305.1359.

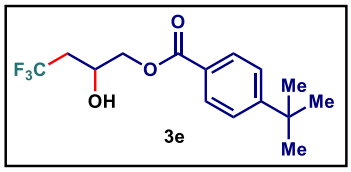

4,4,4-Trifluoro-2-hydroxybutyl 3-methoxybenzoate (**3f**). The title compound **3f** was prepared according to the general procedure **C** starting from allyl benzoate **1f** (0.2 mmol) and CF_3SO_2Na **2** (3 equiv.). Colourless liquid (42 mg, 76% yield), R_f = 0.34 (petroleum ether/EtOAc 80:20).

^{1}H NMR (400 MHz, $CDCl_3$) δ 7.66 – 7.61 (m, 1H), 7.55 (dd, *J* = 2.5, 1.5 Hz, 1H), 7.37 (t, *J* = 8.0 Hz, 1H), 7.13 (ddd, *J* = 8.3, 2.7, 0.9 Hz, 1H), 4.47 – 4.30 (m, 3H), 3.85 (s, 3H), 2.58 (s, 1H), 2.52 – 2.37 (m, 2H). ^{13}C{^{1}H} NMR (100 MHz, $CDCl_3$) δ 166.6 (s), 159.8 (s), 130.8 (s), 129.7 (s), 126.1 (q, *J* = 276.8 Hz), 122.0 (s), 120.0 (s), 114.5 (s), 68.0 (s), 65.0 (q, *J* = 3.1 Hz), 55.6 (s), 38.1 (q, *J* = 28.0 Hz). ^{19}F{^{1}H} NMR (377 MHz, $CDCl_3$) δ -63.51 (s). HRMS (ESI TOF) *m/z* for $C_{12}H_{14}F_3O_4$ $[M + H]^+$ calcd. 279.0844, found 279.0848.

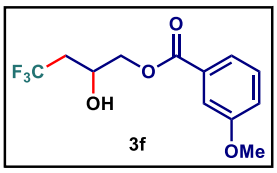

4,4,4-Trifluoro-2-hydroxybutyl 4-(dimethylamino)benzoate (**3g**). The title compound **3g** was prepared according to the general procedure **C** starting from allyl benzoate **1g** (0.2 mmol) and CF_3SO_2Na **2** (3 equiv.). White solid (32 mg, 55% yield), R_f = 0.45 (petroleum ether/EtOAc 70:30), mp 77−79 °C. ^{1}H NMR (400 MHz, $CDCl_3$) δ 7.92 – 7.88 (m, 2H), 6.67 – 6.63 (m, 2H), 4.43 – 4.26 (m, 3H), 3.05 (s, 6H), 2.76 (s, 1H), 2.48 – 2.35 (m, 2H). ^{13}C{^{1}H} NMR (100 MHz, $CDCl_3$) δ 167.2 (s), 153.8 (s), 131.7 (s), 126.2 (q, *J* = 276.8 Hz), 115.8 (s), 110.9 (s), 67.4 (s), 65.3 (q, *J* = 3.1 Hz), 40.2 (s), 38.1 (q, *J* = 27.9 Hz). ^{19}F{^{1}H} NMR (377 MHz, $CDCl_3$) δ -63.51 (s). HRMS (ESI TOF) *m/z* for $C_{13}H_{17}F_3NO_3$ $[M + H]^+$ calcd. 292.1161, found 292.1156.

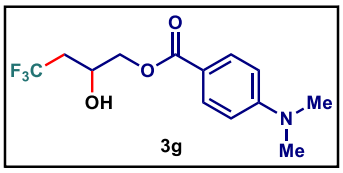

4,4,4-Trifluoro-2-hydroxybutyl 4-nitrobenzoate (**3h**). The title compound **3h** was prepared according to the general procedure **C** starting from allyl benzoate **1h** (0.2 mmol) and CF_3SO_2Na **2** (3 equiv.). Colourless liquid (48 mg, 82% yield), R_f = 0.36 (petroleum ether/EtOAc 70:30). ^{1}H NMR (400 MHz, $CDCl_3$) δ 8.33 – 8.28 (m, 2H), 8.26 – 8.19 (m, 2H), 4.62 – 4.29 (m, 3H), 2.66 – 2.25 (m, 3H). ^{13}C{^{1}H} NMR (100 MHz, $CDCl_3$) δ 164.8 (s), 150.9 (s), 134.9 (s), 131.0 (s), 126.0 (q, *J* = 276.8 Hz), 123.8 (s), 68.5 (s), 64.8 (q, *J* = 3.1 Hz), 38.1 (q, *J* = 28.0 Hz). ^{19}F{^{1}H} NMR (377 MHz, $CDCl_3$) δ -63.48 (s). HRMS (ESI TOF) *m/z* for $C_{11}H_{11}F_3NO_5$ $[M + H]^+$ calcd. 294.0589, found 294.0586.

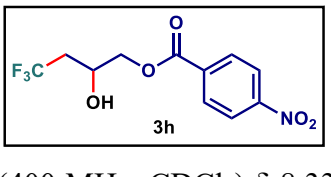

4,4,4-Trifluoro-2-hydroxybutyl 4-cyanobenzoate (**3i**). The title compound **3i** was prepared according to the general procedure **C** starting from allyl benzoate **1i** (0.2 mmol) and CF_3SO_2Na **2** (3 equiv.). White solid (43 mg, 78% yield), R_f = 0.38 (petroleum ether/EtOAc 70:30), mp 62−64 °C. ^{1}H NMR (400 MHz, $CDCl_3$) δ 8.16 – 8.14 (m, 2H), 7.78 – 7.75 (m, 2H), 4.59 – 4.36 (m, 3H), 2.54 – 2.35 (m, 3H). ^{13}C{^{1}H} NMR (100 MHz, $CDCl_3$) δ 165.0 (s), 133.4 (s), 132.5 (s), 130.4 (s),

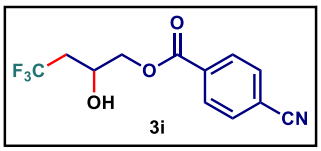

126.0 (q, J = 279.3 Hz), 117.9 (s), 117.0 (s), 68.4 (s), 64.8 (q, J = 3.0 Hz), 38.1 (q, J = 28.0 Hz). $^{19}F\{^{1}H\}$ NMR (377 MHz, $CDCl_3$) δ -63.48 (s). HRMS (ESI TOF) *m/z* for $C_{12}H_{11}F_3NO_3$ $[M + H]^+$ calcd. 274.0691, found 274.0690.

4,4,4-Trifluoro-2-hydroxybutyl 4-formylbenzoate (**3j**). The title compound **3j** was prepared

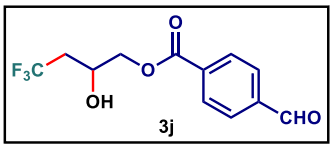

according to the general procedure **C** starting from allyl benzoate **1j** (0.2 mmol) and CF_3SO_2Na **2** (3 equiv.). Colourless liquid (38 mg, 68% yield), R_f = 0.38 (petroleum ether/EtOAc 70:30). ^{1}H NMR (400 MHz, $CDCl_3$) δ 10.11 (s, 1H), 8.22 – 8.20 (m, 2H), 7.98 – 7.6 (m, 2H), 4.50 – 4.36 (m, 3H), 2.58 – 2.37(m, 3H). $^{13}C\{^{1}H\}$ NMR (100 MHz, $CDCl_3$) δ 191.7 (s), 165.6 (s), 139.6 (s), 134.4 (s), 130.5 (s), 129.8 (s), 126.0 (q, J = 276.8 Hz), 68.3 (s), 64.9 (q, J = 3.1 Hz), 38.1 (q, J = 28.0 Hz). $^{19}F\{^{1}H\}$ NMR (377 MHz, $CDCl_3$) δ -63.48 (s). HRMS (ESI TOF) *m/z* for $C_{12}H_{12}F_3O_4$ $[M + H]^+$ calcd. 277.0688, found 277.0684.

4,4,4-Trifluoro-2-hydroxybutyl 4-fluorobenzoate (**3k**). The title compound **3k** was prepared

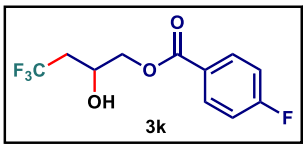

according to the general procedure **C** starting from allyl benzoate **1k** (0.2 mmol) and CF_3SO_2Na **2** (3 equiv.). Colourless liquid (30 mg, 56% yield), R_f = 0.27 (petroleum ether/EtOAc 85:15). ^{1}H NMR (400 MHz, $CDCl_3$) δ 8.08 – 8.03 (m, 2H), 7.14 – 7.10 (m, 2H), 4.43 – 4.31 (m, 3H), 2.81 (s, 1H), 2.50 – 2.37 (m, 2H). $^{13}C\{^{1}H\}$ NMR (100 MHz, $CDCl_3$) δ 166.2 (d, J = 255.0 Hz), 165.8 (s), 132.4 (d, J = 9.4 Hz), 126.1 (q, J = 276.8 Hz), 125.7 (d, J = 3.1 Hz), 115.9 (d, J = 22.1 Hz), 67.9 (s), 64.9 (q, J = 3.1 Hz), 38.0 (q, J = 28.0 Hz). $^{19}F\{^{1}H\}$ NMR (377 MHz, $CDCl_3$) δ -63.53 (s), -104.57 (s). HRMS (ESI TOF) *m/z* for $C_{11}H_{11}F_4O_3$ $[M + H]^+$ calcd. 267.0644, found 267.0641.

4,4,4-Trifluoro-2-hydroxybutyl 2-chlorobenzoate (**3l**). The title compound **3l** was prepared

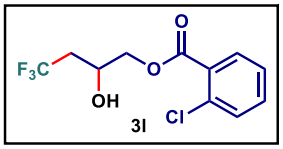

according to the general procedure **C** starting from allyl benzoate **1l** (0.2 mmol) and CF_3SO_2Na **2** (3 equiv.). Colourless liquid (44 mg, 78% yield), R_f = 0.22 (petroleum ether/EtOAc 85:15). ^{1}H NMR (400 MHz, $CDCl_3$) δ 7.85 (ddd, J = 7.7, 1.4, 0.6 Hz, 1H), 7.50 – 7.42 (m, 2H), 7.35 (ddd, J = 7.8, 6.3, 2.3 Hz, 1H), 4.46 (dd, J = 10.9, 3.4 Hz, 1H), 4.39 (s, 1H), 4.33 (dd, J = 10.9, 6.0 Hz, 1H), 2.56 – 2.39 (m, 3H). $^{13}C\{^{1}H\}$ NMR (100 MHz, $CDCl_3$) δ 165.8 (s), 133.7 (s), 133.2 (s), 131.9 (s), 131.3 (s), 129.5 (s), 127.0 (s), 126.0 (q, J = 276.8 Hz), 68.3 (s), 64.7 (q, J = 3.1 Hz), 38.0 (q, J = 28.0 Hz). $^{19}F\{^{1}H\}$ NMR (377 MHz, $CDCl_3$) δ -63.52 (s). HRMS (ESI TOF) *m/z* for $C_{11}H_{11}ClF_3O_3$ $[M + H]^+$ calcd. 283.0349, found 283.0343.

4,4,4-Trifluoro-2-hydroxybutyl 3-bromobenzoate (**3m**). The title compound **3m** was prepared

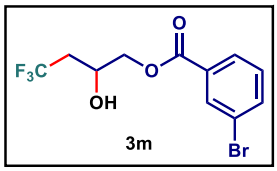

according to the general procedure **C** starting from allyl benzoate **1m** (0.2 mmol) and CF_3SO_2Na **2** (3 equiv.). Colourless liquid (41 mg, 63% yield), R_f = 0.34 (petroleum ether/EtOAc 85:15). ^{1}H NMR (400 MHz, $CDCl_3$) δ 8.17 (t, *J* = 1.7 Hz, 1H), 8.00 – 7.94 (m, 1H), 7.72 (ddd, *J* = 8.0, 2.0, 1.1 Hz, 1H), 7.35 (t, *J* = 7.9 Hz, 1H), 4.56 – 4.23 (m, 3H), 2.62 – 2.24 (m, 3H). ^{13}C{^{1}H} NMR (100 MHz, $CDCl_3$) δ 165.4 (s), 136.6 (s), 132.8 (s), 131.4 (s), 130.3 (s), 128.4 (s), 126.1 (q, *J* = 276.8 Hz), 122.8 (s), 68.2 (s), 64.9 (q, *J* = 3.1 Hz), 38.1 (q, *J* = 28.0 Hz). ^{19}F{^{1}H} NMR (377 MHz, $CDCl_3$) δ -63.49 (s). HRMS (ESI TOF) *m/z* for $C_{11}H_{11}BrF_3O_3$ $[M + H]^+$ calcd. 326.9844, found 326.9849.

4,4,4-Trifluoro-2-hydroxybutyl 2-iodobenzoate (**3n**). The title compound **3n** was prepared

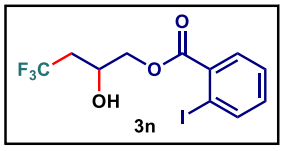

according to the general procedure **C** starting from allyl benzoate **1n** (0.2 mmol) and CF_3SO_2Na **2** (3 equiv.). Colourless liquid (48 mg, 64% yield), R_f = 0.27 (petroleum ether/EtOAc 85:15). ^{1}H NMR (400 MHz, $CDCl_3$) δ 8.01 (dd, *J* = 8.0, 1.0 Hz, 1H), 7.81 (dd, *J* = 7.8, 1.7 Hz, 1H), 7.43 (td, *J* = 7.6, 1.1 Hz, 1H), 7.19 (td, *J* = 7.8, 1.7 Hz, 1H), 4.49 – 4.38 (m, 2H), 4.33 (dd, *J* = 10.9, 5.9 Hz, 1H), 2.56 – 2.36 (m, 3H). ^{13}C{^{1}H} NMR (100 MHz, $CDCl_3$) δ 166.5 (s), 141.5 (s), 134.9 (s), 133.2 (s), 131.4 (s), 128.2 (s), 126.0 (q, *J* = 276.8 Hz), 94.0 (s), 68.5 (s), 64.7 (dd, *J* = 6.2, 3.1 Hz), 38.0 (q, *J* = 28.1 Hz). ^{19}F{^{1}H} NMR (377 MHz, $CDCl_3$) δ -63.47 (s). HRMS (ESI TOF) *m/z* for $C_{11}H_{11}F_3IO_3$ $[M + H]^+$ calcd. 374.9705, found 374.9711.

4,4,4-Trifluoro-2-hydroxybutyl 4-hydroxybenzoate (**3o**). The title compound **3o** was prepared

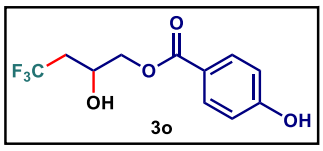

according to the general procedure **C** starting from allyl benzoate **1o** (0.2 mmol) and CF_3SO_2Na **2** (3 equiv.). White solid (27 mg, 51% yield), R_f = 0.22 (petroleum ether/EtOAc 70:30), mp 37−39 °C. ^{1}H NMR (400 MHz, DMSO-*d*$_6$) δ 10.37 (s, 1H), 7.88 – 7.85 (m, 2H), 6.87 – 6.83 (m, 2H), 5.47 (d, *J* = 5.3 Hz, 1H), 4.18 – 4.09 (m, 3H), 2.61 – 2.54 (m, 1H), 2.46 – 2.35 (m, 1H). ^{13}C{^{1}H} NMR (100 MHz, DMSO-*d*$_6$) δ 165.5 (s), 162.1 (s), 131.7 (s), 126.9 (q, *J* = 277.0 Hz), 120.2 (s), 115.4 (s), 67.5 (s), 63.1 (q, *J* = 3.1 Hz), 37.0 (q, *J* = 26.5 Hz). ^{19}F{^{1}H} NMR (377 MHz, DMSO-*d*$_6$) δ -61.74 (s). HRMS (ESI TOF) *m/z* for $C_{11}H_{12}F_3O_4$ $[M + H]^+$ calcd. 265.0688, found 265.0684.

4,4,4-Trifluoro-2-hydroxybutyl 3,4-dimethoxybenzoate (**3p**). The title compound **3p** was prepared according to the general procedure **C** starting from allyl benzoate **1p** (0.2 mmol) and CF_3SO_2Na **2** (3 equiv.). White solid (46 mg, 74% yield), R_f = 0.26 (petroleum ether/EtOAc 70:30), mp 90–92 °C. ^1H NMR (400 MHz, $CDCl_3$) δ 7.67 (dd, *J* = 8.4, 2.0 Hz, 1H), 7.52 (d, *J* = 2.0 Hz, 1H), 6.88 (d, *J* = 8.5 Hz, 1H), 4.43 – 4.29 (m, 3H), 3.94 (s, 3H), 3.92 (s, 3H), 2.73 (s, 1H), 2.50 – 2.35 (m, 2H). $^{13}C\{^1H\}$ NMR (100 MHz, $CDCl_3$) δ 166.6 (s), 153.6 (s), 148.9 (s), 126.1 (q, *J* = 276.8 Hz), 124.0 (s), 121.8 (s), 112.2 (s), 110.4 (s), 67.8 (s), 65.0 (q, *J* = 3.0 Hz), 56.2 (s), 56.1 (s), 38.1 (q, *J* = 27.9 Hz). $^{19}F\{^1H\}$ NMR (377 MHz, $CDCl_3$) δ -63.51 (s). HRMS (ESI TOF) *m/z* for $C_{13}H_{16}F_3O_5$ $[M + H]^+$ calcd. 309.0950, found 309.0951.

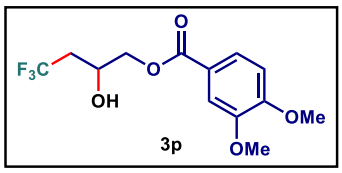

4,4,4-Trifluoro-2-hydroxybutyl 2,4-dichlorobenzoate (**3q**). The title compound **3q** was prepared according to the general procedure **C** starting from allyl benzoate **1q** (0.2 mmol) and CF_3SO_2Na **2** (3 equiv.). White solid (30 mg, 48% yield), R_f = 0.29 (petroleum ether/EtOAc 85:15), mp 67–69 °C. ^1H NMR (400 MHz, $CDCl_3$) δ 7.84 (d, *J* = 8.4 Hz, 1H), 7.51 (d, *J* = 2.0 Hz, 1H), 7.34 (dd, *J* = 8.4, 2.0 Hz, 1H), 4.48 – 4.30 (m, 3H), 2.54 – 2.34 (m, 3H). $^{13}C\{^1H\}$ NMR (100 MHz, $CDCl_3$) δ 164.7 (s), 139.0 (s), 134.8 (s), 132.8 (s), 131.2 (s), 127.6 (s), 127.3 (s), 125.9 (q, *J* = 276.8 Hz), 68.3 (s), 64.5 (q, *J* = 3.1 Hz), 37.9 (q, *J* = 28.1 Hz). $^{19}F\{^1H\}$ NMR (377 MHz, $CDCl_3$) δ -63.52 (s). HRMS (ESI TOF) *m/z* for $C_{11}H_{10}Cl_2F_3O_3$ $[M + H]^+$ calcd. 316.9959, found 316.9954.

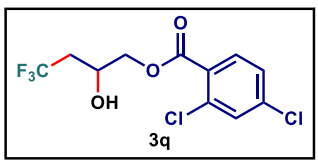

4,4,4-Trifluoro-2-hydroxybutyl 3-bromo-4-methylbenzoate (**3r**). The title compound **3r** was prepared according to the general procedure **C** starting from allyl benzoate **1r** (0.2 mmol) and CF_3SO_2Na **2** (3 equiv.). Colourless liquid (29 mg, 42% yield), R_f = 0.34 (petroleum ether/EtOAc 85:15). ^1H NMR (400 MHz, $CDCl_3$) δ 8.19 (d, *J* = 1.7 Hz, 1H), 7.87 (dd, *J* = 7.9, 1.7 Hz, 1H), 7.32 (d, *J* = 7.9 Hz, 1H), 4.45 – 4.31 (m, 3H), 2.53 (s, 1H), 2.48 – 2.36 (m, 5H). $^{13}C\{^1H\}$ NMR (100 MHz, $CDCl_3$) δ 165.5 (s), 144.2 (s), 133.7 (s), 131.0 (s), 128.8 (s), 128.6 (s), 126.1 (q, *J* = 276.8 Hz), 125.1 (s), 68.1 (s), 65.0 (q, *J* = 3.1 Hz), 38.1 (q, *J* = 27.9 Hz), 23.4 (s). $^{19}F\{^1H\}$ NMR (377 MHz, $CDCl_3$) δ -63.49 (s). HRMS (ESI TOF) *m/z* for $C_{12}H_{13}BrF_3O_3$ $[M + H]^+$ calcd. 341.0000, found 341.0008.

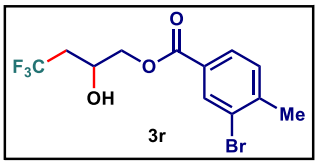

5,5,5-Trifluoro-3-hydroxy-3-methylpentyl benzoate (**3s**). The title compound **3s** was prepared according to the general procedure **C** starting from **1s** (0.2 mmol) and CF_3SO_2Na **2** (3 equiv.). Colourless liquid (40 mg, 73% yield), R_f = 0.22 (petroleum ether/EtOAc 85:15). ^1H NMR (400 MHz, $CDCl_3$) δ 8.03 – 8.00 (m, 2H), 7.59 – 7.55 (m, 1H), 7.46 – 7.42 (m, 2H), 4.53 (t, *J* = 6.6 Hz, 2H), 2.48 – 2.39 (m, 2H), 2.21 (s, 1H), 2.16 – 2.03 (m, 2H), 1.45 (s, 3H). $^{13}C\{^1H\}$ NMR (100 MHz, $CDCl_3$) δ 166.7 (s), 133.3 (s), 130.1 (s), 129.7 (s), 128.6 (s), 126.1 (q, *J* = 277.9 Hz), 69.7 (q, *J* = 1.9 Hz), 61.1 (s), 45.1 (q, *J* = 26.0 Hz), 40.5 (d, *J* = 1.3 Hz), 27.4 (d, *J* = 1.5 Hz). $^{19}F\{^1H\}$ NMR (377 MHz, $CDCl_3$) δ -60.17 (s). HRMS (ESI TOF) *m/z* for $C_{13}H_{15}F_3NaO_3$ $[M + Na]^+$ calcd. 299.0871, found 299.0865.

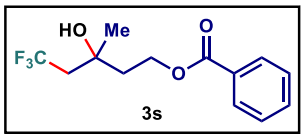

5,5,5-Trifluoro-3-hydroxy-3-methylpentyl 3-methoxybenzoate (**3t**). The title compound **3t** was prepared according to the general procedure **C** starting from **1t** (0.2 mmol) and CF_3SO_2Na **2** (3 equiv.). Colourless liquid (42 mg, 69% yield), R_f = 0.48 (petroleum ether/EtOAc 70:30). δ ^1H NMR (400 MHz, $CDCl_3$) 7.62 – 7.58 (m, 1H), 7.53 (dd, *J* = 2.6, 1.5 Hz, 1H), 7.35 (t, *J* = 8.0 Hz, 1H), 7.11 (ddd, *J* = 8.3, 2.7, 1.0 Hz, 1H), 4.53 (t, *J* = 6.5 Hz, 2H), 3.85 (s, 3H), 2.44 (qd, *J* = 11.4, 1.9 Hz, 2H), 2.21 – 2.01 (m, 3H), 1.45 (s, 3H). $^{13}C\{^1H\}$ NMR (100 MHz, $CDCl_3$) δ 166.6 (s), 159.8 (s), 131.4 (s), 129.6 (s), 126.1 (q, *J* = 277.9 Hz), 122.0 (s), 119.8 (s), 114.1 (s), 69.8 (d, *J* = 2.0 Hz), 61.2 (s), 55.6 (s), 45.1 (q, *J* = 26.1 Hz), 40.5 (d, *J* = 1.3 Hz), 27.5 (d, *J* = 1.6 Hz). $^{19}F\{^1H\}$ NMR (377 MHz, $CDCl_3$) δ -60.15 (s). HRMS (ESI TOF) *m/z* for $C_{14}H_{17}F_3NaO_4$ $[M + Na]^+$ calcd. 329.0977, found 329.0972.

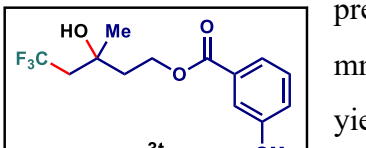

5,5,5-Trifluoro-3-hydroxy-3-methylpentyl 4-nitrobenzoate (**3u**). The title compound **3u** was prepared according to the general procedure **C** starting from **1u** (0.2 mmol) and CF_3SO_2Na **2** (3 equiv.). Colourless liquid (42 mg, 66% yield), R_f = 0.45 (petroleum ether/EtOAc 70:30). ^1H NMR (400 MHz, $CDCl_3$) δ 8.31 – 8.28 (m, 2H), 8.21 – 8.17 (m, 2H), 4.58 (t, *J* = 6.7 Hz, 2H), 2.44 (q, *J* = 11.3 Hz, 2H), 2.18 – 2.06 (m, 2H), 1.99 (s, 1H), 1.46 (s, 3H). $^{13}C\{^1H\}$ NMR (100 MHz, $CDCl_3$) δ 164.8 (s), 150.8 (s), 135.5 (s), 130.8 (s), 126.0 (q, *J* = 278.0 Hz), 123.8 (s), 69.6 (q, *J* = 1.9 Hz), 62.0 (s), 45.2 (q, *J* = 26.1 Hz), 40.3 (s), 27.5 (d, *J* = 1.5 Hz). $^{19}F\{^1H\}$ NMR (377 MHz, $CDCl_3$) δ -60.17 (s). HRMS (ESI TOF) *m/z* for $C_{13}H_{15}F_3NO_5$ $[M + H]^+$ calcd. 322.0902, found 322.0910.

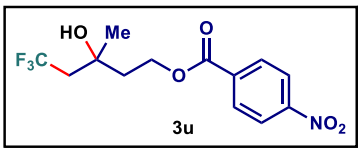

5,5,5-Trifluoro-3-hydroxy-3-methylpentyl pivalate (**3v**). The title compound **3v** was prepared according to the general procedure **C** starting from **1v** (0.2 mmol) and CF_3SO_2Na **2** (3 equiv.). Colourless liquid (29 mg, 56% yield), R_f = 0.31 (petroleum ether/EtOAc 80:20). ^1H NMR (400 MHz, $CDCl_3$) δ 4.25 (t, *J* = 6.4 Hz, 2H), 2.43 – 2.32 (m, 2H), 2.26 (s, 1H), 2.00 – 1.88 (m, 2H), 1.38 (s, 3H), 1.19 (s, 9H). $^{13}C\{^1H\}$ NMR (100 MHz, $CDCl_3$) δ 178.6 (s), 126.1 (q, *J* = 277.9 Hz), 69.7 (q, *J* = 3.9 Hz), 60.7 (s), 45.0 (q, *J* = 26.0 Hz), 40.4 (d, *J* = 1.3 Hz), 38.8 (s), 27.3 (s), 27.2 (s). $^{19}F\{^1H\}$ NMR (377 MHz, $CDCl_3$) δ -60.24 (s). HRMS (ESI TOF) for *m/z* $C_{11}H_{20}F_3O_3$ $[M + H]^+$ calcd. 257.1365, found 257.1363.

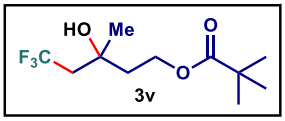

3-Hydroxy-3-methyl-2-(trifluoromethyl)butyl benzoate (**3w**). The title compound **3w** was prepared according to the general procedure **C** starting from **1w** (0.2 mmol) and CF_3SO_2Na **2** (3 equiv.). Colourless liquid (43 mg, 78% yield), R_f = 0.28 (petroleum ether/EtOAc 85:15). ^1H NMR (400 MHz, $CDCl_3$) δ 8.04 – 8.01 (m, 2H), 7.59 – 7.55 (m, 1H), 7.57 – 7.43 (m, 2H), 4.76 (ddd, *J* = 12.2, 3.6, 0.6 Hz, 1H), 4.59 (dd, *J* = 12.3, 6.1 Hz, 1H), 2.68 (qdd, *J* = 9.8, 6.1, 3.6 Hz, 1H), 2.10 (s, 1H), 1.48 (s, 3H), 1.42 (s, 3H). $^{13}C\{^1H\}$ NMR (100 MHz, $CDCl_3$) δ 166.4 (s), 133.4 (s), 129.8 (s), 129.7 (s), 128.6 (s), 126.8 (q, *J* = 282.2 Hz), 70.8 (s), 60.6 (q, *J* = 2.9 Hz), 52.9 (q, *J* = 23.4 Hz), 29.7 (q, *J* = 1.9 Hz), 27.9 (d, *J* = 1.9 Hz). $^{19}F\{^1H\}$ NMR (377 MHz, $CDCl_3$) δ -63.32 (s). HRMS (ESI TOF) *m/z* for $C_{13}H_{16}F_3O_3$ $[M + H]^+$ calcd. 277.1052, found 277.1056.

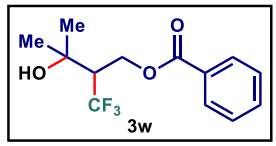

5,5,5-Trifluoro-3-hydroxy-3-methylpentyl 4-methylbenzenesulfonate (**3x**). The title compound **3x** was prepared according to the general procedure **C** starting from **1x** (0.2 mmol) and CF_3SO_2Na **2** (3 equiv.). Colourless liquid (50 mg, 76% yield), R_f = 0.45 (petroleum ether/EtOAc 85:15). ^1H NMR (400 MHz, $CDCl_3$) δ 7.78 (d, *J* = 8.3 Hz, 2H), 7.35 (d, *J* = 8.3 Hz, 2H), 4.07 (t, *J* = 6.3 Hz, 2H), 2.45 (s, 3H), 2.08 – 1.82 (m, 3H), 1.80 – 1.74 (m, 1H), 1.58 – 1.50 (m, 1H), 0.96 (d, *J* = 6.2 Hz, 3H). $^{13}C\{^1H\}$ NMR (100 MHz, $CDCl_3$) δ 145.1 (s), 133.0 (s), 130.1 (s), 128.0 (s), 126.9 (q, *J* = 277.4 Hz), 67.9 (s), 40.0 (q, *J* = 27.3 Hz), 35.4 (s), 24.6 (q, *J* = 2.4 Hz), 21.7 (s), 19.2 (s). $^{19}F\{^1H\}$ NMR (377 MHz, $CDCl_3$) δ -63.23 (s). HRMS (ESI TOF) *m/z* for $C_{13}H_{18}F_3O_4S$ $[M + H]^+$ calcd. 327.0878, found 327.0872.

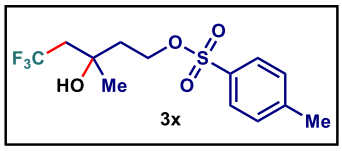

2-((6,6,6-Trifluoro-4-hydroxyhexyl)oxy)isoindoline-1,3-dione (**3y**). The title compound **3y** was prepared according to the general procedure **C** starting from **1y** (0.2 mmol) and CF_3SO_2Na **2** (3 equiv.). White solid (43 mg, 67% yield), R_f = 0.31 (petroleum ether/EtOAc 85:15), mp 73−75 °C. ^1H NMR (400 MHz, $CDCl_3$) δ 7.84 (dd, *J* = 5.5, 3.1 Hz, 2H), 7.75 (dd, *J* = 5.5, 3.1 Hz, 2H), 4.21 (t, *J* = 6.4 Hz, 2H), 2.18 – 2.06 (m, 2H), 1.81 (p, *J* = 6.6 Hz, 2H), 1.69 – 1.61 (m, 4H). $^{13}C\{^1H\}$ NMR (100 MHz, $CDCl_3$) δ 163.8 (s), 134.6 (s), 129.1 (s), 127.3 (q, *J* = 276.3 Hz), 123.7 (s), 78.2 (s), 33.8 (q, *J* = 28.4 Hz), 28.0 (s), 25.0 (s), 21.8 (q, *J* = 3.0 Hz). $^{19}F\{^1H\}$ NMR (377 MHz, $CDCl_3$) δ -66.39 (s). HRMS (ESI TOF) *m/z* for $C_{14}H_{15}F_3NO_4$ $[M + H]^+$ calcd. 318.0953, found 318.0947.

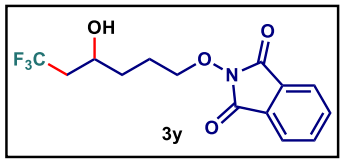

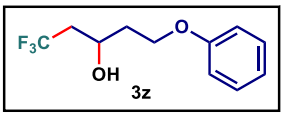

1,1,1-Trifluoro-5-phenoxypentan-3-ol (**3z**). The title compound **3z** was prepared according to the general procedure **C** starting from **1z** (0.2 mmol) and CF_3SO_2Na **2** (3 equiv.). White solid (40 mg, 86% yield), R_f = 0.33 (petroleum ether/EtOAc 90:10), mp 61−63 °C. ^1H NMR (400 MHz, $CDCl_3$) δ 7.32 – 7.26 (m, 2H), 7.00 – 6.96 (m, 1H), 6.93 – 6.90 (m, 2H), 4.34 (tt, *J* = 8.0, 3.9 Hz, 1H), 4.21 (ddd, *J* = 9.6, 7.1, 4.6 Hz, 1H), 4.14 (ddd, *J* = 9.6, 6.3, 4.8 Hz, 1H), 2.59 (s, 1H), 2.42 – 2.30 (m, 2H), 2.05 – 1.98 (m, 2H). $^{13}C\{^1H\}$ NMR (100 MHz, $CDCl_3$) δ 158.5 (s), 129.7 (s), 126.4 (q, *J* = 277.1 Hz), 121.4 (s), 114.6 (s), 65.0 (s), 64.7 (q, *J* = 3.1 Hz), 41.4 (q, *J* = 26.7 Hz), 36.2 (s). $^{19}F\{^1H\}$ NMR (377 MHz, $CDCl_3$) δ -63.42 (s). HRMS (ESI TOF) *m/z* for $C_{11}H_{14}F_3O_2$ $[M + H]^+$ calcd. 235.0946, found 235.0940.

1,1,1-Trifluoro-6-phenoxyhexan-3-ol (**3aa**). The title compound **3aa** was prepared according to the general procedure **C** starting from **1aa** (0.2 mmol) and CF_3SO_2Na **2** (3 equiv.). Colourless liquid (36 mg, 72% yield), R_f = 0.37 (petroleum ether/EtOAc 85:15). ^1H NMR (400 MHz, $CDCl_3$) δ 7.31 – 7.27 (m, 2H), 6.98 – 6.92 (m, 1H), 6.91 – 6.89 (m, 2H), 4.12 – 4.09 (m, 1H), 4.04 – 4.00 (m, 2H), 2.35 – 2.25 (m, 3H), 1.98 – 1.89 (m, 2H), 1.79 – 1.69 (m, 2H). $^{13}C\{^1H\}$ NMR (100 MHz, $CDCl_3$) δ 158.8 (s), 129.6 (s), 126.5 (q, *J* = 277.1 Hz), 121.0 (s), 114.6 (s), 67.6 (s), 66.0 (q, *J* = 3.0 Hz), 41.4 (q, *J* = 26.5 Hz), 34.2 (s), 25.3 (s). $^{19}F\{^1H\}$ NMR (377 MHz, $CDCl_3$) δ -63.46 (s). HRMS (ESI TOF) *m/z* for $C_{12}H_{16}F_3O_2$ $[M + H]^+$ calcd. 249.1102, found 249.1107.

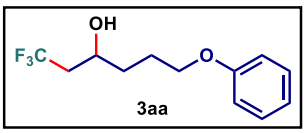

1,1,1-Trifluoro-8-phenoxyoctan-3-ol (**3ab**). The title compound **3ab** was prepared according to the general procedure **C** starting from **1ab** (0.2 mmol) and CF_3SO_2Na **2** (3 equiv.). Colourless liquid (36 mg, 65% yield), R_f = 0.41 (petroleum ether/EtOAc 85:15). ^1H NMR (400 MHz, $CDCl_3$) δ 7.30 – 7.25 (m, 2H), 6.95 – 6.91 (m, 1H), 6.90 – 6.87 (m, 2H), 4.03 – 3.99 (m, 1H), 3.98 – 3.94 (m, 2H), 2.35 – 2.17 (m, 2H), 1.88 (d, *J* = 4.0 Hz, 1H), 1.83 – 1.77 (m, 2H), 1.59 – 1.37 (m, 6H). $^{13}C\{^1H\}$ NMR (100 MHz, $CDCl_3$) δ 159.1 (s), 129.6 (s), 126.6 (q, *J* = 277.2 Hz), 120.7 (s), 114.6 (s), 67.7 (s), 66.2 (q, *J* = 2.9 Hz), 41.3 (q, *J* = 26.4 Hz), 37.2 (s), 29.3 (s), 26.0 (s), 25.1 (s). $^{19}F\{^1H\}$ NMR (377 MHz, $CDCl_3$) δ -63.49 (s). HRMS (ESI TOF) *m/z* for $C_{14}H_{20}F_3O_2$ $[M + H]^+$ calcd. 277.1415, found 277.1410.

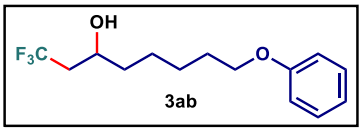

4,4-Difluoro-2-hydroxybutyl benzoate (**3ac**). The title compound **3ac** was prepared according to the general procedure **C** starting from allyl benzoate **1a** (0.2 mmol) and CF_3SO_2Na **2** (3 equiv.). White solid (29 mg, 62% yield), R_f = 0.21 (petroleum ether/EtOAc 85:15), mp 48−50 °C. ^1H NMR (400 MHz, $CDCl_3$) δ 8.05 (dt, *J* = 8.5, 1.5 Hz, 2H), 7.62 – 7.57 (m, 1H), 7.48 – 7.44 (m, 2H), 6.25 – 5.94 (m, 1H), 4.45 – 4.40 (m, 1H), 4.33 – 4.25 (m, 2H), 2.52 (s, 1H), 2.19 – 2.06 (m, 2H). $^{13}C\{^1H\}$ NMR (100 MHz, $CDCl_3$) δ 166.8 (s), 133.6 (s), 129.8 (s), 128.7 (s), 128.7 (s), 115.9 (t, *J* = 238.3 Hz), 68.7 (s), 65.7 (dd, *J* = 8.2, 4.4 Hz), 38.1 (t, *J* = 21.5 Hz). $^{19}F\{^1H\}$ NMR (377 MHz, $CDCl_3$) δ -117.02 (q, *J* = 286.4 Hz). HRMS (ESI TOF) *m/z* for $C_{11}H_{13}F_2O_3$ $[M + H]^+$ calcd. 231.0833, found 231.0824.

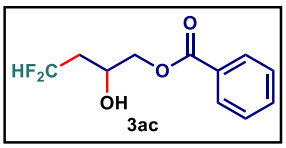

5,5,5-Trifluoro-3-hydroxy-3-methylpentyl thiophene-2-carboxylate (**3ad**). The title compound **3ad** was prepared according to the general procedure **C** starting from **1ad** (0.2 mmol) and CF_3SO_2Na **2** (3 equiv.). Colourless liquid (42 mg, 74% yield), R_f = 0.26 (petroleum ether/EtOAc 85:15). ^1H NMR (400 MHz, $CDCl_3$) δ 7.80 (dd, *J* = 3.8, 1.3 Hz, 1H), 7.57 (dd, *J* = 5.0, 1.2 Hz, 1H), 7.11 (dd, *J* = 5.0, 3.8 Hz, 1H), 4.50 (t, *J* = 6.5 Hz, 2H), 2.44 (qd, *J* = 11.4, 2.4 Hz, 2H), 2.17 – 2.01 (m, 3H), 1.44 (s, 3H). $^{13}C\{^1H\}$ NMR (100 MHz, $CDCl_3$) δ 162.2 (s), 133.8 (s), 133.5 (s), 132.8 (s), 128.0 (s), 126.1 (q, *J* = 277.9 Hz), 69.7 (q, *J* = 1.9 Hz), 61.3 (s), 45.1 (q, *J* = 26.0 Hz), 40.5 (d, *J* = 1.3 Hz), 27.4 (d, *J* = 1.5 Hz). $^{19}F\{^1H\}$ NMR (377 MHz, $CDCl_3$) δ -60.15 (s). HRMS (ESI TOF) *m/z* for $C_{11}H_{13}F_3NaO_3S$ $[M + Na]^+$ calcd. 305.0435, found 305.0427.

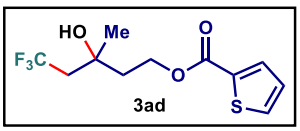

5,5,5-Trifluoro-3-hydroxy-3-methylpentyl furan-2-carboxylate (**3ae**). The title compound **3ae** 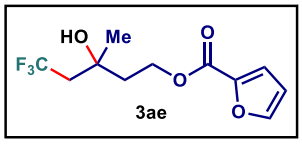

was prepared according to the general procedure **C** starting from **1ae** (0.2 mmol) and CF_3SO_2Na **2** (3 equiv.). Colourless liquid (28 mg, 52% yield), R_f = 0.48 (petroleum ether/EtOAc 85:15). ^1H NMR (400 MHz, $CDCl_3$) δ 7.57 (d, *J* = 0.8 Hz, 1H), 7.17 (d, *J* = 3.5 Hz, 1H), 6.51 (dd, *J* = 3.5, 1.7 Hz, 1H), 4.50 (t, *J* = 6.5 Hz, 2H), 2.43 (q, *J* = 11.4 Hz, 2H), 2.31 (s, 1H), 2.14 – 1.99 (m, 2H), 1.42 (s, 3H). $^{13}C\{^1H\}$ NMR (100 MHz, $CDCl_3$) δ 158.6 (s), 146.7 (s), 144.5 (s), 126.1 (q, *J* = 277.9 Hz), 118.4 (s), 112.1 (s), 69.7 (s), 61.1 (s), 45.0 (q, *J* = 26.1 Hz), 40.2 (d, *J* = 1.2 Hz), 27.3 (s). $^{19}F\{^1H\}$ NMR (377 MHz, $CDCl_3$) δ -60.21 (s). HRMS (ESI TOF) *m/z* for $C_{11}H_{14}F_3O_4$ $[M + H]^+$ calcd. 267.0844, found 267.0842.

4,4,4-Trifluoro-2-hydroxybutyl benzo[b]thiophene-2-carboxylate (**3af**). The title compound 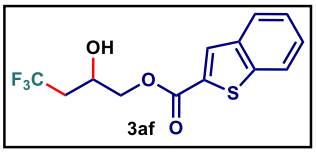

3af was prepared according to the general procedure **C** starting from **1af** (0.2 mmol) and CF_3SO_2Na **2** (3 equiv.). White solid (40 mg, 65% yield), R_f = 0.23 (petroleum ether/EtOAc 85:15), mp 85−87 °C. ^1H NMR (400 MHz, $CDCl_3$) δ 8.11 (s, 1H), 7.88 (t, *J* = 8.7 Hz, 2H), 7.50 – 7.41 (m, 2H), 4.49 – 4.34 (m, 3H), 2.56 – 2.38 (m, 3H); $^{13}C\{^1H\}$ NMR (100 MHz, $CDCl_3$) δ 162.8 (s), 142.5 (s), 138.7 (s), 132.4 (s), 131.3 (s), 127.5 (s), 126.3 (q, *J* = 225.6 Hz), 125.9 (s), 125.3 (s), 122.9 (s), 68.21 (s), 64.9 (q, *J* = 3.1 Hz), 38.0 (q, *J* = 28.0 Hz). $^{19}F\{^1H\}$ NMR (377 MHz, $CDCl_3$) δ -63.47 (s). HRMS (ESI TOF) *m/z* for $C_{13}H_{12}F_3O_3S$ $[M + H]^+$ calcd 305.0459, found 305.0456.

4,4,4-Trifluoro-2-hydroxybutyl 1-methyl-5-(trifluoromethyl)-1H-pyrrole-2-carboxylate (**3ag**). 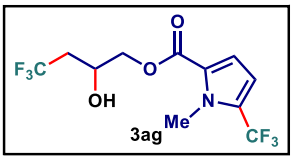

The title compound **3ag** was prepared according to the general procedure **C** starting from **1ag** (0.2 mmol) and CF_3SO_2Na **2** (3 equiv.). Colourless liquid (28 mg, 43% yield), R_f = 0.29 (petroleum ether/EtOAc 85:15). ^1H NMR (400 MHz, $CDCl_3$) δ 6.93 (d, *J* = 4.2 Hz, 1H), 6.55 (d, *J* = 4.2 Hz, 1H), 4.39 – 4.24 (m, 3H), 4.02 (s, 3H), 2.50 (d, *J* = 3.7 Hz, 1H), 2.46 – 2.35 (m, 2H). $^{13}C\{^1H\}$ NMR (150 MHz, $CDCl_3$) δ 160.6 (s), 128.1 (q, *J* = 38.0 Hz), 126.1 (q, *J* = 276.9 Hz), 125.6 (d, *J* = 1.8 Hz), 120.7 (q, *J* = 268.3 Hz), 116.7 (s), 110.7 (q, *J* = 3.5 Hz), 67.2 (s), 64.9 (q, *J* = 3.0 Hz), 38.0 (q, *J* = 28.0 Hz), 33.9 (d, *J* = 1.9 Hz). $^{19}F\{^1H\}$ NMR (377 MHz, $CDCl_3$) δ -59.79 (s), -63.53 (s). HRMS (ESI TOF) *m/z* for $C_{11}H_{12}F_6NO_3$ $[M + H]^+$ calcd. 320.0721, found 320.0720.

5,5,5-Trifluoro-3-hydroxy-3-methylpentyl 1-methyl-5-(trifluoromethyl)-1H-pyrrole-2-carboxylate (**3ah**). The title compound **3ah** was prepared according to the general procedure

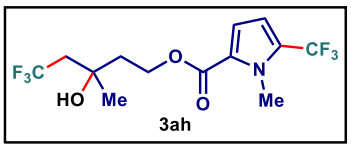

3ah

C starting from **1ah** (0.2 mmol) and CF_3SO_2Na **2** (3 equiv.). Colourless liquid (38 mg, 55% yield), R_f = 0.24 (petroleum ether/EtOAc 85:15). ^1H NMR (400 MHz, $CDCl_3$) δ 6.85 (d, *J* = 4.3 Hz, 1H), 6.53 (d, *J* = 4.2 Hz, 1H), 4.46 (t, *J* = 6.5 Hz, 2H), 4.02 (s, 3H), 2.42 (qd, *J* = 11.3, 1.6 Hz, 2H), 2.16 – 1.95 (m, 3H), 1.43 (s, 3H). $^{13}C\{^1H\}$ NMR (100 MHz, $CDCl_3$) δ 160.7 (s), 127.7 (d, *J* = 37.8 Hz), 126.2 (d, *J* = 1.9 Hz), 126.0 (q, *J* = 277.9 Hz), 120.7 (q, *J* = 268.0 Hz), 116.2 (s), 110.6 (dd, *J* = 7.1, 3.6 Hz), 69.7 (d, *J* = 2.0 Hz), 60.6 (s), 45.1 (q, *J* = 26.1 Hz), 40.4 (s), 33.8 (d, *J* = 2.0 Hz), 27.4 (d, *J* = 1.5 Hz). $^{19}F\{^1H\}$ NMR (377 MHz, $CDCl_3$) δ -59.76 (s), -60.22 (s). HRMS (ESI TOF) *m/z* for $C_{13}H_{16}F_6NO_3$ $[M + H]^+$ calcd. 348.1034, found 348.1031.

(3S,5S,6R,8S,9S,10R,13S,14S,17S)-17-acetyl-5-hydroxy-10,13-dimethyl-6-(trifluoromethyl)hexadecahydro-1H-cyclopenta[a]phenanthren-3-yl benzoate (**3ai**). The title compound **3ai** was prepared according to the general procedure **C** starting from **1ai** (0.2 mmol) and CF_3SO_2Na **2** (3 equiv.). White solid (66 mg, 65% yield), R_f = 0.17 (petroleum ether/EtOAc 85:15), mp 192−194 °C. ^1H NMR (400 MHz, $CDCl_3$) δ 8.02 (d, *J* = 7.1 Hz, 2H), 7.55 (t, *J* = 7.4 Hz, 1H), 7.43 (t, *J* = 7.7 Hz, 2H), 5.41 (tt, *J* = 10.3, 5.0 Hz, 1H), 2.52 (t, *J* = 8.9 Hz, 1H), 2.45 (s, 1H), 2.28 (t, *J* = 12.5 Hz, 2H), 2.12 (s, 3H), 2.05 (dd, *J* = 7.7, 4.7 Hz, 2H), 2.03 – 1.95 (m, 2H), 1.86 – 1.73 (m, 3H), 1.68 (ddd, *J* = 13.3, 8.1, 3.7 Hz, 3H), 1.61 – 1.51 (m, 2H), 1.51 – 1.40 (m, 2H), 1.40 – 1.26 (m, 2H), 1.26 – 1.20 (m, 2H), 1.10 (s, 3H), 0.63 (s, 3H). $^{13}C\{^1H\}$ NMR (100 MHz, $CDCl_3$) δ 209.5 (s), 166.4 (s), 133.1 (s), 130.6 (s), 129.7 (s), 129.5 (dd, *J* = 463.4, 337.3 Hz), 128.5 (s), 76.4 (s), 71.3 (s), 63.8 (s), 56.3 (s), 50.8 (dd, *J* = 50.3, 25.2 Hz), 45.9 (s), 44.4 (s), 39.5 (s), 39.1 (s), 38.8 (s), 33.2 (s), 32.0 (s), 31.6 (s), 26.9 (s), 26.5 (s), 24.4 (s), 23.0 (s), 21.3 (s), 16.5 (dd, *J* = 7.5, 3.7 Hz), 13.7 (s). $^{19}F\{^1H\}$ NMR (377 MHz, $CDCl_3$) δ -60.38 (s). HRMS (ESI TOF) *m/z* for $C_{29}H_{37}F_3NaO_4$ $[M + Na]^+$ calcd. 529.2542, found 529.2542.

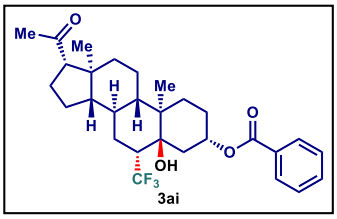

3ai

(3S,5S,6R,8S,9S,10R,13R,14S,17R)-5-hydroxy-10,13-dimethyl-17-((R)-6-methylheptan-2-yl)-6-(trifluoromethyl)hexadecahydro-1H-cyclopenta[a]phenanthren-3-yl benzoate (**3aj**). The title compound **3aj** was prepared according to the general procedure **C** starting from **1aj** (0.2 mmol) and CF_3SO_2Na **2**

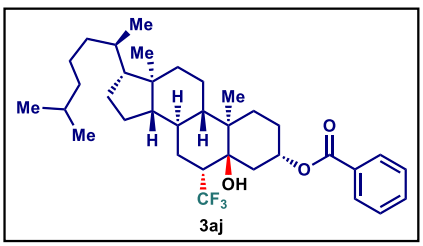

3aj

(3 equiv.). White solid (62 mg, 54% yield), R_f = 0.59 (petroleum ether/EtOAc 85:15), mp 173−175 °C. ^{1}H NMR (600 MHz, $CDCl_3$) δ 8.03 (d, *J* = 7.8 Hz, 2H), 7.55 (t, *J* = 7.4 Hz, 1H), 7.43 (t, *J* = 7.7 Hz, 2H), 5.42 (td, *J* = 11.0, 5.3 Hz, 1H), 2.42 (s, 1H), 2.30 – 2.26 (m, 2H), 2.06 – 2.00 (m, 3H), 1.87 – 1.81 (m, 2H), 1.79– 1.72 (m, 4H), 1.64– 1.56 (m, 3H), 1.51 (td, *J* = 13.1, 6.5 Hz, 1H), 1.46 – 1.41 (m, 1H), 1.41 – 1.32 (m, 4H), 1.31 – 1.24 (m, 2H), 1.22 – 1.18 (m, 1H), 1.16 – 1.13 (m, 3H), 1.11 (s, 3H), 1.10 – 1.07 (m, 2H), 1.01 – 0.96 (m, 1H), 0.91 (d, *J* = 6.5 Hz, 4H), 0.87 (d, *J* = 2.6 Hz, 3H), 0.86 (d, *J* = 2.6 Hz, 2H), 0.68 (s, 3H). ^{13}C{^{1}H} NMR (150 MHz, $CDCl_3$) δ 166.5 (s), 133.1 (s), 130.7 (s), 129.7 (s), 128.4 (s), 127.2 (q, *J* = 280.9 Hz), 76.3 (s), 71.7 (s), 56.4 (s), 56.0 (s), 51.7 (q, *J* = 24.9 Hz), 46.0 (s), 42.9 (s), 40.0 (s), 39.6 (s), 39.4 (s), 38.7 (s), 36.3 (s), 36.0 (s), 33.2 (s), 31.9 (s), 28.4 (s), 28.2 (s), 27.0 (s), 26.5 (s), 24.2 (s), 24.1 (s), 23.0 (s), 22.7 (s), 21.3 (s), 18.8 (s), 16.5 (d, *J* = 3.5 Hz), 12.4 (s). ^{19}F{^{1}H} NMR (565 MHz, $CDCl_3$) δ -61.32 (s). HRMS (ESI TOF) *m/z* for $C_{35}H_{52}F_3O_3$ $[M + H]^+$ calcd. 577.3869, found 577.3863.

Methyl 10-hydroxy-9-(trifluoromethyl)octadecenoate (**3ak**). The title compound **3ak** was prepared according to the general procedure **C** starting from **1ak** (0.2 mmol) and CF_3SO_2Na **2** (3 equiv.). Colourless liquid (36 mg, 47% yield), R_f = 0.27 (petroleum ether/EtOAc 90:10). ^{1}H NMR (600 MHz, $CDCl_3$) δ 3.98 – 3.81 (m, 1H), 3.66 (s, 3H), 2.30 (t, *J* = 7.5 Hz, 2H), 2.24 – 2.02 (m, 1H), 1.70 – 1.34 (m, 11H), 1.35 – 1.21 (m, 16H), 0.87 (t, *J* = 7.0 Hz, 3H). ^{13}C{^{1}H} NMR (150 MHz, $CDCl_3$) δ 174.4 (s), 128.6 (q, *J* = 281.3 Hz), 128.0 (qd, *J* = 281.6, 3.2 Hz), 70.2 (s), 69.6 (d, *J* = 2.5 Hz), 51.6 (s), 48.5 (q, *J* = 22.6 Hz), 48.3 (dq, *J* = 45.4, 22.6 Hz), 48.1 (dd, *J* = 45.5, 22.8 Hz), 34.7 (d, *J* = 11.3 Hz), 34.2 (d, *J* = 2.1 Hz), 34.1 (s), 32.0 (d, *J* = 1.2 Hz), 31.9 (d, *J* = 0.9 Hz), 30.0 (d, *J* = 4.1 Hz), 29.8 (d, *J* = 2.7 Hz), 29.7 (d, *J* = 2.1 Hz), 29.6 (d, *J* = 3.1 Hz), 29.5 (d, *J* = 1.7 Hz), 29.4 (d, *J* = 4.5 Hz), 29.3 (s), 29.2 (s), 29.1 (d, *J* = 2.1 Hz), 29.0 (d, *J* = 3.5 Hz), 28.6 (d, *J* = 13.9 Hz), 27.8 (s), 27.7 (s), 26.4 (d, *J* = 4.2 Hz), 26.3 (s), 26.2 (s), 25.0 (s), 24.9 (d, *J* = 2.1 Hz), 24.8 (d, *J* = 2.0 Hz), 23.1 (d, *J* = 1.7 Hz), 22.8 (s), 22.7 (s), 14.2 (s). ^{19}F{^{1}H} NMR (377 MHz, $CDCl_3$) δ -65.17 (d, *J* = 5.8 Hz), -67.47 (s). HRMS (ESI TOF) *m/z* for $C_{20}H_{38}F_3O_3$ $[M + H]^+$ calcd. 383.2773, found 383.2775.

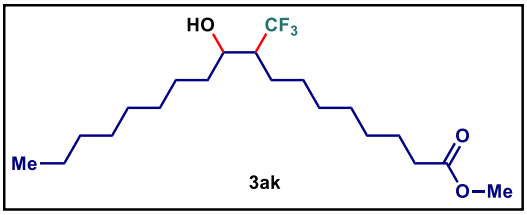

7-Hydroxy-3,7-dimethyl-6-(trifluoromethyl)octyl benzoate (**3al**). The title compound **3al** was prepared according to the general procedure **C** starting from **1al** (0.2 mmol) and CF_3SO_2Na **2** (3 equiv.). Colourless liquid (32 mg, 46% yield), R_f = 0.27 (petroleum ether/EtOAc 90:10). ^1H NMR (600 MHz, $CDCl_3$) δ 8.03 (d, *J* = 7.6 Hz, 2H), 7.55 (t, *J* = 7.4 Hz, 1H), 7.44 (t, *J* = 7.7 Hz, 2H), 4.38 – 4.33 (m, 2H), 2.08 – 2.04 (m, 1H), 1.88-1.79 (m, 1H), 1.76 – 1.72 (m, 1H), 1.67 – 1.62 (m, 3H), 1.61 – 1.54 (m, 2H), 1.50 – 1.44 (m, 1H), 1.34 (s, 3H), 1.30 (s, 3H), 0.99 (dd, *J* = 6.4, 3.6 Hz, 3H). $^{13}C\{^1H\}$ NMR (150 MHz, $CDCl_3$) δ 166.8 (d, *J* = 1.8 Hz), 133.0 (s), 130.5 (s), 129.7 (s), 128.5 (s), 128.3 (q, *J* = 282.1 Hz), 71.6 (d, *J* = 2.3 Hz), 63.4 (d, *J* = 13.4 Hz), 54.0 – 53.5 (m), 37.3 (d, *J* = 16.2 Hz), 35.3 (dd, *J* = 62.7, 35.6 Hz), 30.3 (d, *J* = 12.7 Hz), 29.3 – 28.7 (m), 27.7 (s), 23.3 (dd, *J* = 35.7, 2.3 Hz), 19.5 (d, *J* = 30.1 Hz). $^{19}F\{^1H\}$ NMR (565 MHz, $CDCl_3$) δ -64.86 (d, *J* = 53.7 Hz). HRMS (ESI TOF) *m/z* for $C_{18}H_{25}F_3NaO_3$ $[M + Na]^+$ calcd. 369.1653, found 369.1655.

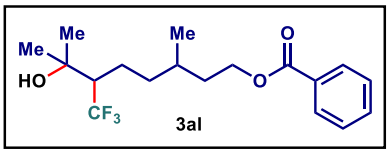

4-Hydroxy-3-(trifluoromethyl)hexyl benzoate (**3xx**). The title compound **3xx** was prepared according to the general procedure **C** starting from benzoate **1am** or **1an** (0.2 mmol) and CF_3SO_2Na **2** (3 equiv.). Colourless liquid, R_f = 0.30 (petroleum ether/EtOAc 85:15). ^1H NMR (400 MHz, $CDCl_3$) δ 8.02 (d, *J* = 7.3 Hz, 2H), 7.59 – 7.54 (m, 1H), 7.44 (t, *J* = 7.8 Hz, 2H), 4.68 – 4.34 (m, 2H), 4.20 – 3.83 (m, 1H), 2.63 – 2.29 (m, 1H), 2.28 – 1.87 (m, 3H), 1.85 – 1.48 (m, 2H), 1.12 – 0.95 (m, 3H). $^{13}C\{^1H\}$ NMR (100 MHz, $CDCl_3$) δ 167.2, 167.0, 166.6, 133.4, 133.3, 133.2, 130.2, 130.1, 130.0, 129.8, 129.7, 129.6, 128.6, 128.5, 127.8 (q, *J* = 280 Hz), 127.5 (q, *J* = 280 Hz), 71.5 (q, *J* = 2.3 Hz), 70.6 (q, *J* = 2.7 Hz), 66.5 (q, *J* = 2.4 Hz), 66.2 (q, *J* = 3.1 Hz), 63.3, 62.9, 62.2, 62.1, 50.1 (q, *J* = 22.9 Hz), 45.4 (q, *J* = 23.6 Hz), 44.6 (q, *J* = 23.7 Hz), 34.1, 33.2 (d, *J* = 1.8 Hz), 28.1, 26.6 (d, *J* = 1.6 Hz), 24.2 (d, *J* = 2.7 Hz), 22.5 (d, *J* = 2.3 Hz), 17.7 (d, *J* = 2.5 Hz), 16.9 (d, *J* = 2.4 Hz), 13.0, 12.3, 10.7, 10.5. $^{19}F\{^1H\}$ NMR (377 MHz, $CDCl_3$) δ -65.21, -65.69, -66.87, -68.13. HRMS (ESI TOF) *m/z* for $C_{14}H_{18}F_3O_3$ $[M + H]^+$ calcd. 291.1208, found 291.1206.

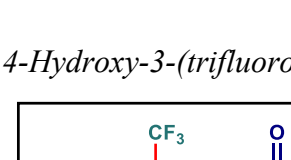

4,4,4-Trifluoro-2-hydroxybutyl 2'-methyl-[1,1'-biphenyl]-2-carboxylate (**5a**). To a solution of **3n** (50 mg, 1.0 equiv.) in toluene/H_2O (1 mL/0.3 mL) at room temperature was added *o*-tolylboronic acid **4a** (1.5 equiv.), $Pd(PPh_3)_4$ (10 mol%) and K_3PO_4 (2.5 equiv.) sequentially under nitrogen atmosphere. The reaction mixture was heated to 80 °C and maintained

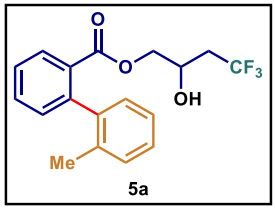

at this temperature for stirring 24 h. After which (monitored by TLC), the reaction mixture was cooled to room temperature and it was filtered through celite bed and the solvent was evaporated under reduce pressure. The residue was purified by column chromatography over silica gel (100-200 mesh) using mixture of petroleum ether/EtOAc as an eluent to afford the desired compound **5a** (37 mg, 82% yield). Yellow liquid, R_f = 0.38 (petroleum ether/EtOAc 80:20). ^{1}H NMR (400 MHz, $CDCl_3$) δ 8.05 (ddd, *J* = 7.8, 4.2, 1.3 Hz, 1H), 7.61 – 7.56 (m, 1H), 7.47 (t, *J* = 7.6 Hz, 1H), 7.34 – 7.27 (m, 3H), 7.23 (dd, *J* = 7.7, 1.1 Hz, 1H), 7.15 (dd, *J* = 7.5, 2.6 Hz, 1H), 4.13 (ddd, *J* = 22.1, 11.4, 3.2 Hz, 1H), 3.91 (ddd, *J* = 22.7, 11.4, 6.2 Hz, 1H), 3.81 – 3.74 (m, 1H), 2.10 (d, *J* = 2.7 Hz, 3H), 2.06 – 1.87 (m, 2H). ^{13}C{^{1}H} NMR (100 MHz, $CDCl_3$) δ 167.9 (d, *J* = 7.6 Hz), 142.4 (d, *J* = 13.5 Hz), 142.2 (d, *J* = 7.2 Hz), 135.6 (d, *J* = 17.5 Hz), 132.3 (d, *J* = 11.9 Hz), 131.2 (d, *J* = 0.6 Hz), 131.1 (d, *J* = 1.0 Hz), 130.0 (d, *J* = 16.7 Hz), 129.7 (d, *J* = 6.2 Hz), 128.7 (d, *J* = 6.5 Hz), 127.9 (d, *J* = 1.6 Hz), 127.7 (d, *J* = 1.4 Hz), 125.8 (dd, *J* = 553.5, 276.8 Hz), 125.8 (d, *J* = 3.7 Hz), 68.5 (d, *J* = 6.7 Hz), 64.2 (d, *J* = 2.1 Hz), 37.3 (q, *J* = 28.1 Hz), 20.1 (d, *J* = 4.4 Hz)**.** ^{19}F{^{1}H} NMR (377 MHz, $CDCl_3$) δ -63.65 (d, *J* = 8.0 Hz). HRMS (ESI TOF) *m/z* for $C_{18}H_{17}F_3NaO_3$ $[M + Na]^+$ calcd. 361.1027, found 361.1021.

4,4,4-Trifluoro-2-hydroxybutyl 2'-methoxy-[1,1'-biphenyl]-2-carboxylate (**5b**). The title compound **5b** was prepared according to the above-mentioned procedure as that of **5a** stating with (2-methoxyphenyl)boronic acid **4b**. Yellow liquid (41 mg, 87% yield), R_f = 0.21 (petroleum ether/EtOAc 80:20). ^{1}H NMR (400 MHz, $CDCl_3$) δ 7.94 (dd, *J* = 7.8, 1.0 Hz, 1H), 7.58 (td, *J* = 7.6, 1.4 Hz, 1H), 7.44 (td, *J* = 7.6, 1.3 Hz, 1H), 7.38 (td, *J* = 8.2, 1.7 Hz, 1H), 7.32 (dd, *J* = 7.7, 0.9 Hz, 1H), 7.28 (dd, *J* = 7.4, 1.6 Hz, 1H), 7.08 (td, *J* = 7.4, 0.9 Hz, 1H), 6.96 (d, *J* = 8.2 Hz, 1H), 4.17 (d, *J* = 8.7 Hz, 1H), 3.93 (s, 1H), 3.87 (s, 1H), 3.73 (s, 3H), 2.04 – 1.87 (m, 2H), 1.59 (s, 1H). ^{13}C{^{1}H} NMR (100 MHz, $CDCl_3$) δ 168.3 (s), 156.1 (s), 138.5 (s), 132.2 (s), 131.6 (s), 131.0 (s), 130.2 (s), 130.1 (s), 129.3 (s), 127.6 (s), 125.9 (q, *J* = 276.8 Hz), 121.1 (s), 110.6 (s), 68.2 (s), 64.3 (s), 55.6 (s), 37.4 (q, *J* = 28.1 Hz). ^{19}F{^{1}H} NMR (377 MHz, $CDCl_3$) δ -63.70 (s). HRMS (ESI TOF) *m/z* for $C_{18}H_{17}F_3O_4$ $[M]^+$ calcd. 354.1079, found 354.1079.

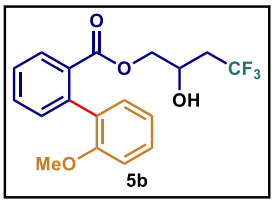

4,4,4-Trifluoro-2-((2-(4-isobutylphenyl)propanoyl)oxy)butyl benzoate (**5c**). To a stirred solution of **3a** (50 mg, 1 equiv.), 2-(4-isobutylphenyl)propanoic acid **4c** (1.5 equiv.) and dimethylaminopyridine, DMAP (10 mol%) in anhydrous CH_2Cl_2 (5 mL) was added N, N′-dicyclohexylcarbodiimide, DCC (1.5 equiv.) at 0 °C, which is then stirred for 5 min at 0 °C and then at room temperature. The progress of the reaction was monitored by TLC. After completion of the reaction, precipitated urea is then filtered off in CH_2Cl_2. The CH_2Cl_2 solution is washed twice with ~ HCl (0.5 N) and with saturated $NaHCO_3$ solution. The combined organic layers were washed with brine solution and dried over anhydrous Na_2SO_4. The crude product was purified by column chromatography over silica gel (100-200 mesh) using mixture of petroleum ether/EtOAc as an eluent to afford **5c**. Colourless liquid (71 mg, 81% yield), R_f = 0.38 (petroleum ether/EtOAc 90:10). ^{1}H NMR (400 MHz, $CDCl_3$) δ 7.98 (dd, *J* = 8.4, 1.3 Hz, 1H), 7.88 (dd, *J* = 8.4, 1.3 Hz, 1H), 7.62 – 7.55 (m, 1H), 7.47 – 7.39 (m, 2H), 7.16 (t, *J* = 8.1 Hz, 2H), 7.03 (d, *J* = 8.1 Hz, 1H), 6.97 (d, *J* = 8.1 Hz, 1H), 5.56 – 5.51 (m, 1H), 4.54 – 4.27 (m, 2H), 3.72 (p, *J* = 7.1 Hz, 1H), 2.62 – 2.41 (m, 2H), 2.40 (d, *J* = 7.2 Hz, 1H), 2.35 (d, *J* = 7.2 Hz, 1H), 1.85 – 1.73 (m, 1H), 1.49 (d, *J* = 7.2 Hz, 3H), 0.87 (d, *J* = 6.6 Hz, 3H), 0.84 (d, *J* = 6.6 Hz, 3H). ^{13}C{^{1}H} NMR (150 MHz, $CDCl_3$) δ 173.7 (s), 173.6 (s), 166.0 (s), 165.9 (s), 140.8 (s), 140.7 (s), 137.1 (s), 137.0 (s), 133.5 (s), 133.4 (s), 129.9 (s), 129.8 (s), 129.5 (s), 129.4 (s), 129.4 (s), 128.6 (s), 128.5 (s), 127.3 (s), 127.2 (s), 125.5 (q, *J* = 276.8 Hz), 125.3 (q, *J* = 277.0 Hz), 65.8 (q, *J* = 2.9 Hz), 65.6 (q, *J* = 2.8 Hz), 64.6 (s), 64.6 (s), 45.3 (s), 45.1 (s), 45.1 (s), 45.0 (s), 35.5 (q, *J* = 29.3 Hz), 35.4 (q, *J* = 29.4 Hz), 30.3 (s), 30.2 (s), 22.5 (s), 22.5 (s), 22.4 (s), 18.3 (s), 18.2 (s). ^{19}F{^{1}H} NMR (377 MHz, $CDCl_3$) δ -63.77 (s), -63.80 (s). HRMS (ESI TOF) *m/z* for $C_{24}H_{27}F_3NaO_4$ $[M+Na]^+$ calcd. 459.1759, found 459.1762.

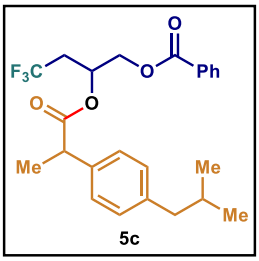

4,4,4-Trifluoro-2-oxobutyl benzoate (**5d**). To a stirred solution of **3a** (50 mg, 1 equiv.), pyridinium chlorochromate (PCC) (1.5 equiv.) was added in anhydrous CH_2Cl_2 (5 mL) then reflux for 14 h. The progress of the reaction was monitored by TLC. After completion of the reaction the solvent was evaporated under reduce pressure. The residue was purified by column chromatography over silica gel (100-200 mesh) using mixture of petroleum ether/EtOAc as an eluent to afford the desired compound **5d**. White solid (38 mg, 76% yield), R_f = 0.28 (petroleum ether/EtOAc 85:15), mp 98−100 °C. ^{1}H NMR (400 MHz, $CDCl_3$) δ 8.09 (dd, *J* = 8.3, 1.2 Hz, 2H), 7.64 – 7.60 (m, 1H), 7.50 – 7.46 (m, 2H), 4.96 (s, 2H), 3.38 (q, *J* = 10.2 Hz, 2H). ^{13}C{^{1}H} NMR (100 MHz, $CDCl_3$) δ 194.0 (q, *J* = 4.8 Hz), 165.8 (s), 133.9 (s), 133.6 (s), 130.1 (s), 128.8 (s), 123.4

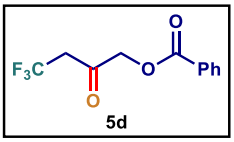

(q, J = 276.9 Hz), 68.4 (q, J = 2.4 Hz), 43.5 (q, J = 29.3 Hz). $^{19}F\{^{1}H\}$ NMR (377 MHz, $CDCl_3$) δ -62.00 (s). HRMS (ESI TOF) *m/z* for $C_{11}H_{10}F_3O_3$ $[M+H]^+$ calcd. 247.0582, found 247.0577.

2.4.5 Appendix II. ^{1}H, $^{13}C\{^{1}H\}$, and $^{19}F\{^{1}H\}$ NMR spectral data of representative compounds

Compound No.	Figure II.X	Data	Page No.
1r	Figure II.1 and II.2	^{1}H and $^{13}C\{^{1}H\}$	73
1af	Figure II.3 and II.4	^{1}H and $^{13}C\{^{1}H\}$	74
1ag	Figure II.5 and II.6	^{1}H and $^{13}C\{^{1}H\}$	75
3a	Figure II.7, II.8 and II.9	^{1}H, $^{13}C\{^{1}H\}$ and $^{19}F\{^{1}H\}$	76
3ac	Figure II.10, II.11 and II.12	^{1}H, $^{13}C\{^{1}H\}$ and $^{19}F\{^{1}H\}$	77
3ag	Figure II.13, II.14, II.15 and II.16	^{1}H, $^{13}C\{^{1}H\}$, $^{19}F\{^{1}H\}$, HOESY	79
5a	Figure II.17, II.18, and II.19	^{1}H, $^{13}C\{^{1}H\}$ and $^{19}F\{^{1}H\}$	81
5b	Figure II.20, II.21, and II.22	^{1}H, $^{13}C\{^{1}H\}$ and $^{19}F\{^{1}H\}$	83
5c	Figure II.23, II.24, and II.25	^{1}H, $^{13}C\{^{1}H\}$ and $^{19}F\{^{1}H\}$	84
5d	Figure II.26, II.27, and II.28	^{1}H, $^{13}C\{^{1}H\}$ and $^{19}F\{^{1}H\}$	86

2.4.6 Copies of ^{1}H, $^{13}C\{^{1}H\}$ and $^{19}F\{^{1}H\}$ NMR Spectra

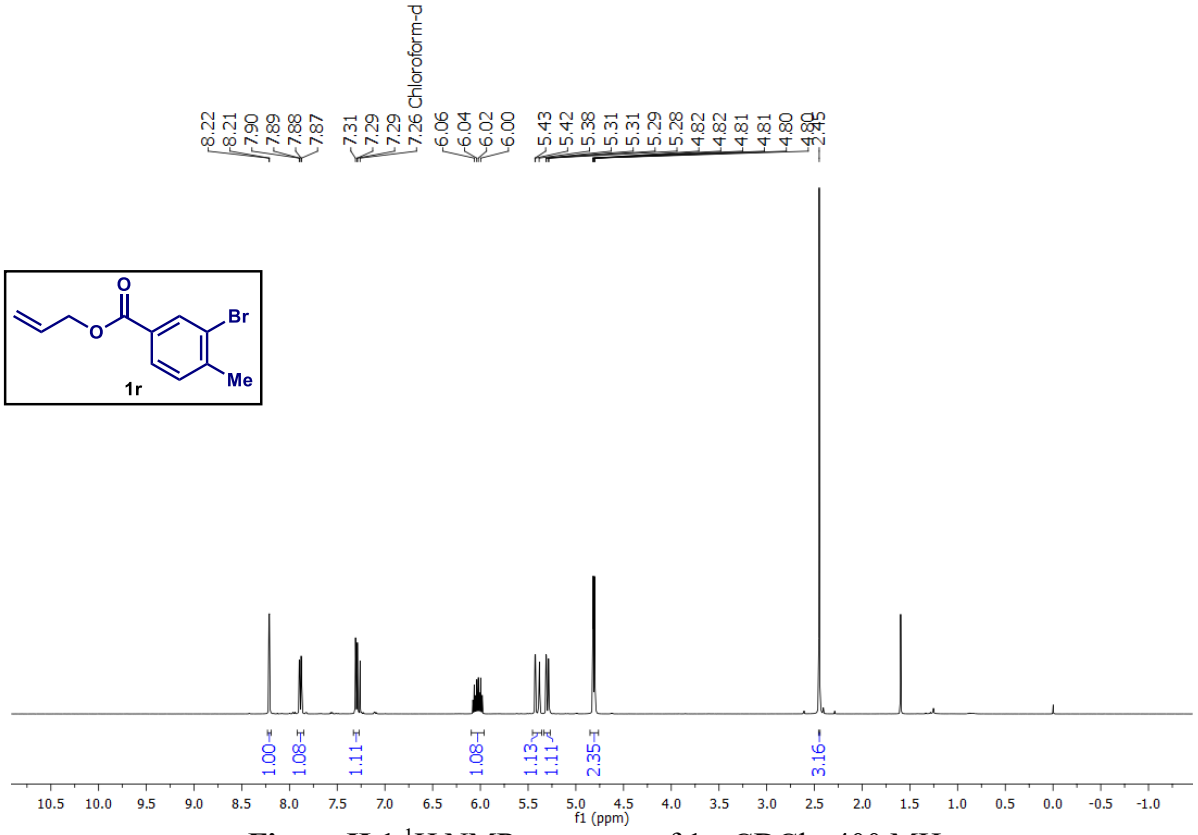

Figure II.1 ^{1}H NMR spectrum of **1r**, $CDCl_3$, 400 MHz

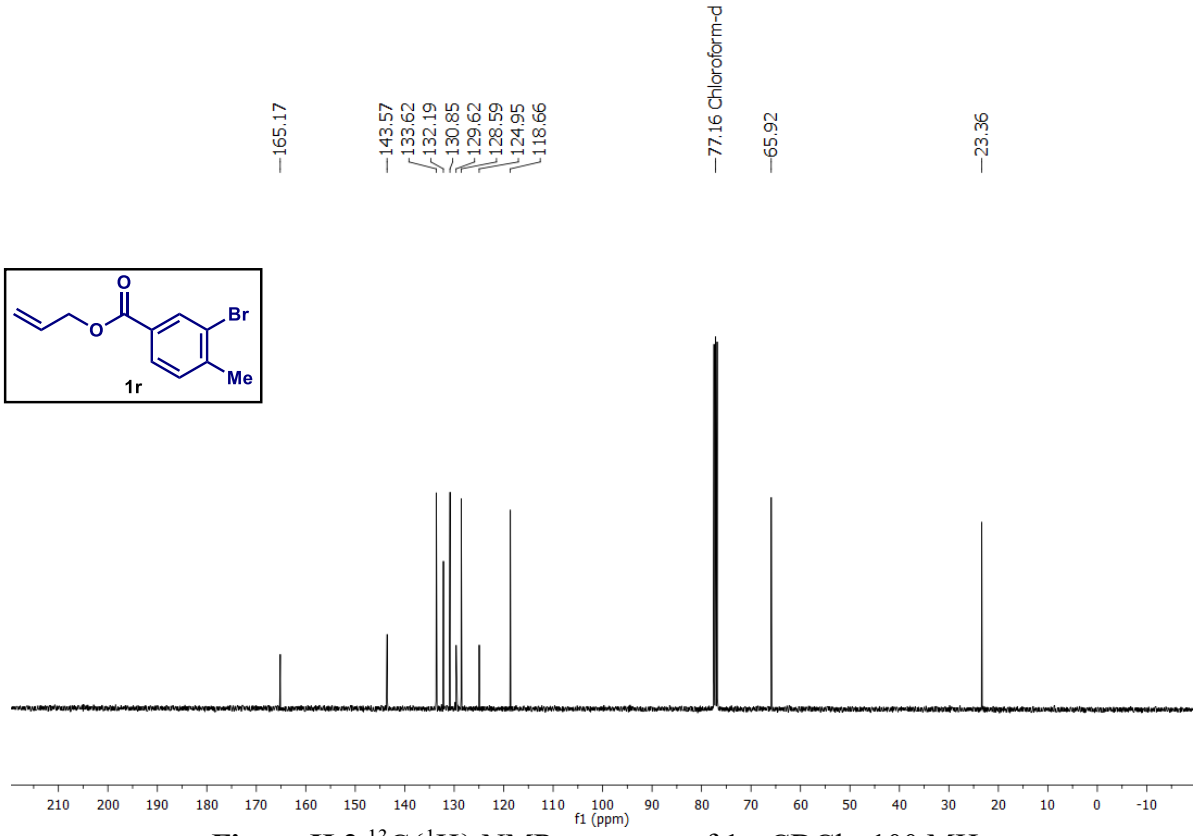

Figure II.2 $^{13}C\{^{1}H\}$ NMR spectrum of **1r**, $CDCl_3$, 100 MHz

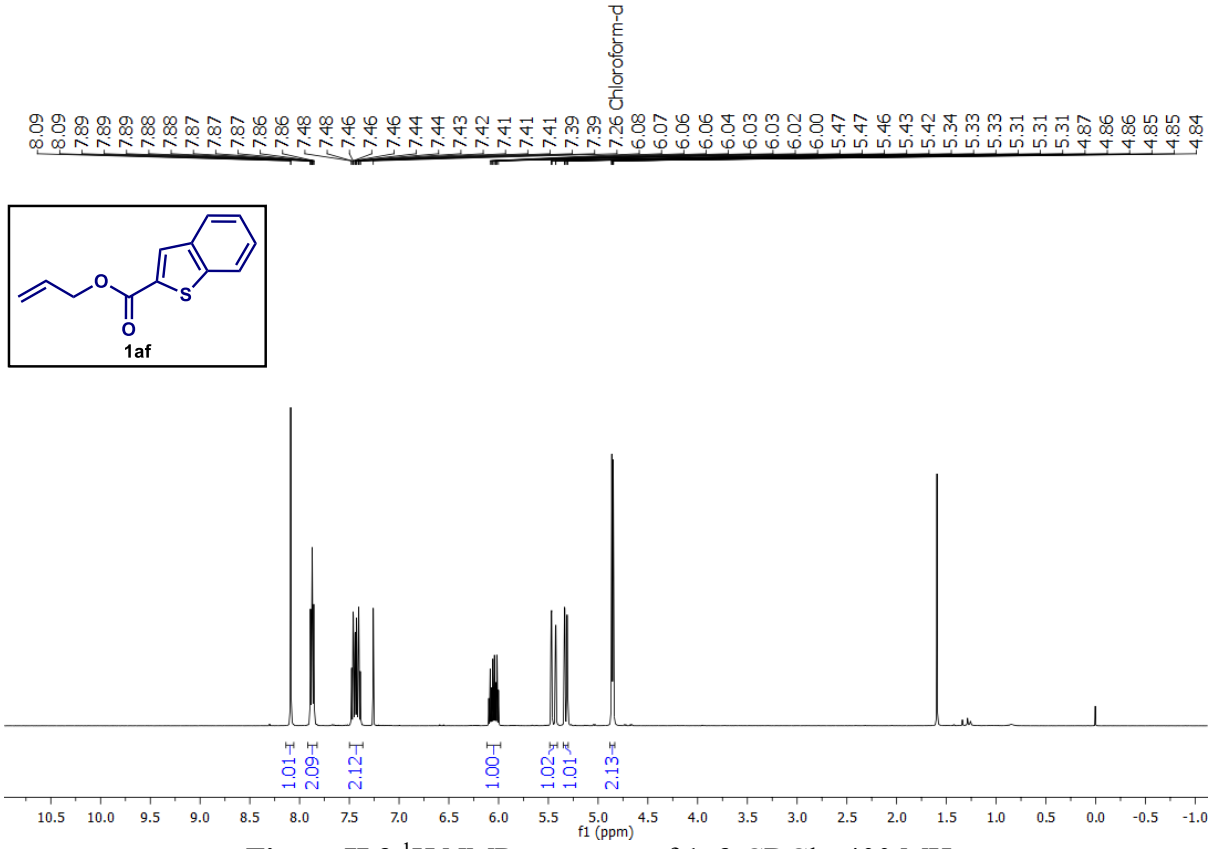

Figure II.3 ^{1}H NMR spectrum of **1af**, $CDCl_3$, 400 MHz

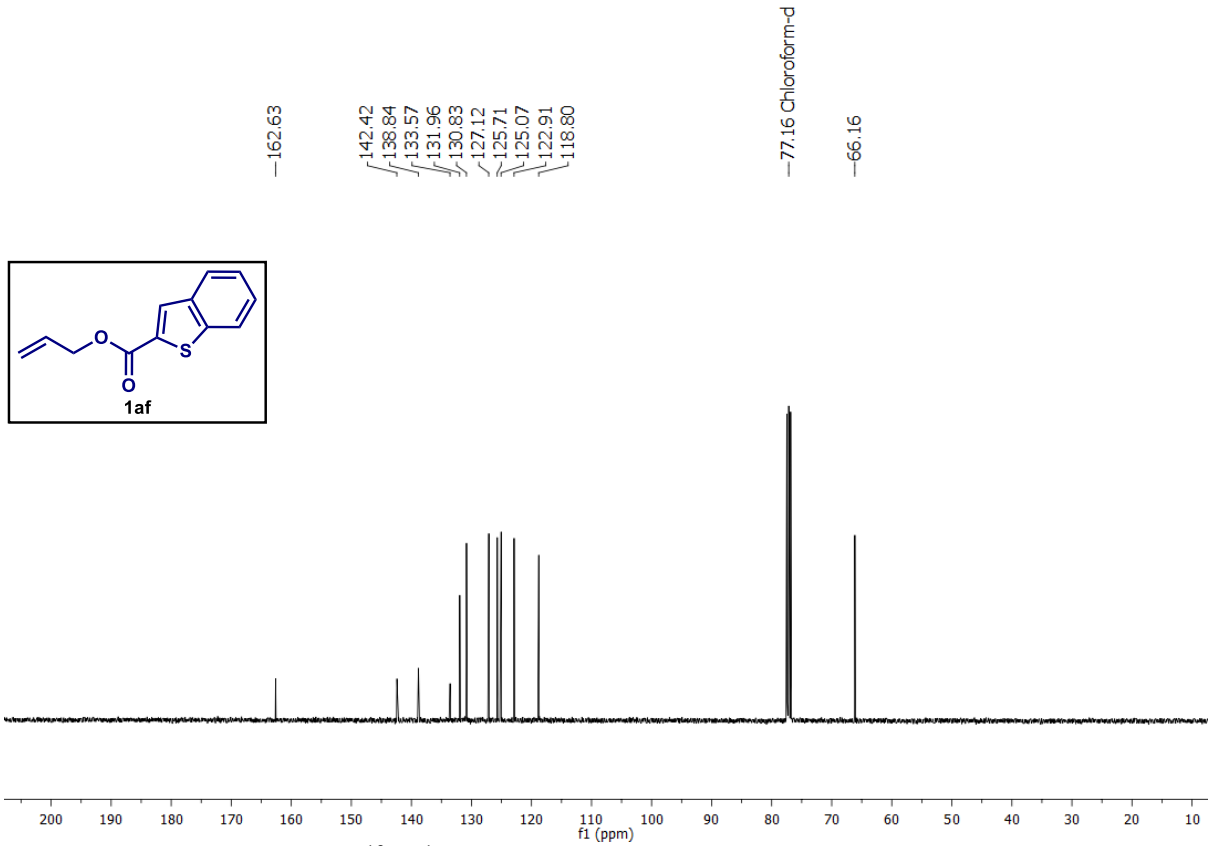

Figure II.4 $^{13}C\{^{1}H\}$ NMR spectrum of **1af**, $CDCl_3$, 100 MHz

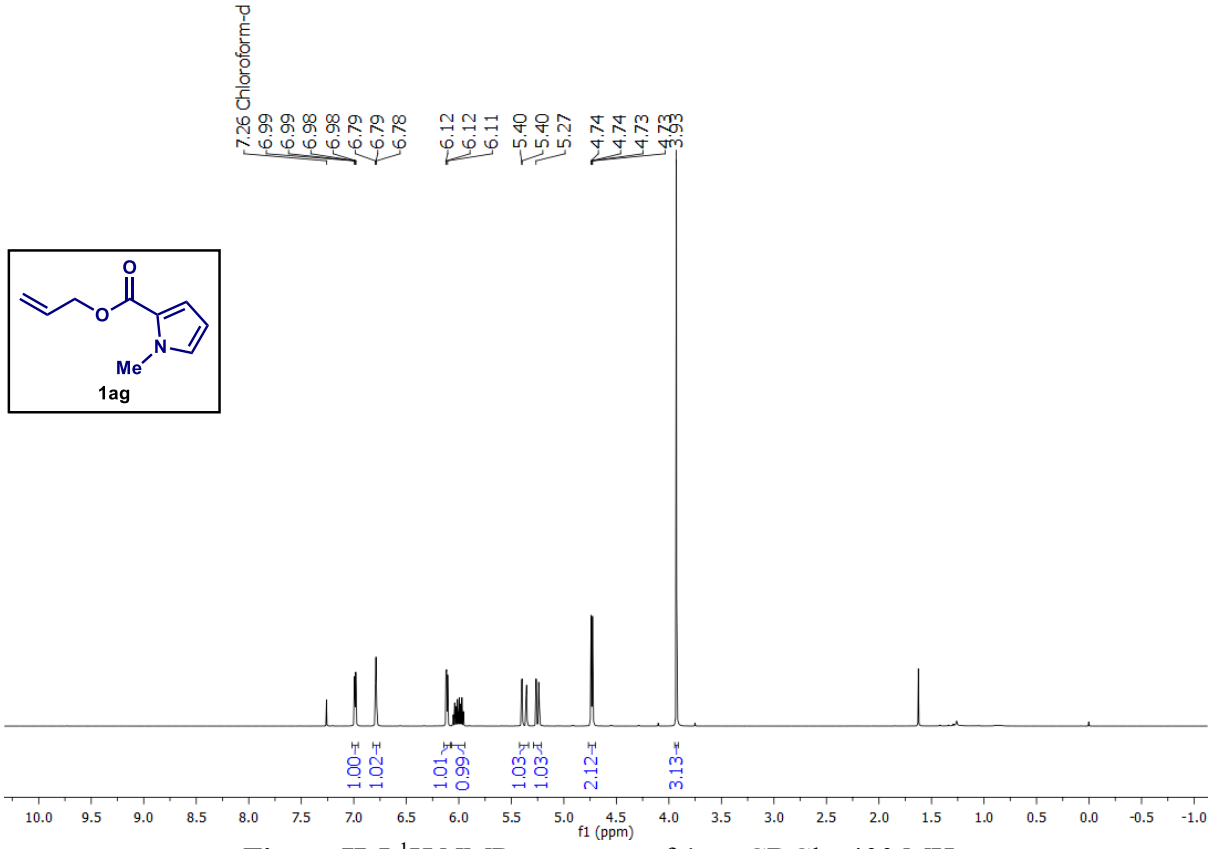

Figure II.5 ^{1}H NMR spectrum of **1ag**, $CDCl_3$, 400 MHz

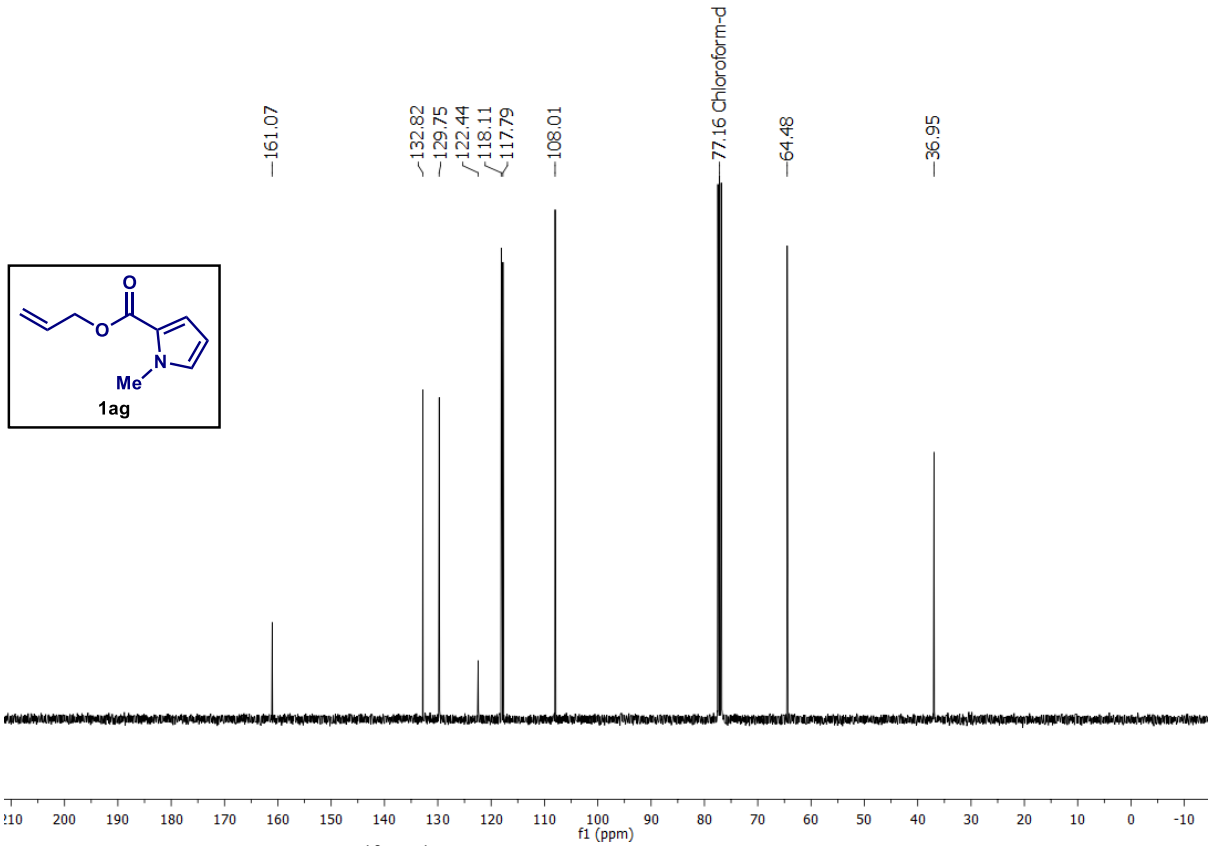

Figure II.6 $^{13}C\{^{1}H\}$ NMR spectrum of **1ag**, $CDCl_3$, 100 MHz

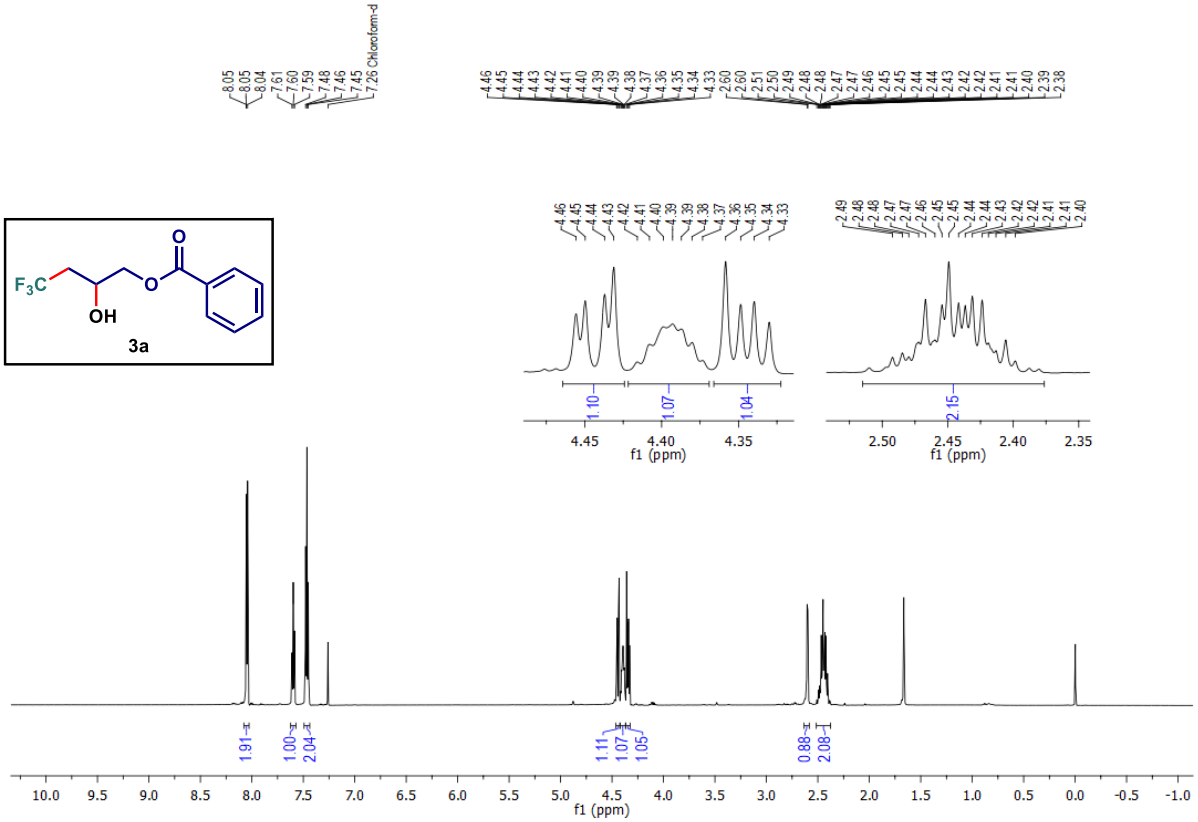

Figure II.7 ^{1}H NMR spectrum of **3a**, $CDCl_3$, 600 MHz

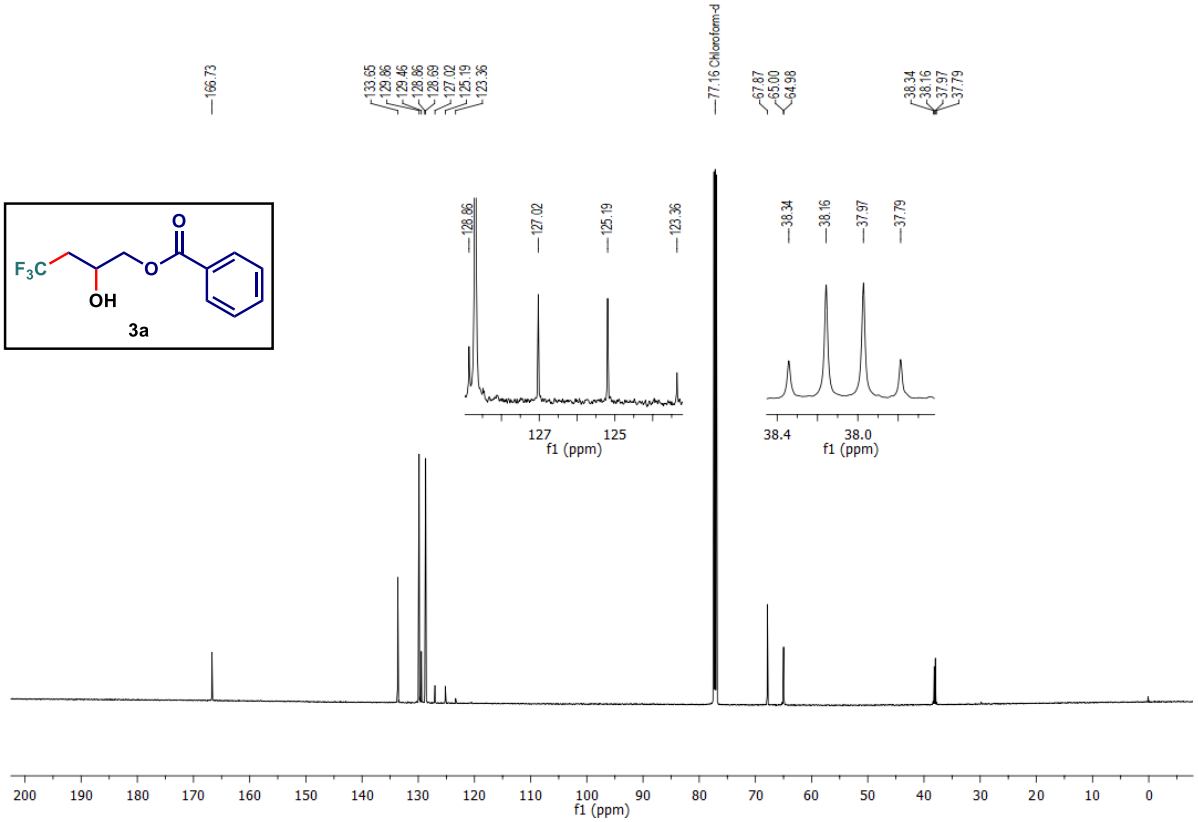

Figure II.8 $^{13}C\{^{1}H\}$ NMR spectrum of **3a**, $CDCl_3$, 150 MHz

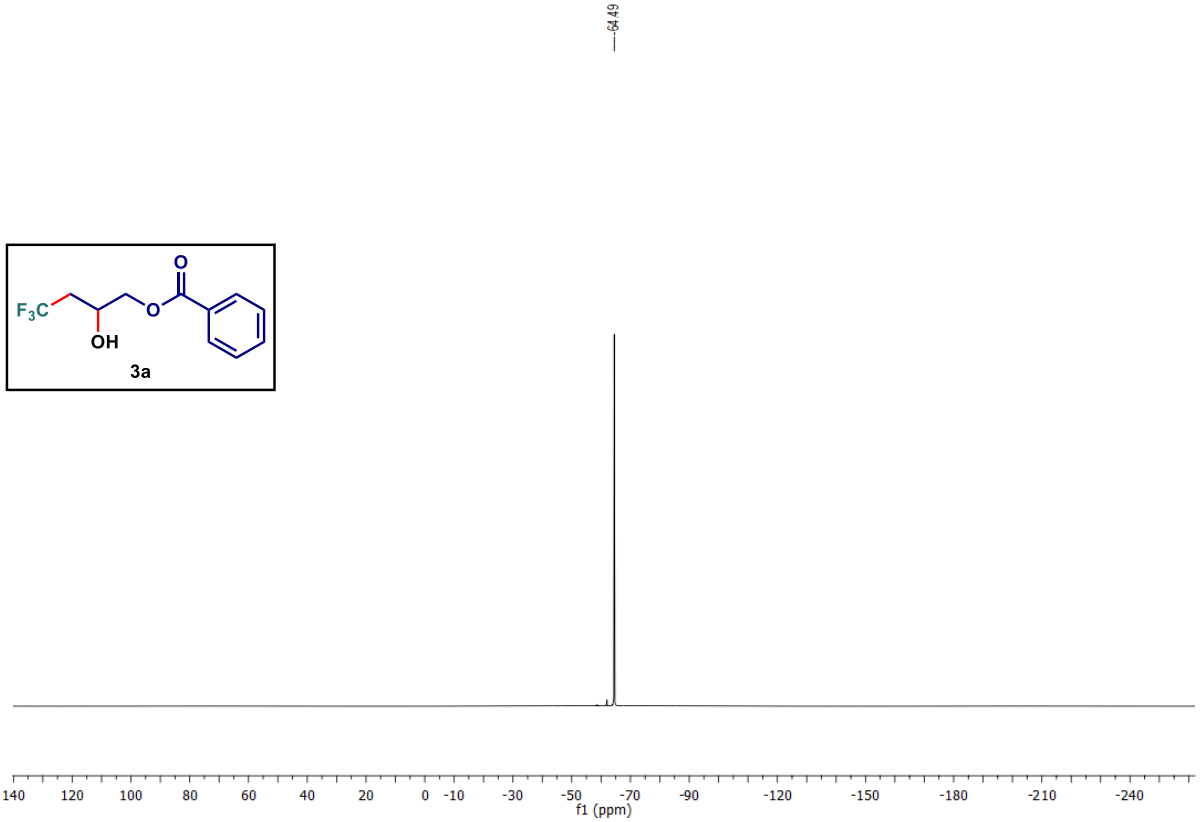

Figure II.9 $^{19}F\{^{1}H\}$ NMR spectrum of **3a**, $CDCl_3$, 565 MHz

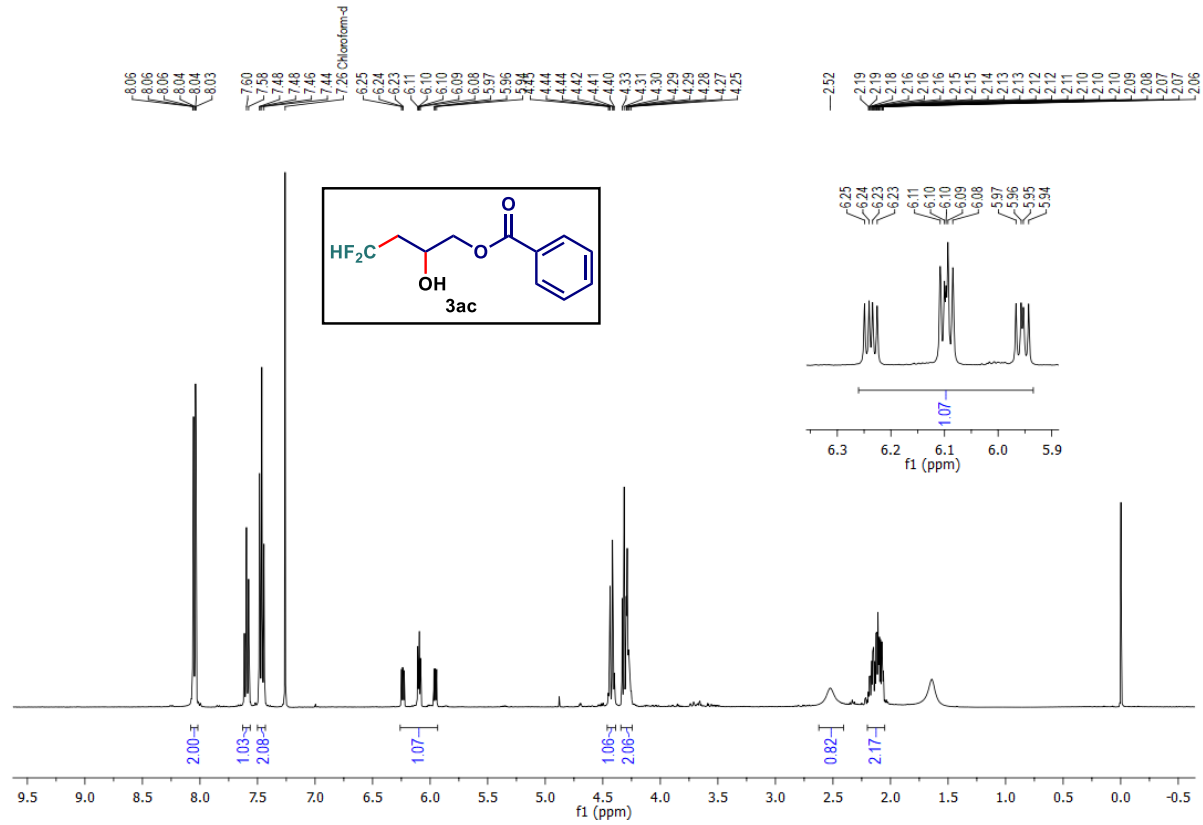

Figure II.10 ^{1}H NMR spectrum of **3ac**, $CDCl_3$, 400 MHz

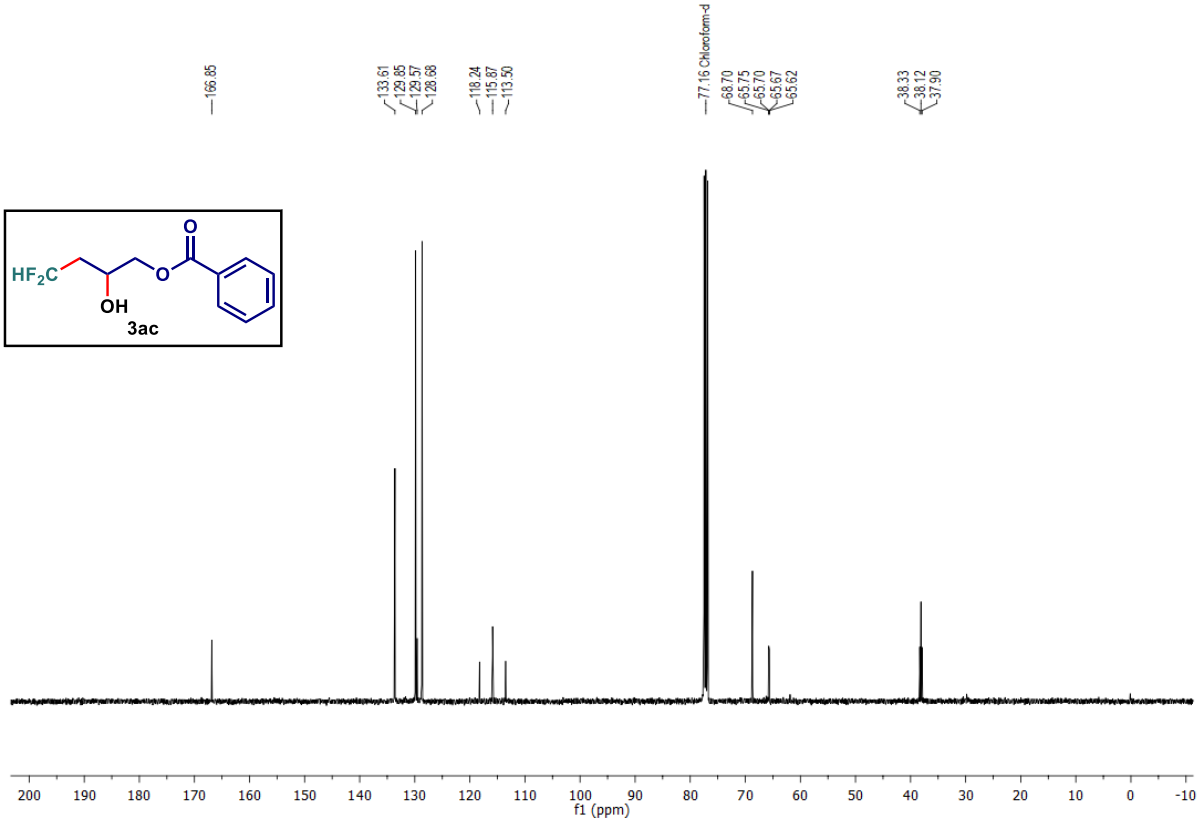

Figure II.11 $^{13}C\{^{1}H\}$ NMR spectrum of **3ac**, $CDCl_3$, 100 MHz

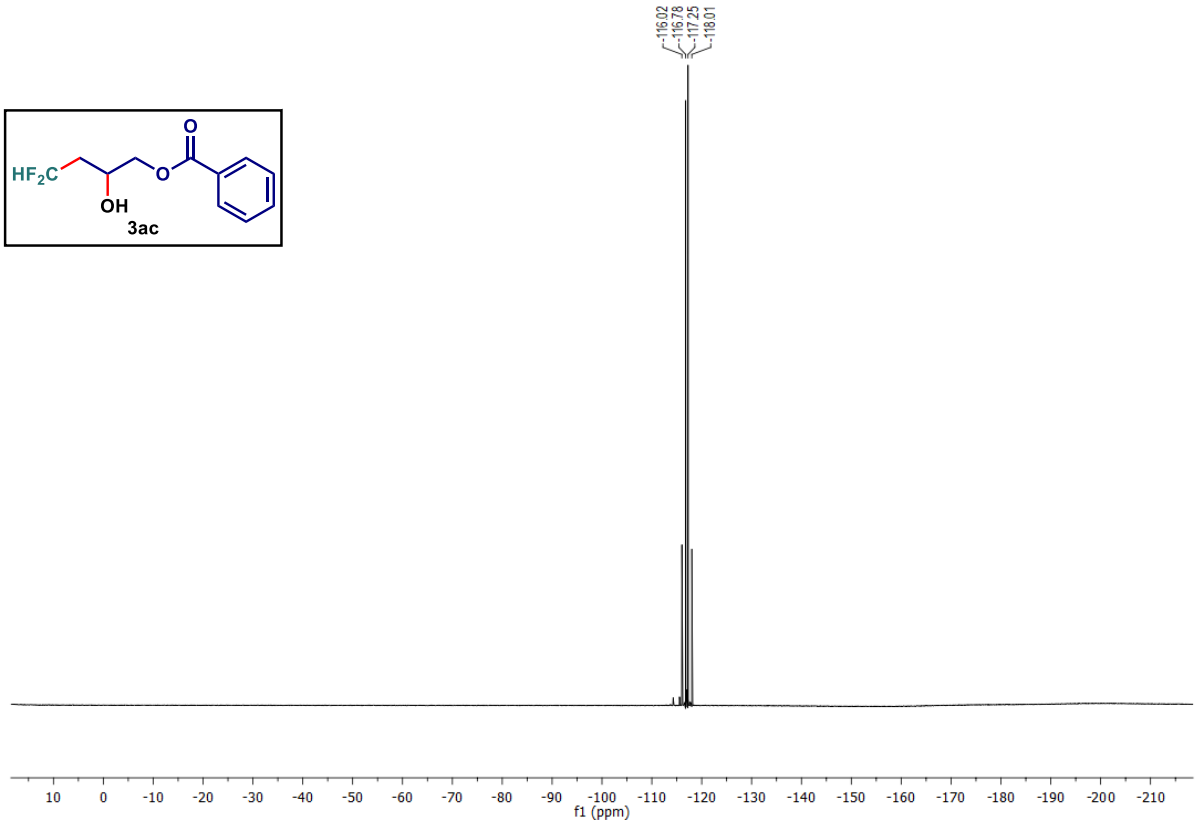

Figure II.12 $^{19}F\{^{1}H\}$ NMR spectrum of **3ac**, $CDCl_3$, 377 MHz

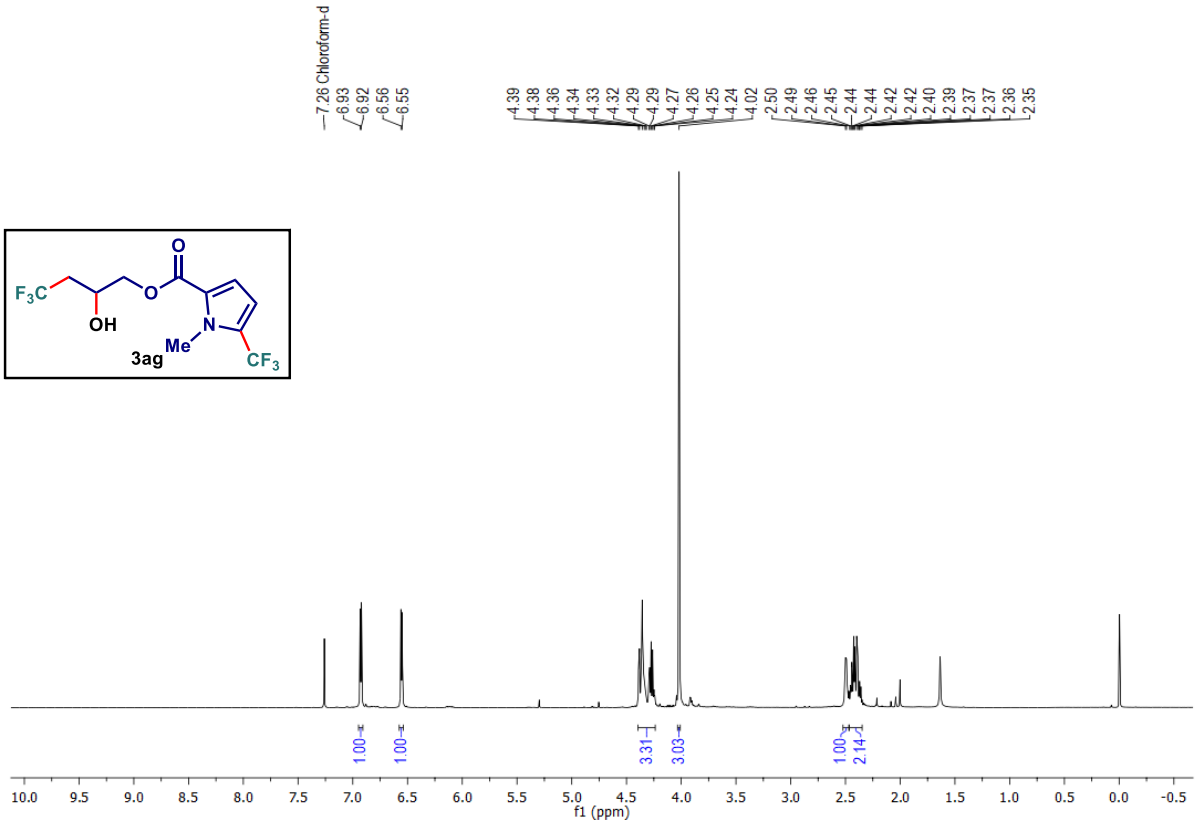

Figure II.13 ^{1}H NMR spectrum of **3ag**, $CDCl_3$, 400 MHz

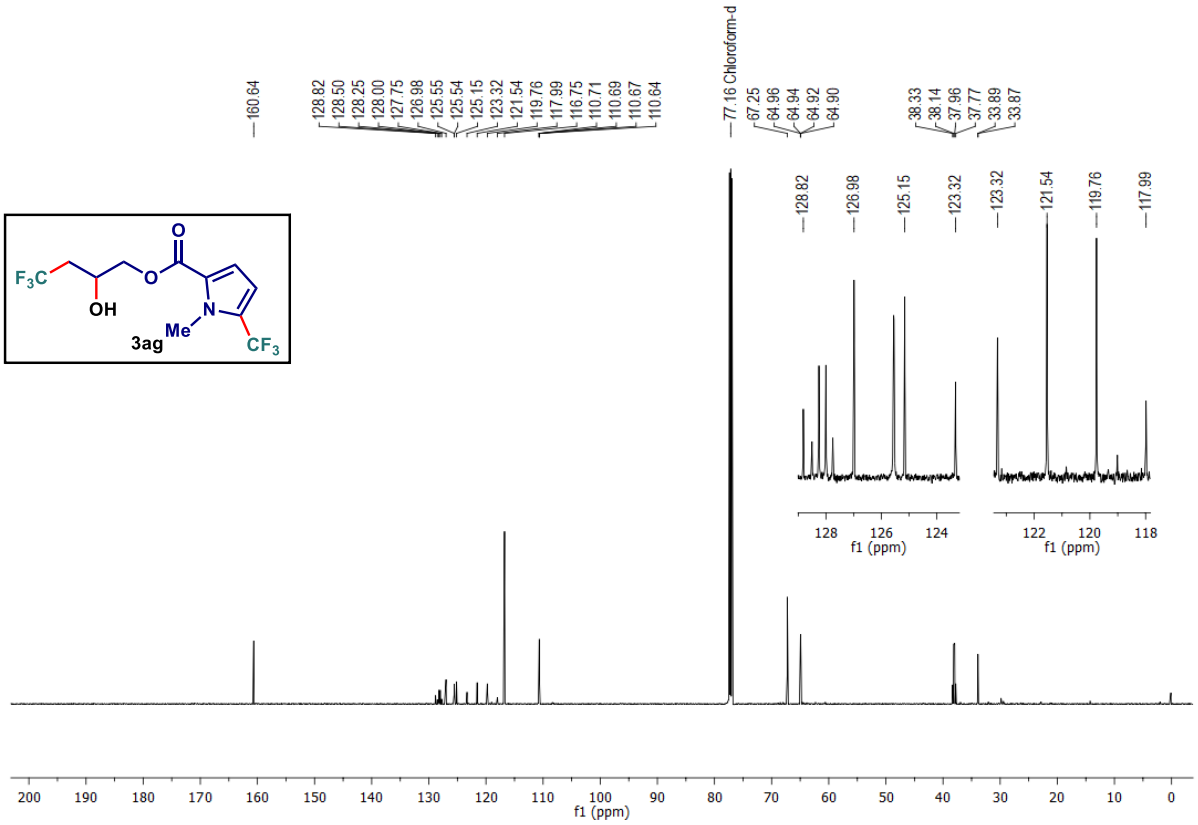

Figure II.14 ^{13}C{^{1}H} NMR spectrum of **3ag**, $CDCl_3$, 100 MHz

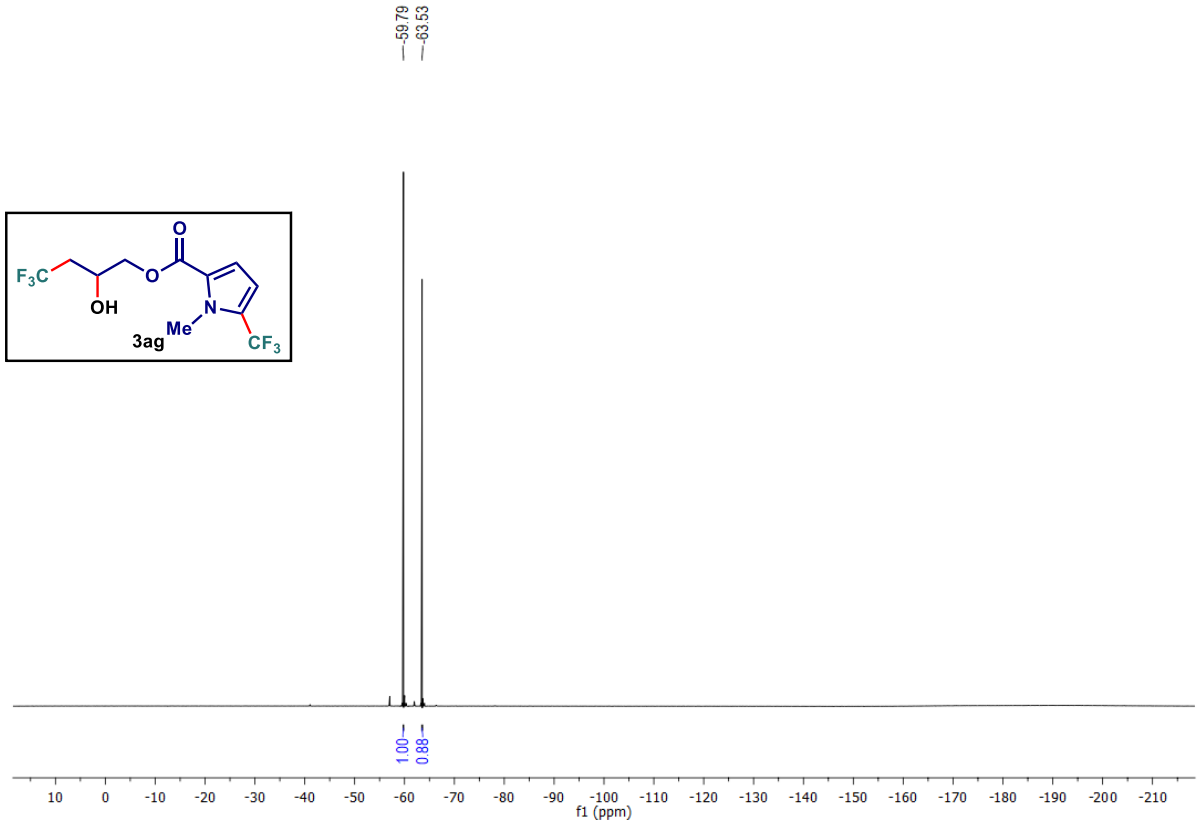

Figure II.15 $^{19}F\{^{1}H\}$ NMR spectrum of **3ag**, $CDCl_3$, 377 MHz

HOESY NMR
^{1}H-^{19}F Correlation

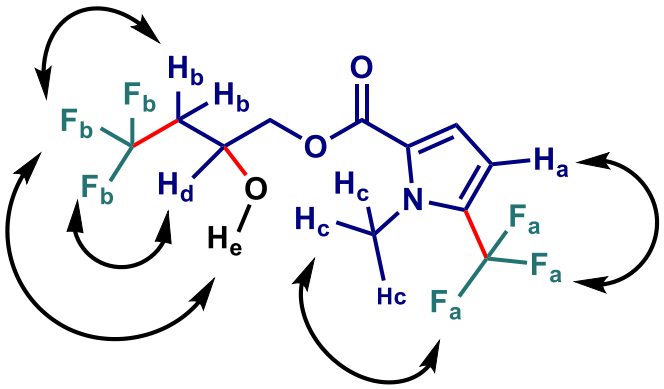

3ag

H_a = 6.55 δ ppm
H_b = 2.40 δ ppm
H_c = 4.02 δ ppm
H_d = 4.39 δ ppm
H_e = 2.50 δ ppm
F_a = -59.80 δ ppm
F_b = -63.53 δ ppm

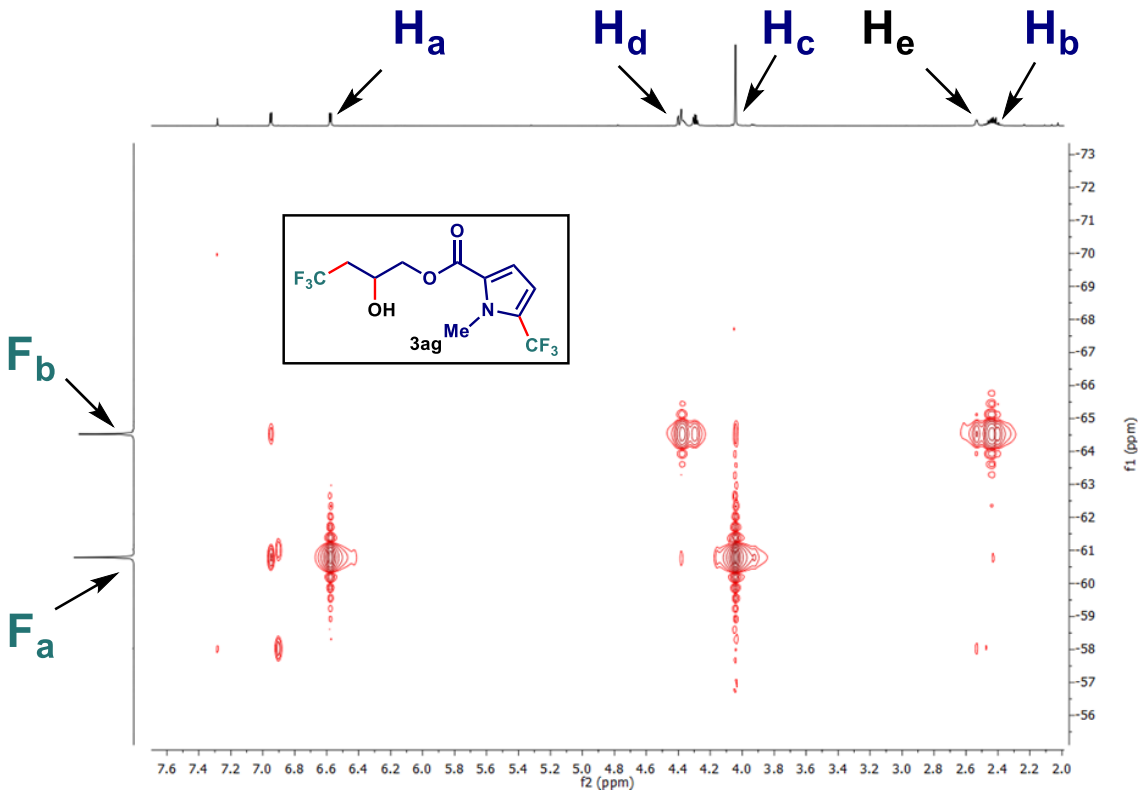

Figure II.16 HOESY (^{1}H-^{19}F) spectrum of **3ag**

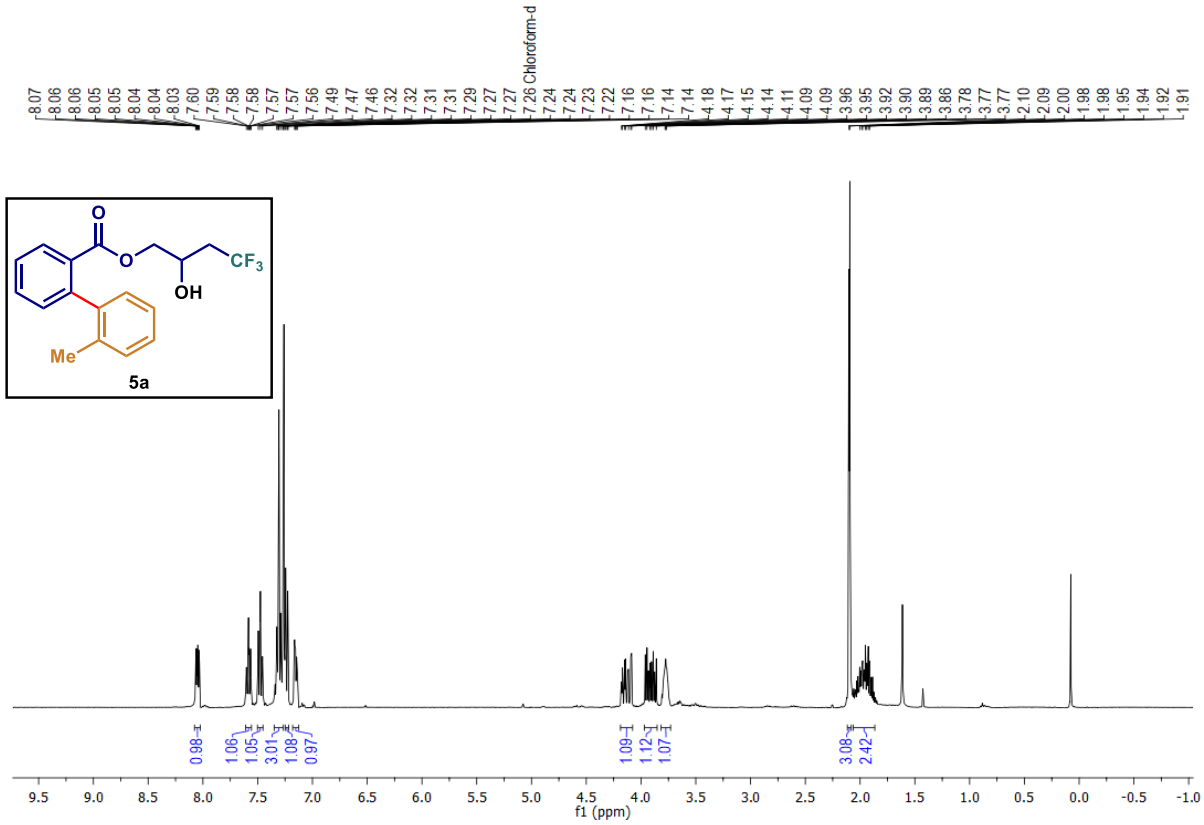

Figure II.17 ^{1}H NMR spectrum of **5a**, $CDCl_3$, 400 MHz

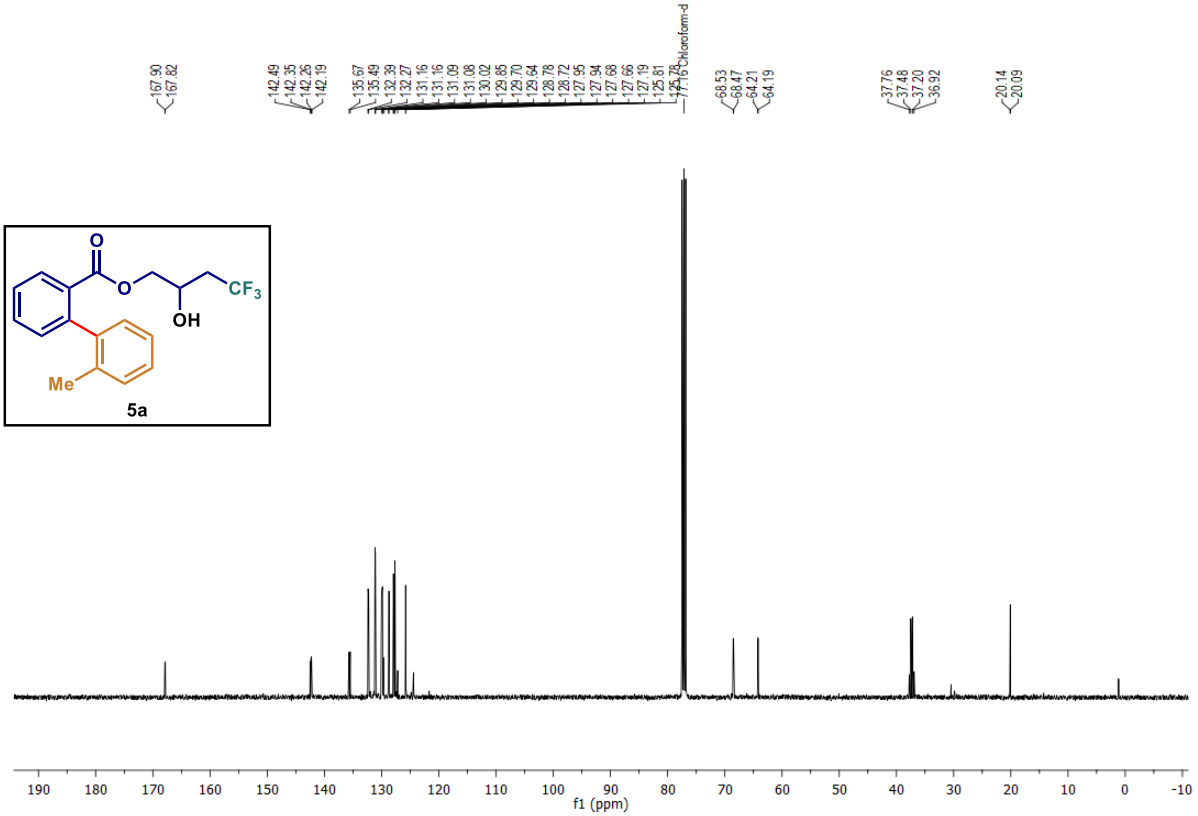

Figure II.18 $^{13}C\{^{1}H\}$ NMR spectrum of **5a**, $CDCl_3$, 100 MHz

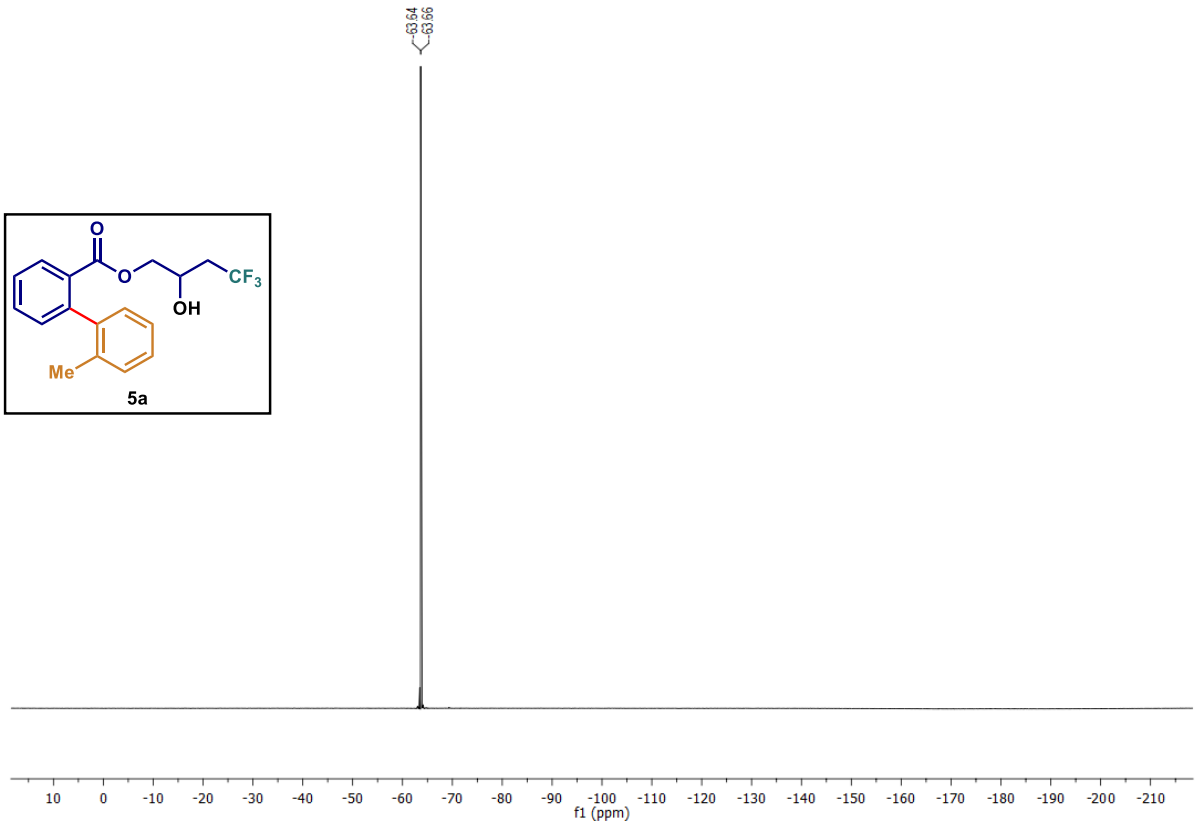

Figure II.19 $^{19}F\{^{1}H\}$ NMR spectrum of **5a**, $CDCl_3$, 377 MHz

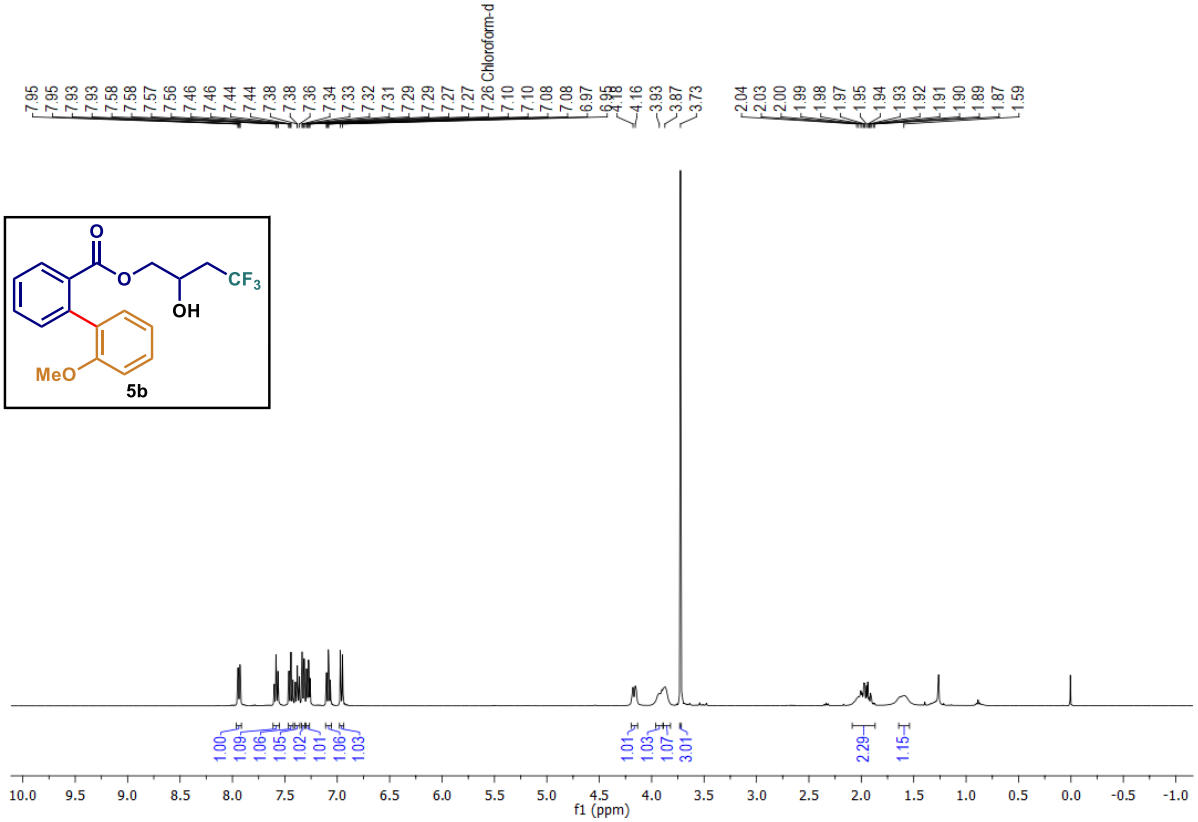

Figure II.20 ^{1}H NMR spectrum of **5b**, $CDCl_3$, 400 MHz

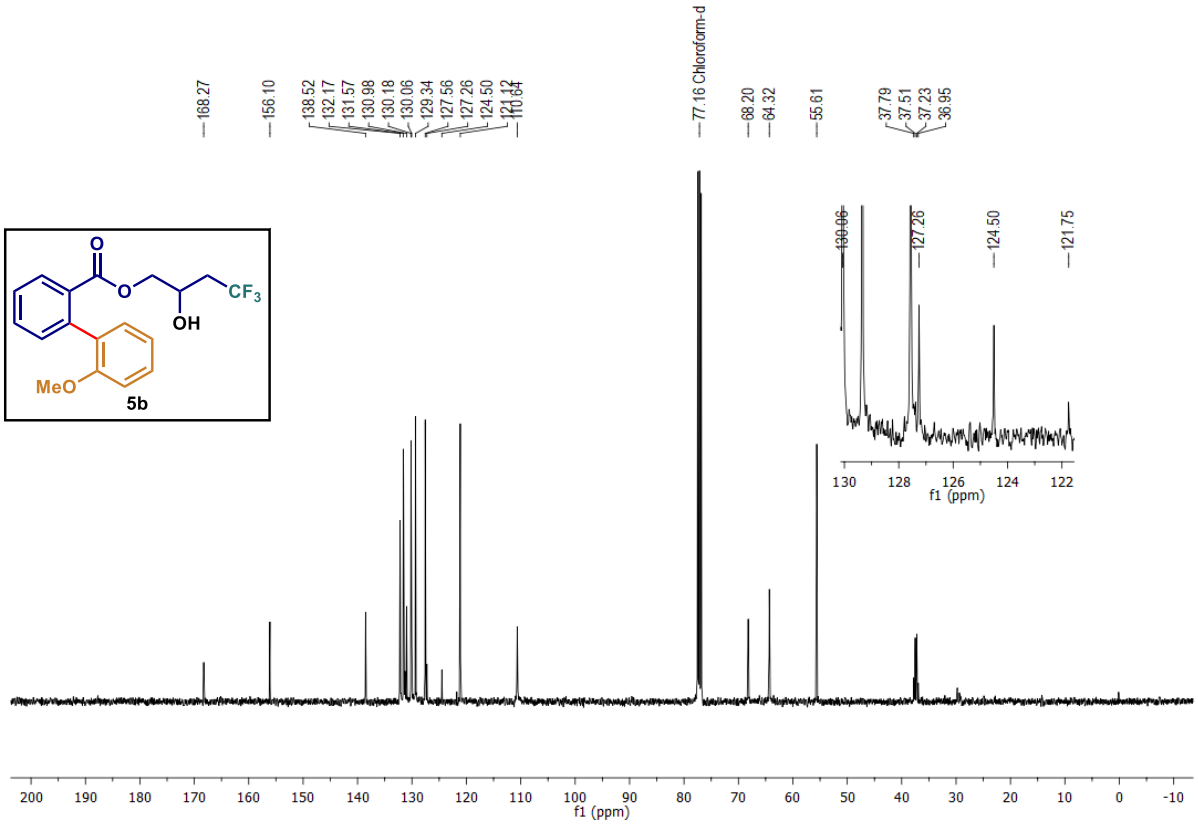

Figure II.21 $^{13}C\{^{1}H\}$ NMR spectrum of **5b**, $CDCl_3$, 100 MHz

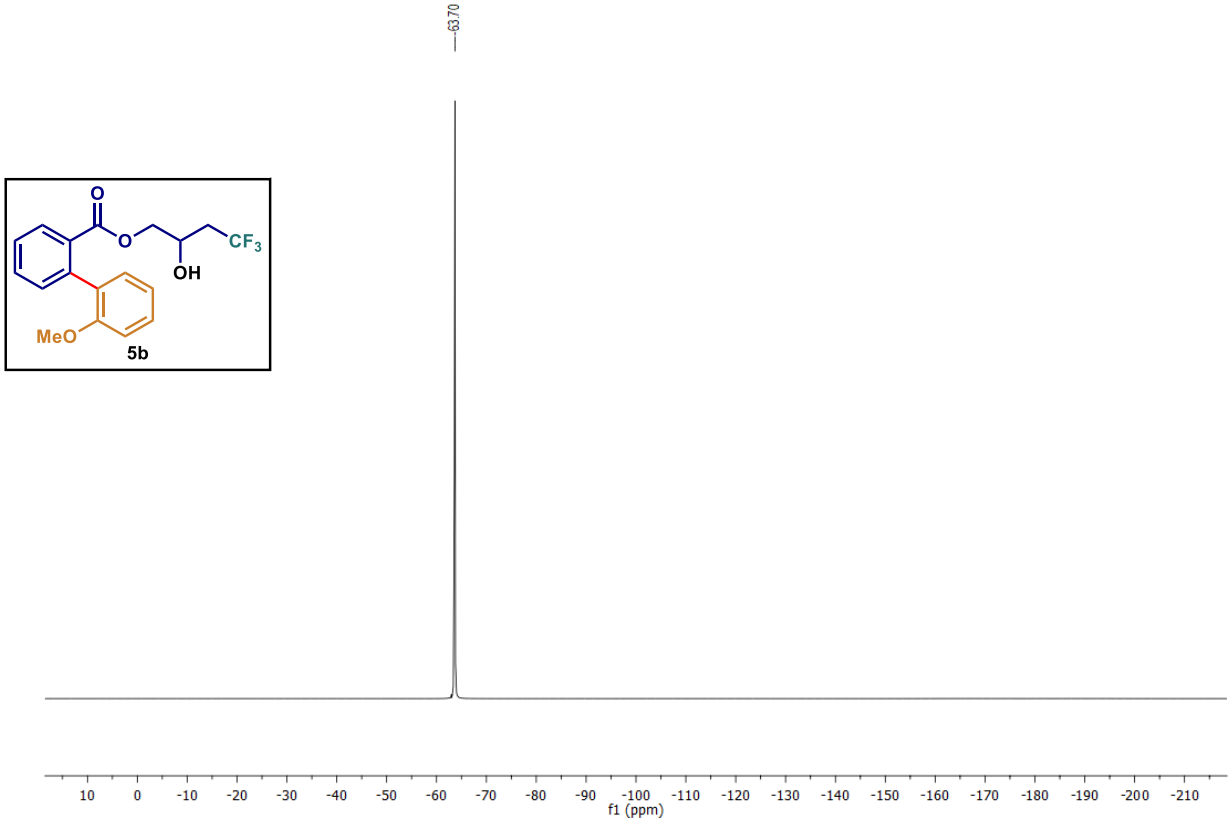

Figure II.22 $^{19}F\{^{1}H\}$ NMR spectrum of **5b**, $CDCl_3$, 377 MHz

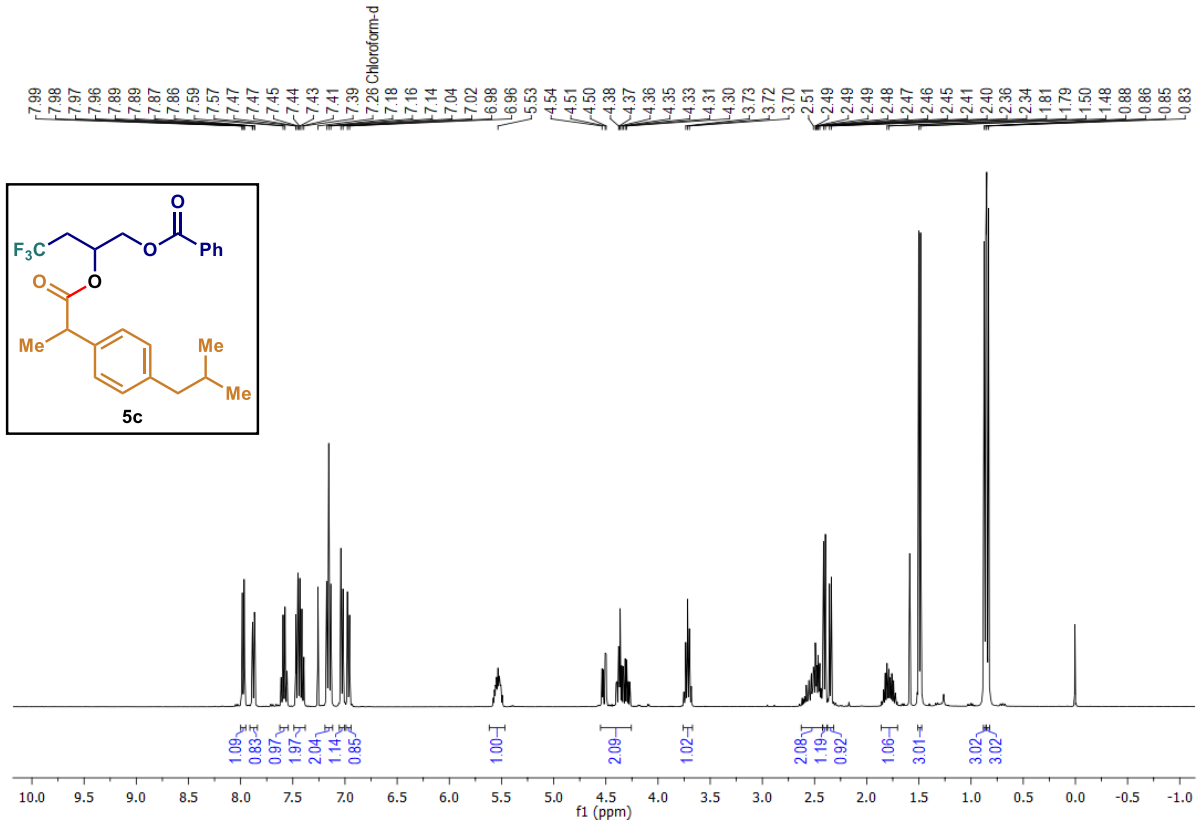

Figure II.23 ^{1}H NMR spectrum of **5c**, $CDCl_3$, 400 MHz

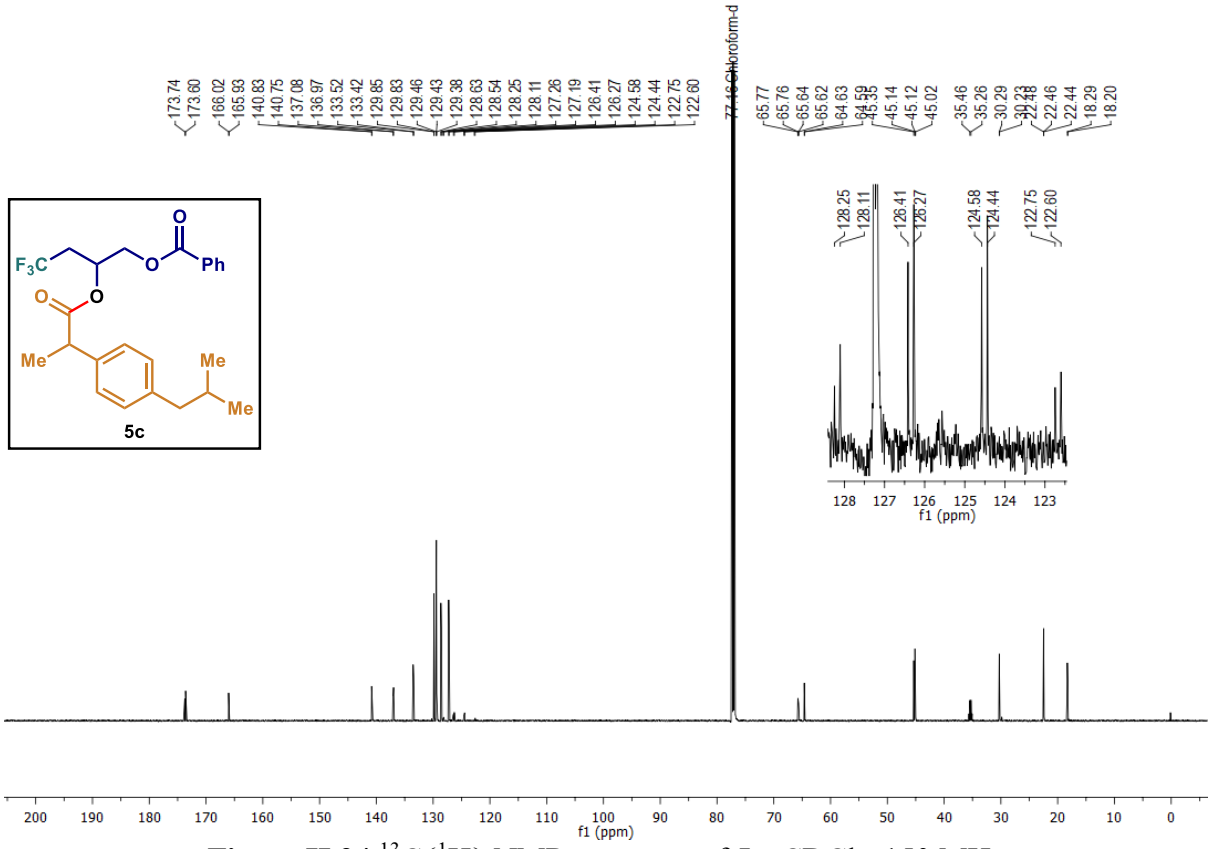

Figure II.24 $^{13}C\{^{1}H\}$ NMR spectrum of **5c**, $CDCl_3$, 150 MHz

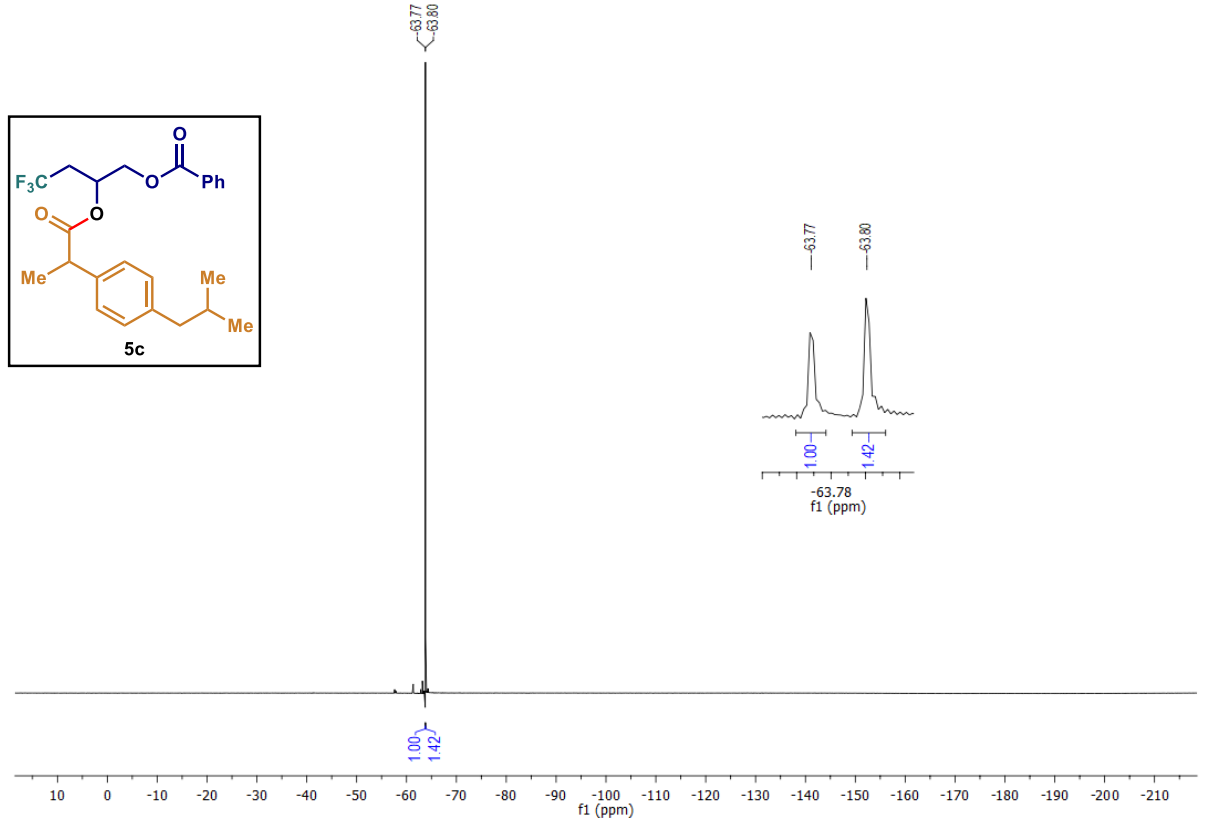

Figure II.25 $^{19}F\{^{1}H\}$ NMR spectrum of **5c**, $CDCl_3$, 377 MHz

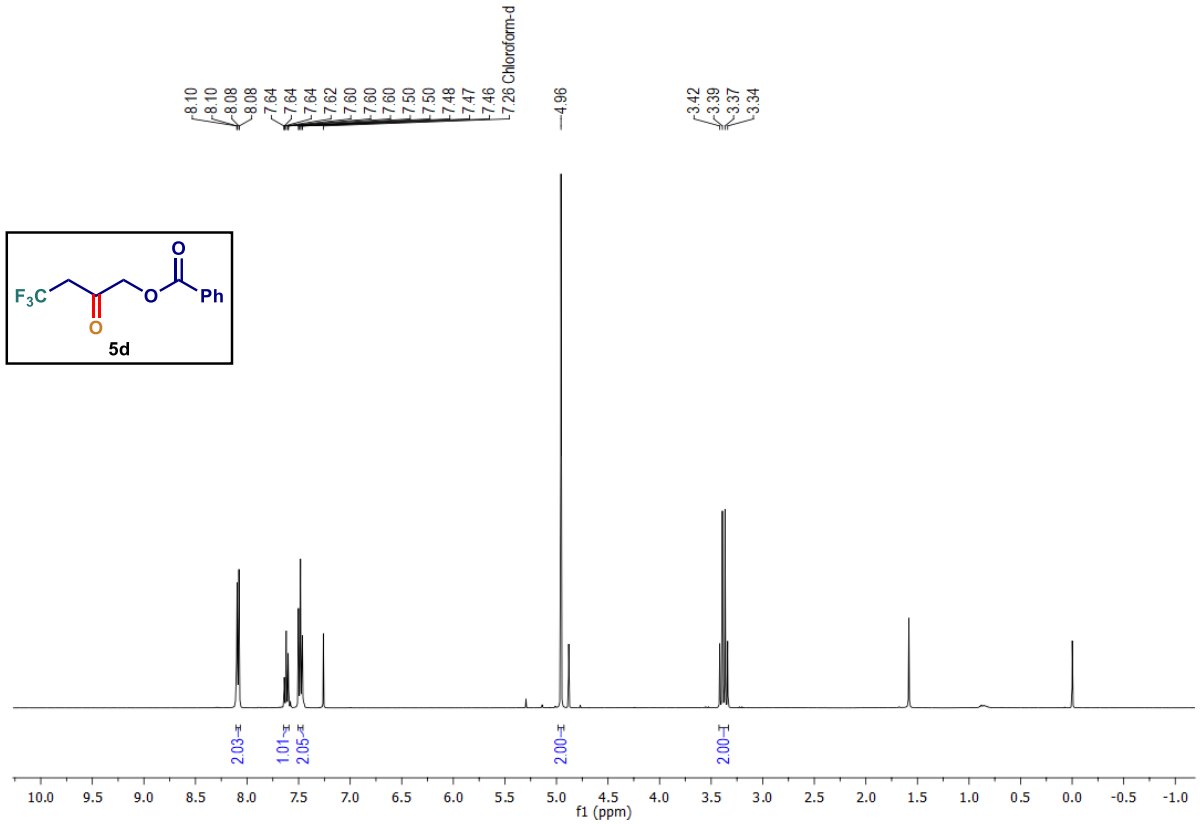

Figure II.26 ^{1}H NMR spectrum of **5d**, $CDCl_3$, 400 MHz

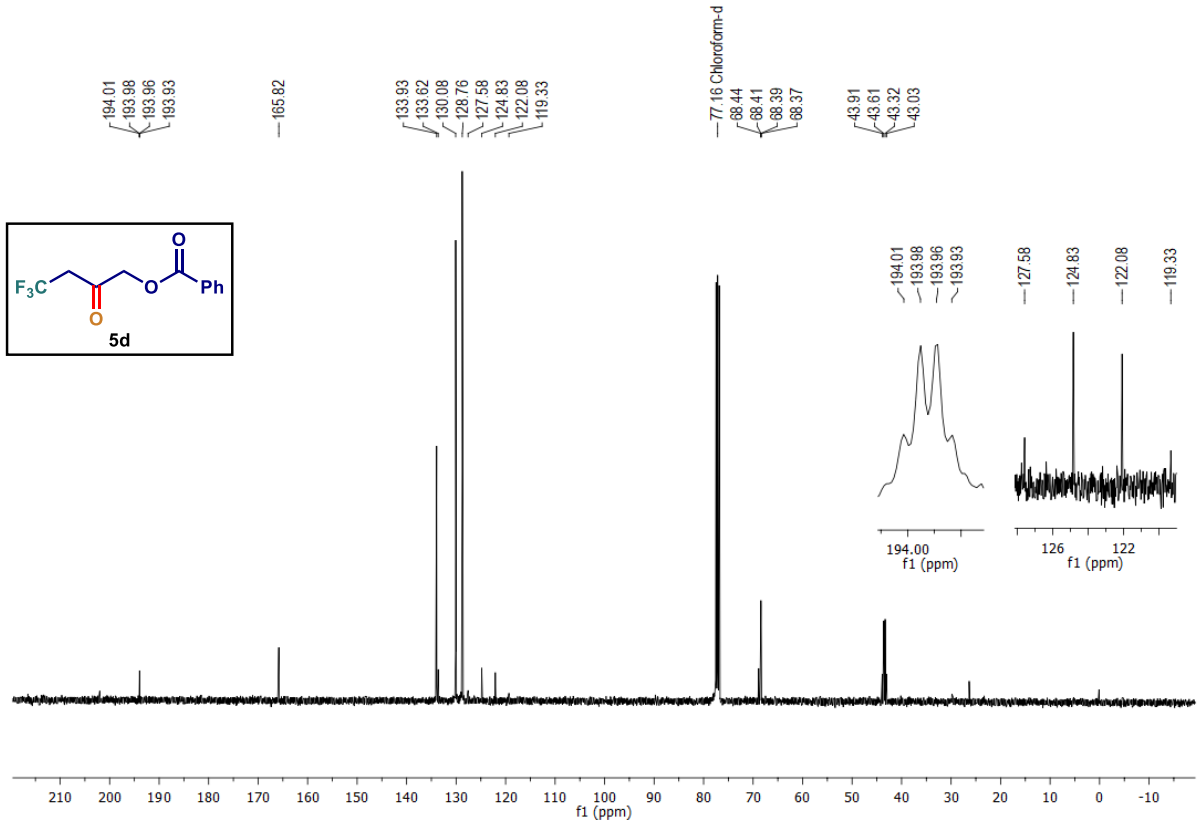

Figure II.27 $^{13}C\{^{1}H\}$ NMR spectrum of **5d**, $CDCl_3$, 100 MHz

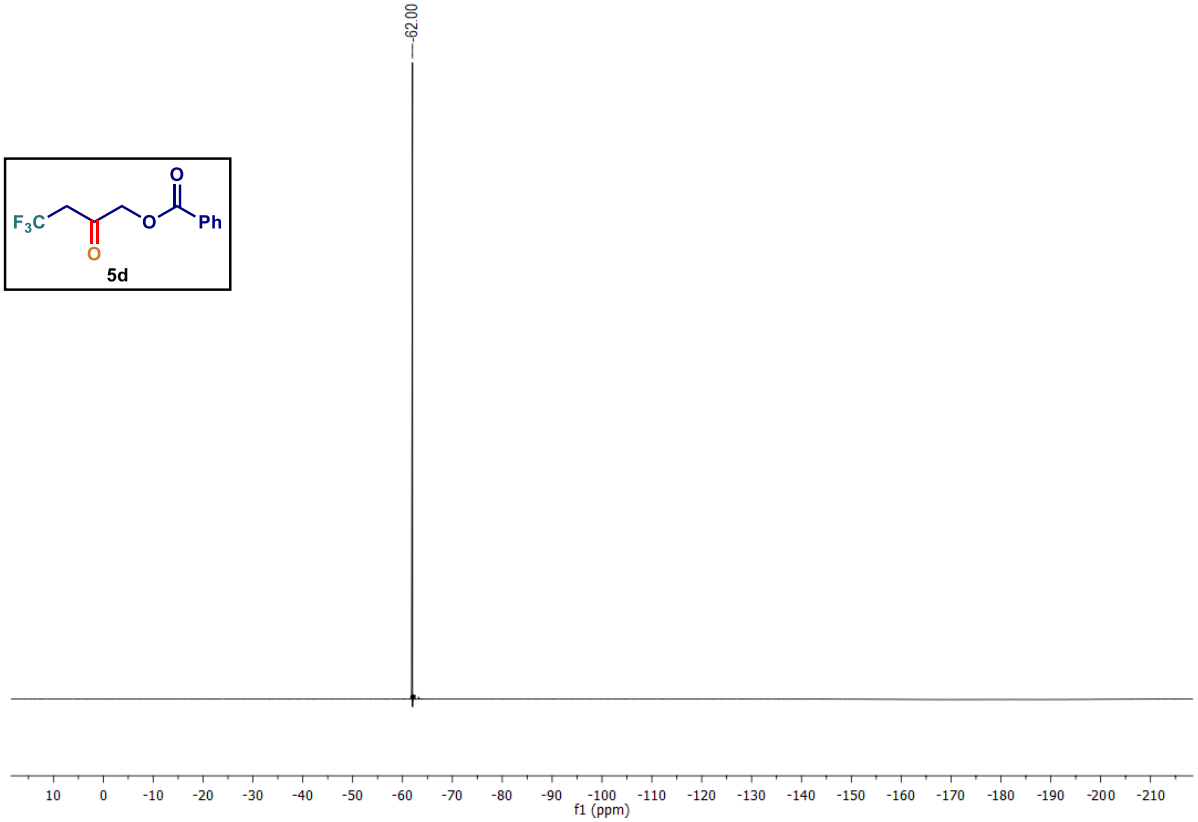

Figure II.28 $^{19}F\{^{1}H\}$ NMR spectrum of **5d**, $CDCl_3$, 377 MHz

2.4.7 Crystal Data of Compound **3ai (CCDC No. 2292952)**

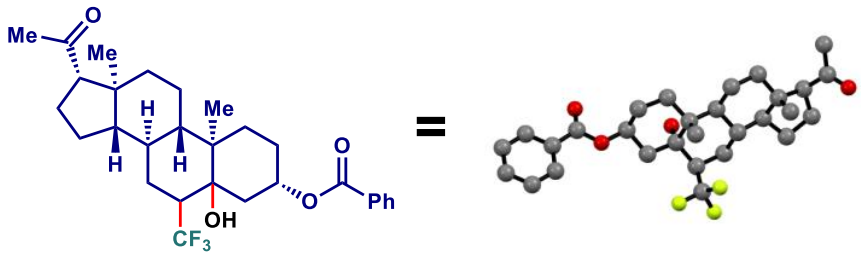

Bond precision: C-C = 0.0088 A Wavelength=1.54178

Cell: a=10.9356(3) b=25.1409(8) c=11.0349(3)
alpha=90 beta=119.473(1) gamma=90

Temperature: 296 K

	Calculated	Reported
Volume	2641.22(13)	2641.22(13)
Space group	P 21	P 21
Hall group	P 2yb	P 2yb
Moiety formula	C29 H37 F3 O4	C29H37F3O4
Sum formula	C29 H37 F3 O4	C29H37F3O4
Mr	506.59	506.59
Dx,g cm-3	1.274	1.274
Z	4	4
Mu (mm-1)	0.809	0.809
F000	1080.0	1080.0
F000'	1083.64	
h,k,lmax	13,31,13	12,30,13
Nref	10466[5359]	8500
Tmin,Tmax		
Tmin'		

Correction method= Not given

Data completeness= 1.59/0.81 Theta(max)= 72.433

R(reflections)= 0.0567(6341) wR2(reflections)= 0.1260(8500)

S = 1.033 Npar= 658

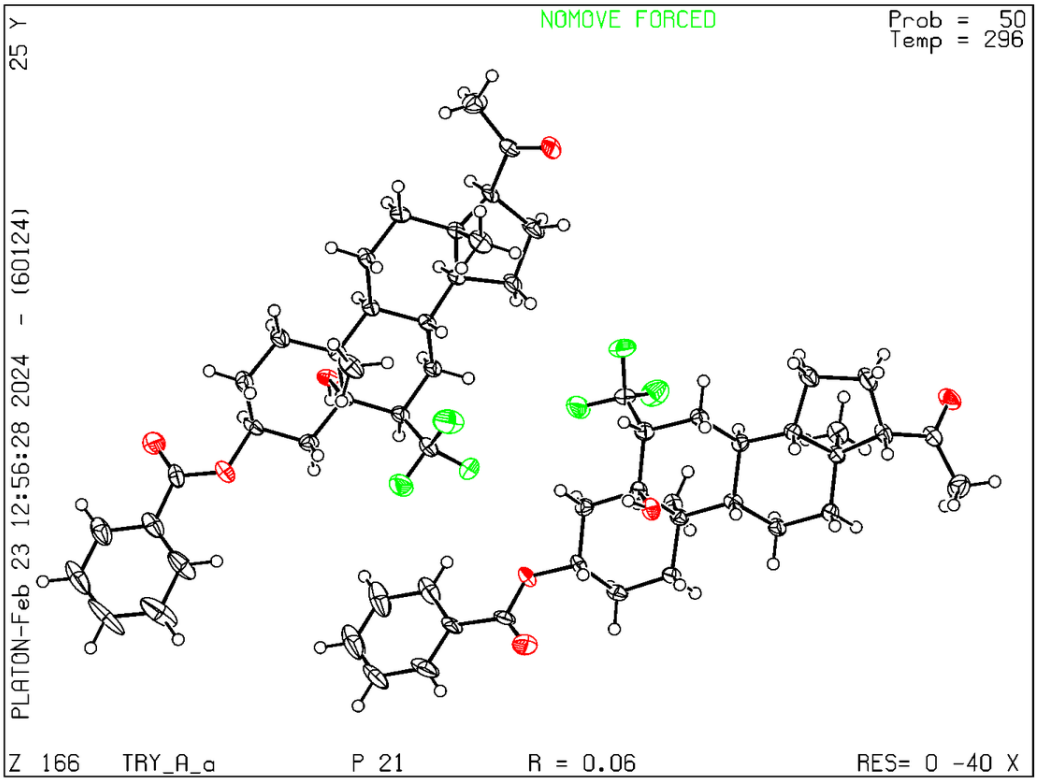

With 50% ellipsoid contour probability

Crystallization: sample was dissolved in a 5% Dichloromethane:hexane system and allowed it to crystalize by solvent diffusion method

Instrumentation used for the crystal measurement: Single-crystal X-ray data of **3ai** were collected at 296 K on a Bruker D8 Venture Duo X-ray diffractometer equipped with Microfocus X-ray source (operated at 50 W; 50 kV/1mA), graded multilayer optics for monochromatic Mo Kα radiation (λ = 0.71073 Å) focused X-ray beam and Photon 100 CMOS chip-based detector system.

2.5 References

1. (a) Kirsch, P. *Modern Fluoroorganic Chemistry*; Wiley-VCH, Weinheim, **2004**. (b) Zhu, W.; Wang, J.; Wang, S.; Gu, Z.; Aceña, J. L.; Izawa, K.; Liu, H.; Soloshonok, V. A. *J. Fluor. Chem.* **2014**, *167*, 37–54.
2. (a) Zhou, Y.; Wang, J.; Gu, Z.; Wang, S.; Zhu, W.; Aceña, J. L.; Soloshonok, V. A.; Izawa, K.; Liu, H. *Chem. Rev.* **2016**, *116*, 422−518. (b) Inoue, M.; Sumii, Y.; Shibata, N. *ACS Omega* **2020**, *5*, 10633–10640.
3. (a) Jeschke, P. *ChemBioChem* **2004**, *5*, 570−589. (b) Ogawa, Y.; Tokunaga, E.; Kobayashi, O.; Hirai, K.; Shibata, N. *iScience* **2020**, *23*, 101467−101489.
4. Hird, M. *Chem. Soc. Rev.* **2007**, *36*, 2070−2095.
5. (a) Ametamey, S. M.; Honer, M.; Schubiger, P. A. *Chem. Rev.* **2008**, *108*, 1501–1516. (b) Francis, F.; Wuest, F. *Molecules* **2021**, *26*, 6478−6502.
6. (a) Mandal, D.; Maji, S.; Pal, T.; Sinha, S. K.; Maiti, D. *Chem. Commun.* **2022**, *58*, 10442–10468. (b) Xiao, H.; Zhang, Z.; Fang, Y.; Zhu, L.; Li, C. *Chem. Soc. Rev.* **2021**, *50*, 6308–6319. (c) Barata-Vallejo, S.; Lantaño, B.; Postigo, A. *Chem. Eur. J.* **2014**, *20*, 16806–16829. (d) Studer, A. *Angew. Chem. Int. Ed.* **2012**, *51*, 8950–8958. (e) Ma, J.-A.; Cahard, D. *J. Fluor. Chem.* **2007**, *128*, 975–996.
7. Zabicky, J., Ed. *Patai's Chemistry of Functional Groups*; The Alkenes, Vol. *2*; Wiley: London, **1970**.
8. (a) Yao, H.; Hu, W.; Zhang, W. *Molecules* **2021**, *26*, 105−135. (b) Lan, X.-W.; Wang, N.-X.; Xing, Y. *Eur. J. Org. Chem.* **2017**, *2017*, 5821–5851.
9. For selective reviews on Trifluoromethylating difunctionalization of alkenes. (a) Egami, H.; Sodeoka, M. *Angew. Chem., Int. Ed.* **2014**, *53*, 8294−8308. (b) Merino, E. X. B.; Nevado, C. *Chem. Soc. Rev.* **2014**, *43*, 6598−6608. (c) Kawamura, S.; Barrio, P.; Fustero, S.; Escorihuela, J.; Han, J.; Soloshonok, V. A.; Sodeoka, M. *Adv. Synth. Catal.* **2023**, *365*, 398–462.
10. Yang, Y.; Liu, Y.; Jiang, Y.; Zhang, Y.; Vicic, D. A. *J. Org. Chem.* **2015**, *80*, 6639–6648.
11. Yang, X.; He, L.; Tsui, G. C. *Org. Lett.* **2017**, *19*, 2446−2449.
12. Jud, W.; Kappe, C. O.; Cantillo, D. *Chem. Eur. J.* **2018**, *24*, 17234–17238.
13. Luo, H.-Q.; Zhang, Z.-P.; Dong, W.; Luo, X.-Z. *Synlett* **2014**, *25*, 1307–1311.
14. (a) Cristina Silva Costa, D. *Arabian J. Chem.* **2020**, *13*, 799–834. (b) Xu, S.; Negishi, E.-i. *Acc. Chem. Res.* **2016**, *49*, 2158–2168.
15. Roth, H. G.; Romero, N. A.; Nicewicz, D. A. *Synlett* **2016**, *27*, 714−723.

16. Shen, W.-G.; Wu, Q.-Y.; Gong, X.-Y.; Aoa, G.-Z.; Liu, F. *Green Chem.* **2019**, *21*, 2983−2987.
17. Li, Q.; Fan, W.; Peng, D.;Meng, B.; Wang, S.; Huang, R.; Liu, S.; Li, S. *ACS Catal.* **2020**, *10*, 4012−4018.
18. (a) Narayanam, J. M. R.; Stephenson, C. R. J. *Chem. Soc. Rev.* **2011**, *40*, 102–113. (b) Xi, Y.; Yi, H.; Lei, A. *Org. Biomol. Chem.* **2013**, *11*, 2387–2403. (c) Prier, C. K.; Rankic, D. A.; MacMillan, D. W. C. *Chem. Rev.* **2013**, *113*, 5322–5363. (d) Staveness, D.; Bosque, I.; Stephenson, C. R. J. Free radical chemistry enabled by visible light-induced electron transfer. *Acc. Chem. Res.* **2016**, *49*, 2295–2306. (e) Shaw, M. H.; Twilton, J.; MacMillan, D. W. C. *J. Org. Chem.* **2016**, *81*, 6898–6926.
19. (a) Gupta, S.; Kundu, A.; Ghosh, S.; Chakraborty, A.; Hajra, A. *Green Chem.*, **2023**, *25*, 8459−8493. (b) Mondal, S.; Ghosh, S.; Hajra, A. *Chem. Commun.* **2024**, *60*, 9659– 9691.
20. Koike, T.; Akita, M. *Chem* **2018**, *4*, 409−437.
21. Yasu, Y.; Koike, T.; Akita, M. *Angew. Chem. Int. Ed.* **2012**, *51*, 9567−9571.
22. Long, W.; Lian, P.; Li, J.; Wan, X. *Org. Biomol. Chem.* **2020**, *18*, 6483–6486.
23. Lee, Y.; Kwon, M. S. *Eur. J. Org. Chem*. **2020**, *2020*, 6028–6043.
24. (a) Dharpure, P. D.; Bhowmick, A.; Warghude, P. K.; Bhat, R. G. *Tetrahedron Lett.* **2020**, *61*, 151407−151415. (b) Bhowmick, A.; Warghude, P. K.; Dharpure, P. D.; Bhat, R. G. *Org. Chem. Front.* **2021**, *8*, 4777–4784. (c) Khade, V. V.; Thube, A. S.; Dharpure, P. D.; Bhat, R. G. *Org. Biomol. Chem.* **2022**, *20*, 1315–1319. (d) Bhowmick, A.; Warghude, P. K.; Bhat, R. G. *Asian J. Org. Chem.* **2022**, *11*, e202200205. (e) Dharpure, P. D.; Behera, M.; Khade, V. V.; Thube, A. S.; Bhat, R. G. *Org. Lett.* **2022**, *24*, 6919−6924. (f) Dharpure, P. D.; Behera, M.; Thube, A. S.; Bhat, R. G. *Chem Asian J.* **2023**, *18*, e202201128. (g) Behera, M.; Dharpure, P. D.; Sahu, A. K.; Bhat, R. G. *ChemRxiv* **2024**, DOI: 10.26434/chemrxiv-2024-sh4gw.
25. CCDC 2292952 (compound **3ai**) contain the supplementary crystallographic data. These data can be obtained free of charge by The Cambridge Crystallographic Data Centre.
26. Tommasino, J.-B.; Brondex, A.; M′edebielle, M.; Thomalla, M.; Langlois, B. R.; Billard, T. *Synlett* **2002**, *10*, 1697−1699.
27. Fukuzumi, S.; Kotani, H.; Ohkubo, K.; Ogo, S.; Tkachenko, N. V.; Lemmetyinen, H. *J. Am. Chem. Soc.*, **2004**, *126*, 1600−1601.
28. White, H. S.; Bard, A. J. *J. Am. Chem. Soc.* **1982**, *104*, 6891–6895.
29. Ren, X.; Liu, Q.; Wang, Z.; Chen, X. *Chin. Chem. Lett.* **2023**, *34*, 107473−107476.
30. Neises, B.; Steglich, W. *Angew. Chem., Int. Ed. Engl.* **1978**, *17*, 522−524.

31. Wang, Q.; Lübcke, M.; Biosca, M.; Hedberg, M.; Eriksson, L.; Himo, F.; Szabo, K. J. *J. Am. Chem. Soc.* **2020**, *142*, 20048−20057.

Chapter 3

Visible Light Driven Organophotoredox Catalyzed Oxidative Functionalization of Styrenes: Synthesis of α-Alkoxylated Ketones

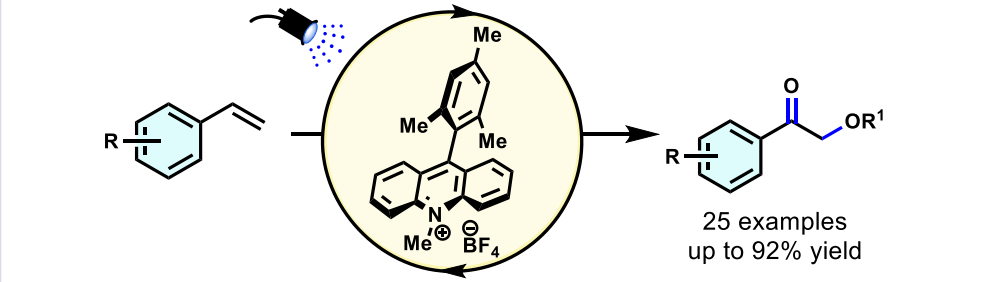

- *Alkene as substrate*
- *Chemical oxidant-free*
- *Transition metal-free*
- *Organophotocatalyst*
- *Broad scope*
- *Scalable and feasible under sunlight*

Visible Light Driven Organophotoredox Catalyzed Oxidative Functionalization of Styrenes: Synthesis of α-Alkoxylated Ketones

3

This chapter presents a mild, transition metal-free approach for the synthesis of α-alkoxylated ketones, employing organophotoredox catalysis and readily available, inexpensive styrene feedstocks. The reaction proceeds via the oxidative functionalization of styrenes using molecular oxygen (O_2) as the oxidant. While previous methods have primarily relied on activated substrates such as ketones, enols, or enolates, yet the direct transformation of styrenes into α-alkoxylated ketones has not been reported to the best of our knowledge. Herein, we demonstrate for the first time the use of styrenes as starting materials for this transformation. The developed protocol features a broad substrate scope, tolerating a variety of styrene derivatives and alcohols. Moreover, the resulting α-alkoxylated ketones can be further functionalized to access valuable α-keto amide, highlighting the synthetic utility of the method. The reaction is scalable and can be performed efficiently under natural sunlight as well. Based on the control experiments, fluorescence quenching studies, and cyclic voltammetry analysis a plausible reaction mechanism has been proposed.

3.1 Introduction

The carbonyl group is a cornerstone in organic chemistry, serving as a key structural unit in a wide range of functional groups, including amides, carboxylic acids, carbamates, and ketones.[1] Its importance spans across fundamental education in organic chemistry to advanced applications in fields such as materials science, biochemistry, and drug discovery.[2] Within this broad class, the ketone moiety exerts a profound influence on the pharmacodynamic and pharmacokinetic profiles of drug molecules, contributing significantly to their efficacy and target specificity (Figure 3.1).[3] Additionally, the ketones hold a particularly prominent position in industrially relevant substances such as dyes, fragrances, and flavoring agents.[4] Beyond their structural ubiquity, ketones are highly valued as reactive intermediates in organic synthesis and for the synthesis of natural product-inspired compounds.[5] Their electrophilic carbonyl center enables a broad range of classical and contemporary transformations, including well-established reactions such as the Mannich, Wittig, Grignard, and Passerini reactions, along with

oxidative and reductive processes such as the Baeyer–Villiger oxidation and Wolff–Kishner–Huang reduction.[2a] Given this wide-ranging relevance, the development of efficient, practical methods for the synthesis of ketones from abundant feedstock chemicals has long been a subject of considerable interest in both academic and industrial research.[6]

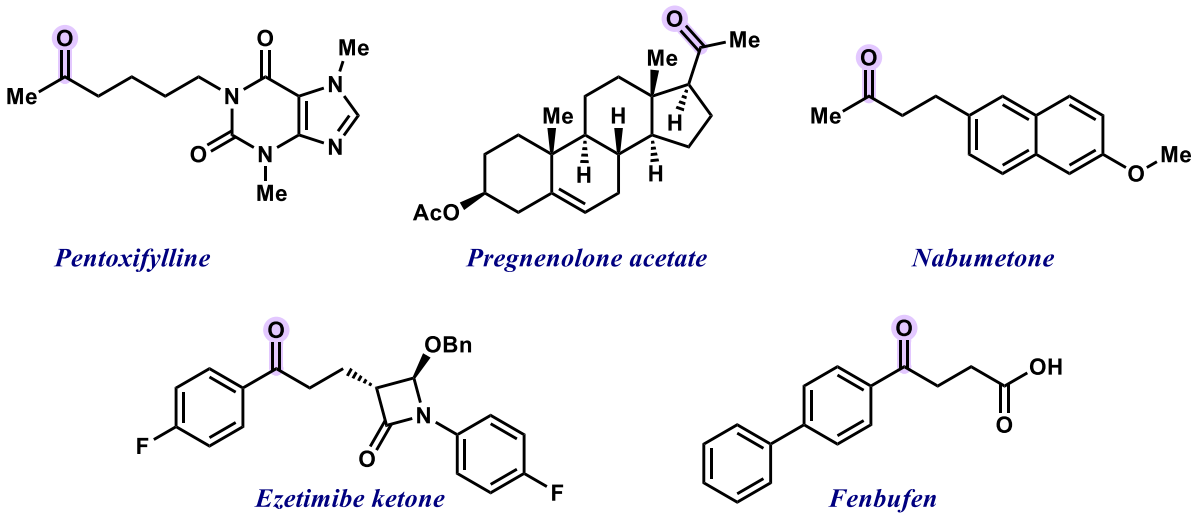

Figure 3.1 Selected bioactive molecules containing ketone moiety

Alkenes represent a class of hydrocarbons that are both economically accessible and abundantly available, primarily sourced from the refinement of petroleum and natural gas. Owing to their structural simplicity and reactivity, they serve as indispensable feedstocks in numerous industrial processes and synthetic organic methodologies. [7] Specially, the synthesis of carbonyl compounds from alkenes is of immense importance in organic chemistry.[8] A prominent example is the hydroformylation of olefins, a key industrial process that facilitates the production of higher aldehydes from alkenes, particularly within the fine chemicals sector.[9] The Wacker oxidation, an industrially significant aerobic oxidation of olefins to carbonyl compounds mediated by palladium and copper in aqueous conditions, has been employed for the large-scale production of acetaldehyde from ethylene.[10] Such transformations commonly employ noble metal salts as catalysts for double bond activation; however, the frequent requirement for high catalyst loadings can raise economic and sustainability concerns.

Photoredox chemistry has emerged as a viable alternative to conventional techniques, enabling transformations which are usually inaccessible from the traditional pathways.[11] Also, it has been effectively employed to address the limitations associated with the conventional methods for the synthesis of carbonyl/α-functionalized carbonyl compound **2** usually

photoredox chemistry avoids the use of toxic reagents and effectively minimizes the side-product formation (Scheme 3.1).[12]

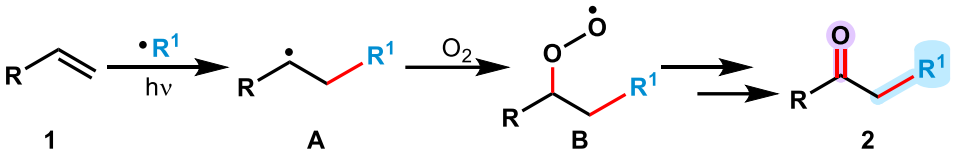

Scheme 3.1 General representation for the visible-light promoted α-functionalized carbonyl compounds

In 2007, Itoh and co-workers reported a visible-light-promoted synthesis of phenacyl iodide **2** from the reaction of styrenes **1** and iodine using fluorescent lamps (Scheme 3.2).[13] Through systematic investigation and optimization of the reaction conditions, they identified FMS-16 (a mesoporous silica material) as an effective catalyst and molecular oxygen (O_2) as the terminal oxidant. The same group later modified the reaction conditions for the formation of phenacyl halides, demonstrating that a small amount of water could effectively replace FSM-16. Furthermore, they extended the protocol to the synthesis of phenacyl bromides via the aerobic photo-oxidation of styrenes using 48% aqueous HBr.[14]

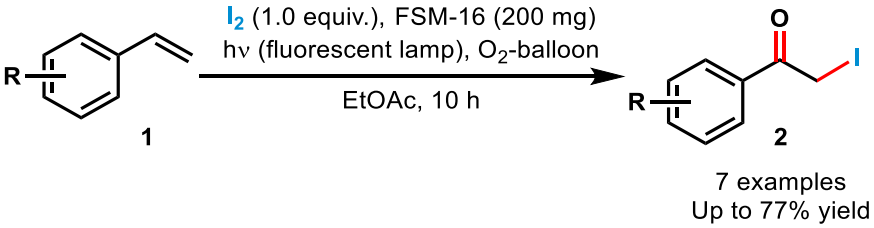

Scheme 3.2 The visible light promoted synthesis of α-iodoketones

In contrast to iodination and bromination, chlorination is often regarded as more challenging, primarily due to the lower reactivity of chlorine sources, especially when employing traditionally inert inorganic halides such as potassium salts (KX). In 2019, Zhu and co-workers introduced an elegant, operationally straightforward, and safe approach for synthesizing α-haloketones **2**, employing potassium bromide (KBr) and potassium chloride (KCl) as benign halogen sources (Scheme 3.3).[15]

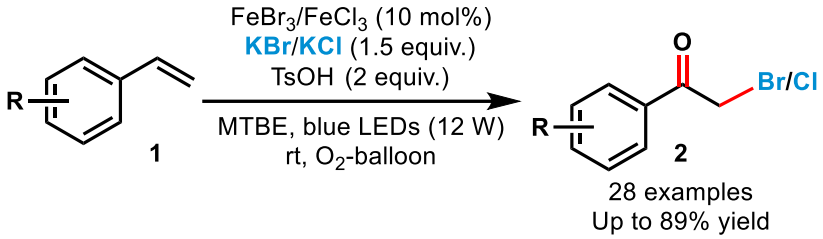

Scheme 3.3 The visible light promoted synthesis of *α*-iodoketones

The protocol involved an iron catalyzed reaction of alkenes with KBr or KCl under blue LEDs irradiation, with molecular oxygen serving as the terminal oxidant and methyl *tert*-butyl ether (MTBE) as a solvent. This approach effectively circumvented the safety risks associated with handling halogenated electrophiles such as Cl_2, Br_2, NCS, and NBS. The method afforded a variety of *α*-bromo- and *α*-chloroketones **2** in moderate to very good yields.

In 2014, the Yadav research group successfully employed substituted thiophenols **2** for the difunctionalization of styrenes, enabling the synthesis of *α*-sulfinyl ketones **3** (Scheme 3.4A).[16] They carried out the reaction of styrenes bearing various electron-withdrawing or electron-donating substituents with aryl mercaptans **2** in the presence of eosin Y and under the irradiation of visible light (green LEDs), affording the desired *α*-sulfinyl ketones **3** in good to excellent yields. Subsequently, in 2017, Niu and coworkers reported the successful synthesis of a series of α-sulfonyl ketones **5** through the reaction of olefins with sulfonyl chlorides **4** in acetonitrile, employing $Ir(ppy)_2(dtbbpy)PF_6$ as a photocatalyst under visible-light irradiation and ambient air (Scheme 3.4B).[17] In 2019, the Zhu research group disclosed the conversion of alkenes to *β*-ketone/hydroxy sulfones **7** and **8** from the reaction of styrenes and sulfonyl hydrazides **6** employing methylene blue (MB) as a photocatalyst, DABCO as a base, ethanol as a solvent and oxygen as a terminal oxidant under blue light irradiation (Scheme 3.4C).[18] Meanwhile, Wei and co-workers reported a catalyst-free method for the synthesis of *β*-oxo sulfones **10** via visible light-induced oxysulfonylation of alkenes using arylazo sulfones **9** and molecular oxygen under blue LEDs irradiation (Scheme 3.4D).[19]

Zhu research group developed a synthetic protocol for *α*-aryl ketones 3 starting from styrenes **1** and arylhydrazines **2**, using methylene blue as the photocatalyst, and DABCO as a base under blue light irradiation (Scheme 3.5).[20]

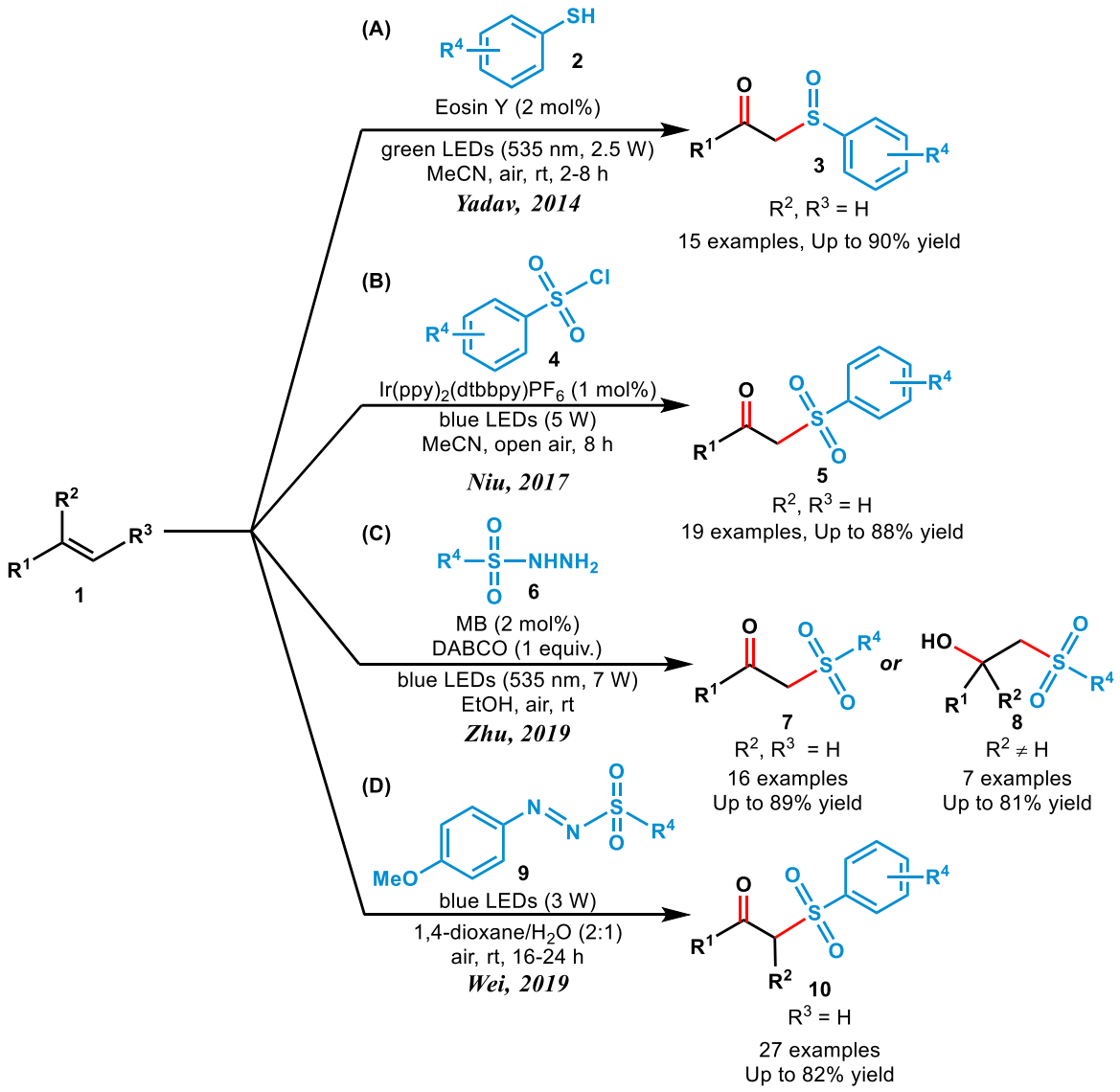

Scheme 3.4 The visible light mediated synthesis of α-sulfinyl/ sulfonyl ketones

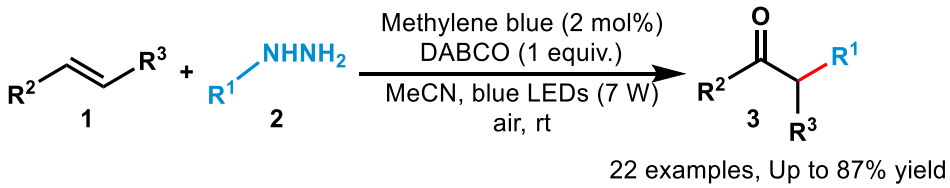

Scheme 3.5 Visible-light induced synthesis of ketones

This strategy has also been extended to the synthesis of α-azido ketones. In 2018, the Wei group reported the synthesis of α-azido ketones **3** from the reaction of olefins with trimethylsilyl azide ($TMSN_3$), employing rose bengal as the photocatalyst, diphenyl diselenide

(PhSeSePh) as the catalyst, and molecular oxygen as the oxidant under blue LEDs irradiation (Scheme 3.6).[21]

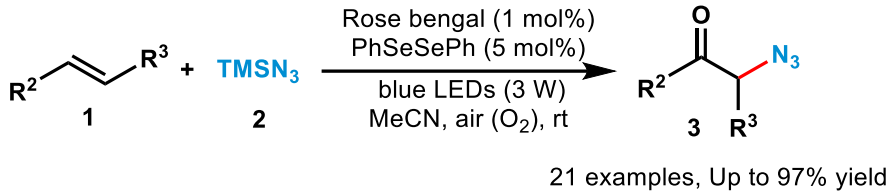

Scheme 3.6 Visible-light-induced oxyazidation of alkenes

Nan and coworkers developed a method for the synthesis of α-thiocyanato ketones **3** via the difunctionalization of olefins, employing the non-toxic and cost-effective Na_2-Eosin Y as the photocatalyst and molecular oxygen as the oxidant (Scheme 3.7).[22]

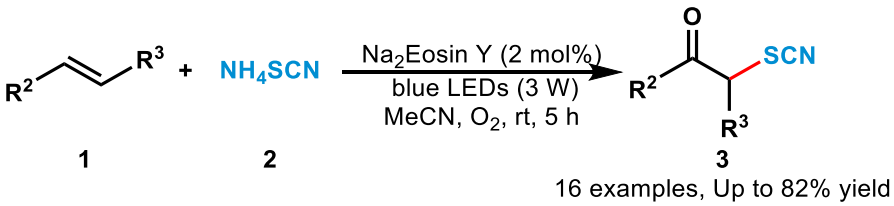

Scheme 3.7 Visible-light-induced synthesis of α-thiocyanato ketones

As illustrated, the synthesis of various α-functionalized ketones such as α-halo, sulfinyl/sulfonyl, aryl, azido, and thiocyanato ketones from alkenes have been well-documented in the literature. However, the direct synthesis of α-alkoxylated carbonyl compounds from readily available alkenes has not yet been reported. α-Alkoxylated carbonyl compounds are valuable synthetic building blocks, playing a pivotal role in the development of bioactive molecules such as adrenergic blockers and HIV-1 integrase inhibitors.[23] Additionally, these compounds serve as vital precursors in the synthesis of chiral alcohols, rendering them indispensable in asymmetric synthesis.[24] As a result, a wide range of synthetic methodologies have been developed to access these valuable molecules with high efficiency. Traditionally, the synthesis of α-alkoxylated carbonyl compounds has greatly relied on an umpolung strategy involving ketone or enol substrates **1** and **4**, with hypervalent iodine compounds serving as oxidants and alcohols functioning as both solvents and nucleophiles (Scheme 3.8).[25]

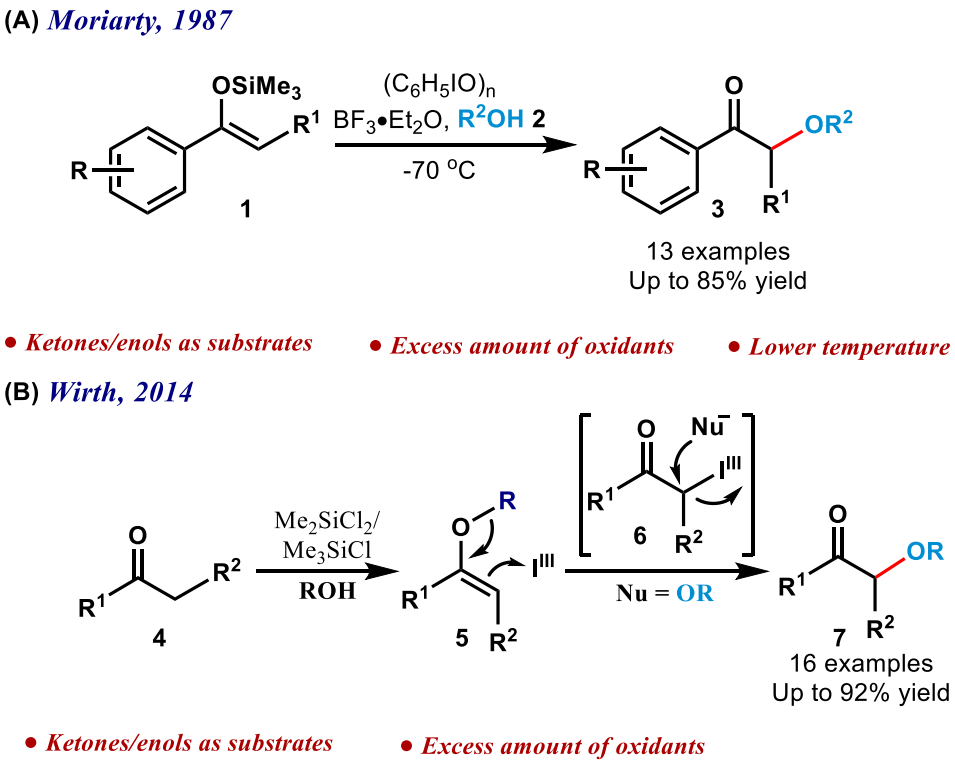

Scheme 3.8 Synthesis of α-alkylated ketones from ketones/enols

However, these approaches required the use of excess amount of oxidant, which in turn resulted in limited functional group compatibility and posed challenges with respect to substrate scope and selectivity. Furthermore, the methodologies often necessitated the prior generation of enolates from ketones, adding an additional synthetic step.

In 2021, Dagousset and coworkers reported a photoredox-mediated strategy for the synthesis of α-alkoxylated carbonyl compounds via the reaction of silyl enol ethers **1** with *N*-alkoxypyridinium salts **2** under visible-light irradiation (Scheme 3.9).[26]

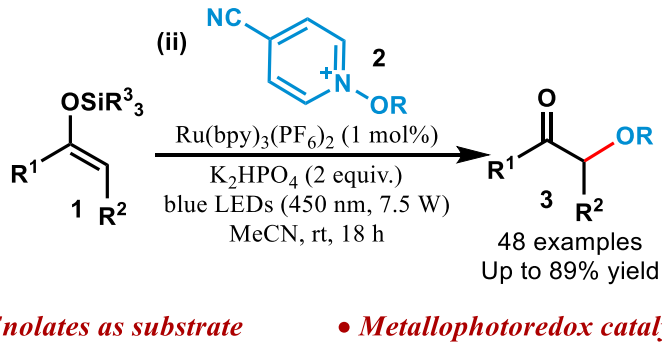

Scheme 3.9 Photoredox approach for α-alkoxylation from enols

However, this approach required the synthesis of radical precursors (*N*-alkoxypyridinium salts) and the use of a precious metal-based photocatalyst, $[Ru(bpy)_3(PF_6)_2]$.

Recently, Rong and coworkers developed an electrochemical approach for the synthesis of α-alkoxylated ketones **2** via the reaction of enol acetates **1** with free alcohols in an undivided cell, employing platinum (Pt) electrodes as both the cathode and anode.[27] The reaction was conducted under constant current conditions in acetonitrile (MeCN), with *n*-Bu_4NBF_4 serving as the supporting electrolyte (Scheme 3.10). Although this method avoids the use of chemical oxidants, it is constrained by the high cost of platinum electrodes and the necessity for pre-functionalized enol acetate substrates.

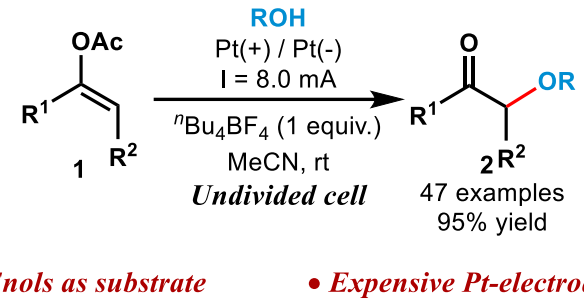

Scheme 3.10 Electro-organic synthesis approach for α-alkoxylation from enols

The synthesis of α-alkoxylated ketones has traditionally relied on carbonyl-containing substrates, such as ketones, enols, or enolates. However, to the best of our knowledge, their preparation directly from inexpensive feedstocks like styrene has not yet been explored. In this regard, we hypothesized that α-alkoxylated ketones **2** could be synthesized through the oxidative functionalization of alkenes with alcohol via organophotoredox catalysis under the irradiation of visible-light and metal-free conditions (Scheme 3.11).

Scheme 3.11 Hypothesis for the oxidative functionalization of alkenes to α-alkoxylated ketones

3.2 Results and Discussions

Table 3.1 Optimization of reaction conditions for α-alkoxylated ketone formation[a]

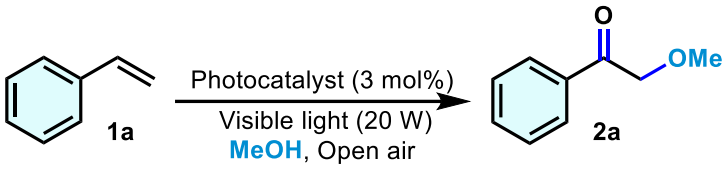

Sr. no.	Light (nm)	Photocatalyst	Solvent	Yield(%)[b]
1	405	Mes-Acr-Me·ClO_4	MeOH	36
2	427	Mes-Acr-Me·ClO_4	MeOH	52
3	440	Mes-Acr-Me·ClO_4	MeOH	58
4	456	Mes-Acr-Me·ClO_4	MeOH	62
5	467	Mes-Acr-Me·ClO_4	MeOH	65
6	525	Mes-Acr-Me·ClO_4	MeOH	55
7	**467**	**Mes-Acr-Me·BF_4**	**MeOH**	**68, 86,[c] (82)[d]**
8	467	2,4,6-Triphenylpyrylium·BF_4	MeOH	<10
9	467	EosinY	MeOH	ND
10	467	Rhodamine B	MeOH	ND
11	467	Rhodamine 6G	MeOH	ND
12	467	Fluorescein	MeOH	ND
13	467	Rose Bengal	MeOH	ND
14	467	Erythrosine B	MeOH	ND
15	467	Mes-Acr-Me·BF_4	MeCN	48[e]
16	467	Mes-Acr-Me·BF_4	DMF	ND[e]
17	467	Mes-Acr-Me·BF_4	DMSO	ND[e]

Standard reaction conditions: [a]**1a** (0.4 mmol), Photocatalyst (3 mol%), solvent (3 mL), Kessil LEDs (nm, 20 W) for 8 h at room temperature (rt). [b]Determined by ^{1}H NMR analysis using 1,3,5-Trimethoxybenzene as an internal standard. [c]O_2-purging (10 min). [d]Isolated yield after column chromatography. [e]MeOH (0.5 mL). ND = Not Detected.

To evaluate our hypothesis, we commenced the optimization of reaction conditions for the synthesis of α-alkoxylated ketones **2a** using styrene **1a** as the model substrate, with 9-mesityl-10-methylacridinium perchlorate (Mes-Acr-Me·ClO_4) as the photocatalyst and methanol serving as both the solvent and nucleophile. Initially, various light sources of different wavelengths were screened (427 nm, 440 nm, 456 nm, 467 nm, and 525 nm) (Table 3.1, Entries 1–6). Though the desired product **2a** was obtained under all tested conditions, blue LEDs (467 nm) afforded the desired product **2a** in highest yield (65%, Table 3.1, Entry 5). Encouraged

with this initial result, we further screened various photocatalysts such as Mes-Acr-Me·BF_4, 2,4,6-triphenylpyrylium·BF_4, eosin Y, rhodamine B, rhodamine 6G, fluorescein, rose bengal, and erythrosine B using blue LED (467 nm) (Table 3.1, Entries 7–14). Among all, photocatalysts Mes-Acr-Me·X (X = ClO_4 or BF_4) delivered the *α*-methoxylated product **2a** in significant yields of 55% and 68%, respectively (Table 3.1, Entries 6 and 7), while triphenylpyrylium·BF_4 afforded **2a** in poor yield (10%, Table 3.1, Entry 8). Subsequently, different solvents such as MeCN, DMF, and DMSO were evaluated using MeOH (0.5 mL) as a co-solvent. The reaction worked only in MeCN by affording the desired product **2a** albeit in modest yield (48%, Table 3.1, Entries 15–17). Later we screened the reaction by purging molecular oxygen for 10 minutes and interestingly the reaction afforded the desired product in very good yield (86%, Table 3.1, Entry 7 condition c). After the detailed screening, styrene **1a** (0.4 mmol), Mes-Acr-Me·BF_4 (2 mol%) in methanol (serving as both solvent and nucleophile), in presence of O_2 (10-minute purge) under the irradiation with Kessil blue LEDs (467 nm, 20 W) at room temperature proved to optimum reaction condition to obtain desired *α*-methoxylated product **2a**.

Having established the optimum reaction conditions, we then evaluated the substrate scope to assess the generality of the protocol for the synthesis of different *α*-alkoxylated ketones (Table 3.2). A series of electronically neutral and electron-rich styrenes (**1a**–**1f**) smoothly underwent the transformation under the optimized reaction conditions to afford the corresponding *α*-alkoxylated ketones (**2a**–**2f**) in moderate to very good yields (up to 87%, Table 3.2). Additionally, styrene bearing an electron-donating acetoxy group **1g** reacted smoothly to deliver the desired product **2g** in good yield (76%, Table 3.2). Furthermore, styrenes bearing electron-withdrawing groups such as –CN, –CO_2Me, –CO_2Et and –$CO_2{}^i$Pr (**1h**–**1j**) also performed well under the optimized reaction conditions, delivering the corresponding products (**2h**–**2j**) in good to excellent yields (up to 92%, Table 3.2). Moreover, styrenes bearing electron-deactivating substituents such as fluoro, chloro, bromo, and trifluoromethyl groups (**1l**–**1p**) were reacted smoothly under the reaction conditions to afford the corresponding products (**2l**–**2p**) in good to very good yields (up to 88%, Table 3.2). Notably, the styrene **1q** bearing electron withdrawing nitro (–NO_2) group exclusively offered the corresponding *α*-di-methoxylated ketone product **2q** in good yield (Table 3.2).

Table 3.2 Substrate scope of α-alkoxylated ketone products.[a]

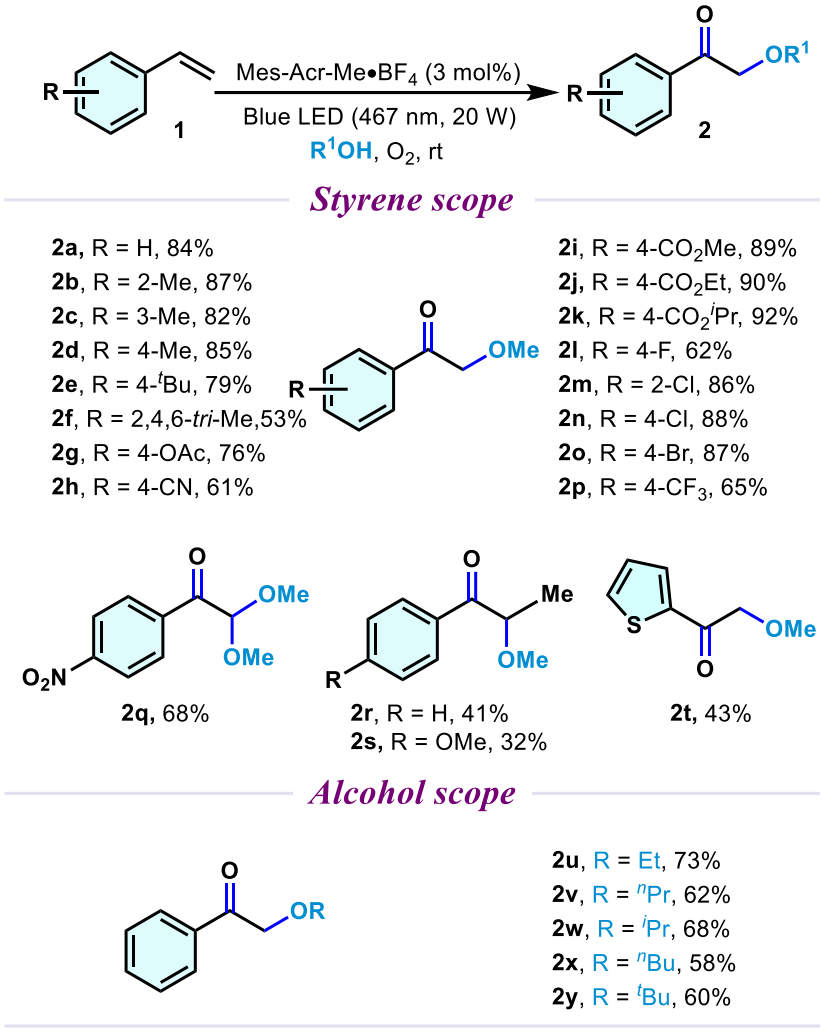

Reaction conditions: : [a]**1** (0.4 mmol), Mes-Acr-Me·BF_4 (3 mol%), **R^1OH** (3 mL), Kessil blue LEDs (467 nm, 20 W) room temperature (rt), O_2-purging (10 min). [b]Isolated yield after purification by column chromatography.

Furthermore, β-methyl styrene derivatives **1r** and **1s** also underwent successful transformation under the optimized reaction conditions, affording the α-methoxylated ketone products **2r** and **2s** in modest yields (Table 3.2). Additionally, heteroaryl substrate 2-vinylthiophene **1t** underwent the transformation successfully, delivering the desired product **2t** in moderate yield (43%, Table 3.2). Later, various alcohols such as ethanol, *n*-propanol, *i*-propanol, *n*-butanol, and *t*-butanol were explored and all of them reacted with styrene **1a** to afford the corresponding α-alkoxylated ketone products (**2u**-**2y**) successfully in moderate to good yields (up to 73%, Table 3.2).

Having demonstrated the generality of the developed protocol for the synthesis of broad range of α-alkoxylated ketone products, we next explored this protocol under direct exposure of natural sunlight (Scheme 3.12a). This reaction successfully afforded the desired product **2a**

in good yield (76%, Scheme 3.12a). To further evaluate the practicality of the method, we carried out the scale-up reaction using styrene **1a** (1 gram) under the optimized reaction conditions to obtain the corresponding product **2a** in a good yield (68%, Scheme 3.12b).

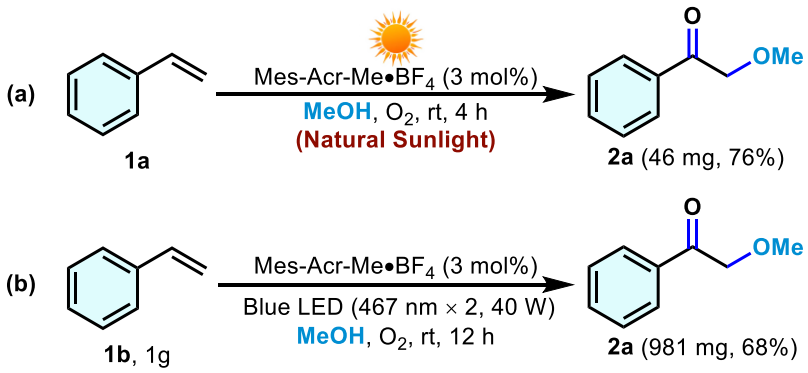

Scheme 3.12 Reaction under direct exposure of sunlight and gram scale synthesis

Subsequently, in order to explore practicality of the synthesized compounds, the *α*-methoxylated ketone product **2a** was subjected for the post-synthetic modification with piperidine. Gratifyingly corresponding *α*-keto amide **4a** was obtained in very good yield (Scheme 3.13).

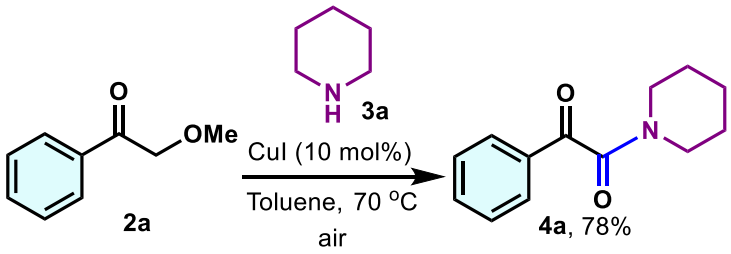

Scheme 3.13 Post synthetic modification of **2a** to synthesize *α*-keto amide **4a**

In order to gain a deeper understanding of the reaction mechanism, a few control experiments were performed systematically (Scheme 3.14). When compound **1a** was subjected to the standard reaction conditions in the absence of either light or the photocatalyst, no product formation was observed (Scheme 3.14a and 3.14b).

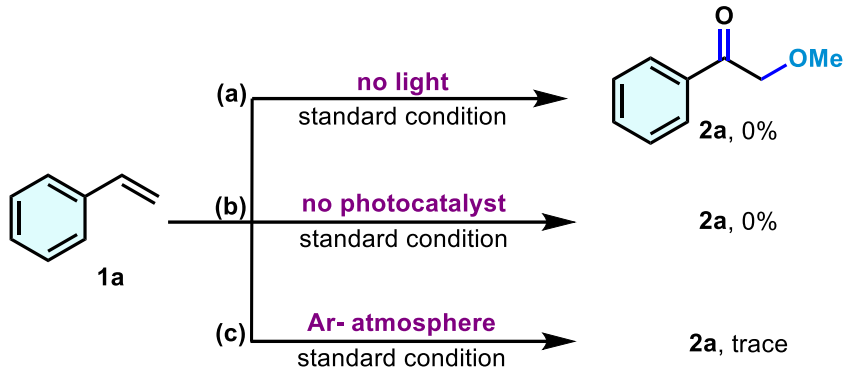

◆ ***Light, photocatalyst, and molecular oxygen (air) are essential components***

Scheme 3.14 Control experiments

Additionally, the reaction in the argon atmosphere failed to give the desired product **2a** (Scheme 3.14c). These results clearly highlighted the essential roles of light, photocatalyst, and molecular oxygen in this transformation.

As indicated by the above experiment, molecular oxygen (air) plays a critical role in this transformation. To determine the specific reactive oxygen species involved during reaction we planned to carry out few experiments. In order to confirm the presence of singlet oxygen or the superoxide radical anion, the reaction was first carried out in the presence of known singlet oxygen quenchers, DABCO and NaN_3 (Scheme 3.15a and b).[28, 29] The reaction afforded the desired product **2a** in the presence of DABCO; however, desired product **2a** was formed when NaN_3 was used. Additionally, when the reaction was conducted in the presence of the base DMAP, product **2a** was obtained in 72% yield (Scheme 3.15d). In contrast, the reaction in the presence of H_2O (10 equiv.) furnished the desired product **2a** in poor yield (10%, Scheme 3.15d). These findings clearly indicate that the azide nucleophile may inhibit the reaction, while the base does not significantly influence the reaction outcome and the yield of the desired product **2a**. Collectively, the data suggest that singlet oxygen is unlikely to play a role in the reaction mechanism. Subsequently, the reaction was conducted in the presence of *p*-benzoquinone, a well-known quencher of superoxide radical anion, under otherwise standard conditions. The inhibition of the desired product **2a** formation supported for the involvement of the superoxide radical anion in the reaction pathway (Scheme 3.15e).[30]

Furthermore, the reaction of **1a** in the presence of radical quenchers 2,6-di-*tert*-butyl-4-methylphenol (BHT) or (2,2,6,6-tetramethylpiperidin-1-yl)oxyl (TEMPO) failed to afford and reduced the yield of the desired product **2a** respectively (Scheme 3.16a and b). The α-keto methyl radical–TEMPO adduct was detected using high-resolution mass spectrometric

(HRMS) analysis (Figure 3.2). These results support the involvement of radical intermediate **B** in the reaction pathway.

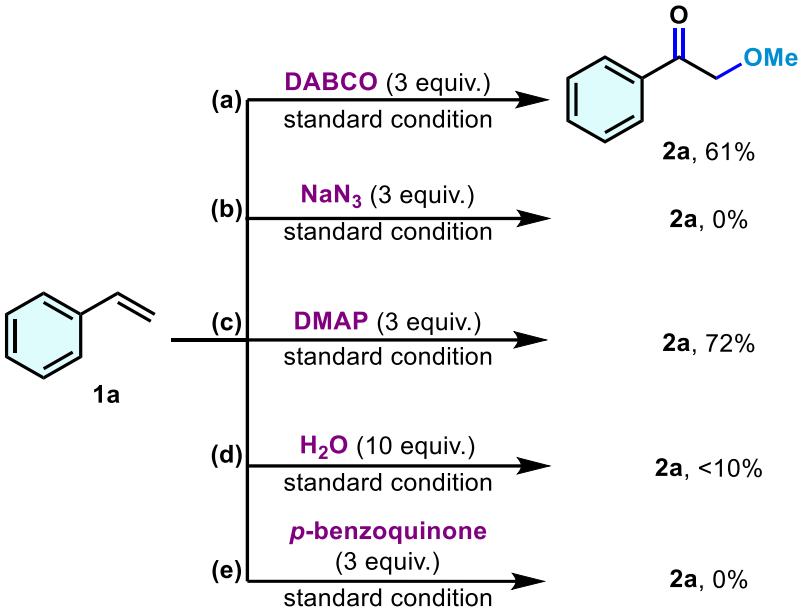

Scheme 3.15 Control experiments to identify the oxygen species involved

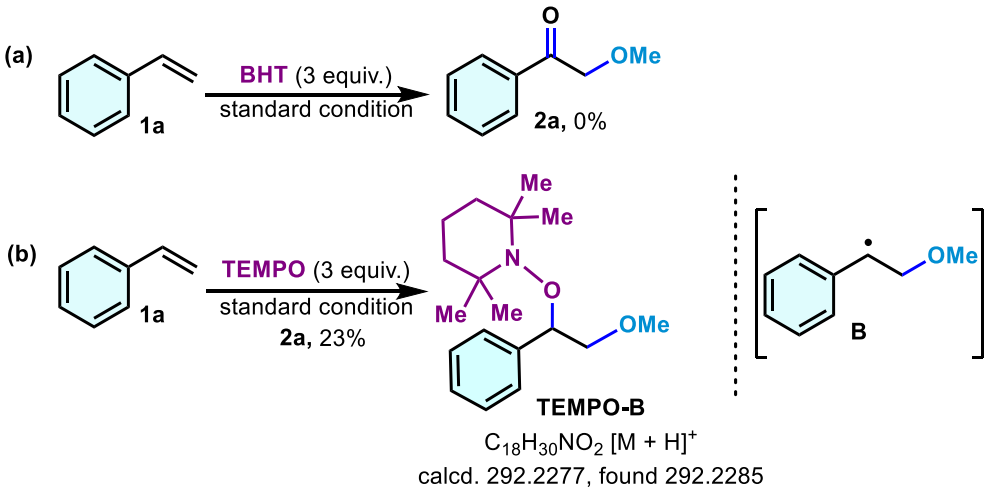

Scheme 3.16 Radical trapping experiment with BHT and TEMPO

The fluorescence quenching experiment of the excited state photocatalyst (Acr*) with styrene **1a** suggested the interaction of (Acr*) with styrene (Figure 3.3A). The ability of photoexcited photocatalyst Acr* to undergo Single Electron Transfer (SET) with styrene was further supported by the oxidation potential of styrene (E_{ox} = +1.84 V vs SCE) (Figure 3.3B), which is lower than the reduction potential of Acr* (E_{red*} = +2.08 V vs SCE).[24] Thus, implying the

possibility of reductive quenching cycle of photocatalyst.

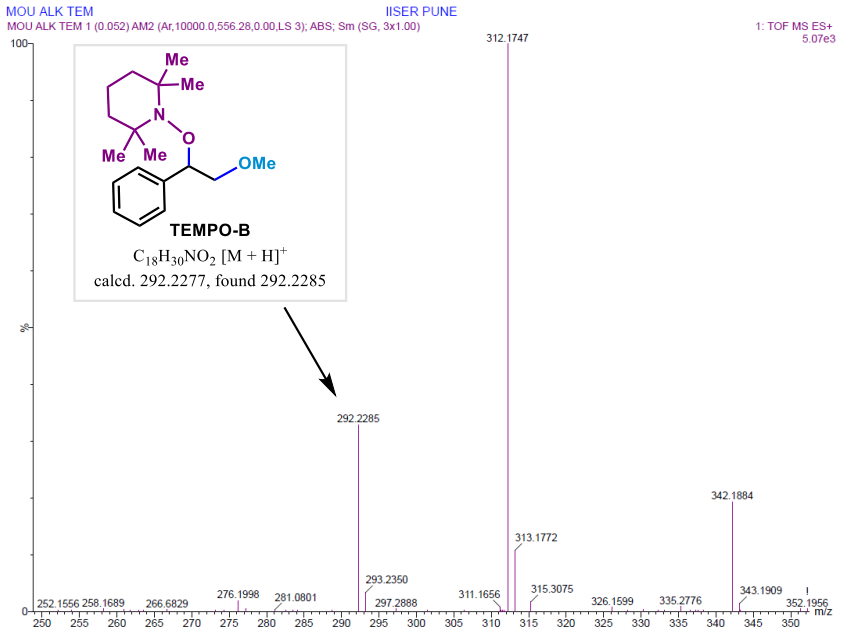

Figure 3.2 HRMS spectrum of radical adduct of **B** with TEMPO

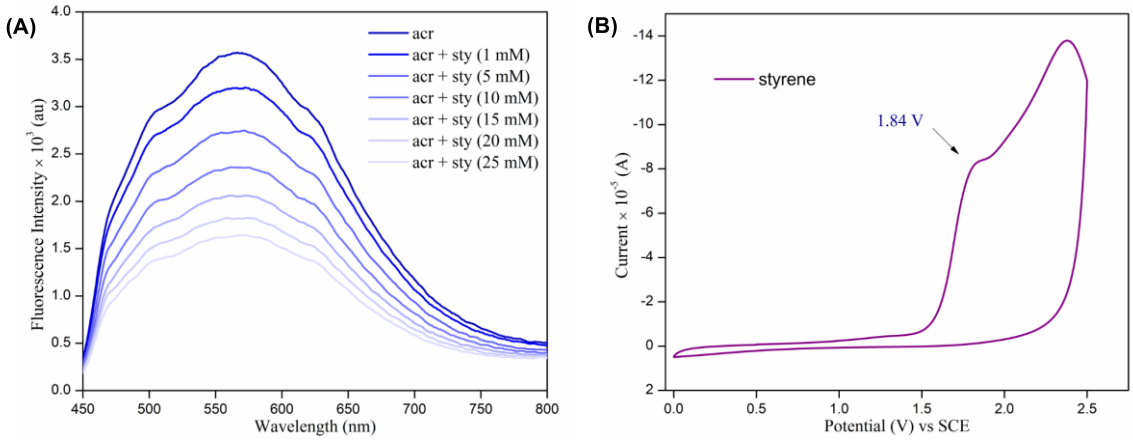

Figure 3.3 (A) Fluorescence spectra of Mes-Acr-Me$^+$ (10 μM) with increasing concentration of **1a**. (B) Cyclic voltammogram of styrene: E_p = +0.1.84 V (vs SCE in MeCN). Sample was prepared with 100 mM analyte and 100 mM $TBAPF_6$ electrolyte solution in MeCN with a scan rate of 100 mV/s. Cyclic voltammetry (CV) was performed using a CHI (model 600E) electrochemical analyzer/workstation. A three-electrode setup was used, consisting of a 3 mm dia. glassy carbon working electrode (Part no- CHI104, CH Instruments), platinum wire counter electrode (CHI115, CH Instruments), and a Calomel reference electrode (Part no-CHI150, CH Instruments).

Based on the control experiments, fluorescence quenching, cyclic voltammetric studies, and relevant literature precedents, a plausible reaction mechanism is proposed (Scheme 3.17).[31] Upon irradiation with blue light, the photocatalyst Acr is excited to its active state (Acr*). The excited Acr* species (E_{red*} = +2.08 V vs SCE) undergoes a single electron transfer (SET) with styrene **1a** (E_{ox} = +1.84 V vs SCE) via a reductive quenching pathway, resulting in the formation of Acr radical anion ($Acr^{\bullet-}$) and styrene radical cation **A**. This SET process is supported by the fluorescence quenching experiment and cyclic voltammetry data (Figure 3.3). The resulting $Acr^{\bullet-}$ then undergoes a subsequent single electron transfer (SET) with the molecular oxygen, superoxide radical anion ($O_2^{\bullet-}$), while simultaneously regenerating the ground-state Acr, thus completing the photocatalytic cycle. Meanwhile, the intermediate **A** reacts with methanol to form intermediate **B**. The radical adduct of intermediate **B** with TEMPO was detected by high-resolution mass spectrometry (HRMS), providing evidence for its formation. Subsequently, the intermediate **B** reacts with $O_2^{\bullet-}$ leading to intermediate **C,** which then undergoes protonation forming intermediate **D** and subsequent dehydration, ultimately leading to the formation of the desired α-alkoxylated ketone product **2a** (Scheme 3.17).

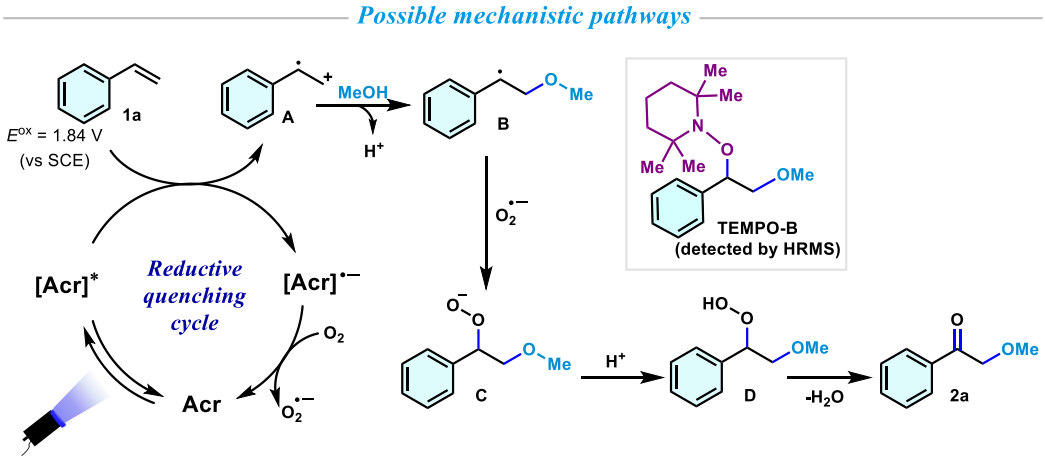

Scheme 3.17 Probable reaction mechanism for the formation of α-alkoxylated product

3.3 Conclusion

In summary, we have successfully demonstrated a transition metal-free, visible light promoted direct synthesis of α-alkoxylated ketone from readily available inexpensive feedstock chemical styrene at room temperature. A nontoxic and inexpensive acridinium organophotoredox catalyst has been utilized for the operationally simple and mild protocol. The methodology showed broad substrate scope with respect to styrene and alcohols. The post synthetic

modification of the synthesized product has been demonstrated for the synthesis of α-keto amide. Also, the protocol has been proved to be scalable on gram quantity and it works smoothly under direct exposure of sunlight. A series of control experiments, fluorescence quenching and cyclic voltammetry studies proved that transformation is driven via reductive quenching mechanistic cycle.

3.4 Experimental Section

3.4.1 General Details

Unless otherwise noted, all the starting materials and reagents were purchased from commercial suppliers (Sigma-Aldrich, TCI, Alfa Aesar, Spectrochem and BLD Pharm) and were used as received. Thin-layer chromatography (TLC) was performed using silica gel 60 GF_{254} precoated aluminum backed plates (2.5 mm). Visualization was accomplished by irradiation with UV light at 254 nm. The column chromatography was performed using silica gel (100–200 mesh) eluting with petroleum ether and ethyl acetate. The NMR spectra were recorded using tetramethylsilane as the internal standard. ^{1}H NMR spectra were recorded at 400 MHz, $^{19}F\{^{1}H\}$ NMR spectra were recorded at 377 MHz and $^{13}C\{^{1}H\}$ NMR spectra were recorded at 100 MHz (400 MHz Bruker and Jeol NMR instruments) unless otherwise noted. Chemical shifts (δ) are reported in ppm downfield from $CDCl_3$ (δ = 7.26 ppm) for ^{1}H NMR and relative to the central $CDCl_3$ resonance (δ = 77.16 ppm) for $^{13}C\{^{1}H\}$ NMR spectroscopy. For ^{1}H NMR, data are reported as follows: chemical shift, multiplicity (s = singlet, d = doublet, t = triplet, q = quartet, p = pentet, s = sextet, h = heptet, m = multiplet, br = broad), coupling constants (*J*) are given in Hz and integration. ^{13}C NMR spectra were recorded with complete proton decoupling. Mass samples were analyzed by high-resolution mass spectrometry (HRMS)-ESI TOF. Fluorescence emission spectra were obtained on a RF-6000 Spectrofluorophotometer from Shimadzu in a 3 mL, Hellma fluorescence cuvette (path length 1.0 cm). All photocatalytic reactions were performed under blue LEDs (Kessil PR160L series Blue LEDs. The reaction mixture was taken in a borosilicate glass and irradiated from 5 cm away from the LEDs. The reaction temperature is maintained 25-30 ^{o}C throughout the reaction by using external cooling fans.

List of starting materials used for the synthesis of *α*-alkoxylated ketones:

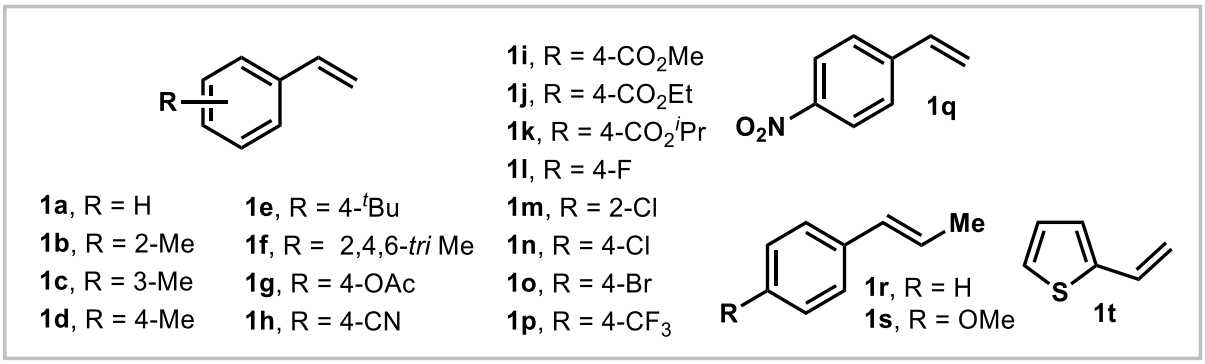

3.4.2 General Experimental Procedure

3.4.2A. General Procedure A (GP A) for the organophotoredox catalyzed synthesis of *α*-alkoxylated ketones **2**:

To an oven-dried reaction tube equipped with a stir bar styrene **1** (0.4 mmol, 1 equiv.), Mes-Acr-Me·BF_4 (3 mol %), and ROH (3 mL) were added. The reaction mixture was purged with O_2 balloon for 10 minutes. Then the reaction mixture was irradiated with 467 nm Kessil PR-160L Blue LED (50% intensity *i.e.* 20 W), from ~5 cm away under open air and stirred at room temperature (under the continuous flow of fan to maintain the temperature at 25–30 °C) for 4 h (monitored by TLC). After completion of the reaction, the reaction mixture was filtered and concentrated under vacuum to obtain the crude product. The crude residues were purified by column chromatography over silica gel using mixture of petroleum ether/EtOAc as an eluent to afford corresponding pure desired *α*-alkoxylated ketones **2.**

3.4.2B General Procedure B (GP B) Procedure for the synthesis of *α*-methoxylated ketone **2a** under the exposure of natural sunlight: To an oven-dried reaction tube equipped with a stir bar styrene **1a** (0.4 mmol, 1 equiv.), Mes-Acr-Me·BF_4 (3 mol %), and MeOH (3 mL) were added. The reaction mixture was purged with O_2 balloon for 10 minutes. Then the reaction mixture was stirred under natural sunlight for 4 h (monitored by TLC). After completion of the reaction, the reaction mixture was filtered and concentrated under vacuum to obtain the crude product. The crude residues were purified by column chromatography over silica gel using mixture of petroleum ether/EtOAc as an eluent to afford corresponding pure desired *α*-methoxylated ketone **2a** in 76%.

3.4.2C. General Procedure C (**GP C**) for the scale-up synthesis of *α*-methoxylated ketone **2a**: To an oven-dried 100 mL reaction flask equipped with a stir bar styrene **1a** (1g, 1 equiv.), Mes-Acr-Me·BF_4 (3 mol %), and MeOH (10 mL) were added. Then the reaction mixture was irradiated with Kessil PR-160L blue LEDs (467 nm, 100% intensity *i.e.* 40 W × 2), from ~5 cm away under open air and stirred at room temperature (under the continuous flow of fan to maintain the temperature at 25–30 °C) for 24 h (monitored by TLC). After completion of the reaction, the reaction mixture was filtered and concentrated under vacuum to obtain the crude product. The crude residues were purified by column chromatography over silica gel using mixture of petroleum ether/EtOAc as an eluent to afford corresponding pure desired *α*-methoxylated ketone **2a** in 68%.

3.4.3 Product Characterization Data

2-methoxy-1-phenylethan-1-one (**2a**): The compound **2a** was prepared following the General Procedure A (GP A). Colourless liquid (50 mg, 84% yield), R_f = 0.40 (petroleum ether/EtOAc 85:15). ^{1}H NMR (400 MHz, $CDCl_3$) δ 7.95 – 7.92 (m, 2H), 7.61 – 7.56 (m, 1H), 7.47 (dd, *J* = 8.3, 7.0 Hz, 2H), 4.71 (s, 2H), 3.51 (s, 3H). ^{13}C{^{1}H} NMR (100 MHz, $CDCl_3$) δ 196.3, 135.0, 133.7, 128.9, 128.0, 75.4, 59.6. HRMS (ESI-TOF) *m/z* for $C_9H_{10}NaO_2$, $[M + Na]^+$ calcd. 173.0578; found: 173.0575.

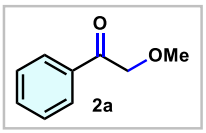

2-methoxy-1-phenylethan-1-one (**2b**): The compound **2b** was prepared following the General Procedure A (GP A). Colourless liquid (57 mg, 87% yield), R_f = 0.43 (petroleum ether/EtOAc 85:15). ^{1}H NMR (400 MHz, $CDCl_3$) δ 7.57 (dd, *J* = 7.7, 1.4 Hz, 1H), 7.40 (td, *J* = 7.5, 1.4 Hz, 1H), 7.30 – 7.25 (m, 2H), 4.56 (s, 2H), 3.49 (s, 3H), 2.52 (s, 3H). ^{13}C{^{1}H} NMR (100 MHz, $CDCl_3$) δ 200.4, 138.7, 135.4, 132.2, 131.9, 128.3, 125.8, 76.7, 59.5, 21.2. HRMS (ESI TOF) *m/z* for $C_{10}H_{12}NaO_2$ $[M + Na]^+$ calcd. 187.0735, found 187.0732.

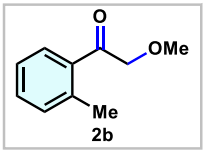

2-methoxy-1-(m-tolyl)ethan-1-one (**2c**): The compound **2c** was prepared following the General Procedure A (GP A). Colourless liquid (54 mg, 82% yield), R_f = 0.33 (petroleum ether/EtOAc 85:15). ^{1}H NMR (400 MHz, $CDCl_3$) δ 7.77 – 7.69 (m, 2H), 7.42 – 7.33 (m, 2H), 4.71 (s, 2H), 3.51 (s, 3H), 2.41 (s, 3H). ^{13}C{^{1}H} NMR (100 MHz, $CDCl_3$) δ 196.4, 138.8, 135.0, 134.5, 128.7, 128.4, 125.1, 75.4, 59.6,

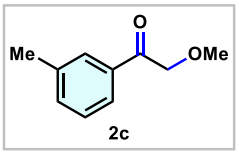

21.5. HRMS (ESI TOF) *m/z* for $C_{10}H_{12}NaO_2$ $[M + Na]^+$ calcd. 187.0735, found 187.0733.

2-methoxy-1-(p-tolyl)ethan-1-one (**2d**): The compound **2d** was prepared following the General Procedure A (GP A). Colourless liquid (56 mg, 85% yield), R_f = 0.33 (petroleum ether/EtOAc 85:15). ^{1}H NMR (400 MHz, $CDCl_3$) δ 7.87 – 7.81 (m, 2H), 7.29 – 7.23 (m, 2H), 4.68 (s, 2H), 3.50 (s, 3H), 2.41 (s, 3H). $^{13}C\{^1H\}$ NMR (100 MHz, $CDCl_3$) δ 195.9, 144.6, 132.5, 129.5, 128.1, 75.3, 59.6, 21.8. HRMS (ESI TOF) *m/z* for $C_{10}H_{12}NaO_2$ $[M + Na]^+$ calcd. 187.0735, found 187.0736.

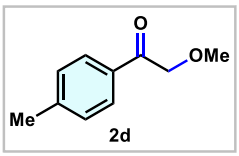

1-(4-(tert-butyl)phenyl)-2-methoxyethan-1-one (**2e**): The compound **2e** was prepared following the General Procedure A (GP A). Colourless liquid (70 mg, 79% yield), R_f = 0.43 (petroleum ether/EtOAc 85:15). ^{1}H NMR (400 MHz, $CDCl_3$) δ 7.89 – 7.86 (m, 2H), 7.50 – 7.46 (m, 2H), 4.69 (s, 2H), 3.50 (s, 3H), 1.34 (s, 9H). $^{13}C\{^1H\}$ NMR (100 MHz, $CDCl_3$) δ 195.9, 157.5, 132.4, 127.9, 125.8, 75.4, 59.6, 35.3, 31.2. HRMS (ESI TOF) *m/z* for $C_{13}H_{18}NaO_2$ $[M + Na]^+$ calcd. 229.1204, found 229.1207.

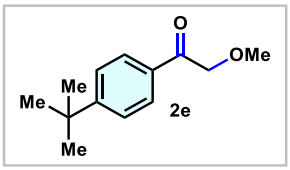

1-mesityl-2-methoxyethan-1-one (**2f**): The compound **2f** was prepared following the General Procedure A (GP A). Colourless liquid (41 mg, 53% yield), R_f = 0.46 (petroleum ether/EtOAc 85:15). ^{1}H NMR (400 MHz, $CDCl_3$) δ 6.84 (s, 2H), 4.30 (s, 2H), 3.49 (s, 3H), 2.28 (s, 3H), 2.22 (s, 6H). $^{13}C\{^1H\}$ NMR (100 MHz, $CDCl_3$) δ 207.6, 139.2, 136.1, 133.6, 128.6, 78.6, 59.5, 21.2, 19.1. HRMS (ESI TOF) *m/z* for $C_{12}H_{16}NaO_2$ $[M + Na]^+$ calcd. 215.1048, found 215.1045.

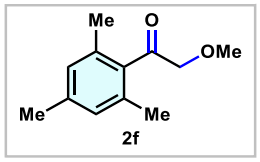

4-(2-methoxyacetyl)phenyl acetate (**2g**): The compound **2g** was prepared following the General Procedure A (GP A). Colourless liquid (63 mg, 76% yield), R_f = 0.23 (petroleum ether/EtOAc 75:25). ^{1}H NMR (400 MHz, $CDCl_3$) δ 8.00 – 7.97 (m, 2H), 7.23 – 7.19 (m, 2H), 4.68 (s, 2H), 3.50 (s, 3H), 2.33 (s, 3H). $^{13}C\{^1H\}$ NMR (100 MHz, $CDCl_3$) δ 195.2, 168.9, 154.8, 132.5, 129.7, 122.1, 75.4, 59.6, 21.3. HRMS (ESI TOF) *m/z* for $C_{11}H_{12}NaO_4$ $[M + Na]^+$ calcd. 231.0633, found 231.0639.

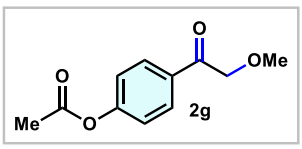

4-(2-methoxyacetyl)benzonitrile (**2h**): The compound **2h** was prepared following the General Procedure A (GP A). Colourless liquid (43 mg, 61% yield), R_f = 0.26 (petroleum ether/EtOAc 75:25). ^{1}H NMR (400 MHz, $CDCl_3$) δ 8.05 – 8.03 (m, 2H), 7.79 – 7.77 (m, 2H), 4.67 (s, 2H), 3.50 (s, 3H). $^{13}C\{^1H\}$ NMR (100 MHz, $CDCl_3$) δ 195.4, 137.9, 132.7, 128.7, 117.9, 117.0, 75.8, 59.7. HRMS (ESI TOF) *m/z* for $C_{10}H_9NNaO_2$ $[M + Na]^+$ calcd. 198.0531, found 198.0536.

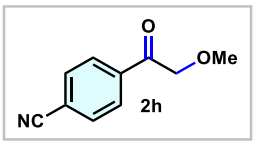

methyl 4-(2-methoxyacetyl)benzoate (**2i**): The compound **2i** was prepared following the General Procedure A (GP A). Colourless liquid (74 mg, 89% yield), R_f = 0.20 (petroleum ether/EtOAc 85:15). ^{1}H NMR (400 MHz, $CDCl_3$) δ 8.17 – 8.11 (m, 2H), 8.02 – 7.95 (m, 2H), 4.71 (s, 2H), 3.95 (s, 3H), 3.51 (s, 3H). $^{13}C\{^1H\}$ NMR (100 MHz, $CDCl_3$) δ 196.0, 166.2, 138.1, 134.4, 130.1, 128.0, 75.7, 59.7, 52.7. HRMS (ESI TOF) *m/z* for $C_{11}H_{12}NaO_4$ $[M + Na]^+$ calcd. 231.0633, found 231.0639.

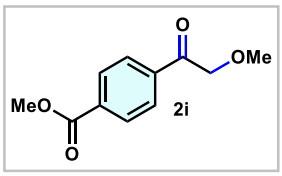

ethyl 4-(2-methoxyacetyl)benzoate (**2j**): The compound **2j** was prepared following the General Procedure A (GP A). Colourless liquid (80 mg, 90% yield), R_f = 0.26 (petroleum ether/EtOAc 85:15). ^{1}H NMR (400 MHz, $CDCl_3$) δ 8.12 (d, *J* = 8.4 Hz, 2H), 7.97 (d, *J* = 8.5 Hz, 2H), 4.71 (s, 2H), 4.40 (q, *J* = 7.1 Hz, 2H), 3.50 (s, 3H), 1.40 (t, *J* = 7.1 Hz, 3H). $^{13}C\{^1H\}$ NMR (100 MHz, $CDCl_3$) δ 196.0, 165.7, 138.0, 134.8, 130.0, 127.9, 75.6, 61.6, 59.6, 14.4. HRMS (ESI TOF) *m/z* for $C_{12}H_{14}NaO_4$ $[M + Na]^+$ calcd. 245.0790, found 245.0791.

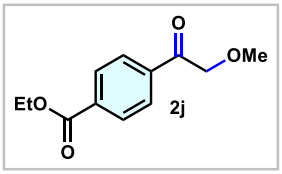

isopropyl 4-(2-methoxyacetyl)benzoate (**2k**): The compound **2k** was prepared following the General Procedure A (GP A). Colourless liquid (87 mg, 92% yield), R_f = 0.33 (petroleum ether/EtOAc 85:15). ^{1}H NMR (400 MHz, $CDCl_3$) δ 8.12 (d, *J* = 8.4 Hz, 2H), 7.97 (d, *J* = 8.4 Hz, 2H), 5.27 (p, *J* = 6.3 Hz, 1H), 4.71 (s, 2H), 3.51 (s, 3H), 1.38 (d, *J* = 6.2 Hz, 6H). $^{13}C\{^1H\}$ NMR (100 MHz, $CDCl_3$) δ 196.1, 165.2, 138.0, 135.2, 130.0, 127.9, 75.6, 69.3, 59.6, 22.0. HRMS (ESI TOF) *m/z* for $C_{13}H_{16}NaO_4$ $[M + Na]^+$ calcd. 259.0946, found 259.0951.

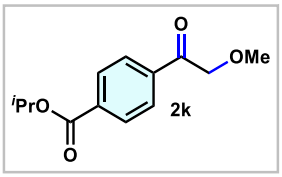

1-(4-fluorophenyl)-2-methoxyethan-1-one (**2l**): The compound **2l** was prepared following the

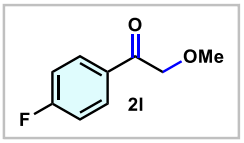

General Procedure A (GP A). Colourless liquid (42 mg, 62% yield), R_f = 0.30 (petroleum ether/EtOAc 85:15). ^{1}H NMR (400 MHz, $CDCl_3$) δ 8.01 – 7.96 (m, 2H), 7.17 – 7.12 (m, 2H), 4.66 (s, 2H), 3.50 (s, 3H). $^{13}C\{^1H\}$ NMR (100 MHz, $CDCl_3$) δ 194.9, 166.1 (d, J = 255.4 Hz), 130.8 (d, J = 9.3 Hz), 130.4 (d, J = 7.7 Hz), 116.0 (d, J = 22.0 Hz), 75.5, 59.6. $^{19}F\{^1H\}$ NMR (377 MHz, $CDCl_3$) δ -104.03. HRMS (ESI TOF) *m/z* for $C_9H_9FNaO_2$ $[M + Na]^+$ calcd. 191.0484, found 191.0488.

1-(2-chlorophenyl)-2-methoxyethan-1-one (**2m**): The compound **2m** was prepared following

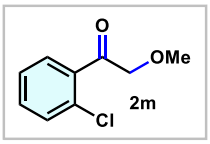

the General Procedure A (GP A). Colourless liquid (64 mg, 86% yield), R_f = 0.36 (petroleum ether/EtOAc 85:15). ^{1}H NMR (400 MHz, $CDCl_3$) δ 7.55 – 7.50 (m, 1H), 7.44 – 7.40 (m, 2H), 7.34 (ddd, J = 7.5, 5.3, 3.4 Hz, 1H), 4.59 (s, 2H), 3.48 (s, 3H). $^{13}C\{^1H\}$ NMR (100 MHz, $CDCl_3$) δ 200.1, 136.9, 132.4, 131.5, 130.6, 129.6, 127.1, 77.7, 59.6. HRMS (ESI TOF) *m/z* for $C_9H_9ClNaO_2$ $[M + Na]^+$ calcd. 207.0189, found 207.0182.

1-(4-chlorophenyl)-2-methoxyethan-1-one (**2n**): The compound **2n** was prepared following the

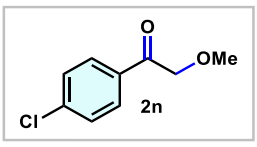

General Procedure A (GP A). Colourless liquid (65 mg, 88% yield), R_f = 0.36 (petroleum ether/EtOAc 85:15). ^{1}H NMR (400 MHz, $CDCl_3$) δ 7.90 – 7.87 (m, 2H), 7.46 – 7.42 (m, 2H), 4.65 (s, 2H), 3.49 (s, 3H). $^{13}C\{^1H\}$ NMR (100 MHz, $CDCl_3$) δ 195.3, 140.1, 133.2, 129.5, 129.2, 75.5, 59.6. HRMS (ESI TOF) *m/z* for $C_9H_9ClNaO_2$ $[M + Na]^+$ calcd. 207.0189, found 207.0185.

1-(4-bromophenyl)-2-methoxyethan-1-one (**2o**): The compound **2o** was prepared following the

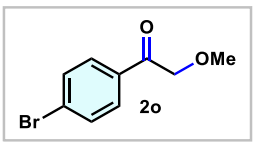

General Procedure A (GP A). Colourless liquid (80 mg, 87% yield), R_f = 0.33 (petroleum ether/EtOAc 85:15). ^{1}H NMR (400 MHz, $CDCl_3$) δ 7.84 – 7.79 (m, 2H), 7.64 – 7.60 (m, 2H), 4.65 (s, 2H), 3.50 (s, 3H). $^{13}C\{^1H\}$ NMR (100 MHz, $CDCl_3$) δ 195.5, 133.7, 132.2, 129.6, 128.9, 75.5, 59.6. HRMS (ESI TOF) *m/z* for $C_9H_9BrNaO_2$ $[M + Na]^+$ calcd. 250.9684, found 250.9689.

2-methoxy-1-(4-(trifluoromethyl)phenyl)ethan-1-one (**2p**): The compound **2p** was prepared following the General Procedure A (GP A). Colourless liquid (57 mg, 65% yield), R_f = 0.20 (petroleum ether/EtOAc 90:10). ^{1}H NMR (400 MHz, $CDCl_3$) δ 8.06 (d, *J* = 8.1 Hz, 2H), 7.75 (d, *J* = 8.3 Hz, 2H), 4.70 (s, 2H), 3.51 (s, 3H). $^{13}C\{^1H\}$ NMR (100 MHz, $CDCl_3$) δ 195.7, 137.6, 129.4, 128.5, 125.9 (q, *J* = 3.8 Hz), 124.3 (q, *J* = 273.2 Hz), 75.7, 59.7. $^{19}F\{^1H\}$ NMR (377 MHz, $CDCl_3$) δ -63.24. HRMS (ESI TOF) *m/z* for $C_{10}H_9F_3NaO_2$ $[M + Na]^+$ calcd. 241.0452, found 241.0456.

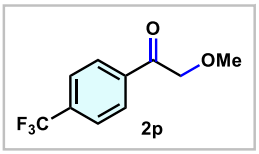

2,2-dimethoxy-1-(4-nitrophenyl)ethan-1-one (**2q**): The compound **2q** was prepared following the General Procedure A (GP A). Colourless liquid (61 mg, 68% yield), R_f = 0.39 (petroleum ether/EtOAc 85:15). ^{1}H NMR (400 MHz, $CDCl_3$) δ 8.24 – 8.21 (m, 2H), 7.66 – 7.62 (m, 2H), 5.47 (s, 1H), 3.34 (s, 6H). $^{13}C\{^1H\}$ NMR (100 MHz, $CDCl_3$) δ 148.1, 145.2, 130.9, 128.0, 123.6, 101.7, 52.8. HRMS (ESI TOF) *m/z* for $C_{10}H_{11}NNaO_5$ $[M + Na]^+$ calcd. 248.0535, found 248.0531.

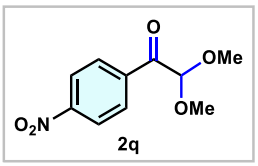

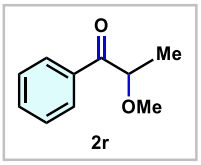

2-methoxy-1-phenylpropan-1-one (**2r**): The compound **2r** was prepared following the General Procedure A (GP A). Colourless liquid (27 mg, 41% yield), R_f = 0.48 (petroleum ether/EtOAc 85:15). ^{1}H NMR (400 MHz, $CDCl_3$) δ 8.09 – 8.02 (m, 2H), 7.62 – 7.55 (m, 1H), 7.48 (dd, *J* = 8.3, 7.0 Hz, 2H), 4.63 (q, *J* = 6.9 Hz, 1H), 3.39 (s, 3H), 1.49 (d, *J* = 6.9 Hz, 3H). $^{13}C\{^1H\}$ NMR (100 MHz, $CDCl_3$) δ 200.7, 133.5, 130.4, 128.9, 128.8, 80.4, 57.4, 18.6. HRMS (ESI TOF) *m/z* for $C_{10}H_{12}NaO_2$ $[M + Na]^+$ calcd. 187.0735, found 187.0733.

2-methoxy-1-(4-methoxyphenyl)propan-1-one (**2s**): The compound **2s** was prepared following the General Procedure A (GP A). Colourless liquid (25 mg, 32% yield), R_f = 0.20 (petroleum ether/EtOAc 90:10). ^{1}H NMR (400 MHz, $CDCl_3$) δ 8.08 – 8.05 (m, 2H), 6.96 – 6.92 (m, 2H), 4.56 (q, *J* = 6.9 Hz, 1H), 3.88 (s, 3H), 3.37 (s, 3H), 1.48 (d, *J* = 6.8 Hz, 3H). $^{13}C\{^1H\}$ NMR (100 MHz, $CDCl_3$) δ 199.3, 163.8, 131.3, 127.9, 113.9, 80.5, 57.4, 55.6, 18.9. HRMS (ESI TOF) *m/z* for $C_{11}H_{14}NaO_3$ $[M + Na]^+$ calcd. 217.0841, found 217.0847.

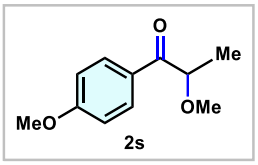

2-methoxy-1-(thiophen-2-yl)ethan-1-one (**2t**): The compound **2t** was prepared following the General Procedure A (GP A). Colourless liquid (27 mg, 43% yield), R_f = 0.27 (petroleum ether/EtOAc 85:15). ^{1}H NMR (400 MHz, $CDCl_3$) δ 7.85 (dd, *J* = 3.8, 1.1 Hz, 1H), 7.68 (dd, *J* = 4.9, 1.1 Hz, 1H), 7.15 (dd, *J* = 5.0, 3.8 Hz, 1H), 4.55 (s, 2H), 3.51 (s, 3H). ^{13}C{^{1}H} NMR (100 MHz, $CDCl_3$) δ 189.9, 141.1, 134.1, 132.6, 128.2, 75.9, 59.7. HRMS (ESI TOF) *m/z* for $C_7H_8NaO_2S$ [M + Na]$^+$ calcd. 179.0143, found 179.0140.

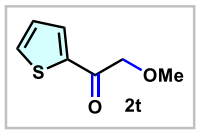

2-ethoxy-1-phenylethan-1-one (**2u**): The compound **2u** was prepared following the General Procedure A (GP A). Colourless liquid (48 mg, 73% yield), R_f = 0.42 (petroleum ether/EtOAc 85:15). ^{1}H NMR (400 MHz, $CDCl_3$) δ 7.96 – 7.93 (m, 2H), 7.60 – 7.56 (m, 1H), 7.49 – 7.44 (m, 2H), 4.74 (s, 2H), 3.65 (q, *J* = 7.0 Hz, 2H), 1.29 (t, *J* = 7.0 Hz, 3H). ^{13}C{^{1}H} NMR (100 MHz, $CDCl_3$) δ 196.7, 135.1, 133.6, 128.8, 128.0, 73.7, 67.4, 15.2. HRMS (ESI TOF) *m/z* for $C_{10}H_{12}NaO_2$ [M + Na]$^+$ calcd. 187.0735, found 187.0739.

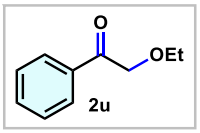

1-phenyl-2-propoxyethan-1-one (**2v**): The compound **2v** was prepared following the General Procedure A (GP A). Colourless liquid (44 mg, 62% yield), R_f = 0.34 (petroleum ether/EtOAc 85:15). ^{1}H NMR (400 MHz, $CDCl_3$) δ 7.96 – 7.94 (m, 2H), 7.60 – 7.56 (m, 1H), 7.49 – 7.44 (m, 2H), 4.73 (s, 2H), 3.54 (t, *J* = 6.7 Hz, 2H), 1.68 (h, *J* = 7.2 Hz, 2H), 0.95 (t, *J* = 7.4 Hz, 3H). ^{13}C{^{1}H} NMR (100 MHz, $CDCl_3$) δ 196.9, 135.2, 133.6, 128.8, 128.1, 74.0, 73.7, 23.0, 10.6. HRMS (ESI TOF) *m/z* for $C_{11}H_{14}NaO_2$ [M + Na]$^+$ calcd. 201.0891, found 201.0893.

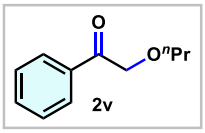

2-isopropoxy-1-phenylethan-1-one (**2w**): The compound **2w** was prepared following the General Procedure A (GP A). Colourless liquid (48 mg, 68% yield), R_f = 0.32 (petroleum ether/EtOAc 85:15). ^{1}H NMR (400 MHz, $CDCl_3$) δ 7.97 – 7.94 (m, 2H), 7.60 – 7.55 (m, 1H), 7.49 – 7.44 (m, 2H), 4.73 (s, 2H), 3.73 (hept, *J* = 6.2 Hz, 1H), 1.25 (d, *J* = 6.1 Hz, 6H). ^{13}C{^{1}H} NMR (100 MHz, $CDCl_3$) δ 197.1, 135.3, 133.5, 128.8, 128.2, 72.8, 71.5, 22.0. HRMS (ESI TOF) *m/z* for $C_{11}H_{14}NaO_2$ [M + Na]$^+$ calcd. 201.0891, found 201.0895.

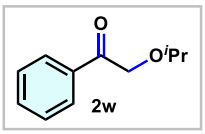

2-butoxy-1-phenylethan-1-one (**2x**): The compound **2x** was prepared following the General Procedure A (GP A). Colourless liquid (45 mg, 58% yield), R_f = 0.41 (petroleum ether/EtOAc 90:10). ^{1}H NMR (400 MHz, $CDCl_3$) δ 7.96 – 7.94 (m, 2H), 7.60 – 7.56 (m, 1H), 7.49 – 7.44 (m, 2H), 4.72 (s, 2H), 3.57 (t, *J* = 6.6 Hz, 2H), 1.68 – 1.61 (m, 2H), 1.40 (dq, *J* = 14.7, 7.4 Hz, 2H), 0.92 (t, *J* = 7.4 Hz, 3H). ^{13}C{^{1}H} NMR (100 MHz, $CDCl_3$) δ 196.9, 135.2, 133.6, 128.8, 128.1, 74.0, 71.9, 31.8, 19.4, 14.0. HRMS (ESI TOF) *m/z* for $C_{12}H_{16}NaO_2$ $[M + Na]^+$ calcd. 215.1048, found 215.1053.

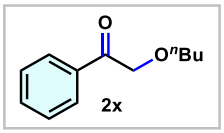

2-(tert-butoxy)-1-phenylethan-1-one (**2y**): The compound **2y** was prepared following the General Procedure A (GP A). Colourless liquid (46 mg, 60% yield), R_f = 0.41 (petroleum ether/EtOAc 90:10). ^{1}H NMR (400 MHz, $CDCl_3$) δ 8.03 – 7.91 (m, 2H), 7.62 – 7.52 (m, 1H), 7.50 – 7.43 (m, 2H), 4.66 (s, 2H), 1.28 (s, 9H). ^{13}C{^{1}H} NMR (100 MHz, $CDCl_3$) δ 197.3, 135.6, 133.3, 128.7, 128.3, 74.7, 66.4, 27.6. HRMS (ESI TOF) *m/z* for $C_{12}H_{16}NaO_2$ $[M + Na]^+$ calcd. 215.1048, found 215.1051.

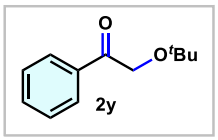

1-phenyl-2-(piperidin-1-yl)ethane-1,2-dione (**4a**): The compound **4a** was prepared following the reported literature procedure.[27] Brown solid (56 mg, 78% yield), R_f = 0.37 (petroleum ether/EtOAc 75:25). ^{1}H NMR (400 MHz, $CDCl_3$) δ 7.96 – 7.93 (m, 2H), 7.66 – 7.61 (m, 1H), 7.51 (t, *J* = 7.7 Hz, 2H), 3.72 – 3.69 (m, 2H), 3.30 – 3.27 (m, 2H), 1.69 (p, *J* = 2.9 Hz, 4H), 1.57 – 1.51 (m, 2H). ^{13}C{^{1}H} NMR (100 MHz, $CDCl_3$) δ 192.1, 165.6, 134.8, 133.4, 129.7, 129.1, 47.2, 42.3, 26.3, 25.6, 24.5. HRMS (ESI TOF) *m/z* for $C_{13}H_{16}NO_2$ $[M + H]^+$ calcd. 218.1181, found 218.1183.

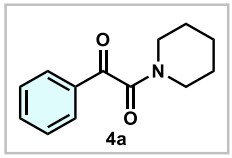

3.4.4 Appendix III. ^{1}H and $^{13}C\{^{1}H\}$ NMR spectral data of representative compounds

Compound No.	Figure III.X	Data	Page No.
2a	Figure III.1 and III.2	^{1}H and $^{13}C\{^{1}H\}$	119
2f	Figure III.3 and III.4	^{1}H and $^{13}C\{^{1}H\}$	120
2h	Figure III.5 and III.6	^{1}H and $^{13}C\{^{1}H\}$	121
2s	Figure III.7 and III.8	^{1}H and $^{13}C\{^{1}H\}$	122
2t	Figure III.9 and III.10	^{1}H and $^{13}C\{^{1}H\}$	123
2u	Figure III.11 and III.12	^{1}H and $^{13}C\{^{1}H\}$	124
2v	Figure III.13 and III.14	^{1}H and $^{13}C\{^{1}H\}$	125
2w	Figure III.15 and III.16	^{1}H and $^{13}C\{^{1}H\}$	126
2x	Figure III.17 and III.18	^{1}H and $^{13}C\{^{1}H\}$	127
4a	Figure III.19 and III.20	^{1}H and $^{13}C\{^{1}H\}$	128

3.4.5 Copies of ^{1}H and $^{13}C\{^{1}H\}$ NMR Spectra

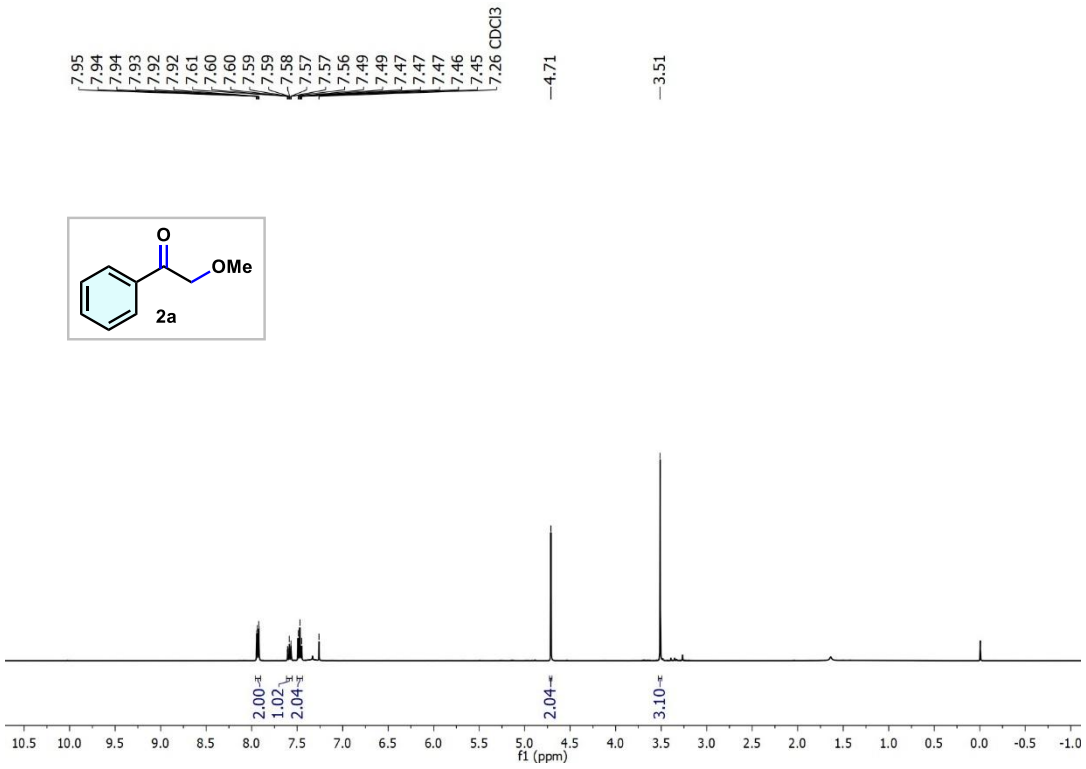

Figure III.1 ^{1}H NMR spectrum of **2a**, $CDCl_3$, 400 MHz

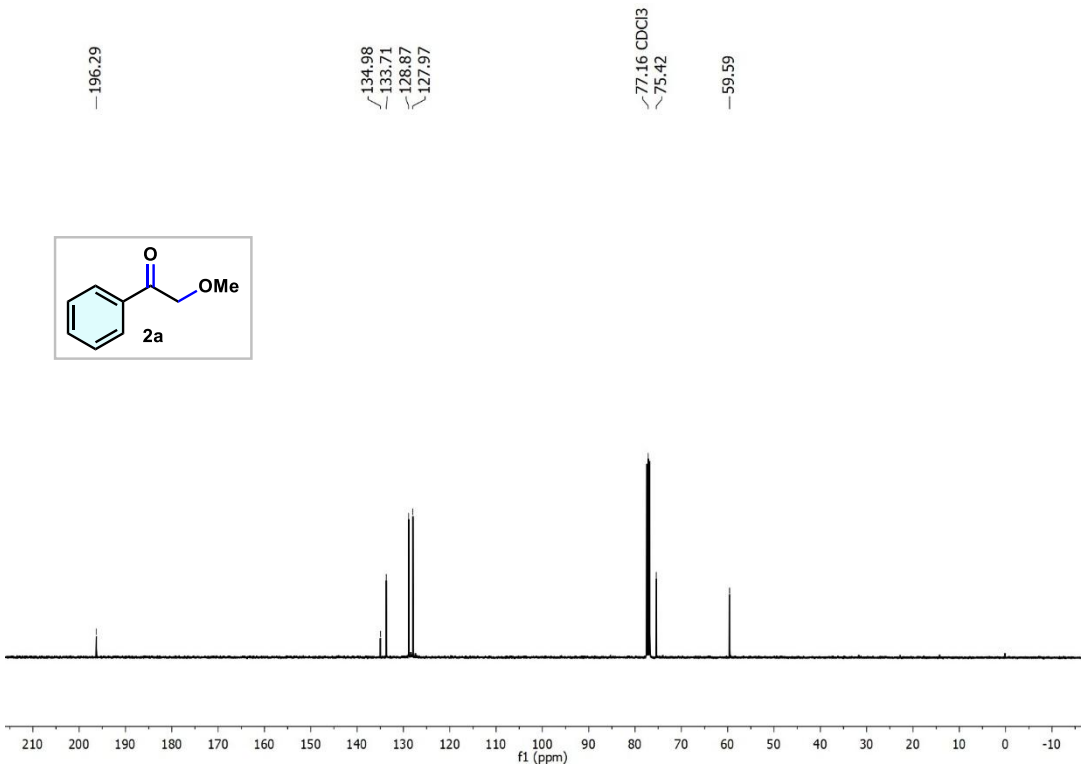

Figure III.2 $^{13}C\{^{1}H\}$ NMR spectrum of **2a**, $CDCl_3$, 100 MHz

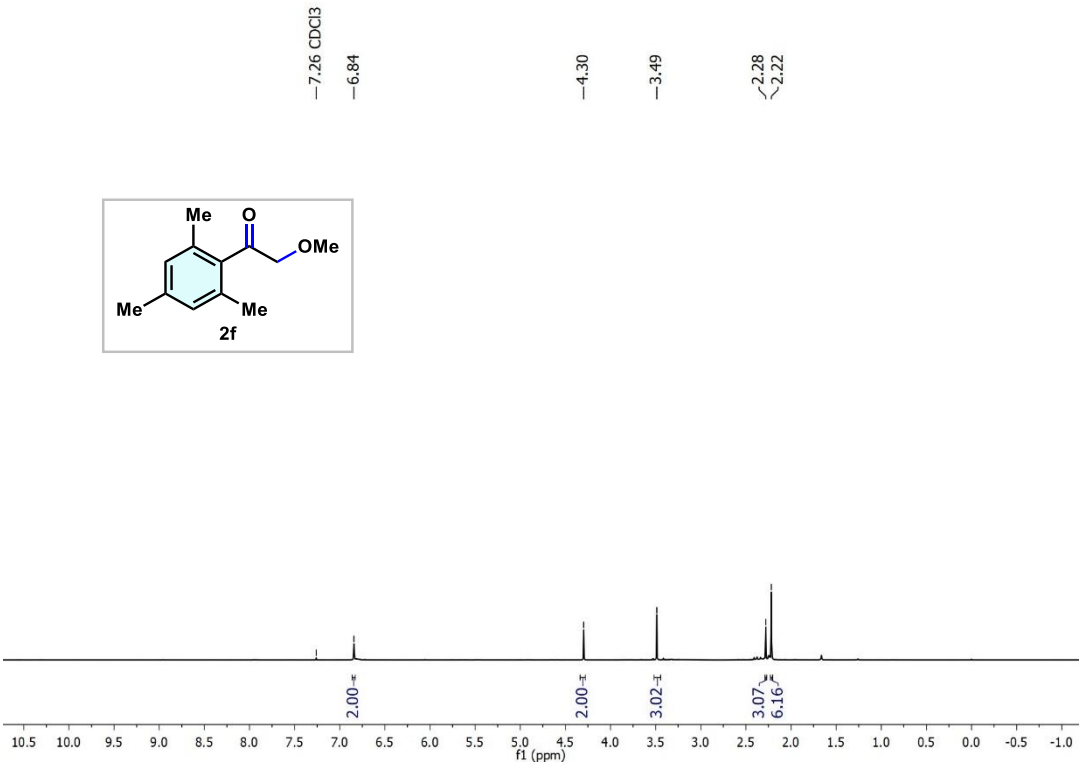

Figure III.3 ^{1}H NMR spectrum of **2f**, $CDCl_3$, 400 MHz

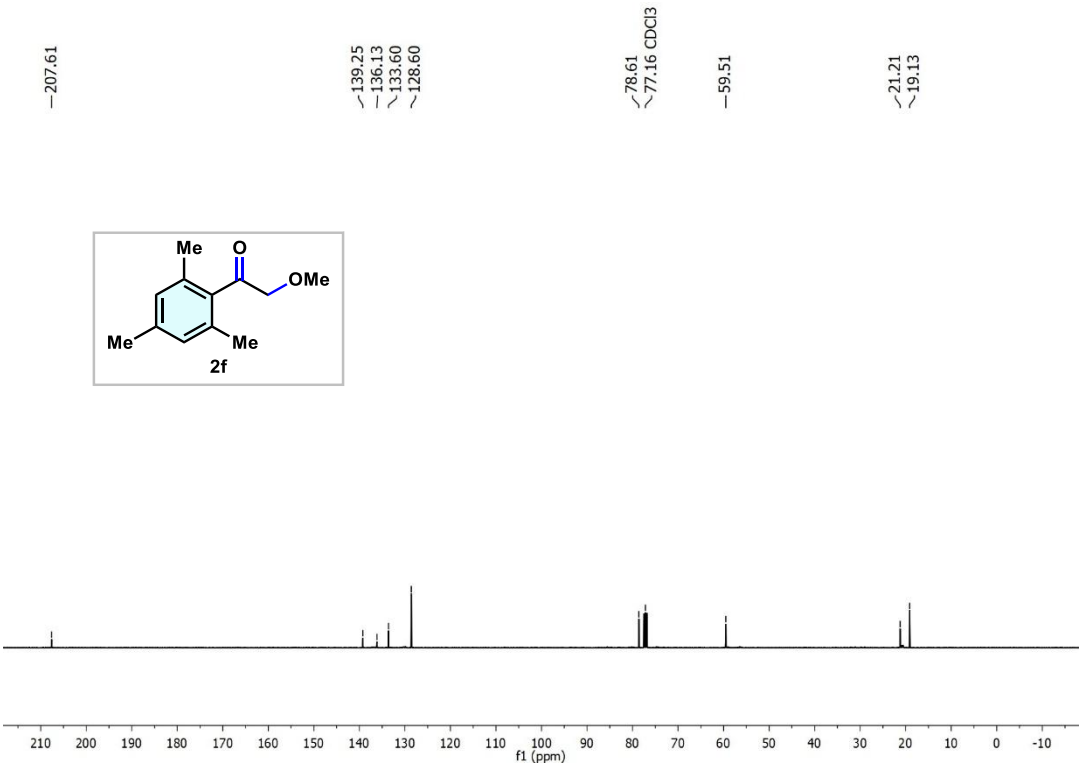

Figure III.4 $^{13}C\{^{1}H\}$ NMR spectrum of **2f**, $CDCl_3$, 100 MHz

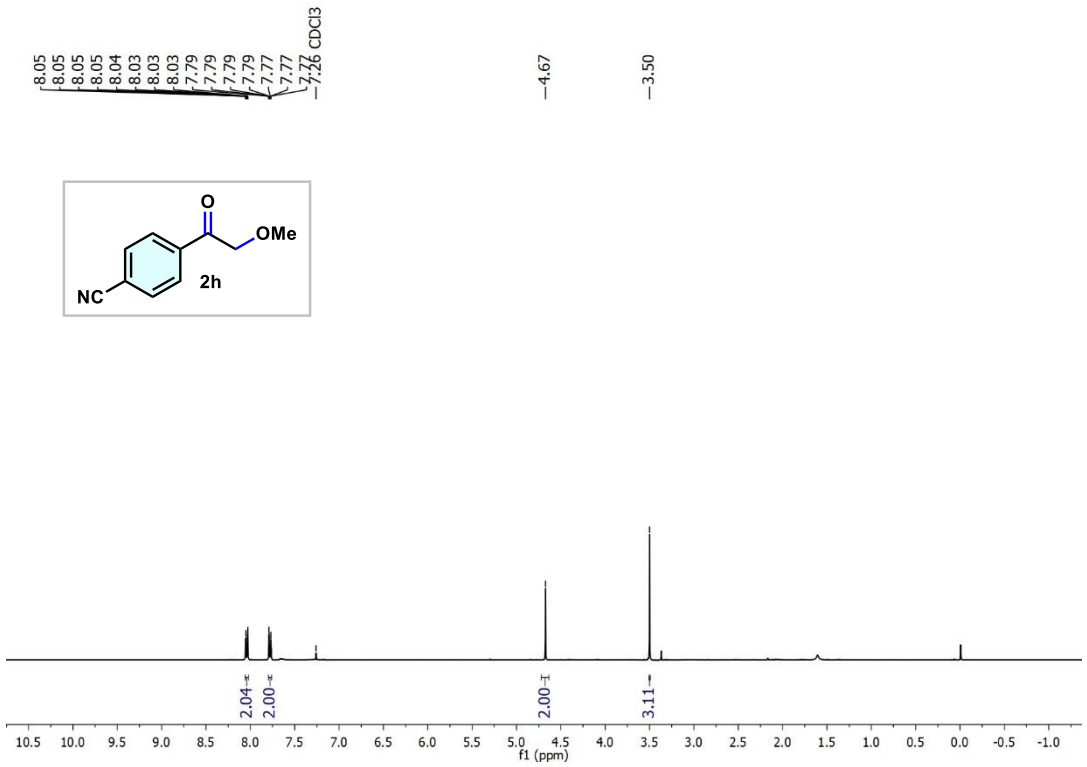

Figure III.5 ^{1}H NMR spectrum of **2h**, $CDCl_3$, 400 MHz

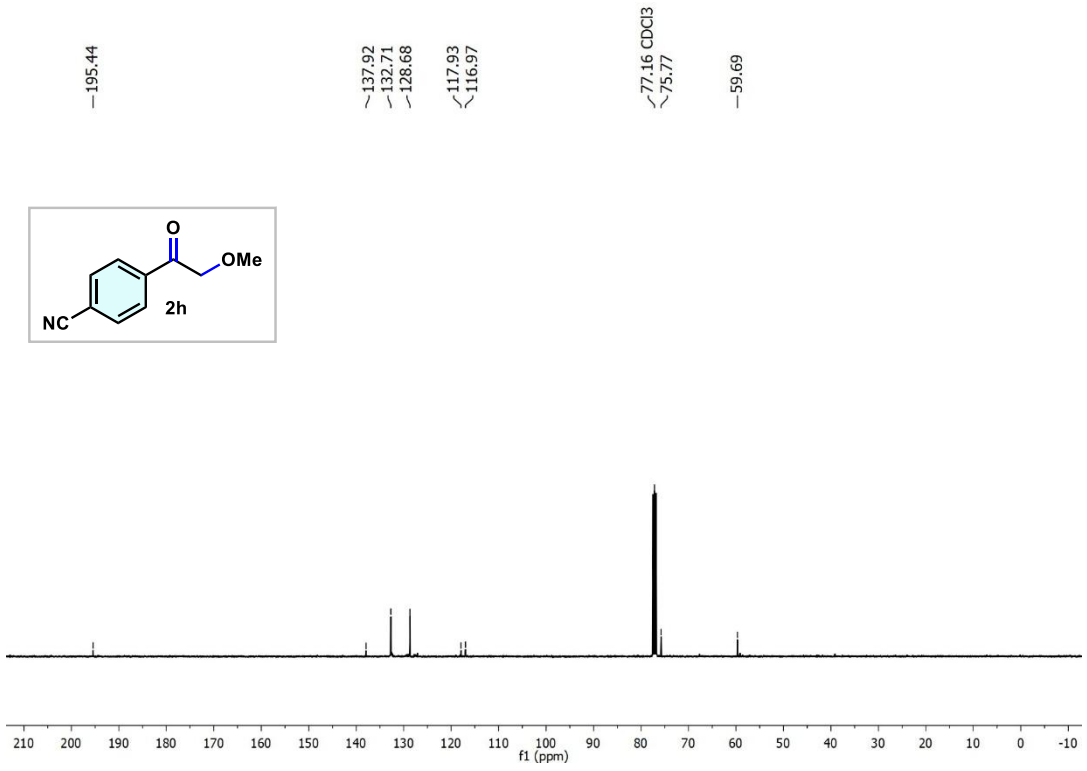

Figure III.6 $^{13}C\{^{1}H\}$ NMR spectrum of **2h**, $CDCl_3$, 100 MHz

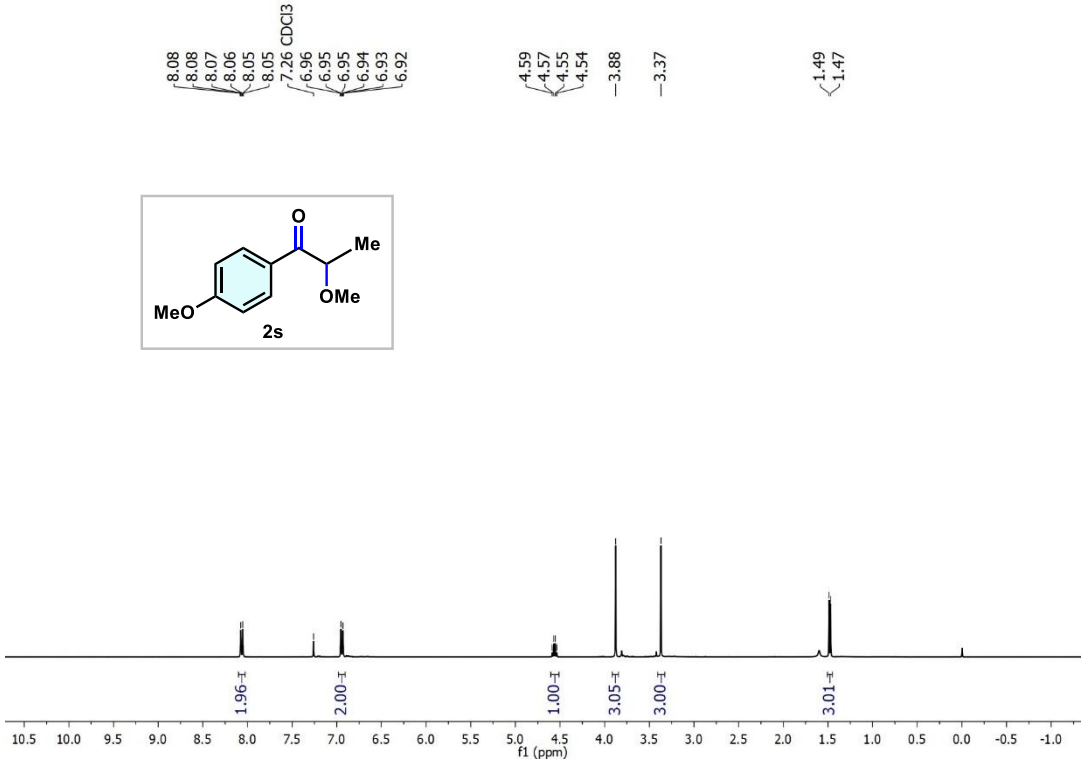

Figure III.7 ^{1}H NMR spectrum of **2s**, $CDCl_3$, 400 MHz

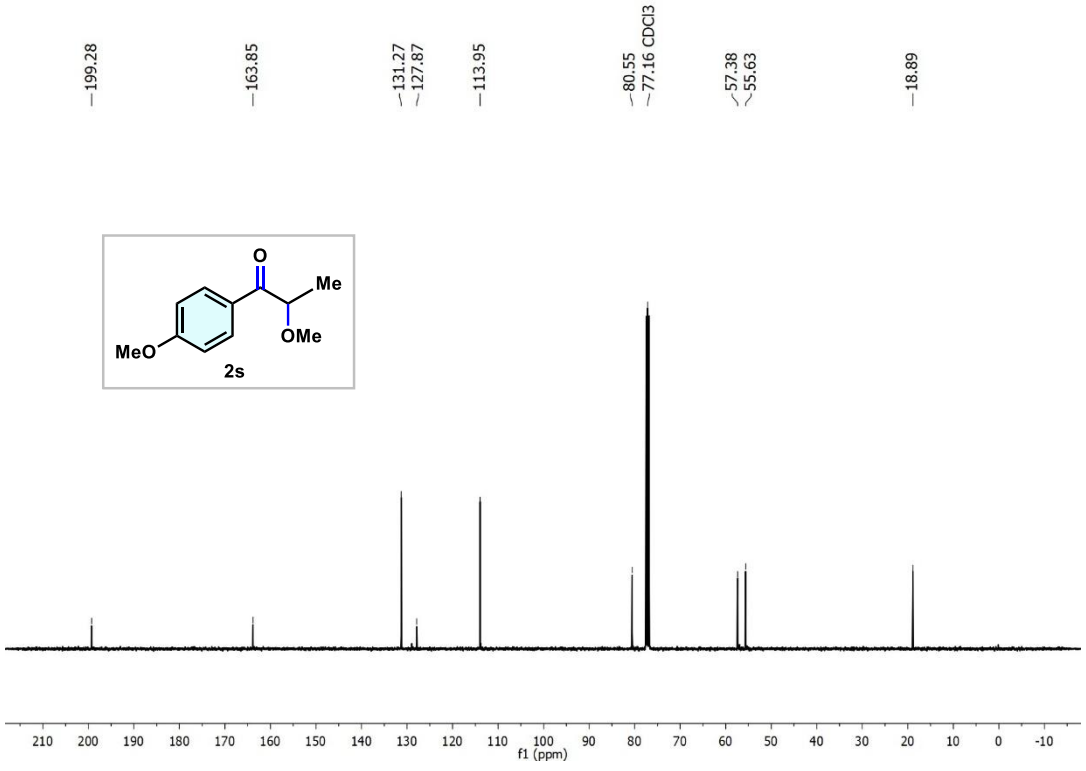

Figure III.8 $^{13}C\{^{1}H\}$ NMR spectrum of **2s**, $CDCl_3$, 100 MHz

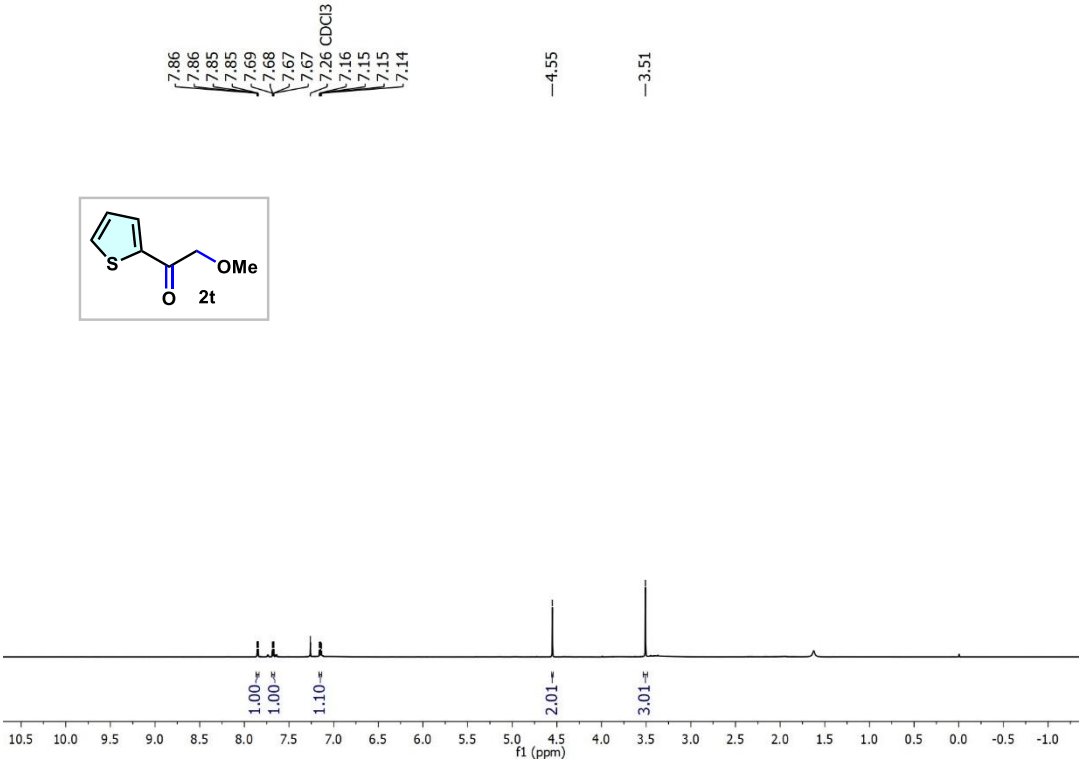

Figure III.9 ^{1}H NMR spectrum of **2t**, $CDCl_3$, 400 MHz

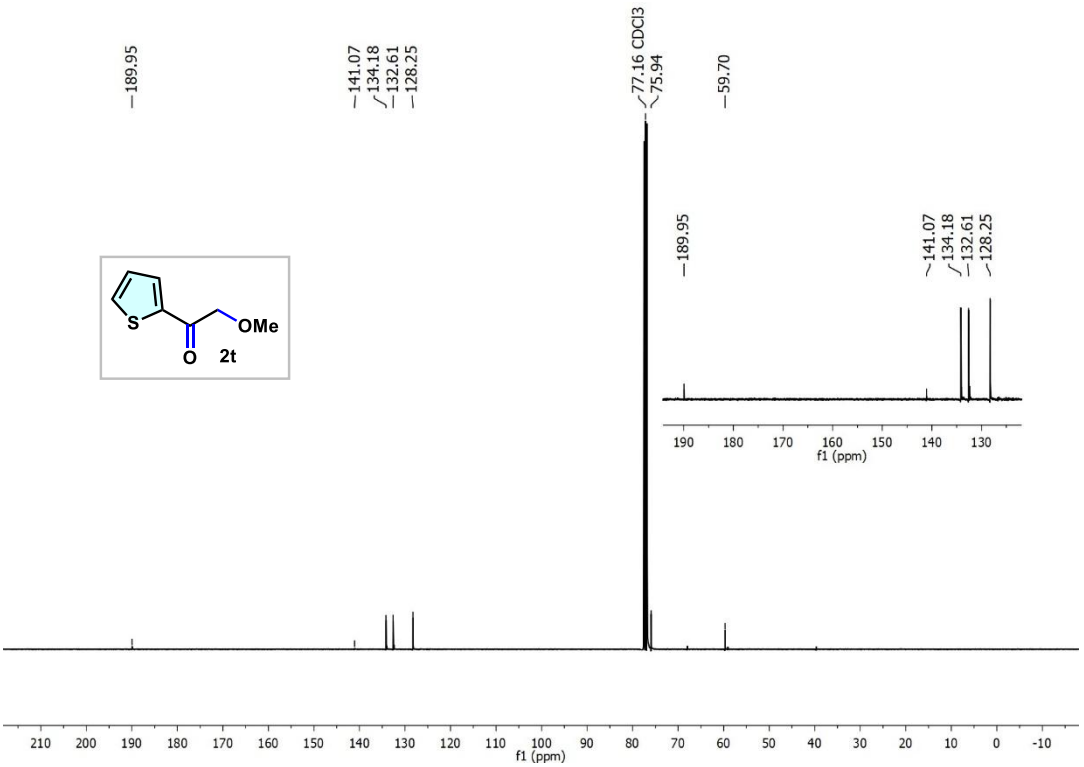

Figure III.10 ^{13}C{^{1}H} NMR spectrum of **2t**, $CDCl_3$, 100 MHz

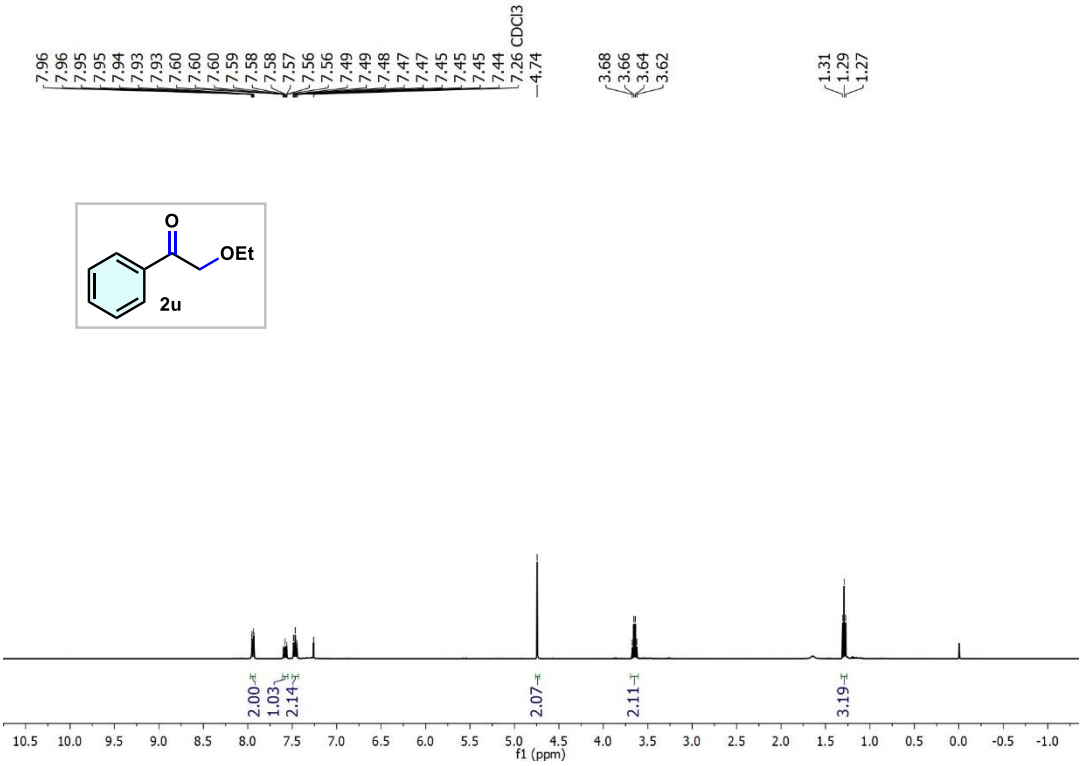

Figure III.11 ^{1}H NMR spectrum of **2u**, $CDCl_3$, 400 MHz

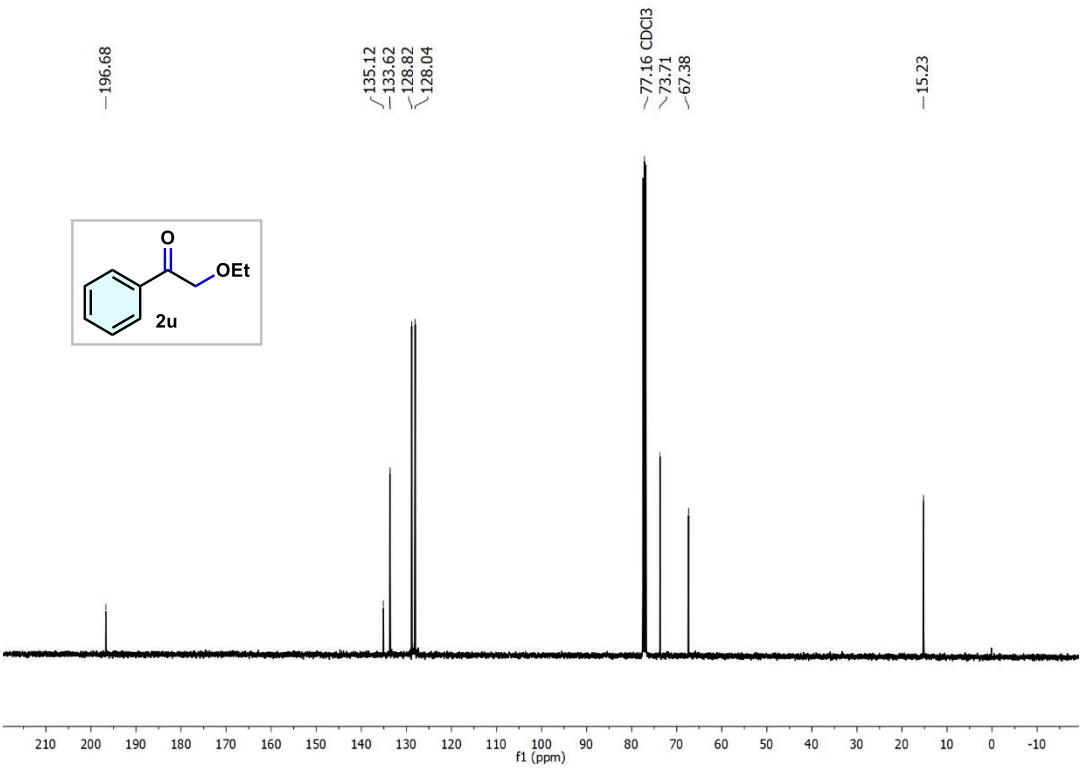

Figure III.12 $^{13}C\{^{1}H\}$ NMR spectrum of **2u**, $CDCl_3$, 100 MHz

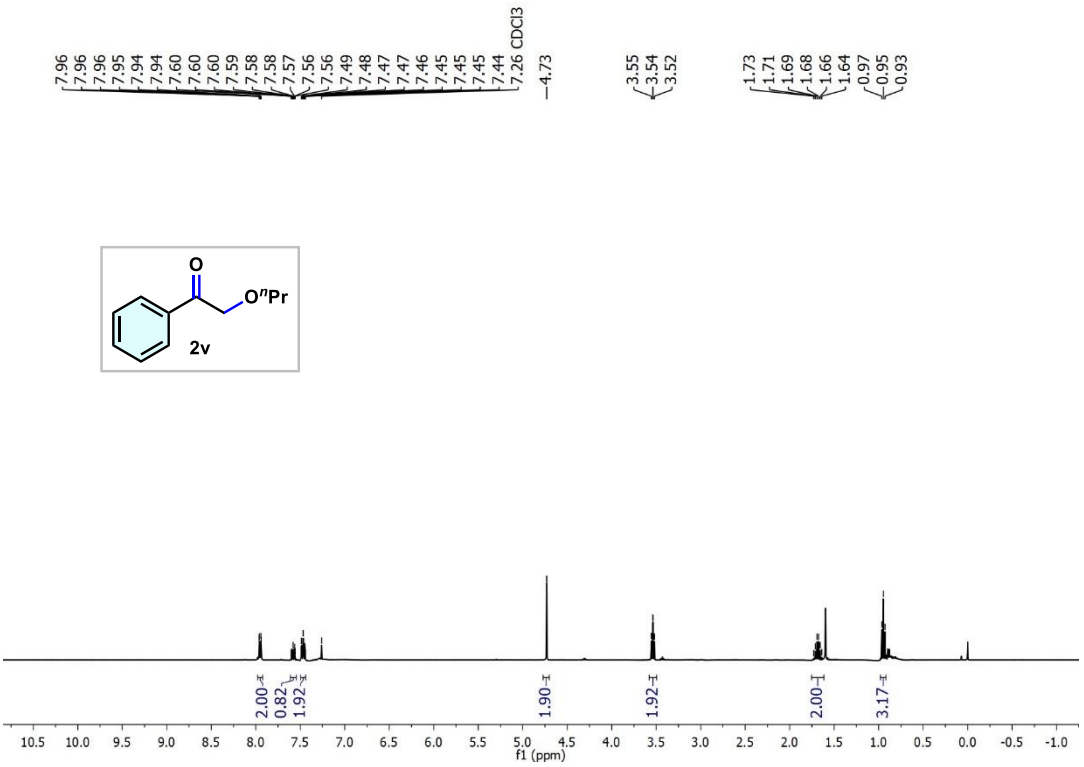

Figure III.13 ^{1}H NMR spectrum of **2v**, $CDCl_3$, 400 MHz

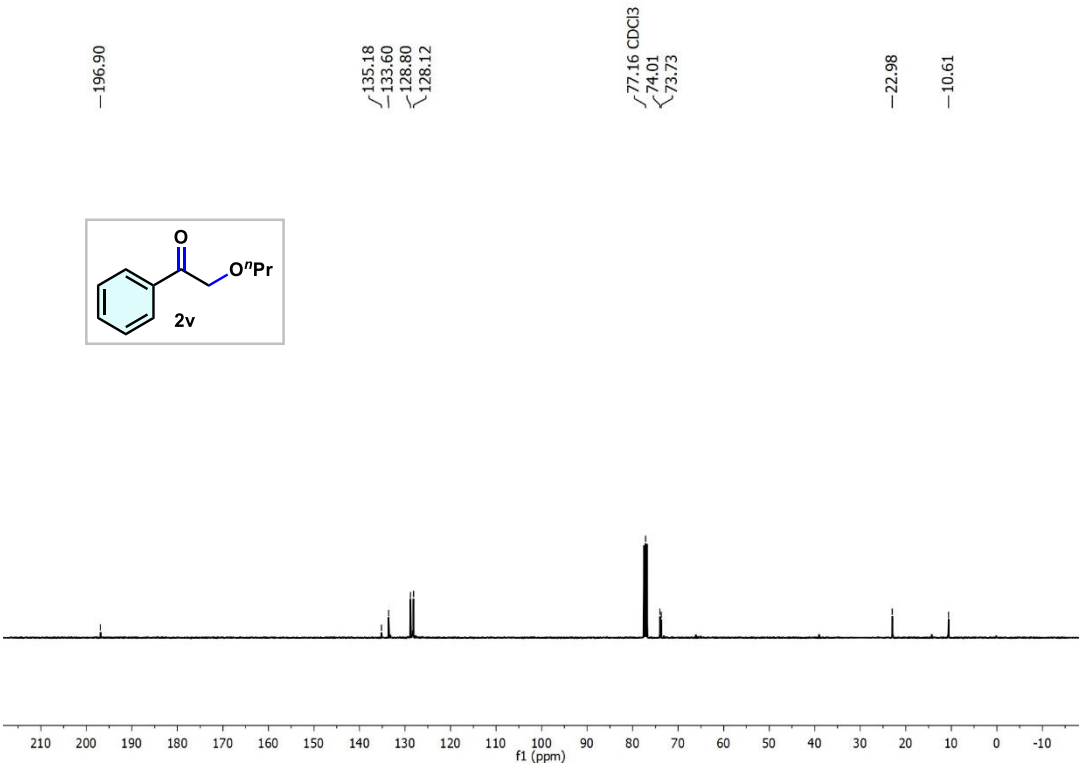

Figure III.14 ^{13}C{^{1}H} NMR spectrum of **2u**, $CDCl_3$, 100 MHz

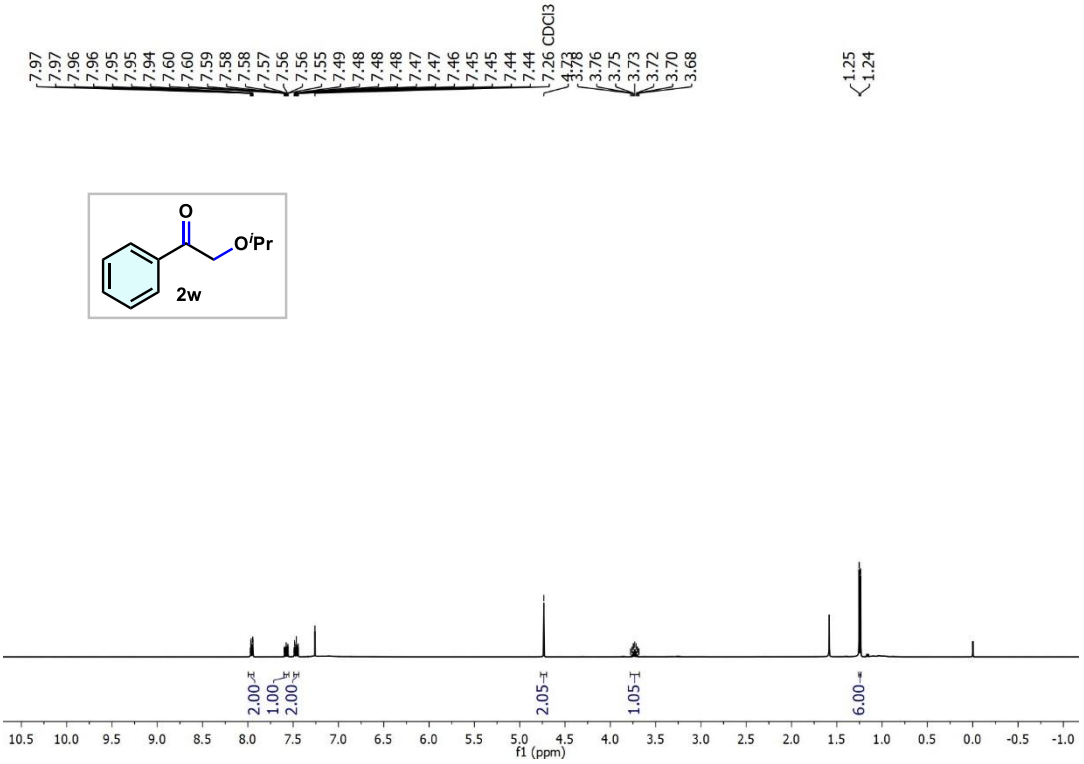

Figure III.15 ^{1}H NMR spectrum of **2w**, $CDCl_3$, 400 MHz

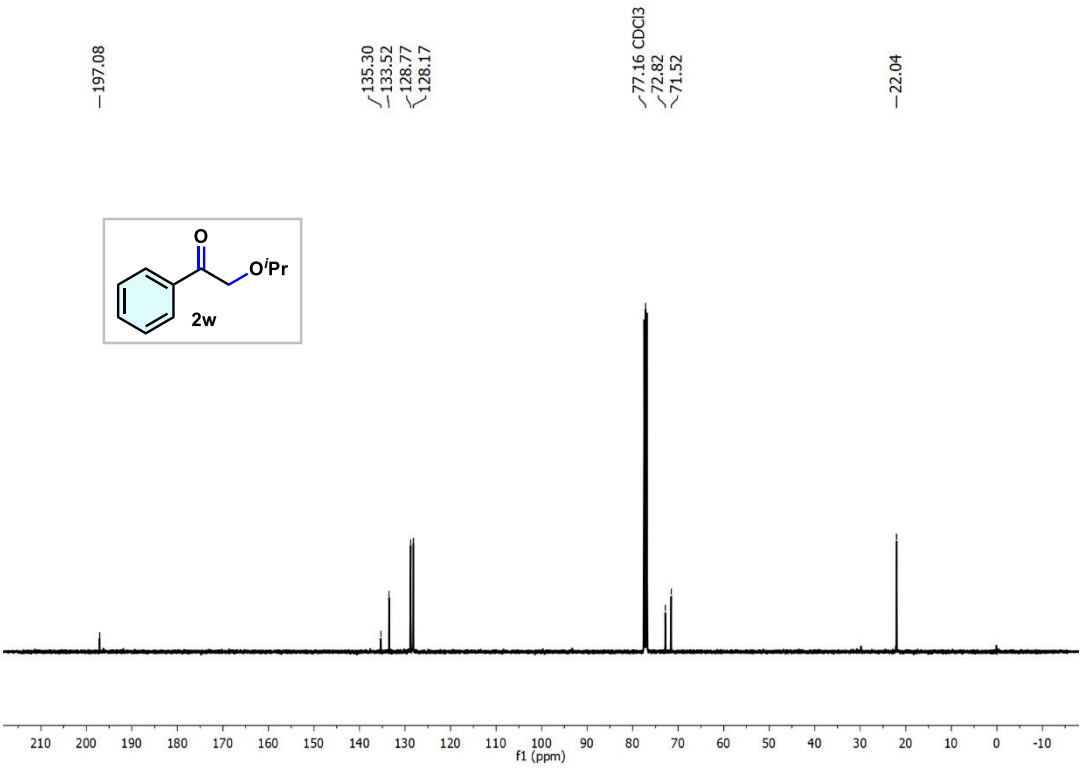

Figure III.16 ^{13}C{^{1}H} NMR spectrum of **2w**, $CDCl_3$, 100 MHz

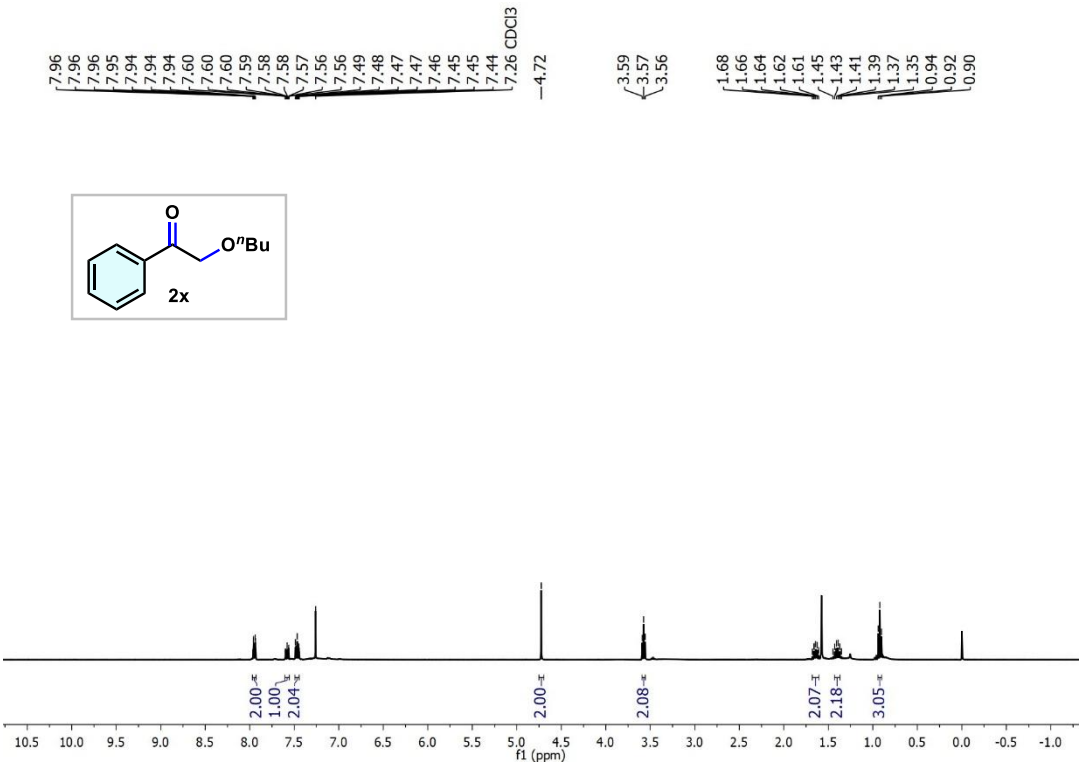

Figure III.17 ^{1}H NMR spectrum of **2x**, $CDCl_3$, 400 MHz

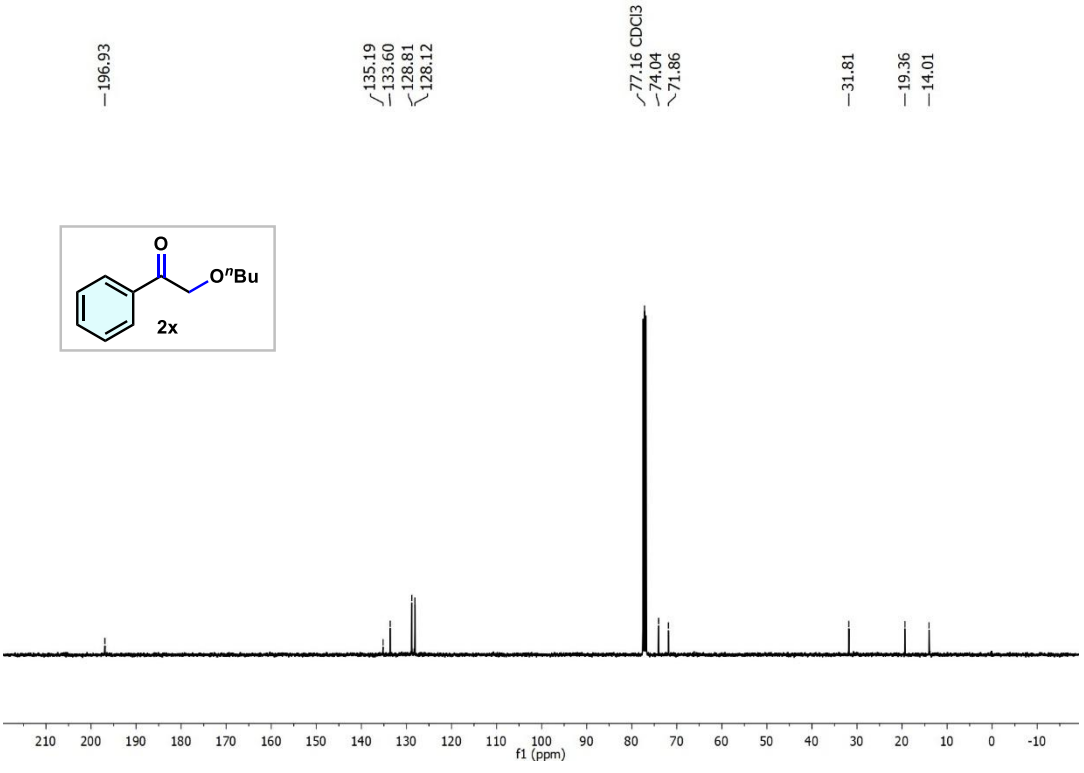

Figure III.18 $^{13}C\{^{1}H\}$ NMR spectrum of **2x**, $CDCl_3$, 100 MHz

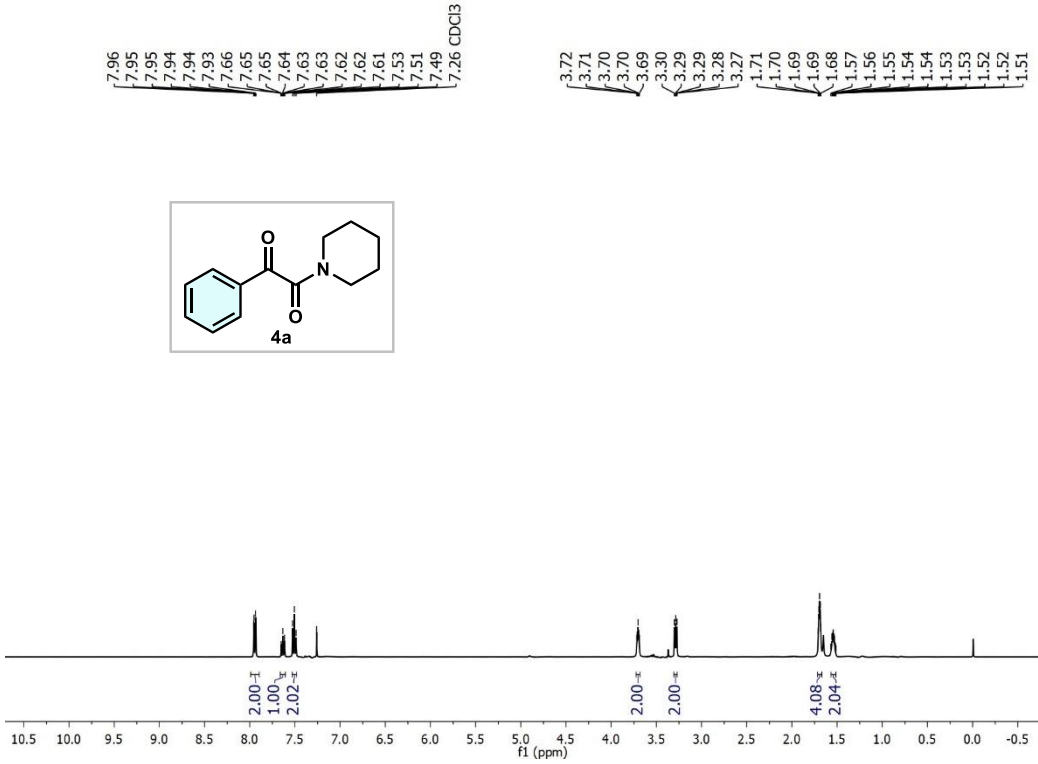

Figure III.19 ^{1}H NMR spectrum of **4a**, $CDCl_3$, 400 MHz

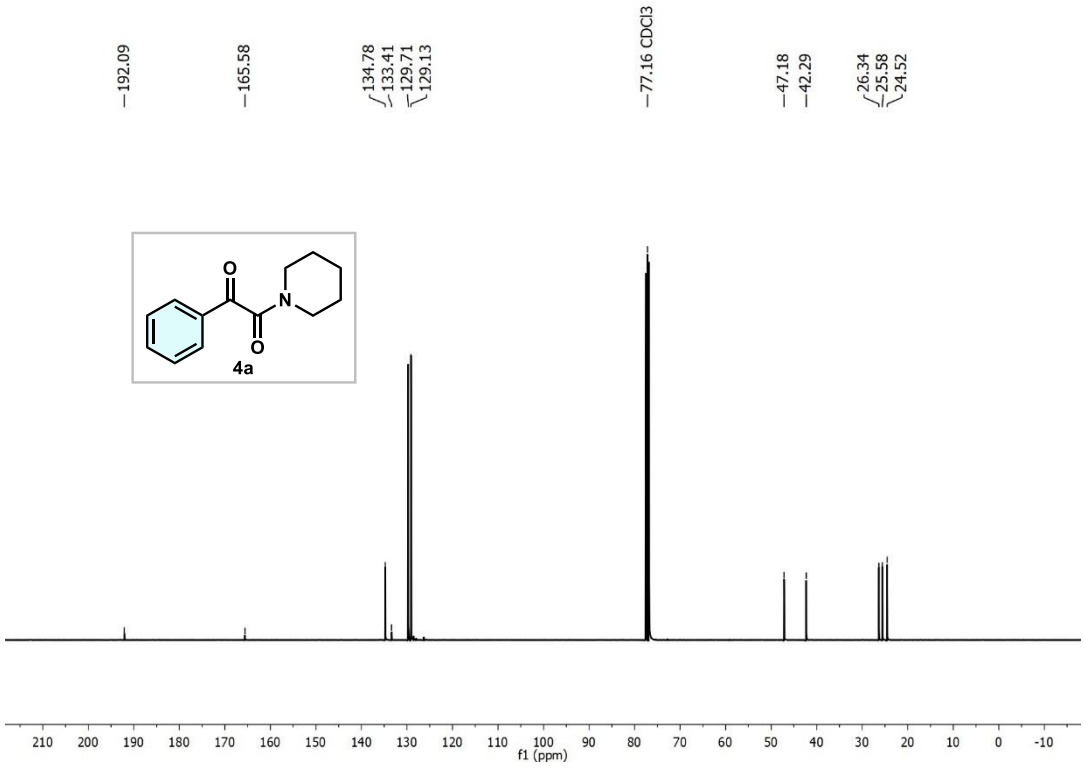

Figure III.20 $^{13}C\{^{1}H\}$ NMR spectrum of **4a**, $CDCl_3$, 100 MHz

3.5 References

1) (a) Otera, J. (ed.) *Modern Carbonyl Chemistry*, Wiley-VCH, **2000**. (b) Carey, F. A.; Sundberg, R. J. *Advanced Organic Chemistry*, *Part A: Structure and Mechanisms*, 5th ed.; Springer: New York, **2007**.
2) (a) Smith, M. B.; March, J. *March's Advanced Organic Chemistry: Reactions, Mechanisms, and Structure*, 6th ed.; Wiley-Inter science: Hoboken, NJ, **2007,** pp 1234–1267. (b) Clayden, J.; Greeves, N.; Warren, S.; Wothers, P. *Organic Chemistry*, 1st ed.; Oxford University Press: Oxford, **2001**. (c) Bruice, P. Y. *Organic Chemistry*, 8th ed.; Pearson Education, **2016**. (d) Berg, J. M.; Tymoczko, J. L.; Stryer, L. *Biochemistry*, 8th ed.; W.H. Freeman, **2015**.
3) (a) Blakemore, D. C.; Castro, L.; Churcher, I.; Rees, D. C.; Thomas, A. W.; Wilson, D. M.; Wood, A. *Nat. Chem.* **2018**, *10*, 383−394. (b) Huo, T.; Zhao, X.; Cheng, Z.; Wei, J.; Zhu, M.; Dou, X.; Jiao, N. *Acta. Pharm. Sin. B* **2024**, *14*, 1030−1076.
4) (a) Tan, Y.; Siebert, K. J. *J. Agric. Food Chem.* **2004**, *52*, 3057–3064. (b) Guo, H.; Chang, S.; Jia, L.; Wang, Z. *Flavour Fragr. J.* **2021**, *36*, 1–12.
5) For selected recent reviews on the application of ketones in organic synthesis, see: (a) Zhou, Q.-Q.; Zou, Y.-Q.; Lu, L.-Q.; Xiao, W.-J. *Angew. Chem. Int. Ed.* **2019**, *58*, 1586–1604. (b) Foley, D. J.; Waldmann, H. *Chem. Soc. Rev.* **2022**, *51*, 4094−4120. (c) Wright, T. B.; Evans, P. A. *Chem. Rev.* **2021**, *121*, 9196−9242. (d) Huang, Z.; Lim, H. N.; Mo, F.; Young, M. C.; Dong, G. *Chem. Soc. Rev.* **2015**, *44*, 7764−7786. (e) Péter, A.; Agasti, S.; Knowles, O.; Pye, E.; Procter, D. J. *Chem. Soc. Rev.* **2021**, *50*, 5349−5365.
6) (a) Ruzi, R.; Liu, K.; Zhu, C.; Xie, J. *Nat. Commun.* **2020**, *11*, 3312–3320. (b) Pan, C.; Jia, X.; Cheng, J. *Synthesis* **2012**, *44*, 677−685. (c) Kloetzing, R. J.; Krasovskiy, A.; Knochel, P. *Chem.-Eur. J.* **2007**, *13*, 215−227. (d) Allen, L. A. T.; Raclea, R.-C.; Natho, P.; Parsons, P. J. *Org. Biomol. Chem.* **2021**, *19*, 498−513.
7) (a) Zabicky, J., Ed. *Patai's Chemistry of Functional Groups; The Alkenes,* Vol. 2; Wiley: London, **1970**. (b) Lan, X. W.; Wang, N. X.; Xing, Y. *Eur. J. Org. Chem.* **2017**, *2017*, 5821−5851. (c) Bao, X.; Li, J.; Jiang, W.; Huo, C. *Synthesis* **2019**, *51*, 4507−4530. (d) Das, S.; Lai, D.; Mallick, A.; Roy, S. *ChemistrySelect* **2016**, *4*, 691–695.
8) Siegel, H.; Eggersdorfer, M. *Ullmann's Encyclopedia of Industrial Chemistry*, ed. M. Bohnet, VCH, Weinheim, 6th edn, **2003**, vol. *18*, p. 739.

9) (a) Agbossou, F.; Carpentier, J.-F.; Mortreux, A. *Chem. Rev.* **1995**, *95*, 2485–2506. (b) Franke, R.; Selent, D.; Börner, A. *Chem. Rev.* **2012**, *112*, 5675–5732.

10) (a) Smidt, J.; Hahner, W.; Jima, R.; Sedlmeier, J.; Sieber, R.; Rüttinger, R.; Kojer, K. *Angew. Chem.* 1959, 71, 176–182. (b) Smidt, J.; Hafner, W.; Jira, R.; Sieber, R.; Sedlmeier, J.; Sabel, A. *Angew. Chem. Int. Ed. Engl.* **1962**, *1*, 80–88. (c) Jira, R. *Angew. Chem. Int. Ed.* **2009**, *48*, 9034–9037.

11) (a) Nicewicz, D. A.; MacMillan, D. W. C. *Science* **2008**, *322*, 77−80. (b) Narayanam, J. M. R.; Stephenson, C. R. J. *Chem. Soc. Rev.* **2011**, *40*, 102−113. (c) Prier, C. K.; Rankic, D. A.; MacMillan, D. W. C. *Chem. Rev.* **2013**, *113*, 5322–5363. (d) Romero, N. A.; Nicewicz, D. A. *Chem. Rev.* **2016**, *116*, 10075–10166.

12) (a) Gong, X.; Zhu, C.; Ye, L.-W. *Org. Biomol. Chem.* **2020**, *18*, 1843–1850. (b) Chalotra, N.; Sultan, S.; Shah, B. A. *Asian J. Org. Chem.* **2020**, *9*, 863−881.

13) Nakayama, H.; Itoh, A. *Tetrahedron Lett.* **2007**, *48*, 1131–1133.

14) Nobuta, T.; Hirashima, S.; Tada, N.; Miura, T.; Itoh, A. *Synlett* **2010**, *15*, 2325–2329.

15) Luo, Z.; Meng, Y. G.; Gong, X. C.; Wu, J.; Zhang, Y. L.; Ye, L. W.; Zhu, C. *Chin. J. Chem.* **2020**, *38,* 173–177.

16) Keshari, T.; Yadav, V. K.; Srivastava, V. P.; Yadav, L. D. S. *Green Chem.* **2014**, *16*, 3986–3992.

17) Niu, T. F.; Cheng, J.; Zhuo, C. L.; Jiang, D. Y.; Shu, X. G.; Ni, B. Q. *Tetrahedron Lett.* **2017**, *58*, 3667–3671.

18) Wu, J.; Zhang, Y. L.; Gong, X. C.; Meng, Y. G.; Zhu, C. Y. *Org. Biomol. Chem.* **2019**, *17*, 3507–3513.

19) Liu, Q. S.; Liu, F.; Yue, H. L.; Zhao, X. H.; Li, J. S.; Wei, W. *Adv. Synth. Catal.* **2019**, *361*, 5277–5282.

20) Ding, Y.; Zhang, W. K.; Li, H.; Meng, Y. G.; Zhang, T.; Chen, Q. Y.; Zhu, C. Y. *Green Chem.* **2017**, *19*, 2941–2944.

21) Wei, W.; Cui, H. H.; Yue, H. L.; Yang, D. S. *Green Chem.* **2018**, *20*, 3197–3202. 22) Nan, G. M.; Yue, H. L. *Synlett*, **2018**, *29*, 1340–1345.

22) (a) Wei, S.; Messerer, R.; Tsogoeva, S. B. *Chem. Eur. J.* **2011**, *17*, 14380−14384. (b) Baez-Santos, Y. M.; Barraza, S. J.; Wilson, M. W.; Agius, M. P.; Mielech, A. M.; Davis, N. M.; Baker, S. C.; Larsen, S. D.; Mesecar, A. D. *J. Med. Chem.* **2014**, *57*, 2393−2412.

23) (a) Addis, D.; Shaikh, N.; Zhou, S.; Das, S.; Junge, K.; Beller, M. *Chem.−Asian J.* **2010**, *5*, 1687−1691. (b)Eagon, S.; Ball-Jones, N.; Haddenham, D.; Saavedra, J.; DeLieto, C.;

Buckman, M.; Singaram, B. *Tetrahedron Lett.* **2010**, *51*, 6418−6421. (c) Lowicki, D.; Bezlada, A.; Mlynarski, J. *Adv. Synth. Catal.* **2014**, *356*, 591−595.

24) (a) Moriarty, R. M.; Prakash, O.; Duncan, M. P.; Vaid, R. K. *J. Org. Chem.* **1987**, *52*, 150–153. (b) Yu, H.; Xu, Y.; Fang, Y.; Dong, R. *Eur. J. Org. Chem.* **2016**, *2016*, 5257−5262. (c) Mizar, P.; Wirth, T. *Angew. Chem. Int. Ed.* **2014**, *53*, 5993−5997.

25) (a) Moriarty, R. M.; Prakash, O.; Duncan, M. P.; Vaid, R. K. *J. Org. Chem.* **1987**, *52*, 150–153. (b) Yu, H.; Xu, Y.; Fang, Y.; Dong, R. *Eur. J. Org. Chem.* **2016**, *2016*, 5257−5262. (c) Mizar, P.; Wirth, T. *Angew. Chem. Int. Ed.* **2014**, *53*, 5993−5997.

26) Banoun, C.; Bourdreux, F.; Magnier, E.; Dagousset, G. *Org. Lett.* **2021**, *23*, 8926–8930.

27) Wu, F.; Guo, Y.; Ren, Z., Chen, Z.; Liu, X.; Wang, C.; Rong, L. *J. Org. Chem.* **2023**, *88*, 8825−8834.

28) (a) Guo, J.-T.; Yang, D.-C.; Guan, Z.; He, Y.-H. *J. Org. Chem.* **2017**, *82*, 1888–1894. (b) Fujiya, A.; Tanaka, M.; Yamaguchi, E.; Tada, N.; Itoh, A. *J. Org. Chem.* **2016**, *81*, 7262−7270. (c) Maia da Silva Santos, B.; dos Santos Dupim, M.; Paula de Souza, C.; Messias Cardozo, T.; Gadini Finelli, F. *Beilstein J. Org. Chem.* **2021,** *17,* 2959–2967.

29) (a) Bancirova, M. *Luminescence* **2011**, *26*, 685–688. (b) Harbour, J. R.; Issler, S. L. *J. Am. Chem. Soc.* **1982**, *104*, 903–905.

30) Pelaez, M.; Falaras, P.; Likodimos, V.; O'shea, K.; De la Cruz, A.; Dunlop, P. S. M.; Byrne, J. A.; Dionysiou, D. D. *J. Mol. Catal. A Chem.* **2016**, *425*, 183–189.

31) Sarró, P.; Ji, Y.; Gallego-Gamo, A.; Gimbert-Suriñach, C.; Vallribera, A.; Granados, A. *Org. Chem. Front.* **2025**, *12*, 3475−3492.

Chapter 4

Visible Light Driven Organophotoredox Catalyzed Oxidative Functionalization of Styrenes: Synthesis of 1,4-Diketones

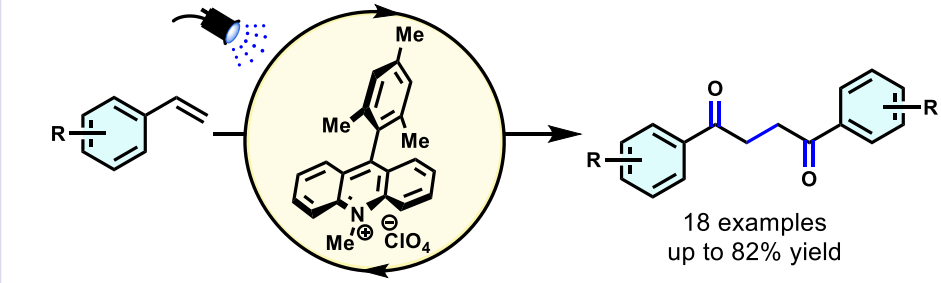

- *Visible light mediated*
- *Transition metal-free*
- *Organophotocatalyst*
- *Broad substrate scope*
- *Post-synthetic application to heterocycles*

Visible Light Driven Organophotoredox Catalyzed Oxidative Functionalization of Styrenes: Synthesis of 1,4-Diketones

4

This chapter outlines a mild, transition metal-free, organophotoredox-catalyzed strategy for the synthesis of 1,4-diketones from readily available and cost-effective styrene derivatives. Compared to their 1,3- and 1,5-diketone counterparts, the synthesis of 1,4-diketones presents greater challenges, primarily due to the inherent polarity mismatch of carbonyl synthetic equivalents, making them less intuitive targets. Recent advances in the construction of 1,4-dicarbonyl frameworks have predominantly focused on umpolung strategies that utilize pre-existing carbonyl-containing fragments. In contrast, transformations involving non-carbonyl precursors to generate carbonyl functionalities in-situ remain relatively underexplored. A facile protocol is established to access 1,4-diketones via the oxidative functionalization of styrenes followed by dimerization. The developed protocol demonstrates a broad substrate scope, tolerating a wide variety of styrene derivatives. Moreover, the resulting diketones can be further applied for the synthesis of valuable heterocyclic compounds, highlighting the synthetic utility of the method. The reaction is scalable and proceeds efficiently under the exposure of natural sunlight. A plausible reaction mechanism is proposed and supported by control experiments, fluorescence quenching studies, and cyclic voltammetry analysis.

4.1 Introduction

1,4-carbonyls are important organic frameworks with significant applications across medicinal chemistry, food science, and polymer technology (Figure 4.1).[1] 1,4-Carbonyl compounds are pivotal intermediates in organic synthesis, renowned for their versatility in constructing a diverse array of heterocyclic compounds, including furans, pyrroles, thiophenes, and pyridazines.[2] These heterocycles are integral to numerous applications in pharmaceuticals, agrochemicals, and materials science due to their unique chemical and physical properties.[3] Consequently, the development of novel methods for the synthesis of 1,4-dicarbonyl compounds remains a highly desirable pursuit in the field of organic chemistry.[4] However, the synthesis of 1,4-dicarbonyl is more challenging and therefore less easily conceptualized

compared to that of 1,3- or 1,5-dicarbonyl compounds (Figure 4.2A, B). Due to the inherent polarity mismatch of carbonyl synthetic equivalents, they present a valuable retrosynthetic challenge that stimulates the creativity of synthetic chemists.[5]

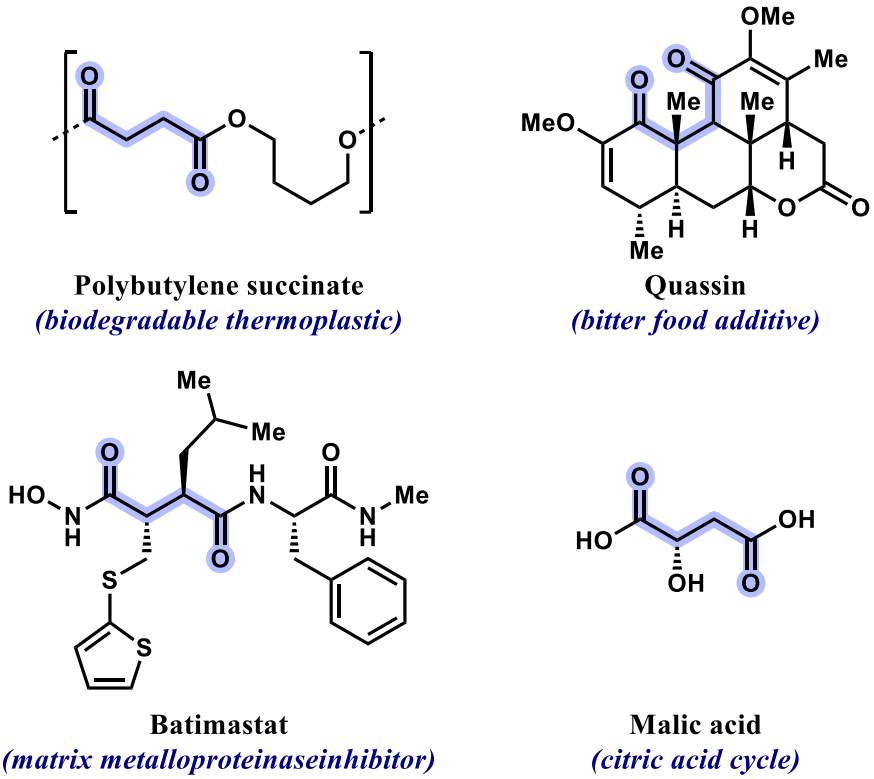

Figure 4.1 Representative examples of useful 1,4-dicarbonyl compounds

Over the past decades, this problem has been addressed by multiple methods (Figure 4.2C), which include organocatalytic Stetter reactions,[6] oxidative enolate coupling,[7] coupling of pre-functionalized carbonyls[8] and Claisen rearrangement–cleavage cascades[9]. Recent advances in forming 1,4-dicarbonyls largely focused on radical Stetter-type approaches or enolate umpolung reactions employing enolonium intermediates, that utilizes the bond formation strategy between existing carbonyl fragments under irradiation of visible/UV- light.[10]

In 2019, Gilmour and coworkers introduced a bioinspired radical umpolung strategy that enabled an intermolecular radical Stetter reaction between α-keto acids **1** and α,β-unsaturated aldehydes **2** (Scheme 4.1). The transformation involved the *in-situ* formation of iminium ions through secondary amine activation, followed by the generation of a photoactive electron donor–acceptor (EDA) complex with α-keto carboxylic acids. Upon visible-light excitation, this complex underwent single electron transfer (SET), leading to rapid decarboxylation (loss of CO_2) and subsequent radical–radical recombination to afford 4-ketoaldehydes **3**.[11]

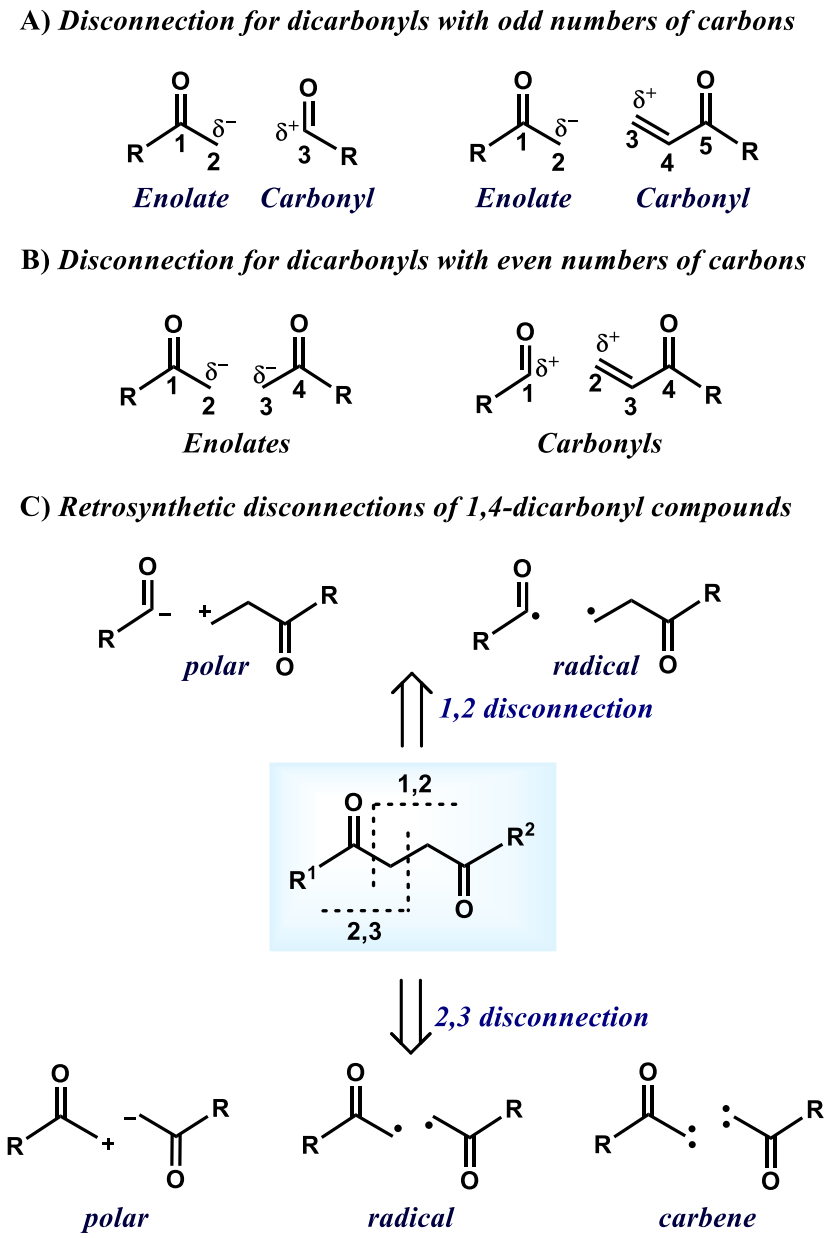

Figure 4.2 Retrosynthetic disconnections for dicarbonyl compounds

Yu and coworkers developed an enantioselective radical hydroacylation of enals **2** with *α*-keto acids **1**, enabled by a dual photoredox/amine catalytic system (Scheme 4.2).[12] In this methodology, acyl radicals derived from *α*-keto acids react with iminium ions formed *in-situ* from cinnamaldehyde derivatives and a chiral amine catalyst (**A1**). The reaction proceeds in the presence of the photocatalyst $Ru(bpz)_3(PF_6)_2$ under white LEDs irradiation at −20 °C, over 60 hours. This approach offers an efficient and enantioselective route to 1,4-dicarbonyl compounds such as keto aldehydes **3** and represents a valuable alternative and complementary strategy to the traditional Stetter reaction.

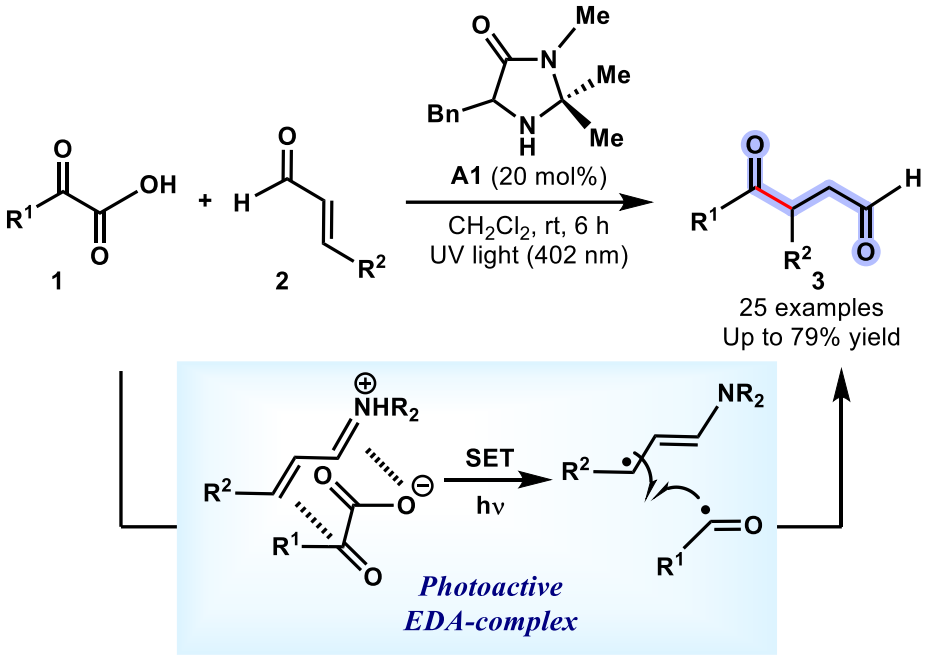

Scheme 4.1 Radical Stetter reaction for 1,4-dicarbonyl synthesis

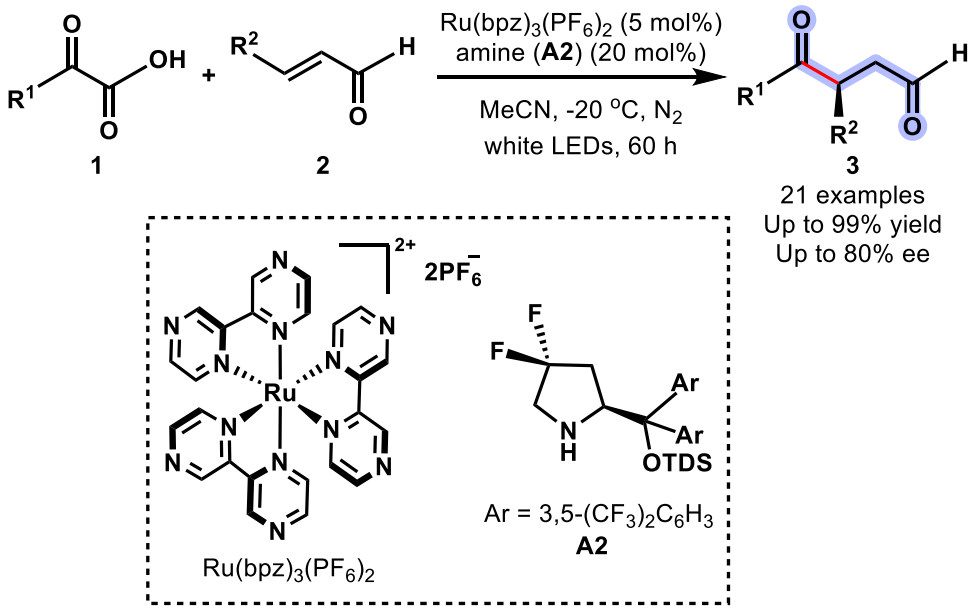

Scheme 4.2 Photoredox/amine cocatalysis for the enantioselective radical hydroacylation of enals with α-ketoacids

Melchiorre and coworkers developed a visible-light-mediated organocatalytic strategy for the enantioselective conjugate addition of acyl radicals to enals **1**, enabling the synthesis of valuable 1,4-dicarbonyl compounds **3** (Scheme 4.3).[13] In this approach, acyl radicals are

generated from 4-acyl-1,4-dihydropyridines **2** upon visible-light irradiation. Concurrently, enals **1** are activated through iminium ion formation with a chiral amine catalyst **A2**. The resulting stereoselective radical trapping delivers enantioenriched, acyclic 1,4-dicarbonyl compounds **3** with high efficiency and selectivity.

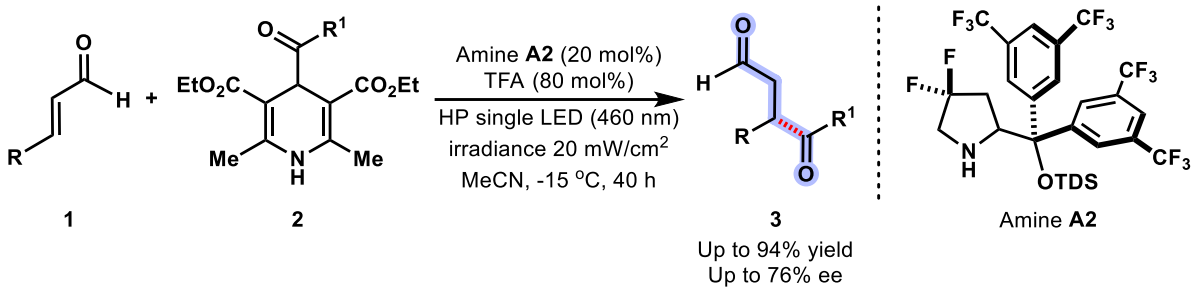

Scheme 4.3 Photochemical organocatalytic acyl radical addition to enals

A recent advancement by Wu and coworkers demonstrated the direct incorporation of two carbonyl groups across both an alkene double bond, achieving 1,2-dicarbonylation via photocatalysis using orgnophotocatalyst such as 4CzIPN to access diketones **3** (Scheme 4.4A).[14] The key mechanistic feature involves the association of the $[N(n\text{-}Bu)_4]^+$ cation with the alkyl anion intermediate, which effectively suppresses protonation. Simultaneously, the α-keto acid **1** is activated to participate in an electrophilic addition step. Notably, the α-keto acid serves a dual role: acting both as the acyl radical source and as the electrophilic partner. By fine-tuning the reductive and electrophilic properties of the acyl precursor, the researchers successfully achieved unsymmetric 1,4-dicarbonylation of alkenes **2** as well (Scheme 4.4B).

Nevertheless, the transformation or coupling of non-carbonyl precursors to construct 1,4-dicarbonyl compounds via the oxidative functionalization of alkenes remains relatively underexplored. Alkenes are inexpensive and readily available hydrocarbons, commonly sourced from petroleum and natural gas, rendering them highly valuable feedstocks for both industrial processes and synthetic organic chemistry.[14] Therefore, the development of methods for their direct functionalization holds considerable synthetic importance.[15]

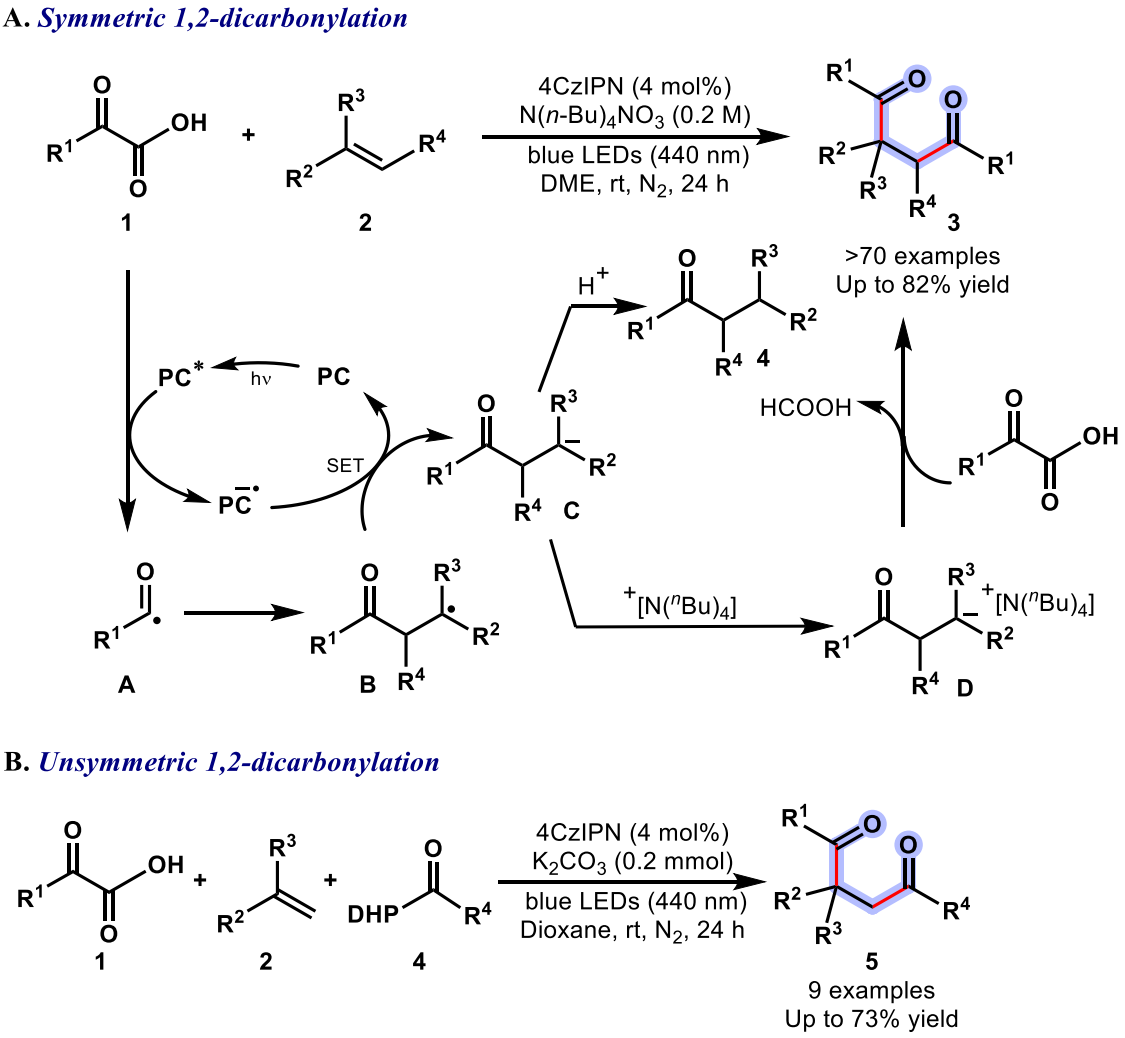

Scheme 4.4 Visible light mediated direct 1,2-dicarbonylation of alkenes for 1,4-diketones

The oxidative coupling of styrenes to form 1,4-diketones **2** is also relatively rare. Roy and coworkers reported an oxidative functionalization of styrenes **1** to access 1,4-diketones **2** using polyoxometalate POM $(NH_4)_{42}[Mo^{VI}_{72}Mo^{V}_{60}O_{372}(CH_3COO)_{30}(H_2O)_{72}]$•hydrate as a catalyst in the presence of conc. HCl (cat.) and UV-light (8W) (Scheme 4.5).[16] While this method demonstrates the feasibility of such a transformation, however, it is limited to several practical constraints, including the requirement for prior synthesis of POM, the use of corrosive reagents such as concentrated hydrochloric acid, high-energy UV irradiation, and a relatively narrow substrate scope.

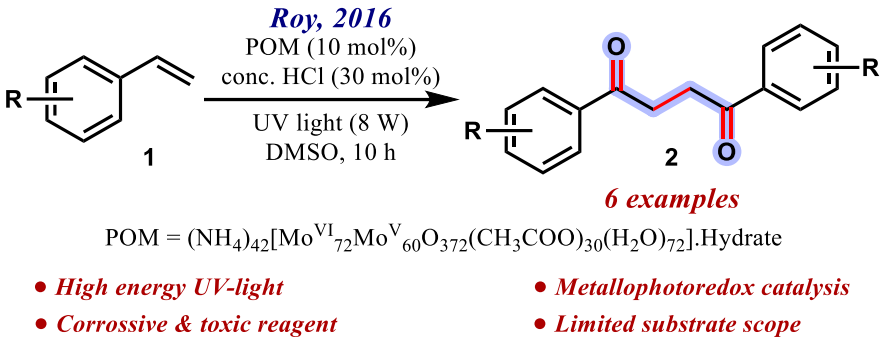

Scheme 4.5 Metallophotoredox catalysis approach for 1,4-dicarbonyl synthesis

Visible-light-driven photoredox catalysis has emerged over the past two decades as a sustainable and powerful tool in synthetic organic chemistry, owing to its operational simplicity, mild reaction conditions, and elegant scope.[17] Based on the literature survey, olefins have been rarely utilized for directly constructing the 1,4-dicarbonyl saffold. Building on our ongoing interest in organophotoredox-catalyzed methodologies utilizing readily available alkenes,[18] we hypothesized that under suitable visible light condition 1,4-diketones could be synthesized directly from styrene by looking into their oxidation potential and reactivity patterns.

In this chapter, we disclose a straightforward and efficient protocol for the direct synthesis of 1,4-diketones from styrenes via organophotoredox catalysis under blue LEDs irradiation (Scheme 4.6).

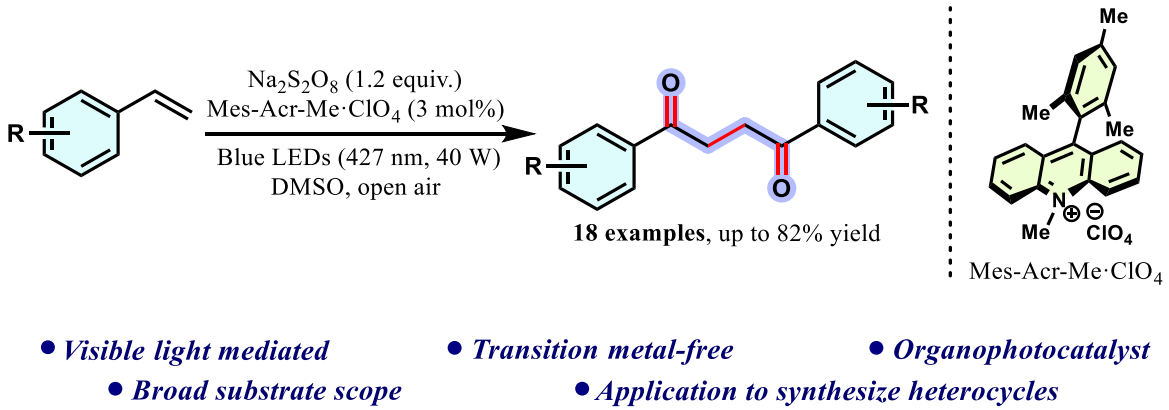

Scheme 4.6 Visible light mediated organophotoredox catalyzed synthesis of 1,4-diketones

4.2 Results and Discussions

To validate our hypothesis, we initiated the optimization of reaction conditions for the synthesis of 1,4-diketones using 4-chlorostyrene **1a** as a model substrate in dimethyl sulfoxide (DMSO) as solvent under the irradiation with 427 nm blue LEDs (40 W) for 8 hours. A range

of organophotocatalysts was evaluated, including Acr-Mes-BF_4, Acr-Mes-ClO_4, 2,4,6-triphenylpyrylium•BF_4, Eosin Y, Rose Bengal, Rhodamine 6G, Rhodamine B, fluorescein, and riboflavin. The desired product **2a** was obtained in moderate yields (up to 55%) in all cases except with Rose Bengal (Table 4.1, Entries 1–9). Among the tested photocatalysts, Acr-Mes-ClO_4 provided the highest yield of the product **2a** (Table 4.1, Entry 2).

Table 4.1 Optimization of reaction conditions for 1,4-diketone synthesis[a]

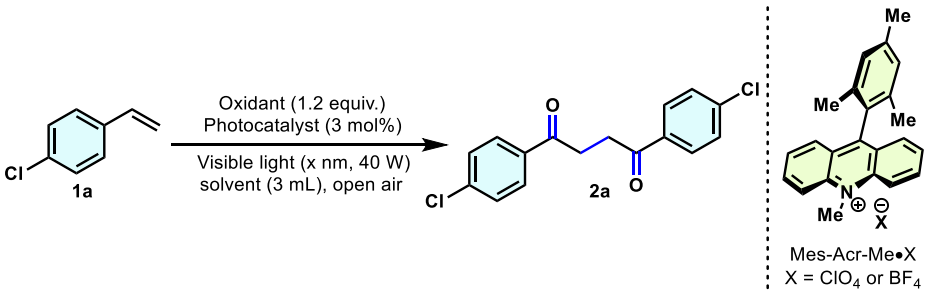

Sr. No.	Photocatalyst	Solvent	Oxidant	Light (nm)	Yield(%)[b]
1	Mes-Acr-Me·BF_4	DMSO	-	427	53
2	Mes-Acr-Me·ClO_4	DMSO	-	427	55
3	2,4,6-Triphenylpyrylium•BF_4	DMSO	-	427	42
4	EosinY	DMSO	-	427	40
5	Rose bengal	DMSO	-	427	ND
6	Rhodamine 6G	DMSO	-	427	52
7	Rhodamine B	DMSO	-	427	48
8	Fluoroscein	DMSO	-	427	21
9	Riboflavin	DMSO	-	427	32
10	$Ru(bpy)_3.2PF_6$	DMSO	-	427	<10
11	Mes-Acr-Me·ClO_4	Toluene	-	427	ND
12	Mes-Acr-Me·ClO_4	1,4-Dioxane	-	427	ND
13	Mes-Acr-Me·ClO_4	EtOAc	-	427	ND
14	Mes-Acr-Me·ClO_4	THF	-	427	ND
15	Mes-Acr-Me·ClO_4	DCE	-	427	ND
16	Mes-Acr-Me·ClO_4	DCM	-	427	ND
17	Mes-Acr-Me·ClO_4	DMF	-	427	37
18	Mes-Acr-Me·ClO_4	MeCN	-	427	11

19	Mes-Acr-Me·ClO_4	DMSO:MeCN (1:5)	-	427	43
20	Mes-Acr-Me·ClO_4	DMSO	$(NH_4)_2S_2O_8$	427	68
21	Mes-Acr-Me·ClO_4	DMSO	$K_2S_2O_8$	427	70
22	**Mes-Acr-Me·ClO_4**	**DMSO**	**$Na_2S_2O_8$**	**427**	**74(67)[c]**
23	Mes-Acr-Me·ClO_4	DMSO	TBHP	427	49
24	Mes-Acr-Me·ClO_4	DMSO	BIOAc	427	56
25	Mes-Acr-Me·ClO_4	DMSO	$Na_2S_2O_8$	440	66
26	Mes-Acr-Me·ClO_4	DMSO	$Na_2S_2O_8$	456	63
27	Mes-Acr-Me·ClO_4	DMSO	$Na_2S_2O_8$	467	57
28	Mes-Acr-Me·ClO_4	DMSO	$Na_2S_2O_8$	525	43

Standard reaction conditions: [a]**1a** (0.4 mmol), Oxidant (1.2 equiv.), Photocatalyst (3 mol%) in Solvent (3 mL), Visible light (xx nm, 40 W) for 8 h at room temperature (rt). [b]Determined by ^{1}H NMR analysis using 1,3,5-Trimethoxybenzene as an internal standard. [c]Isolated yield after column chromatography. ND = Not Detected.

Additionally, the use of the metallophotocatalyst Ru(bpy)$_3$·2PF_6 resulted the desired product **2a** in a poor yield (Table 4.1, Entry 10). Subsequently, in presence of Mes-Acr-Me·ClO_4 as the fixed photocatalyst, a variety of solvents were evaluated, including toluene, 1,4-dioxane, ethyl acetate (EtOAc), tetrahydrofuran (THF), dichloroethane (DCE), and dichloromethane (DCM). However, none of these solvents afforded product **2a** (Table 4.1, Entries 11–16). The use of dimethyl formamide (DMF) and acetonitrile (MeCN) led to poor to modest yields (Up to 37%, Table 4.1, Entries 17 and 18). Moreover, the reaction in mixture of DMSO and MeCN (1:5) slightly improved yield of product **2a** (43%, Table 4.1, Entry 19). Subsequently, various oxidants such as $(NH_4)_2S_2O_8$, $K_2S_2O_8$, $Na_2S_2O_8$, *tert*-butyl hydroperoxide (TBHP), and 1-acetoxy-1,2-benziodoxol-3(1*H*)-one (BIOAc) were evaluated (Table 4.1, Entries 20–24). Among these, $Na_2S_2O_8$ provided the desired product **2a** in highest yield (74%, Table 4.1, Entry 22). Later, we screened the light sources with different wavelengths (440 nm, 456 nm, 467 nm, and 525 nm LEDs) to see the overall effect on the outcome of the yield of desired product **2a** (Table 4.1, Entries 25–28). A progressive decrease in the yield of **2a** was observed with the increasing wavelength and among all 427 nm proved to be most suitable. Furthermore, we varied the equivalents of the oxidant to examine the optimum amount (Table 4.2, Entries 1–3) and we observed that 1.2 equiv. proved to be optimum for the smooth transformation to afford **2a** in highest yield (Table 4.2, Entry 2). We have also evaluated the effect of reaction time on

the overall outcome of the yield of product **2a** (Table 4.3, Entries 1–3), with the highest yield of 74% observed at 8 h (Table 4.3, Entry 2).

Table 4.2 Optimization of equivalents of oxidants[a]

Sr. No.	$Na_2S_2O_8$ (x equiv.)	2a Yield(%)[b]
1	0.6 equiv.	61
2	**1.2 equiv.**	**74**
3	2.0 equiv.	68

Standard reaction conditions: [a]**1a** (0.4 mmol), $Na_2S_2O_8$ (x equiv.), Mes-Acr-Me•ClO_4 (3 mol%) in DMSO (3 mL), Kessil Blue LEDs (427 nm, 40 W) for 8 h at room temperature (rt). [b]Determined by ^{1}H NMR analysis using 1,3,5-Trimethoxybenzene as an internal standard.

Based on the exhaustive screening, 4-chlorostyrene (**1a**, 0.2 mmol), $Na_2S_2O_8$ (1.2 equiv.), and Acr-Mes-ClO_4 (3 mol%) in DMSO (3 mL), irradiation with blue LEDs (427 nm, 40 W) under ambient air at room temperature for 8 h proved to be the optimum reaction condition to obtain the desired product **2a**.

Table 4.3 Optimization of reaction time[a]

Sr. No.	Time (h)	2a Yield(%)[b]
1	4	58
2	**8**	**74**
3	12	72

Standard reaction conditions: [a]**1a** (0.4 mmol), $Na_2S_2O_8$ (1.2 equiv.), Mes-Acr-Me•ClO_4 (3 mol%) in DMSO (3 mL), Kessil Blue LEDs (427 nm, 40 W) for x h at room temperature (rt).

Having obtained the optimum reaction conditions, we further proceeded to investigate the substrate scope to evaluate the practicality and generality of the developed protocol. Under the optimized conditions, a range of electronically neutral and electron-rich styrenes (**1b**–**1f**) successfully underwent the transformation, affording the corresponding 1,4-diketone products (**2b**–**2f**) in good yields (up to 68%, Table 4.4). Additionally, styrenes bearing electron-donating

substituents such as methoxy, phenoxy, and acetoxy groups (**1g**–**1i**) reacted efficiently under the optimized conditions, affording the corresponding products (**2g**–**2i**) in moderate to very good yields (up to 80%, Table 4.4).

Table 4.4 Substrate scope of 1,4-Diketones[a]

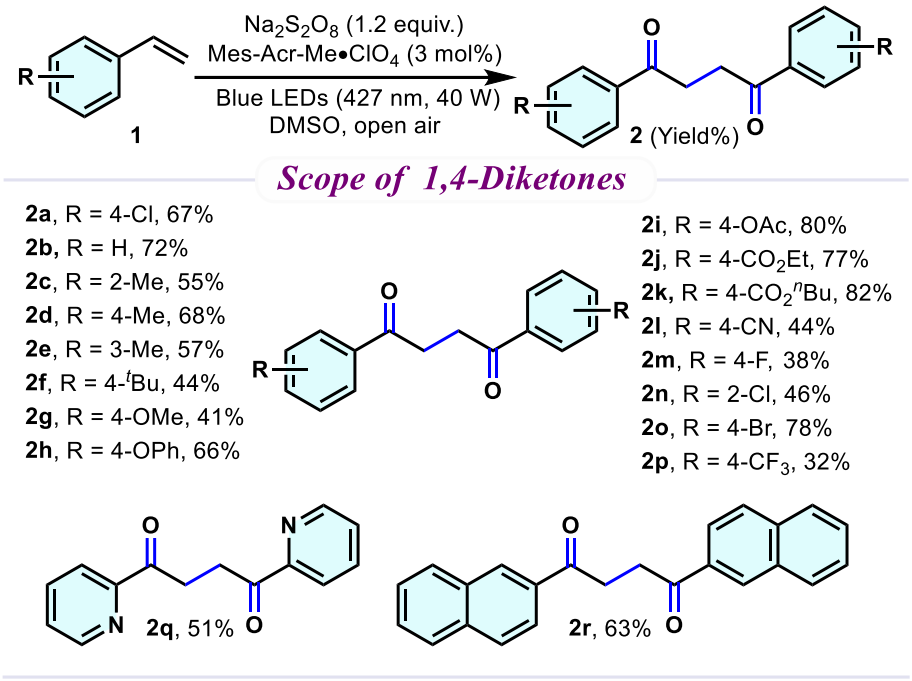

Reaction conditions: [a]**1** (0.4 mmol), $Na_2S_2O_8$ (1.2 equiv.), Mes-Acr-Me•ClO_4 (3 mol%), DMSO (2 mL), blue LEDs (427 nm, 40 W), rt, open air. [b]Isolated yield after column chromatography.

Furthermore, styrenes bearing electron-withdrawing groups such as –CO_2Et, –$CO_2{}^n$Bu, and –CN (**1j**–**1l**) also performed well under the optimized reaction conditions, delivering the corresponding products (**2j**–**2l**) in moderate to excellent yields, (up to 82%, Table 4.4). Notably, styrenes bearing electron-deactivating substituents such as fluoro, chloro, bromo, and trifluoromethyl groups (**1a**, **1m**–**1q**) were well-tolerated under the reaction conditions, affording the corresponding products (**2a**, **2m**–**2p**) in modest to good yields (up to 78%, Table 4.4). Additionally, heteroaryl and polyaromatic substrates such as 2-vinylpyridine **1q** and 2-vinylnaphthalene **1r** also underwent the transformation successfully, delivering the desired products (**2q** and **2r**) in moderate yields (up to 63%, Table 4.4).

Having demonstrated the broad applicability of the developed protocol for the synthesis of 1,4-diketones, we next explored its performance under the direct exposure of natural sunlight. This reaction successfully afforded the desired product **2a** in good yield (Scheme 4.7a). To further evaluate the practicality of the method, we carried out the scale-up reaction on a gram

quantity (1 g, compound **1b**) under the optimum reaction conditions to afford the corresponding product **2b** in a moderate yield (63%, Scheme 4.7b).

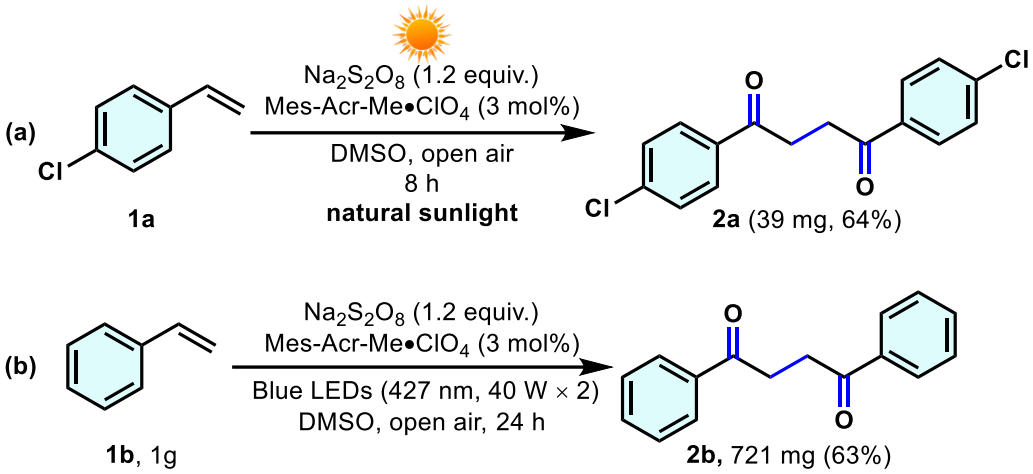

Scheme 4.7 Reaction under natural sunlight and gram scale synthesis

Subsequently, we directed our efforts toward the post-synthetic modification of the representative compound **2b** (Scheme 4.8).

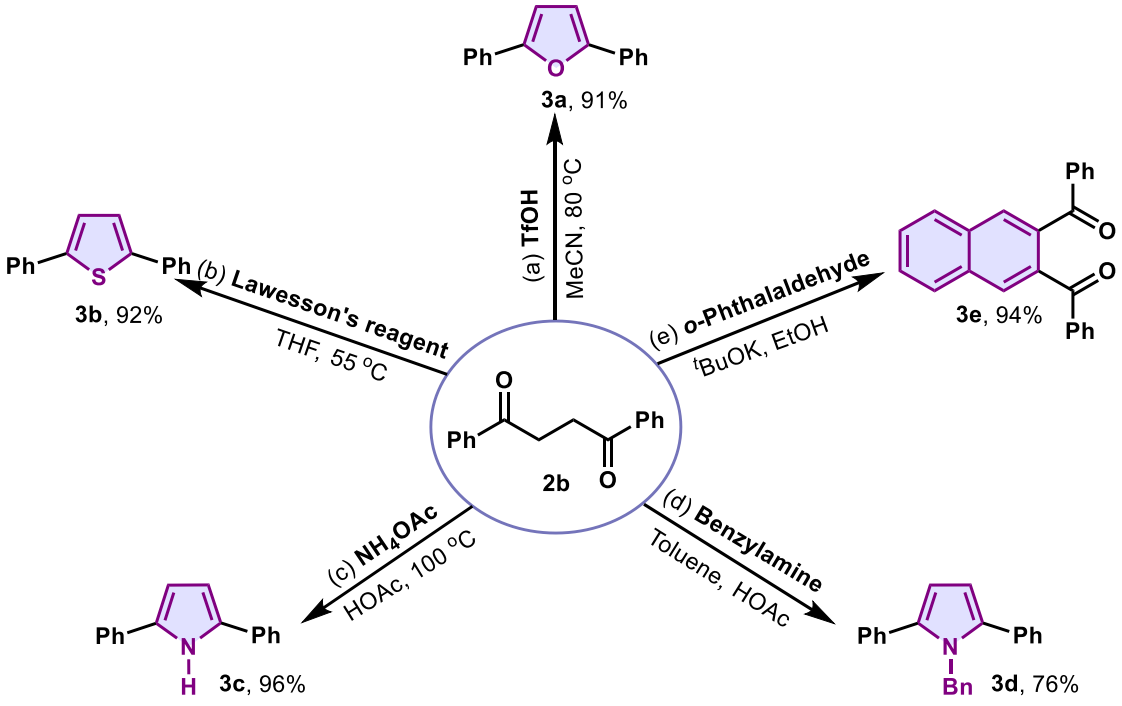

Scheme 4.8 Post synthetic modification of 1,4-diketone product **2b**

Leveraging its versatility, compound **2b** was employed as a key precursor for the synthesis of a variety of synthetically valuable and high-value heterocyclic scaffolds, including furan, thiophene, and pyrrole derivatives, in accordance with slightly modified established literature procedures.[19]

Treatment of compound **2b** with trifluoromethanesulfonic acid (TfOH) afforded 2,5-diphenylfuran **3a** in excellent yield, as illustrated in (Scheme 4.8a).[19a] Additionally, the substituted thiophene derivative **3b** was efficiently synthesized through the reaction of compound **2b** with Lawesson's reagent (Scheme 4.8b). [19b] Furthermore, the corresponding 2,5-diphenyl-substituted *N*H-pyrrole **3c** and *N*-benzyl pyrrole **3d** were obtained in good and quantitative yields, respectively (Scheme 4.8c and d).[19c] The reaction of compound **2b** with *o*-phthalaldehyde furnished naphthalene-2,3-diylbis(phenylmethanone) **3e** in excellent yield (Scheme 4.8e).[19d] Gratifyingly, the synthesized compound **2o** serves as a valuable intermediate for the synthesis of *Ombitasvir*, a potent NS5A inhibitor used in the treatment of Hepatitis C virus infection (Scheme 4.9).[20]

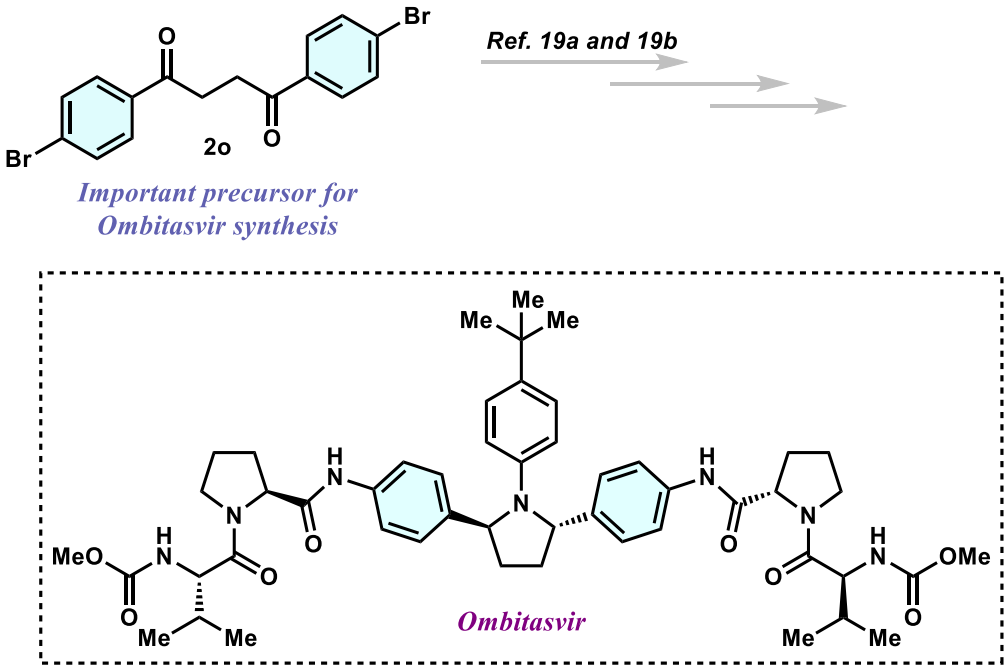

Scheme 4.9 Plausible biological application to synthesize *Ombitasvir*

To gain a deeper understanding of the reaction mechanism, a series of control experiments were performed (Scheme 4.10). When compound **1a** was subjected to the standard conditions in the absence of either light or the photocatalyst, no product formation was observed (Scheme

4.10a and 4.10b). Additionally, omitting the oxidant from the reaction resulted in only trace amounts of the desired product **2a** (Scheme 4.10c). These results highlighted the essential roles of light, photocatalyst, and oxidant in the transformation. Furthermore, conducting the reaction under an inert atmosphere completely suppressed product **2a** formation (Scheme 4.10d), whereas performing the reaction in the presence of molecular oxygen (using an O_2 balloon) delivered product **2a** in slightly reduced yield (Scheme 4.10e). Subsequently, the reaction was performed under an inert atmosphere in the presence of water; however, no formation of the desired product **2a** was observed (Scheme 4.10f). Furthermore, when the reaction was carried out under standard conditions with added water in open air, the product **2a** was obtained in very low yield (<10%) (Scheme 4.10g). Thus, implying that moisture might not involve in the reaction. These observations suggest that moisture is unlikely to play a significant role in the reaction mechanism and rules out the possibility of moisture as a potential source of oxygen in the product.

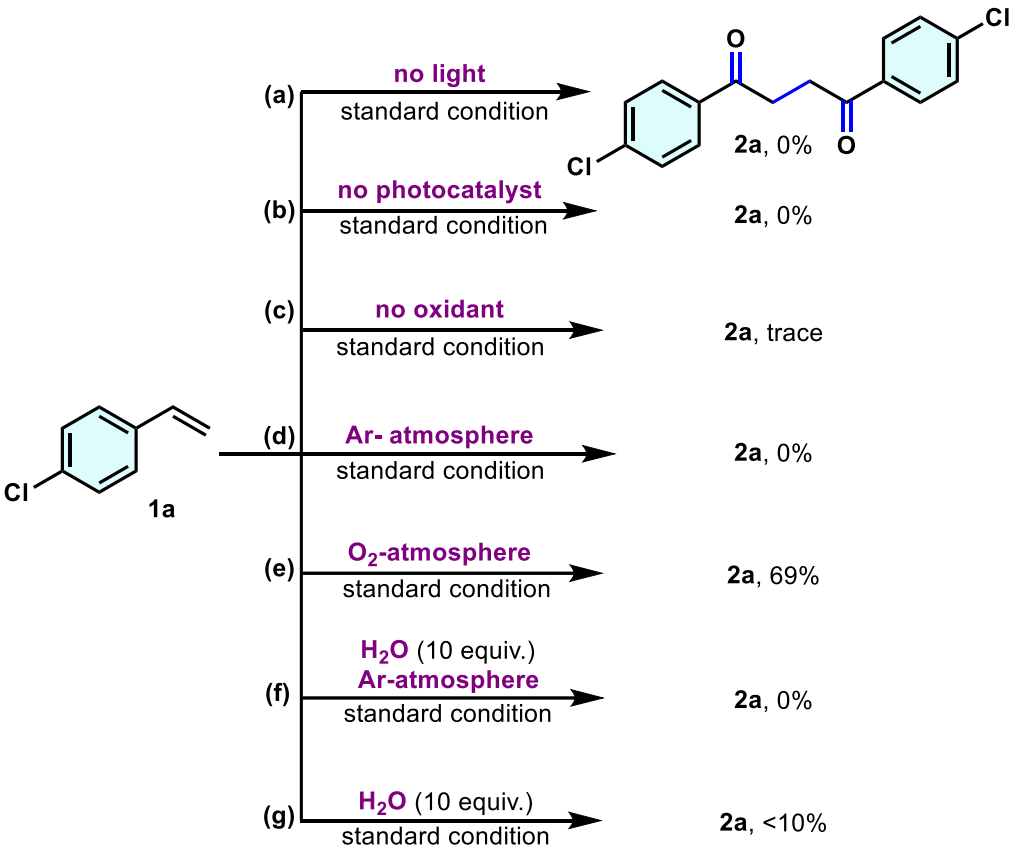

- ***Light, photocatalyst, oxidant, and molecular oxygen (air) are essential components***
- ***Rules out moisture as a potential source of oxygen in the product.***

Scheme 4.10 Control experiments

As suggested by the above experiment, molecular oxygen (air) may play a crucial role in the

reaction. To identify the specific reactive oxygen species involved is whether singlet oxygen or superoxide radical anion. We first conducted the reaction in the presence of a well-known singlet oxygen quencher, DABCO (Scheme 4.11a).[21] The absence of product **2a** formation in the presence of DABCO suggests the potential involvement of either singlet oxygen or a single electron transfer (SET)-mediated process. Furthermore, when the reaction was performed in the presence of the base DMAP, the formation of the corresponding product **2a** was not observed (Scheme 4.11b). Thus, suggesting the involvement of a SET process. Furthermore, when the reaction was carried out under standard conditions in the presence of sodium azide (NaN_3), a well-known singlet oxygen quencher, the desired product **2a** was obtained in 42% yield (Scheme 4.11c).[22] This result suggests that singlet oxygen is not involved in the reaction mechanism. Subsequently, the reaction was conducted in the presence of *p*-benzoquinone, a well-known quencher of superoxide radical anions, under otherwise standard conditions. The absence of the desired product **2a** indicated the plausible involvement of the superoxide radical anion in the reaction pathway (Scheme 4.11d).[23]

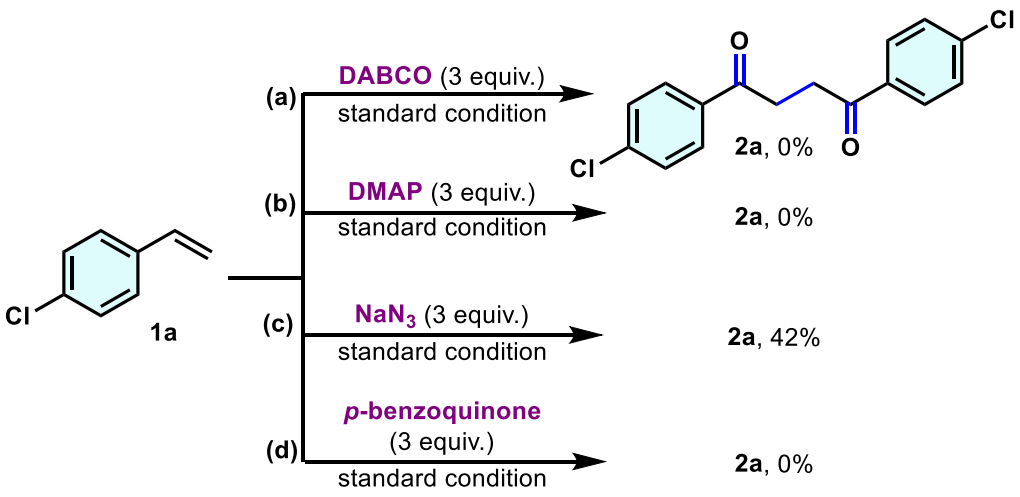

Scheme 4.11 Control experiments to identify the oxygen species involved

Furthermore, the reaction of styrene **1a** in the presence of radical quenchers 2,6-di-tert-butyl-4-methylphenol (BHT) or (2,2,6,6-tetramethylpiperidin-1-yl)oxyl (TEMPO) failed to afford the desired product **2a** in either case (Scheme 4.12).

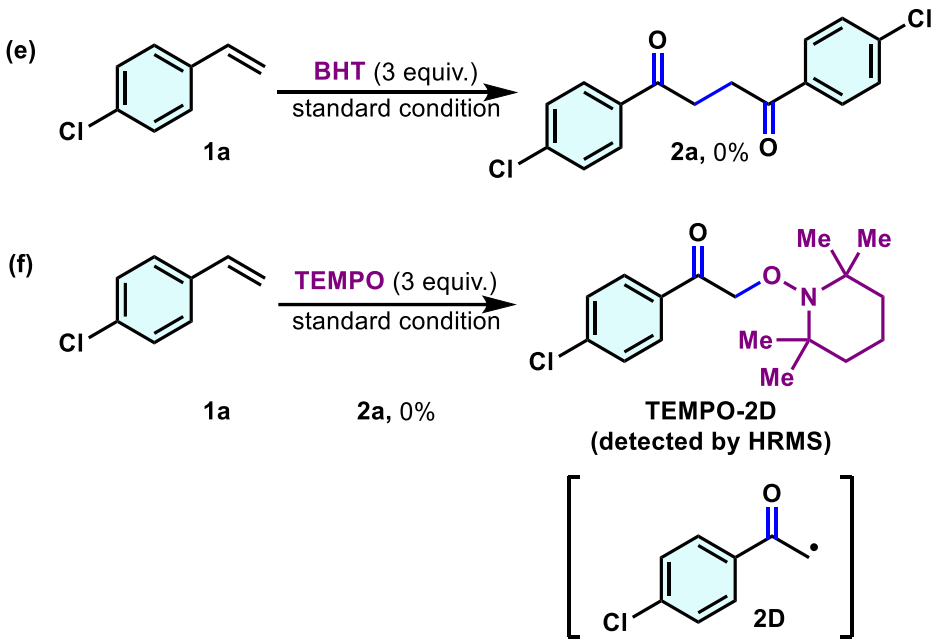

Scheme 4.12 Radical trapping experiment with BHT and TEMPO

However, the α-keto methyl radical–TEMPO adduct was detected by high-resolution mass spectrometry (HRMS) (Figure 4.3), thereby confirming the radical nature of the transformation and the involvement of radical intermediate **2D** in the reaction pathway.

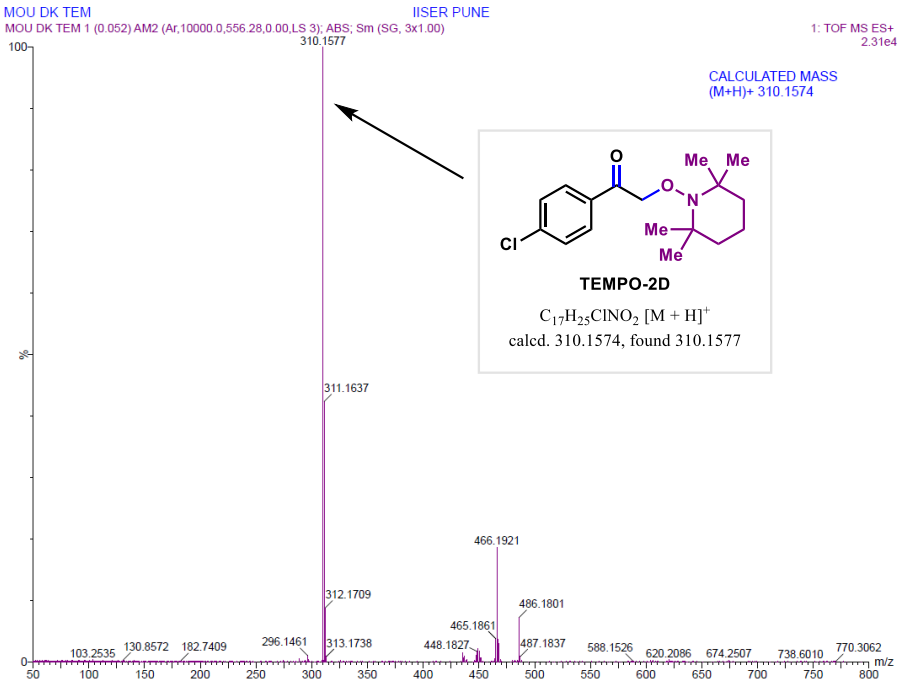

Figure 4.3 HRMS spectrum of radical adduct of **2D** with TEMPO

To investigate whether substrate styrene **1b**, or oxidant $Na_2S_2O_8$ interacts with the excited state photocatalyst (Acr*), we conducted a fluorescence quenching experiment and plotted the corresponding Stern–Volmer graph (Figure 4.4). The results demonstrated that styrene **1b** interacts with Acr* and not with the oxidant $Na_2S_2O_8$. The ability of Acr* to undergo single electron transfer (SET) with styrene was further supported by the oxidation potential of styrene (E_{ox} = +1.84 V vs SCE), which is lower than the reduction potential of Acr* (E_{red*} = 2.06 V vs SCE).[24]

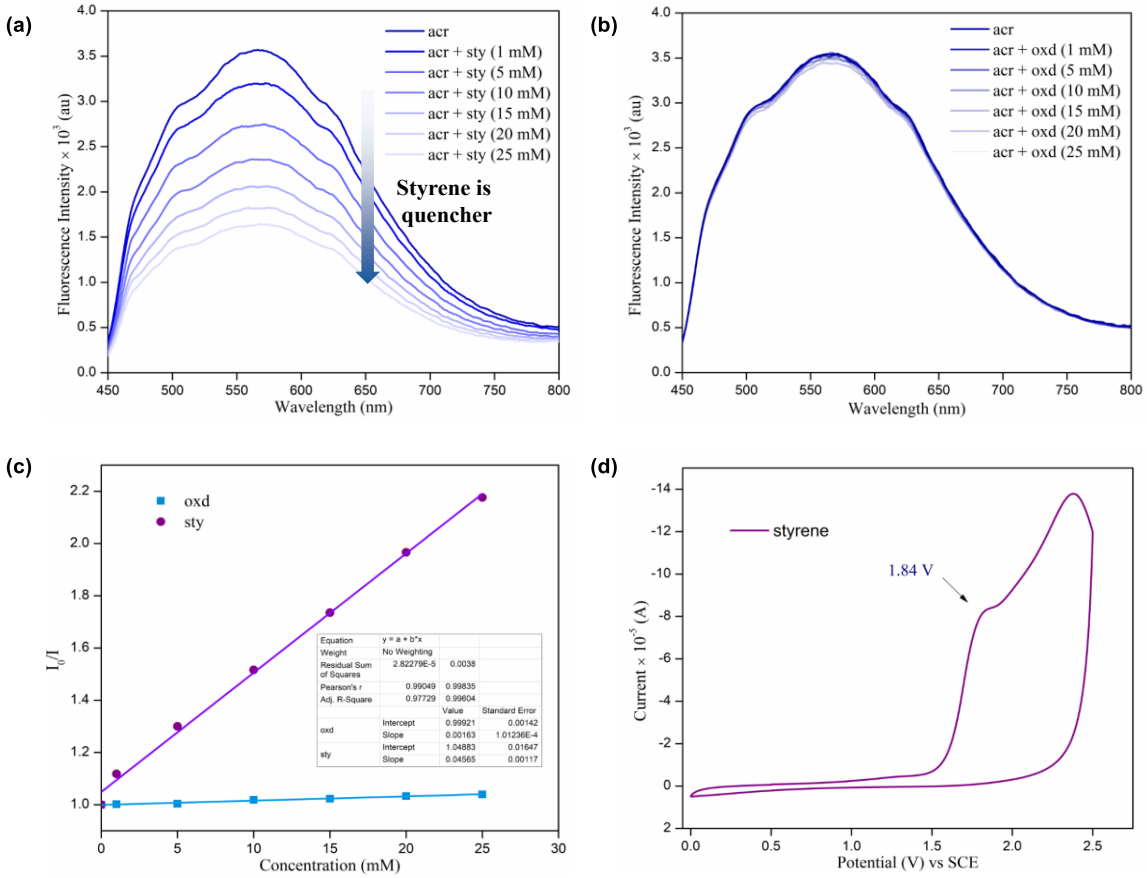

Figure 4.4 (a) Fluorescence spectra of Mes-Acr-Me^+ (10 μM) with increasing concentration of **1a**. (b) Fluorescence spectra of Mes-Acr-Me^+ (10 μM) with increasing concentration of oxidant $Na_2S_2O_8$. (c) Steady-state Stern–Volmer quenching plot of Mes-Acr-Me^+ (10 μM) with varying concentrations of **1a**/oxidant $Na_2S_2O_8$. (d) Cyclic voltammogram of styrene: E_p = +0.1.84 V (vs SCE in MeCN). Sample was prepared with 100 mM analyte and 100 mM $TBAPF_6$ electrolyte solution in MeCN with a scan rate of 100 mV/s. Cyclic voltammetry (CV) was performed using a CHI (model 600E) electrochemical analyzer/workstation. A three-electrode setup was used, consisting of a 3 mm dia. glassy carbon working electrode (Part no-CHI104, CH Instruments), platinum wire counter electrode (CHI115, CH Instruments), and a

Calomel reference electrode (Part no- CHI150, CH Instruments).

Based on the control experiments, Stern–Volmer analysis, cyclic voltammetry studies, and relevant literature precedents, a plausible reaction mechanism is proposed (Scheme 4.13). [16,25] Upon irradiation with blue light, the photocatalyst Acr is excited to its active state (Acr*). The excited Acr* species (E_{red*} =2.06 V vs SCE) further undergoes a single electron transfer (SET) with styrene **1b** (E_{ox} = +1.84 V vs SCE) via a reductive quenching pathway, resulting in the formation of Acr radical anion ($Acr^{\bullet-}$) and styrene radical cation **A**. This SET process is supported by Stern–Volmer quenching experiments and cyclic voltammetry data (Figure 4.4). The resulting $Acr^{\bullet-}$ then undergoes a subsequent single electron transfer (SET) with either the oxidant $Na_2S_2O_8$ or molecular oxygen, generating $SO_4^{\bullet-}/SO_4^{2-}$ or superoxide radical anion ($O_2^{\bullet-}$) respectively, while simultaneously regenerating the ground-state Acr, thus completing the photocatalytic cycle. Meanwhile, the intermediate **A** reacts with $O_2^{\bullet-}$ to form intermediate **B**, which undergoes SET, protonation and subsequent dehydration, affording intermediate **C** and ultimately leading to the formation of intermediate **D**. The radical adduct of intermediate **D** with TEMPO was detected by high-resolution mass spectrometry (HRMS), providing evidence for its formation. Subsequently, intermediate **D** undergoes tail-to-tail dimerization to furnish the desired 1,4-diketone product **2b**.

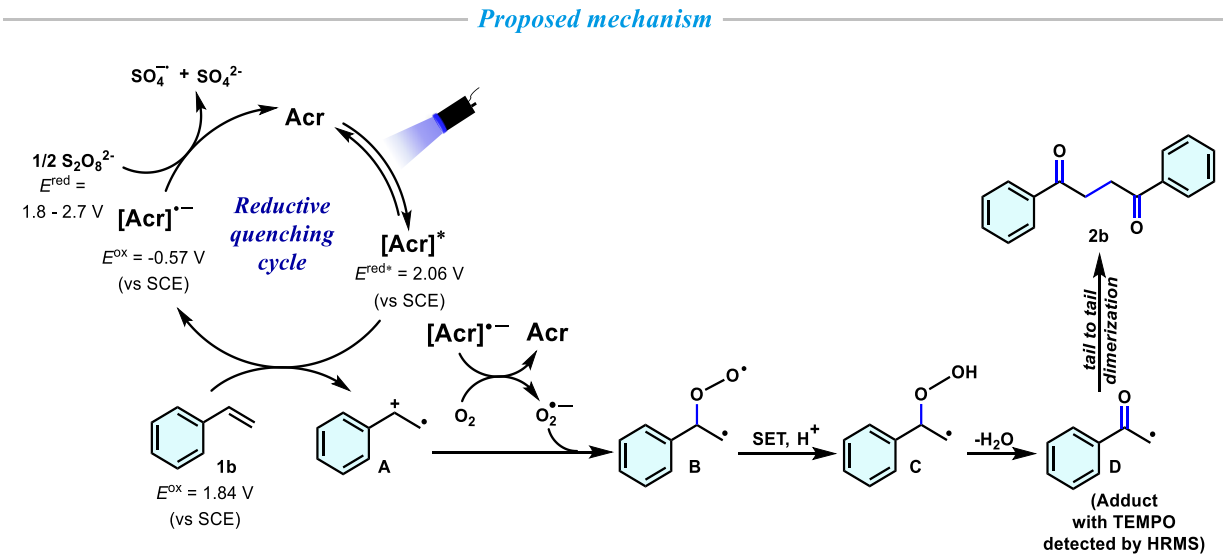

Scheme 4.13 Proposed reaction mechanism for 1,4-diketone synthesis

4.3 Conclusion

In summary, we have successfully demonstrated a transition metal-free, visible light promoted

direct synthesis of 1,4-deketones from readily available inexpensive and commercially viable styrene at room temperature. A non-toxic and inexpensive acridinium organophotoredox catalyst has been utilized as the photoredox catalyst for this operationally simple and mild protocol. The methodology showed the broad substrate scope with respect to styrene. The post synthetic modifications of the synthesized products have been demonstrated in the synthesis of different heterocyclic compounds such as furan, thiophene, pyrrol and naphthalene derivatives. Also, the protocol has been proved to be scalable and it works smoothly under direct exposure of sunlight. A series of control experiments, fluorescence quenching and cyclic voltammetry studies proved that transformation is driven via reductive quenching mechanistic cycle.

4.4 Experimental Section

4.4.1 General Details

Unless otherwise noted, all the starting materials and reagents were purchased from commercial suppliers (Sigma-Aldrich, TCI, Alfa Aesar, Spectrochem and BLD Pharm) and were used as received. Thin-layer chromatography (TLC) was performed using silica gel 60 GF_{254} precoated aluminum backed plates (2.5 mm). Visualization was accomplished by irradiation with UV light at 254 nm. The column chromatography was performed using silica gel (100–200 mesh) eluting with petroleum ether and ethyl acetate. The NMR spectra were recorded using tetramethylsilane as the internal standard. ^{1}H NMR spectra were recorded at 400 MHz, $^{19}F\{^{1}H\}$ NMR spectra were recorded at 377 MHz and $^{13}C\{^{1}H\}$ NMR spectra were recorded at 100 MHz (400 MHz Bruker and Jeol NMR instruments) unless otherwise noted. Chemical shifts (δ) are reported in ppm downfield from $CDCl_3$ (δ = 7.26 ppm) for ^{1}H NMR and relative to the central $CDCl_3$ resonance (δ = 77.16 ppm) for $^{13}C\{^{1}H\}$ NMR spectroscopy. For ^{1}H NMR, data are reported as follows: chemical shift, multiplicity (s = singlet, d = doublet, t = triplet, q = quartet, p = pentet, s = sextet, h = heptet, m = multiplet, br = broad), coupling constants (*J*) are given in Hz and integration. ^{13}C NMR spectra were recorded with complete proton decoupling. Mass samples were analyzed by high-resolution mass spectrometry (HRMS)-ESI TOF. Fluorescence emission spectra were obtained on a RF-6000 Spectrofluorophotometer from Shimadzu in a 3 mL, Hellma fluorescence cuvette (path length 1.0 cm). All photocatalytic reactions were performed under blue LEDs (Kessil PR160L series Blue LEDs. The reaction mixture was taken in a borosilicate glass and irradiated from 5 cm away from the LEDs. The reaction temperature is maintained 25-30 ^{o}C throughout the reaction by using external cooling fans.

List of starting materials used for the synthesis of and 1,4-diketones:

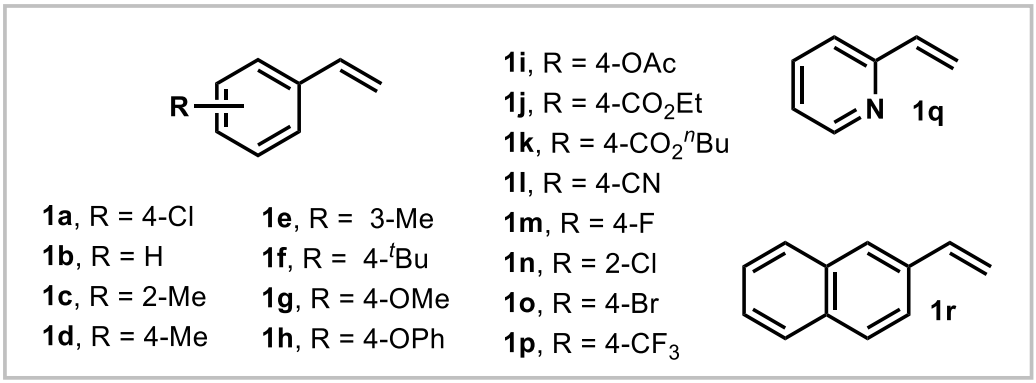

4.4.2 General Experimental Procedure

4.4.2A General Procedure A (GP A) for the organophotoredox catalyzed synthesis of 1,4-diketones **2**:

To an oven-dried reaction tube equipped with a stir bar styrene **1** (0.4 mmol, 1 equiv.), $Na_2S_2O_8$ (1.2 equiv.), Mes-Acr-Me·ClO_4 (3 mol %), and DMSO (3 mL) were added. Then the reaction mixture was irradiated with 427 nm Kessil PR-160L Blue LED (100% intensity *i.e.* 40 W), from ~5 cm away under open air and stirred at room temperature (under the continuous flow of fan to maintain the temperature at ~25–30 °C) for 8 h (monitored by TLC). After completion of the reaction, the reaction mixture was subjected to work up via pouring to ice cold water then separated using CH_2Cl_2. The combined organic layers were dried over anhydrous Na_2SO_4. After filtration, the filtrate was concentrated under reduced pressure. Then, the crude residue was purified by column chromatography over silica gel (100–200 mesh size) using mixture of petroleum ether/EtOAc as an eluent to afford the corresponding desired 1,4-diketones **2**.

4.4.2B General Procedure B (GP B) for the synthesis of 1,4-diketone **2a** under natural sunlight: To an oven-dried reaction tube equipped with a stir bar styrene **1** (0.4 mmol, 1 equiv.), $Na_2S_2O_8$ (1.2 equiv.), Mes-Acr-Me·ClO_4 (3 mol %), and DMSO (3 mL) were added. Then the reaction mixture was stirred under natural sunlight for 8 h (monitored by TLC). After completion of the reaction, the reaction mixture was subjected to work up via pouring to ice cold water then separated via using CH_2Cl_2. The combined organic layers were dried by anhydrous Na_2SO_4. After filtration, the filtrate was condensed under reduced pressure. Then, the crude residue was purified by column chromatography over silica gel (100–200 mesh size) using mixture of petroleum ether/EtOAc as an eluent to afford the corresponding desired 1,4-diketones **2a** in (39 mg, 64%).

4.4.2C General Procedure C (GP C) for the scale-up synthesis of 1,4-diketone **2a**:

To an oven-dried 100 mL reaction flask equipped with a stir bar styrene **1a** (1g, 1 equiv.), $Na_2S_2O_8$ (1.2 equiv.), Mes-Acr-Me·ClO_4 (3 mol %), and DMSO (10 mL) were added. Then the reaction mixture was irradiated with Kessil PR-160L Blue LED (427 nm, 100% intensity *i.e.* 40 W × 2), from ~5 cm away under open air and stirred at room temperature (under the continuous flow of fan to maintain the temperature at 25–30 °C) for 24 h (monitored by TLC). After completion of the reaction, the reaction mixture was subjected to work up via pouring to ice cold water then separated with CH_2Cl_2. The combined organic layers were dried by anhydrous Na_2SO_4. After filtration, the filtrate was condensed under reduced pressure. Then, the crude residue was purified by column chromatography over silica gel (100–200 mesh size) using mixture of petroleum ether/EtOAc as an eluent to afford the corresponding desired 1,4-diketone **2a** in (721 mg, 63%).

4.4.3 Product Characterization Data

1,4-bis(4-chlorophenyl)butane-1,4-dione (**2a**): The compound **2a** was prepared following the

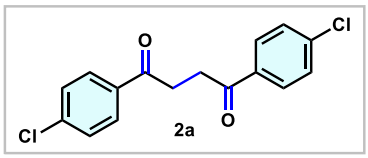

General Procedure A (GP A). White solid (41 mg, 67% yield), R_f = 0.30 (petroleum ether/EtOAc 90:10). ^{1}H NMR (400 MHz, $CDCl_3$) δ 7.99 – 7.96 (m, 4H), 7.48 – 7.44 (m, 4H), 3.42 (s, 4H). $^{13}C\{^1H\}$ NMR (100 MHz, $CDCl_3$) δ 197.5, 139.8, 135.1, 129.7, 129.1, 32.6. HRMS (ESI TOF) *m/z* for $C_{16}H_{13}Cl_2O_2$ $[M + H]^+$ calcd. 307.0293, found 307.0298.

1,4-diphenylbutane-1,4-dione (**2b**): The compound **2b** was prepared following the General

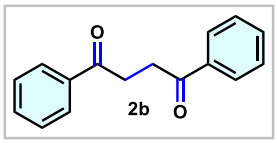

Procedure A (GP A). White solid (34 mg, 72% yield), R_f = 0.30 (petroleum ether/EtOAc 90:10). ^{1}H NMR (400 MHz, $CDCl_3$) δ 8.06 – 8.03 (m, 4H), 7.60 – 7.56 (m, 2H), 7.48 (ddd, *J* = 8.2, 6.7, 1.3 Hz, 4H), 3.47 (s, 4H). $^{13}C\{^1H\}$ NMR (100 MHz, $CDCl_3$) δ 198.9, 136.9, 133.3, 128.7, 128.3, 32.7. HRMS (ESI TOF) *m/z* for $C_{16}H_{15}O_2$ $[M + H]^+$ calcd. 239.1072, found 239.1070.

1,4-di-o-tolylbutane-1,4-dione (**2c**): The compound **2c** was prepared following the General

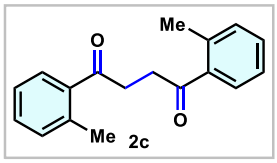

Procedure A (GP A). White solid (29 mg, 55% yield), R_f = 0.38 (petroleum ether/EtOAc 90:10). ^{1}H NMR (400 MHz, $CDCl_3$) δ 7.80 (dd, *J* = 7.7, 1.1 Hz, 2H), 7.38 (td, *J* = 7.5, 1.3 Hz, 2H), 7.30 (d, *J* = 7.6 Hz, 2H), 7.25 (d, *J* = 6.8 Hz, 2H), 3.34 (s, 4H), 2.50 (s, 6H). $^{13}C\{^1H\}$ NMR (100 MHz, $CDCl_3$)

δ 202.8, 138.2, 138.0, 132.0, 131.4, 128.7, 125.8, 35.8, 21.4. HRMS (ESI TOF) *m/z* for $C_{18}H_{19}O_2$ $[M + H]^+$ calcd. 267.1385, found 267.1381.

1,4-di-p-tolylbutane-1,4-dione (**2d**): The compound **2d** was prepared following the General Procedure A (GP A). White solid (36 mg, 68% yield), R_f = 0.33 (petroleum ether/EtOAc 90:10). ^{1}H NMR (400 MHz, $CDCl_3$) δ 7.94 (d, *J* = 8.3 Hz, 4H), 7.27 (d, *J* = 9.1 Hz, 4H), 3.43 (s, 4H), 2.42 (s, 6H). $^{13}C\{^1H\}$ NMR (100 MHz, $CDCl_3$) δ 198.6, 144.0, 134.5, 129.4, 128.4, 32.7, 21.8. HRMS (ESI TOF) *m/z* for $C_{18}H_{19}O_2$ $[M + H]^+$ calcd. 267.1385, found 267.1387.

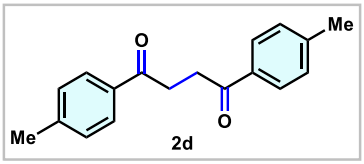

1,4-di-m-tolylbutane-1,4-dione (**2e**): The compound **2e** was prepared following the General Procedure A (GP A). White solid (31 mg, 57% yield), R_f = 0.36 (petroleum ether/EtOAc 90:10). ^{1}H NMR (400 MHz, $CDCl_3$) δ 7.85 – 7.83 (m, 4H), 7.39 – 7.36 (m, 4H), 3.45 (s, 4H), 2.42 (s, 6H). $^{13}C\{^1H\}$ NMR (100 MHz, $CDCl_3$) δ 199.1, 138.5, 137.0, 134.0, 128.8, 128.6, 125.5, 32.8, 21.5. HRMS (ESI TOF) *m/z* for $C_{18}H_{19}O_2$ $[M + H]^+$ calcd. 267.1385, found 267.1389.

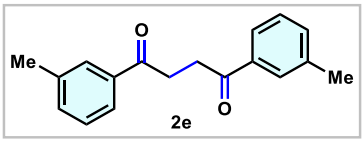

1,4-bis(4-(tert-butyl)phenyl)butane-1,4-dione (**2f**): The compound **2f** was prepared following the General Procedure A (GP A). White solid (31 mg, 44% yield), R_f = 0.43 (petroleum ether/EtOAc 90:10). ^{1}H NMR (400 MHz, $CDCl_3$) δ 8.00 – 7.96 (m, 4H), 7.51 – 7.48 (m, 4H), 3.44 (s, 4H), 1.35 (s, 18H). $^{13}C\{^1H\}$ NMR (100 MHz, $CDCl_3$) δ 198.7, 157.0, 134.4, 128.2, 125.7, 32.7, 31.2, 29.9. HRMS (ESI TOF) *m/z* for $C_{24}H_{31}O_2$ $[M + H]^+$ calcd. 351.2324, found 351.2327.

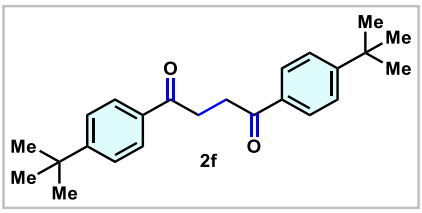

1,4-bis(4-methoxyphenyl)butane-1,4-dione (**2g**): The compound **2g** was prepared following the General Procedure A (GP A). White solid (25 mg, 41% yield), R_f = 0.43 (petroleum ether/EtOAc 90:10). ^{1}H NMR (400 MHz, $CDCl_3$) δ 8.04 – 8.00 (m, 4H), 6.97 – 6.93 (m, 4H), 3.88 (s, 6H), 3.40 (s, 4H). $^{13}C\{^1H\}$ NMR (100 MHz, $CDCl_3$) δ 197.6, 163.7, 130.5, 130.1, 113.9, 55.6, 32.5. HRMS (ESI TOF) *m/z* for $C_{18}H_{18}NaO_4$ $[M + Na]^+$ calcd. 321.1102, found 321.1102.

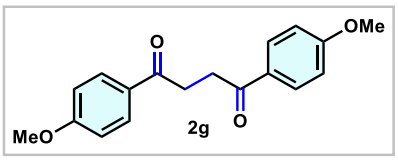

1,4-bis(4-phenoxyphenyl)butane-1,4-dione (**2h**): The compound **2h** was prepared following the General Procedure A (GP A). White solid (56 mg, 66% yield), R_f = 0.25 (petroleum ether/EtOAc 90:10). ^{1}H NMR (400 MHz, $CDCl_3$) δ 8.04 – 8.00 (m, 4H), 7.43 – 7.38 (m, 4H), 7.22 – 7.18 (m, 2H), 7.10 – 7.06 (m, 4H), 7.04 – 7.00 (m, 4H), 3.41 (s, 4H). ^{13}C{^{1}H} NMR (100 MHz, $CDCl_3$) δ 197.5, 162.2, 155.7, 131.6, 130.5, 130.2, 124.7, 120.3, 117.5, 32.5. HRMS (ESI TOF) *m/z* for $C_{28}H_{23}O_4$ $[M + H]^+$ calcd. 423.1596, found 423.1597.

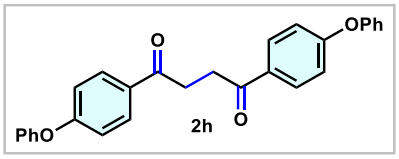

Succinylbis(4,1-phenylene) diacetate (**2i**): The compound **2i** was prepared following the General Procedure A (GP A). White solid (57 mg, 80% yield), R_f = 0.40 (petroleum ether/EtOAc 60:40). ^{1}H NMR (400 MHz, $CDCl_3$) δ 8.09 – 8.06 (m, 4H), 7.23 – 7.20 (m, 4H), 3.44 (s, 4H), 2.33 (s, 6H). ^{13}C{^{1}H} NMR (100 MHz, $CDCl_3$) δ 197.5, 169.0, 154.6, 134.5, 129.9, 122.0, 32.7, 21.3. HRMS (ESI TOF) *m/z* for $C_{20}H_{19}O_6$ $[M + H]^+$ calcd. 355.1182, found 355.1180.

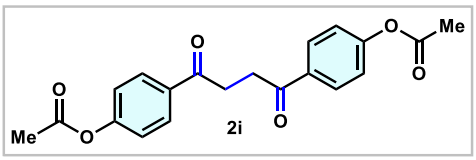

diethyl 4,4'-succinyldibenzoate (**2j**): The compound **2j** was prepared following the General Procedure A (GP A). White solid (59 mg, 77% yield), R_f = 0.20 (petroleum ether/EtOAc 80:20). ^{1}H NMR (400 MHz, $CDCl_3$) δ 8.17 – 8.14 (m, 4H), 8.10 – 8.07 (m, 4H), 4.42 (q, *J* = 7.1 Hz, 4H), 3.50 (s, 4H), 1.42 (t, *J* = 7.1 Hz, 6H). ^{13}C{^{1}H} NMR (100 MHz, $CDCl_3$) δ 198.2, 165.9, 139.9, 134.5, 130.0, 128.2, 61.6, 33.0, 14.4. HRMS (ESI TOF) *m/z* for $C_{22}H_{23}O_6$ $[M + H]^+$ calcd. 383.1495, found 383.1494.

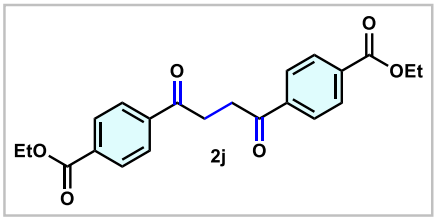

dibutyl 4,4'-succinyldibenzoate (**2k**): The compound **2k** was prepared following the General Procedure A (GP A). White solid (72 mg, 82% yield), R_f = 0.30 (petroleum ether/EtOAc 80:20). ^{1}H NMR (400 MHz, $CDCl_3$) δ 8.15 (d, *J* = 8.5 Hz, 4H), 8.08 (d, *J* = 8.5 Hz, 4H), 4.36 (t, *J* = 6.6 Hz, 4H), 3.50 (s, 4H), 1.81 – 1.74 (m, 4H), 1.54 – 1.45 (m, 4H), 0.99 (t, *J* = 7.4 Hz, 6H). ^{13}C{^{1}H} NMR (100 MHz, $CDCl_3$) δ 198.2, 166.0, 139.9, 134.6, 130.0, 128.2, 65.5, 33.0, 30.9, 19.4, 13.9. HRMS (ESI TOF) *m/z* for $C_{26}H_{31}O_4$ $[M + H]^+$ calcd. 439.2121, found

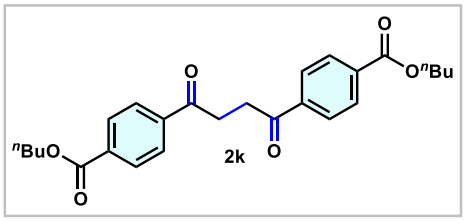

439.2120.

4,4'-Succinyldibenzonitrile (**2l**): The compound **2l** was prepared following the General Procedure A (GP A). White solid (25 mg, 44% yield), R_f = 0.36 (petroleum ether/EtOAc 60:40). ^{1}H NMR (400 MHz, $CDCl_3$) δ 8.13 – 8.10 (m, 4H), 7.82 – 7.80 (m, 4H), 3.48 (s, 4H). $^{13}C\{^1H\}$ NMR (100 MHz, $CDCl_3$) δ 197.1, 139.6, 132.7, 128.7, 118.0, 105.3, 32.9. HRMS (ESI TOF) *m/z* for $C_{18}H_{13}N_2O_2$ $[M + H]^+$ calcd. 289.0977, found 289.0971.

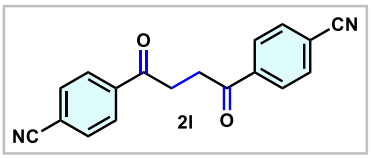

1,4-bis(4-fluorophenyl)butane-1,4-dione (**2m**): The compound **2m** was prepared following the General Procedure A (GP A). White solid (21 mg, 38% yield), R_f = 0.25 (petroleum ether/EtOAc 90:10). ^{1}H NMR (400 MHz, $CDCl_3$) δ 8.09 – 8.04 (m, 4H), 7.18 – 7.13 (m, 4H), 3.43 (s, 4H). $^{13}C\{^1H\}$ NMR (100 MHz, $CDCl_3$) δ 197.2 (s), 166.0 (d, *J* = 254.9 Hz), 133.3 (s), 130.9 (d, *J* = 9.4 Hz), 115.9 (d, *J* = 21.9 Hz), 32.6 (s). $^{19}F\{^1H\}$ NMR (377 MHz, $CDCl_3$) δ -105.10. HRMS (ESI TOF) *m/z* for $C_{16}H_{13}F_2O_2$ $[M + H]^+$ calcd. 275.0884, found 275.0888.

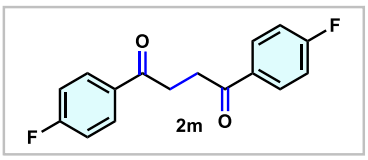

1,4-bis(2-chlorophenyl)butane-1,4-dione (**2n**): The compound **2n** was prepared following the General Procedure A (GP A). White solid (28 mg, 46% yield), R_f = 0.29 (petroleum ether/EtOAc 90:10). ^{1}H NMR (400 MHz, $CDCl_3$) δ 7.63 – 7.61 (m, 2H), 7.45 – 7.32 (m, 6H), 3.41 (s, 4H). $^{13}C\{^1H\}$ NMR (100 MHz, $CDCl_3$) δ 201.6, 139.1, 132.0, 131.1, 130.7, 129.5, 127.1, 37.4. HRMS (ESI TOF) *m/z* for $C_{16}H_{13}Cl_2O_2$ $[M + H]^+$ calcd. 307.0293, found 307.0292.

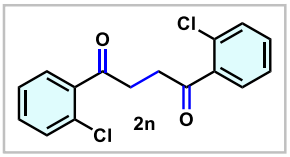

1,4-bis(4-bromophenyl)butane-1,4-dione (**2o**): The compound **2o** was prepared following the General Procedure A (GP A). White solid (62 mg, 78% yield), R_f = 0.26 (petroleum ether/EtOAc 90:10). ^{1}H NMR (400 MHz, $CDCl_3$) δ 7.91 – 7.88 (m, 4H), 7.64 – 7.61 (m, 4H), 3.41 (s, 4H). $^{13}C\{^1H\}$ NMR (100 MHz, $CDCl_3$) δ 197.7, 135.5, 132.1, 129.8, 128.6, 32.6. HRMS (ESI TOF) *m/z* for $C_{16}H_{13}Br_2O_2$ $[M + H]^+$ calcd. 394.9282, found 394.9285.

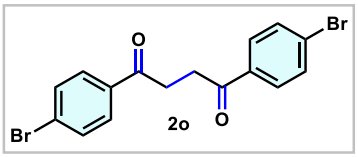

1,4-bis(4-(trifluoromethyl)phenyl)butane-1,4-dione (**2p**): The compound **2p** was prepared following the General Procedure A (GP A). White solid (24 mg, 32% yield), R_f = 0.23 (petroleum ether/EtOAc 90:10). ^{1}H NMR (400 MHz, $CDCl_3$) δ 8.14 (d, *J* = 8.1 Hz, 4H), 7.77 (d, *J* = 8.2 Hz, 4H), 3.50 (s, 4H). $^{13}C\{^1H\}$ NMR (100 MHz, $CDCl_3$) δ 197.6, 139.4, 134.8 (q, *J* = 32.7 Hz), 128.6, 125.9 (q, *J* = 3.7 Hz), 123.7 (q, *J* = 272.9 Hz), 32.9. $^{19}F\{^1H\}$ NMR (377 MHz, $CDCl_3$) δ -63.13. HRMS (ESI TOF) *m/z* for $C_{18}H_{13}F_6O_2$ $[M + H]^+$ calcd. 375.0820, found 375.0821.

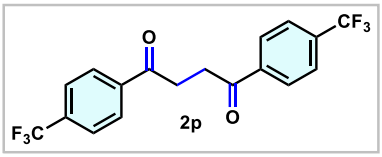

1,4-di(pyridin-2-yl)butane-1,4-dione (**2q**): The compound **2q** was prepared following the General Procedure A (GP A). White solid (25 mg, 51% yield), R_f = 0.40 (petroleum ether/EtOAc 60:40). ^{1}H NMR (400 MHz, $CDCl_3$) δ 8.71 (ddd, *J* = 4.7, 1.6, 0.9 Hz, 2H), 8.04 (dt, *J* = 7.9, 1.0 Hz, 2H), 7.83 (td, *J* = 7.7, 1.7 Hz, 2H), 7.48 (ddd, *J* = 7.6, 4.8, 1.2 Hz, 2H), 3.70 (s, 4H). $^{13}C\{^1H\}$ NMR (100 MHz, $CDCl_3$) δ 200.6, 153.4, 149.1, 137.0, 127.3, 122.0, 32.2. HRMS (ESI TOF) *m/z* for $C_{14}H_{13}N_2O_2$ $[M + H]^+$ calcd. 241.0977, found 241.0976.

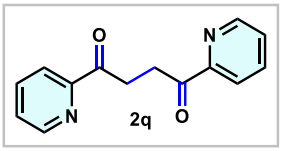

1,4-di(naphthalen-2-yl)butane-1,4-dione (**2r**): The compound **2r** was prepared following the General Procedure A (GP A). White solid (43 mg, 63% yield), R_f = 0.23 (petroleum ether/EtOAc 90:10). ^{1}H NMR (400 MHz, $CDCl_3$) δ 8.62 (s, 2H), 8.11 (dd, *J* = 8.6, 1.7 Hz, 2H), 8.01 (d, *J* = 8.0 Hz, 2H), 7.91 (dd, *J* = 12.0, 8.3 Hz, 4H), 7.64 – 7.55 (m, 4H), 3.68 (s, 4H). $^{13}C\{^1H\}$ NMR (100 MHz, $CDCl_3$) δ 198.9, 135.8, 134.3, 132.7, 130.1, 129.8, 128.6, 127.9, 126.9, 124.0, 33.0. HRMS (ESI TOF) *m/z* for $C_{24}H_{19}O_2$ $[M + H]^+$ calcd. 339.1385, found 339.1383.

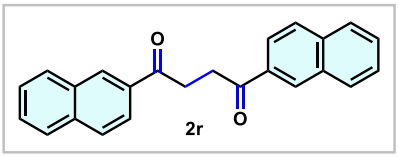

2,5-diphenylfuran (**3a**): The compound **3a** was prepared with slight modifications to a previously reported procedure.[18a] To an oven-dried reaction flask containing **2b** (50 mg, 0.21 mmol), MeCN (3 mL) and TfOH (1.1 equiv.) were added. The reaction mixture was heated to 85 °C overnight. The reaction was quenched by Sat. $NaHCO_3$ and extracted by DCM. The combined organic layers were dried by anhydrous Na_2SO_4. After filtration, the filtrate was condensed under reduced pressure. Then, the crude residue was purified by column chromatography over silica gel (100–200 mesh size) using mixture of petroleum ether/EtOAc as an eluent to obtain **3a**. White solid (42 mg, 91% yield),

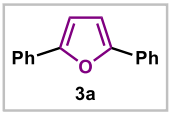

R_f = 0.46 (petroleum ether/EtOAc 98:2). ^{1}H NMR (400 MHz, $CDCl_3$) δ 7.77 – 7.74 (m, 4H), 7.41 (dd, *J* = 8.5, 7.0 Hz, 4H), 7.30 – 7.27 (m, 2H), 6.75 (s, 2H). $^{13}C\{^1H\}$ NMR (100 MHz, $CDCl_3$) δ 153.5, 130.9, 128.9, 127.5, 123.9, 107.4. HRMS (ESI TOF) *m/z* for $C_{16}H_{13}O$ $[M + H]^+$ calcd. 221.0966, found 221.0967.

2,5-diphenylthiophene (**3b**): The compound **3b** was prepared with slight modifications to a previously reported procedure.[18b] To an oven-dried reaction flask containing **2b** (50 mg, 0.21 mmol), THF (3 mL) and Lawesson's reagent (1.1 equiv.) were added. The reaction mixture was heated to 55 ºC for 5 h. The reaction mixture was condensed and the residue was purified by column chromatography over silica gel (100–200 mesh size) using mixture of petroleum ether/EtOAc as an eluent to obtain **3b**. White solid (46 mg, 92% yield), R_f = 0.46 (petroleum ether/EtOAc 98:2). ^{1}H NMR (400 MHz, $CDCl_3$) δ 7.64 – 7.61 (m, 4H), 7.40 – 7.36 (m, 4H), 7.30 – 7.26 (m, 4H). $^{13}C\{^1H\}$ NMR (100 MHz, $CDCl_3$) δ 143.8, 134.4, 129.1, 127.6, 125.8, 124.1. HRMS (ESI TOF) *m/z* for $C_{16}H_{13}S$ $[M + H]^+$ calcd. 237.0783, found 237.0780.

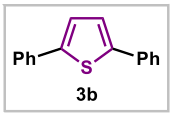

3b

2,5-diphenyl-1H-pyrrole (**3c**): The compound **3c** was prepared with slight modifications to a previously reported procedure.[18c] To an oven-dried reaction flask containing **2b** (50 mg, 0.21 mmol), NH_4OAc (5 equiv.) and HOAc (1.5 mL) were added. The reaction mixture was refluxed at 100 ºC overnight. The reaction mixture was cooled to rt and poured into ice-water. The solid was collected and washed with H_2O. The solid was dried to afford **3c**. White solid (44 mg, 96% yield), R_f = 0.27 (petroleum ether/EtOAc 95:5). ^{1}H NMR (400 MHz, $CDCl_3$) δ 8.66 (s, 1H), 7.58 (d, *J* = 7.2 Hz, 4H), 7.44 (t, *J* = 7.6 Hz, 4H), 7.29 (d, *J* = 7.5 Hz, 2H), 6.64 (d, *J* = 2.6 Hz, 2H). $^{13}C\{^1H\}$ NMR (100 MHz, $CDCl_3$) δ 133.3, 132.6, 129.1, 126.5, 123.9, 108.1. HRMS (ESI TOF) *m/z* for $C_{16}H_{14}N$ $[M + H]^+$ calcd. 220.1126, found 220.1125.

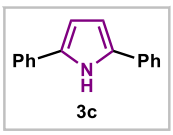

3c

1-benzyl-2,5-diphenyl-1H-pyrrole (**3d**): The compound **3d** was prepared with slight modifications to a previously reported procedure.[18d] To an oven-dried reaction flask containing **2b** (50 mg, 0.21 mmol), benzylamine, (1.2 equiv.), HOAc (2-5 drops) and toluene (2 mL) were added. The reaction mixture was refluxed at 100 ºC overnight. The reaction mixture was cooled to rt, and solvent was removed under reduced pressure and the residue was purified by column chromatography over silica gel (100–200 mesh size) using mixture of petroleum ether/EtOAc as an eluent to obtain

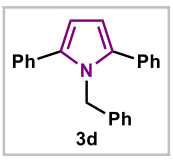

3d

3d. White solid (49 mg, 76% yield), R_f = 0.33 (petroleum ether/EtOAc 95:5). ^{1}H NMR (400 MHz, $CDCl_3$) δ 7.37 – 7.28 (m, 8H), 7.27 – 7.26 (m, 1H), 7.25 – 7.23 (m, 1H), 7.15 – 7.07 (m, 3H), 6.67 – 6.65 (m, 2H), 6.36 (s, 2H), 5.24 (s, 2H). $^{13}C\{^1H\}$ NMR (100 MHz, $CDCl_3$) δ 139.4, 136.9, 133.8, 129.2, 128.5, 128.4, 127.1, 126.9, 126.1, 109.8, 48.8. HRMS (ESI TOF) *m/z* for $C_{23}H_{20}N$ $[M + H]^+$ calcd. 310.1596, found 310.1599.

naphthalene-2,3-diylbis(phenylmethanone) (**3e**): The compound **3e** was prepared was prepared with slight modifications to a previously reported procedure.[18e] To an oven-dried reaction flask containing **2b** (50 mg, 0.21 mmol), *o*-phthalaldehyde (1.1 equiv.) and EtOH (3 mL) were added. Subsequently, ^{t}BuOK (2.5 equiv.) was added slowly. Then the reaction was stirred at rt overnight. The reaction mixture was quenched by H_2O and extracted by EtOAc for 3 times. The combined organic layers were dried by anhydrous Na_2SO_4. After filtration, the filtrate was condensed under reduced pressure. Then, the crude residue was purified by column chromatography over silica gel (100–200 mesh size) using mixture of petroleum ether/EtOAc as an eluent to obtain **3e**. Colourless liquid (66 mg, 94% yield), R_f = 0.28 (petroleum ether/EtOAc 80:20). ^{1}H NMR (400 MHz, $CDCl_3$) δ 8.10 (s, 2H), 7.97 – 7.92 (m, 2H), 7.83 – 7.80 (m, 4H), 7.69 – 7.64 (m, 2H), 7.57 – 7.53 (m, 2H), 7.44 – 7.39 (m, 4H). $^{13}C\{^1H\}$ NMR (100 MHz, $CDCl_3$) δ 196.5, 137.5, 137.1, 133.2, 133.1, 130.9, 130.1, 128.9, 128.8, 128.5. HRMS (ESI TOF) *m/z* for $C_{24}H_{17}O_2$ $[M + H]^+$ calcd. 337.1229, found 337.1230.

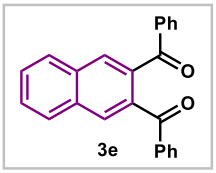

4.4.4 Appendix IV. ^{1}H and $^{13}C\{^1H\}$ NMR spectral data of representative compounds

Compound No.	Figure IV.X	Data	Page No.
2a	Figure IV.1 and IV.2	^{1}H and $^{13}C\{^1H\}$	161
2g	Figure IV.3 and IV.4	^{1}H and $^{13}C\{^1H\}$	162
2h	Figure IV.5 and IV.6	^{1}H and $^{13}C\{^1H\}$	163
2q	Figure IV.7 and IV.8	^{1}H and $^{13}C\{^1H\}$	164
2r	Figure IV.9 and IV.10	^{1}H and $^{13}C\{^1H\}$	165
3a	Figure IV.11 and IV.12	^{1}H and $^{13}C\{^1H\}$	166
3b	Figure IV.13 and IV.14	^{1}H and $^{13}C\{^1H\}$	167
3c	Figure IV.15 and IV.16	^{1}H and $^{13}C\{^1H\}$	168
3d	Figure IV.17 and IV.18	^{1}H and $^{13}C\{^1H\}$	169
3e	Figure IV.19 and IV.20	^{1}H and $^{13}C\{^1H\}$	170

4.4.5 Copies of ^{1}H and $^{13}C\{^{1}H\}$ NMR Spectra

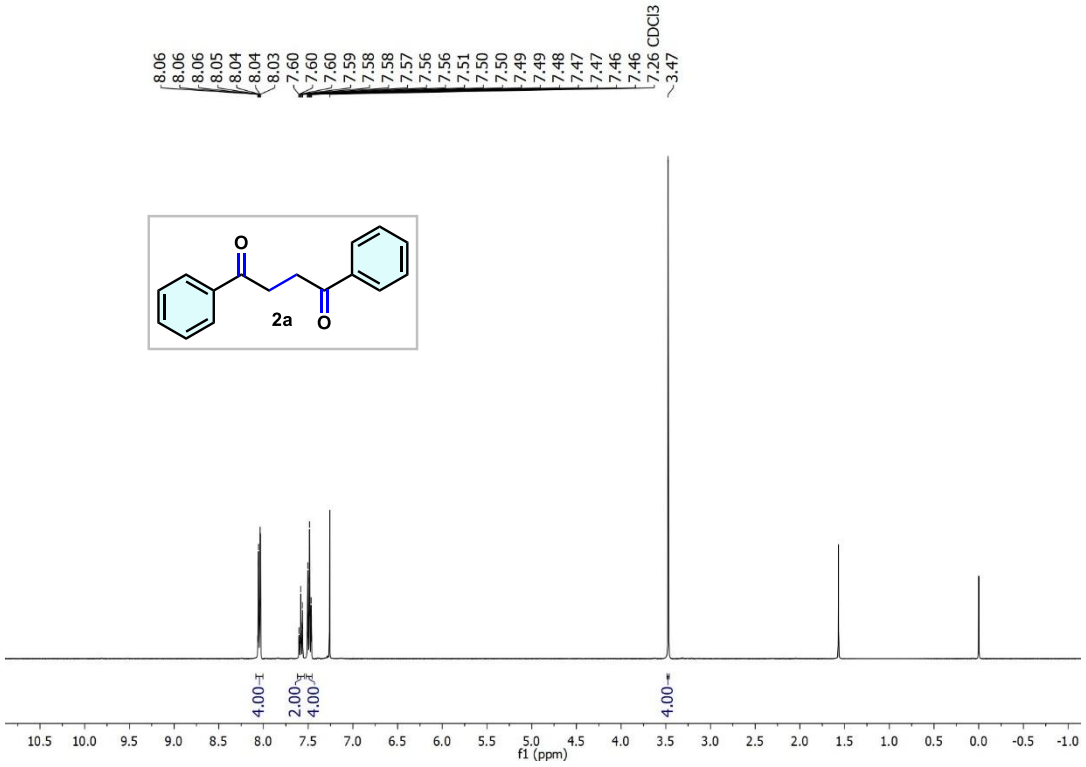

Figure IV.1 ^{1}H NMR spectrum of **2a**, $CDCl_3$, 400 MHz

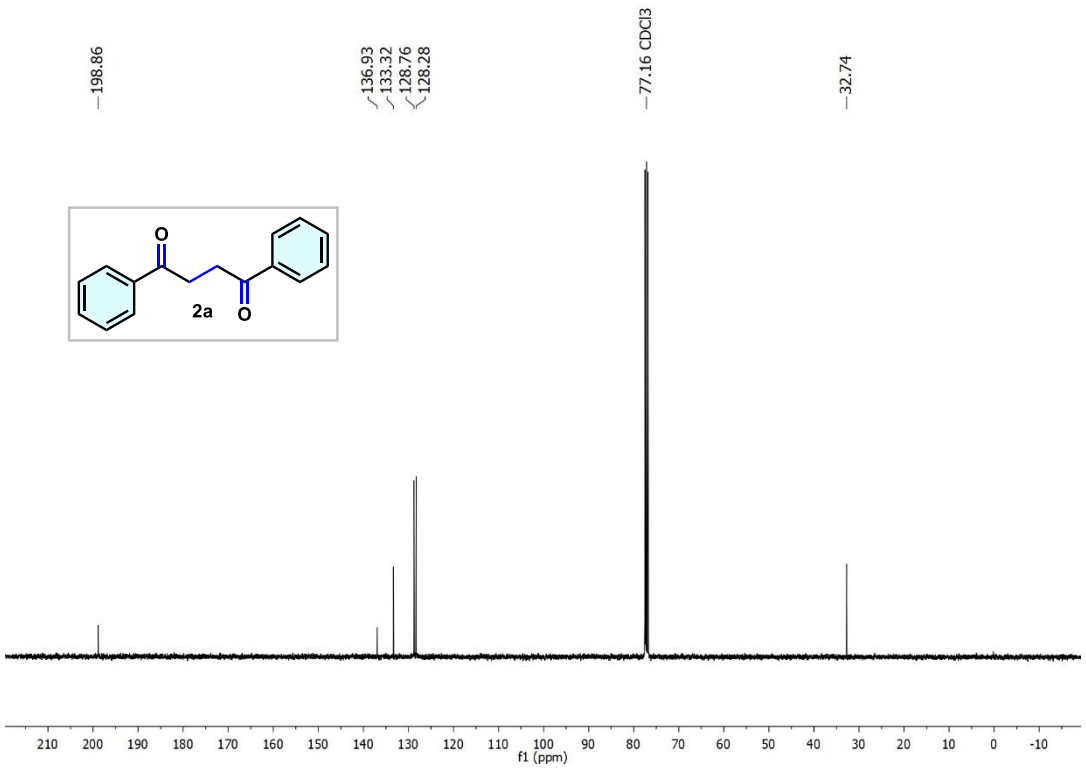

Figure IV.2 $^{13}C\{^{1}H\}$ NMR spectrum of **2a**, $CDCl_3$, 100 MHz

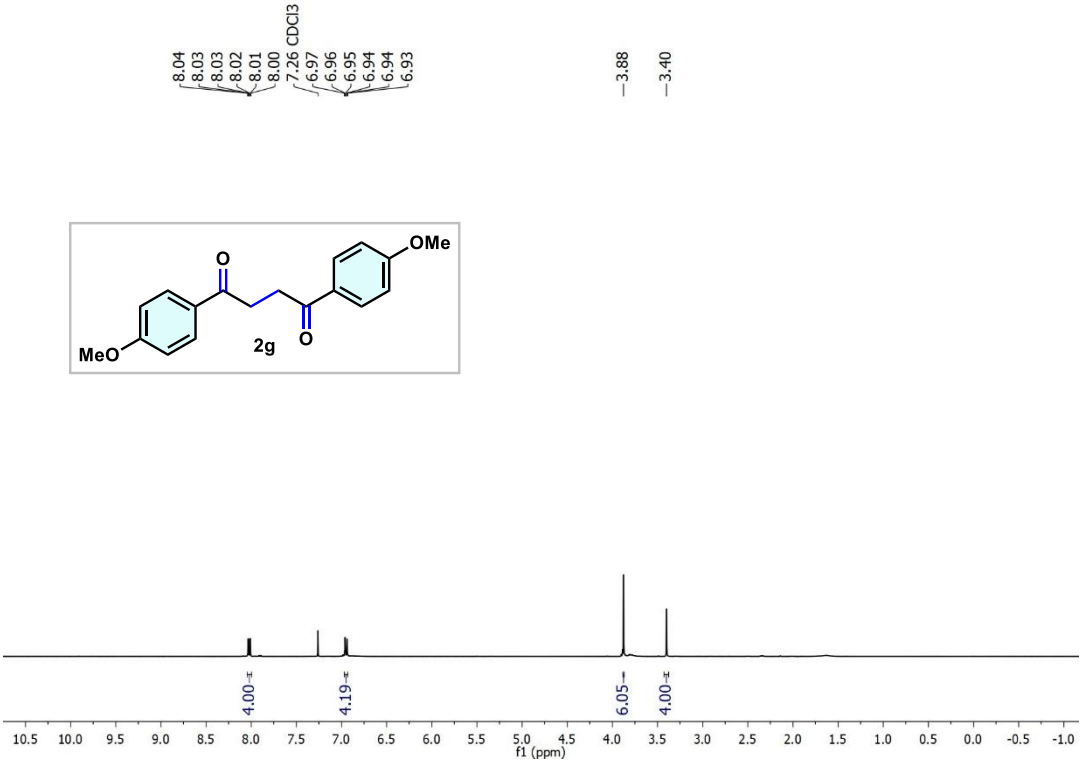

Figure IV.3 ^{1}H NMR spectrum of **2g**, $CDCl_3$, 400 MHz

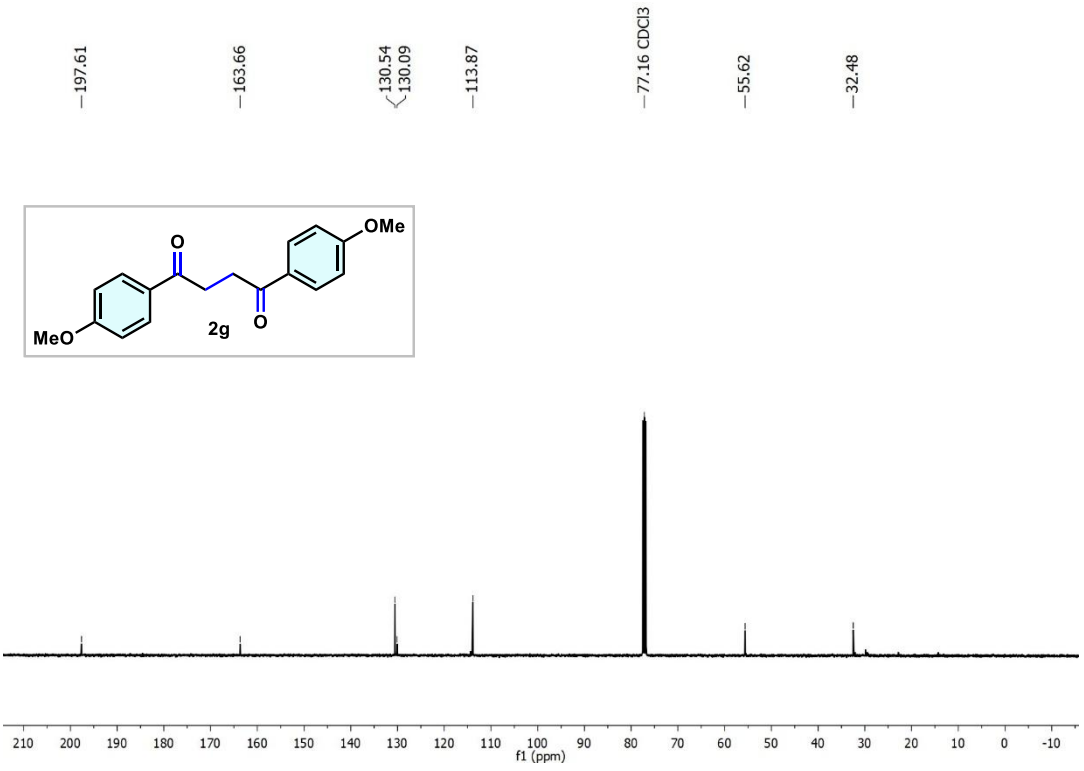

Figure IV.4 $^{13}C\{^{1}H\}$ NMR spectrum of **2g**, $CDCl_3$, 100 MHz

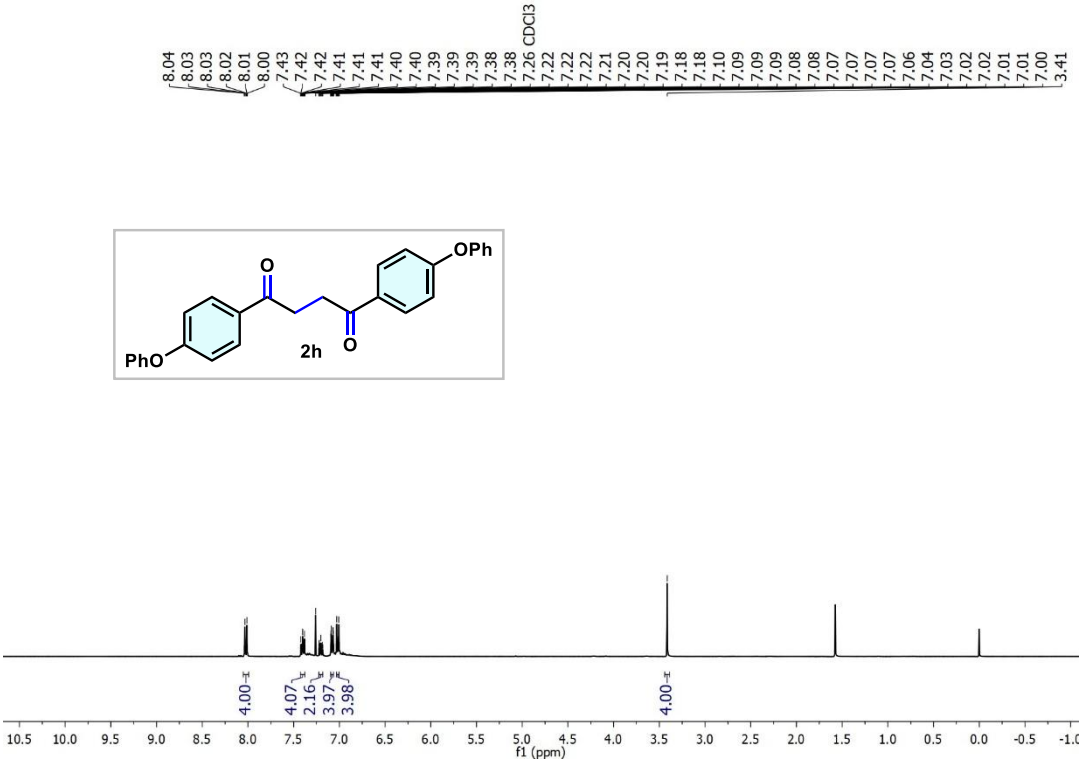

Figure IV.5 ^{1}H NMR spectrum of **2h**, $CDCl_3$, 400 MHz

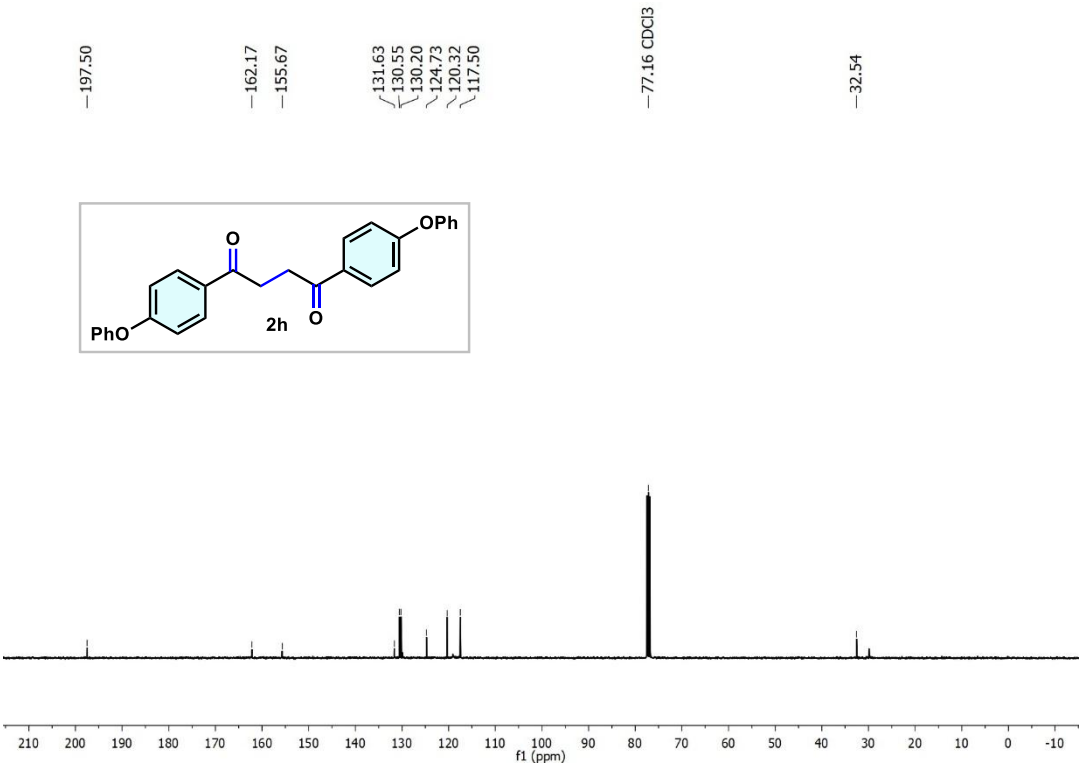

Figure IV.6 $^{13}C\{^{1}H\}$ NMR spectrum of **2h**, $CDCl_3$, 100 MHz

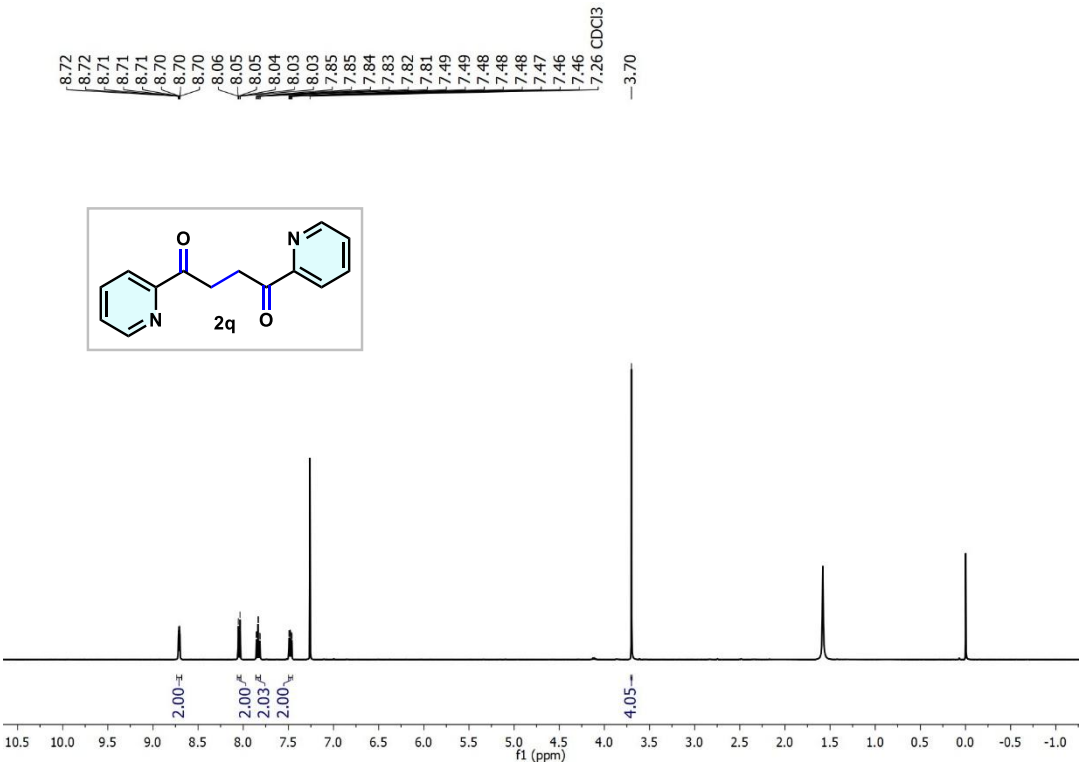

Figure IV.7 ^{1}H NMR spectrum of **2q**, $CDCl_3$, 400 MHz

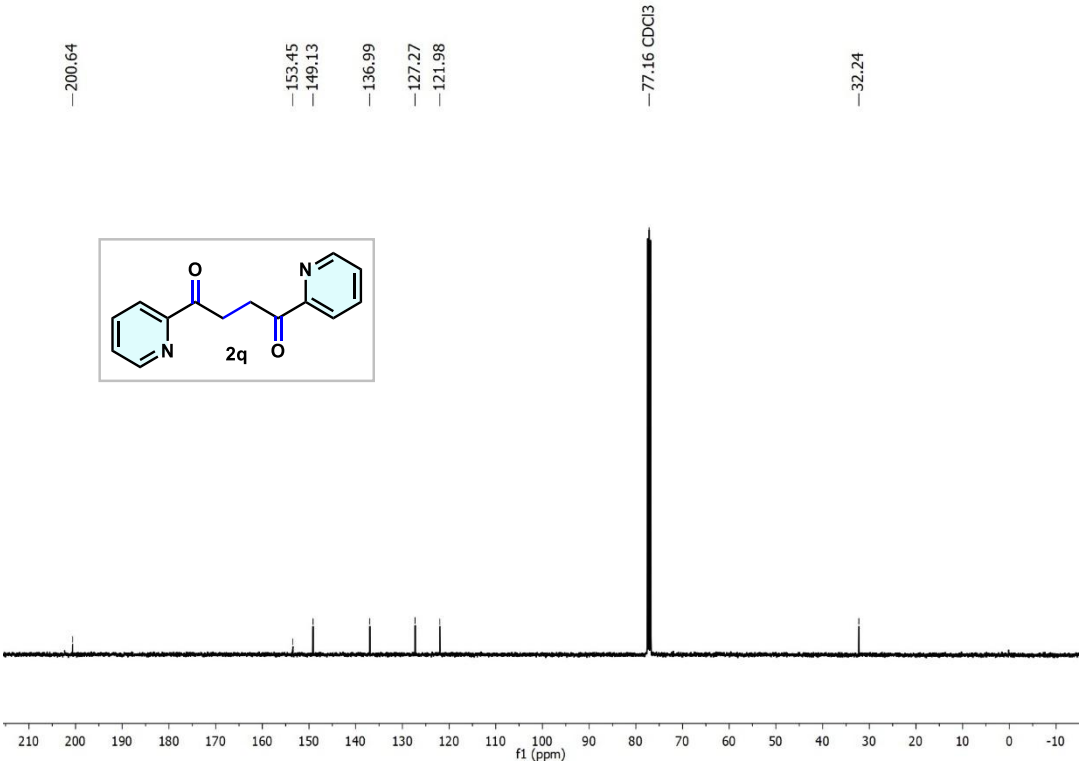

Figure IV.8 $^{13}C\{^{1}H\}$ NMR spectrum of **2q**, $CDCl_3$, 100 MHz

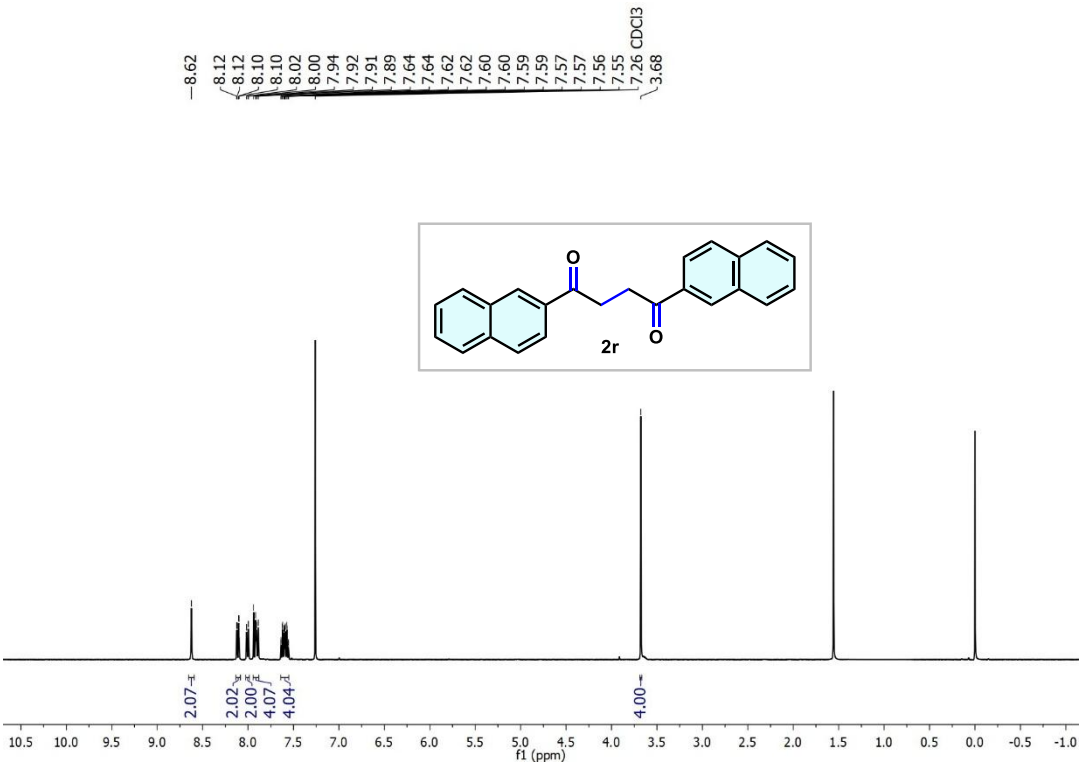

Figure IV.9 ^{1}H NMR spectrum of **2r**, $CDCl_3$, 400 MHz

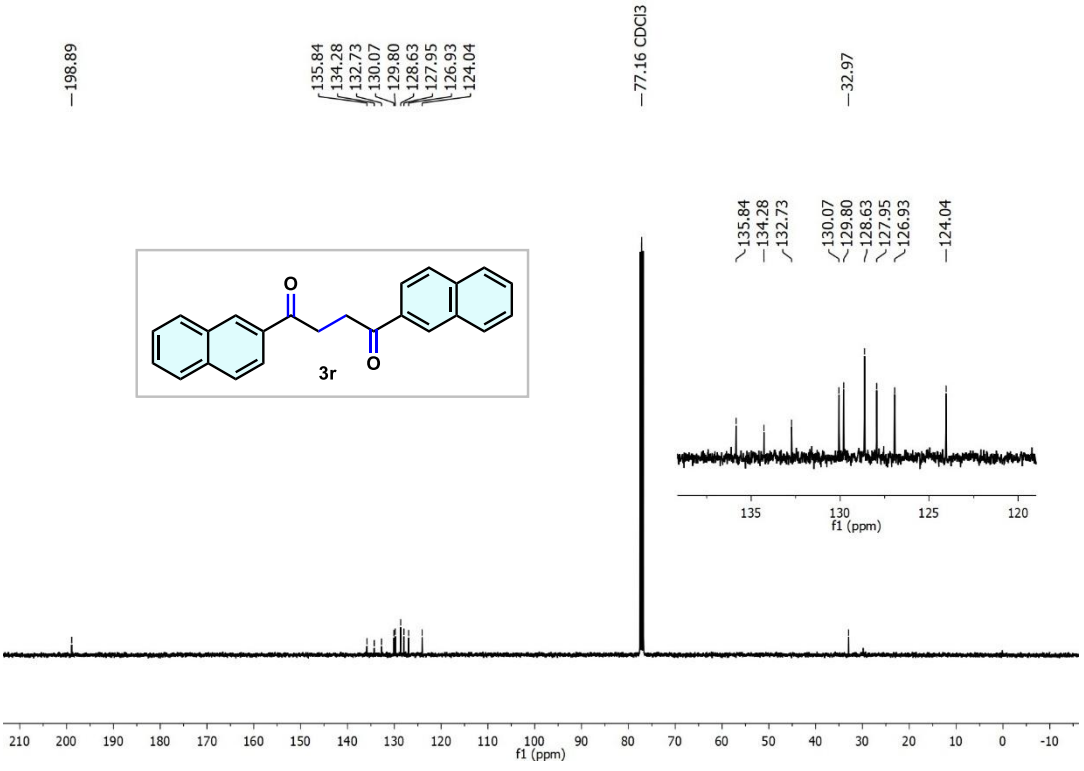

Figure IV.10 $^{13}C\{^{1}H\}$ NMR spectrum of **2r**, $CDCl_3$, 100 MHz

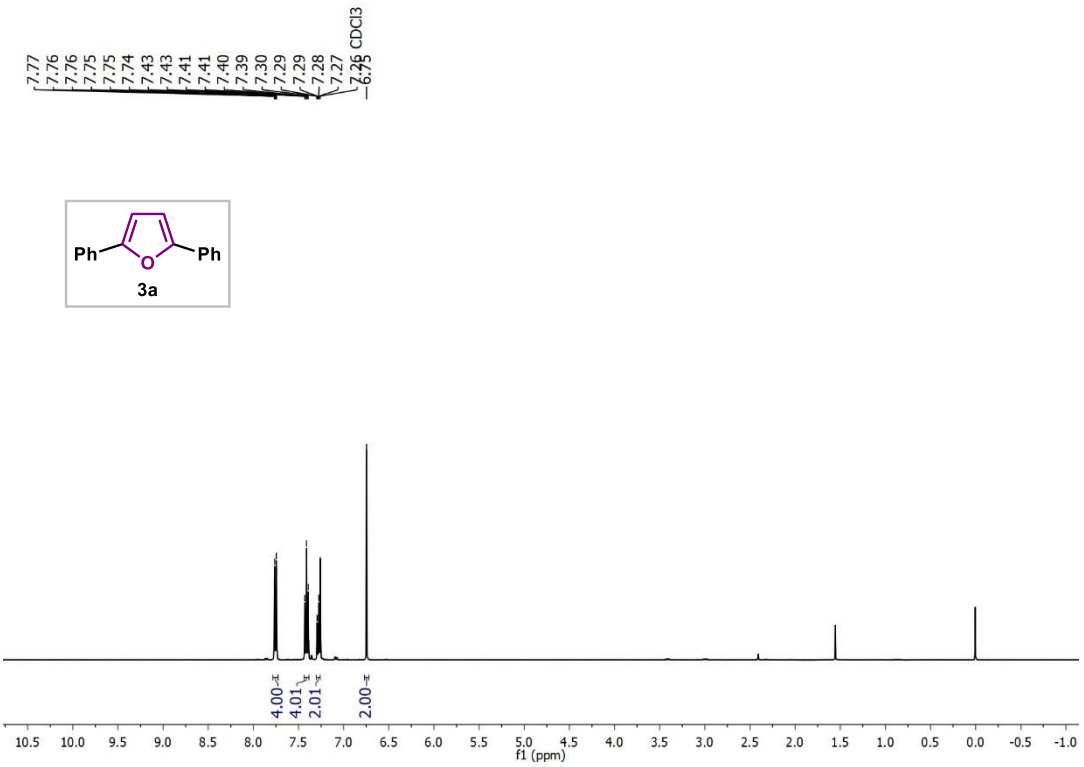

Figure IV.11 ^{1}H NMR spectrum of **3a**, $CDCl_3$, 400 MHz

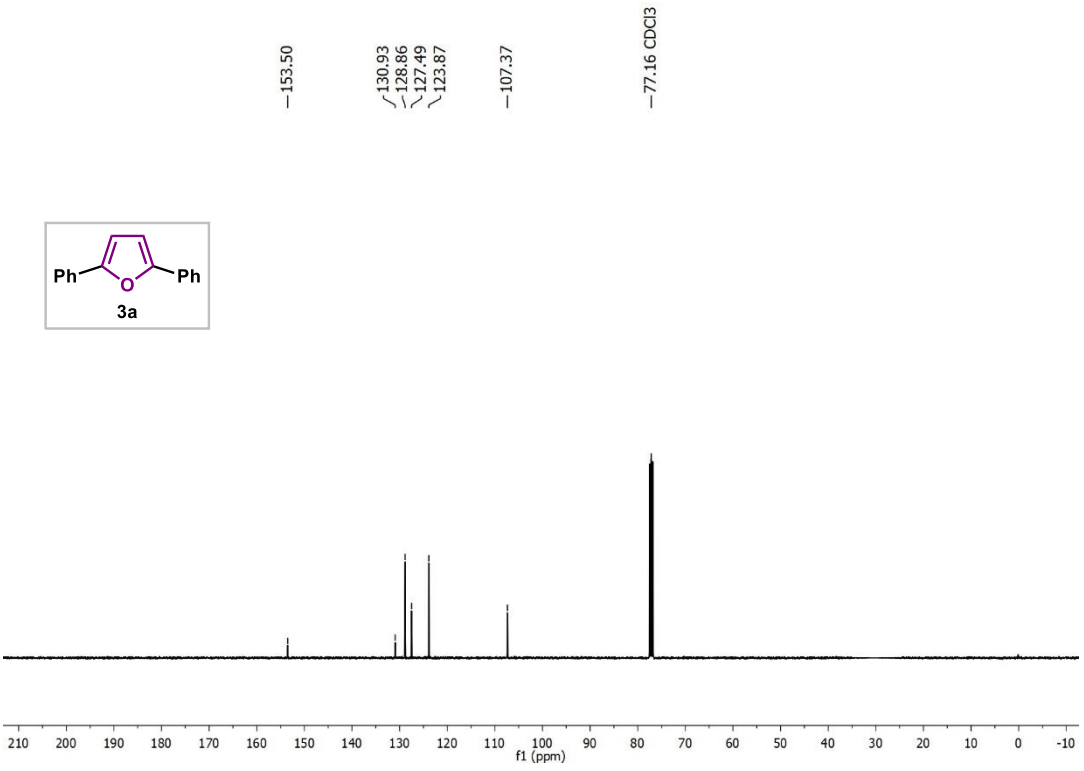

Figure IV.12 $^{13}C\{^{1}H\}$ NMR spectrum of **3a**, $CDCl_3$, 100 MHz

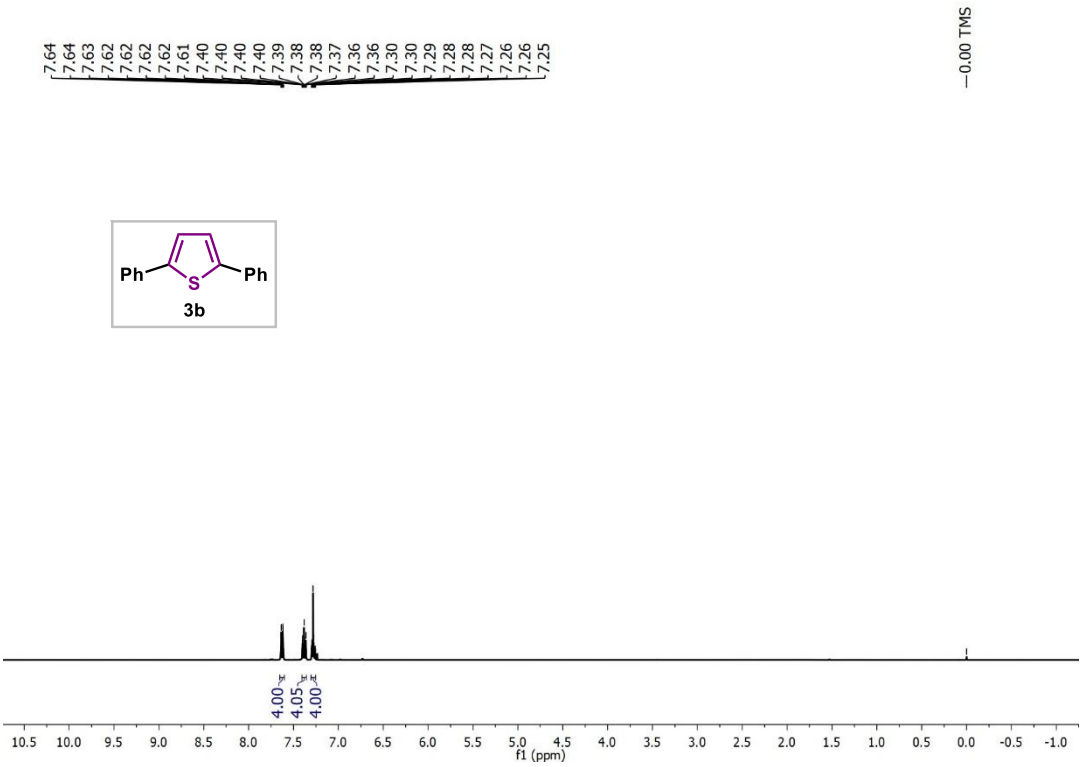

Figure IV.13 ^{1}H NMR spectrum of **3b**, $CDCl_3$, 400 MHz

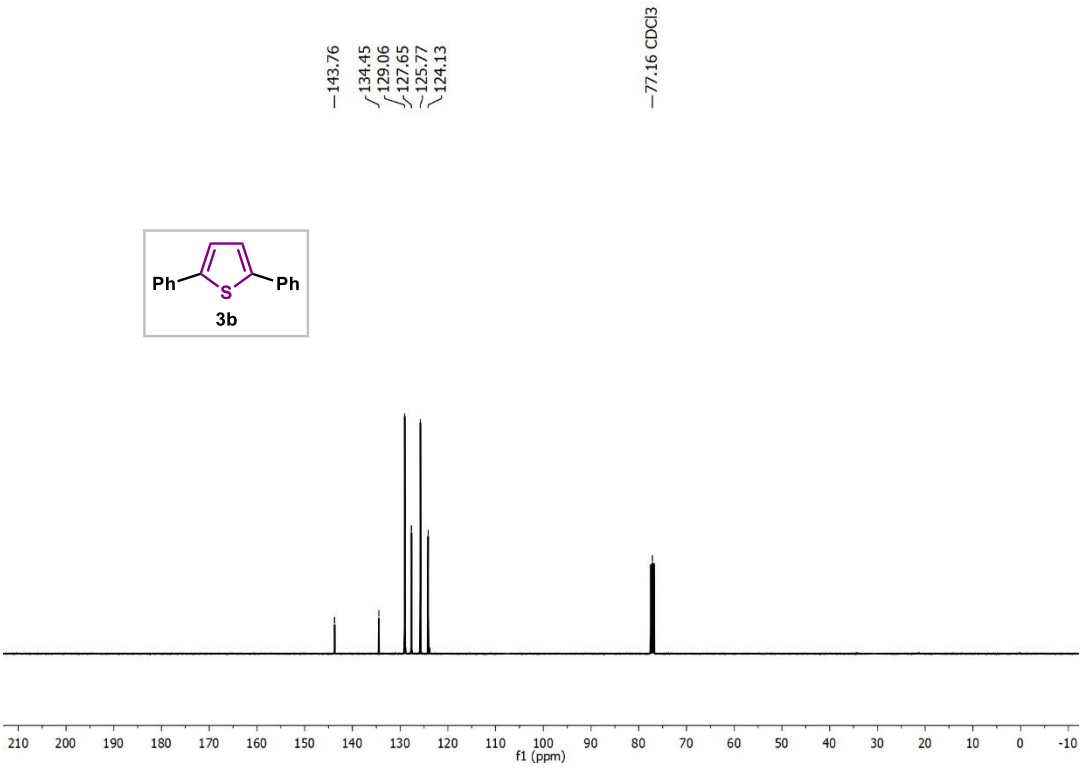

Figure IV.14 $^{13}C\{^{1}H\}$ NMR spectrum of **3b**, $CDCl_3$, 100 MHz

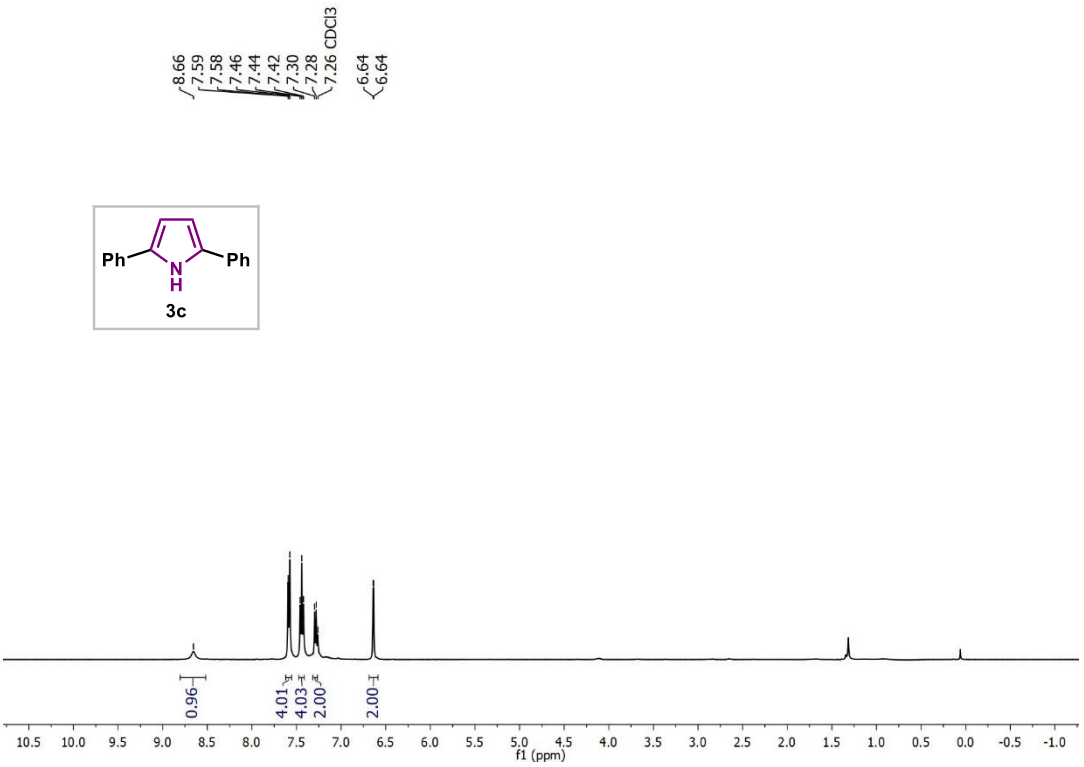

Figure IV.15 ^{1}H NMR spectrum of **3c**, $CDCl_3$, 400 MHz

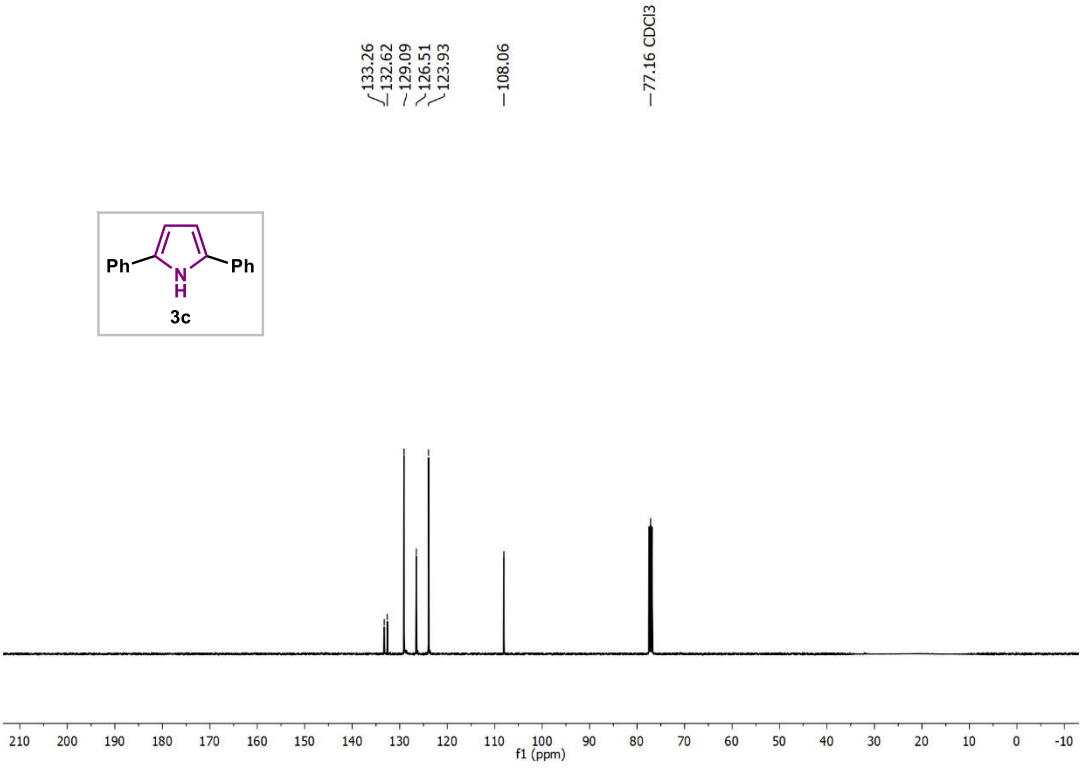

Figure IV.16 $^{13}C\{^{1}H\}$ NMR spectrum of **3c**, $CDCl_3$, 100 MHz

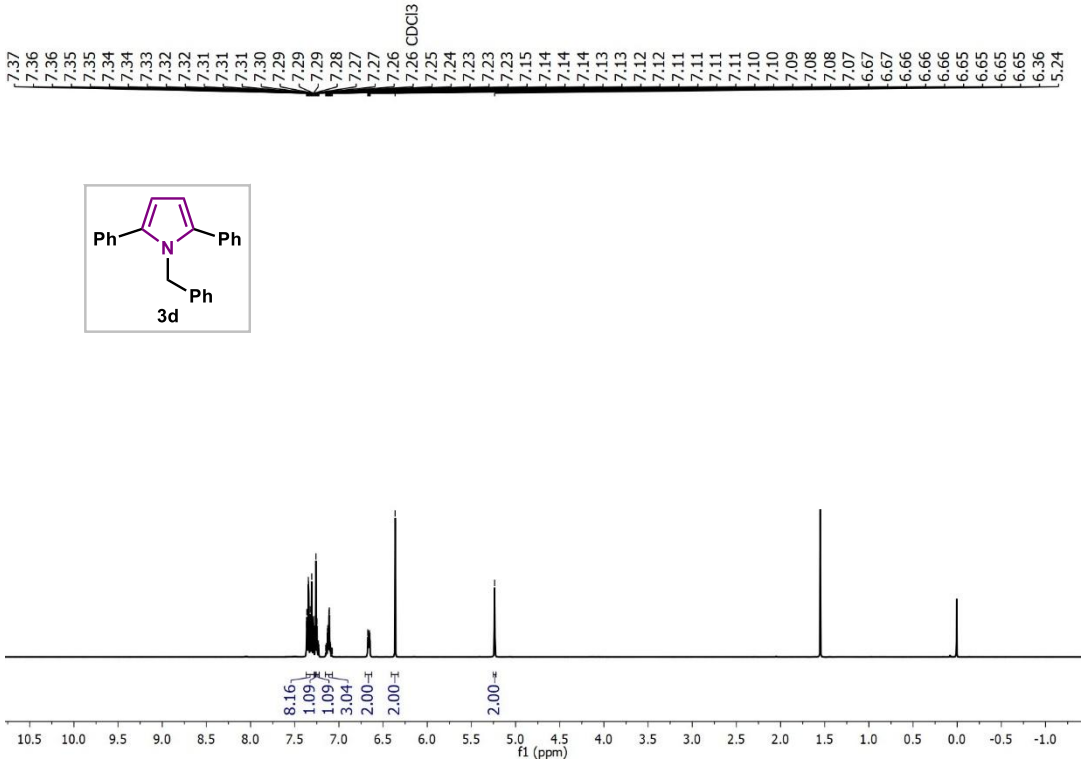

Figure IV.17 ^{1}H NMR spectrum of **3d**, $CDCl_3$, 400 MHz

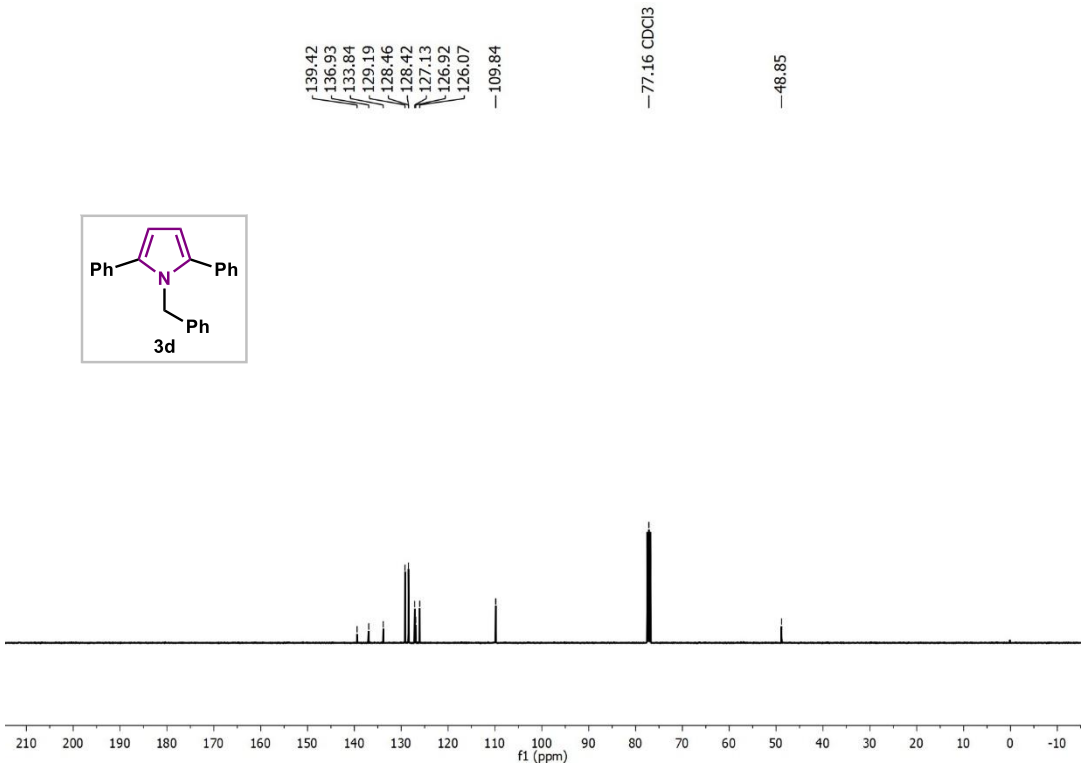

Figure IV.18 $^{13}C\{^{1}H\}$ NMR spectrum of **3d**, $CDCl_3$, 100 MHz

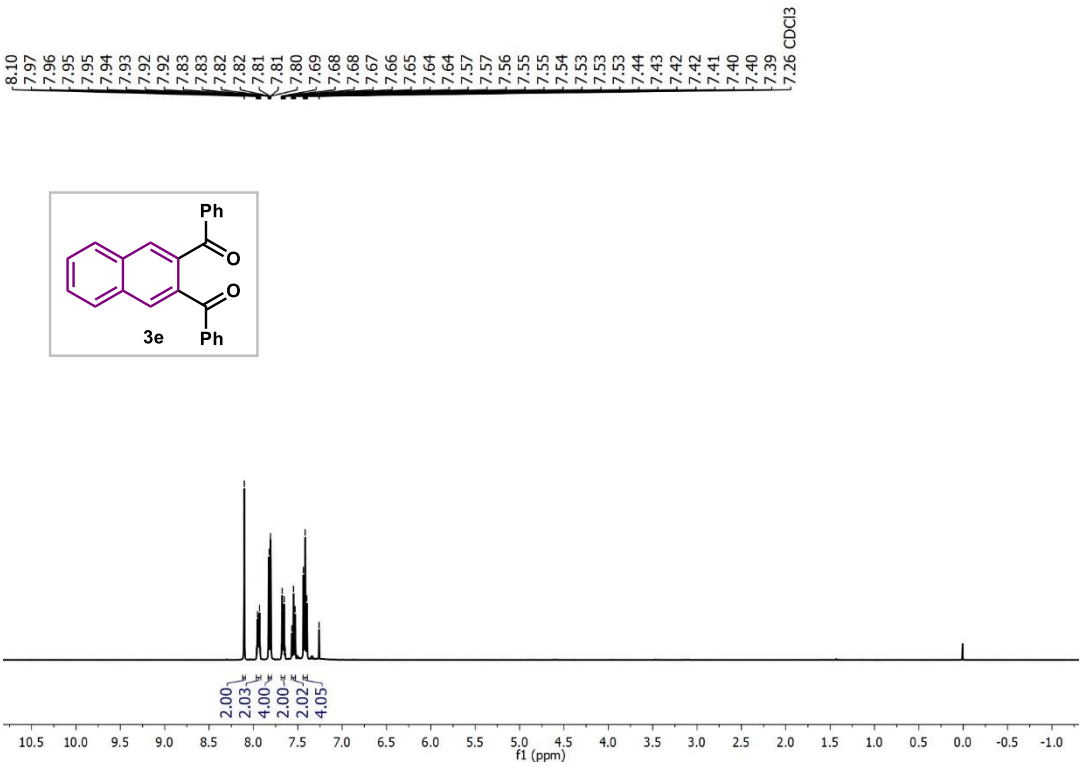

Figure IV.19 ^{1}H NMR spectrum of **3e**, $CDCl_3$, 400 MHz

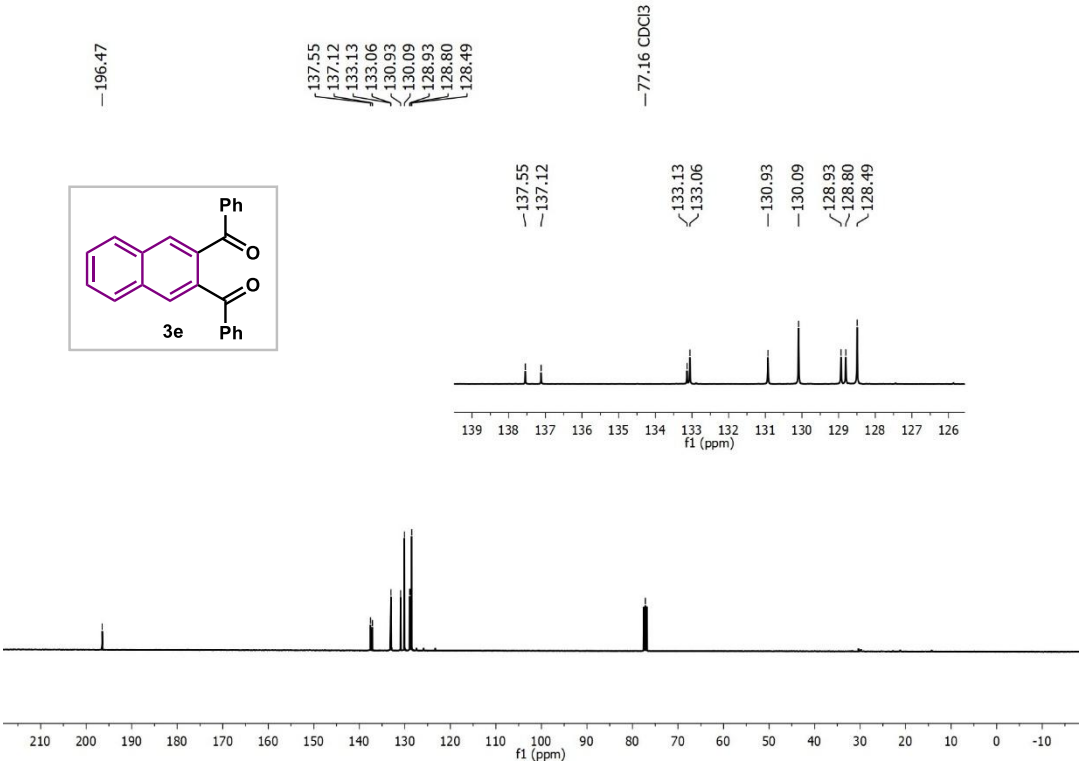

Figure IV.20 $^{13}C\{^{1}H\}$ NMR spectrum of **3e**, $CDCl_3$, 100 MHz

4.7 References:

1) (a) Fujisawa, T.; Igeta, K.; Odake, S.; Morita, Y.; Yasuda, J.; Morikawa, T. *Bioorg. Med. Chem.* **2002**, *10*, 2569–2581. (b) Tokiwa, Y.; Calabia, B. P.; Ugwu, C. U.; Aiba, S. *Int. J. Mol. Sci.* **2009**, *10*, 3722–3742.
2) (a) Knorr, L. *Chem. Ber.* **1884**, *17*, 1635−1642. (b) Paal, C. *Chem. Ber.* **1885**, *18*, 367−371. (c) Amarnath, V.; Anthony, D. C.; Amarnath, K.; Valentine, W. M.; Wetterau, L. A.; Graham, D. G. *J. Org. Chem.* **1991**, *56*, 6924−6931.
3) (a) Kabir, E.; Uzzaman, M. *Results Chem.* **2022**, *4*, 100606−100616. (b) Amin, A.; Qadir, T.; Sharma, P.; Jeelani, I.; Abe, H. *Open Med. Chem. J.* **2022**, *16*, e187410452209010.
4) Lemmerer, M.; Schupp, M.; Kaiser, D.; Maulide, N. *Nat. Synth.* **2022**, *1*, 923−935.
5) (a) Corey, E. J.; Seebach, D. *Angew. Chem. Int. Ed.* **1965**, *4*, 1077–1078. (b) Seebach, D. *Angew. Chem. Int. Ed.* **1979**, *18*, 239–258.
6) (a) Yetra, S. R.; Patra, A.; Biju, A. T. *Synthesis* **2015**, *47*, 1357–1378. (b) Heravi, M. M.; Zadsirjan, V.; Kafshdarzadeh, K.; Amiri, Z. *Asian J. Org. Chem.* **2020**, *9*, 1999–2034.
7) (a) Arava, S.; Kumar, J. N.; Maksymenko, S.; Iron, M. A.; Parida, K. N.; Fristrup, P.; Szpilman, A. M. *Angew. Chem. Int. Ed.* **2017**, *56*, 2599−2603. (b) DeMartino, M. P.; Chen, K.; Baran, P. S. *J. Am. Chem. Soc.* **2008**, *130*, 11546–11560. (c) Amaya, T.; Maegawa, Y.; Masuda, T.; Osafune, Y.; Hirao, T. *J. Am. Chem. Soc.* **2015**, *137*, 10072–10075.
8) (a) Cuccu, F.; Serusi, L.; Luridiana, A.; Secci, F.; Caboni, P.; Aitken, D. J.; Frongia, A. *Org. Lett.* **2019**, *21*, 7755–7758. (b) Zhang, H.; Wang, Z.; Wang, Z.; Chu, Y.; Wang, S.; Hui, X.-P. *ACS Catal.* **2022**, *9*, 5510–5516.
9) Carman, L.; Kwart, L. D.; Hudlicky, T. *Synth. Commun.* **1986**, *16*, 169–182.
10) (a) Cheng, Y.-Y.; Yu, J.-X.; Lei, T.; Hou, H.-Y.; Chen, B.; Tung, C.-H.; Wu, L.-Z. *Angew. Chem. Int. Ed.* **2021**, *60*, 26822–26828. (b) Che, C.; Qian, Z.; Wu, M.; Zhao, Y.; Zhu, G. *J. Org. Chem.* **2018**, *83*, 5665–5673.
11) Morack, T.; Mück-Lichtenfeld, C.; Gilmour, R. *Angew. Chem. Int. Ed.* **2019**, *58*, 1208–1212.
12) Zhao, J.-J.; Zhang, H.-H.; Shen, X.; Yu, S. *Org. Lett.* **2019**, *21*, 913–916.
13) Goti, G.; Bieszczad, B.; Vega-Peñaloza, A.; Melchiorre, P. *Angew. Chem. Int. Ed.* **2019**, *58*, 1213–1217.

14) Cheng, Y.-Y.; Yu, J.-X.; Lei, T.; Hou, H.-Y.; Chen, B.; Tung, C.H.; Wu, L.-Z. *Angew. Chem. Int. Ed.* **2021**, *60*, 26822–26828.

15) (a) Lan, X. W.; Wang, N. X.; Xing, Y. *Eur. J. Org. Chem.* **2017**, *2017*, 5821−5851. (b) Bao, X.; Li, J.; Jiang, W.; Huo, C. *Synthesis* **2019**, *51*, 4507−4530

16) Das, S.; Lai, D.; Mallick, A.; Roy, S. *ChemistrySelect* **2016**, *4*, 691 –695.

17) (a) König, B. *Eur. J. Org. Chem.* **2017**, *2017*, 1979–1981. (b) Akita, M.; Ceroni, P.; Stephenson, C. R. J.; Masson, G. *J. Org. Chem.* **2023**, *88*, 6281– 6283.

18) (a) Behera, M.; Dharpure, P. D.; Sahu, A. K.; Bhat, R. G. *J. Org. Chem.* **2024**, *89*, 14695−14709. (b) Bhowmick, A.; Chatterjee, A.; Pathak, S. S.; Bhat, R. G. *Chem. Commun.* **2023**, *59*, 11875–11878.

19) (a) Stauffer, F.; Neier, R. *Org. Lett.* **2000**, *2*, 3535–3537. (b) Kaleta, Z.; Makowski, B. T.; Soós, T.; Dembinski, R. *Org. Lett.* **2006**, *8*, 1625–1628. (c) Yamaguchi, M.; Fujiwara, S.; Manabe, K. *Org. Lett*. **2019**, 21, 6972−6977. (d) Can Üsküp, H.; Yıldız, T.; Onar, H. Ç.; Hasdemir, B. *ACS Omega* **2023**, *8*, 14047–14052. (e) Clement, J. A.; Mohanakrishnan, A. K. *Tetrahedron* **2010**, *66*, 2340−2350.

20) Yang, B.; Lu, S.; Wang, Y.; Zhu, S. *Nat Commun* **2022**, *13*, 1858−1869.

21) (a) Guo, J.-T.; Yang, D.-C.; Guan, Z.; He, Y.-H. *J. Org. Chem.* **2017**, *82*, 1888–1894. (b) Fujiya, A.; Tanaka, M.; Yamaguchi, E.; Tada, N.; Itoh, A. *J. Org. Chem.* **2016**, *81*, 7262−7270. (c) Maia da Silva Santos, B.; dos Santos Dupim, M.; Paula de Souza, C.; Messias Cardozo, T.; Gadini Finelli, F. *Beilstein J. Org. Chem.* **2021,** *17,* 2959–2967.

22) (a) Bancirova, M. *Luminescence* **2011**, *26*, 685–688. (b) Harbour, J. R.; Issler, S. L. *J. Am. Chem. Soc.* **1982**, *104*, 903–905.

23) Pelaez, M.; Falaras, P.; Likodimos, V.; O'shea, K.; De la Cruz, A.; Dunlop, P. S. M.; Byrne, J. A.; Dionysiou, D. D. *J. Mol. Catal. A Chem.* **2016**, *425*, 183–189.

24) Fukuzumi, S.; Kotani, H.; Ohkubo, K.; Ogo, S.; Tkachenko,N. V.; Lemmetyinen, H. *J. Am. Chem. Soc.* **2004**, *126*, 1600−1601.

25) Sarró, P.; Ji, Y.; Gallego-Gamo, A.; Gimbert-Suriñach, C.; Vallribera, A.; Granados, A. *Org. Chem. Front.* **2025**, *12*, 3475−3492.

Chapter 5

Harnessing Aryl Thiocyanate: A Circular Chemical Approach to Thiocyano-Thioesters from Cyclic Thioacetals

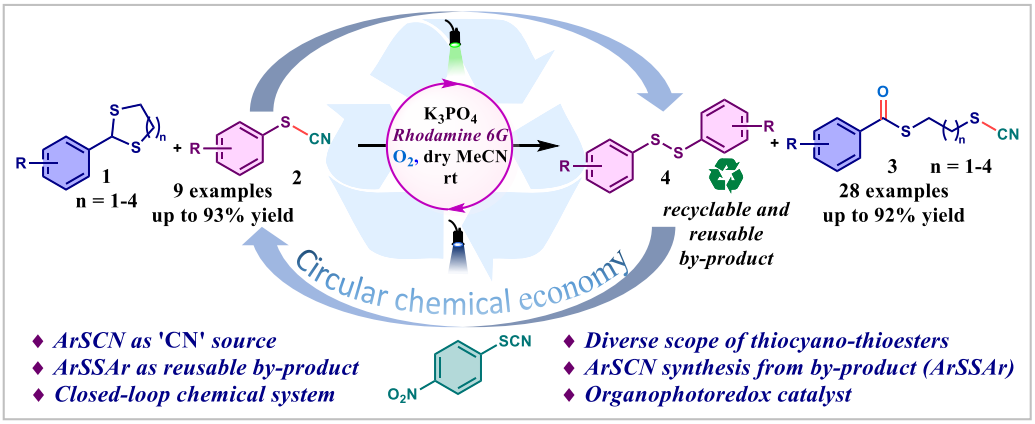

Harnessing Aryl Thiocyanate: A Circular Chemical Approach to Thiocyano-Thioesters from Cyclic Thioacetals

5

An expedient sustainable and transition metal-free approach has been developed to access thiocyano-thioesters, leveraging the power of organophotoredox catalysis and visible light. Using aryl thiocyanate as an organic 'CN' source, this method enables the direct transformation of cyclic thioacetals with remarkable efficiency. Notably, the process embodies the principles of circular chemistry by repurposing the by-product, diaryl disulfide, into a recyclable and reusable precursor for the synthesis of aryl thiocyanate as well. This strategy boasts broad functional group tolerance, seamlessly accommodating 5- to 8-membered cyclic thioacetals, and is readily scalable to gram quantity. The mechanistic insights, supported by the fluorescence quenching studies, cyclic voltammetry, and control experiments, provide a deeper understanding of the reaction pathway, further underscoring the synthetic utility of this approach.

5.1 Introduction:

The remarkable versatility of the cyano group in organic transformations stems from the nucleophilic nature of the nitrogen lone pairs, the π-coordination ability of the C≡N triple bond, and the intrinsic electrophilicity of the carbon center (Figure 5.1A). The cyano group is a highly versatile synthetic handle, facilitating the formation of diverse functional groups, including carboxylic acids, amides, imines, aldehydes, ketones, and amines (Figure 5.1B). [1] The cyano group containing organic compounds has often been utilized as a versatile precursor to synthesize various heterocyclic compounds such as tetrazoles, oxazoles, and isoquinolines.[2] Moreover, the cyano-capped organic compounds are integral to various cutting-edge technologies, including organic solar cells (OSCs), organic light-emitting diodes (OLEDs), nonlinear optics (NLO), light conversion agents, organic fluorescent probes, and photoredox catalysis.[3] Additionally, the cyano group is abundantly found in natural products and commercially significant materials such as dyes, agrochemicals, and pharmaceuticals.[4]

Given their importance in diverse applications, considerable progress has been made in

achieving cyanation with a range of cyanating reagents. In light of growing concerns regarding environmental sustainability and toxicity, there has been a remarkable paradigm shift from the use of traditional cyanating reagents—such as potassium cyanide (KCN), sodium cyanide (NaCN), zinc cyanide [$Zn(CN)_2$], and potassium ferrocyanide ($K_4[Fe(CN)_6]$)—toward relatively safer alternatives like metal thiocyanates.[5] While this transition marks significant progress, certain limitations persist, as some of these reagents still generate stoichiometric metal waste and may inadvertently release the highly toxic and volatile hydrogen cyanide (HCN).

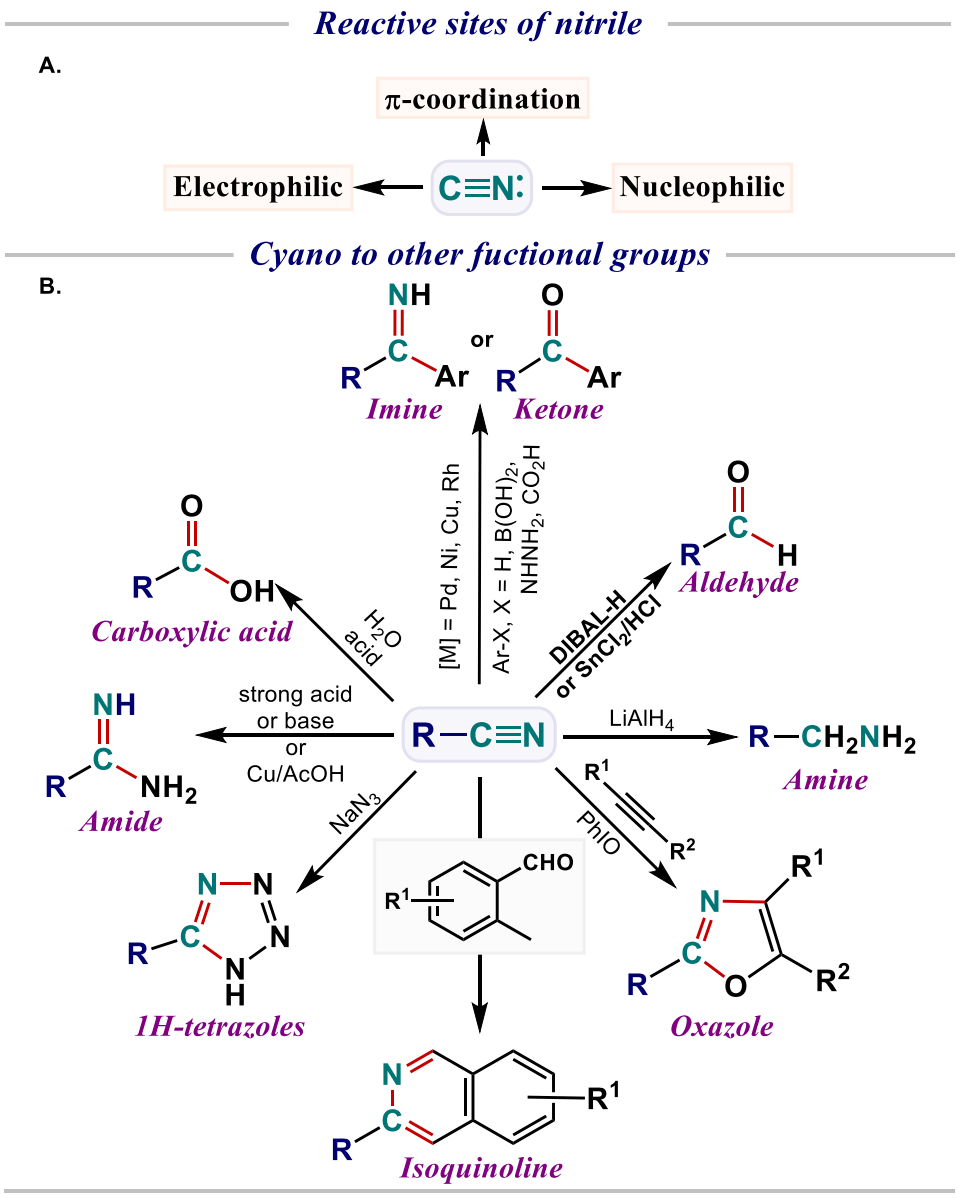

Figure 5.1 The cyano group as a versatile precursor for diverse functional group transformations.

To overcome these persistent challenges and promote a greener, more sustainable approach

to cyanation, researchers have been exploring a diverse range of non-metallic organo-cyanating reagents. Unlike the coordinative bonding in metal complexes, the presence of a covalent C–C bond in these reagents ensures a strongly bound cyano group, preventing the spontaneous release of cyanide. Among them, the most promising candidates are benzyl nitrile, acetonitrile, ethyl cyanoacetate, 2,3-diaminomaleonitrile, cyanohydrin, trimethylsilyl cyanide (TMSCN), propanedinitrile, and isocyanides, which offer alternative cyanation pathways while addressing the environmental and safety concerns associated with conventional methods.[6]

The first documented use of nitriles as cyanide sources dates back to 1998, when Cheng and coworkers reported a palladium/zinc-mediated nitrile transfer from organic nitriles to bromoarenes forming ArCN compounds, particularly with *ortho*-disubstituted bromoarenes (Scheme 5.1).[6a] The mechanism involves the cooperation of two metals, palladium and zinc, with the former responsible for C−C bond formation and the latter for the bond cleavage of the C−C bond of the nitrile solvents and the transfer of the nitrile-group to aryl halides.

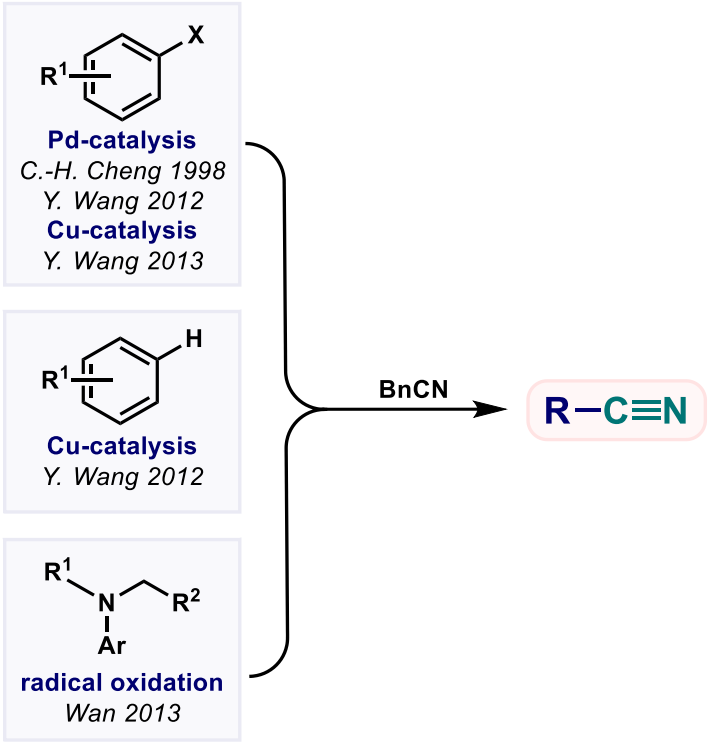

Scheme 5.1 Representative examples on cyanation of different compounds with benzyl nitriles

In 2012 and 2013, Wang and coworkers investigated cyanation reactions using benzyl cyanide and successfully demonstrated the palladium or copper-catalyzed cyanation of aryl halides (Scheme 5.1).[6b,c] In the year 2012, The same research group reported a copper-catalyzed cyanation of arenes using benzyl nitrile as a cyanide anion surrogate, leading to the

formation of aromatic nitriles (Scheme 5.1). [6d] The cascade process involves a copper-catalyzed aerobic oxidation of benzyl cyanide, followed by retro-cyanohydrination and a copper-catalyzed aerobic oxidative C–H functionalization.

In 2013, the Wan research group reported an oxidative α-cyanation of tertiary amines (Scheme 5.1).[6e] The reaction features the formation of α-aminoalkyl radicals and benzoyl cyanide as key intermediates. The proposed mechanism involves a nucleophilic attack of the α-aminoalkyl radical on the C–N bond of PhCOCN, followed by an elimination step that furnishes the desired α-aminonitrile along with an acyl radical.

Compared to cyanates, organic thiocyanates have garnered greater interest as cyanide sources. In 1983, Cava and coworkers reported the synthesis of 2-arylmalononitriles from aryl nitriles using 2-chlorobenzyl thiocyanate (Scheme 5.2).[7]

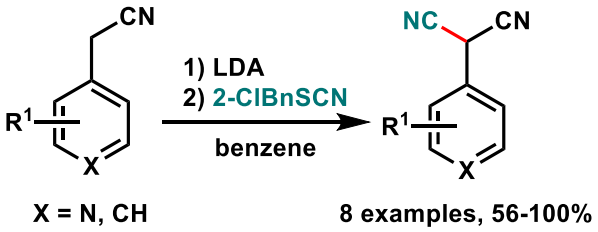

Scheme 5.2 Selected examples on cyanation of different compounds with organic nitriles

In 2006, Liebeskind and coworkers reported the cyanation of boronic acids via a palladium-catalyzed, copper(I)-mediated coupling of benzyl thiocyanate with boronic acids (Scheme 5.3). Their study demonstrated that various thiocyanates could undergo coupling with boronic acids in the presence of a catalytic amount of palladium and a stoichiometric quantity of copper(I) carboxylate. The copper(I) carboxylate plays a dual role: the soft Cu(I) ion acts as a thiophilic agent, facilitating polarization of the palladium-thiolate bond, while simultaneously enabling borophilic activation by coordination of the carboxylate to the trivalent boron atom. However, its applicability is constrained by the requirement for a transition metal catalyst and stoichiometric amounts of a copper co-catalyst under elevated temperatures.[8]

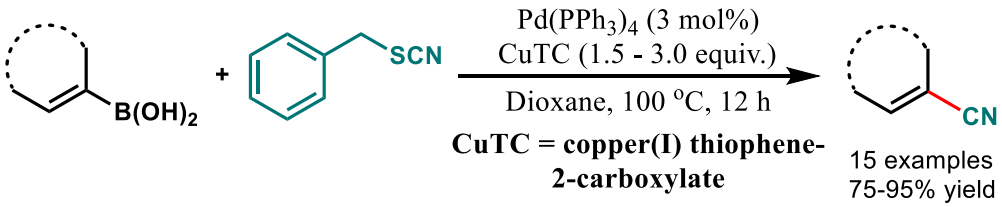

Scheme 5.3 Palladium-catalyzed, copper(I)-mediated coupling of boronic acids with benzyl thiocyanate

In 2018, Vaghasiya and coworkers have reported an oxidative cyanation on aryl boronic acid derivatives using various simple indole-based thiocyanates, catalyzed by a new *N*,*N*,*N*-trimethyl-2-(sulfooxy)ethanaminium palladium(II) chloride (IL-$PdCl_4$) catalyst (Scheme 5.4).[9]

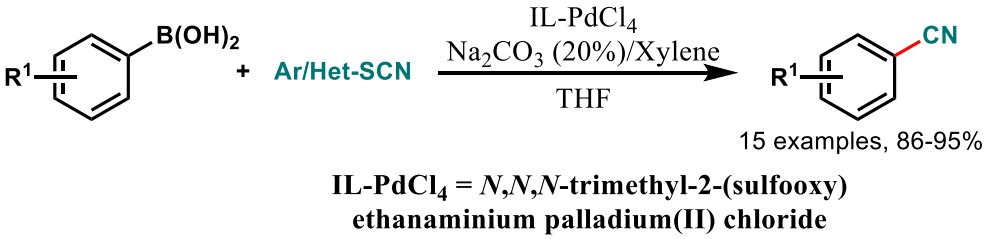

Scheme 5.4 IL-$PdCl_4$ catalyzed cyanation on arylboronic acid.

Although, C Mes-Acr-Me·ClO_4 CN bond formation has been extensively studied, the construction of X–CN bonds (X = N, S, O) has received comparatively less attention.[10,11] Owing to the unique reactivity of the XCN group, especially its behavior as a leaving group, these compounds are often classified as organic pseudohalides. Although relatively rare, several thiocyanate-containing natural products have been isolated and investigated for their biological activities (Figure 5.2).[12]

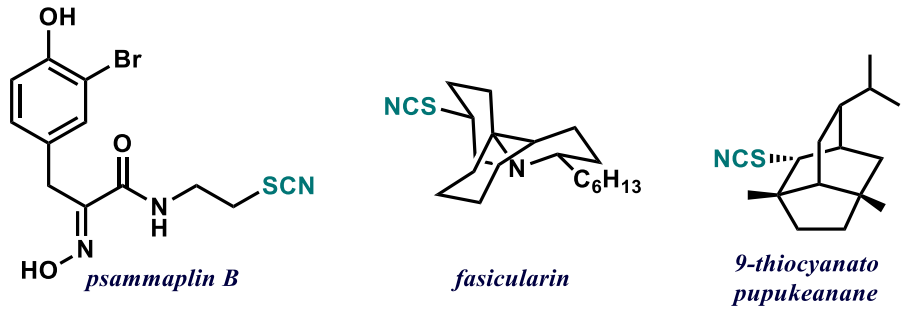

Figure 5.2 Representative examples of thiocyanate-containing natural products.

The thiocyanates bearing compounds are ubiquitous moieties in numerous pharmaceutical molecules known to exhibit antimicrobial activities.[13] For example, 2-amino-4-thiocyanatobenzothiazole derivatives exhibit distinguished *anti*-helmintic and *anti*-fungal activities while 4-phenoxyphenoxyethyl thiocyanate and 2,4-dichlorophenoxyethyl thiocyanate are efficient inhibitors of *Trypanosoma cruzi* proliferation (Figure 5.3).[14] Moreover, the thiocyanate moiety acts as a versatile synthon for the synthesis of a wide range of valuable compounds, including thiocarbamates, sulfonyl cyanides, sulfonic acids, sulfonyl

chlorides, thioesters, sulfides, and various related heterocycles (Figure 4.4).[15]

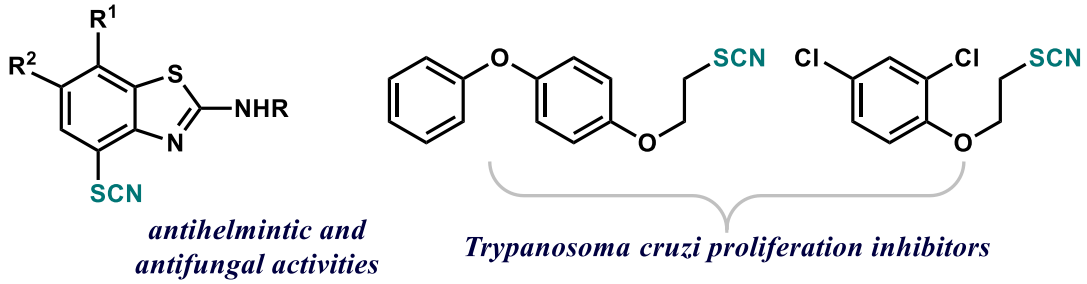

Figure 5.3 Selected examples of bioactive compounds containing the S–CN moiety.

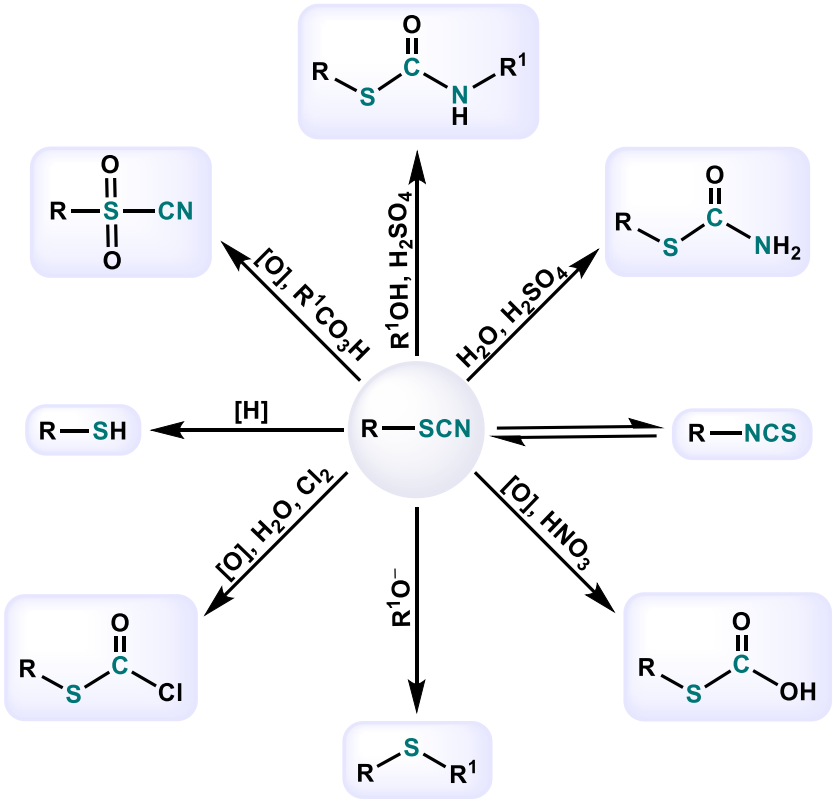

Figure 5.4 The thiocyanate group as a versatile precursor for diverse functional group transformations

Visible-light photoredox catalysis has revolutionized synthetic organic chemistry by enabling mild, sustainable, and selective transformations through single-electron transfer (SET) pathways. Since its resurgence in 2008, this strategy has unlocked diverse bond-forming reactions using environmentally benign visible light as the energy source.[16] As a result, numerous cyanation strategies have been developed under visible-light irradiation over the past decade.[17] Most reported methods focus on the cyanation of aryl and benzyl substrates, while cyanation involving heteroatoms remains relatively rare. In 2018, Guo and co-workers reported

a rose bengal catalyzed method for the cyanation of thiols, using NH_4SCN as the cyanide source to afford the corresponding thiocyanates (Scheme 5.5).[18] A broad range of thiophenols bearing both electron-donating and electron-withdrawing groups were well tolerated, delivering the desired thiocyanates in good to excellent yields. Notably, several of the synthesized thiocyanate derivatives serve as key scaffolds in medicinal chemistry. Radical trapping experiments further supported CN bond formation via C–S bond cleavage in NH_4SCN.

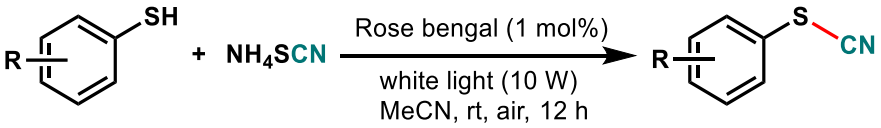

Scheme 5.5 Visible light mediated rose bengal catalyzed cyanation of thiols.

Previously, we investigated the reactivity of dithiolanes/dithianes with NaSCN as a cyanating agent to directly synthesize thiocyano-thioesters.[19] Organic thiocyanates are valuable motifs in organic synthesis, and similarly, thioesters play a vital role in biosynthetic processes, including protein and nucleic acid synthesis. They are also used in drug delivery, biomolecule labeling, and as acyl radical equivalents in acyl transfer reactions.[20]

Environmental challenges from waste generation and limited chemical resources are prompting chemists to adopt sustainable approaches, focusing on recycling, reusing, and redesigning chemical processes. By integrating circular economy principles, reusing by-products as starting materials, the reliance on virgin chemicals can be reduced, and waste generation can be minimized as well.[21] To address issues in thiocyano-thioester synthesis, such as the usage of excess reagent and in turn generation of stochiometric water soluble waste may not be attractive from environmental hazard point view. In this regard, we aim to use organic cyanating sources, enabling the reuse of by-products in subsequent transformations so as to avoid or minimize the waste generation.[22]

To the best of our knowledge, there are no reports till date on the use of aryl thiocyanates (ArSCN) as a radical cyanating source in photoinduced transformations. We hypothesized that aryl thiocyanates can serve as an ideal source for generating CN radicals under visible light irradiation, with the organic by-product, diaryl disulfide, being recycled for the synthesis of additional aryl thiocyanates, thus aligning with circular economy principles. Here, in this chapter we present, for the first time, the use of aryl thiocyanates as an efficient cyanating agent under visible-light organophotoredox catalysis to synthesize thiocyano-thioesters from cyclic thioacetals. The diaryl disulfides formed in the reaction are effectively recycled to produce

various aryl thiocyanates (Scheme 5.6).

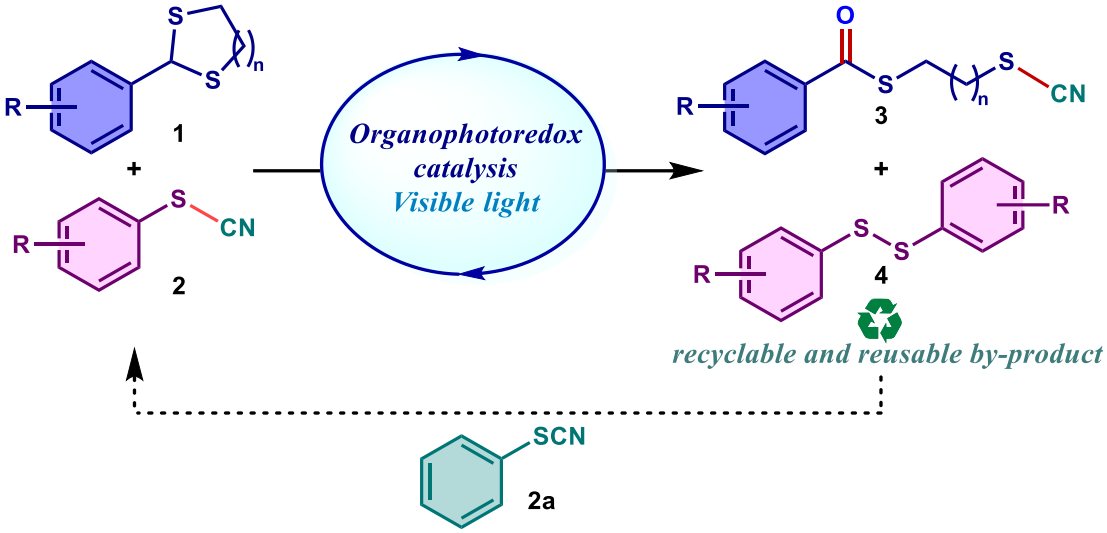

Scheme 5.6 Our hypothesis: Circular chemical economy approach for the synthesis of thiocyano-thioesters using aryl thiocyanates

5.2 Results and Discussions

To validate our hypothesis, we initiated reaction optimization using cyclic thioacetal **1a** and phenyl thiocyanate **2a** as model substrates. After systematic evaluation of various conditions, the optimal condition was identified as Rhodamine 6G (2 mol%) as the organophotoredox catalyst, K_3PO_4 as the base, in anhydrous MeCN (3 mL), under O_2-atmosphere and irradiation with Kessil green LEDs (525 nm, 20 W) at room temperature. Gratifyingly, the reaction efficiently afforded the desired thiocyano thioester **3a** in 89% yield (Table 5.1, Entry 1). We found that replacing K_3PO_4 with other bases such as K_2CO_3 and Na_2CO_3 reduced afforded the desired product **3a** in lower yield or it failed to afford the desired product **3a** respectively (Table 5.1, Entries 2-3). Subsequently, we evaluated various monochromatic visible light sources (427 nm, 440 nm, 456 nm, and 467 nm) in place of 525 nm. A noticeable decline in the yield of product **3a** was observed with decreasing wavelength (Table 5.1, Entry 4). Among all, green LEDs (525 nm, 20 W) proved to be efficient by affording the desired compound **3a** in very good yield (Table 5.1, Entry 1). To further optimize the reaction, various organophotocatalysts such as Eosin Y, Rhodamine B, and Mes-Acr-$MeClO_4$ (9-Mesityl-10-methylacridinium perchlorate) were screened, furnishing product **3a** in up to 61% (Table 5.1, Entry 5). Transition metal photocatalysts, such as the Ru-polypyridyl complex, also yielded the desired product **3a**, albeit in moderate yield (64%, Table 5.1, Entry 6). Among all the photocatalysts tested,

Rhodamine 6G (Rh6G) was the most effective, delivering **3a** in the highest yield (89%, Table 5.1, Entry 1). We subsequently evaluated various solvents, including 1,4-dioxane, THF, DCE, and DCM, all of which led to a significant drop in the yield of the desired product **3a** (Table 5.1, Entry 7).

Table 5.1 Optimization of reaction conditions for thiocyano-thioester formation.[a]

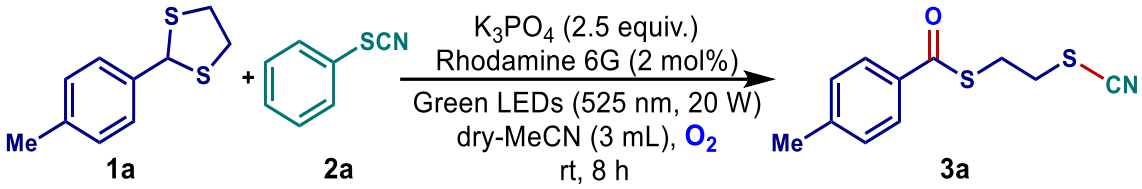

Entry	Deviations from standard condition	Yield (%)[b]
1	None	89(82)[c]
2	Na_2CO_3 instead of K_3PO_4 as a base	ND
3	K_2CO_3 instead of K_3PO_4 as a base	45
4	427 nm *or* 440 nm *or* 456 *or* 467 nm instead of 525 nm	Up to 72[d]
5	Eosin Y or Rhodamine B or Mes-Acr-ClO_4 as a photocatalyst	Up to 61
6	$[Ru(bpy)_3](PF_6)_2$ instead of Rh6G	64
7	1,4-Dioxane *or* THF *or* DCE *or* DCM as a solvent	Up to 23
8	Rhodamine 6G (1 or 4 mol%) instead of 2 mol%	78 or 80
9	Dry-MeCN (2 mL or 4 mL) instead of 3 mL	83 or 79
10	K_3PO_4 (1 equiv. or 5 equiv.) instead of 2.5 equiv.	67 or 72
11	1 or 3 equiv. of **2a** instead of 1.1 equiv.	82 or 85
12	4 h or 12 h instead of 8 h	62 or 86
13	Open air	81
14	No light	NR
15	No photocatalyst	NR
16	No base	ND
17	Ar-balloon	NR

Standard reaction conditions: [a]**1a** (0.2 mmol), PhSCN **2a** (1.1 equiv.), K_3PO_4 (2.5 equiv.), Rhodamine 6G (2 mol%), O_2- balloon, dry-MeCN (3 mL), Kessil Green LEDs (525 nm, 20 W) for 8 h at room temperature (rt). [b]Determined by ^1H NMR analysis using 1,3,5-Trimethoxybenzene as an internal standard. [c]Isolated yield. [d]1,2-diphenyldisulfide formation was not observed. ND = Not Detected. NR = No Reaction.

Among them, anhydrous acetonitrile proved to be the most effective (Table 5.1, Entry 1). Adjusting the photocatalyst loading to 1 or 4 mol% furnished the desired product **3a** in slightly diminished yields and 2 mol% of Rhodamine 6G (Rh6G) proved to be optimum to deliver **3a** in highest yield (Table 5.1, Entries 1 and 8). Later, changing the solvent volume to 2 or 4 mL also led to decreased yields of **3a** (Table 5.1, Entry 9). Variations in the amount of K_3PO_4 (1 or 5 equiv.) and PhSCN (1 or 3 equiv.) showed no significant effect on the yield of **3a** (Table 5.1, Entries 10 and 11). Altering the reaction time to 4 h or 12 h similarly resulted in reduced yields (Table 5.1, Entry 12). Additionally, the reaction under ambient atmosphere, rather than an O_2-enriched environment, afforded a lower yield, likely due to partial deprotection of **1a** to the corresponding aldehyde (Table 5.1, Entry 13).[23] Control experiments confirmed the necessity of light, photocatalyst, base, and oxygen, as the desired product **3a** was not formed in the absence of light or photocatalyst or base or under inert atmosphere (Table 5.1, Entries 14-17). Collectively, these investigations established the optimized reaction conditions: cyclic thioacetal **1a** (0.2 mmol), phenyl thiocyanate **2a** (1.1 equiv.), K_3PO_4 (2.5 equiv.), and Rhodamine 6G (2 mol%) in anhydrous acetonitrile (3 mL), irradiation with green LEDs (525 nm, 20 W) under an O_2 atmosphere at room temperature.

Having obtained the optimized reaction conditions, we next explored the substrate scope to evaluate the practicality and generality of the protocol. Various para-substituted dithiolane substrates, containing both electronically neutral and electron-rich groups such as −Me, −H, −OMe, and $-N(Et)_2$, successfully delivered the corresponding thiocyano-thioester products (**3a**–**3d**) in excellent yields (up to 92%, Table 5.2). Additionally, dithiolanes bearing electron-withdrawing groups (−CN, $-NO_2$) and electron-deactivating substituents (−F, −Cl, −Br, and $-CF_3$) also performed well, affording the desired products (**3e**–**3j**) in very good yields (up to 88%, Table 5.2). Furthermore, various *ortho*-substituted (−Me, −Br) and *meta*-substituted (−Br) dithiolanes reacted smoothly, affording the corresponding products (**3k**–**3m**) in very good yields, reaching up to 84% (Table 5.2). In addition, substrates bearing allyl, propargyl, and tosyl-protected hydroxyl groups were well tolerated under the optimized conditions, affording the desired products (**3n**–**3p**) in very good yields (up to 88%, Table 5.2). Additionally, dithiolanes featuring di- or tri-substitution on the phenyl ring reacted smoothly to afford the corresponding thiocyano-thioester products (**3q**–**3t**) in good to excellent yields (up to 92%, Table 5.2). Moreover, heterocyclic thioacetals derived from thiophene and benzofuran

Table 5.2 Substrate scope of thiocyano-thioester products.[a]

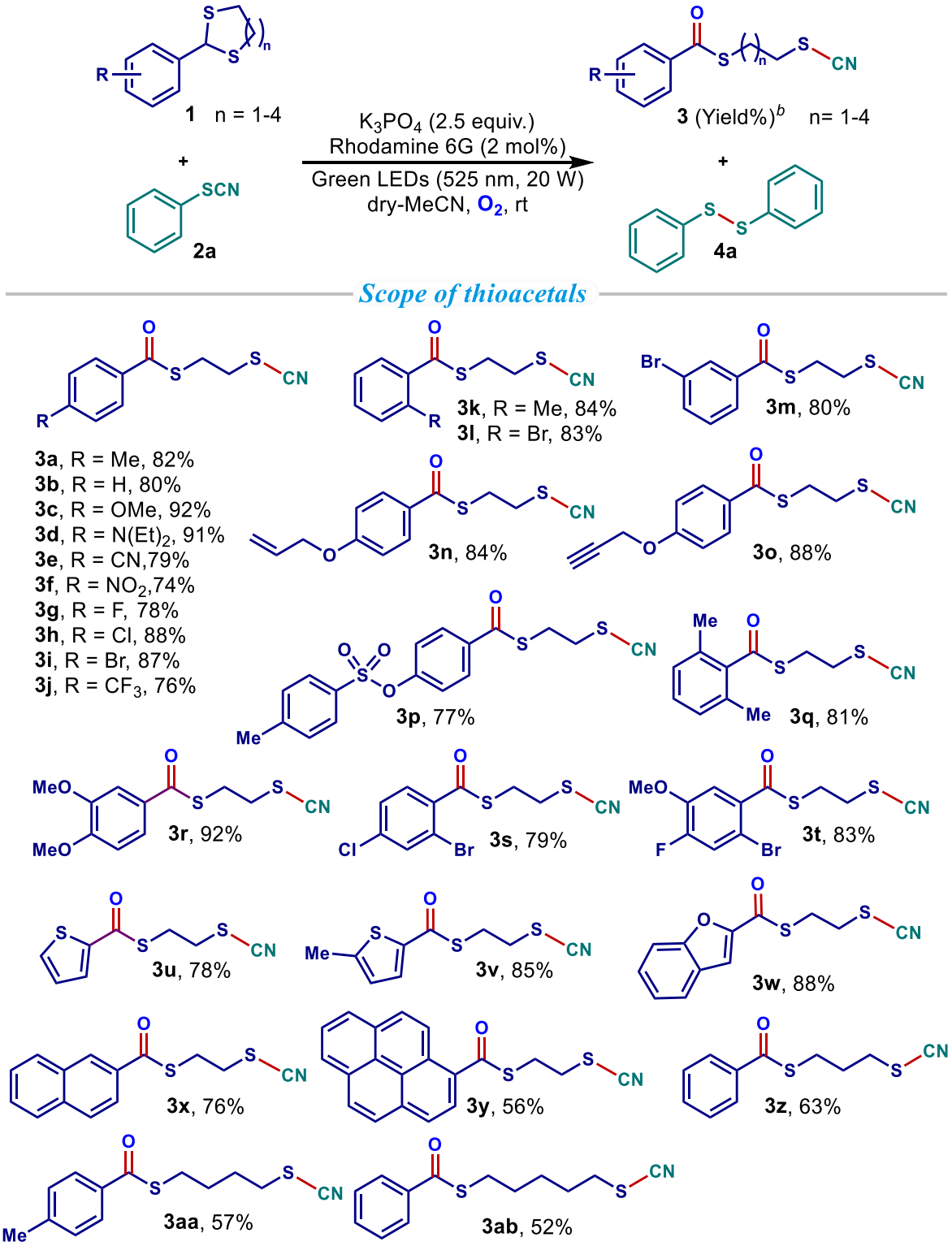

Reaction conditions: [a]**1** (0.2 mmol), PhSCN **2a** (1.1 equiv.), K_3PO_4 (2.5 equiv.), Rhodamine 6G (2 mol%), O_2-balloon, dry-MeCN (3 mL), Kessil Green LEDs (525 nm, 20 W) at room temperature (rt). [b]Isolated yield after purification by column chromatography.

carboxaldehydes reacted efficiently, affording the desired products (**3u**–**3w**) in good to very good yields (up to 88%, Table 5.2). Gratifyingly, polycyclic aromatic substrates such as naphthalene and pyrene furnished the desired products (**3x**, **3y**) in moderate to good yields (up to 76%, Table 5.2).

Table 5.3 Screening of 'CN' sources for thiocyano-thioester product.[a]

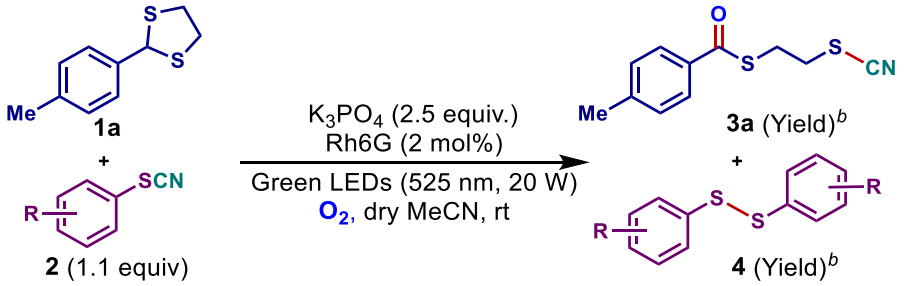

Scope of 'CN' sources

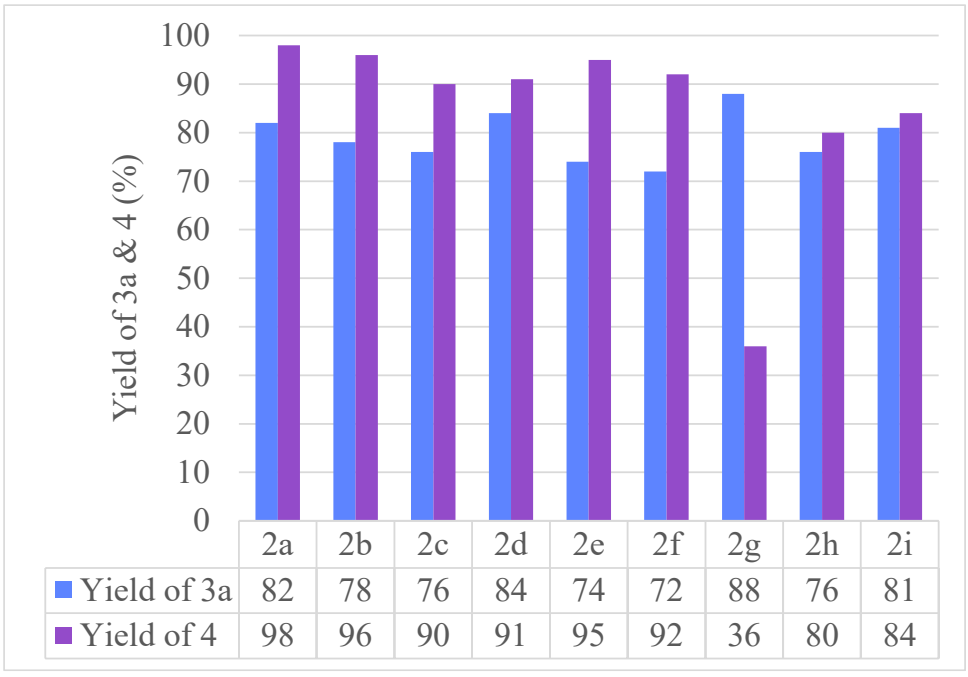

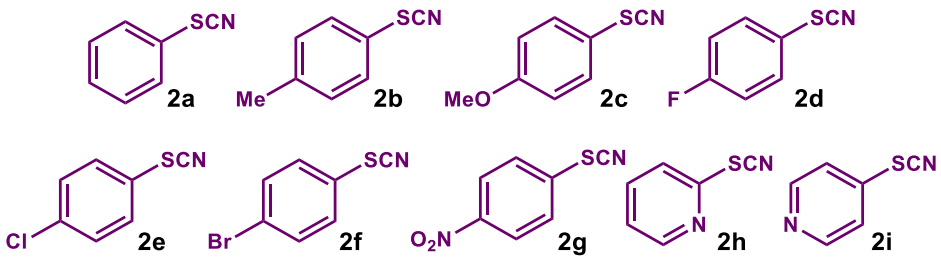

Reaction conditions: [a]**1a** (0.2 mmol), ArSCN **2** (1.1 equiv.), K_3PO_4 (2.5 equiv.), Rhodamine 6G (2 mol%), O_2-balloon, dry-MeCN (3 mL), Kessil Green LEDs (525 nm, 20 W) at room temperature (rt). [b]Isolated yield after purification by column chromatography.

Subsequently, we investigated the reaction by varying the ring size of thioacetals (ranging from 5- to 8-membered rings) under the optimized conditions, resulting in the corresponding thiocyano-thioester products (**3z**, **3aa**, and **3ab**) in moderate to good yields (up to 63%, Table 5.2). It is important to note that the by-product, diphenyldisulfide **4a**, was successfully isolated in quantitative yields in all cases.

To examine the impact of substituents on the phenyl ring of thiocyanate on the outcome of yield of the thiocyano-thioester product **3a**, the reaction was performed with various substituted phenyl thiocyanates. We carefully assessed the yields of **3a** along with the by-product diaryl disulfides **4** (Table 5.3). The electron-neutral and electron-donating groups on phenyl thiocyanates (**2a**–**2c**) provided the desired product **3a** in good yields (up to 82%, Table 5.3). Furthermore, phenyl thiocyanates with electron-deactivating halogen substituents (−F, −Cl, −Br) (**2d**–**2f**) afforded the corresponding product **3a** in very good yields (up to 84%, Table 5.3). Phenyl thiocyanate **2g**, bearing the electron-withdrawing $-NO_2$ group, provided the product **3a** in excellent yield (88%, Table 5.3). Furthermore, pyridine thiocyanates **2h** and **2i** afforded **3a** in good yields (up to 81%, Table 5.3). Notably, the corresponding aryl disulfides **4a**-**4i** (by-products) were also isolated in very good to nearly quantitative yields (up to 98%, Table 5.3).

To validate our hypothesis of implementing circular economy principles through the reuse of by-products diaryl disulfides, we started optimization of reaction condition using the isolated diaryl disulfide **4a** with 4-NO_2-PhSCN **2g** as model substrates. The reaction of diaryl disulfide **4a** with 4-NO_2-PhSCN **2g** under blue LED irradiation (427 nm, 40 W), offered the desired product phenyl thiocyanate **2a** in excellent yield (88%, Table 5.4, Entry 1). The presence of photocatalyst Rhodamine 6G or O_2 atmosphere had a little effect on the outcome of the yield of **2a**, although the reaction time increased to 24 h (Table 5.4, Entries 2 and 3). Conducting the reaction under Ar-atmosphere also gave the desired product **2a** in very good yield (Table 5.4, Entry 4). When the reaction was performed in the absence of light (also wrapped the flask with aluminium foil), the desired product **2a** was obtained in 82% yield after 12 h (Table 5.4, Entry 5). Screening bases such as Na_2CO_3 and K_2CO_3 resulted in either no product formation or a decrease in yield (Table 5.4, Entries 6 and 7). Solvents like toluene and DMF were also tested, but they led to a reduction in yield of **2a** (Table 5.4, Entries 8 and 9). Testing various monochromatic light sources (440 nm, 456 nm, 467 nm, and 525 nm) revealed that decreasing the light wavelength resulted in a decrease in product formation (Table 5.4, Entry 10). When 2-pyridyl disulfide **4h** and phenyl thiocyanate **2a** were treated in the absence of light, the reaction did not proceed at all (Table 5.4, Entry 12). However, when irradiated with 427 nm light, the desired product **2h** was formed with an 86% yield (Table 5.4, Entry 12). Collectively, the

optimized conditions were chosen to be the reaction of disulfide **4** with thiocyanate **2a** or **2g** (2.1 equiv.) in presence of K_3PO_4 (2.5 equiv.) as a base and MeCN as a solvent under irradiation of 427 nm blue LEDs.

Table 5.4 Optimization of reaction conditions for thiocyanate formation.[a]

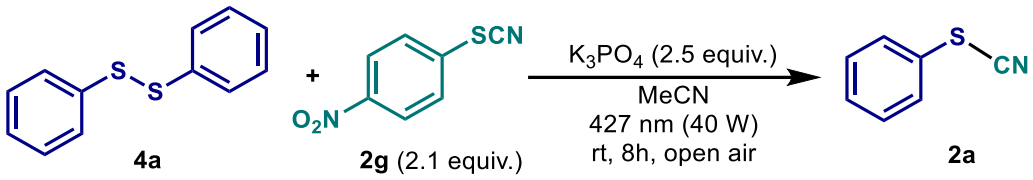

Entry	Deviations standard condition	Yield (%)[b]
1	None	88
2	Rh6G	86[c]
3	O_2-balloon	83[c]
4	Ar-balloon	85
5	No light	82[d]
6	Na_2CO_3 as a base	ND
7	K_2CO_3 as a base	64
8	Toluene as a solvent	43
9	DMF as a solvent	71
10	440 nm *or* 456 nm *or* 467 nm *or* 525 nm instead of 427 nm	82, 74, 68, 52
11	**4h** and **2a** instead of **4a** and **2g** respectively	NR[e]
12	**4h** and **2a** instead of **4a** and **2g** respectively	86[d]

Reaction condition: [a]**4a** (0.2 mmol), PhSCN **2a** (2.1 equiv.), K_3PO_4 (2.5 equiv.), in MeCN (3 mL), Kessil Blue LEDs (427 nm, 40 W) at room temperature (rt), open to air. [b]Isolated yield after purification by column chromatography. [c]24 h instead of 8 h. [d]product **2h** was obtained, 12 h. [e]Reaction without light. ND = Not Detected. NR = No Reaction.

Then, the generality of this protocol was tested by reacting different aryl disulfides with PhSCN (**2a**) or 4-NO_2-PhSCN (**2g**). Gratifyingly, the corresponding aryl thiocyanates (**2b**–**2j**) were obtained in excellent yields (up to 93%, Table 5.5). This strategy effectively enabled the conversion of diaryl disulfide by-products **4** into valuable aryl thiocyanates **2**, which were successfully employed as reagents in subsequent transformations. This approach not only demonstrates efficient resource utilization but also minimizes dependence on virgin chemical

feedstocks.

Table 5.5 Substrate scope of arylthiocyanate products.[a]

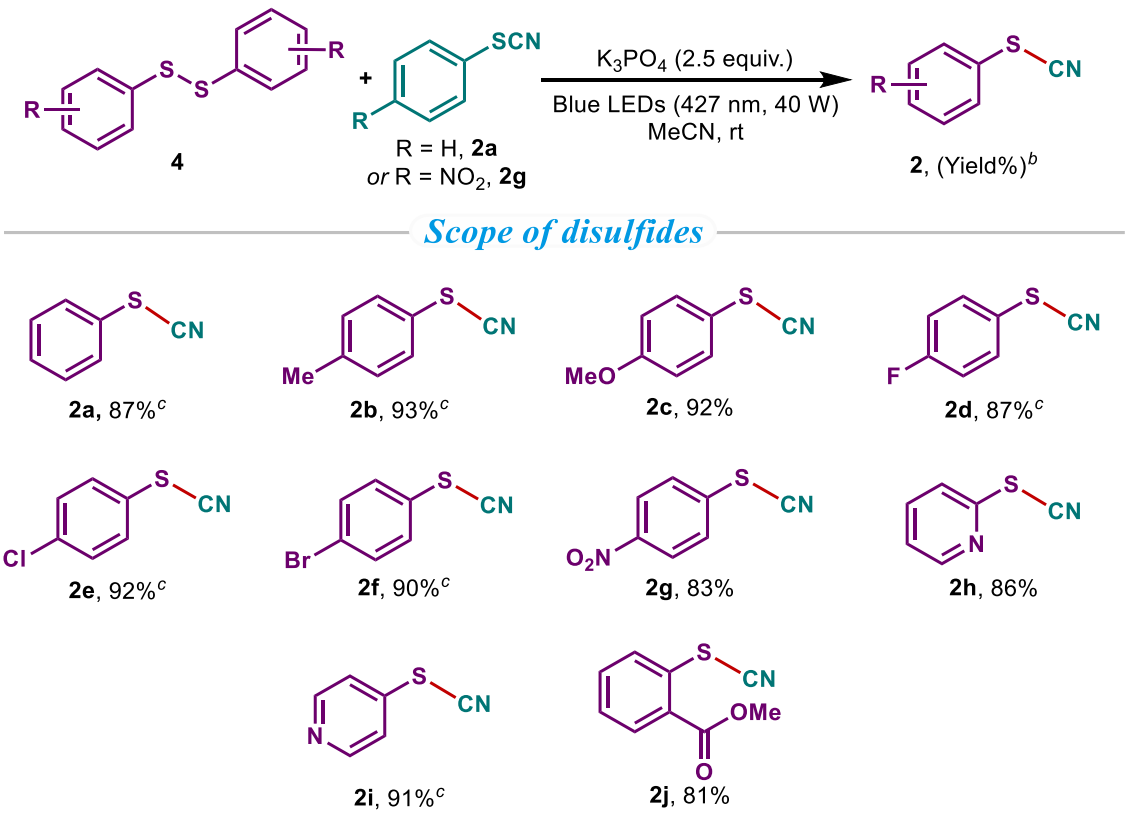

Reaction conditions: [a]**4** (0.2 mmol), PhSCN **2a** (2.1 equiv.), K_3PO_4 (2.5 equiv.), in dry-MeCN (3 mL), Kessil Blue LEDs (427 nm, 40 W) at room temperature (rt). [b]Isolated yield after purification by column chromatography. [c]4-NO_2-PhSCN **2g** (2.1 equiv.) was used instead of **2a**.

To gain insight into the reaction mechanism, we systematically conducted a series of control experiments. To probe the role of reactive oxygen species, we conducted control experiments using well-established singlet oxygen quenchers, DABCO and NaN_3 (Scheme 5.7a, b).[24] In both cases, the formation of product **3a** was observed, suggesting that singlet oxygen might not have involved in the reaction mechanism. However, when the reaction was carried out in the presence of the well-known superoxide radical anion quencher *p*-benzoquinone, no formation of the desired product **3a** was observed under otherwise standard conditions. This result suggests that the superoxide radical anion might play a crucial role in the reaction pathway (Scheme 5.7c).[25]

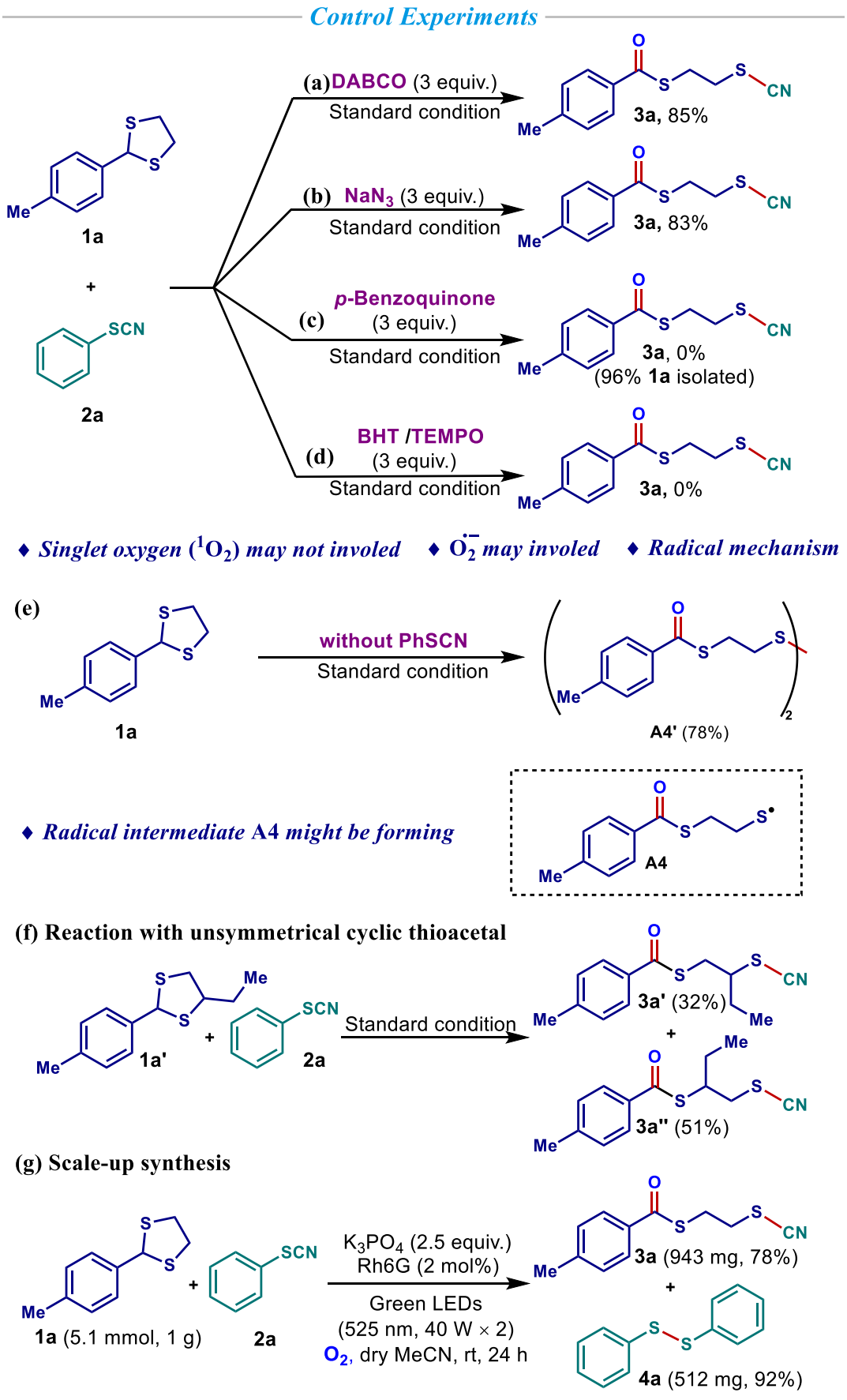

Scheme 5.7 Control experiments and scale-up synthesis of thiocyano-thioester

The reaction of dithiolane **1a** in the presence of BHT/TEMPO (radical quenchers) did not proceed, thereby confirming the radical nature of the transformation (Scheme 5.7d). Additionally, when the reaction was carried out without PhSCN under the standard conditions, we observed the formation of the disulfide-linked dithioester product **A4'** from **1a**. This suggests the involvement of the thiyl radical **A4** in the reaction mechanism (Scheme 5.7e). Moreover, when the unsymmetrical cyclic thioacetal **1a'** was reacted with phenyl thiocyanate **2a** under the standard conditions, the corresponding thiocyano-thioester products **3a'** and **3a''** were obtained in 32% and 51% yields, respectively (Scheme 5.7f). In addition, the protocol was successfully scaled up on a gram scale (5.1 mmol, 1 g), affording the desired product **3a** in 78% yield (Scheme 5.7g).

To know whether the substrate or the combination of substrates involving in direct excitation under the visible light irradiation, we have recorded the UV-Visible absorption spectra (Figure 5.5).

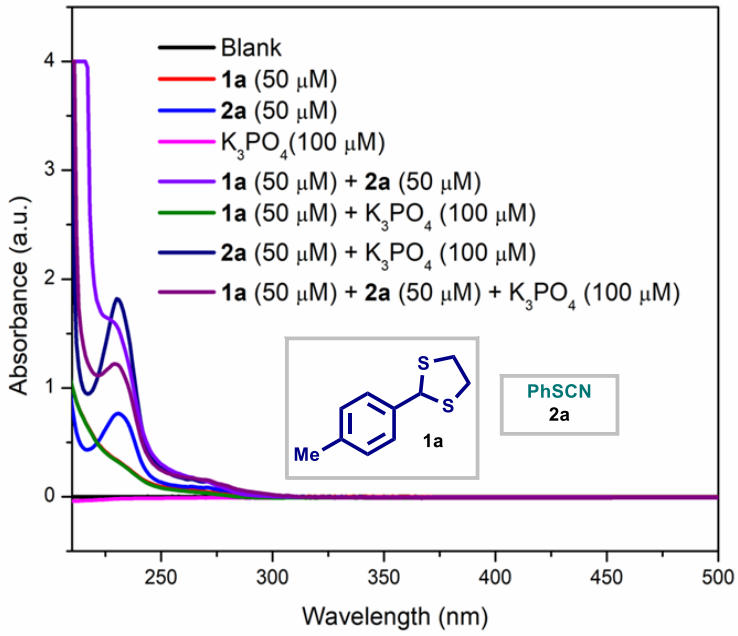

Figure 5.5 UV-Vis absorption spectra of each component **1a** (50 mM in 2 mL MeCN), **2a** (50 mM in 2 mL MeCN), K_3PO_4 (100 mM in 2 mL MeCN), and their mixture **1a** (50 mM) + K_3PO_4 (100 mM) in 2 mL MeCN, **2a** (50 mM) + K_3PO_4 (100 mM) in 2 mL MeCN, **1a** (50 mM) + **2a** (50 mM) in 2 mL MeCN, **1a** (50 mM) + **2a** (50 mM) + K_3PO_4 (100 mM) in 2 mL MeCN.

UV-Visible absorption experiment reveals that neither the individual components (**1a**, **2a**, or K_3PO_4) nor their mixtures exhibit absorbance in the visible light range (380–700 nm). Therefore, these components do not undergo photoexcitation under visible light, ruling out the possibility of product formation through direct excitation of the substrates.

To investigate whether dithioacetal **1a**, thiocyanate **2a**, or K_3PO_4 interact with the excited state photocatalyst (Rh6G*), we conducted a fluorescence quenching experiment and plotted the corresponding Stern–Volmer graph (Figure 5.6). The results demonstrated that K_3PO_4 interacts more efficiently with Rh6G* compared to **1a** and **2a**. The ability of Rh6G* to undergo Single Electron Transfer (SET) with K_3PO_4 was further supported by the oxidation potential of K_3PO_4 (E^{ox} = +0.85 V vs SCE),[26] which is lower than the reduction potential of Rh6G* (E^{red*} = +1.39 V vs SCE).[27] Additionally, the reduction potential of Rh6G* is lower than the oxidation potentials of thioacetal **1a** (E^{ox} = +1.71 V vs SCE) and 4-Cl-PhSCN (E^{ox} = +2.45 V vs SCE). Cyclic voltammograms recorded for substrates **1a** and 4-Cl-PhSCN in the presence of K_3PO_4 revealed an increase in the oxidation potential of **1a** from E^{ox} = +1.42 V vs Ag/Ag^+ to E^{ox} = +1.60 V vs Ag/Ag^+, suggesting that K_3PO_4 interacts with **1a** following the oxidation of K_3PO_4 (Figure 5.7).

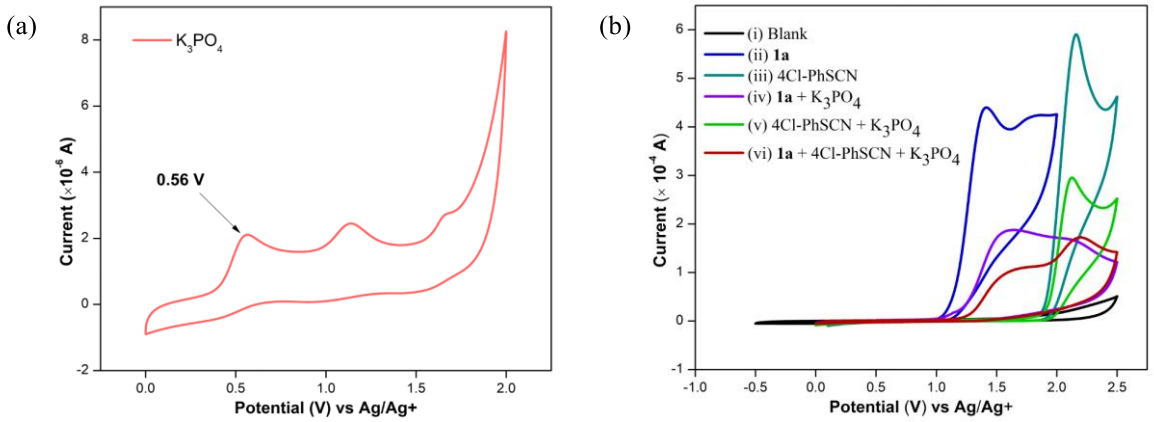

Figure 5.6 (a) Cyclic voltammogram of K_3PO_4: E_p = +0.56 V (vs $Ag/AgNO_3$ (0.01 M) in MeCN). (b) (i) Blank, $^nBu_4NClO_4$ (100 mM), (ii) thioacetal **1a,** (iii) 4Cl-PhSCN **2e**, (iv) **1a** + K_3PO_4, (v) 4Cl-PhSCN **2e** + K_3PO_4, (vi) **1a** + 4Cl-PhSCN **2e** + K_3PO_4. Samples were prepared with analyte (10 mM) and $^nBu_4NClO_4$ (100 mM) electrolyte solution in MeCN and recorded with a scan rate of 100 mV/s. The cyclic voltammetry (CV) was performed using a CHI (model 600E) electrochemical analyzer/workstation. A three-electrode setup was used, consisting of a 3 mm dia. glassy carbon working electrode (Part no- CHI104, CH Instruments), platinum wire counter electrode (Part no- CHI115, CH Instruments), and non-aqueous $Ag/AgNO_3$ (0.01 M) reference electrode w/ porous teflon tip (Part no- CHI112, CH Instruments). The measured potentials were recorded with respect to an $Ag/AgNO_3$ (0.01 M) reference electrode.

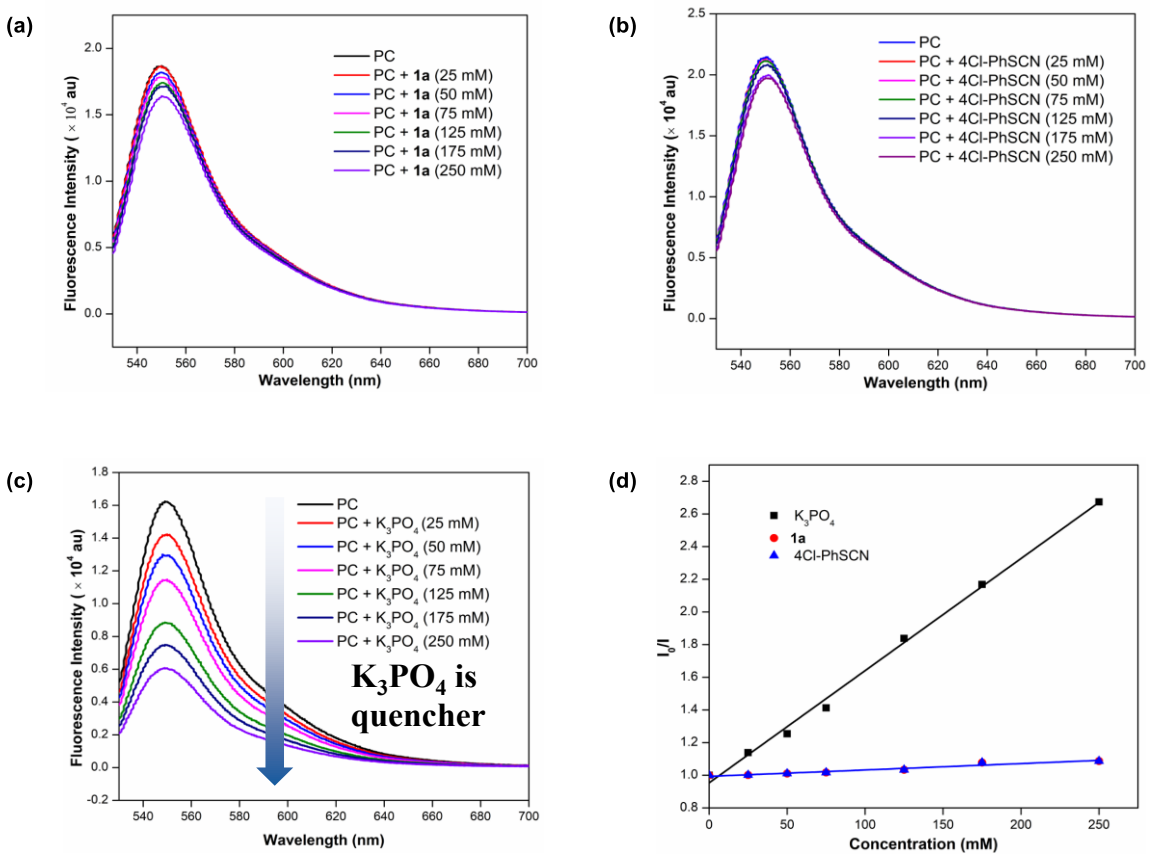

Figure 5.7 (a) Fluorescence spectra of Rh6G (10 μM) with increasing concentration of **1a**. (b) Fluorescence spectra of Rh6G (10 μM) with increasing concentration of 4-Cl-PhSCN **2e**. (c) Fluorescence spectra of Rh6G (10 μM) with increasing in the concentration of K_3PO_4. (d) Steady-state Stern–Volmer quenching plot of Rh6G (10 μM) with varying concentrations of **1a**/**2e**/ K_3PO_4.

.

Based on the control experiments, Stern–Volmer plot, cyclic voltammetry studies and preceding literature,[19,28] a possible reaction mechanism has been illustrated in (Scheme 5.8). Upon irradiation with green light, the photocatalyst Rh6G is excited to its active state (Rh6G*). The excited Rh6G* species (E^{red*} = +1.39 V vs SCE) undergoes a single electron transfer (SET) with K_3PO_4 (E^{ox} = +0.85 V vs SCE) via a reductive quenching pathway, generating the Rh6G radical anion ($Rh6G^{\bullet-}$) and the $[K_3PO_4]^{\bullet+}$ radical cation. This SET process is supported by cyclic voltammetry data and Stern–Volmer quenching studies (Figures 5.6 and 5.7). The resulting $Rh6G^{\bullet-}$ then engages in another SET event with molecular oxygen to produce the superoxide radical anion ($O_2^{\bullet-}$) and regenerate ground-state Rh6G, thereby completing the photocatalytic cycle. Meanwhile, the reactive $[K_3PO_4]^{\bullet+}$ species interacts with dithiolane **1a** to generate intermediate **A1**, which undergoes ring opening to form intermediate **A2**. The nucleophilic

superoxide radical anion ($O_2^{\bullet-}$) subsequently attacks the electrophilic carbon center in **A2**, leading to the formation of intermediate **A3**. Proton abstraction by base K_3PO_4 followed by the elimination of O_2 generates a thiyl radical intermediate **A4** (the dimer of **A4** has been isolated and analyzed by NMR, Scheme 5.7e).[28] This thiyl radical **A4** then reacts with phenyl thiocyanate (PhSCN) to afford the desired thiocyano-thioester product **3a**, along with diphenyl disulfide **4a** as a by-product.

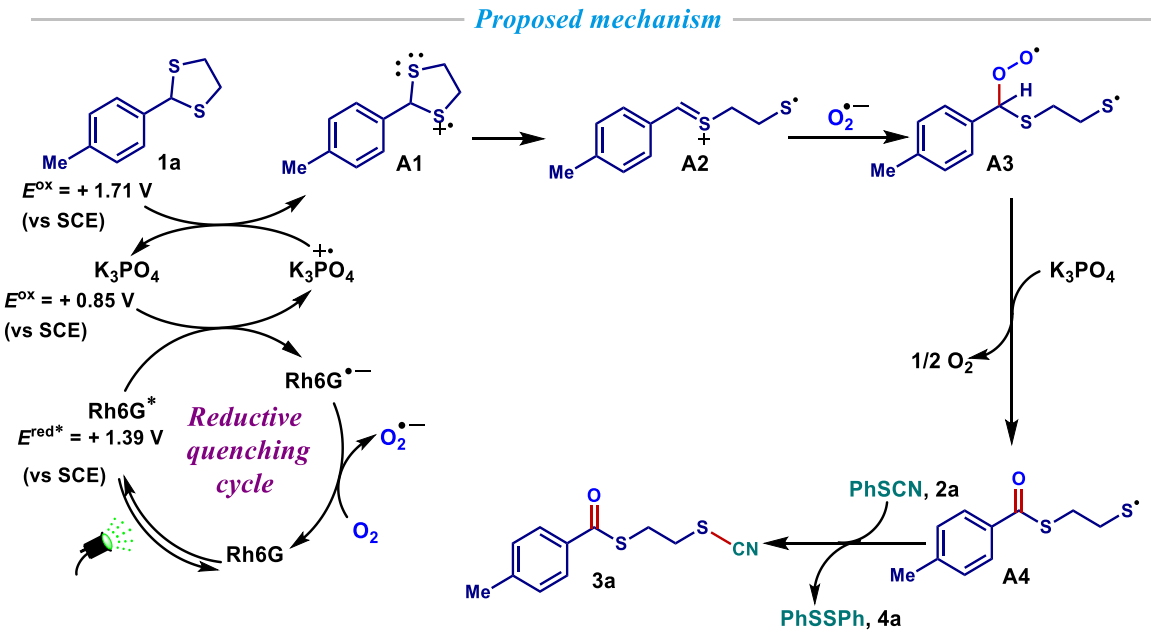

Scheme 5.8 Proposed reaction mechanism for thiocyano-thioester formation

Additionally, to propose a possible reaction mechanism for the thiocyanate formation from disulfides, we conducted a series of control experiments, including radical trapping studies using TEMPO and BHT (Schemes 5.9 and 5.10). Radical adducts were successfully detected with both BHT and TEMPO (Figures 5.8–5.11), suggesting that the reaction might proceeds through a radical pathway.

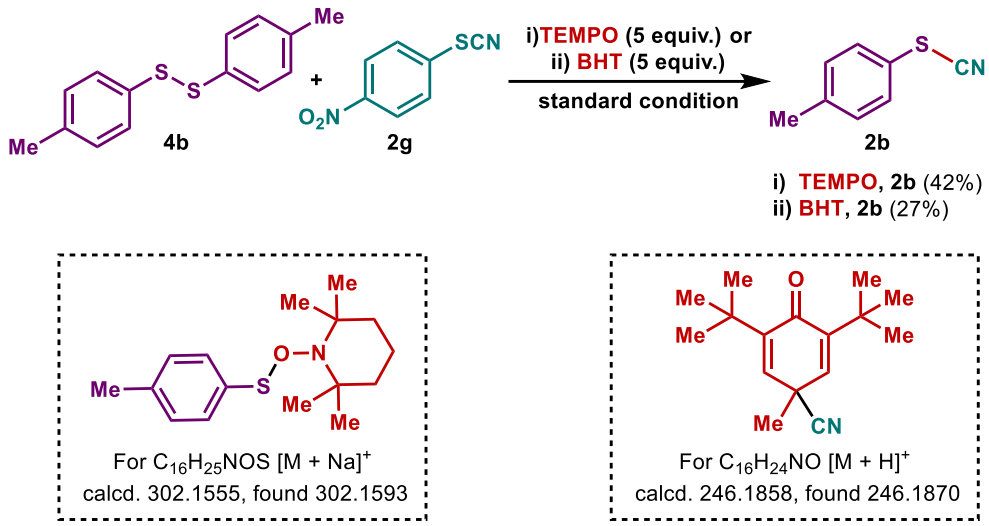

Scheme 5.9 Radical trapping experiment for reaction of **4b** with **2g**

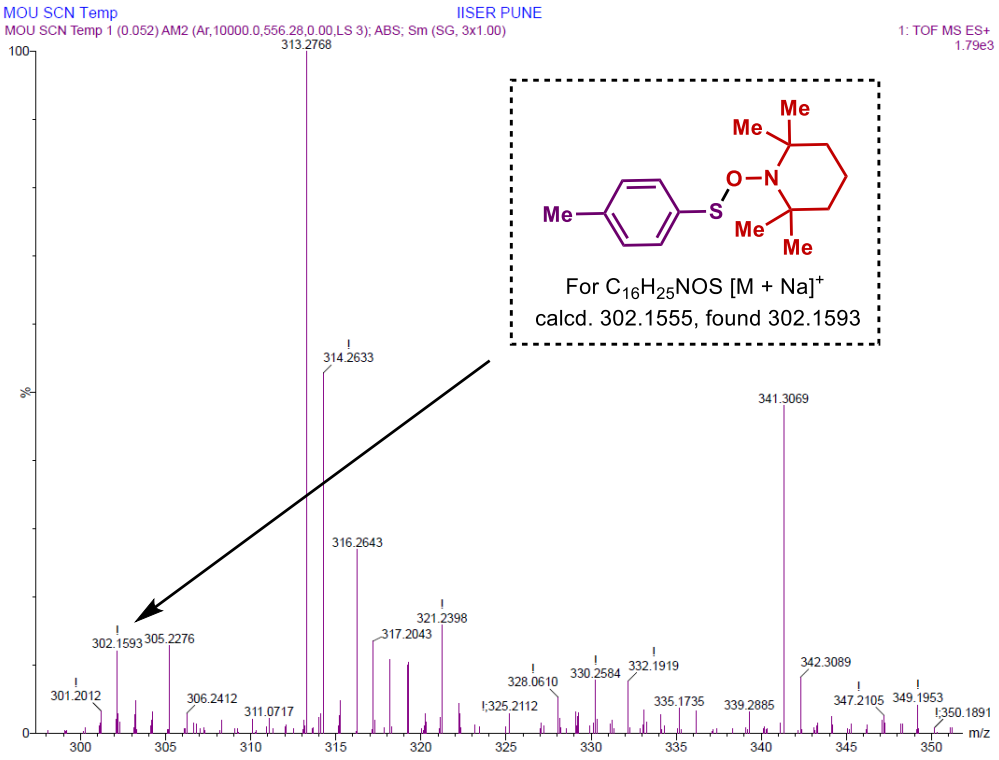

Figure 5.8 HRMS spectrum of TEMPO trapped radical intermediate

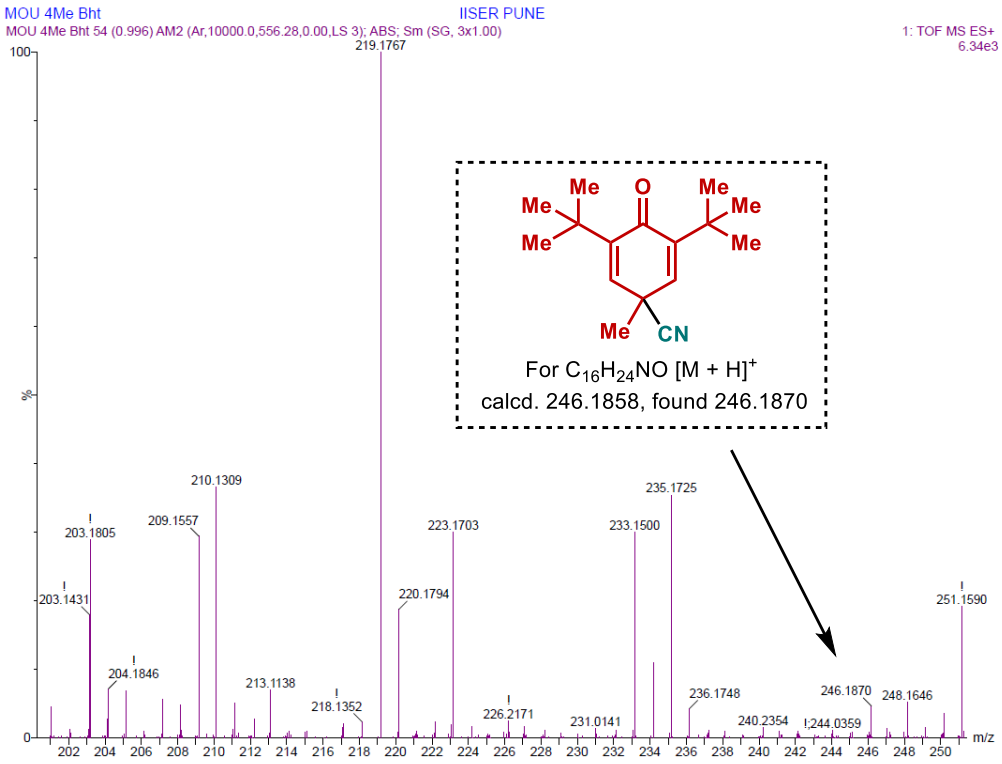

Figure 5.9 HRMS spectrum of BHT trapped radical intermediate.

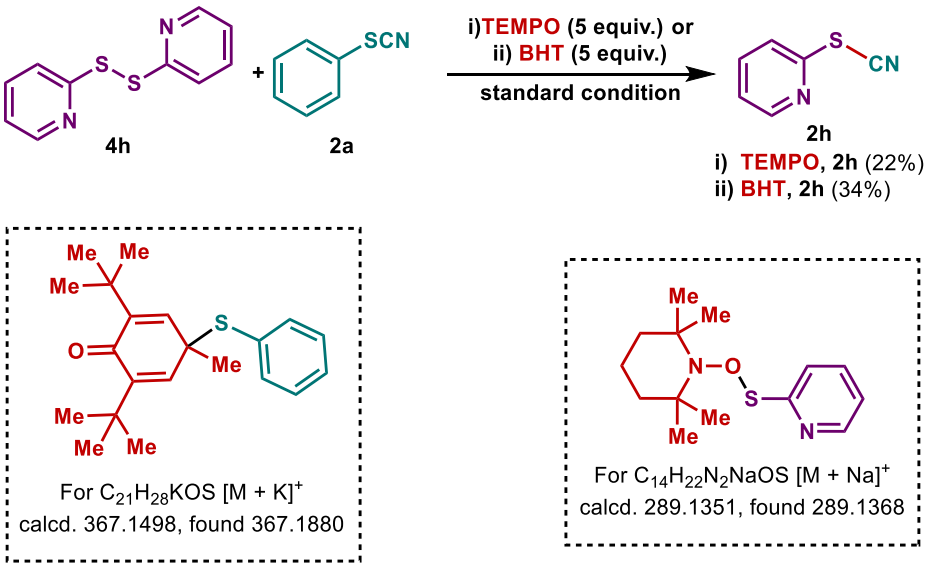

Scheme 5.10 Radical trapping experiment for the reaction of **4h** with **2a**

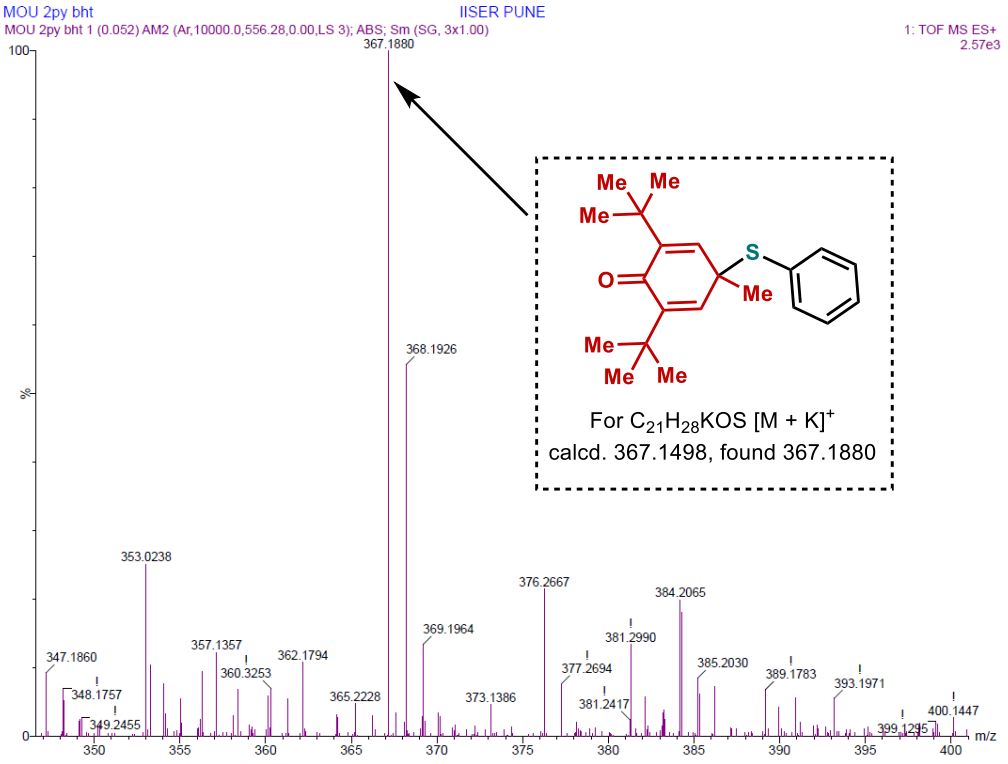

Figure 5.10 HRMS spectrum of BHT trapped radical intermediate.

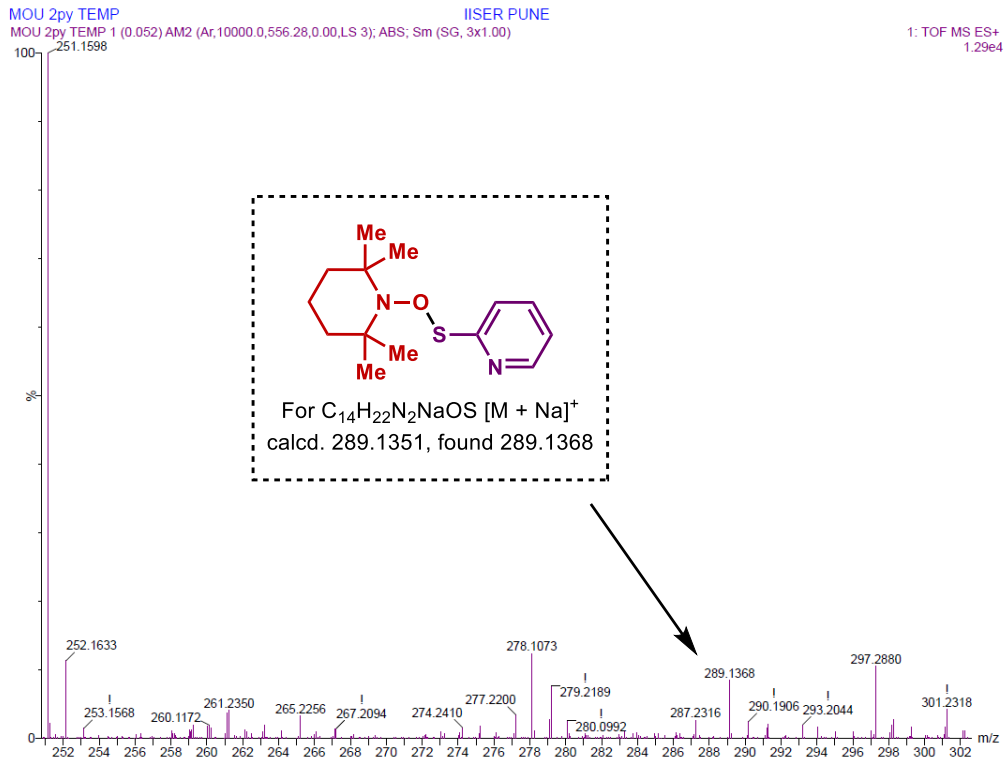

Figure 5.11 HRMS spectrum of TEMPO trapped radical intermediate.

Further UV-Visible absorption experiments were conducted (Figure 5.12 and 5.13). The absorption spectra revealed that the individual components (**4a** or **2g**) absorb only below 380 nm (blue and cyan curves, Figure 5.12). Notably, the mixture of **2g** and K_3PO_4 exhibited a pronounced bathochromic shift into the visible region, with a new absorption maximum (λ_{max}) appearing around 486 nm and extending up to 550 nm (pink curve, Figure 5.12). In contrast, no such shift was observed for the mixtures of **4a** with K_3PO_4 (green curve, Figure 5.12) or **4a** with **2g** (violet curve, Figure 5.12). These observations strongly suggest the formation of a new photoactive electron donor–acceptor (EDA) complex between **2g** and K_3PO_4.

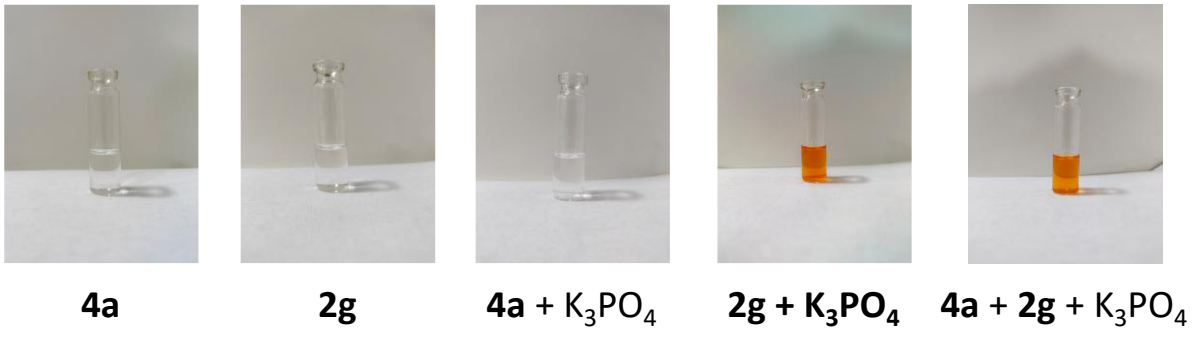

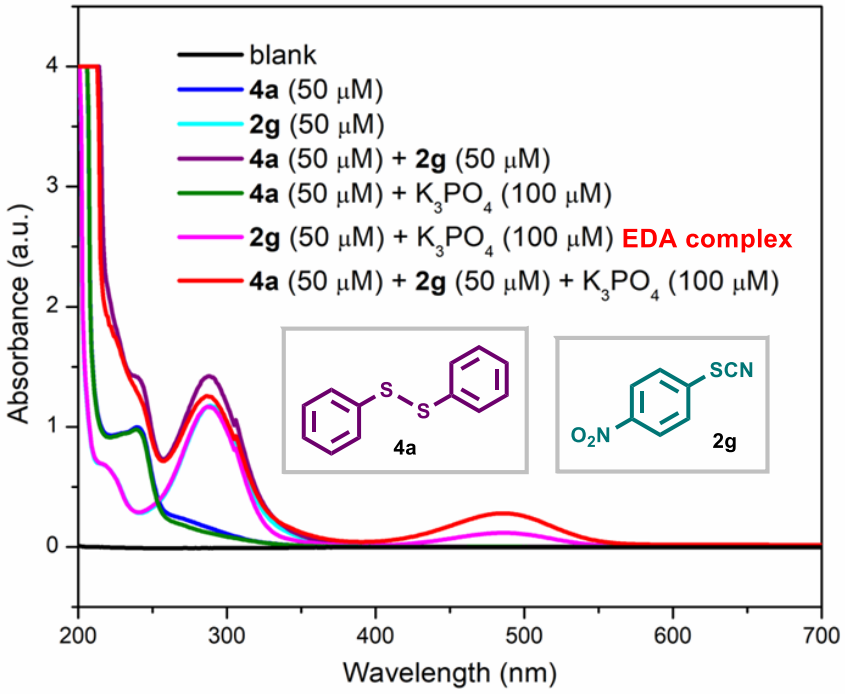

Figure 5.12 UV-Vis absorption spectra of individual components **4a** (50 μM in 2 mL MeCN), **2g** (50 μM in 2 mL MeCN), and their mixture **4a** (50 μM) + **2g** (50 μM) in 2 mL MeCN, **4a** (50 μM) + K_3PO_4 (100 μM) in 2 mL MeCN, **2g** (50 μM) + K_3PO_4 (100 μM) in 2 mL MeCN, **4a** (50 μM) + **2g** (50 μM) + K_3PO_4 (100 μM) in 2 mL MeCN.

The absorption spectra further reveal that the individual components (**4h** and **2a**) absorb only below 310 nm (violet and cyan curves, Figure 5.13). Interestingly, the mixture of **4h** and K_3PO_4 displays a notable bathochromic shift into the visible region, with a new absorption peak (λ_{max}) appearing around 370 nm and extending to 430 nm (green curve, Figure 5.13). In contrast, no such shift is observed in the mixtures of **2a** with K_3PO_4 (blue curve, Figure 5.13) or **4h** with **2a** (pink curve, Figure 5.13). These results suggest that **4h** and K_3PO_4 form a new photoactive electron donor–acceptor (EDA) complex. Moreover, when the reaction between **4h** and **2a** was halted after 6 hours, a new intermediate was isolated and characterized by NMR and HRMS, revealing its structure as the heterodisulfide **4ha** (Scheme 5.11). Thus, further supporting the light-induced cleavage of disulfide **4h** to generate a thiyl radical.

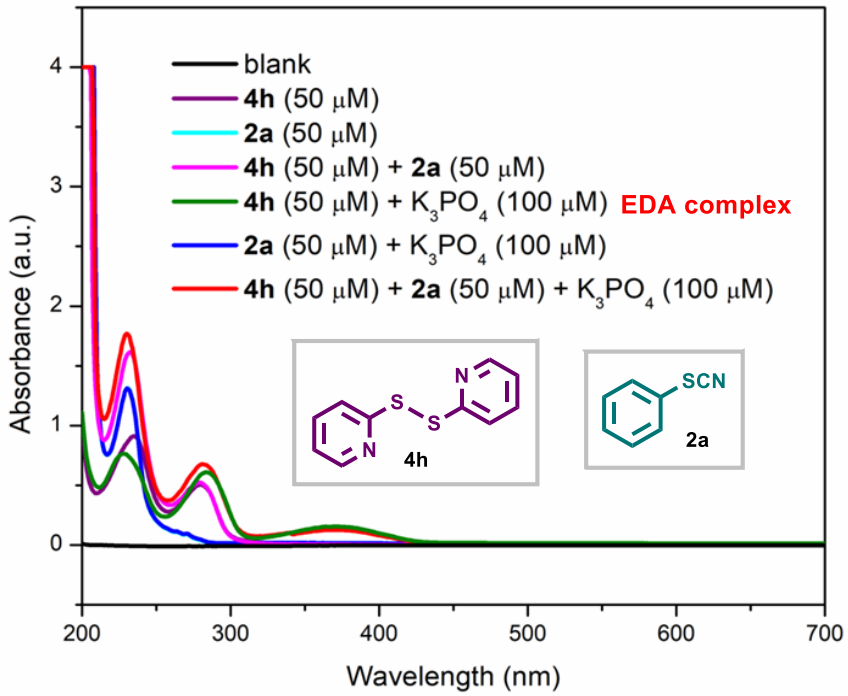

Figure 5.13 UV-Vis absorption spectra of individual components **4h** (50 μM in 2 mL MeCN), **2a** (50 μM in 2 mL MeCN), and their mixture **4h** (50 μM) + **2a** (50 μM) in 2 mL MeCN, **4h** (50 μM) + K_3PO_4 (100 μM) in 2 mL MeCN, **2a** (50 μM) + K_3PO_4 (100 μM) in 2 mL MeCN, **4h** (50 μM) + **2a** (50 μM) + K_3PO_4 (100 μM) in 2 mL MeCN.

Based on the results of these control experiments, UV-Visible absorption experiments and literature report[29] we have proposed two possible mechanisms for the formation of thiocyanates (Scheme 5.12). The reaction of **4a** and **2g** proceeds through the formation of an electron donor-acceptor (EDA) complex between **2g** and K_3PO_4. This complex undergoes single electron

transfer (SET) with or without visible light irradiation, resulting in the formation of PO_4^{2-}, 4-NO_2-phenyl thiolate anion **2g'**, and the CN radical ($CN^{\bullet}$). The $CN^{\bullet}$ then reacts with disulfide **4a** to yield thiocyanate **2a** (Scheme 5.12A).

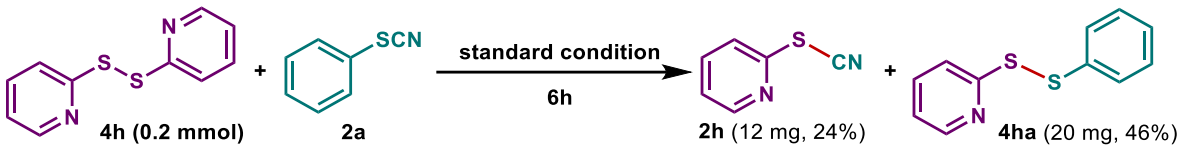

Scheme 5.11 Isolation of the intermediate heterodisulfide **4ha.**

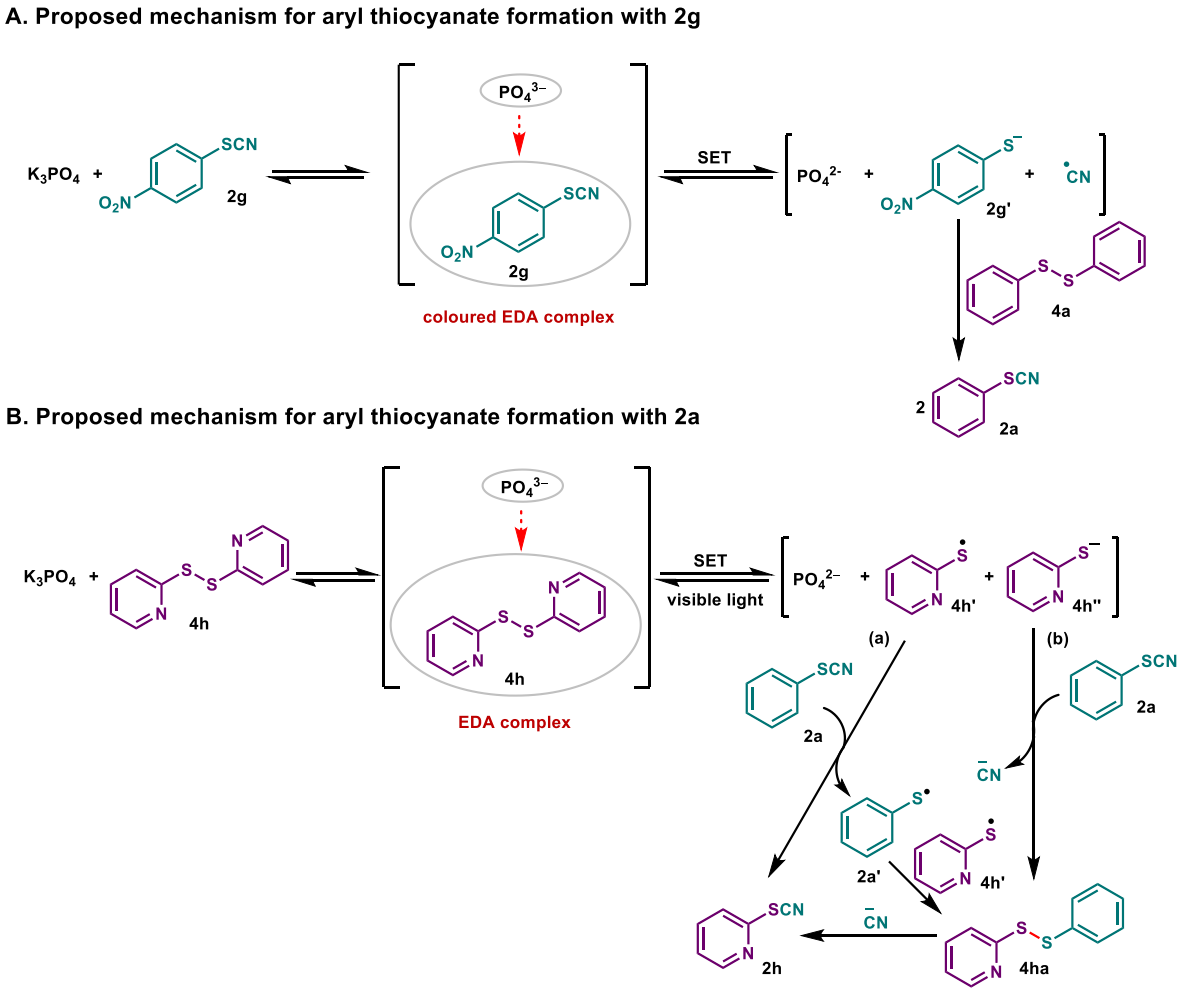

Scheme 5.12 Proposed reaction mechanism for thiocyanate formation.

However, for the reaction involving **4h** and **2a**, it is proposed that an EDA complex forms between **4h** and K_3PO_4 (Scheme 5.12B). Following this, visible light-mediated single electron transfer (SET) occurs from K_3PO_4 to disulfide **4h**, resulting in the formation of PO_4^{2-}, 2-pyridyl

thiyl radical **4h'**, and 2-pyridyl thiolate anion **4h''**. Two potential pathways (a and b) can lead to the formation of thiocyanate **2h**. The first pathway involves the reaction of the 2-pyridyl thiyl radical **4h'** with phenyl thiocyanate **2a**, leading to the formation of 2-pyridyl thiocyanate **2h** and the generation of phenyl thiyl radical **2a'** (Scheme 5.12Ba). This phenyl thiyl radical **2a'** may then react with the 2-pyridyl thiyl radical **4h'**, forming heterodisulfide **4ha**. The second pathway suggests the reaction of 2-pyridyl thiolate anion **4h''** with phenyl thiocyanate **2a**, resulting in the formation of heterodisulfide **4ha** and the generation of the cyanide anion (CN^-) (Scheme 5.12Ba). Subsequently, the formed heterodisulfide **4ha** may react with CN^-, ultimately yielding the desired product **2h**.

5.3 Conclusion

In summary, aryl thiocyanates have been demonstrated as a sustainable alternative source of organic 'CN' for the cyanation of cyclic thioacetals. The by-products, diaryl disulfides, were isolated and efficiently recycled to synthesize various aryl thiocyanates in excellent yields. Moreover, the synthesized aryl thiocyanates were effectively utilized to access thiocyano thioesters. This approach highlights the practical application of both by-products and products in a framework of circular economy, reducing the need for virgin chemicals. The protocol is applicable to a broad range of substrates, including both thioacetals and disulfides. The method utilizes visible light (Green and Blue LEDs) as a clean energy source, eliminating the need for external chemical oxidizing agents. Control experiments, UV-Visible absorption spectroscopic data, fluorescence quenching, and cyclic voltammetry studies support the conclusion that the transformation proceeds via a reductive quenching mechanistic cycle.

5.4 Experimental Section

5.4.1 General Details

Reagent Information: Unless otherwise noted, all reactions were carried out with distilled and dried solvents using oven-dried glassware under dry Argon atmosphere. All the starting materials and reagents were purchased from commercial suppliers (Sigma-Aldrich, TCI, Alfa Aesar, Spectrochem, BLD Pharm and Chemscene) and were used as received. Thin-layer chromatography (TLC) was performed using silica gel 60 GF_{254} precoated aluminum backed plates (2.5 mm). Visualization was accomplished by irradiation with UV light at 254 nm and 2,4-dinitrophenyl hydrazine (DNP) staining agent. The column chromatography was performed using silica gel (100−200 mesh) eluting with petroleum ether and ethyl acetate.

Analytical Information: All isolated compounds were characterized by proton (^1H) and carbon $^{13}C\{^1H\}$ NMR spectra recorded on a Bruker Avance III HD Ascend spectrometer (400 MHz). The NMR spectra were recorded using tetramethylsilane as the internal standard. ^1H NMR spectra were recorded at 400 MHz, $^{19}F\{^1H\}$ NMR spectra were recorded at 377 MHz and $^{13}C\{^1H\}$ NMR spectra were recorded at 100 MHz. Chemical shifts (δ) are reported in ppm downfield from $CDCl_3$ (δ = 7.26 ppm) for ^1H NMR and relative to the central $CDCl_3$ resonance (δ = 77.16 ppm) for $^{13}C\{^1H\}$ NMR spectroscopy. For ^1H NMR, data are reported as follows: chemical shift, multiplicity (s = singlet, d = doublet, t = triplet, q = quartet, p = pentet, s = sextet, h = heptet, m = multiplet, br = broad), coupling constants (*J*) are given in Hz and integration. Mass samples were analyzed by high-resolution mass spectrometry (HRMS)-ESI TOF. Using an open glass capillary, melting points were recorded on a BUCHI M-560 melting point apparatus, and are not corrected. UV-Visible absorption spectra were recorded on the JUV-1900 UV-Vis Spectrophotometer. Fluorescence emission spectra were obtained on a RF-6000 Spectrofluorophotometer from Shimadzu in a 3 mL, Hellmafluorescence cuvette (path length 1.0 cm). All photocatalytic reactions were performed under (Kessil PR160L series Green LEDs (525 nm, 20 W), Blue LEDs (427 nm, 40 W) and IBRA Pure 20 W Blue LED Flood Light, IP Rating: IP66). The reaction mixture was taken in a borosilicate glass and irradiated from 5 cm away from the LEDs. The reaction temperature is maintained 25-30 °C throughout the reaction by using external cooling fans.

5.4.2 Experimental Procedures

5.4.2A General Procedure A (GP A) for the synthesis of cyclic thioacetals 1: (protection of aldehyde).[27] To a round bottom flask containing SiO_2, PPA (6.5 w/w %) DCM (10 mL) was added and stirred well for 15 min. After that DCM was evaporated to obtain a well-mixed SiO_2-PPA mixture. To this mixture, DCM (15 mL), aldehyde (1 equiv.; 1.5 mmol) and alkane-1, n-dithiol were added and stirred for 6 h at room temperature. After completion of the reaction (monitored by TLC) the solution was filtered through cotton. The filtrate was treated with saturated KOH solution (15 mL) and stirred for 30 min to quench excess dithiols. After which, solution was extracted with dichloromethane (3 x 20 mL). The combined organic layers were dried over anhydrous sodium sulphate, filtered, and concentrated under reduced pressure. The crude product was further purified by column chromatography over silica gel to afford the corresponding compound **1**.

5.4.2B General Procedure B (GP B) for the synthesis of aryl thiocyanates (2a-2i).[30] Aryl thiol (1.0 mmol) was first reacted with SO_2Cl_2 (1.1 mmol) at 0 ^oC in dry CH_2Cl_2 under Ar-atm in presence of triethylamine (1.2 mmol). After stirring of solution for 30 min at 0 ^oC, the CH_2Cl_2 was removed by evaporation and replaced with MeCN, followed by the slow addition of TMSCN (1.1 mmol). The resulting brown solution was stirred at 25 ^oC for 1 h (monitored by TLC) and concentrated under vacuum. The crude residues were purified by column chromatography over silica gel using mixture of petroleum ether/EtOAc as an eluent to afford corresponding pure aryl thiocyanate products (**2a**−**2i**).

5.4.2C General Procedure C (GP C) for the synthesis of diaryl disulfide 4j.[31] Arylthiophenol (1.78 mmol, 300 mg), anhydrous potassium carbonate (1.2 equiv.), and MeCN (10 mL) were sequentially added in a round bottom flask (50 mL) and the resulting mixture was stirred at room temperature under air for 24 h. The completion of reaction was monitored by TLC. The mixture was filtered and concentrated under vacuum to obtain the crude product. The crude residues were purified by column chromatography over silica gel using mixture of petroleum ether/EtOAc as an eluent to afford corresponding pure diaryl disulfide product **4j**.

5.4.2D General Procedure D (GP D) for the photoredox catalyzed synthesis of thiocyano-thioesters 3. An oven-dried round bottom flask equipped with a stir bar was charged with cyclic thioacetal **1** (0.2 mmol, 1 equiv.), K_3PO_4 (0.5 mmol, 2.5 equiv.), ArSCN **2** (2.2 mmol, 1.1 equiv.) Rhodamine 6G (2 mol%), dry MeCN (4 mL). The reaction mixture was initially

purged with O_2 for 5 min and the oxygen atmosphere was maintained throughout the reaction (using an oxygen balloon). The reaction mixture was stirred under the irradiation of green LEDs (525 nm, 20 W) at room temperature for 8 h (monitored by TLC). After completion of the reaction, the solvent was removed under reduced pressure and the crude residue was purified by column chromatography over silica gel (100−200 mesh) using mixture of petroleum ether/EtOAc as an eluent to afford the corresponding product **3** and by-products diaryl disulfides **4** in quantitative yield.

(*Note- The presence of moisture and the impurity of alkanedithiol in cyclic thioacetal **1** greatly influences the yield of reaction. Dry solvent is must to avoid the deprotection of cyclic thioacetal to corresponding aldehydes. The reaction mixture was taken in a borosilicate glass and irradiated with Kessil PR160L series Green LEDs (525 nm, 20 W) from 5 cm away from the LEDs. The reaction temperature was maintained 25-30 °C throughout the reaction by using external cooling fans.*)

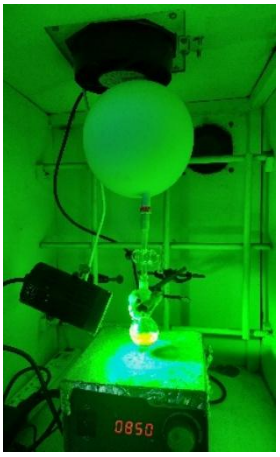

Figure 5.14 Reaction setup for the synthesis of thiocyano-thioester **3** under Green LEDs

5.4.2E General Procedure E (GP E) for the synthesis of aryl thiocyanates 2. An oven-dried reaction tube equipped with a stir bar was charged with diaryl disulfide **4** (0.2 mmol, 1 equiv.), K_3PO_4 (0.5 mmol, 2.5 equiv.), PhSCN **2a** *or* 4-NO_2-PhSCN **2g** (0.42 mmol, 2.1 equiv.) MeCN (3 mL). The reaction mixture was stirred room temperature under the irradiation of blue LEDs (427 nm, 40 W) for 8 h (monitored by TLC). After completion of the reaction, the solvent was removed under reduced pressure and the crude residue was purified by column chromatography over silica gel (100−200 mesh) using mixture of petroleum ether/EtOAc as an eluent to afford the corresponding **2**.

Figure 5.15 Reaction setup for the synthesis of aryl thiocyanates **2** under Blue LEDs

5.4.2F General Procedure F (**GP F**) for the photoredox catalyzed scale-up synthesis of thiocyano-thioester **3a**. An oven-dried 100 mL round bottom flask equipped with a stir bar was charged with cyclic thioacetal **1a** (5.1 mmol, 1 g, 1 equiv.), K_3PO_4 (12.75 mmol, 2.5 equiv.), ArSCN **2** (11.2 mmol, 1.1 equiv.) Rhodamine 6G (2 mol%), dry MeCN (20 mL). The reaction mixture was initially purged with O_2 for 5 min and the oxygen atmosphere was maintained throughout the reaction (using an oxygen balloon). The reaction mixture was stirred under the irradiation of green LEDs (525 nm, 40 W × 2) at room temperature for 24 h (monitored by TLC). After completion of the reaction, the solvent was removed under reduced pressure and the crude residue was purified by column chromatography over silica gel using mixture of petroleum ether/EtOAc as an eluent to afford the corresponding **3a** (943 mg, 78%) and corresponding by-products diphenyl disulfide **4a** (512 mg, 92%). (*Note- The presence of moisture and the impurity of alkanedithiol in cyclic thioacetal **1a** greatly influences the yield of reaction. Dry solvent is must to avoid the deprotection of cyclic thioacetal to corresponding aldehydes. The reaction mixture was taken in a borosilicate glass and irradiated with Kessil PR160L series Green LEDs (525 nm, 40 W × 2) from 5 cm away from the LEDs. The reaction temperature was maintained 25-30 °C throughout the reaction by using external cooling fans.*)

Figure 5.16 Reaction setup for the scale-up synthesis of **3a** under Green LEDs

5.4.3 Product Characterization Data

2-(phenyldisulfaneyl)pyridine (**4ha**): The compound **4ha** was prepared following the General Procedure E (GP E) for 6 h. Colourless liquid (20 mg, 46% yield), R_f = 0.45 (petroleum ether/EtOAc 95:05). ^{1}H NMR (400 MHz, $CDCl_3$) δ 8.53 – 8.41 (m, 1H), 7.73 – 7.56 (m, 2H), 7.56 – 7.48 (m, 2H), 7.40 – 7.25 (m, 2H), 7.28 – 7.18 (m, 1H), 7.09 (ddd, *J* = 7.2, 4.8, 1.4 Hz, 1H). ^{13}C{^{1}H} NMR (100 MHz, $CDCl_3$) δ 159.8, 149.7, 137.4, 136.2, 129.3, 127.4, 127.4, 121.0, 119.7. HRMS (ESI TOF) *m/z* for $C_{11}H_{10}NS_2$ $[M + H]^+$ calcd. 220.0255, found 220.0267.

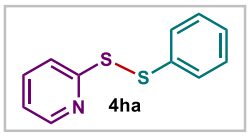

S,S'-(disulfanediylbis(ethane-2,1-diyl)) bis(4-methylbenzothioate) (**A4'**): The compound **A4'** was prepared following the General Procedure D (GP D) without PhSCN. White solid (33 mg, 78% yield), R_f = 0.44 (petroleum ether/EtOAc 85:15). ^{1}H NMR (400 MHz, $CDCl_3$) δ 7.89 – 7.84 (m, 4H), 7.24 (d, *J* = 7.9 Hz, 4H), 3.46 – 3.39 (m, 4H), 3.02 – 2.96 (m, 4H), 2.41 (s, 6H). ^{13}C{^{1}H} NMR (100 MHz, $CDCl_3$) δ 191.0, 144.6, 134.5, 129.5, 127.5, 29.1, 21.8. HRMS (ESI TOF) *m/z* for $C_{20}H_{23}O_2S_4$ $[M + H]^+$ calcd. 423.0581, found 423.0583.

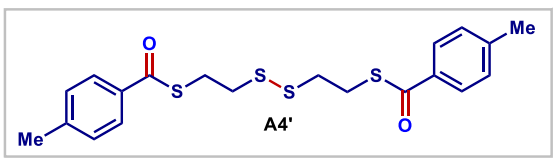

4-ethyl-2-(p-tolyl)-1,3-dithiolane (**1a'**): The compound **1a'** was prepared following the General Procedure A (GP A). Colourless liquid (987 mg, 88% yield), R_f = 0.38 (petroleum ether/EtOAc 99:1). ^{1}H NMR (400 MHz, $CDCl_3$) δ 7.46 – 7.38 (m, 2H), 7.12 (d, *J* = 7.9 Hz, 2H), 5.64 (s, 1H), 3.81 (dqd, *J* = 78.5, 7.1, 4.9 Hz, 1H), 3.44 (ddd, *J* = 58.9, 11.6, 5.0 Hz, 1H), 3.13 (ddd, *J* = 40.1, 11.6, 7.1 Hz, 1H), 2.33 (s, 3H), 1.89 (pd, *J* = 7.3, 3.2 Hz, 1H), 1.79 (pd, *J* = 7.3, 1.6 Hz, 1H), 1.06 (q, *J* = 7.4 Hz, 3H). ^{13}C{^{1}H} NMR (100 MHz, $CDCl_3$) δ 139.0 (d, *J* = 15.0 Hz), 137.2 (d, *J* = 121.3 Hz), 129.3, 128.0 (d, *J* = 20.1 Hz), 59.3 (d, *J* = 19.5 Hz), 55.8 (d, *J* = 107.5 Hz), 44.6 (d, *J* = 56.0 Hz), 28.3 (d, *J* = 30.9 Hz), 21.3 (d, *J* = 2.1 Hz), 13.5 (d, *J* = 7.3 Hz). HRMS (ESI TOF) *m/z* for $C_{12}H_{17}S_2$ $[M + H]^+$ calcd. 225.0772, found 225.0767.

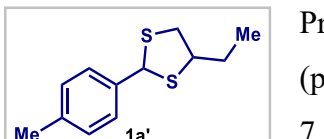

S-(2-thiocyanatoethyl) 4-methylbenzothioate (**3a**): The compound **3a** was prepared following the General Procedure D (GP D). Colourless liquid (39 mg, 82% yield), R_f = 0.43 (petroleum ether/EtOAc 85:15). ^{1}H NMR (400 MHz, $CDCl_3$) δ 7.86 – 7.83 (m, 2H), 7.26 (d, *J* = 7.9 Hz, 2H), 3.46 – 3.42 (m, 2H), 3.22 – 3.19 (m, 2H), 2.41 (s, 3H). ^{13}C{^{1}H} NMR

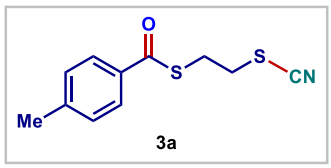

(100 MHz, $CDCl_3$) δ 190.2, 145.1, 133.8, 129.5, 127.5, 111.6, 33.6, 29.0, 21.8. HRMS (ESI TOF) *m/z* for $C_{11}H_{12}NOS_2$ $[M + H]^+$ calcd. 238.0360, found 238.0362.

S-(2-thiocyanatoethyl) benzothioate (**3b**): The compound **3b** was prepared following the General Procedure D (GP D). White solid (36 mg, 80% yield), R_f = 0.42 (petroleum ether/EtOAc 85:15). ^1H NMR (400 MHz, $CDCl_3$) δ 7.97 – 7.94 (m, 2H), 7.63 – 7.59 (m, 1H), 7.50 – 7.46 (m, 2H), 3.49 – 3.45 (m, 2H), 3.24 – 3.21 (m, 2H). $^{13}C\{^1H\}$ NMR (100 MHz, $CDCl_3$) δ 190.7, 136.4, 134.1, 129.0, 127.5, 111.6, 33.6, 29.1. HRMS (ESI TOF) *m/z* for $C_{10}H_{10}NOS_2$ $[M + H]^+$ calcd. 224.0204, found 224.0200.

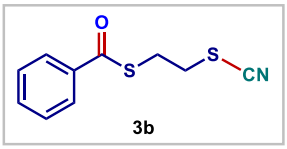

3b

S-(2-thiocyanatoethyl) 4-methoxybenzothioate (**3c**): The compound **3c** was prepared following the General Procedure D (GP D). White solid (47 mg, 92% yield), R_f = 0.27 (petroleum ether/EtOAc 85:15). ^1H NMR (400 MHz, $CDCl_3$) δ 7.94 – 7.90 (m, 2H), 6.95 – 6.91 (m, 2H), 3.87 (s, 3H), 3.43 (dd, *J* = 8.4, 6.4 Hz, 2H), 3.20 (dd, *J* = 8.3, 6.4 Hz, 2H). $^{13}C\{^1H\}$ NMR (100 MHz, $CDCl_3$) δ 189.0, 164.3, 129.7, 129.2, 114.1, 111.7, 55.7, 33.7, 28.9. HRMS (ESI TOF) *m/z* for $C_{11}H_{12}NO_2S_2$ $[M + H]^+$ calcd. 254.0309, found 254.0303.

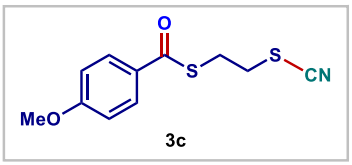

3c

S-(2-thiocyanatoethyl) 4-(diethylamino)benzothioate (**3d**): The compound **3d** was prepared following the General Procedure D (GP D). Brown solid (54 mg, 91% yield), R_f = 0.28 (petroleum ether/EtOAc 85:15). ^1H NMR (400 MHz, $CDCl_3$) δ 7.82 (d, *J* = 8.8 Hz, 2H), 6.61 (d, *J* = 8.8 Hz, 2H), 3.41 (p, *J* = 7.1 Hz, 6H), 3.20 (dd, *J* = 8.7, 6.1 Hz, 2H), 1.20 (t, *J* = 7.0 Hz, 6H). $^{13}C\{^1H\}$ NMR (100 MHz, $CDCl_3$) δ 187.6, 152.0, 130.0, 123.0, 111.9, 110.3, 44.7, 34.1, 28.7, 12.6. HRMS (ESI TOF) *m/z* for $C_{14}H_{19}N_2OS_2$ $[M + H]^+$ calcd. 295.0939, found 295.0934.

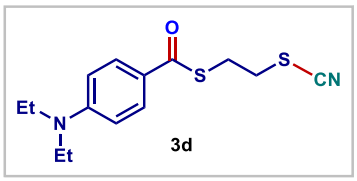

3d

S-(2-thiocyanatoethyl) 4-cyanobenzothioate (**3e**): The compound **3e** was prepared following the General Procedure D (GP D). White solid (39 mg, 79% yield), R_f = 0.25 (petroleum ether/EtOAc 80:20). ^1H NMR (400 MHz, $CDCl_3$) δ 8.06 – 8.03 (m, 2H), 7.79 – 7.77 (m, 2H), 3.51 (dd, *J* = 8.2, 6.5 Hz, 2H), 3.23 (dd, *J* = 8.3, 6.3 Hz, 2H). $^{13}C\{^1H\}$ NMR (100 MHz, $CDCl_3$) δ 189.6, 139.4, 132.8, 127.9, 117.7, 117.4, 111.3, 33.3, 29.4. HRMS (ESI TOF) *m/z* for $C_{11}H_9N_2OS_2$ [M

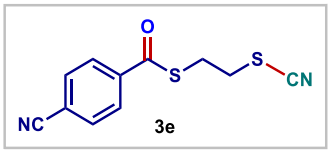

3e

+ H]$^+$ calcd. 249.0156, found 249.0151.

S-(2-thiocyanatoethyl) 4-nitrobenzothioate (**3f**): The compound **3f** was prepared following the General Procedure D (GP D). White solid (40 mg, 74% yield), R_f = 0.28 (petroleum ether/EtOAc 80:20). ^{1}H NMR (400 MHz, $CDCl_3$) δ 8.35 – 8.31 (m, 2H), 8.14 – 8.10 (m, 2H), 3.53 (dd, *J* = 8.2, 6.5 Hz, 2H), 3.25 (dd, *J* = 8.1, 6.5 Hz, 2H). ^{13}C{^{1}H} NMR (100 MHz, $CDCl_3$) δ 189.4, 151.0, 140.8, 128.6, 124.2, 111.3, 33.2, 29.6. HRMS (ESI TOF) *m/z* for $C_{10}H_9N_2O_3S_2$ [M + H]$^+$ calcd. 269.0055, found 269.0054.

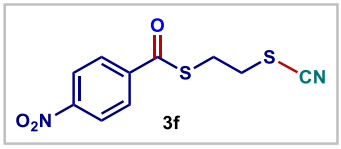

S-(2-thiocyanatoethyl) 4-fluorobenzothioate (**3g**): The compound **3g** was prepared following the General Procedure D (GP D). Colourless liquid (38 mg, 78% yield), R_f = 0.43 (petroleum ether/EtOAc 85:15). ^{1}H NMR (400 MHz, $CDCl_3$) δ 8.01 – 7.96 (m, 2H), 7.18 – 7.12 (m, 2H), 3.49 – 3.45 (m, 2H), 3.24 – 3.20 (m, 2H). ^{13}C{^{1}H} NMR (100 MHz, $CDCl_3$) δ 189.2, 166.4 (d, *J* = 256.3 Hz), 132.7 (d, *J* = 3.1 Hz), 130.1 (d, *J* = 9.5 Hz), 116.2 (d, *J* = 22.1 Hz), 111.5, 33.6, 29.2. ^{19}F{^{1}H} NMR (377 MHz, $CDCl_3$) δ -103.37. HRMS (ESI TOF) *m/z* for $C_{10}H_9FNOS_2$ [M + H]$^+$ calcd. 242.0110, found 242.0112.

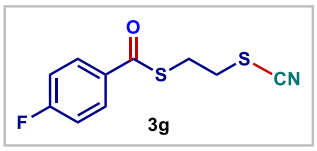

S-(2-thiocyanatoethyl) 4-chlorobenzothioate (**3h**): The compound **3h** was prepared following the General Procedure D (GP D). White solid (45 mg, 88% yield), R_f = 0.43 (petroleum ether/EtOAc 85:15). ^{1}H NMR (400 MHz, $CDCl_3$) δ 7.90 – 7.88 (m, 2H), 7.46 – 7.44 (m, 2H), 3.49 – 3.45 (m, 2H), 3.24 – 3.20 (m, 2H). ^{13}C{^{1}H} NMR (100 MHz, $CDCl_3$) δ 189.6, 140.6, 134.7, 129.3, 128.8, 111.5, 33.5, 29.2. HRMS (ESI TOF) *m/z* for $C_{10}H_9ClNOS_2$ [M + H]$^+$ calcd. 257.9814, found 257.9814.

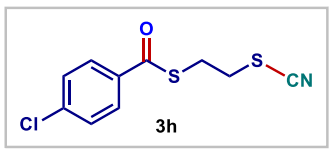

S-(2-thiocyanatoethyl) 4-bromobenzothioate (**3i**): The compound **3i** was prepared following the General Procedure D (GP D). White solid (53 mg, 83% yield), R_f = 0.43 (petroleum ether/EtOAc 85:15). ^{1}H NMR (400 MHz, $CDCl_3$) δ 7.83 – 7.80 (m, 2H), 7.64 – 7.60 (m, 2H), 3.49 – 3.45 (m, 2H), 3.23 – 3.20 (m, 2H). ^{13}C{^{1}H} NMR (100 MHz, $CDCl_3$) δ 189.8, 135.1, 132.3, 129.3, 128.9, 111.5, 33.5, 29.2. HRMS (ESI TOF) *m/z* for $C_{10}H_8BrNNaOS_2$ [M + Na]$^+$ calcd. 325.9108, found 325.9105.

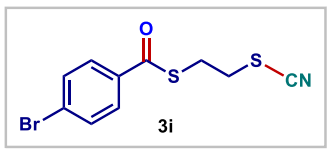

S-(2-thiocyanatoethyl) 4-(trifluoromethyl)benzothioate (**3j**): The compound **3j** was prepared following the General Procedure D (GP D). White solid (44 mg, 76% yield), R_f = 0.43 (petroleum ether/EtOAc 85:15). ^{1}H NMR (400 MHz, $CDCl_3$) δ 8.06 (d, *J* = 7.9 Hz, 2H), 7.75 (d, *J* = 7.8 Hz, 2H), 3.53 – 3.49 (m, 2H), 3.25 – 3.22 (m, 2H). ^{13}C{^{1}H} NMR (100 MHz, $CDCl_3$) δ 190.0, 139.1, 135.4 (q, *J* = 32.9 Hz), 127.9, 126.1 (q, *J* = 3.7 Hz), 123.5 (q, *J* = 272.9 Hz), 111.4, 33.4, 29.4. ^{19}F{^{1}H} NMR (377 MHz, $CDCl_3$) δ -63.21. HRMS (ESI TOF) *m/z* for $C_{11}H_9F_3NOS_2$ [M + H]$^+$ calcd. 292.0078, found 292.0076.

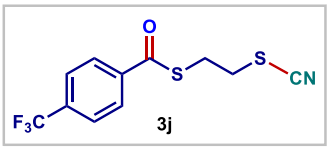

S-(2-thiocyanatoethyl) 2-methylbenzothioate (**3k**): The compound **3k** was prepared following the General Procedure D (GP D). Colourless liquid (40 mg, 84% yield), R_f = 0.48 (petroleum ether/EtOAc 85:15). ^{1}H NMR (400 MHz, $CDCl_3$) δ 7.80 (d, *J* = 7.9 Hz, 1H), 7.43 (td, *J* = 7.6, 1.2 Hz, 1H), 7.27 (t, *J* = 7.8 Hz, 2H), 3.43 (dd, *J* = 8.5, 6.4 Hz, 2H), 3.23 (dd, *J* = 8.3, 6.3 Hz, 2H), 2.50 (s, 3H). ^{13}C{^{1}H} NMR (100 MHz, $CDCl_3$) δ 192.6 (s), 137.5 (s), 136.4 (s), 132.5 (s), 132.0 (s), 128.9 (s), 126.1 (s), 111.6 (s), 33.6 (s), 29.6 (s), 20.9 (s). HRMS (ESI TOF) *m/z* for $C_{11}H_{12}NOS_2$ [M + H]$^+$ calcd. 238.0360, found 238.0361.

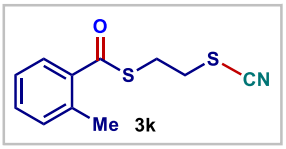

S-(2-thiocyanatoethyl) 2-bromobenzothioate (**3l**): The compound **3l** was prepared following the General Procedure D (GP D). White solid (50 mg, 83% yield), R_f = 0.37 (petroleum ether/EtOAc 85:15). ^{1}H NMR (400 MHz, $CDCl_3$) δ 7.67 – 7.62 (m, 2H), 7.43 – 7.33 (m, 2H), 3.47 (dd, *J* = 8.4, 6.4 Hz, 2H), 3.26 (dd, *J* = 8.3, 6.3 Hz, 2H). ^{13}C{^{1}H} NMR (100 MHz, $CDCl_3$) δ 191.7 (s), 138.6 (s), 134.4 (s), 133.0 (s), 129.4 (s), 127.6 (s), 119.2 (s), 111.5 (s), 33.3 (s), 30.2 (s). HRMS (ESI TOF) *m/z* for $C_{10}H_8BrNNaOS_2$ [M + Na]$^+$ calcd. 323.9128, found 323.9126.

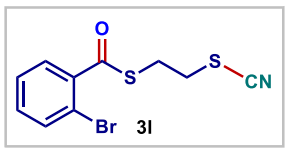

S-(2-thiocyanatoethyl) 3-bromobenzothioate (**3m**): The compound **3m** was prepared following the General Procedure D (GP D). Colourless liquid (48 mg, 80% yield), R_f = 0.43 (petroleum ether/EtOAc 85:15). ^{1}H NMR (400 MHz, $CDCl_3$) δ 8.07 (t, *J* = 1.8 Hz, 1H), 7.93 – 7.85 (m, 1H), 7.73 (ddd, *J* = 8.0, 1.9, 1.0 Hz, 1H), 7.36 (t, *J* = 7.9 Hz, 1H), 3.48 (dd, *J* = 8.3, 6.4 Hz, 2H), 3.22 (dd, *J* = 8.3, 6.4 Hz, 2H). ^{13}C{^{1}H} NMR (100 MHz, $CDCl_3$) δ 189.5 (s), 138.0 (s), 137.0 (s), 130.5 (s), 130.4 (s), 126.1 (s), 123.2 (s), 111.5 (s), 33.5 (s), 29.3 (s). HRMS (ESI TOF) *m/z* for $C_{10}H_9BrNOS_2$ [M + H]$^+$ calcd. 301.9309, found 301.9304.

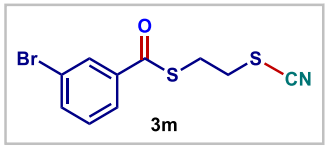

S-(2-thiocyanatoethyl) 4-(allyloxy)benzothioate (**3n**): The compound **3n** was prepared following the General Procedure D (GP D). White solid (47 mg, 84% yield), R_f = 0.38 (petroleum ether/EtOAc 85:15). ^{1}H NMR (400 MHz, $CDCl_3$) δ 7.91 (d, *J* = 8.9 Hz, 2H), 6.95 (d, *J* = 8.9 Hz, 2H), 6.04 (ddt, *J* = 17.2, 10.5, 5.3 Hz, 1H), 5.42 (dq, *J* = 17.3, 1.5 Hz, 1H), 5.33 (dt, *J* = 10.5, 1.3 Hz, 1H), 4.60 (dt, *J* = 5.3, 1.5 Hz, 2H), 3.43 (dd, *J* = 8.4, 6.4 Hz, 2H), 3.20 (dd, *J* = 8.3, 6.4 Hz, 2H). ^{13}C{^{1}H} NMR (100 MHz, $CDCl_3$) δ 189.0, 163.3, 132.4, 129.7, 129.3, 118.5, 114.8, 111.7, 69.1, 33.7, 29.0. HRMS (ESI TOF) *m/z* for $C_{13}H_{13}NNaO_2S_2$ [M + Na]$^+$ calcd. 302.0285, found 302.0284.

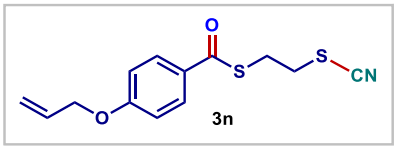

S-(2-thiocyanatoethyl) 4-(prop-2-yn-1-yloxy)benzothioate (**3o**): The compound **3o** was prepared following the General Procedure D (GP D). White solid (49 mg, 88% yield), R_f = 0.28 (petroleum ether/EtOAc 85:15). ^{1}H NMR (400 MHz, $CDCl_3$) δ 7.97 – 7.90 (m, 2H), 7.05 – 6.99 (m, 2H), 4.76 (d, *J* = 2.4 Hz, 2H), 3.44 (dd, *J* = 8.4, 6.4 Hz, 2H), 3.21 (dd, *J* = 8.3, 6.4 Hz, 2H), 2.56 (t, *J* = 2.4 Hz, 1H). ^{13}C{^{1}H} NMR (100 MHz, $CDCl_3$) δ 189.1, 162.1, 129.9, 129.7, 115.0, 111.7, 77.6, 76.5, 56.1, 33.7, 29.0. HRMS (ESI TOF) *m/z* for $C_{13}H_{11}NNaO_2S_2$ [M + Na]$^+$ calcd. 300.0129, found 300.0135.

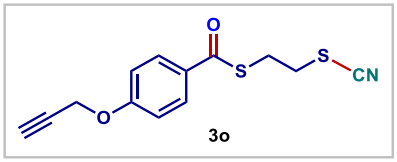

S-(2-thiocyanatoethyl) 4-(tosyloxy)benzothioate (**3p**): The compound **3p** was prepared following the General Procedure D (GP D). Light orange solid (61 mg, 77% yield), R_f = 0.22 (petroleum ether/EtOAc 80:20). ^{1}H NMR (400 MHz, $CDCl_3$) δ 7.94 – 7.87 (m, 2H), 7.71 (d, *J* = 8.4 Hz, 2H), 7.33 (d, *J* = 8.1 Hz, 2H), 7.15 – 7.07 (m, 2H), 3.46 (dd, *J* = 8.3, 6.4 Hz, 2H), 3.20 (dd, *J* = 8.2, 6.4 Hz, 2H), 2.46 (s, 3H). ^{13}C{^{1}H} NMR (100 MHz, $CDCl_3$) δ 189.4, 153.7, 146.0, 134.9, 132.1, 130.1, 129.2, 128.6, 122.9, 111.5, 33.5, 29.3, 21.9. HRMS (ESI TOF) *m/z* for $C_{17}H_{16}NO_4S_3$ [M + H]$^+$ calcd. 394.0241, found 394.0249.

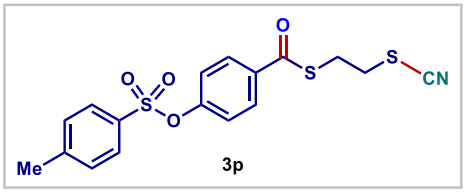

S-(2-thiocyanatoethyl) 2,6-dimethylbenzothioate (**3q**): The compound **3q** was prepared following the General Procedure D (GP D). Colourless liquid (41 mg, 81% yield), R_f = 0.47 (petroleum ether/EtOAc 85:15). ^{1}H NMR (400 MHz, $CDCl_3$) δ 7.21 (t, *J* = 7.6 Hz, 1H), 7.04 (d, *J* = 7.6 Hz, 2H), 3.47 (dd, *J* = 8.7, 6.3 Hz, 2H), 3.27 (dd, *J* = 8.4, 6.3 Hz, 2H), 2.31 (s, 6H). ^{13}C{^{1}H} NMR

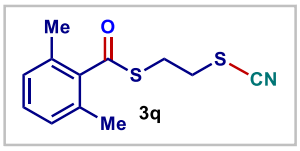

(100 MHz, $CDCl_3$) δ 196.7 (s), 139.5 (s), 133.8 (s), 130.0 (s), 127.9 (s), 111.4 (s), 33.5 (s), 29.6 (s), 19.2 (s). HRMS (ESI TOF) *m/z* for $C_{12}H_{13}NNaOS_2$ $[M + Na]^+$ calcd. 274.0336, found 274.0331.

S-(2-thiocyanatoethyl) 3,4-dimethoxybenzothioate (**3r**): The compound **3r** was prepared following the General Procedure D (GP D). White solid (52 mg, 92% yield), R_f = 0.26 (petroleum ether/EtOAc 90:10). ^1H NMR (400 MHz, $CDCl_3$) δ 7.62 (dd, *J* = 8.4, 2.1 Hz, 1H), 7.42 (d, *J* = 2.1 Hz, 1H), 6.88 (d, *J* = 8.5 Hz, 1H), 3.93 (s, 3H), 3.91 (s, 3H), 3.44 – 3.41 (m, 2H), 3.21 – 3.18 (m, 2H). $^{13}C\{^1H\}$ NMR (100 MHz, $CDCl_3$) δ 189.1, 154.0, 149.1, 129.2, 122.1, 111.6, 110.4, 109.5, 56.2, 56.1, 33.7, 29.0. HRMS (ESI TOF) *m/z* for $C_{12}H_{13}NNaO_3S_2$ $[M + Na]^+$ calcd. 306.0235, found 306.0236.

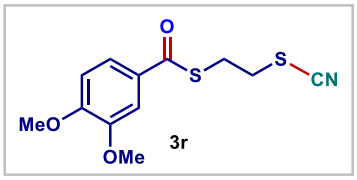

S-(2-thiocyanatoethyl) 2-bromo-4-chlorobenzothioate (**3s**): The compound **3s** was prepared following the General Procedure D (GP D). Colourless liquid (53 mg, 79% yield), R_f = 0.45 (petroleum ether/EtOAc 85:15). ^1H NMR (400 MHz, $CDCl_3$) δ 7.60 – 7.58 (m, 2H), 7.34 (dd, *J* = 8.6, 2.5 Hz, 1H), 3.49 (dd, *J* = 8.5, 6.2 Hz, 2H), 3.26 (dd, *J* = 8.5, 6.2 Hz, 2H). $^{13}C\{^1H\}$ NMR (100 MHz, $CDCl_3$) δ 190.7 (s), 139.9 (s), 135.5 (s), 133.9 (s), 132.9 (s), 129.2 (s), 117.1 (s), 111.3 (s), 33.2 (s), 30.2 (s). HRMS (ESI TOF) *m/z* for $C_{10}H_8BrClNOS_2$ $[M + H]^+$ calcd. 335.8918, found 335.8913.

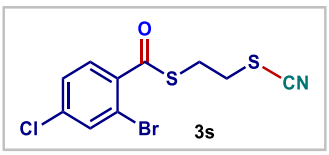

S-(2-thiocyanatoethyl) 2-bromo-4-fluoro-5-methoxybenzothioate (**3t**): The compound **3t** was prepared following the General Procedure D (GP D). Colourless liquid (58 mg, 83% yield), R_f = 0.30 (petroleum ether/EtOAc 80:20). ^1H NMR (400 MHz, $CDCl_3$) δ 7.37 (d, *J* = 10.3 Hz, 1H), 7.27 (d, *J* = 8.4 Hz, 1H), 3.93 (s, 3H), 3.48 (dd, *J* = 8.2, 6.4 Hz, 2H), 3.26 (dd, *J* = 8.1, 6.3 Hz, 2H). $^{13}C\{^1H\}$ NMR (100 MHz, $CDCl_3$) δ 190.5 (s), 153.9 (d, *J* = 258.1 Hz), 147.3 (d, *J* = 10.8 Hz), 134.5 (d, *J* = 4.2 Hz), 122.2 (d, *J* = 21.7 Hz), 114.3 (d, *J* = 3.2 Hz), 111.6 (s), 109.6 (d, *J* = 8.5 Hz), 56.8 (s), 33.3 (s), 30.4 (s). $^{19}F\{^1H\}$ NMR (377 MHz, $CDCl_3$) δ -126.23 (s). HRMS (ESI TOF) *m/z* for $C_{11}H_9BrFNNaO_2S_2$ $[M + Na]^+$ calcd. 371.9140, found 371.9139.

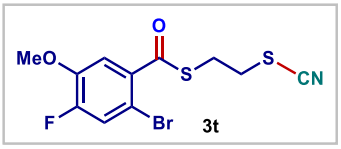

S-(2-thiocyanatoethyl) thiophene-2-carbothioate (**3u**): The compound **3u** was prepared following the General Procedure D (GP D). Colourless liquid (36 mg, 78% yield), R_f = 0.37 (petroleum ether/EtOAc 85:15). ^{1}H NMR (400 MHz, $CDCl_3$) δ 7.82 (dd, *J* = 3.9, 1.2 Hz, 1H), 7.67 (dd, *J* = 4.9, 1.2 Hz, 1H), 7.14 (dd, *J* = 5.0, 3.9 Hz, 1H), 3.45 (dd, *J* = 8.5, 6.2 Hz, 2H), 3.22 (dd, *J* = 8.5, 6.2 Hz, 2H). ^{13}C{^{1}H} NMR (100 MHz, $CDCl_3$) δ 182.6, 141.2, 133.8, 132.0, 128.3, 111.5, 33.7, 29.7. HRMS (ESI TOF) *m/z* for $C_8H_8NOS_3$ $[M + H]^+$ calcd. 229.9768, found 229.9761.

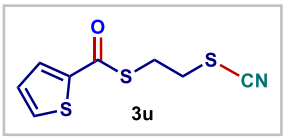

S-(2-thiocyanatoethyl) 5-methylthiophene-2-carbothioate (**3v**): The compound **3v** was prepared following the General Procedure D (GP D). White solid (41 mg, 85% yield), R_f = 0.40 (petroleum ether/EtOAc 85:15). ^{1}H NMR (400 MHz, $CDCl_3$) δ 7.63 (d, *J* = 3.8 Hz, 1H), 6.80 (dd, *J* = 3.8, 1.1 Hz, 1H), 3.42 (dd, *J* = 8.4, 6.3 Hz, 2H), 3.21 (dd, *J* = 8.3, 6.3 Hz, 2H), 2.54 (s, 3H). ^{13}C{^{1}H} NMR (100 MHz, $CDCl_3$) δ 182.0, 150.1, 138.6, 132.6, 127.0, 111.6, 33.8, 29.1, 16.1. HRMS (ESI TOF) *m/z* for $C_9H_9NNaOS_3$ $[M + Na]^+$ calcd. 265.9744, found 265.9742.

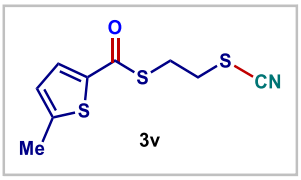

S-(2-thiocyanatoethyl) benzofuran-2-carbothioate (**3w**): The compound **3w** was prepared following the General Procedure D (GP D). Pale yellow solid (46 mg, 88% yield), R_f = 0.42 (petroleum ether/EtOAc 85:15). ^{1}H NMR (400 MHz, $CDCl_3$) δ 7.73 – 7.71 (m, 1H), 7.61 – 7.57 (m, 2H), 7.51 (ddd, *J* = 8.4, 7.2, 1.3 Hz, 1H), 7.34 (ddd, *J* = 8.0, 7.1, 1.0 Hz, 1H), 3.53 – 3.49 (m, 2H), 3.26 – 3.23 (m, 2H). ^{13}C{^{1}H} NMR (100 MHz, $CDCl_3$) δ 181.0, 155.8, 150.5, 128.8, 126.9, 124.4, 123.5, 112.6, 112.3, 111.4, 33.6, 28.6. HRMS (ESI TOF) *m/z* for $C_{12}H_9NNaO_2S_2$ $[M + H]^+$ calcd. 285.9972, found 285.9977.

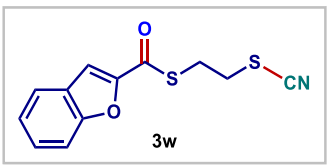

S-(2-thiocyanatoethyl) naphthalene-2-carbothioate (**3x**): The compound **3x** was prepared following the General Procedure D (GP D). White solid (42 mg, 76% yield), R_f = 0.43 (petroleum ether/EtOAc 85:15). ^{1}H NMR (400 MHz, $CDCl_3$) δ 8.52 (d, *J* = 1.1 Hz, 1H), 7.98 (ddd, *J* = 8.5, 6.4, 1.6 Hz, 2H), 7.92 – 7.88 (m, 2H), 7.61 (dddd, *J* = 20.1, 8.2, 6.9, 1.4 Hz, 2H), 3.54 – 3.51 (m, 2H), 3.29 – 3.25 (m, 2H). ^{13}C{^{1}H} NMR (100 MHz, $CDCl_3$) δ 190.7, 136.2, 133.7, 132.5, 129.8, 129.2, 129.0, 128.9, 128.0, 127.3, 123.1, 111.6, 33.7, 29.2. HRMS (ESI TOF) *m/z* for $C_{14}H_{12}NOS_2$ $[M + H]^+$ calcd. 274.0360, found 274.0354.

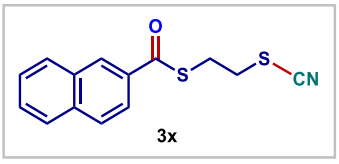

S-(2-thiocyanatoethyl) pyrene-2-carbothioate (**3y**): The compound **3y** was prepared following the General Procedure D (GP D). Brown solid (39 mg, 56% yield), R_f = 0.32 (petroleum ether/EtOAc 85:15). ^{1}H NMR (400 MHz, $CDCl_3$) δ 8.88 (d, *J* = 9.4 Hz, 1H), 8.51 (d, *J* = 8.1 Hz, 1H), 8.25 (dd, *J* = 7.6, 1.5 Hz, 2H), 8.22 (d, *J* = 9.4 Hz, 1H), 8.16 (t, *J* = 8.0 Hz, 2H), 8.08 – 8.04 (m, 2H), 3.61 – 3.58 (m, 2H), 3.37 – 3.34 (m, 2H). ^{13}C{^{1}H} NMR (100 MHz, $CDCl_3$) δ 192.7, 134.7, 131.1, 130.6, 130.4, 130.20, 130.1, 128.8, 127.1, 126.9, 126.8, 126.7, 126.5, 124.9, 124.3, 124.2, 124.1, 111.7, 33.7, 30.2. HRMS (ESI TOF) *m/z* for $C_{20}H_{13}NNaOS_2$ $[M + Na]^+$ calcd. 370.0336, found 370.0336.

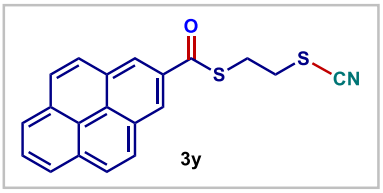

S-(3-thiocyanatopropyl) benzothioate (**3z**): The compound **3z** was prepared following the General Procedure D (GP D). Colourless liquid (30 mg, 63% yield), R_f = 0.42 (petroleum ether/EtOAc 85:15). ^{1}H NMR (400 MHz, $CDCl_3$) δ 7.96 (dd, *J* = 8.4, 1.3 Hz, 2H), 7.62 – 7.57 (m, 1H), 7.49 – 7.44 (m, 2H), 3.23 (t, *J* = 6.8 Hz, 2H), 3.06 (t, *J* = 7.1 Hz, 2H), 2.23 (p, *J* = 6.9 Hz, 2H). ^{13}C{^{1}H} NMR (100 MHz, $CDCl_3$) δ 191.4, 136.7, 133.8, 128.9, 127.4, 112.0, 32.7, 30.1, 26.8. HRMS (ESI TOF) *m/z* for $C_{11}H_{12}NOS_2$ $[M + H]^+$ calcd. 238.0360, found 238.0365.

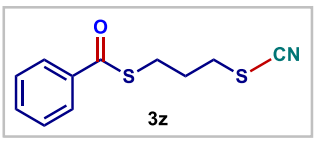

S-(4-thiocyanatobutyl) 4-methylbenzothioate (**3aa**): The compound **3aa** was prepared following the General Procedure D (GP D). Colourless liquid (30 mg, 57% yield), R_f = 0.42 (petroleum ether/EtOAc 90:10). ^{1}H NMR (400 MHz, $CDCl_3$) δ 7.86 (d, *J* = 8.3 Hz, 2H), 7.25 (d, *J* = 8.4 Hz, 2H), 3.09 (t, *J* = 7.1 Hz, 2H), 3.00 (t, *J* = 7.1 Hz, 2H), 2.41 (s, 3H), 2.03 – 1.92 (m, 2H), 1.90 – 1.79 (m, 2H). ^{13}C{^{1}H} NMR (100 MHz, $CDCl_3$) δ 191.4, 144.5, 134.5, 129.4, 127.4, 112.2, 33.6, 29.0, 28.2, 27.9, 21.8. HRMS (ESI TOF) *m/z* for $C_{13}H_{15}NNaOS_2$ $[M + Na]^+$ calcd. 288.0493, found 288.0489.

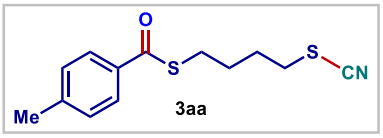

S-(5-thiocyanatopentyl) benzothioate (**3ab**): The compound **3aa** was prepared following the General Procedure D (GP D). Colourless liquid (28 mg, 52% yield), R_f = 0.40 (petroleum ether/EtOAc 85:15). ^{1}H NMR (400 MHz, $CDCl_3$) δ 7.98 – 7.95 (m, 2H), 7.60 – 7.55 (m, 1H), 7.47 – 7.43 (m, 2H), 3.09 (t, *J* = 7.2 Hz, 2H), 2.96 (t, *J* = 7.2 Hz, 2H), 1.89 (dt, *J* = 14.8, 7.4 Hz, 2H), 1.74 (dt, *J* = 14.5, 7.2 Hz, 2H), 1.63 – 1.56 (m, 2H). ^{13}C{^{1}H} NMR (100 MHz, $CDCl_3$) δ 192.0 (s), 137.2 (s), 133.5 (s), 128.8 (s), 127.3 (s), 112.3 (s), 33.9 (s), 29.5 (s), 29.1 (s), 28.6

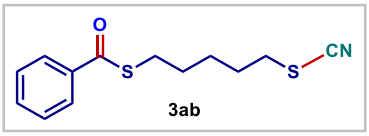

(s), 27.2 (s). HRMS (ESI TOF) *m/z* for $C_{13}H_{15}NNaOS_2$ $[M + Na]^+$ calcd. 288.0493, found 288.0493.

S-(2-thiocyanatobutyl) 4-methylbenzothioate (**3a'**): The compound **3a'** was prepared following

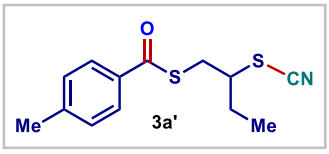

the General Procedure D (GP D). Colourless liquid (17 mg, 32% yield), R_f = 0.30 (petroleum ether/EtOAc 95:5). ^{1}H NMR (400 MHz, $CDCl_3$) δ 7.86 (d, *J* = 8.3 Hz, 2H), 7.27 (d, *J* = 7.0 Hz, 2H), 3.57 – 3.37 (m, 2H), 3.22 (dtd, *J* = 9.0, 6.8, 4.7 Hz, 1H), 2.42 (s, 3H), 2.07 (dqd, *J* = 14.7, 7.4, 4.7 Hz, 1H), 1.81 (ddq, *J* = 14.6, 9.1, 7.3 Hz, 1H), 1.13 (t, *J* = 7.3 Hz, 3H). $^{13}C\{^1H\}$ NMR (100 MHz, $CDCl_3$) δ 190.3, 145.1, 133.9, 129.6, 127.6, 110.6, 52.9, 34.4, 27.6, 21.9, 11.7. HRMS (ESI TOF) *m/z* for $C_{13}H_{15}NNaOS_2$ $[M + Na]^+$ calcd. 288.0493, found 288.0490.

S-(1-thiocyanatobutan-2-yl) 4-methylbenzothioate (**3a''**): The compound **3a''** was prepared

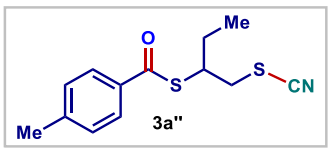

following the General Procedure D (GP D). White solid (27 mg, 51% yield), R_f = 0.24 (petroleum ether/EtOAc 95:5). ^{1}H NMR (400 MHz, $CDCl_3$) δ 7.85 (d, *J* = 8.3 Hz, 2H), 7.26 (d, *J* = 8.0 Hz, 2H), 3.93 (ddt, *J* = 8.7, 7.3, 5.1 Hz, 1H), 3.44 (dd, *J* = 13.3, 5.3 Hz, 1H), 3.29 (dd, *J* = 13.3, 7.3 Hz, 1H), 2.42 (s, 3H), 2.03 (dqd, *J* = 14.6, 7.4, 4.8 Hz, 1H), 1.84 (ddt, *J* = 14.2, 8.5, 7.2 Hz, 1H), 1.09 (t, *J* = 7.4 Hz, 3H). $^{13}C\{^1H\}$ NMR (100 MHz, $CDCl_3$) δ 190.3, 145.0, 134.1, 129.6, 127.6, 112.4, 45.8, 39.5, 25.4, 21.9, 11.5. HRMS (ESI TOF) *m/z* for $C_{13}H_{15}NNaOS_2$ $[M + Na]^+$ calcd. 288.0493, found 288.0492.

1,2-diphenyldisulfane (**4a**): The compound **4a** was prepared following the General Procedure

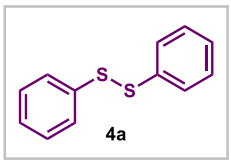

D (GP D). White solid (23 mg, 98% yield), R_f = 0.52 (petroleum ether/EtOAc 99:1). ^{1}H NMR (400 MHz, $CDCl_3$) δ 7.51 (dd, *J* = 8.0, 2.2 Hz, 4H), 7.31 (td, *J* = 8.0, 7.6, 1.7 Hz, 4H), 7.23 (td, *J* = 7.1, 1.3 Hz, 2H). $^{13}C\{^1H\}$ NMR (100 MHz, $CDCl_3$) δ 137.2, 129.2, 127.7, 127.3. HRMS (ESI TOF) *m/z* for $C_{12}H_{11}S_2$ $[M + H]^+$ calcd. 219.0302, found 219.0300.

1,2-di-p-tolyldisulfane (**4b**): The compound **4b** was prepared following the General Procedure

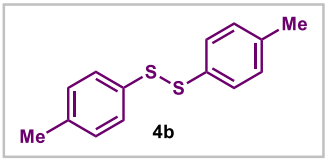

D (GP D). White solid (26 mg, 96% yield), R_f = 0.48 (petroleum ether/EtOAc 99:1). ^{1}H NMR (400 MHz, $CDCl_3$) δ 7.39 (d, *J* = 8.2 Hz, 4H), 7.11 (d, *J* = 8.0 Hz, 4H), 2.32 (s, 6H). $^{13}C\{^1H\}$ NMR (100 MHz, $CDCl_3$) δ 137.6, 134.0, 129.9, 128.7, 21.2. HRMS (ESI TOF) *m/z* for $C_{14}H_{15}S_2$ [M +

H]$^+$ calcd. 247.0615, found 247.0611.

1,2-bis(4-methoxyphenyl)disulfane (**4c**): The compound **4c** was prepared following the General Procedure D (GP D). Yellow liquid (28 mg, 90% yield), R_f = 0.35 (petroleum ether/EtOAc 95:5). ^{1}H NMR (400 MHz, $CDCl_3$) δ 7.44 – 7.36 (m, 4H), 6.87 – 6.80 (m, 4H), 3.80 (s, 6H). $^{13}C\{^1H\}$ NMR (100 MHz, $CDCl_3$) δ 160.1, 132.8, 128.6, 114.8, 55.5. HRMS (ESI TOF) *m/z* for $C_{14}H_{15}O_2S_2$ [M + H]$^+$ calcd. 279.0513, found 279.0508.

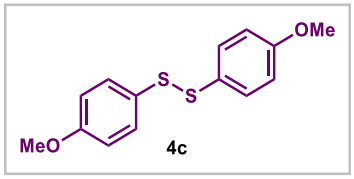

4c

1,2-bis(4-fluorophenyl)disulfane (**4d**): The compound **4d** was prepared following the General Procedure D (GP D). Colourless liquid (25 mg, 91% yield), R_f = 0.55 (petroleum ether/EtOAc 99:1). ^{1}H NMR (400 MHz, $CDCl_3$) δ 7.47 – 7.42 (m, 4H), 7.04 – 6.98 (m, 4H). $^{13}C\{^1H\}$ NMR (100 MHz, $CDCl_3$) δ 162.8 (d, *J* = 248.2 Hz), 132.3 (d, *J* = 3.3 Hz), 131.4 (d, *J* = 8.2 Hz), 116.4 (d, *J* = 22.3 Hz). $^{19}F\{^1H\}$ NMR (377 MHz, $CDCl_3$) δ -113.48. HRMS (ESI TOF) *m/z* for $C_{12}H_9F_2S_2$ [M + H]$^+$ calcd. 255.0114, found 255.0113.

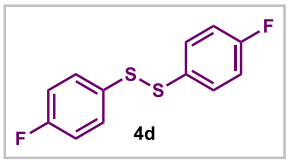

4d

1,2-bis(4-chlorophenyl)disulfane (**4e**): The compound **4e** was prepared following the General Procedure D (GP D). White solid (30 mg, 95% yield), R_f = 0.60 (petroleum ether/EtOAc 99:1). ^{1}H NMR (400 MHz, $CDCl_3$) δ 7.42 – 7.38 (m, 4H), 7.29 – 7.26 (m, 4H). $^{13}C\{^1H\}$ NMR (100 MHz, $CDCl_3$) δ 137.1, 129.2, 127.7, 127.3. HRMS (ESI TOF) *m/z* for $C_{12}H_9Cl_2S_2$ [M + H]$^+$ calcd. 286.9523, found 286.9520.

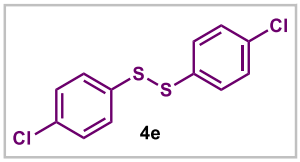

4e

1,2-bis(4-bromophenyl)disulfane (**4f**): The compound **4f** was prepared following the General Procedure D (GP D). White solid (38 mg, 92% yield), R_f = 0.57 (petroleum ether/EtOAc 99:1). ^{1}H NMR (400 MHz, $CDCl_3$) δ 7.45 – 7.41 (m, 4H), 7.35 – 7.32 (m, 4H). $^{13}C\{^1H\}$ NMR (100 MHz, $CDCl_3$) δ 135.9, 132.4, 129.5, 121.7. HRMS (ESI TOF) *m/z* for $C_{12}H_9Br_2S_2$ [M + H]$^+$ calcd. 374.8512, found 374.8508.

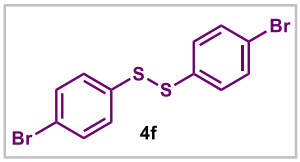

4f

1,2-bis(4-nitrophenyl)disulfane (**4g**): The compound **4g** was prepared following the General Procedure D (GP D). Yellow solid (12 mg, 36% yield), R_f = 0.48 (petroleum ether/EtOAc 85:15). ^{1}H NMR (400 MHz, DMSO-d_6) δ 8.19 – 8.16 (m, 4H), 7.76 – 7.72 (m, 4H). ^{13}C{^{1}H} NMR (100 MHz, DMSO-d_6) δ 146.6, 143.6, 126.8, 124.6. HRMS (ESI TOF) *m/z* for $C_{12}H_9N_2O_4S_2$ [M + H]$^+$ calcd. 309.0004, found 309.0002.

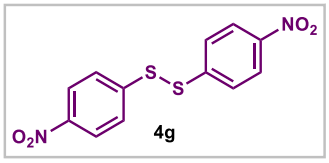

1,2-di(pyridin-2-yl)disulfane (**4h**): The compound **4h** was prepared following the General Procedure D (GP D). White solid (19 mg, 80% yield), R_f = 0.21 (petroleum ether/EtOAc 85:15). ^{1}H NMR (400 MHz, $CDCl_3$) δ 8.46 (dt, *J* = 4.7, 1.3 Hz, 2H), 7.64 – 7.58 (m, 4H), 7.10 (ddd, *J* = 6.7, 4.8, 2.1 Hz, 2H). ^{13}C{^{1}H} NMR (100 MHz, $CDCl_3$) δ 159.1, 149.7, 137.5, 121.2, 119.8. HRMS (ESI TOF) *m/z* for $C_{10}H_9N_2S_2$ [M + H]$^+$ calcd. 221.0207, found 221.0201.

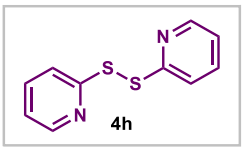

1,2-di(pyridin-4-yl)disulfane (**4i**): The compound **4i** was prepared following the General Procedure D (GP D). Off white solid (23 mg, 94% yield), R_f = 0.59 (petroleum ether/EtOAc 100:0). ^{1}H NMR (400 MHz, $CDCl_3$) δ 7.45 – 7.41 (m, 4H), 7.35 – 7.32 (m, 4H). ^{13}C{^{1}H} NMR (100 MHz, $CDCl_3$) δ 135.9, 132.4, 129.6, 121.7. HRMS (ESI TOF) *m/z* for $C_{10}H_9N_2S_2$ [M + H]$^+$ calcd. 221.0207, found 221.0203.

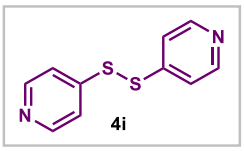

dimethyl 2,2'-disulfanediyldibenzoate (**4j**): The compound **4j** was prepared following the General Procedure C (GP C). White solid (185 mg, 62% yield), R_f = 0.45 (petroleum ether/EtOAc 85:15). ^{1}H NMR (400 MHz, $CDCl_3$) δ 8.06 (dd, *J* = 7.8, 1.6 Hz, 2H), 7.75 (dd, *J* = 8.2, 1.2 Hz, 2H), 7.41 (ddd, *J* = 8.3, 7.3, 1.5 Hz, 2H), 7.23 (td, *J* = 7.5, 1.1 Hz, 2H), 3.99 (s, 6H). ^{13}C{^{1}H} NMR (100 MHz, $CDCl_3$) δ 167.1, 140.5, 133.2, 131.6, 127.4, 126.0, 125.6, 52.5. HRMS (ESI TOF) *m/z* for $C_{16}H_{15}O_4S_2$ [M + H]$^+$ calcd. 335.0412, found 335.0410.

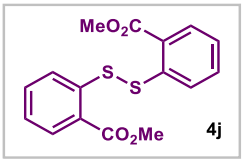

Thiocyanatobenzene (**2a**): The compound **2a** was prepared following the General Procedure E (GP E). Yellow liquid (47 mg, 87% yield), R_f = 0.37 (petroleum ether/EtOAc 95:5). ^{1}H NMR (400 MHz, $CDCl_3$) δ 7.56 – 7.51 (m, 2H), 7.46 – 7.41 (m, 3H). ^{13}C{^{1}H} NMR (100 MHz, $CDCl_3$) δ 130.4, 130.2, 129.7, 124.6, 110.7. HRMS (ESI TOF) *m/z* for C_7H_6NS [M + H]$^+$ calcd. 136.0221, found 136.0218.

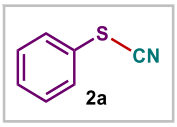

1-methyl-4-thiocyanatobenzene (**2b**): The compound **2b** was prepared following the General Procedure E (GP E). Yellow liquid (55 mg, 83% yield), R_f = 0.37 (petroleum ether/EtOAc 95:5). ^{1}H NMR (400 MHz, $CDCl_3$) δ 7.45 – 7.41 (m, 2H), 7.24 (d, *J* = 7.6 Hz, 2H), 2.38 (s, 3H). $^{13}C\{^1H\}$ NMR (100 MHz, $CDCl_3$) δ 140.4, 131.1, 130.9, 120.7, 111.2, 21.3. HRMS (ESI TOF) *m/z* for C_8H_8NS $[M + H]^+$ calcd. 150.0377, found 150.0374.

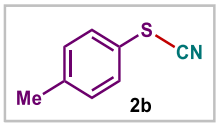

1-methoxy-4-thiocyanatobenzene (**2c**): The compound **2c** was prepared following the General Procedure E (GP E). White solid (61 mg, 92% yield), R_f = 0.18 (petroleum ether/EtOAc 85:15). ^{1}H NMR (400 MHz, $CDCl_3$) δ 7.52 – 7.48 (m, 2H), 6.96 – 6.92 (m, 2H), 3.83 (s, 3H). $^{13}C\{^1H\}$ NMR (100 MHz, $CDCl_3$) δ 161.4, 133.9, 116.0, 113.9, 111.7, 55.7. HRMS (ESI TOF) *m/z* for C_8H_8NOS $[M + H]^+$ calcd. 166.0327, found 166.0325.

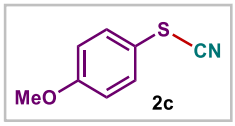

1-fluoro-4-thiocyanatobenzene (**2d**): The compound **2d** was prepared following the General Procedure E (GP E). Colourless liquid (53 mg, 87% yield), R_f = 0.37 (petroleum ether/EtOAc 95:5). ^{1}H NMR (400 MHz, $CDCl_3$) δ 7.59 – 7.53 (m, 2H), 7.18 – 7.12 (m, 2H). $^{13}C\{^1H\}$ NMR (100 MHz, $CDCl_3$) δ 163.8 (d, *J* = 252.0 Hz), 133.4 (d, *J* = 8.8 Hz), 119.4 (d, *J* = 3.6 Hz), 117.8 (d, *J* = 22.8 Hz), 110.7. $^{19}F\{^1H\}$ NMR (377 MHz, $CDCl_3$) δ -109.60. HRMS (ESI TOF) *m/z* for C_7H_4FNNaS $[M + Na]^+$ calcd. 175.9946, found 175.9939.

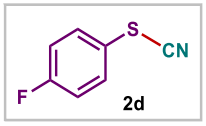

1-chloro-4-thiocyanatobenzene (**2e**): The compound **2e** was prepared following the General Procedure E (GP E). White solid (62 mg, 92% yield), R_f = 0.37 (petroleum ether/EtOAc 95:5). ^{1}H NMR (400 MHz, $CDCl_3$) δ 7.49 – 7.46 (m, 2H), 7.44 – 7.40 (m, 2H). $^{13}C\{^1H\}$ NMR (100 MHz, $CDCl_3$) δ 136.3, 131.6, 130.6, 122.9, 110.1. HRMS (ESI TOF) *m/z* for C_7H_5ClNS $[M + H]^+$ calcd. 169.9831, found 169.9827.

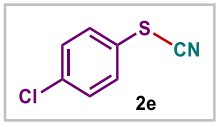

1-bromo-4-thiocyanatobenzene (**2f**): The compound **2f** was prepared following the General Procedure E (GP E). Pink solid (77 mg, 90% yield), R_f = 0.47 (petroleum ether/EtOAc 85:15). ^{1}H NMR (400 MHz, $CDCl_3$) δ 7.59 – 7.56 (m, 2H), 7.42 – 7.38 (m, 2H). $^{13}C\{^1H\}$ NMR (100 MHz, $CDCl_3$) δ 133.5, 131.6, 124.3, 123.6, 109.9. HRMS (ESI TOF) *m/z* for C_7H_5BrNS $[M + H]^+$ calcd. 213.9326, found 213.9322.

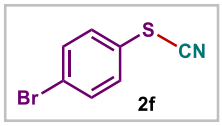

1-nitro-4-thiocyanatobenzene (**2g**): The compound **2g** was prepared following the General Procedure E (GP E). White solid (60 mg, 83% yield), R_f = 0.37 (petroleum ether/EtOAc 85:15). ^{1}H NMR (400 MHz, $CDCl_3$) δ 8.32 – 8.29 (m, 2H), 7.69 – 7.65 (m, 2H). $^{13}C\{^1H\}$ NMR (100 MHz, $CDCl_3$) δ 148.1, 133.5, 128.8, 125.2, 108.2. HRMS (ESI TOF) *m/z* for $C_7H_5N_2O_2S$ $[M + H]^+$ calcd. 181.0072, found 181.0070.

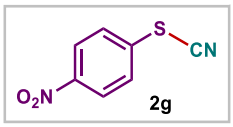

2-thiocyanatopyridine (**2h**): The compound **2h** was prepared following the General Procedure E (GP E). Brown liquid (47 mg, 86% yield), R_f = 0.43 (petroleum ether/EtOAc 85:15). ^{1}H NMR (400 MHz, $CDCl_3$) δ 8.52 (ddd, *J* = 4.8, 1.9, 0.9 Hz, 1H), 7.77 (td, *J* = 7.8, 1.9 Hz, 1H), 7.61 (dt, *J* = 8.2, 1.0 Hz, 1H), 7.29 – 7.26 (m, 1H). $^{13}C\{^1H\}$ NMR (100 MHz, $CDCl_3$) δ 150.7, 150.2, 138.6, 122.9, 122.1, 109.2. HRMS (ESI TOF) *m/z* for $C_6H_5N_2S$ $[M + H]^+$ calcd. 137.0173, found 137.0165.

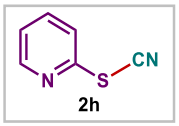

4-thiocyanatopyridine (**2i**): The compound **2i** was prepared following the General Procedure E (GP E). White solid (50 mg, 91% yield), R_f = 0.37 (petroleum ether/EtOAc 95:5). ^{1}H NMR (400 MHz, $CDCl_3$) δ 7.59 – 7.56 (m, 2H), 7.42 – 7.39 (m, 2H). $^{13}C\{^1H\}$ NMR (100 MHz, $CDCl_3$) δ 133.6, 131.7, 124.3, 123.6, 110.0. HRMS (ESI TOF) *m/z* for $C_6H_5N_2S$ $[M + H]^+$ calcd. 137.0173, found 137.0171.

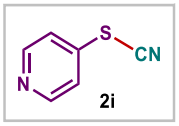

methyl 2-thiocyanatobenzoate (**2j**): The compound **2j** was prepared following the General Procedure E (GP E). White solid (63 mg, 81% yield), R_f = 0.26 (petroleum ether/EtOAc 95:5). ^{1}H NMR (400 MHz, $CDCl_3$) δ 8.11 (dd, *J* = 7.8, 1.6 Hz, 1H), 7.90 (dd, *J* = 8.2, 1.1 Hz, 1H), 7.63 (ddd, *J* = 8.2, 7.3, 1.6 Hz, 1H), 7.41 (td, *J* = 7.6, 1.1 Hz, 1H), 3.95 (s, 3H). $^{13}C\{^1H\}$ NMR (100 MHz, $CDCl_3$) δ 166.6, 134.2, 131.7, 131.0, 127.9, 127.7, 126.2, 111.7, 53.0. HRMS (ESI TOF) *m/z* for $C_9H_8NO_2S$ $[M + H]^+$ calcd. 194.0276, found 194.0273.

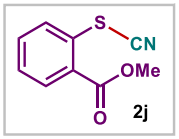

5.4.4 Appendix V. Copies of **^{1}H** and **^{13}C{^{1}H}** NMR spectra of representative compounds

Compound No.	Figure V.X	Data	Page No.
A4'	Figure V.1 and V.2	^{1}H and ^{13}C{^{1}H}	219
1a'	Figure V.3 and V.4	^{1}H and ^{13}C{^{1}H}	220
2a	Figure V.5 and V.6	^{1}H and ^{13}C{^{1}H}	221
3a	Figure V.7 and V.8	^{1}H and ^{13}C{^{1}H}	222
3a'	Figure V.9 and V.10	^{1}H and ^{13}C{^{1}H}	223
3a"	Figure V.11 and V.12	^{1}H and ^{13}C{^{1}H}	224
3aa	Figure V.13 and V.14	^{1}H and ^{13}C{^{1}H}	225
3ab	Figure V.15 and V.16	^{1}H and ^{13}C{^{1}H}	226
4a	Figure V.17 and V.18	^{1}H and ^{13}C{^{1}H}	227
4ha	Figure V.19 and V.20	^{1}H and ^{13}C{^{1}H}	228

5.5 Copies of ^{1}H and $^{13}C\{^{1}H\}$ NMR Spectra

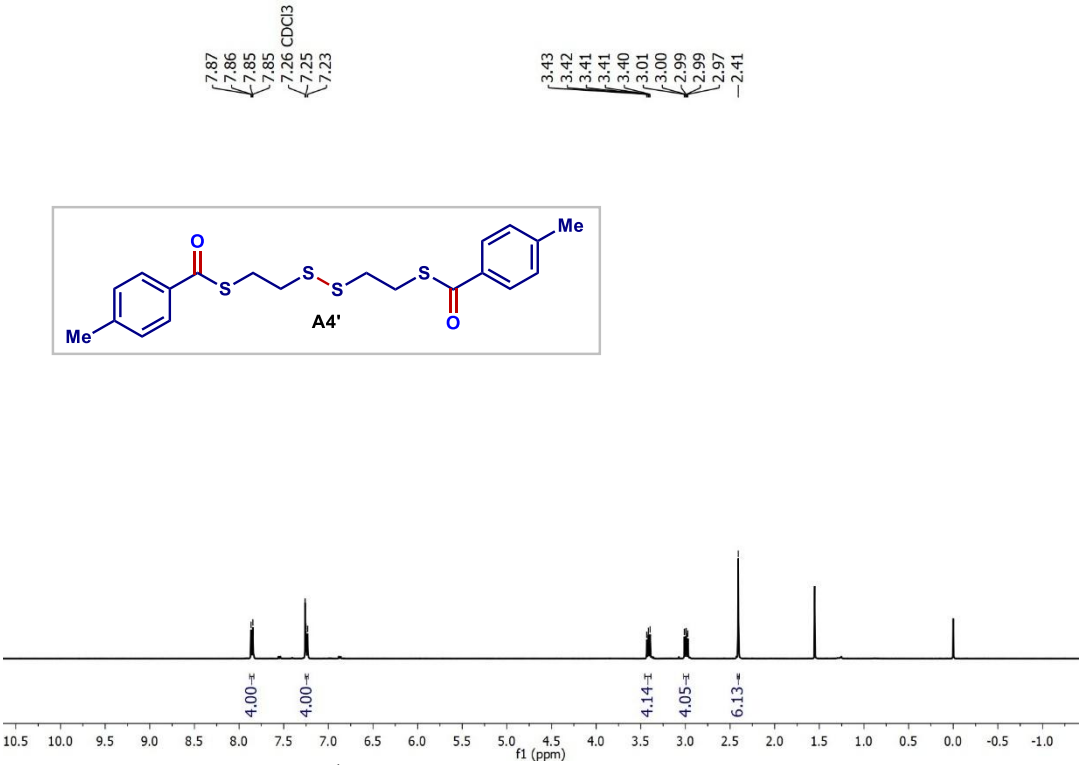

Figure V.1 ^{1}H NMR spectrum of **A4'**, $CDCl_3$, 400 MHz

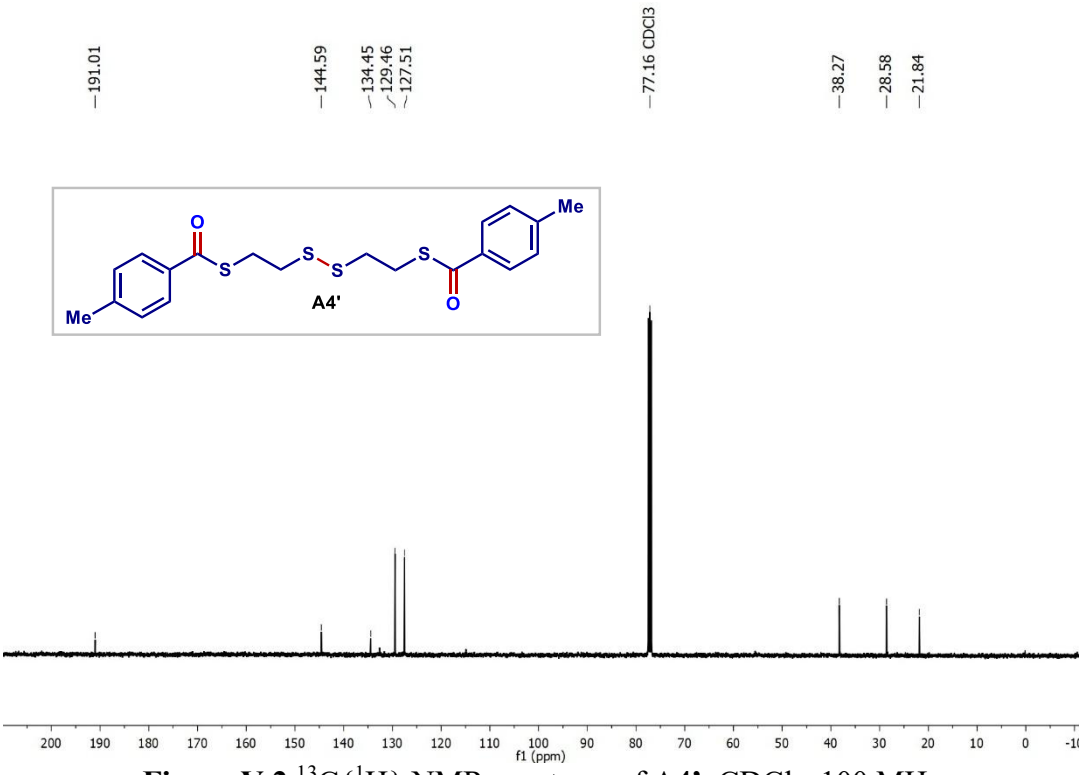

Figure V.2 $^{13}C\{^{1}H\}$ NMR spectrum of **A4'**, $CDCl_3$, 100 MHz

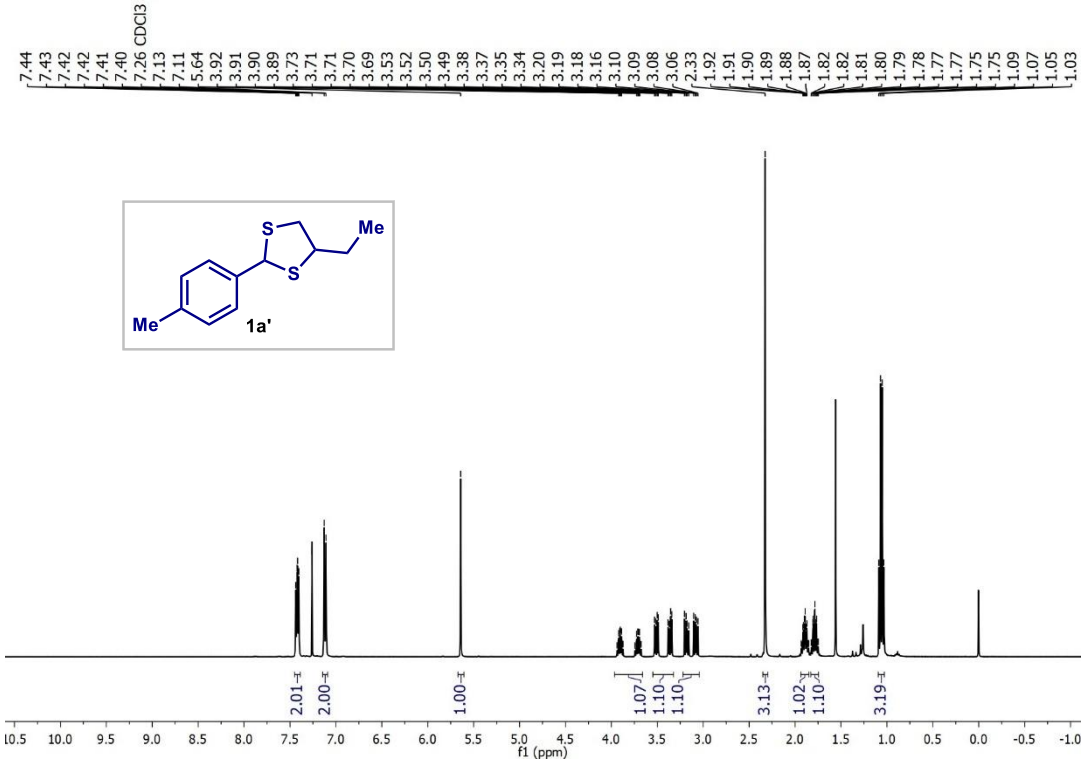

Figure V.3 ^{1}H NMR spectrum of **1a'**, $CDCl_3$, 400 MHz

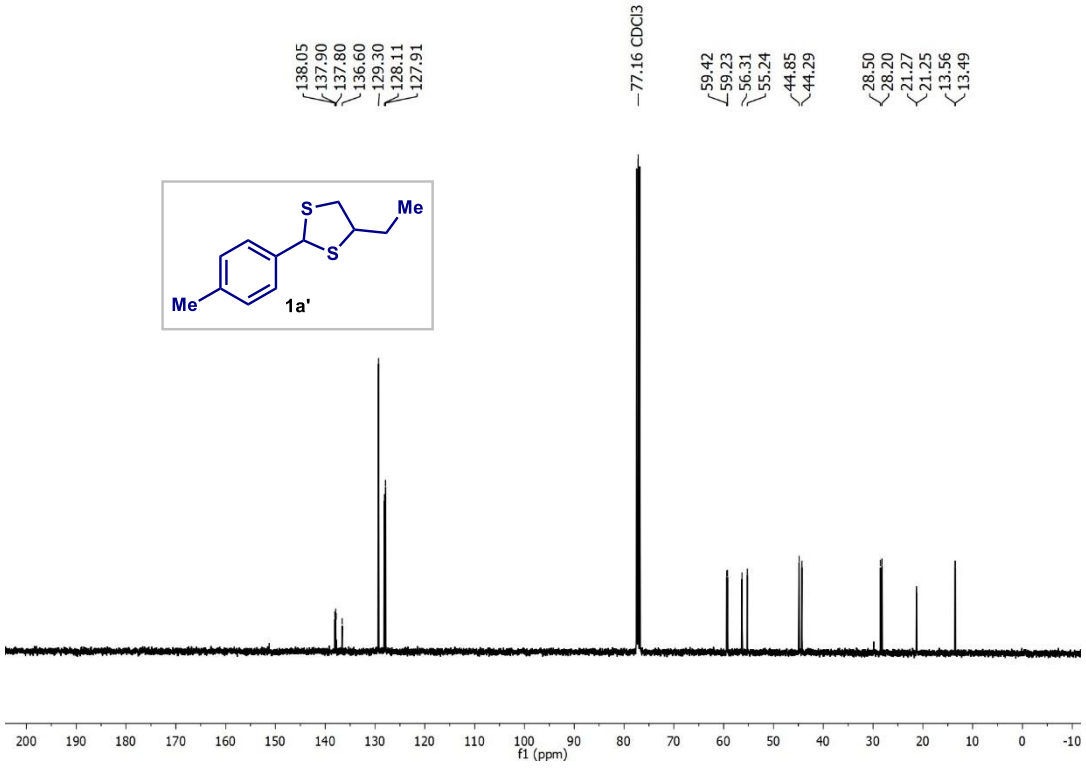

Figure V.4 $^{13}C\{^{1}H\}$ NMR spectrum of **1a'**, $CDCl_3$, 100 MHz

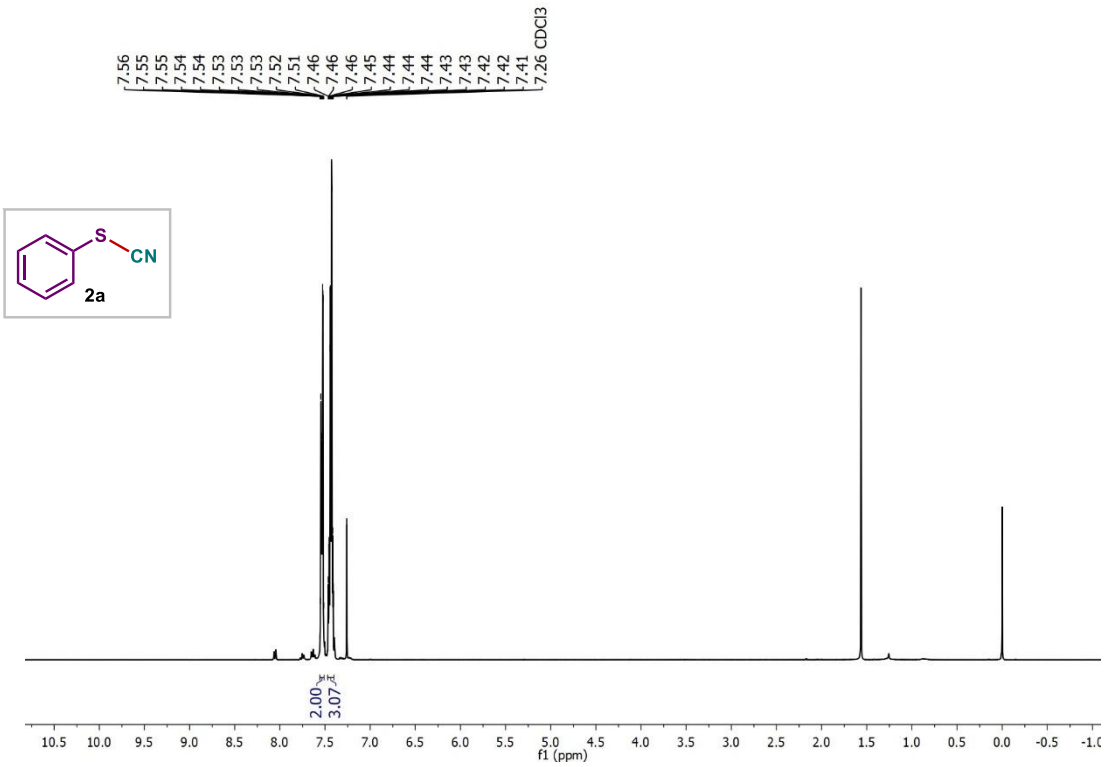

Figure V.5 ^{1}H NMR spectrum of **2a**, $CDCl_3$, 400 MHz

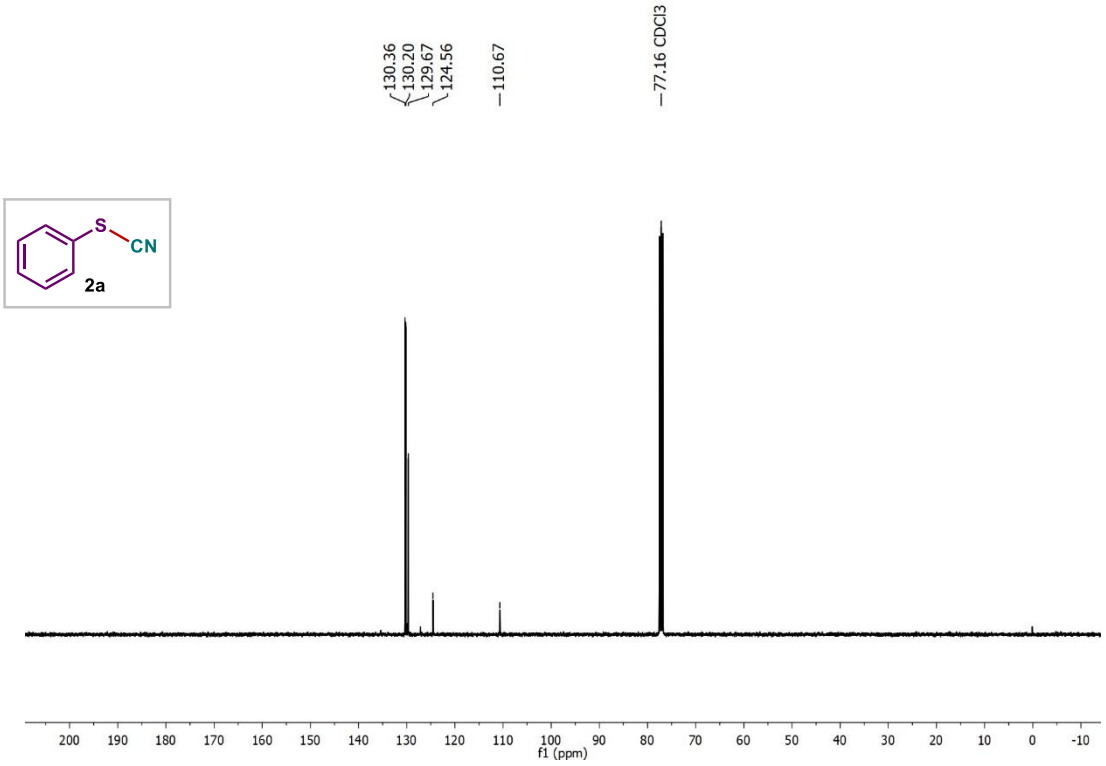

Figure V.6 $^{13}C\{^{1}H\}$ NMR spectrum of **2a**, $CDCl_3$, 100 MHz

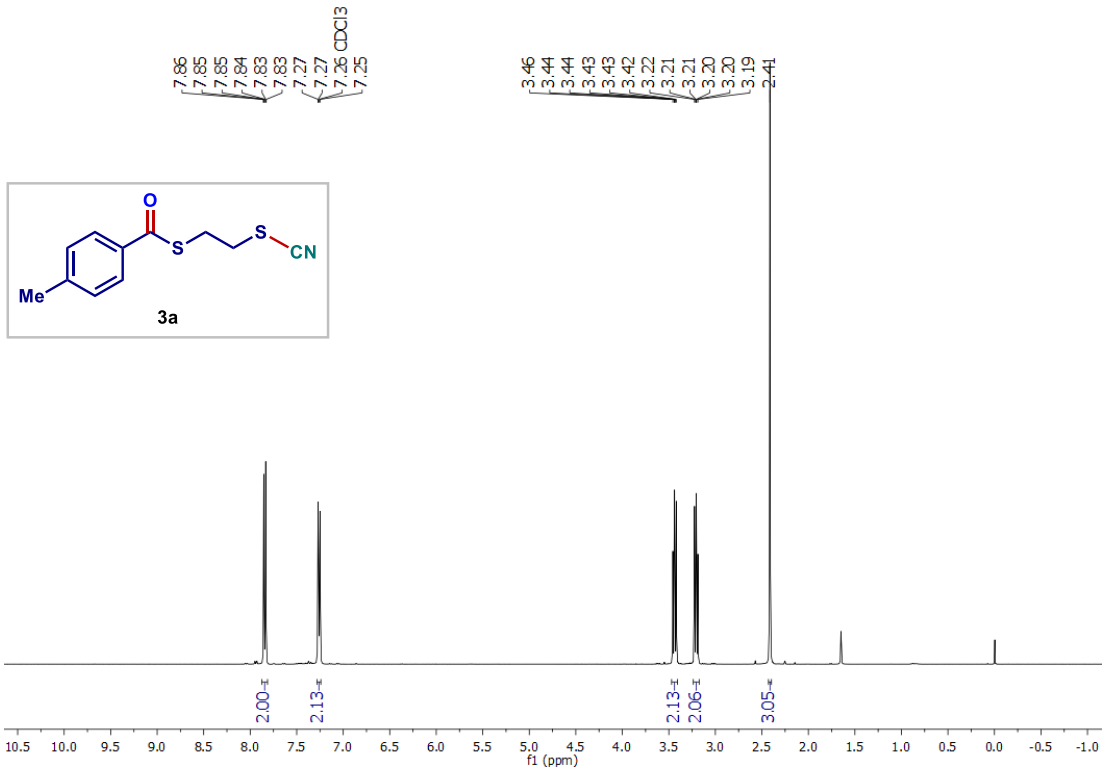

Figure V.7 ^{1}H NMR spectrum of **3a**, $CDCl_3$, 400 MHz

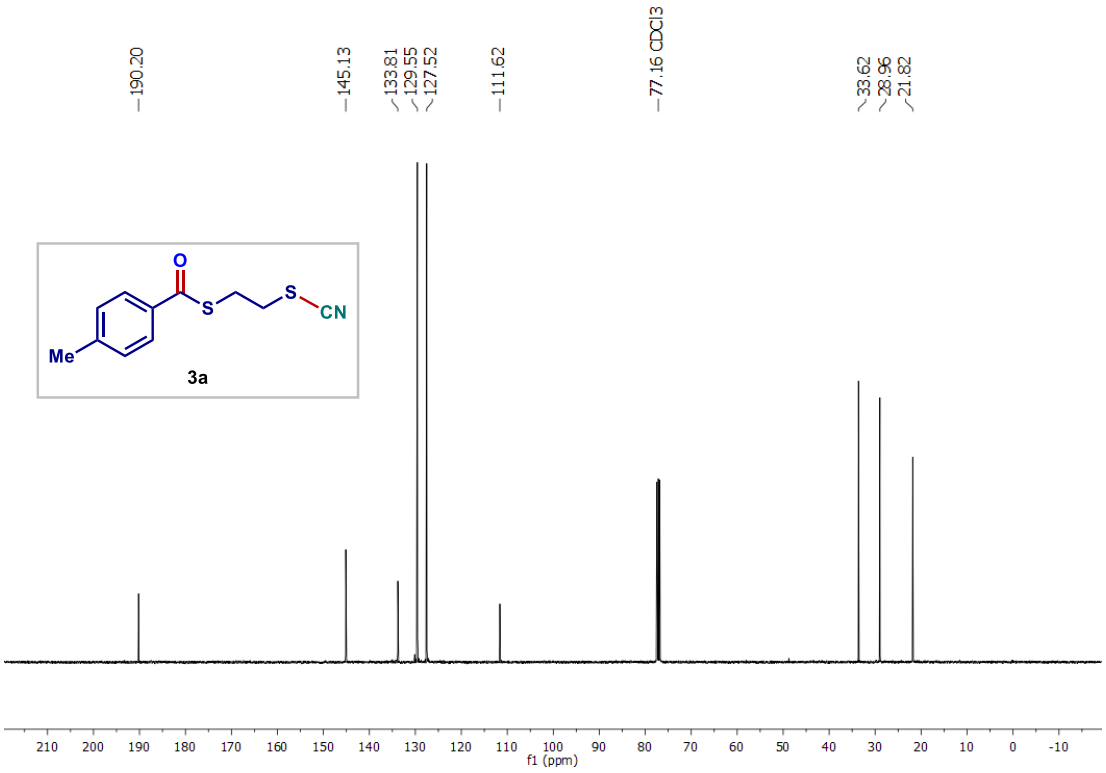

Figure V.8 $^{13}C\{^{1}H\}$ NMR spectrum of **3a**, $CDCl_3$, 100 MHz

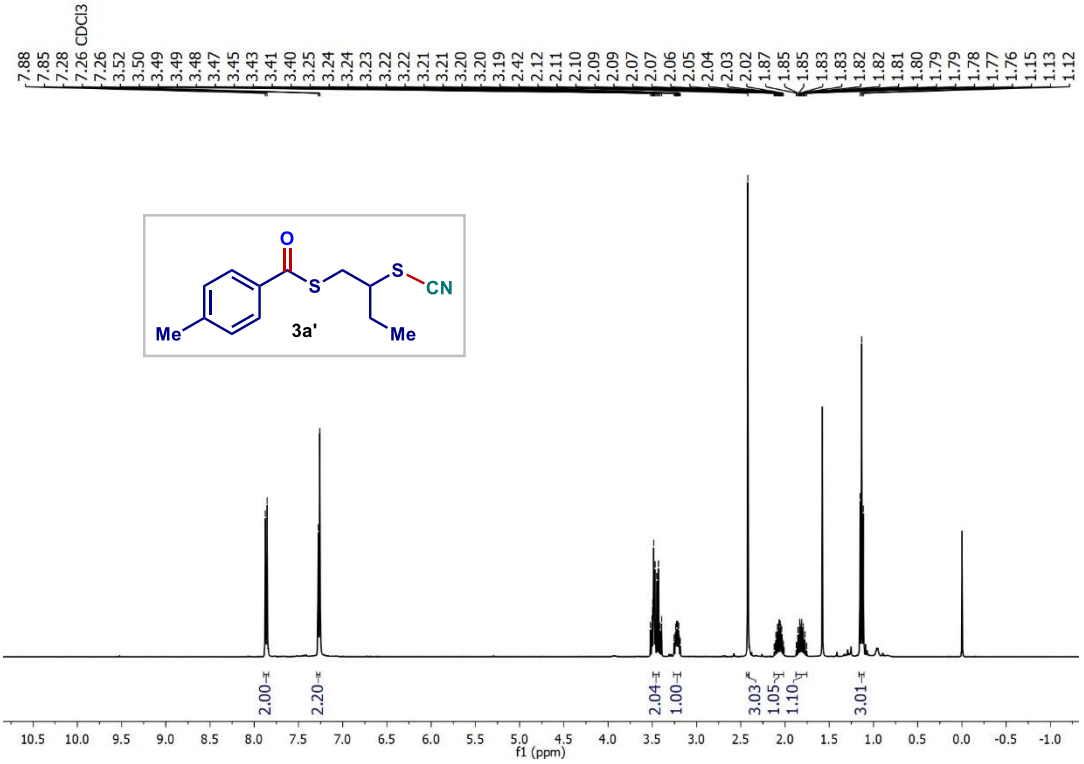

Figure V.9 ^{1}H NMR spectrum of **3a'**, $CDCl_3$, 400 MHz

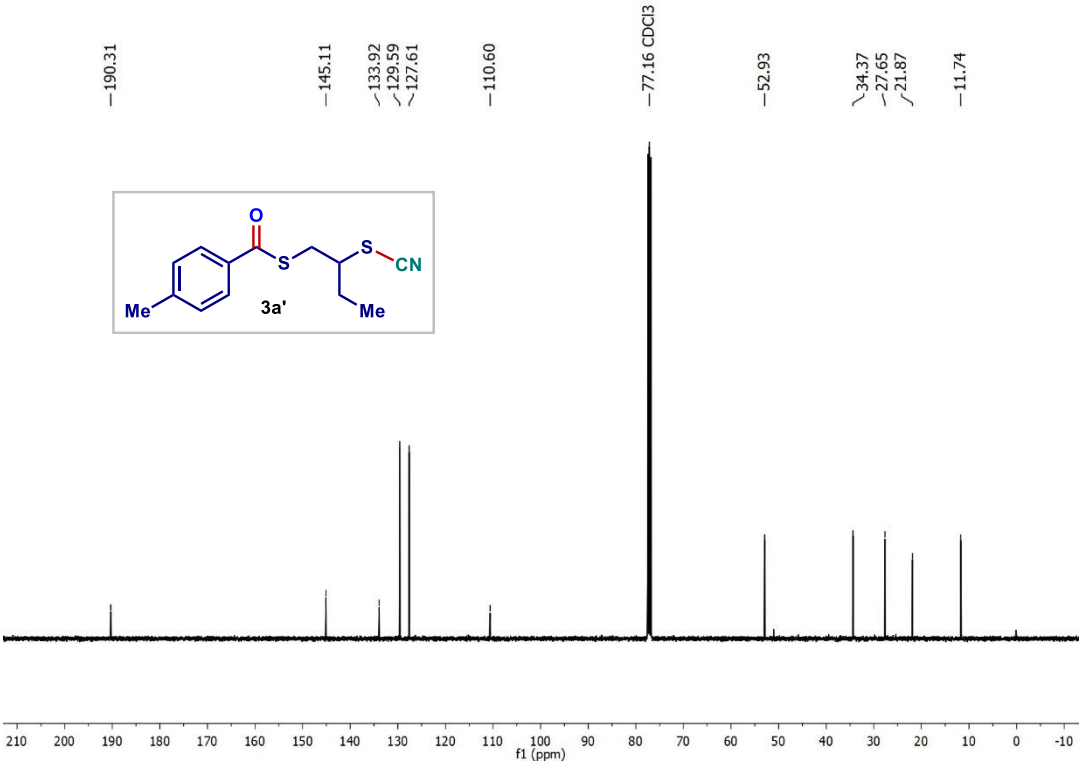

Figure V.10 $^{13}C\{^{1}H\}$ NMR spectrum of **3a'**, $CDCl_3$, 100 MHz

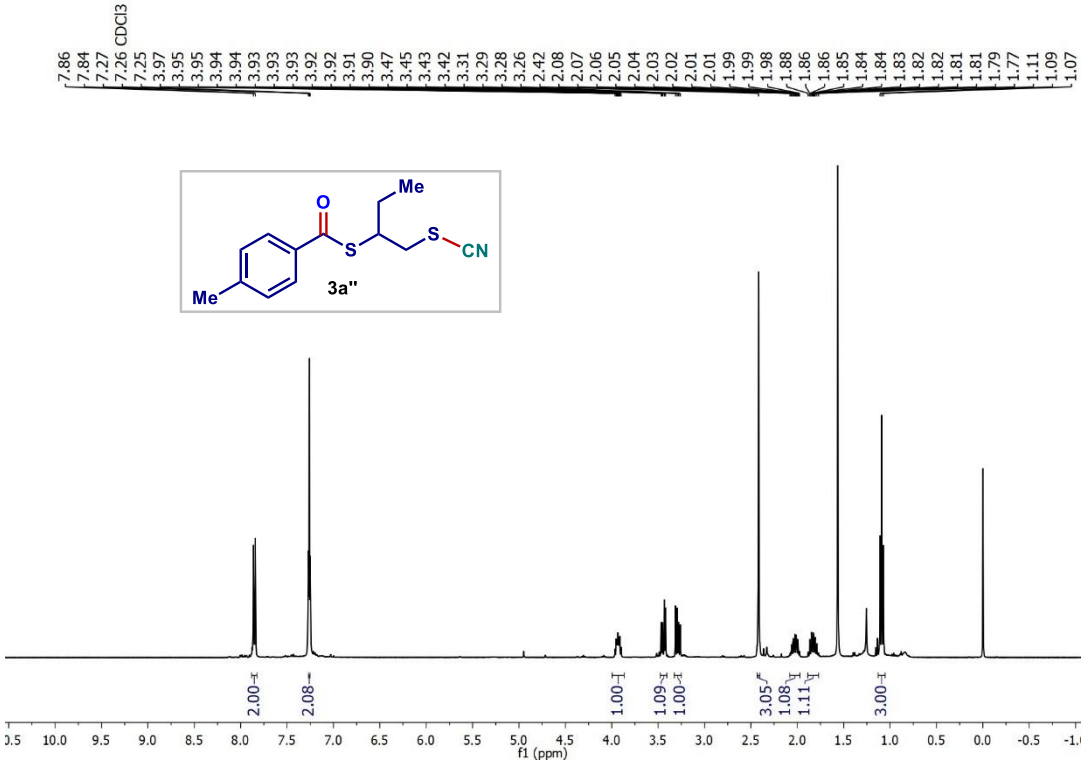

Figure V.11 ^{1}H NMR spectrum of **3a''**, $CDCl_3$, 400 MHz

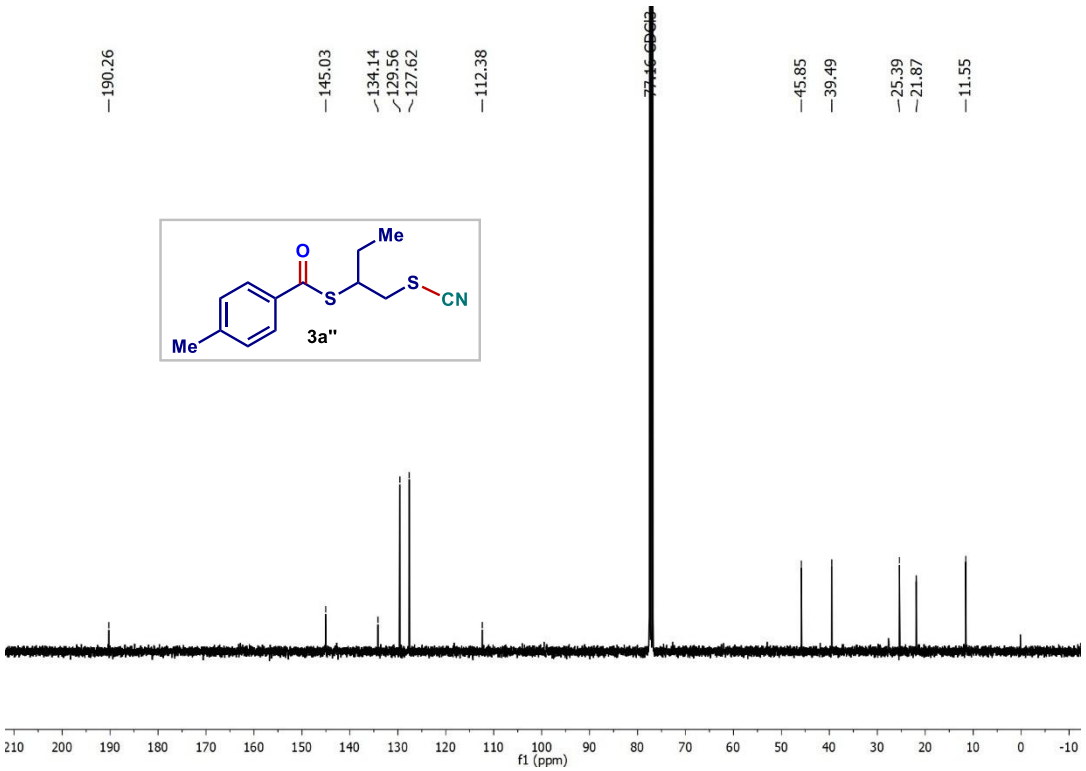

Figure V.12 ^{13}C{^{1}H} NMR spectrum of **3a''**, $CDCl_3$, 100 MHz

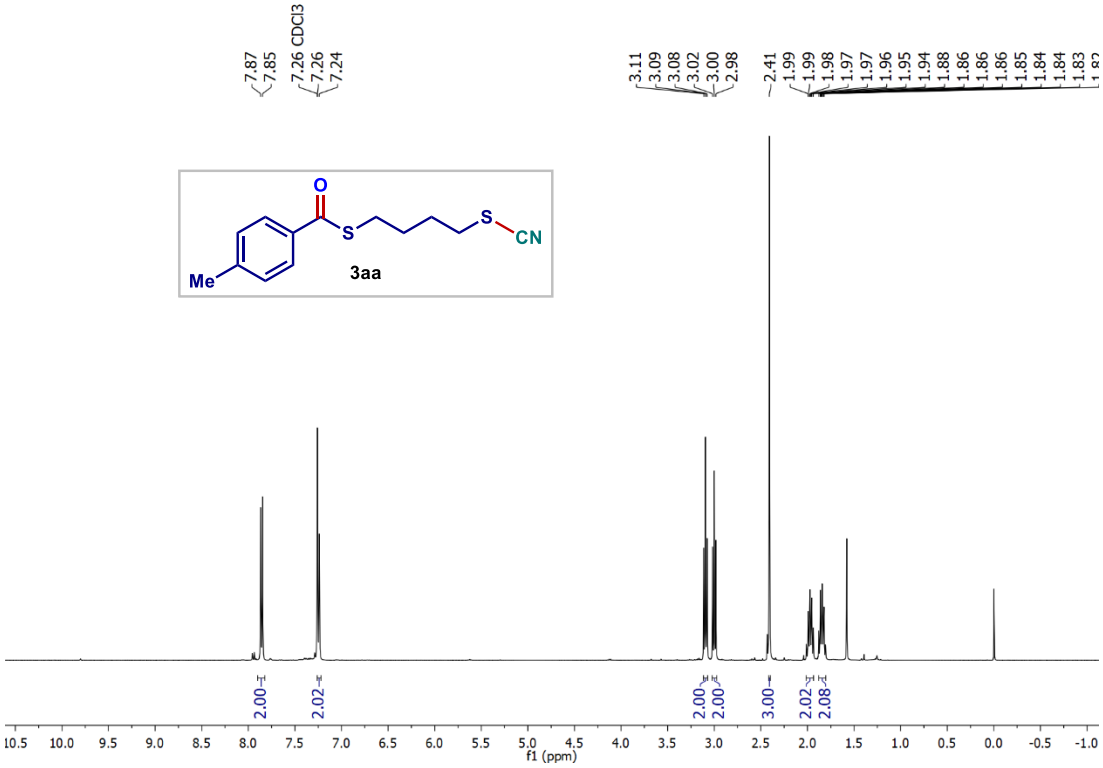

Figure V.13 ^{1}H NMR spectrum of **3aa**, $CDCl_3$, 400 MHz

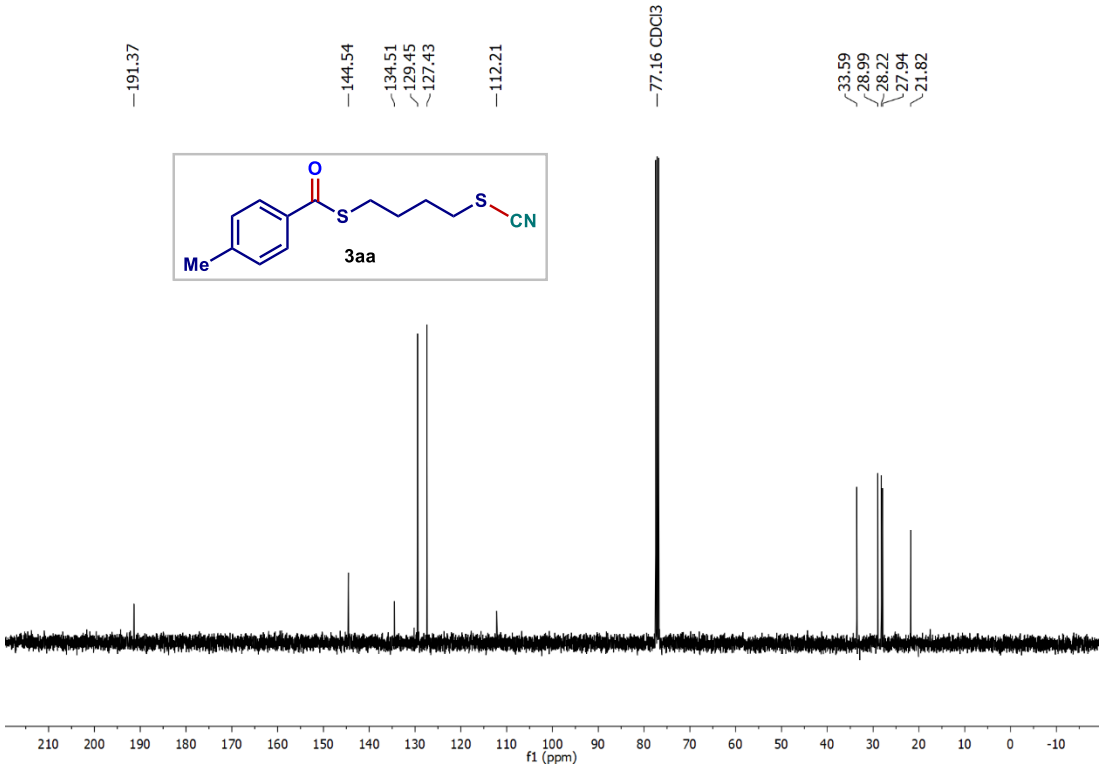

Figure V.14 $^{13}C\{^{1}H\}$ NMR spectrum of **3aa**, $CDCl_3$, 100 MHz

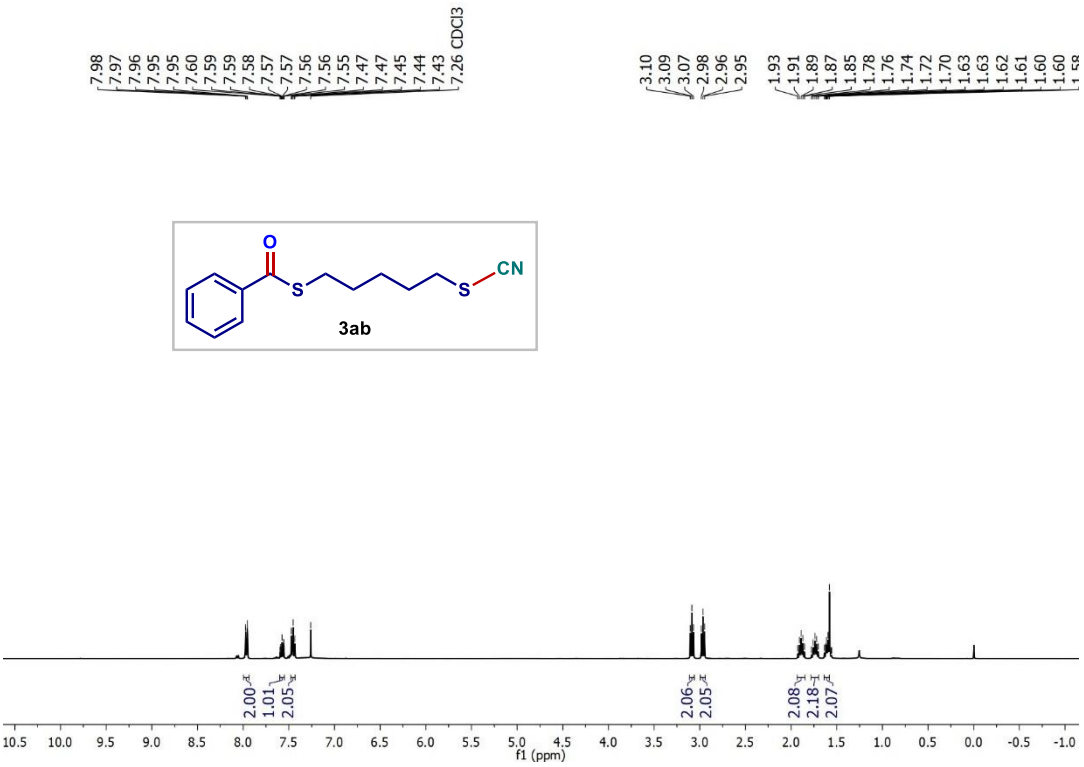

Figure V.15 ^{1}H NMR spectrum of **3ab**, $CDCl_3$, 400 MHz

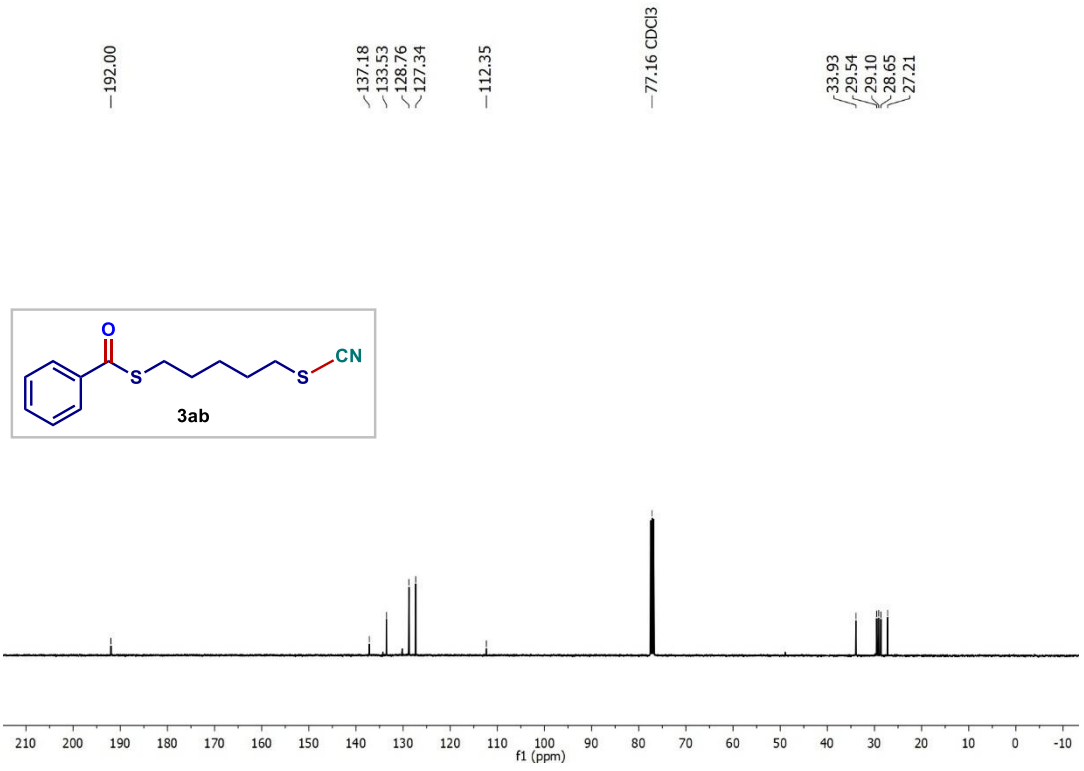

Figure V.16 $^{13}C\{^{1}H\}$ NMR spectrum of **3ab**, $CDCl_3$, 100 MHz

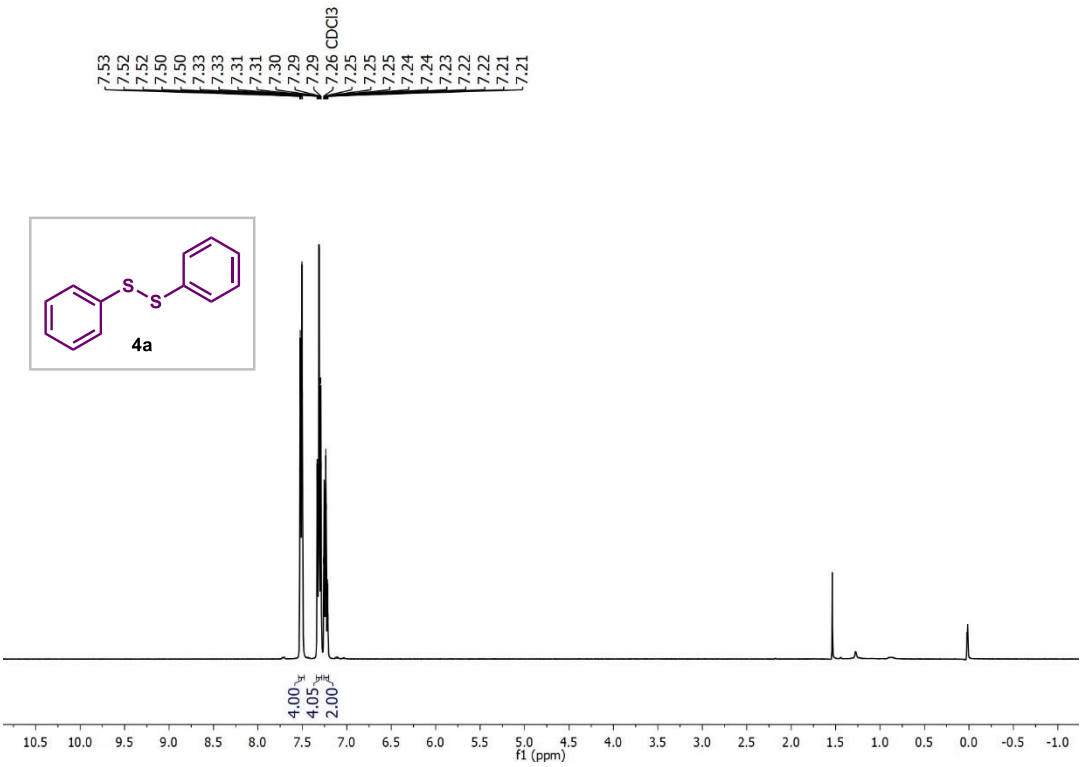

Figure V.17 ^{1}H NMR spectrum of **4a**, $CDCl_3$, 400 MHz

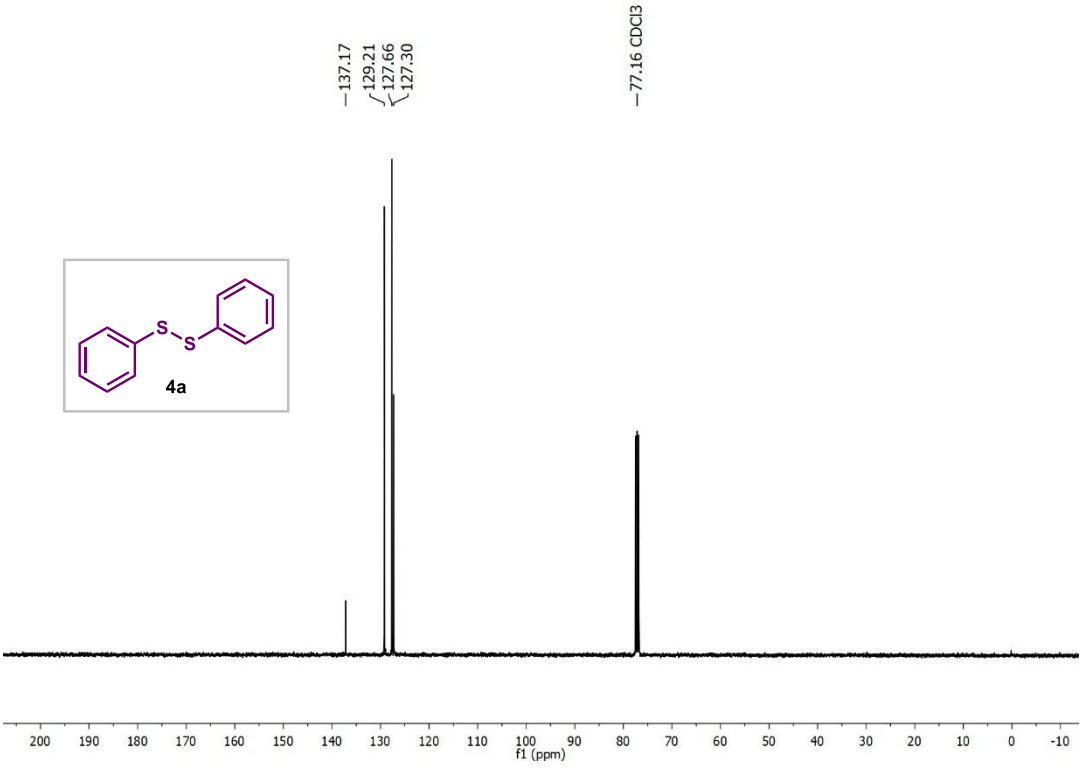

Figure V.18 $^{13}C\{^{1}H\}$ NMR spectrum of **4a**, $CDCl_3$, 100 MHz

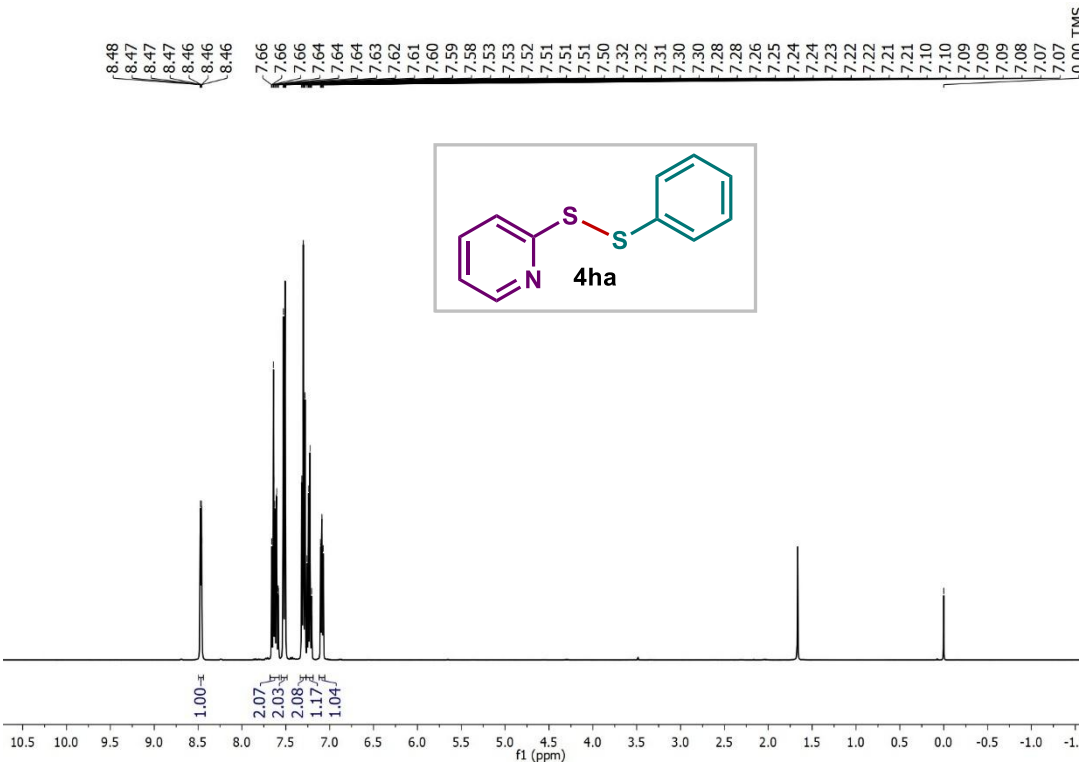

Figure V.19 ^{1}H NMR spectrum of **4ha**, $CDCl_3$, 400 MHz

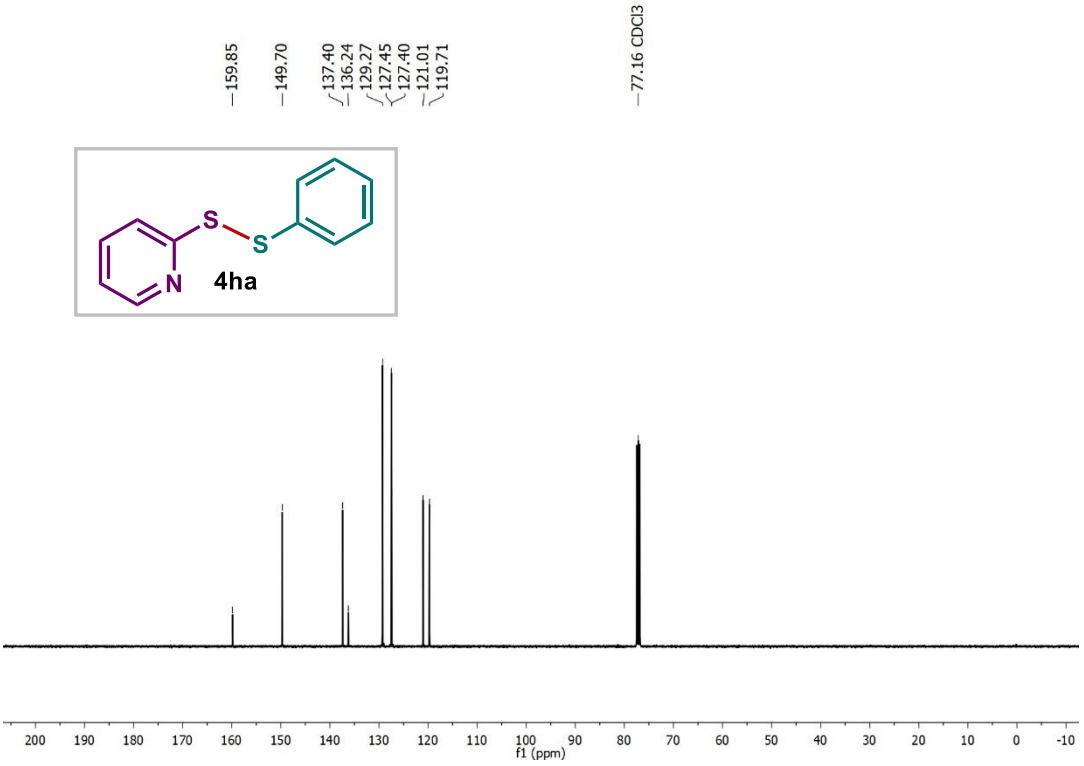

Figure V.20 $^{13}C\{^{1}H\}$ NMR spectrum of **4ha**, $CDCl_3$, 100 MHz

5.6 References:

1) (a) *Chemistry of the cyano group*, (Ed.: Z. Rappoport), Wiley, London, **1970**. (b) R. C. Larock, *Comprehensive organic transformations*, Wiley-VCH, New York, **1989**, p 819. (b) Rakshit, A.; Dhara, H. N.; Sahoo, A. K.; Patel, B. K. *Chem. Asian J.* **2022**, *17*, e202200792. (c) Xia, Y.; Jiang, H.; Wu, W. *Eur. J. Org. Chem.* **2021**, *2021*, 6658–6669.
2) (a) Wang, H.; Zhao, C.; Burešová, Z.; Bureš, F.; Liu, J. *J. Mater. Chem. A* **2023**, *11*, 3753–3770. (b) Demko, Z. P.; Sharpless, K. B. *J. Org. Chem.*, **2001**, *66*, 7945–7950. (c) Saito, A.; Taniguchi, A.; Kambara, Y.; Hanzawa, Y. *Org. Lett.*, **2013**, *15*, 2672–2675. (d) Shuai, S.; Mao, J.; Zhou, F.; Yan, Q.; Chen, L.; Li, J.; Walsh, P. J.; Liang, G. *J. Org. Chem.*, **2024**, *89*, 6793–6797.
3) H. Wang, C. Zhao, Z. Burešová, F. Bureš, J. Liu, *J. Mater. Chem. A* **2023**, *11*, 3753–3770.
4) (a) Fleming, F. F.; Yao, L.; Ravikumar, P. C.; Funk, L.; Shook, B. C. *J. Med. Chem.* **2010**, *53*, 7902–7917. (b) Liu, J. -R.; Gao, Y.; Jin, B.; Guo, D.; Deng, F.; Bian, Q.; Zhang, H. -F.; Han, X. -Y.; Ali, A. S.; Zhang, M. -Z.; Zhang, W. -H.; Gu, Y. -C. *Mar. Drugs* **2023**, *21*, 103–116. (c) Bhattacharya, R.; Flora, S. J. *Handbook of toxicology of chemical warfare agents*; Gupta, R. C. Ed.; Academic Press: Boston, **2009**; pp 255−270.
5) (a) Nauth, A. M.; Opatz, T.; *Org. Biomol. Chem.* **2019**, *17*, 11–23.
6) (a) Luo, F.-H.; Chu, C.-I.; Cheng, C.-H. *Organometallics* **1998**, *17*, 1025−1030. (b) Wen, Q.; Jin, J.; Hu, B. Lu, P. Wang, Y. *RSC Adv.* **2012**, *2*, 6167−6169. (c) Wen, Q.; Jin, J.; Mei, Y.; Lu, P.; Wang, Y. *Eur. J. Org. Chem.* **2013**, *2013*, 4032−4036. (d) Jin, J.; Wen, Q.; Lu, P.; Wang, Y. *Chem. Commun.* **2012**, *48*, 9933−9935. (e) Zhang, C.; Liu, C.; Shao, Y.; Bao, X.; Wan, X. *Chem. – Eur. J.* **2013**, *19*, 17917−17925.
7) Davis, W. A.; Cava, M. P. *J. Org. Chem.* **1983**, *48*, 2774–2775.
8) Zhang, Z.; Liebeskind, L. S. *Org. Lett.* **2006**, *8*, 4331–4333.
9) Vaghasiya, B. K.; Satasia, S. P.; Thummar, R. P.; Kamani, R. D.; Avalani, J. R.; Sapariya, N. H.; Raval, D. K.; *J. Sulfur Chem.* **2018**, *39*, 1–9.
10) (a) Kim, J.; Kim, H. J.; Chang, S. *Angew. Chem. Int. Ed.* **2012**, *51*, 11948–11959. (b) Yan, G.; Zhang, Y.; Wang, J. *Adv. Synth. Catal.* **2017**, *359*, 4068–4105. (c) Najam, T.; Shah, S. S. A.; Mehmood, K.; Din, A. U.; Rizwan, S.; Ashfaq, M.; Shaheen, S.; Waseem, A. *Inorg. Chim. Acta*, **2018**, *469*, 408–423.
11) Yu, J.-T.; Teng, F.; Cheng, J. *Adv. Synth. Catal.* **2017**, *359*, 26–38.

12) (a) Castanheiro, T.; Suffert, J.; Donnard, M.; Gulea, M. *Chem. Soc. Rev.* **2016**, *45*, 494–505. (b) Cros, F.; Pelotier, B.; Piva, O. *Synthesis* **2010**, *2010*, 233–238.

13) Grishchuk, B. D., Prodanchuk, N. G., Sinchenko, V. G.; Gorbovoi, P. M.; Kudrik, E. Y. *Pharm. Chem. J.* **1994**, *28*, 657–659.

14) (a) Szajnman, S. H.; Yan, W.; Bailey, B. N.; Docampo, R.; Elhalem, E.; Rodriguez, J. B. *J. Med. Chem.*, **2000**, *43*, 1826–1840. (b) Elhalem, E.; Bailey, B. N.; Docampo, R.; Ujvary, I.; Szajnman, S. H.; Rodriguez, J. B. *J. Med. Chem.* **2002**, *45*, 3984–3999. (c) Yasman; Edrada, R. A.; Wray, V.; Proksch, P. *J. Nat. Prod.* **2003**, *66*, 1512–1514. (d) Munirajasekhar, D.; Himaja, M.; Mali, S. V. *Int. Res. J. Pharm*. **2011**, *2*, 114-117.

15) Furukawa, M.; Suda, T.; Tsukamoto, A.; Hayashi, S. *Synthesis* **1975**, *3*, 165–167.

16) (a) König, B. *Eur. J. Org. Chem.* **2017**, *2017*, 1979–1981. (b) Akita, M.; Ceroni, P.; Stephenson, C. R. J.; Masson, G. *J. Org. Chem.* **2023**, *88*, 6281–6283.

17) Patel, R. I.; Sharma, S.; Sharma, A. *Org. Chem. Front.* **2021**, *8*, 3166–3200.

18) Guo, W.; Tan, W.; Zhao, M.; Zheng, L.; Tao, K.; Chen, D.; Fan, X. *Org. Chem.* **2018**, *83*, 6580 –6588.

19) Dharpure, P. D.; Behera, M.; Khade, V. V.; Thube, A. S.; Bhat, R. G. *Org. Lett.* **2022**, *24*, 6919–6924.

20) Franke, J.; Hertweck, C. *Cell Chem. Biol.* **2016**, *23*, 1179–1192.

21) (a) Clark, J. H.; Farmer, T. J.; Herrero-Davila, L.; Sherwood, J. *Green Chem.* **2016**, *18*, 3914–3934. (b) Haas, W.; Krausmann, F.; Wiedenhofer, D.; Heinz, M.; *J. Ind. Ecol.* **2015**, *19*, 765–777.

22) (a) Saxena, B.; Patel, R. I.; Sharma, A. *Green Chem.* **2024**, *26*, 11650–11661. (b) Patel, R. I.; Saxena, B.; Sharma, A. *Green Chem.* **2024**, *26*, 10265–10274.

23) Dharpure, P. D.; Bhowmick, A.; Warghude, P. K.; Bhat, R. G. *Tetrahedron Lett.* **2020**, *61*, 151407–151415.

24) (a) Guo, J.-T.; Yang, D.-C.; Guan, Z.; He, Y.-H. *J. Org. Chem.* **2017**, *82*, 1888–1894. (b) Bancirova, M. *Luminescence* **2011**, *26*, 685–688. (c) Harbour, J. R.; Issler, S. L. *J. Am. Chem. Soc.* **1982**, *104*, 903–905.

25) Pelaez, M.; Falaras, P.; Likodimos, V.; O'shea, K.; De la Cruz, A.; Dunlop, P. S. M.; Byrne, J. A.; Dionysiou, D. D. *J. Mol. Catal. A Chem.* **2016**, *425*, 183–189.

26) *The measured potentials were recorded with respect to an Ag/AgNO₃ (0.01 M) reference electrode. The values of redox potentials (vs Ag/AgNO₃) are converted into those vs SCE by addition of 0.29 V.* Mann, C. K.; Barnes, K. K. *Electrochemical Reactions in Non-aqueous Systems*, Mercel Dekker, New York, **1970**.

27) Dharpure, P. D.; Behera, M.; Thube, A. S.; Bhat, R. G. *Chem. Asian J.* **2023**, *18*, e202201128.

28) (a) Dietrich, A.; Buschmann, V.; Müller, C.; Sauer, M. *Rev. Mol. Biotechno.* **2002**, *82*, 211–231. (b) Doose, S.; Neuweiler, H.; Sauer, M. *ChemPhysChem* **2009**, *10*, 1389–1398.

29) Li, Z.; Wang, S.; Huo, Y.; Wang, B.; Yan, J.; Guo, Q. *Org. Chem. Front.* **2021**, *8*, 3076–3081.

30) Still, I. W. J.; Watson, I. D. G. An efficient synthetic route to aryl thiocyanates from arenesulfinates. *Synth. Commun.* **2001**, *31*, 1355-1359.

31) Zhu, X.; Xie, Z.; Chen, X.; Mu, M.; Wu, H.; Sun, M.; Yang, J.; Wanga, L.; Wang, Z. *J. Org. Chem.* **2024**, *89*, 14940–14950.

Summary

Alkenes are one of the most abundant and inexpensive carbon feedstocks easily accessible from natural resources. Most importantly their unique reactivity in radical oxidative difunctionalization reactions have been widely utilized for the synthesis of myriads of highly functionalized compounds for applications in the synthesis of bioactive molecules and materials science. Similarly, the cyclic thioacetals are widely used as protecting groups for carbonyl compounds and for enabling umpolung reactivity. In this regard, photoredox catalysis has been an indispensable tool in organic synthesis for more than a decade now for its simple, mild, sustainable, and unique reactivity. Although, the metallophotoredox catalysis play a crucial role in organic synthesis, however, their less abundance, cost, and toxicity challenge their diverse applications. In this regard, reliance of organophotoredox catalysis has been growing not only for the metal-free reason, but for the distinct reactivity profiles allowing access to unique transformations and a broader range of substrates. Also, organophotoredox catalysis have demonstrated the capabilities of constructing the interesting and useful scaffolds that were inaccessible or difficult via traditional synthetic approaches.

The initial three working chapters described the oxidative difunctionalization of alkenes to synthesize high valued functionalized products such as β-hydroxy trifluoromethylated alcohols, α-alkoxylated ketones, and the 1,4-diketones. Initially, we described an approach for the β-hydroxy trifluoromethylation designed to be applicable to previously unapproachable unactivated alkenes (both terminal and internal), under transition metal-free and mild reaction conditions under the irradiation of visible light. Subsequently, the synthetically and pharmaceutically useful α-alkoxylated ketones were synthesized using styrene as the substrate for the first time via visible light organophotoredox catalysis and the method did not rely on any external chemical oxidant. The previous procedures relied on the pre-functionalized enol or enolate substrates. Additionally, 1,4-diketones, which are otherwise difficult to synthesize due to the inherent polarity mismatch of the existing carbonyl synthons, were synthesised directly from styrene utilising the strength of organophotoredox catalysis. The last working chapter disclosed the selective cleavage of single C–S bond of cyclic thioacetals to synthesize rearranged functionalized products using organophotoredox catalysis under visible light irradiation. For the first time, the aryl thiocyanate has been employed as an organic cyanating reagent under visible light irradiation and transition metal-free conditions. The generated by-product diaryl disulfide has been efficiently repurposed as a recyclable and reusable substrate for the sustainable synthesis of aryl thiocyanate, thus supporting the circular chemical

economy.

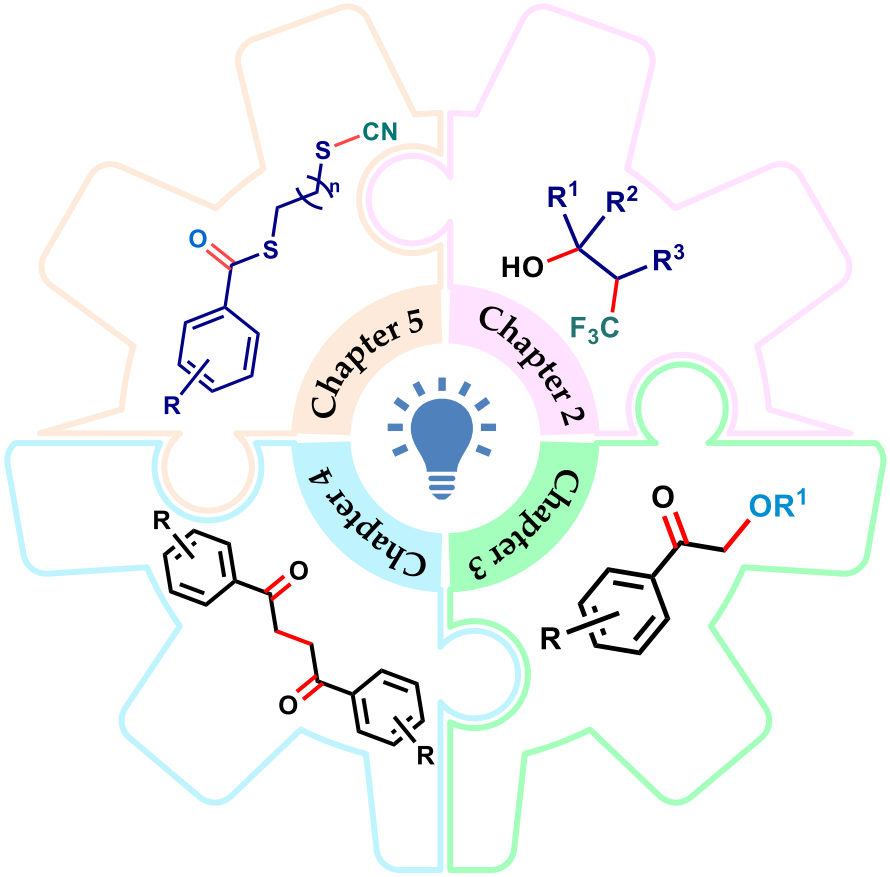

The protocols were developed through the extensive optimization, involving systematic screening of reagents, photocatalysts, solvents, oxidants, bases, additives, light sources, stoichiometry, and the reaction time. The scope and generality of each transformation were demonstrated by synthesizing a broad library of substrates. The synthetic utility was further validated through post-synthetic derivatization and methods proved to be scalable. A key focus of the study was mechanistic investigation, which included a series of well-designed control experiments to identify potential intermediates, supported by HRMS and EPR/ESR analyses. Complementary photophysical and electrochemical studies—UV-Visible absorption, photoluminescence quenching, and cyclic voltammetry experiments supports the proposed plausible reaction mechanisms.

Check for updates

ACES Asian Chemical Editorial Society

doi.org/10.1002/asia.202500423

CHEMISTRY AN ASIAN JOURNAL Research Article

www.chemasianj.org

Aryl Thiocyanate as an Organic 'CN' Source: Access to Thiocyano-Thioesters from Cyclic Thioacetals

Mousumi Behera,[a] Shubham Y. Shukla,[a] Pankaj D. Dharpure,[a] and Ramakrishna G. Bhat*[a]

A facile, transition metal-free method has been developed for the synthesis of thiocyano–thioesters. It employs cyclic thioacetals and aryl thiocyanate as an organic 'CN' source, facilitated by organophotocatalyst under the visible light irradiation. Additionally, the diaryl disulfide by-products have been efficiently repurposed as a recyclable and reusable substrates for the sustainable synthesis of aryl thiocyanates, supporting the circular chemical economy. This method exhibits broad functional group tolerance and is applicable to five- to eight-membered cyclic thioacetals. The method also proved to be scalable on gram quantity. A series of control experiments, fluorescence quenching, and cyclic voltammetry analysis supported the proposed reaction mechanism.

1. Introduction

The cyano group is known for its rich and diverse reactivity thus making it as a versatile precursor to access various functional groups such as carboxylic acids, aldehydes, amines, amidines, amides, tetrazoles, oxazoles, and isoquinolines.[1] Furthermore, the cyano group is prevalent in numerous natural products and commercially available materials, such as dyes, agrochemicals, and pharmaceuticals.[2] Additionally, the cyano-capped organic compounds play a crucial role in diverse applications of organic electronics and related technologies such as organic solar cells (OSCs), organic light-emitting diodes (OLEDs), nonlinear optics (NLO), light conversion agents, organic fluorescent probes, and photoredox catalysis.[3] Consequently, significant progress has been made to achieve cyanation by employing a range of cyanating reagents.

Considering environmental impacts and toxicity, there has been a notable transition from the use of conventional cyanating reagents such as KCN, NaCN, $Zn(CN)_2$, and $K_4[Fe(CN)_6]$ to relatively safer metal thiocyanates.[4a] However, some of these reagents generate stoichiometric metal waste and/or release hazardous HCN. In order to overcome these perennial problems, various nonmetallic organo cyanating reagents have been explored for the cyanation including acetone cyanohydrin, trimethylsilyl cyanide (TMSCN), propanedinitrile, ethyl cyanoacetate, and isocyanides.[4b] Additionally, benzyl nitrile and benzyl thiocyanate have also been utilized as organocyanating reagents in metal catalysis (Scheme 1A).[5] However, these transformations either require stoichiometric amounts of transition metal catalysts or metal salts as oxidants at elevated temperature. Furthermore, constructing X—CN bonds (X = N, S, and O) has been relatively less explored in comparison to the extensively studied C—CN bond formation.[6,7]

Visible light photoredoxcatalysis has emerged as one of the most dynamic and transformative areas since 2008.[8] Over the past decade numerous cyanation strategies have been developed under visible light irradiation.[9] However, despite significant progress, to the best of our knowledge, there are no reports till date on the use of aryl thiocyanates (ArSCN) as a radical cyanating source in photoinduced transformations.

Previously, we investigated the reactivity of dithiolanes and dithianes with a super-stoichiometric amount of NaSCN as a cyanating agent to synthesize thiocyano–thioesters.[10] Organic thiocyanates serve as valuable synthetic intermediates for the preparation of various sulfur-containing compounds.[11a] They have garnered significant interest due to their notable biological activities, particularly their antimicrobial and antiproliferative properties.[11b,c] Similarly, thioesters play a vital role in biosynthetic pathways, including protein and nucleic acid synthesis, and find applications in drug delivery, biomolecule labeling, and as acyl radical equivalents in acyl transfer reactions.[12]

The growing environmental challenges of waste generation and limited chemical resources necessitate alternative sustainable strategies in organic synthesis. Integrating circular economy principles by repurposing products and by-products as starting materials reduces reliance on virgin chemicals and minimizes waste through closed-loop chemical processes.[13] To address challenges in thiocyano–thioester synthesis while promoting sustainability, we sought to employ an organic cyanating source that enables the reutilization of its by-product in subsequent transformations.[14] We propose that aryl thiocyanates can effectively generate 'CN' radicals under visible light irradiation, while the resulting by-product, diaryl disulfide, can be recycled to synthesize a diverse range of aryl thiocyanates, thereby aligning with circular economy principles. Herein, we report for the first time the use of aryl thiocyanates as an efficient cyanating source under visible light organophotoredox catalytic condition to

[a] M. Behera, S. Y. Shukla, P. D. Dharpure, Prof. Dr. R. G. Bhat
Department of Chemistry, Indian Institute of Science Education and Research (IISER) Pune, Dr. Homi Bhabha Road, NCL Colony, Pashan, Pune, Maharashtra 411008, India
E-mail: rgb@iiserpune.ac.in

Shubham Y. Shukla and Pankaj D. Dharpure contributed equally to this work.

Supporting information for this article is available on the WWW under https://doi.org/10.1002/asia.202500423

© 2025 Wiley-VCH GmbH

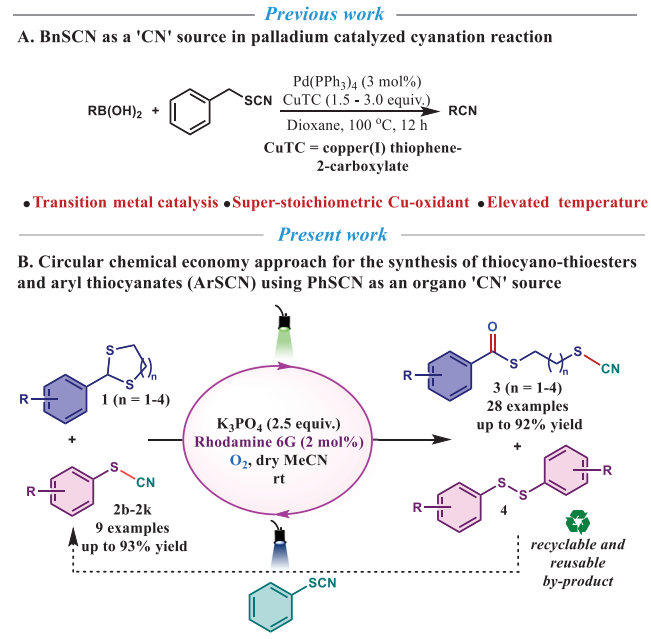

Scheme 1. Synthetic strategies for cyanation using organothiocyanates.

access thiocyano–thioesters from cyclic thioacetals. Furthermore, the diaryl disulfides generated in the reaction are effectively recycled in a circular manner to synthesize a diverse range of aryl thiocyanates (Scheme 1B).[15a]

2. Results and Discussion

To validate the hypothesis, we commenced with the reaction optimization studies with cyclic thioacetal **1a** and phenyl thiocyanate **2a** as model substrates. After the initial systematic and detailed investigation of the reaction conditions, Rhodamine 6G (2 mol%) as an organophotoredox catalyst and K_3PO_4 as a base in anhydrous MeCN (3 mL), Kessil green LEDs (525 nm, 20 W) under O_2-atmosphere at room temperature proved to be advantageous for accessing the desired thiocyano–thioester **3a** in very good yield (89%, Table 1, Entry 1). We observed that the reaction in presence of different bases such as K_2CO_3 or Na_2CO_3 (instead of K_3PO_4) either did not afford or led to a decrease in the yield of the desired product **3a** (Table 1, Entries 2, 3 and see Supporting Information, S6,S7, Table S2 for details). Later, we screened different monochromatic visible light sources with varied wavelengths and we observed that yield of **3a** dropped with decrease in wavelength (Table 1, Entry 4, and see Supporting Information, S6,S7, Table S2, Entries 8-12 for details). Among all, green LEDs (525 nm, 20 W) proved to be efficient by affording the desired compound **3a** in very good yield (Table 1, Entry 1). To further optimize the reaction conditions, we screened different organophotocatalysts such as Eosin Y, Rhodamine B, and few others. In all the cases, desired product **3a** was formed in poor to moderate yields (up to 61%, Table 1, Entry 5 and see Supporting Information, S6,S7, Table S2, Entries 13–19 for details). The transition metal photocatalysts such as Ru-polypyridyl complex also afforded the desired product **3a** in 64% yield (Table 1, Entry 6). Among all the photocatalysts screened, Rhodamine 6G (Rh6G) proved to be the most efficient to obtain **3a** in highest yield (89%, Table 1, Entry 1). Later, we screened different solvents such as DMF and few other solvents (see Table 1, Entry 7 and see Supporting Information, S6,S7, Table S2, Entries 22-28 for details), among all anhydrous acetonitrile proved to be an advantageous (see Table 1, Entry 1). Further, the photocatalyst loading was varied (1 or 4 mol%), we observed slightly reduction in the yields of **3a** (Table 1, Entry 8 and see Supporting Information, S8, Appendix I). Later, we looked into the effect of solvent concentration (2 or 4 mL) and we observed a decrease in the yield of **3a** (Table 1, Entry 9 and see Supporting Information, S8, Appendix II). Moreover, we varied the equivalents of K_3PO_4 (1 or 5 equiv), however there was no improvement in the yield of **3a** (Table 1, Entry 10 and see Supporting Information, S8, Appendix III). Furthermore, the stoichiometric amount of PhSCN was varied (1 or 3 equiv) and we observed that there were no significant changes in the

Table 1. Optimization of reaction conditions.[a]

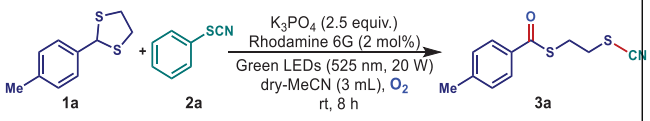

Entry	Deviations from Standard Condition	Yield (%)[b]
1	**None**	**89(82)**[c]
2	Na_2CO_3 instead of K_3PO_4 as a base	ND[d]
3	K_2CO_3 instead of K_3PO_4 as a base	45[d]
4	427 nm instead of 525 nm	72[e]
5	Eosin Y or Rhodamine B or Mes-Acr•ClO_4 as a photocatalyst	up to 61
6	$[Ru(bpy)_3](PF_6)_2$ instead of Rh6G	64
7	DMF as a solvent	NR
8	Rhodamine 6G (1 or 4 mol%) instead of 2 mol%	77 or 80
9	Dry-MeCN (2 mL or 4 mL) instead of 3 mL	83 or 79
10	K_3PO_4 (1 equiv or 5 equiv) instead of 2.5 equiv	67 or 72
11	1 or 3 equiv of **2a** instead of 1.1 equiv	82 or 85
12	4 or 12 h instead of 8 h	62 or 86
13	Open air	81
14	No light	NR
15	No photocatalyst	NR
16	No base	ND
17	Ar-balloon	NR

Standard reaction conditions: [a]**1a** (0.2 mmol), PhSCN **2a** (1.1 equiv), K_3PO_4 (2.5 equiv), Rhodamine 6G (2 mol%), O_2- balloon, dry-MeCN (3 mL), Kessil Green LEDs (525 nm, 20 W) for 8 h at room temperature (rt). [b]Determined by ^1H NMR analysis using 1,3,5-trimethoxybenzene as an internal standard. [c]Isolated yield. [d]Rhodamine 6G (4 mol%), MeCN (2 mL), Blue LEDs (20 W) were used. [e]1,2-Diphenyldisulfide formation was not observed. ND = Not Detected. NR = No Reaction.

© 2025 Wiley-VCH GmbH

1861471x, 0, Downloaded from https://acesonlinelibrary.wiley.com/doi/10.1002/asia.202500423 by Indian Institute Of Science Education And Research Pune, Wiley Online Library on [23/06/2025]. See the Terms and Conditions (https://onlinelibrary.wiley.com/terms-and-conditions) on Wiley Online Library for rules of use; OA articles are governed by the applicable Creative Commons License

yield of **3a** (Table 1, Entry 11 and see Supporting Information, S9, Appendix IV). Later, we examined the influence of the reaction time (4 or 12 h) and we noted the decrease in the yield of **3a** (Table 1, Entry 12 and see Supporting Information, S9,S10, Appendix V). Additionally, we observed that the reaction proceeds under open atmosphere (instead of O_2) affording the desired product **3a** in relatively lower yield as compared to the presence of dioxygen (Table 1, Entry 13). This is probably due to the deprotection of **1a** to corresponding aldehyde as a side product.[15b] Further, the reaction in the absence of light, while maintaining the other standard reaction conditions did not furnish the desired product **3a** (Table 1, Entry 14). The reaction did not proceed in the absence of photocatalyst as well as base (Table 1, Entries, 15 and 16). As expected, the reaction under inert atmosphere (Ar) while maintaining the other initial optimized reaction conditions did not give the desired product **3a** (Table 1, Entry 17). These experimental results strongly support that light, photocatalyst, base, and oxygen are essential for the smooth transformation to access **3a**. Based on the exhaustive screening, cyclic thioacetal **1a** (0.2 mmol) and phenyl thiocyanate **2a** (1.1 equiv), K_3PO_4 (2.5 equiv), Rh6G (2 mol%) in anhydrous MeCN (3 mL), Green LEDs (525 nm, 20 W) under O_2 atmosphere at room temperature proved to be the optimum reaction condition.

Having optimized the reaction condition, we further explored the substrate scope for achieving the practicality and generality of the protocol. Different *para*-substituted electronically neutral as well as electron-rich dithiolane substrates (**1a**–**1d**) under the optimized reaction conditions furnished the corresponding thiocyano–thioester products (**3a**–**3d**) in excellent yields (up to 92%, Scheme 2). Further, dithiolanes (**1e**–**1j)** containing electron withdrawing substituents (—CN, —NO_2) and electron deactivating groups (—F, —Cl, —Br, and —CF_3) have also worked well to give the desired products (**3e—3j**) in very good yields (up to 88%, Scheme 2). Furthermore, various *ortho* and *meta* substituted substrates (**1k**–**1m**) reacted smoothly to afford the corresponding desired products (**3k**–**3m**) in very good yields (up to 84%). In addition, substrates (**1n**,–**1p**) containing allyl, propargyl, and tosyl protected hydroxyl group also well tolerated under optimized reaction conditions to afford the desired products (**3n**,–**3p**) in very good yields (up to 88%, Scheme 2). Additionally, dithiolanes (**1q**–**1t**) bearing disubstitution and trisubstitution on the phenyl ring reacted smoothly to obtain the corresponding thiocyano–thioesters products (**3q**–**3t**) in good to excellent yields (up to 92%, Scheme 2). Moreover, heterocyclic thioacetals derived from thiophene and benzofuran carboxaldehydes (**1u**–**1w)** worked well to give the desired products (**3u**–**3w)** in good to very good yields (up to 88%, Scheme 2). Gratifyingly, polycyclic aromatics **1x**, **1y** naphthalene and pyrene substrates afforded the desired products **3x**, **3y** in moderate to good yields (up to 76%, Scheme 2). Later, we explored the reaction by varying the ring size of thioacetals (from 5 to 8 membered rings, **1z**, **1aa**, and **1ab**) under the optimized reaction to obtain the corresponding thiocyano–thioester products **3z**, **3aa,** and **3ab** in moderate to good yields (up to 63%, Scheme 2). It is very important to highlight that we have successfully isolated the by-product diphenyldisulfide **4a** in quantitative yields in all the cases.

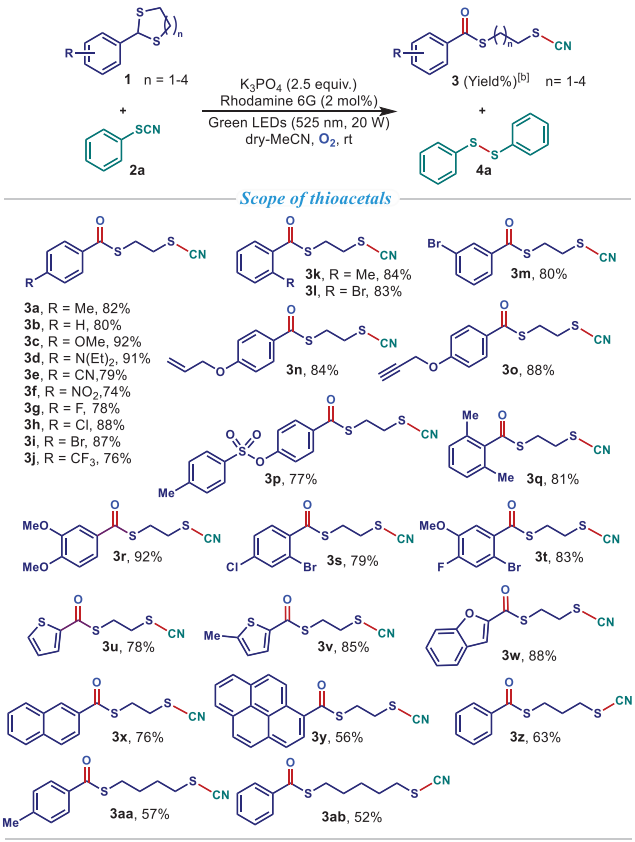

Scheme 2. Substrate scope of thiocyano–thioester products.[a] (Reaction conditions: [a]**1** (0.2 mmol), PhSCN **2a** (1.1 equiv), K_3PO_4 (2.5 equiv), Rhodamine 6G (2 mol%), O_2-balloon, dry-MeCN (3 mL), and Kessil Green LEDs (525 nm, 20 W) at room temperature (rt). [b]Isolated yield after purification by column chromatography).

To decipher the influence of substituents on the phenyl ring of thiocyanate on the yield of thiocyano–thioester product **3a**, the reaction was carried out by varying substituents on phenyl thiocyanates. We carefully evaluated the yields of **3a** as well as the by-product diaryl disulfides **4** (Scheme 3). The electro-neutral and electron donating group on phenyl thiocyanate **2a**–**2c** furnished the desired product **3a** in good yields (up to 82%, Scheme 3). Moreover, phenyl thiocyanate having electron deactivating halo substituents (—F, —Cl, and —Br) **2d**–**2f** gave the corresponding product **3a** in very good yields (up to 84%, Scheme 3). The electron withdrawing —NO_2 group bearing phenyl thiocyanate **2g** offered the product **3a** in very good yield (88%, Scheme 3). Moreover, pyridine thiocyanates **2h** and **2i** furnished **3a** in good yield (up to 81%, Scheme 3). Gratifyingly, we have also isolated the corresponding aryl disulfides **4a**–**4i** (by-products) in very good to almost quantitative yields (up to 98%, see Scheme 3).

To validate the hypothesis on circular economy and reuse of the by-product, we subjected reaction of all the isolated diaryl disulfides with PhSCN **2a** or 4-NO_2-PhSCN **2g** under irradiation of blue LEDs (427 nm, 40 W) for better yields (for detail optimization, see Supporting Information, S11, Table S3). Gratifyingly, we obtained the corresponding aryl thiocyanates **2b**–**2j** in excellent yields (up to 93%, Scheme 4). The protocol

© 2025 Wiley-VCH GmbH

1861471x, 0, Downloaded from https://acesonlinelibrary.wiley.com/doi/10.1002/asia.202500423 by Indian Institute Of Science Education And Research Pune, Wiley Online Library on [23/06/2025]. See the Terms and Conditions (https://onlinelibrary.wiley.com/terms-and-conditions) on Wiley Online Library for rules of use; OA articles are governed by the applicable Creative Commons License

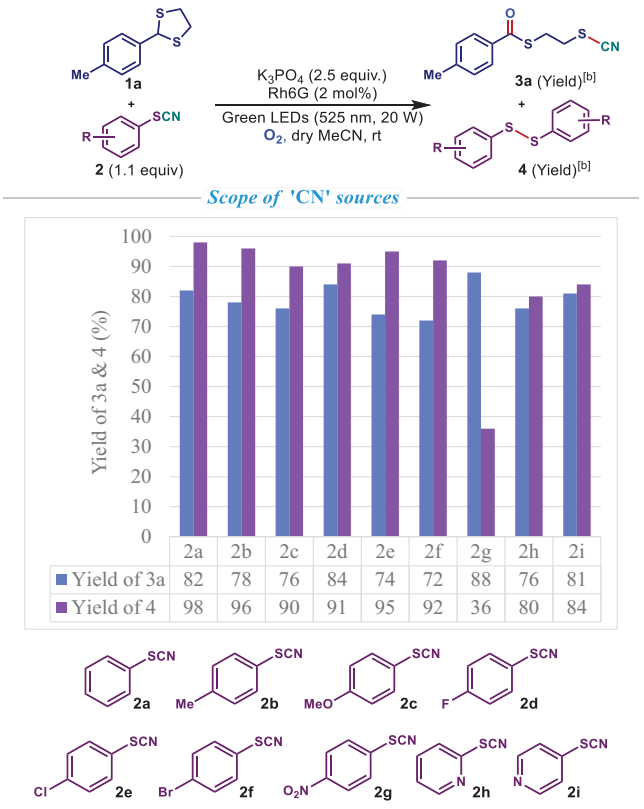

Scheme 3. Screening of 'CN' sources for thiocyano–thioester product.[a] (Reaction conditions:[a] **1a** (0.2 mmol), ArSCN **2** (1.1 equiv), K_3PO_4 (2.5 equiv), Rhodamine 6G (2 mol%), O_2-balloon, dry-MeCN (3 mL), and Kessil Green LEDs (525 nm, 20 W) at room temperature (rt).[b] Isolated yield after purification by column chromatography).

successfully enabled the conversion of isolated by-product diaryl disulfides **4** into various aryl thiocyanates **2** that have been utilized as reagents for the transformation in a circular manner. This reduces the reliance on virgin chemicals (either disulfides or thiocyanates).

To shed light into the reaction mechanism, we carried out a few control experiments systematically. Firstly, to investigate the reactive oxygen species involved during the reaction, we carried out the reaction in presence of well-known singlet oxygen quenchers such as DABCO and NaN_3 (Scheme 5a,b).[16] We observed the formation of **3a** in both the cases, thus clearly indicating that the singlet oxygen might not involve in the reaction. However, the reaction in the presence of well-known superoxide radical anion quencher *p*-benzoquinone while maintaining the other standard reaction conditions did not furnish the desired product **3a**. This result indicates that superoxide radical anion may be involving in the reaction pathway (Scheme 5c).[17] The reaction of dithiolane **1a** in the presence of BHT/TEMPO (radical quencher) did not work, thus confirming the radical nature of the transformation (Scheme 5d). Further, when we performed a reaction without PhSCN under standard reaction condition we obtained the disulfide linked di-thioester product **A4'** from **1a**. Thus, indicating the involvement of thiyl radical **A4** in the reaction (Scheme 5e).

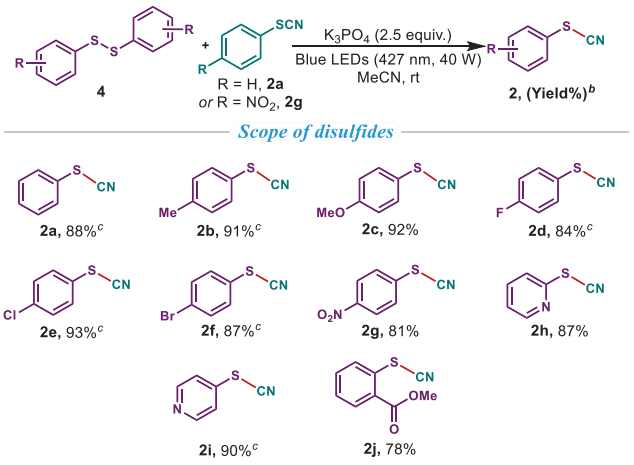

Scheme 4. Substrate scope of thiocyanate products.[a] (Reaction conditions: [a]**4** (0.2 mmol), PhSCN **2a** (2.1 equiv), K_3PO_4 (2.5 equiv), in MeCN (3 mL), Kessil Blue LEDs (427 nm, 40 W) at room temperature (rt), 12 h.[b] Isolated yield after purification by column chromatography. [c] 4-NO_2-PhSCN **2g** (2.1 equiv) was used instead of **2a**, 8 h.).

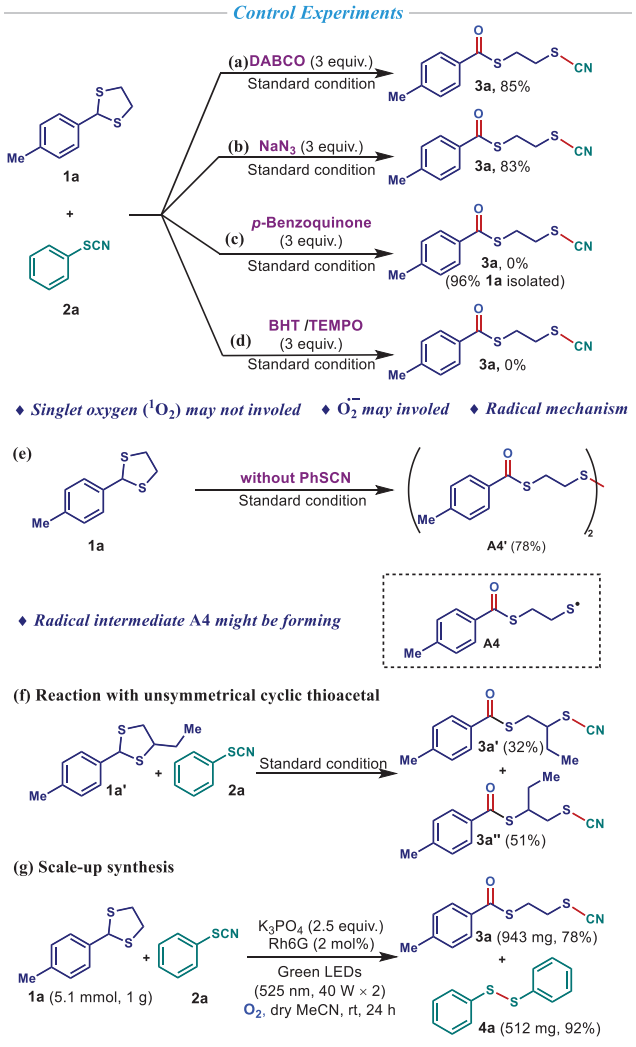

Scheme 5. Control experiments and scale-up synthesis.

© 2025 Wiley-VCH GmbH

1861471x, 0, Downloaded from https://aces.onlinelibrary.wiley.com/doi/10.1002/asia.202500423 by Indian Institute Of Science Education And Research Pune, Wiley Online Library on [23/06/2025]. See the Terms and Conditions (https://onlinelibrary.wiley.com/terms-and-conditions) on Wiley Online Library for rules of use; OA articles are governed by the applicable Creative Commons License

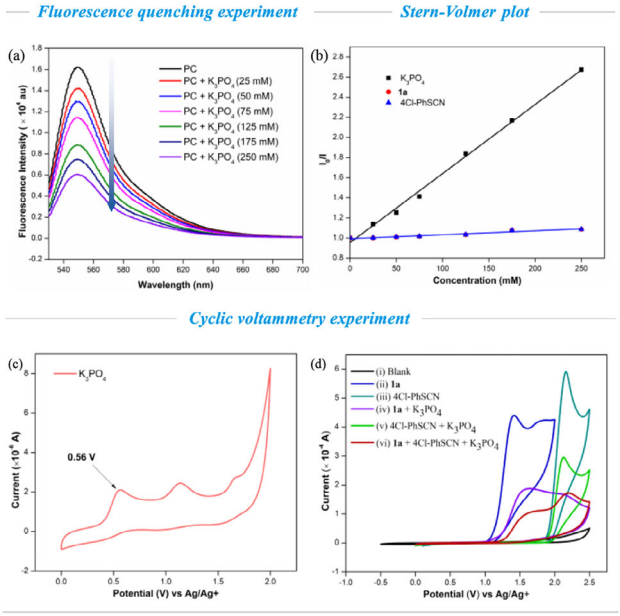

Figure 1. (a) Fluorescence quenching study. (b) Stern–Volmer plot. (c and d) Cyclic voltammetry experiment.

Furthermore, the reaction of unsymmetrical cyclic thioacetal **1a′** with phenyl thiocyanate **2a** under standard conditions, afforded the corresponding thiocyano–thioester products **3a′** and **3a″** in 32% and 51%, respectively, (Scheme 5f). Additionally, the scalability of this protocol was demonstrated on a gram scale (5.1 mmol, 1 g) to access desired product **3a** in a 78% yield (Scheme 5g).

To confirm whether dithioacetal **1a** or thiocyanate **2a** or K_3PO_4 is interacting with the excited state photocatalyst (Rh6G*), we carried out the fluorescence quenching experiment and corresponding Stern–Volmer graph has been plotted (Figure 1a,b and see Supporting Information, S20, Figure S15 for details). This study revealed that K_3PO_4 is effectively interacting with Rh6G* than with **1a** and **2a**. The efficiency of Rh6G* to involve in Single Electron Transfer (SET) with K_3PO_4 was further supported by the oxidation potential of K_3PO_4 (E^{ox} = +0.85 V vs SCE)[18] which is less than the reduction potential of Rh6G* (E^{red*} = +1.39 V vs SCE) (Figure 1c).[19] It is also observed that the reduction potential of Rh6G* is less than the oxidation potential of thioacetal **1a** (E^{ox} = 1.71 V vs SCE) and 4Cl-PhSCN (E^{ox} = 2.45 V vs SCE). Further, cyclic voltammograms were recorded for substrate **1a** and 4Cl-PhSCN in presence of K_3PO_4. It was observed that oxidation potential of **1a** increased from (E^{ox} = 1.42 V vs Ag/Ag^+) to (E^{ox} = 1.60 V vs Ag/Ag^+) in the presence of K_3PO_4, implying interaction of K_3PO_4 with **1a** after the oxidation of K_3PO_4 (Figure 1d and see Supporting Information, S20,S21, Figure S16 for details).

Based on the control experiments, Stern–Volmer plot, cyclic voltammetry studies and preceding literature,[10,20] a possible reaction mechanism has been depicted in (Scheme 6). It is proposed that upon irradiation with green light, the photocatalyst Rh6G will get excited to Rh6G*. This excited species Rh6G* (E^{red*} = +1.39 V vs SCE) will involve in SET process with K_3PO_4 (E^{ox} = +0.85 V vs SCE) via reductive quenching pathway to

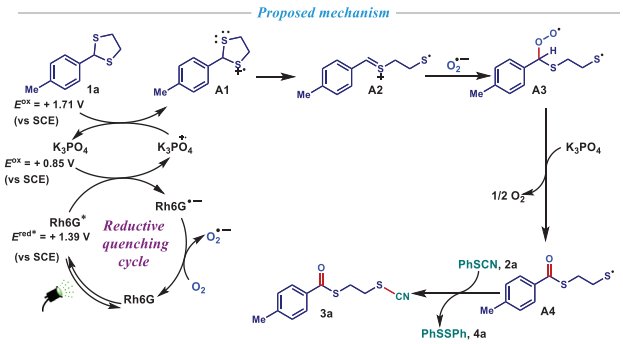

Scheme 6. Proposed reaction mechanism for thiocyano–thioester formation.

generate the photocatalyst radical anion ($Rh6G^{\bullet-}$) and $[K_3PO_4]^{\bullet+}$. This SET event was suggested by the Stern–Volmer experimental studies and cyclic voltammetry experiment (Figure 1). Further, $Rh6G^{\bullet-}$ takes part in another SET event with oxygen to generate a superoxide radical anion ($O_2^{\bullet-}$) and the ground-state Rh6G, thus completing the photocatalytic cycle. Alongside, the reactive radical cation species - $[K_3PO_4]^{\bullet+}$ reacts with dithiolane **1a** to form an intermediate **A1**. Then **A1** would further undergo ring opening to form intermediate **A2**. Later, the nucleophilic superoxide anion ($O_2^{\bullet-}$) will attack on the intermediate **A2** at the electrophilic carbon to generate intermediate **A3**. Further, K_3PO_4 abstracts a proton and the subsequent removal of O_2 generates thiyl radical intermediate **A4** (the dimer of **A4** has been isolated and analyzed by ^1H, ^{13}C NMR, HRMS, Scheme 5e).[20] Further, this intermediate reacts with PhSCN **2a** to form the desired thiocyano–thioester product **3a** along with the formation of diphenyl disulfide **4a** as a by-product.

Additionally, to propose a possible reaction mechanism for the thiocyanate formation from disulfide, we performed a few control experiments (see Supporting Information, S11–S16, Scheme S1–S3) such as radical trapping experiments with TEMPO and BHT. The results indicated that the reaction is going via radical pathway. Further, UV-vis absorption experiments were performed (see Supporting Information, S18,S19, Figures S13,S14) and the absorption spectra revealed that the individual components (**4a** or **2g**) absorb only below 380 nm (see Supporting Information, S18, Figure S13). Hence, these compounds (**4a**, **2g**) are not photoactive under visible light. In addition, the mixture of **2g** and K_3PO_4 exhibits a pronounced bathochromic shift into the visible region, with a new absorption peak (λ_{max}) appearing around 486 nm and extending up to 550 nm (see Supporting Information, S18, Figure S13, pink curve). In contrast, no such shift was observed for the mixtures of **4a** with K_3PO_4 (see Supporting Information, S18, Figure S13, green curve) or **4a** with **2g** (see Supporting Information, S18, Figure S13, violet curve). These findings suggest that **2g** and K_3PO_4 form a new photoactive electron donor–acceptor (EDA) complex. Further, the absorption spectra revealed that the individual components (**4h** or **2a**) absorb only below 310 nm (see Supporting Information, S19, Figure S14). Hence, these compounds (**4h**, **2a**) are not photoactive under visible light as well. Notably, the mixture of **4h** and K_3PO_4 exhibits a significant bathochromic shift into the visible region,

© 2025 Wiley-VCH GmbH

1861471x, 0, Downloaded from https://acesonlinelibrary.wiley.com/doi/10.1002/asia.202500423 by Indian Institute Of Science Education And Research Pune, Wiley Online Library on [23/06/2025]. See the Terms and Conditions (https://onlinelibrary.wiley.com/terms-and-conditions) on Wiley Online Library for rules of use; OA articles are governed by the applicable Creative Commons License

with a new absorption peak (λ_{max}) emerging around 370 nm and extending up to 430 nm (see Supporting Information, S19, Figure S14, green curve). In contrast, no such shift was observed for the mixtures of **2a** with K_3PO_4 (see Supporting Information, S19, Figure S14, blue curve) or **4h** with **2a** (see Supporting Information, S19, Figure S14, pink curve). These findings indicate that **4h** and K_3PO_4 likely form a new photoactive electron donor–acceptor (EDA) complex in situ. Moreover, when the reaction of **4h** with **2a** was stopped (after 6 h), a new intermediate that was isolated proved to be heterodisulfide **4ha** (see Supporting Information, S14–S16, Scheme S3 and Figures S9–S11). This result further supported the light-induced cleavage of disulfide **4h** to generate a thiyl radical followed by reaction with phenyl thiocyanate **2a** to afford heterodisulfide **4ha**.

Based on these control experiments, UV-vis absorption experiments and literature report[22] we have proposed two possible pathways for the formation of thiocyanates **2** (for details see Supporting Information, S22, Figure S18A,B).

3. Conclusion

In summary, aryl thiocyanates have been utilized as sustainable alternative organic 'CN' source for the cyanation of cyclic thioacetals. Diaryl disulfides formed as by-products were isolated and successfully reused for synthesizing various aryl thiocynates in excellent yields. Likewise, different aryl thiocyanates synthesized were effectively employed for accessing thiocyano–thioesters. We have demonstrated the utility of both by-products as well as products formed for the further utility in circular manner and abiding the principle of circular economy, thus reducing the dependency of the virgin chemicals. This protocol proved to be applicable to a wide variety of substrates with respect to thioacetals as well as disulfides. The methods worked under the irradiation of visible light (Green and Blue LEDs) as clean energy source and do not rely on external chemical oxidizing reagent. A series of control experiments, UV-vis absorption spectroscopic, fluorescence quenching, and cyclic voltammetric studies proved that thiocyano-thioester formation is driven via reductive quenching mechanistic cycle.

Supporting Information

General experimental procedures, the detailed optimization of the reaction conditions, fluorescence quenching plot, cyclic voltammograms, UV-vis absorption spectra, general characterization data, and copies of ^{1}H, $^{13}C\{^{1}H\}$ and $^{19}F\{^{1}H\}$ NMR spectra (PDF). The authors have cited additional references within the Supporting Information.[20,21]

Acknowledgements

Ramakrishna G. Bhat thanks Science and Engineering Research Board, Department of Science and Technology (SERB-DST), New Delhi, Government of India (CRG/2023/004226) for the generous research grant. The authors also thank IISER Pune for financial assistance. Mousumi Behera and Shubham Y. Shukla thank IISER Pune and Pankaj D. Dharpure thanks CSIR, New Delhi for the fellowship.

Conflict of Interests

The authors declare no conflict of interest.

Data Availability Statement

The data that support the findings of this study are available in the supplementary material of this article.

Keywords: 'CN' source · Aryl thiocyanate · Circular chemical economy · Cyclic thioacetals · Thiocyano–thioesters

[1] a) *Chemistry of the Cyano Group*, (Ed: Z. Rappoport), Wiley, London, England **1970**; b) R. C. Larock, *Comprehensive Organic Transformations*, Wiley-VCH, New York **1989**, pp. 819; c) Z. P. Demko, K. B. Sharpless, *J. Org. Chem.* **2001**, *66*, 7945–7950; d) W. He, C. Li, L. Zhang, *J. Am. Chem. Soc.* **2011**, *133*, 8482–8485; e) C. Si, A. G. Myers, *Angew. Chem., Int. Ed.* **2011**, *50*, 10409–10413; f) A. Rakshit, H. N. Dhara, A. K. Sahoo, B. K. Patel, *Chem. Asian J.* **2022**, *17*, e202200792.
[2] a) C. Scotti, J. W. Barlow, *Nat. Prod. Commun.* **2022**, *17*, 1–24; b) J.-R. Liu, Y. Gao, B. Jin, D. Guo, F. Deng, Q. Bian, H.-F. Zhang, X.-Y. Han, A.S. Ali, M.-Z. Zhang, W.-H. Zhang, Y.-C. Gu, *Mar. Drugs* **2023**, *21*, 103–116; c) W.-C. Chen, S. Nachimuthu, J.-C. Jiang, *Sci. Rep.* **2017**, *7*, 4979–4991; d) F. F. Fleming, L. Yao, P. C. Ravikumar, L. Funk, B. C. Shook, *J. Med. Chem.* **2010**, *53*, 7902–7917.
[3] H. Wang, C. Zhao, Z. Burešová, F. Bureš, J. Liu, *J. Mater. Chem. A* **2023**, *11*, 3753–3770.
[4] a) R. Bhattacharya, S. J. Flora, *Handbook of Toxicology of Chemical Warfare Agents*, (Ed: R. C. Gupta), Academic Press, Boston **2009**, pp. 255–270; b) A. M. Nauth, T. Opatz, *Org. Biomol. Chem.* **2019**, *17*, 11–23.
[5] a) J. Jin, Q. Wen, P. Lu, Y. Wang, *Chem. Commun.* **2012**, *48*, 9933–9935; b) Z. Zhang, L. S. Liebeskind, *Org. Lett.* **2006**, *8*, 4331–4333.
[6] a) J. Kim, H. J. Kim, S. Chang, *Angew. Chem., Int. Ed.* **2012**, *51*, 11948–11959; b) G. Yan, Y. Zhang, J. Wang, *Adv. Synth. Catal.* **2017**, *359*, 4068–4105; c) T. Najam, S. S. A. Shah, K. Mehmood, A. U. Din, S. Rizwan, M. Ashfaq, S. Shaheen, A. Waseem, *Inorg. Chim. Acta* **2018**, *469*, 408–423.
[7] J.-T. Yu, F. Teng, J. Cheng, *Adv. Synth. Catal.* **2017**, *359*, 26–38.
[8] a) B. König, *Eur. J. Org. Chem.* **2017**, *2017*, 1979–1981; b) M. Akita, P. Ceroni, C. R. J. Stephenson, G. Masson, *J. Org. Chem.* **2023**, *88*, 6281–6283.
[9] R. I. Patel, S. Sharma, A. Sharma, *Org. Chem. Front.* **2021**, *8*, 3166–3200.
[10] P. D. Dharpure, M. Behera, V. V. Khade, A. S. Thube, R. G. Bhat, *Org. Lett.* **2022**, *24*, 6919–6924. Though the strategy found to be convenient, the usage of excess reagent and in turn generation of stochiometric water soluble waste may not be attractive from environmental hazard point view.
[11] a) T. Castanheiro, J. Suffert, M. Donnard, M. Gulea, *Chem. Soc. Rev.* **2016**, *45*, 494–505; b) B. D. Grishchuk, N. G. Prodanchuk, V. G. Sinchenko, P. M. Gorbovoi, E. Y. Kudrik, *Pharm. Chem. J.* **1994**, *28*, 657–659; c) S. H. Szajnman, W. Yan, B. N. Bailey, R. Docampo, E. Elhalem, J. B. Rodriguez, *J. Med. Chem.* **2000**, *43*, 1826–1840.
[12] J. Franke, C. Hertweck, *Cell Chem. Biol.* **2016**, *23*, 1179–1192.
[13] a) J. H. Clark, T. J. Farmer, L. Herrero-Davila, J. Sherwood, *Green Chem.* **2016**, *18*, 3914–3934; b) W. Haas, F. Krausmann, D. Wiedenhofer, M. Heinz, *J. Ind. Ecol.* **2015**, *19*, 765–777.
[14] a) B. Saxena, R. I. Patel, A. Sharma, *Green Chem.* **2024**, *26*, 11650–11661; b) R. I. Patel, B. Saxena, A. Sharma, *Green Chem.* **2024**, *26*, 10265–10274.

© 2025 Wiley-VCH GmbH

1861471x, 0, Downloaded from https://acess.onlinelibrary.wiley.com/doi/10.1002/asia.202500423 by Indian Institute Of Science Education And Research Pune, Wiley Online Library on [23/06/2025]. See the Terms and Conditions (https://onlinelibrary.wiley.com/terms-and-conditions) on Wiley Online Library for rules of use; OA articles are governed by the applicable Creative Commons License

[15] a) M. Behera, S. Y. Shukla, P. D. Dharpure, R. G. Bhat, *ChemRxiv* **2025**, 1–6. DOI: 10.26434/chemrxiv-2025-p2cbf; b) P. D. Dharpure, A. Bhowmick, P. K. Warghude, R. G. Bhat, *Tetrahedron Lett.* **2020**, *61*, 151407–151415.
[16] a) J.-T. Guo, D.-C. Yang, Z. Guan, Y.-H. He, *J. Org. Chem.* **2017**, *82*, 1888–1894; b) M. Bancirova, *Luminescence* **2011**, *26*, 685–688; c) J. R. Harbour, S. L. Issler, *J. Am. Chem. Soc.* **1982**, *104*, 903–905.
[17] M. Pelaez, P. Falaras, V. Likodimos, K. O'shea, A. De la Cruz, P. S. M. Dunlop, J. A. Byrne, D. D. Dionysiou, *J. Mol. Catal. A Chem.* **2016**, *425*, 183–189.
[18] The measured potentials were recorded with respect to an $Ag/AgNO_3$ (0.01 M) reference electrode. The values of redox potentials (vs $Ag/AgNO_3$) are converted into those vs SCE by addition of 0.29 V.C. K. Mann, K. K. Barnes, *Electrochemical Reactions in Nonaqueous Systems*, Marcel Dekker, New City, New York **1970**.
[19] a) A. Dietrich, V. Buschmann, C. Müller, M. Sauer, *Rev. Mol. Biotechnol.* **2002**, *82*, 211–231; b) S. Doose, H. Neuweiler, M. Sauer, *ChemPhysChem* **2009**, *10*, 1389–1398.
[20] P. D. Dharpure, M. Behera, A. S. Thube, R. G. Bhat, *Chem.-Asian J.* **2023**, *18*, e202201128.
[21] a) I. W. J. Still, I. D. G. Watson, *Synth. Commun.* **2001**, *31*, 1355–1359; b) X. Zhu, Z. Xie, X. Chen, M. Mu, H. Wu, M. Sun, J. Yang, L. Wanga, Z. Wang, *J. Org. Chem.* **2024**, *89*, 14940–14950; c) C. K. Mann, K. K. Barnes, *Electrochemical Reactions in Nonaqueous Systems*, Marcel Dekker, New City, New York **1970**.
[22] Z. Li, S. Wang, Y. Huo, B. Wang, J. Yan, Q. Guo, *Org. Chem. Front.* **2021**, *8*, 3076–3081.

Manuscript received: March 10, 2025
Revised manuscript received: May 6, 2025
Version of record online: ■■, ■■

© 2025 Wiley-VCH GmbH

1861471x, 0, Downloaded from https://acesonlinelibrary.wiley.com/doi/10.1002/asia.202500423 by Indian Institute Of Science Education And Research Pune, Wiley Online Library on [23/06/2025]. See the Terms and Conditions (https://onlinelibrary.wiley.com/terms-and-conditions) on Wiley Online Library for rules of use; OA articles are governed by the applicable Creative Commons License

JOC The Journal of Organic Chemistry

pubs.acs.org/joc Article

Visible Light-Induced Organophotoredox-Catalyzed β-Hydroxytrifluoromethylation of Unactivated Alkenes

Mousumi Behera, Pankaj D. Dharpure, Ajit K. Sahu, and Ramakrishna G. Bhat*

Cite This: J. Org. Chem. 2024, 89, 14695−14709 Read Online

ACCESS | Metrics & More | Article Recommendations | Supporting Information

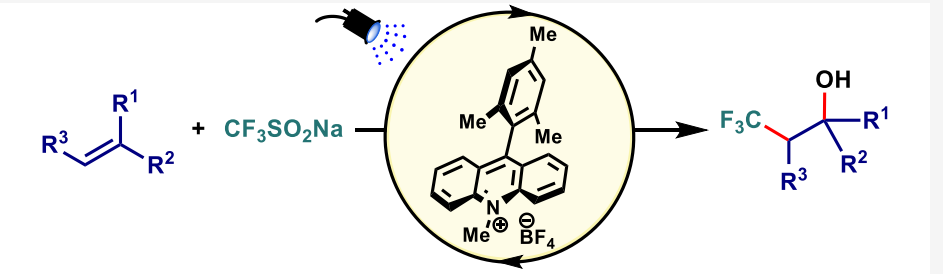

♦ Transition metal-free ♦ Organic photocatalyst ♦ Diverse functional group tolerance
♦ Functionalization of natural products ♦ Terminal & internal alkenes ♦ Up to 86% yield

ABSTRACT: Herein, we report a mild transition metal-free organophotoredox-catalyzed approach for β-hydroxytrifluoromethylation of unactivated alkenes using CF_3SO_2Na and acridinium salt. The protocol is compatible with various mono-, di-, and trisubstituted aliphatic unactivated alkenes containing numerous functional groups and natural product derivatives. Further, the postsynthetic modifications of the synthesized trifluoromethylated products have been demonstrated through cross-coupling and functional group interconversion reactions. The method proved to be scalable and it works smoothly under the direct exposure of sunlight. A plausible mechanism has been proposed based on the fluorescence quenching experiment and cyclic voltammetry analysis.

Downloaded via IISER PUNE on June 23, 2025 at 13:57:37 (UTC).
See https://pubs.acs.org/sharingguidelines for options on how to legitimately share published articles.

INTRODUCTION

Trifluoromethylation is one of the key transformations in organic synthesis. Incorporating a trifluoromethyl group into the organic molecules drastically amplifies electronegativity, polarizability and various pharmacokinetic properties such as lipophilicity, metabolic stability and bioavailability.[1] Consequently, the number of trifluoromethylated organic compounds have been increasing in pharmaceuticals,[1b−d] agrochemicals,[1e,f] functional materials (liquid crystal displays, LCDs),[1g] and useful tracers for positron emission tomography (PET) imaging.[1h,i] Thus, over the years extensive efforts have been made to develop synthetic strategies for the trifluoromethylation of diverse organic molecules.[2] Among these, alkenes are one of the easily accessible, abundant and robust carbon feedstocks to synthesize commodity chemicals. More importantly, the unique reactivity of alkenes in difunctionalization reactions has proven to be useful in synthetic transformations to construct a wide range of compounds.[3] Specifically, the direct hydroxy trifluoromethylative difunctionalization of activated alkenes such as styrene derivatives has been explored via transition metal catalysis and also through other conventional methods to access trifluoromethylated alcohols.[4] However, the direct difunctionalization leading to trifluoromethylation of unactivated alkenes has been elusive in the literature probably due to the relative inertness of unactivated alkenes. This might be due to their higher oxidation potential compared to styrenes.[5a,b] Consequently, there are only a few reports available in the literature for the direct hydroxytrifluoromethylation of unactivated alkenes.[5c,d] However, these transformations either rely on transition metal catalyst or require elevated temperature.

Over the recent years, the visible light photoredox catalysis has made significant contribution as a useful and alternative tool to access myriads of organic compounds.[6] In this regard, photocatalytic trifluoromethylative difunctionalization of alkenes has emerged as a new synthetic methodology.[7] Recently, in 2020, Wan research group has developed a metallaphotocatalyzed [$Mn(acac)_3$] protocol for hydroxytrifluoromethylation of unactivated alkenes (Scheme 1a).[8] Despite the synthetic utility of transition metal photocatalysts, organo-

Received: April 22, 2024
Revised: September 19, 2024
Accepted: September 25, 2024
Published: October 9, 2024

© 2024 American Chemical Society

https://doi.org/10.1021/acs.joc.4c00967
J. Org. Chem. 2024, 89, 14695−14709

Scheme 1. Approaches for the Synthesis of β-Trifluoromethyl Alcohols

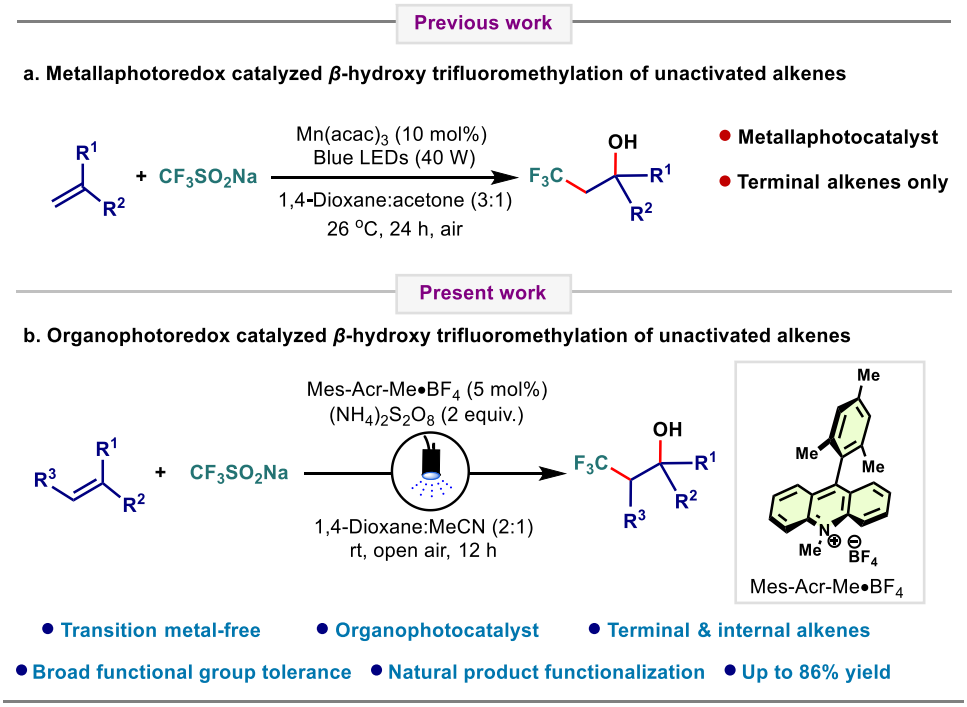

photoredox catalysts are preferred due to their environmental viability and sustainability.[9]

Interestingly, to the best of our knowledge there are no reports for the organophotoredox-catalyzed β-hydroxytrifluoromethylation of unactivated alkenes in the literature. As a part of our ongoing research program dedicated to organophotoredox catalysis, we sought to develop a transition metal free strategy for accessing β-trifluoromethylated alcohols of unactivated alkenes using an organophotoredox catalyst under visible light.[10] Herein, we report the organophotoredox-catalyzed direct hydroxy trifluoromethylation of unactivated alkenes under visible light irradiation at room temperature (Scheme 1b).[10g]

RESULTS AND DISCUSSION

We commenced our reaction optimization studies with allyl benzoate **1a** and sodium trifluoromethanesulfinate **2** as model substrates. Upon systematic and detailed investigation of the reaction conditions, Mes-Acr-Me·BF_4 (5 mol %) as an organophotoredox catalyst and $(NH_4)_2S_2O_8$ as an oxidant in 1,4-Dioxane/MeCN (2:1, 3 mL) using Kessil blue LEDs (467 nm, 20 W) under open air proved to be advantageous for accessing the desired hydroxytrifluoromethylated product **3a** in very good yield (77%, Table 1, Entry 1). Importantly, no product formation was observed in the absence of light, photocatalyst, oxidant, and under argon atmosphere (Table 1, Entries 2−5). To further optimize the reaction conditions, we screened different organophotocatalysts such as Eosin Y, Rhodamine 6G (Rh6G), Riboflavin, Fluorescein, and others (see Supporting Information, S3, Table S2 for details). However, all these afforded the desired trifluoromethylated product **3a** albeit in lower yield and among all Mes-Acr-Me·BF_4 proved to be the most advantageous to obtain **3a** in higher yield (Table 1, Entry 1). Notably, the transition metal photocatalyst $Ru(bpy)_3{\cdot}2PF_6$ did not afford the desired product (Table 1, Entry 6). Subsequent screening of solvents

Table 1. Optimization of Reaction Conditions[a]

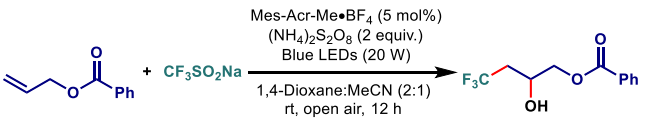

entry	deviations from standard condition	yield (%)[b]
1	**none**	77 (65)[c]
2	no light	NR
3	no photocatalyst	NR
4	no oxidant	NR
5	Ar-atm instead of open air	NR
6[d]	$Ru(bpy)_3.2PF_6$ instead of Mes-Acr-Me·BF_4	ND
7	MeCN as a solvent	55
8	1,4-dioxane as a solvent	60

[a]**Standard reaction conditions**: **1a** (0.2 mmol), CF_3SO_2Na **2** (3 equiv), $(NH_4)_2S_2O_8$ (2 equiv), Mes-Acr-Me·BF_4 (5 mol %) in 1,4-Dioxane:MeCN (2:1, 3 mL), Kessil Blue LEDs (467 nm, 20 W) for 12 h at room temperature (rt). [b]Determined by ^1H NMR analysis using 1,3,5-Trimethoxybenzene as an internal standard. [c]Isolated yield. [d]Blue LEDs (20 W) and MeCN instead of Kessil Blue LEDs and Dioxane:MeCN (2:1, 3 mL) respectively. NR = No Reaction. ND = Not Detected.

including polar aprotic as well as protic, nonpolar, and halogenated ones such as acetonitrile or 1,4-dioxane, among others, lowered the yield of **3a** (Table 1, Entries 7, 8 and see Supporting Information, S4, Table S3 for details). We observed the highest yield of **3a** in mixture of 1,4-Dioxane:MeCN (Table 1, Entry 1). Later, various oxidants like $PhI(OAc)_2$, $Na_2S_2O_8$, $K_2S_2O_8$ and TBHP were screened (see Supporting Information, S4, Table S4 for details) and among all $(NH_4)_2S_2O_8$ proved to be the most efficient (Table 1, Entry 1). Further, various monochromatic Blue LEDs were screened (see Supporting Information, S5, Table S5 for details) among all Blue LED 467 nm proved to be best by

https://doi.org/10.1021/acs.joc.4c00967
J. Org. Chem. 2024, 89, 14695−14709

Table 2. Substrate Scope of β-Trifluoromethyl Alcohols[a]

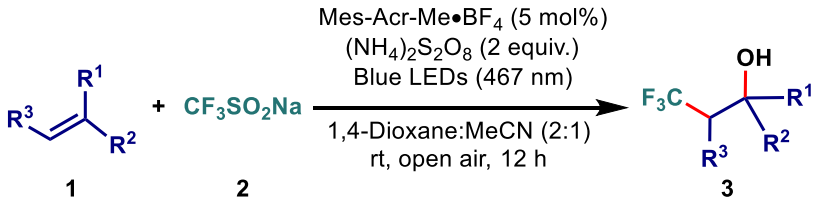

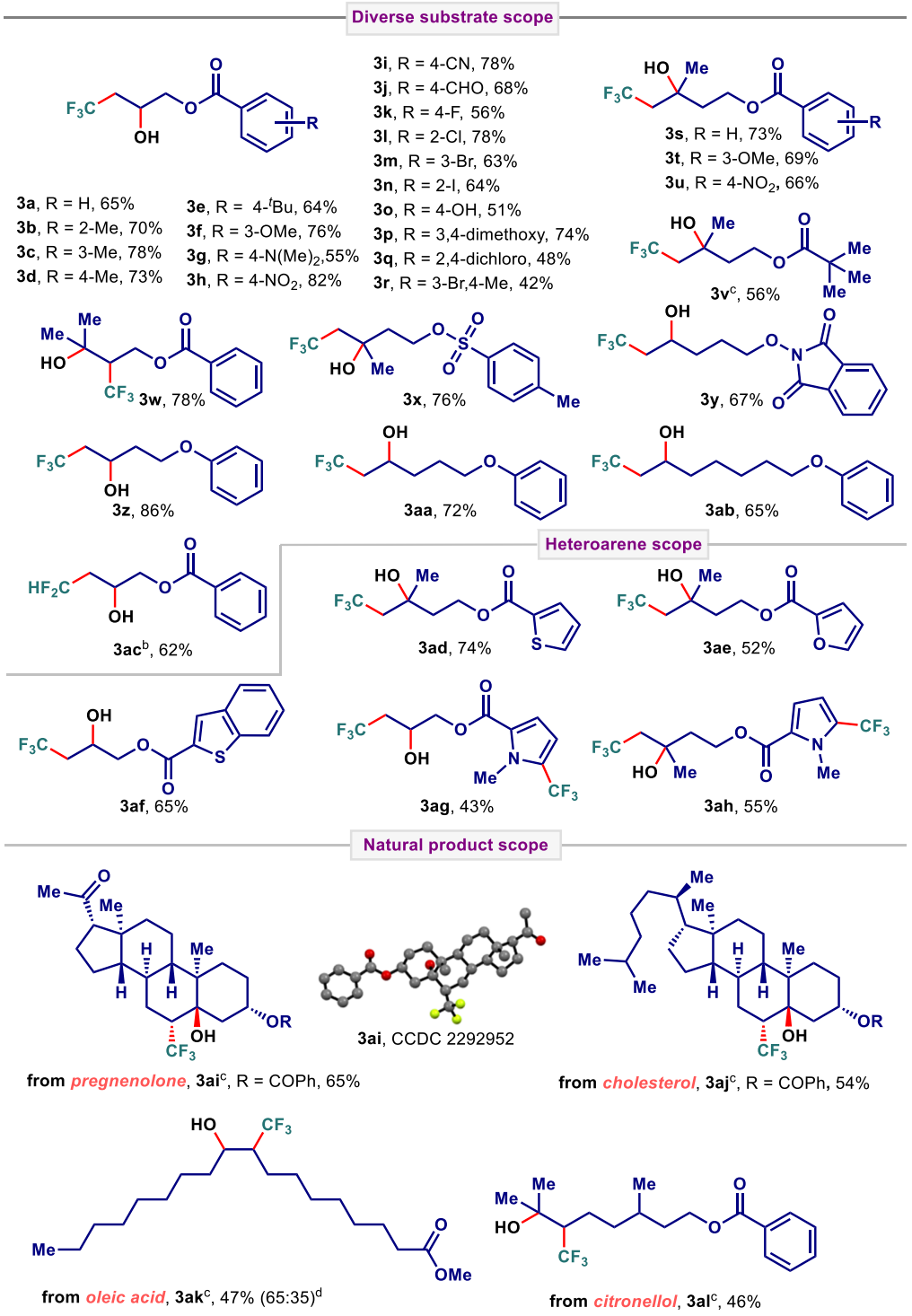

[a]**Reaction conditions**: **1** (0.2 mmol), CF_3SO_2Na **2** (3 equiv), $(NH_4)_2S_2O_8$ (2 equiv), Mes-Acr-Me·BF_4 (5 mol %), 1,4-Dioxane:MeCN (2:1, 3 mL), blue LEDs (467 nm, 20 W), rt, open air, 12 h. [b]CF_2HSO_2Na **2a** (3 equiv) instead of **2**, 36 h. [c]1,4-Dioxane (3 mL), 36 h. [d]NMR analysis did not allow to conclusively distinguish between *r.r.* or *d.r.*

https://doi.org/10.1021/acs.joc.4c00967
J. Org. Chem. 2024, 89, 14695−14709

Scheme 2. Postsynthetic Application and Scale Up Reaction

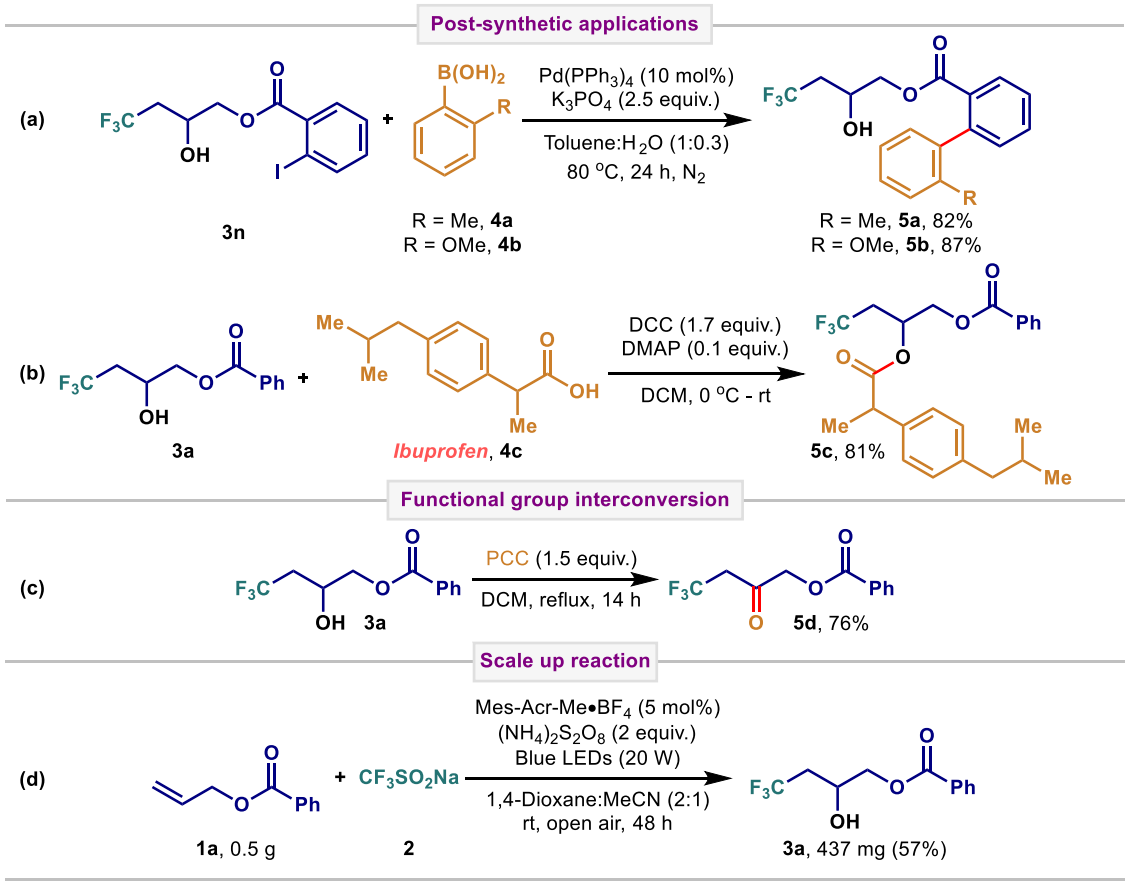

affording compound **3a** in very good yield (Table 1, Entry 1). Based on the exhaustive screening, allyl benzoate **1a** (0.2 mmol), sodium trifluoromethanesulfinate **2** (3 equiv), $(NH_4)_2S_2O_8$ (2 equiv), Mes-Acr-Me·BF_4 (5 mol %), 1,4-Dioxane:MeCN (2:1, 3 mL), and Blue LED (467 nm, 20 W) under open air atmosphere at room temperature for 12 h proved to be the optimum reaction conditions.

Having obtained the optimum reaction condition, we planned to explore the substrate scope for achieving the practicality and generality of the protocol. All the electronically neutral and rich allyl benzoates (**1a**−**1e**) under the optimized reaction conditions afforded the corresponding desired products (**3a**−**3e**) in good yields (up to 78%, Table 2). Additionally, allyl benzoates having electron donating groups such as 3-methoxy **1f** and 4-*N*,*N*-dimethyl amine **1g** reacted smoothly to obtain the corresponding hydroxytrifluoromethylated products (**3f, 3g**) in good yields (up to 76%, Table 2). Further, different allyl benzoates containing electron withdrawing substituents (−NO_2, −CN and −CHO) (**1h**−**1j**) also worked well under the optimized reaction condition to furnish the desired products (**3h**−**3j**) in very good yields (up to 82%, Table 2). Notably, allyl benzoates (**1k**−**1n**) bearing electron deactivating groups such as fluoro, chloro, bromo, and even iodo at *o*/*m*/*p*-positions on the arene ring were compatible under the reaction conditions to afford the corresponding products (**3k**−**n**) in good yields (up to 78%, Table 2). Gratifyingly, these products can be further utilized for different transformations (see below, Scheme 2). Even the arene having unprotected hydroxyl group **1o** reacted smoothly under the reaction conditions to furnish the corresponding trifluoromethylated alcohol **3o** in moderate yield (Table 2). In addition, disubstituted arene derivatives (**1p**−**1r**) gave the desired products (**3p**−**3r**) in moderate to good yields (up to 74%, Table 2). Moreover, 1,1-disubstituted terminal alkene derived benzoates having electron neutral, electron rich as well as electron poor substituents (**1s**−**1u**) furnished the corresponding alcohols (**3s**−**3u**) in moderate to good yields (up to 73%, Table 2). The alkene linked aliphatic ester derivative **1v** afforded the desired product **3v** (56%, Table 2). Additionally, trisubstituted internal alkene **1w** found to be reactive under the reaction condition to give the *anti*-Markonikov adduct **3w** in good yield (78%, Table 2). Later, we explored the alkene substrates containing functional groups such as sulfonate **1x** and oxy-isoindolinedione **1y** under optimized reaction condition to accomplish the corresponding products (**3x**, **3y**) in good yields (up to 76%, Table 2). Furthermore, arene ether linked alkenes with varying chain lengths (**1z, 1aa, 1ab**) underwent hydroxytrifluoromethylation easily to furnish the desired products (**3z**, **3aa**, **3ab**). Further, we obtained *β*-difluoromethyl alcohol product **3ac** by reaction of CF_2HSO_2Na **2a** with **1a**. Moreover, the furan, thiophene and benzothiophene heterocycles having alkene moiety (**1ad**−**1af**) afforded the desired products (**3ad**−**3af**) in moderate to good yields (up to 74%, Table 2). Interestingly, *N*-methylated pyrrole tethered alkenes (**1ag**−**1ah**) gave the bis-trifluoromethylated products (**3ag**−**3ah**) (simultaneous trifluoromethylation of alkene and heterocyclic ring) exclusively unlike the furan and thiophene derived alkenes (up to 55%, Table 2). This might be probably due to the high nucleophilicity of the

https://doi.org/10.1021/acs.joc.4c00967
J. Org. Chem. 2024, 89, 14695−14709

Scheme 3. Control Experiments

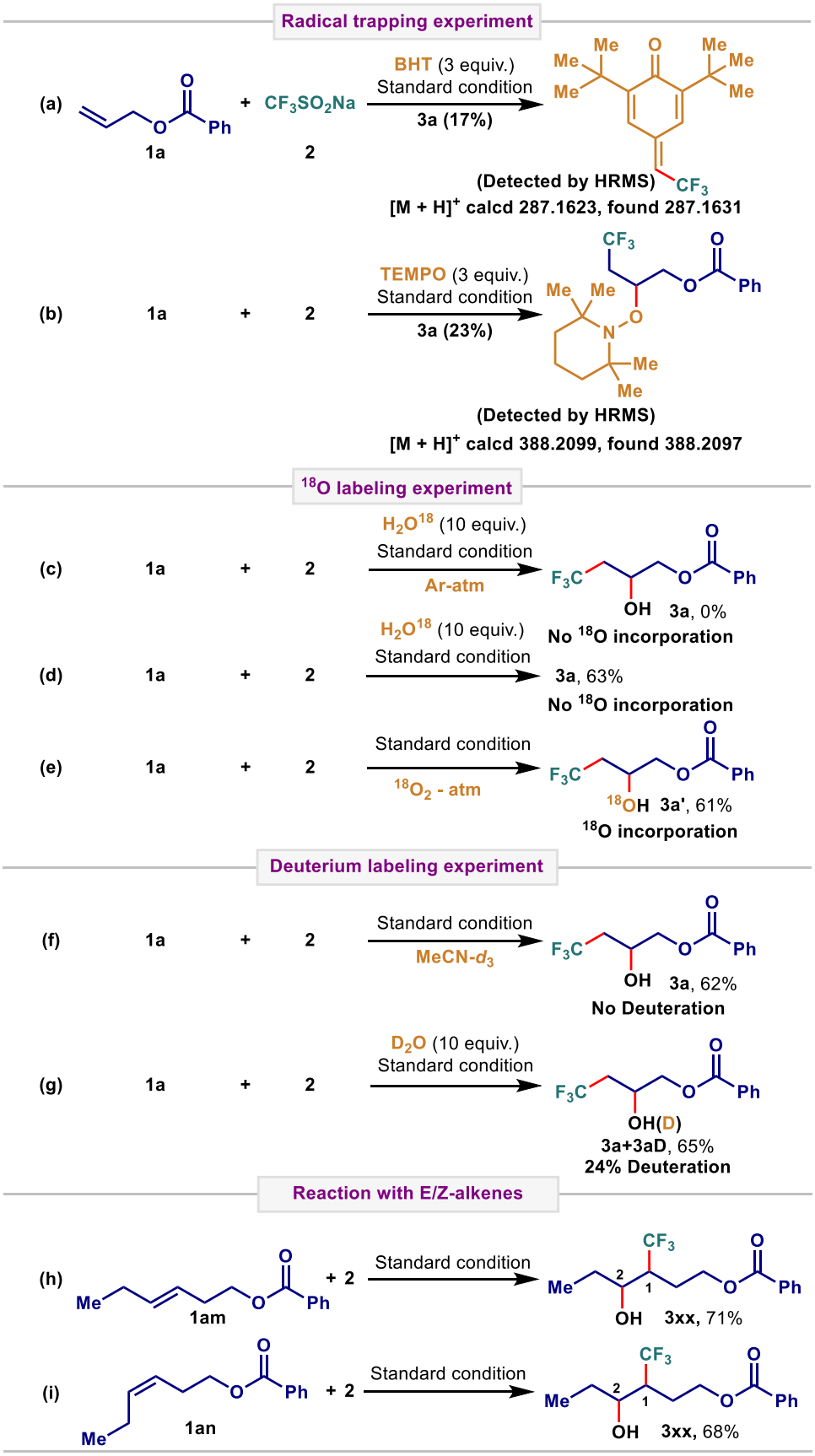

https://doi.org/10.1021/acs.joc.4c00967
J. Org. Chem. 2024, 89, 14695−14709

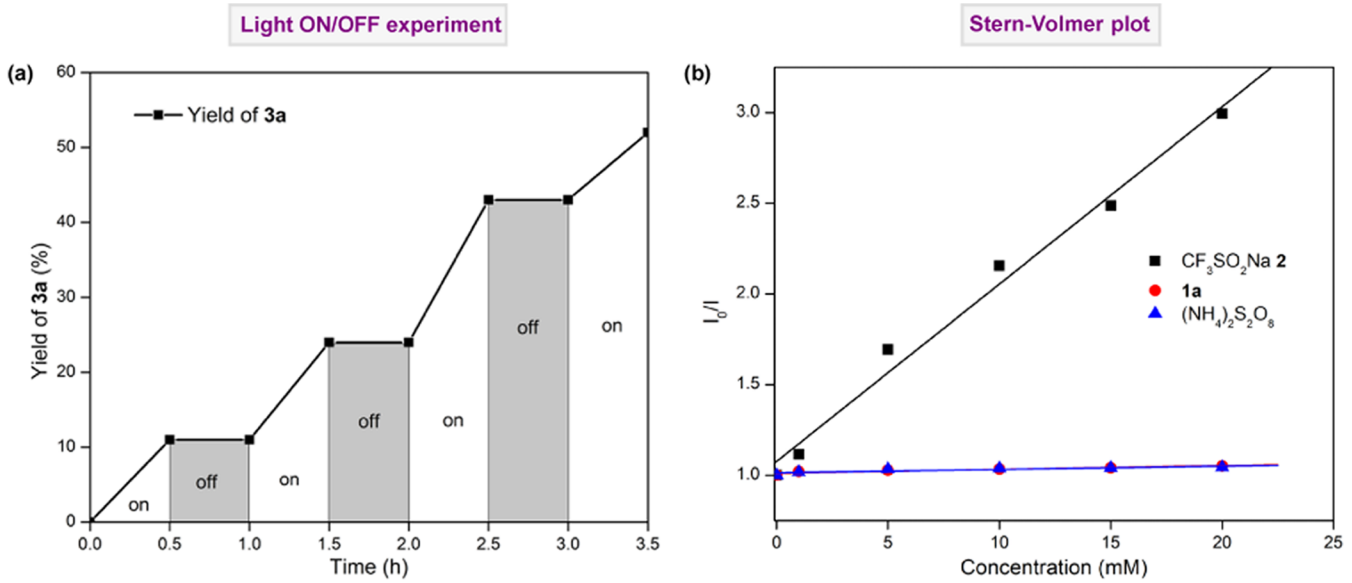

Figure 1. (a) Light ON/OFF experiment. (b) Stern–Volmer plot.

pyrrole ring thus resulting in the photooxidation of the pyrrole ring followed by the trifluoromethylation at the ring.

To further demonstrate the versatility of this protocol, we explored the reaction of commercially available natural products (pregnenolone and cholesterol) derived substrates (**1ai**–**1aj**) under the optimized reaction conditions to give the desired products (**3ai**–**3aj**) (Table 2). Later, the molecular structure of **3ai** has been unambiguously characterized by single crystal X-ray diffraction analysis and it proved the *anti*-addition of hydroxyl and trifluoromethyl group across the double bond.[11] Based on the analogy of **3ai**, we have assigned the stereochemistry of **3aj**. Notably, methyl ester derived from natural omega-nine fatty acid such as oleic acid (*cis*-9-octadecenoic acid) led to the formation of corresponding trifluoromethylated alcohol **3ak**. Furthermore, citronellyl benzoate **1al** (derived from natural citronellol used in perfumes and as a fragrance in cleaning products) also underwent reaction to afford the corresponding trifluoromethylated alcohol **3al** in modest yield (46%, Table 2). Further, we have conducted the reaction with commercially available simple alkenes such as 1-hexene, *cis*-4-octene, *trans*-4-octene and *cis*-cyclooctene. However, in all the cases we have observed that the starting materials getting degraded and we did not observe formation of the corresponding β-hydroxy trifluoromethylated products. To have an insight for these unsuccessful transformations, we recorded the cyclic voltammograms of the starting materials (1-hexene, *cis*-4-octene, *trans*-4-octene and *cis*-cyclooctene) and we found that the oxidation potential of these compounds is ≥2.0 V (see Supporting Information, S20–S22, Figures S22–S25 for details). We presume, these starting materials might be involving in the electron transfer with the excited-state photocatalyst/ground state photocatalyst (Mes-Acr-Me·BF_4* [E_{red*} > 1.8 V vs SCE] and Mes-Acr-Me·BF_4 [E_{ox} = −0.57 V vs SCE]) and getting degraded in the reaction. The optimized hydroxytrifluoromethylation conditions proved to be successful for a wide range of unactivated aliphatic mono-, di-, and trisubstituted alkenes (Table 2).

Having generalized the practicality of the protocol, we further turned our attention toward the postsynthetic modification as an application of this strategy (Scheme 2). We utilized the β-hydroxy trifluoromethylated products (**3a** and **3n**) for different synthetic transformation to access useful organic compounds. The compound **3n** on treatment with aryl boronic acids (**4a** and **4b**) under Suzuki–Miyaura coupling conditions afforded the corresponding coupling products (**5a**, **5b**) in very good yields (up to 87%, Scheme 2a).

Additionally, the synthesized compound **3a** when subjected to esterification with nonsteroidal anti-inflammatory drug (NSAID)-ibuprofen **4c** afforded the corresponding trifluoromethylated ester derivative of ibuprofen **5c** in good yield (81%, Scheme 2b). Further, compound **3a** under the oxidative conditions (in the presence of PCC) furnished the synthetically β-trifluoromethyl ketone **5d** (76%, Scheme 2c). We have also demonstrated the scale-up synthesis of **3a** (437 mg, 57% yield, Scheme 2d). Further, we have also performed the reaction under the direct exposure of natural sunlight as a light source to obtain **3a** (29 mg, 58%, see Supporting Information, S2–S3).

To gain further mechanistic insight into this transformation, we performed a series of control experiments (Scheme 3). To begin with we carried out radical quenching experiment of **1a** with **2** in the presence of radical trapping agents such as BHT and TEMPO under the optimized reaction conditions to obtain the desired product **3a** in poor yields along with the TEMPO/BHT trapped radical intermediates (as confirmed by HRMS, Scheme 3a,b). These results clearly support the *in situ* generation of CF_3 radical **A** as well as trifluoromethylated alkyl radical **B** during the reaction (see Supporting Information, S6 and S7, Scheme S1, Figures S1 and S2). The reaction of **1a** and **2** in the presence of H_2O^{18} under inert atmosphere did not afford the corresponding product **3a** (Scheme 3c, see Supporting Information, S8 and S9, Scheme S2a and Figure S3). However, the reaction of **1a** and **2** in the presence of H_2O^{18} under open air afforded the corresponding desired product **3a** without any incorporation of ^{18}O (Scheme 3d, see Supporting Information, S8 and S9, Scheme S2b and Figure S4). These results ruled out the possibility of moisture as a source of oxygen. Earlier we had observed that reaction did not afford the desired product **3a** under inert atmospheric

https://doi.org/10.1021/acs.joc.4c00967
J. Org. Chem. 2024, 89, 14695–14709

Scheme 4. Plausible Reaction Mechanism

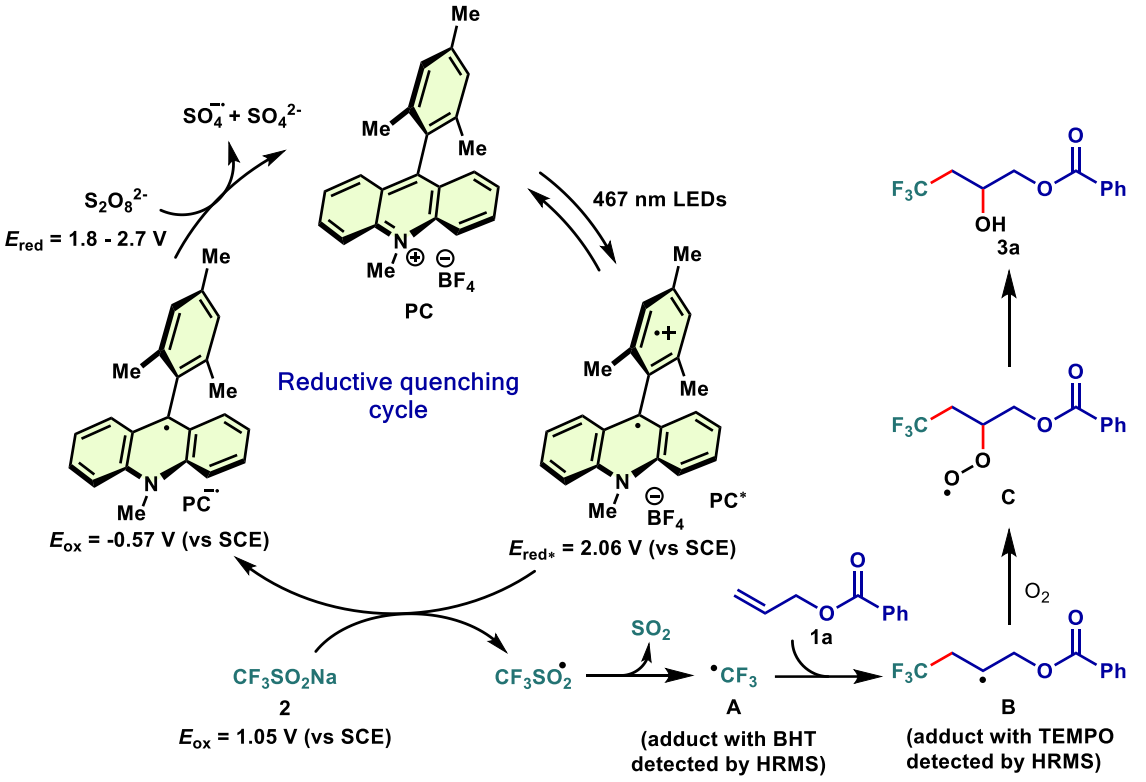

condition while maintaining other optimized reaction condition (Table 1, Entry 5). In addition, we have conducted a reaction of **1a** in the presence of $^{18}O_2$-atmosphere while maintaining other standard conditions. We gratifyingly, obtained the ^{18}O-incorporated product **3a'** (Scheme 3e and see Supporting Information, S10, Figure S5 for HRMS spectrum). These results clearly support the essential requirement of oxygen (air) to drive the reaction. Further, the deuterium labeling experiment in MeCN-d_3 as a solvent was carried out. We obtained the desired product **3a** without the deuterium incorporation (Scheme 3f). The reaction of **1a** and **2** with D_2O (10 equiv) while maintaining the other standard condition furnished the deuterium incorporated product **3aD** along with **3a** (Scheme 3g). These results indicate that probably the moisture present in the solvent is the preliminary source of proton.

To verify the stereochemical outcome of the protocol, we conducted reaction with a pair of *E*/*Z* alkenes **1am** and **1an** using standard reaction conditions to obtain **3xx** exclusively (Scheme 3h,i). Based on the ^{1}H, ^{13}C and ^{19}F{^{1}H} NMR spectral analysis of the products obtained from the reaction of **1am** and **1an** were found to be same product **3xx** (see stacked spectra Supporting Information, S12 and S13, Figures S7−S9). Probably, after the addition of CF_3 radical to the alkene, there may be free rotation of free alkyl radical or even light may be favoring the rotation subsequently leading to product **3xx**.

Further an intermittent illumination (Light ON/OFF) experiment was performed and a correlation between irradiation time and the yield of product **3a** was derived (Figure 1a). No product formation was observed in the absence of light and, we did not see any enhancement in the yield of **3a** thus establishing the light-dependent nature of the reaction. This result clearly eliminates the possibility of a light-initiated radical chain mechanism. This experiment unequivocally proves that the continuous irradiation of light plays a critical role in the product formation.

Later, we performed the fluorescence quenching study of the photocatalyst (Mes-Acr-Me·BF_4) with the varied concentrations of **1a**, **2**, and $(NH_4)_2S_2O_8$ (see Supporting Information, S14−S15, Figures S10−S12 for details). Further, the Stern−Volmer plot proved that the CF_3SO_2Na **2** is a potential fluorescence quencher of the excited state of Mes-Acr-Me·BF_4* (Figure 1b). Also, CF_3SO_2Na is efficiently involved in a SET event with the Mes-Acr-Me·BF_4* and this has been further supported by the oxidation potential of CF_3SO_2Na (**2**) [E_{ox} = 1.05 V vs SCE] which is less than the reduction potential of Mes-Acr-Me·BF_4* [E_{red*} > 1.8 V vs SCE].[12,13]

Based on the results of the control experiments and literature precedence, a plausible visible light mediated radical mechanism for β-hydroxytrifluoromethylation has been outlined (Scheme 4).

It is proposed that Mes-Acr-Me·BF_4 (PC) upon blue light irradiation will generate the excited-state Mes-Acr-Me·BF_4 (PC*) which is known to be a strong oxidant [E_{red*} > 1.8 V vs SCE].[12] Then, PC* undergoes the reductive quenching through single electron transfer (SET) with CF_3SO_2Na **2** [E_{ox} = 1.05 V vs SCE][13] to form trifluoromethyl radical [**A**] (BHT trapped radical adduct detected by HRMS) along with the formation of reduced PC. This radical intermediate [**A**] further reacts with **1a** to generate the radical intermediate [**B**] (TEMPO trapped radical adduct detected by HRMS). This further reacts with O_2 to generate an unstable intermediate [**C**] which further decomposes to furnish the desired product **3a** after proton abstraction. Alongside, the $(NH_4)_2S_2O_8$ [E_{red} = 1.8−2.7 V][14] reacts with the reduced PC [E_{ox} = −0.57 V vs SCE] to regenerate the ground state PC.

https://doi.org/10.1021/acs.joc.4c00967
J. Org. Chem. 2024, 89, 14695−14709

CONCLUSIONS

In summary we have successfully demonstrated a transition metal-free, visible light-induced direct β-hydroxytrifluoromethylation of unactivated alkenes (internal as well as terminal) with Langlois reagent at room temperature. A nontoxic, inexpensive organic dye has been utilized as the photoredox catalyst for this operationally simple and mild β-hydroxytrifluoromethylation. The protocol proved to be practical with good functional group tolerance and a broad substrate scope. Synthetic and practical utility of this approach has been demonstrated by functionalizing natural product derived substrates, the functional group transformation as well as further derivatization of synthesized products. Also, the protocol has been proved to be scalable and it works smoothly under direct exposure of sunlight. A series of control experiments, fluorescence quenching and cyclic voltammetry studies proved that transformation is driven via reductive quenching mechanistic cycle.

EXPERIMENTAL SECTION

General Information. Unless otherwise noted, all the starting materials and reagents were purchased from commercial suppliers (Sigma-Aldrich, TCI, Alfa Aesar, Spectrochem and BLD Pharm) and were used as received. Thin-layer chromatography (TLC) was performed using silica gel 60 GF_{254} precoated aluminum backed plates (2.5 mm). Visualization was accomplished by irradiation with UV light at 254 nm and phosphomolybdic acid (PMA) staining agent. The column chromatography was performed using silica gel (100−200 mesh) eluting with petroleum ether and ethyl acetate. The NMR spectra were recorded using tetramethylsilane as the internal standard. ^{1}H NMR spectra were recorded at 400/600 MHz, ^{19}F NMR spectra were recorded at 377/565 MHz and ^{13}C NMR spectra were recorded at 100/150 MHz (Bruker and Jeol) using tetramethylsilane as the internal standard, unless otherwise noted. Chemical shifts (δ) are reported in ppm downfield from $CDCl_3$ (δ = 7.26 ppm) for ^{1}H NMR and relative to the central $CDCl_3$ resonance (δ = 77.16 ppm) for ^{13}C NMR spectroscopy. For ^{1}H NMR, data are reported as follows: chemical shift, multiplicity (s = singlet, d = doublet, t = triplet, q = quartet, p = pentet, s = sextet, h = heptet, m = multiplet, br = broad), coupling constants (J) are given in Hz and integration. ^{13}C NMR spectra were recorded with complete proton decoupling. Mass samples were analyzed by high-resolution mass spectrometry (HRMS)-ESI TOF. Using an open glass capillary, melting points were recorded on a BUCHI M-560 melting point apparatus, and they are not corrected. Fluorescence emission spectra were obtained on a RF-6000 Spectrofluorophotometer from Shimadzu in a 3 mL, Hellma fluorescence cuvette (path length 1.0 cm). All photocatalytic reactions were performed under blue LEDs (Kessil PR160L series Blue LEDs, and IBRA Pure 20 W Blue LED Flood Light, IP Rating: IP66) and reaction mixture was irradiated from 5 cm away from the LEDs. *Note and Caution! 1. Avoid skin contact, eye contact and inhalation of ammonium persulfate and sodium trifluoromethanesulfinate. 2. Avoid inhalation of the reaction mixture as it may contain SO_2 gas (byproduct of the reaction).*

*General Procedure A for the Synthesis of Compounds **1a−1r, 1w, 1y, 1z, 1aa−1ab,** and **1af−1ag**.* The compounds were synthesized following the previously reported procedure.[15] To an oven-dried reaction tube charged with magnetic stir bar and rubber septum was added DMF (20 mL), benzoic acid or phenol or 2-hydroxyisoindoline-1,3-dione (1 equiv.; 5 mmol), 3-bromoprop-1-ene or 1-bromo-3-methylbut-2-ene or 4-bromobut-1-ene or 5-bromopent-1-ene or 7-bromohept-1-ene (1.5 equiv) and K_2CO_3 (2 equiv) and stirred at room temperature for 12−24 h (monitored by TLC). The reaction mixture was then quenched with water and the product was extracted with ethyl acetate (30 mL × 3). The combined organic layers were washed with brine solution and dried over anhydrous Na_2SO_4. The extract was filtered and evaporated under reduced pressure. The crude products were purified using column chromatography over silica gel to afford **1a−1r, 1w, 1y, 1z, 1aa−1ab, 1af−1ag**.

*General Procedure B for the Synthesis of Compounds **1s−1v, 1x, 1ad−1ae, 1ah,** and **1ai−1al**.* The starting materials **1s−1u, 1ad−1ae, 1ah, 1ai−1al, 1am** and **1an** were synthesized according to the slightly modified reported procedure.[16] To a stirred solution of alcohol (5 mmol, 1 equiv), carboxylic acid (1.5 equiv), and dimethylaminopyridine, DMAP (10 mol %) in anhydrous CH_2Cl_2 (20 mL) was added *N,N′*-dicyclohexylcarbodiimide, DCC (1.5 equiv) at 0 °C, which is then stirred for 5 min at 0 °C and then at room temperature. The progress of the reaction was monitored by TLC. After completion of the reaction, precipitated urea is then filtered off in CH_2Cl_2. The CH_2Cl_2 solution is washed twice with ∼ HCl (0.5 N) and with saturated $NaHCO_3$ solution. The combined organic layers were washed with brine solution and dried over anhydrous Na_2SO_4. The crude product was purified using column chromatography over silica gel to afford **1s−1u, 1ad−1ae, 1ah, 1ai−1al, 1am** and **1an**. The starting materials **1v, 1x** were synthesized according to the reported literature procedure starting from pivaloyl chloride or 4-methylbenzenesulfonyl chloride and 3-methylbut-3-en-1-ol.[17]

*General Procedure C for the Synthesis of **3**.* To an oven-dried reaction tube equipped with a stir bar alkene **1** (0.2 mmol, 1 equiv), CF_3SO_2Na, **2** (3 equiv), $(NH_4)_2S_2O_8$ (2 equiv), Mes-Acr-Me·BF_4 (5 mol %), and 1,4-Dioxane:MeCN (2:1 mL) were added. Then the reaction mixture was irradiated with 467 nm Kessil PR-160L Blue LED (50% intensity), from ∼5 cm away under open air and stirred at room temperature (under the continuous flow of fan to maintain the temperature at 25−30 °C) for 12−36 h (monitored by TLC). After completion of the reaction, the reaction mixture was filtered and the solvent was removed under reduced pressure. Then, the crude residue was purified by column chromatography over silica gel (100−200 mesh size) using mixture of petroleum ether/EtOAc as an eluent to afford the corresponding desired β-trifluoromethyl alcohol product **3**.

*Product Characterization Data. Allyl 3-Bromo-4-methylbenzoate (**1r**).* The title compound **1r** was prepared according to the general procedure **A** starting from 3-bromo-4-methylbenzoic acid (5.0 mmol) and 3-bromoprop-1-ene (1.5 equiv). Colorless liquid (1.17 g, 92% yield), R_f = 0.45 (petroleum ether/EtOAc 95:5). ^{1}H NMR (400 MHz, $CDCl_3$) δ 8.21 (d, J = 1.8 Hz, 1H), 7.89 (dd, J = 7.9, 1.8 Hz, 1H), 7.30 (dd, J = 7.8, 0.8 Hz, 1H), 6.03 (ddt, J = 17.2, 10.4, 5.7 Hz, 1H), 5.40 (dq, J = 17.2, 1.5 Hz, 1H), 5.30 (dq, J = 10.4, 1.3 Hz, 1H), 4.81 (dt, J = 5.7, 1.4 Hz, 2H), 2.45 (s, 3H). ^{13}C{^{1}H} NMR (100 MHz, $CDCl_3$) δ 165.2 (s), 143.6 (s), 133.6 (s), 132.2 (s), 130.8 (s), 129.6 (s), 128.6 (s), 124.9 (s), 118.7 (s), 65.9 (s), 23.4 (s). HRMS (ESI TOF) m/z for $C_{11}H_{12}BrO_2$ $[M + H]^+$ calcd. 255.0021, found 255.0017.

*Allyl Benzo[b]thiophene-2-carboxylate (**1af**).* The title compound **1af** was prepared according to the general procedure **A** starting from benzo[b]thiophene-2-carboxylic acid (5.0 mmol) and 3-bromoprop-1-ene (1.5 equiv). White solid (1.06 g, 97% yield), R_f = 0.43 (petroleum ether/EtOAc 95:5), mp 43−45 °C. ^{1}H NMR (400 MHz, $CDCl_3$) δ 8.09 (d, J = 0.8 Hz, 1H), 7.97−7.80 (m, 2H), 7.61−7.31 (m, 2H), 6.05 (ddt, J = 17.2, 10.4, 5.6 Hz, 1H), 5.45 (dq, J = 17.2, 1.5 Hz, 1H), 5.32 (dq, J = 10.4, 1.3 Hz, 1H), 4.86 (dt, J = 5.7, 1.4 Hz, 2H). ^{13}C{^{1}H} NMR (100 MHz, $CDCl_3$) δ 162.6 (s), 142.4 (s), 138.8 (s), 133.6 (s), 132.0 (s), 130.8 (s), 127.1 (s), 125.7 (s), 125.1 (s), 122.9 (s), 118.8 (s), 66.2 (s). HRMS (ESI TOF) m/z for $C_{12}H_{11}O_2S$ $[M + H]^+$ calcd. 219.0480, found 219.0483.

*Allyl 1-Methyl-1H-pyrrole-2-carboxylate (**1ag**).* The title compound **1ag** was prepared according to the general procedure **A** starting from 1-Methyl-1H-pyrrole-2-carboxylic acid (5.0 mmol) and 3-bromoprop-1-ene (1.5 equiv). Colorless liquid (727 mg, 88% yield), R_f = 0.34 (petroleum ether/EtOAc 95:5). ^{1}H NMR (400 MHz, $CDCl_3$) δ 6.99 (dd, J = 4.0, 1.8 Hz, 1H), 6.79 (t, J = 2.2 Hz, 1H), 6.12 (dd, J = 4.0, 2.5 Hz, 1H), 6.01 (ddt, J = 17.2, 10.7, 5.5 Hz, 1H), 5.38 (dq, J = 17.2, 1.6 Hz, 1H), 5.25 (dq, J = 10.5, 1.4 Hz, 1H), 4.73 (dt, J = 5.5, 1.5 Hz, 2H), 3.93 (s, 3H). ^{13}C{^{1}H} NMR (100 MHz, $CDCl_3$) δ 161.1 (s), 132.8 (s), 129.7 (s), 122.4 (s), 118.1 (s), 117.8 (s), 108.0 (s), 64.5 (s), 36.9 (s). HRMS (ESI TOF) m/z for $C_9H_{12}NO_2$ $[M + H]^+$ calcd. 166.0868, found 166.0871.

https://doi.org/10.1021/acs.joc.4c00967
J. Org. Chem. 2024, 89, 14695−14709

*(E)-hex-3-en-1-yl Benzoate (**1am**).* The title compound **1am** was prepared according to the general procedure **B** starting from benzoic acid (5.0 mmol) and (*E*)-hex-3-en-1-ol (1.5 equiv). Colorless liquid (980 mg, 96% yield), R_f = 0.32 (petroleum ether/EtOAc 95:5). ^{1}H NMR (400 MHz, $CDCl_3$) δ 8.08−8.01 (m, 2H), 7.61−7.52 (m, 1H), 7.48−7.40 (m, 2H), 5.62 (dtt, *J* = 15.3, 6.3, 1.3 Hz, 1H), 5.45 (dtt, *J* = 15.2, 6.8, 1.5 Hz, 1H), 4.32 (t, *J* = 6.8 Hz, 2H), 2.46 (qq, *J* = 6.8, 1.2 Hz, 2H), 2.03 (dtdd, *J* = 8.7, 7.4, 6.2, 1.3 Hz, 2H), 0.97 (t, *J* = 7.5 Hz, 3H). ^{13}C{^{1}H} NMR (100 MHz, $CDCl_3$) δ 166.7, 135.4, 133.0, 130.6, 129.7, 128.4, 124.2, 64.7, 32.2, 25.8, 13.9. HRMS (ESI TOF) *m*/*z* for $C_{13}H_{17}O_2$ $[M + H]^+$ calcd. 205.1229, found 205.1226.

*(Z)-hex-3-en-1-yl Benzoate (**1an**).* The title compound **1an** was prepared according to the general procedure **B** starting from benzoic acid (5.0 mmol) and (*Z*)-hex-3-en-1-ol (1.5 equiv). Colorless liquid (960 mg, 94% yield), R_f = 0.32 (petroleum ether/EtOAc 95:5). 1H NMR (400 MHz, Chloroform-*d*) δ 8.07−8.00 (m, 2H), 7.59−7.51 (m, 1H), 7.47−7.39 (m, 2H), 5.58−5.49 (m, 1H), 5.45−5.36 (m, 1H), 4.32 (t, *J* = 6.9 Hz, 1H), 2.59−2.47 (m, 1H), 2.10 (pd, *J* = 7.6, 1.5 Hz, 1H), 0.97 (t, *J* = 7.5 Hz, 2H). ^{13}C{^{1}H} NMR (100 MHz, $CDCl_3$) δ 166.8, 134.8, 133.0, 130.5, 129.7, 128.5, 123.9, 64.6, 27.0, 20.8, 14.4. HRMS (ESI TOF) *m*/*z* for $C_{13}H_{17}O_2$ $[M + H]^+$ calcd. 205.1229, found 205.1225.

*4,4,4-Trifluoro-2-hydroxybutyl Benzoate (**3a**).* The title compound **3a** was prepared according to the general procedure **C** starting from allyl benzoate **1a** (0.2 mmol) and CF_3SO_2Na **2** (3 equiv). White solid (32 mg, 65% yield), R_f = 0.28 (petroleum ether/EtOAc 85:15), mp 43−45 °C. ^{1}H NMR (600 MHz, $CDCl_3$) δ 8.05−8.03 (m, 2H), 7.60 (t, *J* = 7.4 Hz, 1H), 7.46 (t, *J* = 7.8 Hz, 2H), 4.44 (dd, *J* = 11.2, 3.6 Hz, 1H), 4.42−4.37 (m, 1H), 4.34 (dd, *J* = 11.1, 5.9 Hz, 1H), 2.60 (d, *J* = 4.5 Hz, 1H), 2.52−2.38 (m, 2H). ^{13}C{^{1}H} NMR (150 MHz, $CDCl_3$) δ 166.7 (s), 133.6 (s), 129.9 (s), 129.5 (s), 128.7 (s), 126.1 (q, *J* = 276.7 Hz), 67.9 (s), 65.0 (d, *J* = 2.9 Hz), 38.1 (q, *J* = 27.9 Hz). ^{19}F{^{1}H} NMR (565 MHz, $CDCl_3$) δ 64.49 (s). HRMS (ESI TOF) *m*/*z* for $C_{11}H_{12}F_3O_3$ $[M + H]^+$ calcd. 249.0739, found 249.0741.

*4,4,4-Trifluoro-2-hydroxybutyl 2-Methylbenzoate (**3b**).* The title compound **3b** was prepared according to the general procedure **C** starting from allyl benzoate **1b** (0.2 mmol) and CF_3SO_2Na **2** (3 equiv). Colorless oil (37 mg, 70% yield), R_f = 0.26 (petroleum ether/EtOAc 90:10). ^{1}H NMR (400 MHz, $CDCl_3$) δ 7.92 (dd, *J* = 8.2, 1.4 Hz, 1H), 7.44 (td, *J* = 7.5, 1.4 Hz, 1H), 7.26 (dd, *J* = 7.7, 6.6 Hz, 2H), 4.45−4.28 (m, 3H), 2.61 (s, 3H), 2.53 (d, *J* = 3.3 Hz, 1H), 2.51−2.37 (m, 2H). ^{13}C{^{1}H} NMR (100 MHz, $CDCl_3$) δ 167.5 (s), 140.7 (s), 132.7 (s), 132.1 (s), 130.8 (s), 128.8 (s), 126.1 (q, *J* = 276.8 Hz), 126.0 (s), 67.7 (s), 65.0 (q, *J* = 3.0 Hz), 38.1 (q, *J* = 27.9 Hz), 21.9 (s). ^{19}F NMR (377 MHz, $CDCl_3$) δ −63.52 (s). HRMS (ESI TOF) *m*/*z* for $C_{12}H_{14}F_3O_3$ $[M + H]^+$ calcd. 263.0895, found 263.0889.

*4,4,4-Trifluoro-2-hydroxybutyl 3-Methylbenzoate (**3c**).* The title compound **3c** was prepared according to the general procedure **C** starting from allyl benzoate **1c** (0.2 mmol) and CF_3SO_2Na **2** (3 equiv). Colorless oil (41 mg, 78% yield), R_f = 0.26 (petroleum ether/EtOAc 90:10). ^{1}H NMR (400 MHz, $CDCl_3$) δ 7.85 (m, 2H), 7.40 (d, *J* = 7.8 Hz, 1H), 7.34 (t, *J* = 7.7 Hz, 1H), 4.45−4.31 (m, 3H), 2.61 (s, 1H), 2.49−2.23 (m, 5H). ^{13}C{^{1}H} NMR (100 MHz, $CDCl_3$) δ 166.9 (s), 138.5 (s), 134.4 (s), 130.4 (s), 129.4 (s), 128.6 (s), 127.0 (s), 126.1 (q, *J* = 276.8 Hz), 67.8 (s), 65.0 (d, *J* = 3.1 Hz), 38.1 (q, *J* = 27.9 Hz), 21.4 (s). ^{19}F{^{1}H} NMR (377 MHz, $CDCl_3$) δ −63.51 (s). HRMS (ESI TOF) *m*/*z* for $C_{12}H_{14}F_3O_3$ $[M + H]^+$ calcd. 263.0895, found 263.0894.

*4,4,4-Trifluoro-2-hydroxybutyl 4-Methylbenzoate (**3d**).* The title compound **3d** was prepared according to the general procedure **C** starting from allyl benzoate **1d** (0.2 mmol) and CF_3SO_2Na **2** (3 equiv). White solid (38 mg, 73% yield), R_f = 0.21 (petroleum ether/EtOAc 90:10), mp 54−56 °C. ^{1}H NMR (400 MHz, $CDCl_3$) δ 7.96−7.90 (m, 2H), 7.28−7.23 (m, 2H), 4.45−4.30 (m, 3H), 2.61 (s, 1H), 2.49−2.37 (m, 5H). ^{13}C{^{1}H} NMR (100 MHz, $CDCl_3$) δ 166.8 (s), 144.5 (s), 129.9 (s), 129.4 (s), 126.7 (s), 126.1 (q, *J* = 276.8 Hz), 67.7 (s), 65.1 (q, *J* = 3.0 Hz), 38.1 (q, *J* = 27.9 Hz), 21.8 (s). ^{19}F{^{1}H} NMR (377 MHz, $CDCl_3$) δ −63.52 (s). HRMS (ESI TOF) *m*/*z* for $C_{12}H_{14}F_3O_3$ $[M + H]^+$ calcd. 263.0895, found 263.0888.

*4,4,4-Trifluoro-2-hydroxybutyl 4-(tert-butyl)Benzoate (**3e**).* The title compound **3e** was prepared according to the general procedure **C** starting from allyl benzoate **1e** (0.2 mmol) and CF_3SO_2Na **2** (3 equiv). White solid (39 mg, 64% yield), R_f = 0.26 (petroleum ether/EtOAc 90:10), mp 53−55 °C. ^{1}H NMR (400 MHz, $CDCl_3$) δ 8.00−7.94 (m, 2H), 7.50−7.46 (m, 2H), 4.46−4.30 (m, 3H), 2.60 (d, *J* = 3.9 Hz, 1H), 2.51−2.36 (m, 2H), 1.34 (s, 9H). ^{13}C{^{1}H} NMR (100 MHz, $CDCl_3$) δ 166.8 (s), 157.5 (s), 129.8 (s), 126.6 (s), 126.1 (q, *J* = 276.8 Hz), 125.7 (s), 67.7 (s), 65.1 (q, *J* = 3.0 Hz), 38.1 (q, *J* = 27.9 Hz), 35.3 (s), 31.2 (s). ^{19}F{^{1}H} NMR (377 MHz, $CDCl_3$) δ −63.52 (s). HRMS (ESI TOF) *m*/*z* for $C_{15}H_{20}F_3O_3$ $[M + H]^+$ calcd. 305.1365, found 305.1359.

*4,4,4-Trifluoro-2-hydroxybutyl 3-Methoxybenzoate (**3f**).* The title compound **3f** was prepared according to the general procedure **C** starting from allyl benzoate **1f** (0.2 mmol) and CF_3SO_2Na **2** (3 equiv). Colorless liquid (42 mg, 76% yield), R_f = 0.34 (petroleum ether/EtOAc 80:20). ^{1}H NMR (400 MHz, $CDCl_3$) δ 7.66−7.61 (m, 1H), 7.55 (dd, *J* = 2.5, 1.5 Hz, 1H), 7.37 (t, *J* = 8.0 Hz, 1H), 7.13 (ddd, *J* = 8.3, 2.7, 0.9 Hz, 1H), 4.47−4.30 (m, 3H), 3.85 (s, 3H), 2.58 (s, 1H), 2.52−2.37 (m, 2H). ^{13}C{^{1}H} NMR (100 MHz, $CDCl_3$) δ 166.6 (s), 159.8 (s), 130.8 (s), 129.7 (s), 126.1 (q, *J* = 276.8 Hz), 122.0 (s), 120.0 (s), 114.5 (s), 68.0 (s), 65.0 (q, *J* = 3.1 Hz), 55.6 (s), 38.1 (q, *J* = 28.0 Hz). ^{19}F{^{1}H} NMR (377 MHz, $CDCl_3$) δ −63.51 (s). HRMS (ESI TOF) *m*/*z* for $C_{12}H_{14}F_3O_4$ $[M + H]^+$ calcd. 279.0844, found 279.0848.

*4,4,4-Trifluoro-2-hydroxybutyl 4-(Dimethylamino)benzoate (**3g**).* The title compound **3g** was prepared according to the general procedure **C** starting from allyl benzoate **1g** (0.2 mmol) and CF_3SO_2Na **2** (3 equiv). White solid (32 mg, 55% yield), R_f = 0.45 (petroleum ether/EtOAc 70:30), mp 77−79 °C. ^{1}H NMR (400 MHz, $CDCl_3$) δ 7.92−7.88 (m, 2H), 6.67−6.63 (m, 2H), 4.43−4.26 (m, 3H), 3.05 (s, 6H), 2.76 (s, 1H), 2.48−2.35 (m, 2H). ^{13}C{^{1}H} NMR (100 MHz, $CDCl_3$) δ 167.2 (s), 153.8 (s), 131.7 (s), 126.2 (q, *J* = 276.8 Hz), 115.8 (s), 110.9 (s), 67.4 (s), 65.3 (q, *J* = 3.1 Hz), 40.2 (s), 38.1 (q, *J* = 27.9 Hz). ^{19}F{^{1}H} NMR (377 MHz, $CDCl_3$) δ −63.51 (s). HRMS (ESI TOF) *m*/*z* for $C_{13}H_{17}F_3NO_3$ $[M + H]^+$ calcd. 292.1161, found 292.1156.

*4,4,4-Trifluoro-2-hydroxybutyl 4-Nitrobenzoate (**3h**).* The title compound **3h** was prepared according to the general procedure **C** starting from allyl benzoate **1h** (0.2 mmol) and CF_3SO_2Na **2** (3 equiv). Colorless liquid (48 mg, 82% yield), R_f = 0.36 (petroleum ether/EtOAc 70:30). ^{1}H NMR (400 MHz, $CDCl_3$) δ 8.33−8.28 (m, 2H), 8.26−8.19 (m, 2H), 4.62−4.29 (m, 3H), 2.66−2.25 (m, 3H). ^{13}C{^{1}H} NMR (100 MHz, $CDCl_3$) δ 164.8 (s), 150.9 (s), 134.9 (s), 131.0 (s), 126.0 (q, *J* = 276.8 Hz), 123.8 (s), 68.5 (s), 64.8 (q, *J* = 3.1 Hz), 38.1 (q, *J* = 28.0 Hz). ^{19}F{^{1}H} NMR (377 MHz, $CDCl_3$) δ −63.48 (s). HRMS (ESI TOF) *m*/*z* for $C_{11}H_{11}F_3NO_5$ $[M + H]^+$ calcd. 294.0589, found 294.0586.

*4,4,4-Trifluoro-2-hydroxybutyl 4-Cyanobenzoate (**3i**).* The title compound **3i** was prepared according to the general procedure **C** starting from allyl benzoate **1i** (0.2 mmol) and CF_3SO_2Na **2** (3 equiv). White solid (43 mg, 78% yield), R_f = 0.38 (petroleum ether/EtOAc 70:30), mp 62−64 °C. ^{1}H NMR (400 MHz, $CDCl_3$) δ 8.16−8.14 (m, 2H), 7.78−7.75 (m, 2H), 4.59−4.36 (m, 3H), 2.54−2.35 (m, 3H). ^{13}C{^{1}H} NMR (100 MHz, $CDCl_3$) δ 165.0 (s), 133.4 (s), 132.5 (s), 130.4 (s), 126.0 (q, *J* = 279.3 Hz), 117.9 (s), 117.0 (s), 68.4 (s), 64.8 (q, *J* = 3.0 Hz), 38.1 (q, *J* = 28.0 Hz). ^{19}F{^{1}H} NMR (377 MHz, $CDCl_3$) δ −63.48 (s). HRMS (ESI TOF) *m*/*z* for $C_{12}H_{11}F_3NO_3$ $[M + H]^+$ calcd. 274.0691, found 274.0690.

*4,4,4-Trifluoro-2-hydroxybutyl 4-Formylbenzoate (**3j**).* The title compound **3j** was prepared according to the general procedure **C** starting from allyl benzoate **1j** (0.2 mmol) and CF_3SO_2Na **2** (3 equiv). Colorless liquid (38 mg, 68% yield), R_f = 0.38 (petroleum ether/EtOAc 70:30). ^{1}H NMR (400 MHz, $CDCl_3$) δ 10.11 (s, 1H), 8.22−8.20 (m, 2H), 7.98−7.6 (m, 2H), 4.50−4.36 (m, 3H), 2.58−2.37(m, 3H). ^{13}C{^{1}H} NMR (100 MHz, $CDCl_3$) δ 191.7 (s), 165.6 (s), 139.6 (s), 134.4 (s), 130.5 (s), 129.8 (s), 126.0 (q, *J* = 276.8 Hz), 68.3 (s), 64.9 (q, *J* = 3.1 Hz), 38.1 (q, *J* = 28.0 Hz). ^{19}F{^{1}H} NMR (377 MHz, $CDCl_3$) δ −63.48 (s). HRMS (ESI TOF) *m*/*z* for $C_{12}H_{12}F_3O_4$ $[M + H]^+$ calcd. 277.0688, found 277.0684.

https://doi.org/10.1021/acs.joc.4c00967
J. Org. Chem. 2024, 89, 14695−14709

*4,4,4-Trifluoro-2-hydroxybutyl 4-Fluorobenzoate (**3k**).* The title compound **3k** was prepared according to the general procedure **C** starting from allyl benzoate **1k** (0.2 mmol) and CF_3SO_2Na **2** (3 equiv). Colorless liquid (30 mg, 56% yield), R_f = 0.27 (petroleum ether/EtOAc 85:15). ^1H NMR (400 MHz, $CDCl_3$) δ 8.08−8.03 (m, 2H), 7.14−7.10 (m, 2H), 4.43−4.31 (m, 3H), 2.81 (s, 1H), 2.50−2.37 (m, 2H). $^{13}C\{^1H\}$ NMR (100 MHz, $CDCl_3$) δ 166.2 (d, J = 255.0 Hz), 165.8 (s), 132.4 (d, J = 9.4 Hz), 126.1 (q, J = 276.8 Hz), 125.7 (d, J = 3.1 Hz), 115.9 (d, J = 22.1 Hz), 67.9 (s), 64.9 (q, J = 3.1 Hz), 38.0 (q, J = 28.0 Hz). $^{19}F\{^1H\}$ NMR (377 MHz, $CDCl_3$) δ −63.53 (s), −104.57 (s). HRMS (ESI TOF) m/z for $C_{11}H_{11}F_4O_3$ $[M + H]^+$ calcd. 267.0644, found 267.0641.

*4,4,4-Trifluoro-2-hydroxybutyl 2-Chlorobenzoate (**3l**).* The title compound **3l** was prepared according to the general procedure **C** starting from allyl benzoate **1l** (0.2 mmol) and CF_3SO_2Na **2** (3 equiv). Colorless liquid (44 mg, 78% yield), R_f = 0.22 (petroleum ether/EtOAc 85:15). ^1H NMR (400 MHz, $CDCl_3$) δ 7.85 (ddd, J = 7.7, 1.4, 0.6 Hz, 1H), 7.50−7.42 (m, 2H), 7.35 (ddd, J = 7.8, 6.3, 2.3 Hz, 1H), 4.46 (dd, J = 10.9, 3.4 Hz, 1H), 4.39 (s, 1H), 4.33 (dd, J = 10.9, 6.0 Hz, 1H), 2.56−2.39 (m, 3H). $^{13}C\{^1H\}$ NMR (100 MHz, $CDCl_3$) δ 165.8 (s), 133.7 (s), 133.2 (s), 131.9 (s), 131.3 (s), 129.5 (s), 127.0 (s), 126.0 (q, J = 276.8 Hz), 68.3 (s), 64.7 (q, J = 3.1 Hz), 38.0 (q, J = 28.0 Hz). $^{19}F\{^1H\}$ NMR (377 MHz, $CDCl_3$) δ −63.52 (s). HRMS (ESI TOF) m/z for $C_{11}H_{11}ClF_3O_3$ $[M + H]^+$ calcd. 283.0349, found 283.0343.

*4,4,4-Trifluoro-2-hydroxybutyl 3-Bromobenzoate (**3m**).* The title compound **3m** was prepared according to the general procedure **C** starting from allyl benzoate **1m** (0.2 mmol) and CF_3SO_2Na **2** (3 equiv). Colorless liquid (41 mg, 63% yield), R_f = 0.34 (petroleum ether/EtOAc 85:15). ^1H NMR (400 MHz, $CDCl_3$) δ 8.17 (t, J = 1.7 Hz, 1H), 8.00−7.94 (m, 1H), 7.72 (ddd, J = 8.0, 2.0, 1.1 Hz, 1H), 7.35 (t, J = 7.9 Hz, 1H), 4.56−4.23 (m, 3H), 2.62−2.24 (m, 3H). $^{13}C\{^1H\}$ NMR (100 MHz, $CDCl_3$) δ 165.4 (s), 136.6 (s), 132.8 (s), 131.4 (s), 130.3 (s), 128.4 (s), 126.1 (q, J = 276.8 Hz), 122.8 (s), 68.2 (s), 64.9 (q, J = 3.1 Hz), 38.1 (q, J = 28.0 Hz). $^{19}F\{^1H\}$ NMR (377 MHz, $CDCl_3$) δ −63.49 (s). HRMS (ESI TOF) m/z for $C_{11}H_{11}BrF_3O_3$ $[M + H]^+$ calcd. 326.9844, found 326.9849.

*4,4,4-Trifluoro-2-hydroxybutyl 2-Iodobenzoate (**3n**).* The title compound **3n** was prepared according to the general procedure **C** starting from allyl benzoate **1n** (0.2 mmol) and CF_3SO_2Na **2** (3 equiv). Colorless liquid (48 mg, 64% yield), R_f = 0.27 (petroleum ether/EtOAc 85:15). ^1H NMR (400 MHz, $CDCl_3$) δ 8.01 (dd, J = 8.0, 1.0 Hz, 1H), 7.81 (dd, J = 7.8, 1.7 Hz, 1H), 7.43 (td, J = 7.6, 1.1 Hz, 1H), 7.19 (td, J = 7.8, 1.7 Hz, 1H), 4.49−4.38 (m, 2H), 4.33 (dd, J = 10.9, 5.9 Hz, 1H), 2.56−2.36 (m, 3H). $^{13}C\{^1H\}$ NMR (100 MHz, $CDCl_3$) δ 166.5 (s), 141.5 (s), 134.9 (s), 133.2 (s), 131.4 (s), 128.2 (s), 126.0 (q, J = 276.8 Hz), 94.0 (s), 68.5 (s), 64.7 (dd, J = 6.2, 3.1 Hz), 38.0 (q, J = 28.1 Hz). $^{19}F\{^1H\}$ NMR (377 MHz, $CDCl_3$) δ −63.47 (s). HRMS (ESI TOF) m/z for $C_{11}H_{11}F_3IO_3$ $[M + H]^+$ calcd. 374.9705, found 374.9711.

*4,4,4-Trifluoro-2-hydroxybutyl 4-Hydroxybenzoate (**3o**).* The title compound **3o** was prepared according to the general procedure **C** starting from allyl benzoate **1o** (0.2 mmol) and CF_3SO_2Na **2** (3 equiv). White solid (27 mg, 51% yield), R_f = 0.22 (petroleum ether/EtOAc 70:30), mp 37−39 °C. ^1H NMR (400 MHz, DMSO-d_6) δ 10.37 (s, 1H), 7.88−7.85 (m, 2H), 6.87−6.83 (m, 2H), 5.47 (d, J = 5.3 Hz, 1H), 4.18−4.09 (m, 3H), 2.61−2.54 (m, 1H), 2.46−2.35 (m, 1H). $^{13}C\{^1H\}$ NMR (100 MHz, DMSO-d_6) δ 165.5 (s), 162.1 (s), 131.7 (s), 126.9 (q, J = 277.0 Hz), 120.2 (s), 115.4 (s), 67.5 (s), 63.1 (q, J = 3.1 Hz), 37.0 (q, J = 26.5 Hz). $^{19}F\{^1H\}$ NMR (377 MHz, DMSO-d_6) δ −61.74 (s). HRMS (ESI TOF) m/z for $C_{11}H_{12}F_3O_4$ $[M + H]^+$ calcd. 265.0688, found 265.0684.

*4,4,4-Trifluoro-2-hydroxybutyl 3,4-Dimethoxybenzoate (**3p**).* The title compound **3p** was prepared according to the general procedure **C** starting from allyl benzoate **1p** (0.2 mmol) and CF_3SO_2Na **2** (3 equiv). White solid (46 mg, 74% yield), R_f = 0.26 (petroleum ether/EtOAc 70:30), mp 90−92 °C. ^1H NMR (400 MHz, $CDCl_3$) δ 7.67 (dd, J = 8.4, 2.0 Hz, 1H), 7.52 (d, J = 2.0 Hz, 1H), 6.88 (d, J = 8.5 Hz, 1H), 4.43−4.29 (m, 3H), 3.94 (s, 3H), 3.92 (s, 3H), 2.73 (s, 1H), 2.50−2.35 (m, 2H). $^{13}C\{^1H\}$ NMR (100 MHz, $CDCl_3$) δ 166.6 (s), 153.6 (s), 148.9 (s), 126.1 (q, J = 276.8 Hz), 124.0 (s), 121.8 (s), 112.2 (s), 110.4 (s), 67.8 (s), 65.0 (q, J = 3.0 Hz), 56.2 (s), 56.1 (s), 38.1 (q, J = 27.9 Hz). $^{19}F\{^1H\}$ NMR (377 MHz, $CDCl_3$) δ −63.51 (s). HRMS (ESI TOF) m/z for $C_{13}H_{16}F_3O_5$ $[M + H]^+$ calcd. 309.0950, found 309.0951.

*4,4,4-Trifluoro-2-hydroxybutyl 2,4-Dichlorobenzoate (**3q**).* The title compound **3q** was prepared according to the general procedure **C** starting from allyl benzoate **1q** (0.2 mmol) and CF_3SO_2Na **2** (3 equiv). White solid (30 mg, 48% yield), R_f = 0.29 (petroleum ether/EtOAc 85:15), mp 67−69 °C. ^1H NMR (400 MHz, $CDCl_3$) δ 7.84 (d, J = 8.4 Hz, 1H), 7.51 (d, J = 2.0 Hz, 1H), 7.34 (dd, J = 8.4, 2.0 Hz, 1H), 4.48−4.30 (m, 3H), 2.54−2.34 (m, 3H). $^{13}C\{^1H\}$ NMR (100 MHz, $CDCl_3$) δ 164.7 (s), 139.0 (s), 134.8 (s), 132.8 (s), 131.2 (s), 127.6 (s), 127.3 (s), 125.9 (q, J = 276.8 Hz), 68.3 (s), 64.5 (q, J = 3.1 Hz), 37.9 (q, J = 28.1 Hz). $^{19}F\{^1H\}$ NMR (377 MHz, $CDCl_3$) δ −63.52 (s). HRMS (ESI TOF) m/z for $C_{11}H_{10}Cl_2F_3O_3$ $[M + H]^+$ calcd. 316.9959, found 316.9954.

*4,4,4-Trifluoro-2-hydroxybutyl 3-Bromo-4-methylbenzoate (**3r**).* The title compound **3r** was prepared according to the general procedure **C** starting from allyl benzoate **1r** (0.2 mmol) and CF_3SO_2Na **2** (3 equiv). Colorless liquid (29 mg, 42% yield), R_f = 0.34 (petroleum ether/EtOAc 85:15). ^1H NMR (400 MHz, $CDCl_3$) δ 8.19 (d, J = 1.7 Hz, 1H), 7.87 (dd, J = 7.9, 1.7 Hz, 1H), 7.32 (d, J = 7.9 Hz, 1H), 4.45−4.31 (m, 3H), 2.53 (s, 1H), 2.48−2.36 (m, 5H). $^{13}C\{^1H\}$ NMR (100 MHz, $CDCl_3$) δ 165.5 (s), 144.2 (s), 133.7 (s), 131.0 (s), 128.8 (s), 128.6 (s), 126.1 (q, J = 276.8 Hz), 125.1 (s), 68.1 (s), 65.0 (q, J = 3.1 Hz), 38.1 (q, J = 27.9 Hz), 23.4 (s). $^{19}F\{^1H\}$ NMR (377 MHz, $CDCl_3$) δ −63.49 (s). HRMS (ESI TOF) m/z for $C_{12}H_{13}BrF_3O_3$ $[M + H]^+$ calcd. 341.0000, found 341.0008.

*5,5,5-Trifluoro-3-hydroxy-3-methylpentyl Benzoate (**3s**).* The title compound **3s** was prepared according to the general procedure **C** starting from **1s** (0.2 mmol) and CF_3SO_2Na **2** (3 equiv). Colorless liquid (40 mg, 73% yield), R_f = 0.22 (petroleum ether/EtOAc 85:15). ^1H NMR (400 MHz, $CDCl_3$) δ 8.03−8.00 (m, 2H), 7.59−7.55 (m, 1H), 7.46−7.42 (m, 2H), 4.53 (t, J = 6.6 Hz, 2H), 2.48−2.39 (m, 2H), 2.21 (s, 1H), 2.16−2.03 (m, 2H), 1.45 (s, 3H). $^{13}C\{^1H\}$ NMR (100 MHz, $CDCl_3$) δ 166.7 (s), 133.3 (s), 130.1 (s), 129.7 (s), 128.6 (s), 126.1 (q, J = 277.9 Hz), 69.7 (q, J = 1.9 Hz), 61.1 (s), 45.1 (q, J = 26.0 Hz), 40.5 (d, J = 1.3 Hz), 27.4 (d, J = 1.5 Hz). $^{19}F\{^1H\}$ NMR (377 MHz, $CDCl_3$) δ −60.17 (s). HRMS (ESI TOF) m/z for $C_{13}H_{15}F_3NaO_3$ $[M + Na]^+$ calcd. 299.0871, found 299.0865.

*5,5,5-Trifluoro-3-hydroxy-3-methylpentyl 3-Methoxybenzoate (**3t**).* The title compound **3t** was prepared according to the general procedure **C** starting from **1t** (0.2 mmol) and CF_3SO_2Na **2** (3 equiv). Colorless liquid (42 mg, 69% yield), R_f = 0.48 (petroleum ether/EtOAc 70:30). δ ^1H NMR (400 MHz, $CDCl_3$) 7.62−7.58 (m, 1H), 7.53 (dd, J = 2.6, 1.5 Hz, 1H), 7.35 (t, J = 8.0 Hz, 1H), 7.11 (ddd, J = 8.3, 2.7, 1.0 Hz, 1H), 4.53 (t, J = 6.5 Hz, 2H), 3.85 (s, 3H), 2.44 (qd, J = 11.4, 1.9 Hz, 2H), 2.21−2.01 (m, 3H), 1.45 (s, 3H). $^{13}C\{^1H\}$ NMR (100 MHz, $CDCl_3$) δ 166.6 (s), 159.8 (s), 131.4 (s), 129.6 (s), 126.1 (q, J = 277.9 Hz), 122.0 (s), 119.8 (s), 114.1 (s), 69.8 (d, J = 2.0 Hz), 61.2 (s), 55.6 (s), 45.1 (q, J = 26.1 Hz), 40.5 (d, J = 1.3 Hz), 27.5 (d, J = 1.6 Hz). $^{19}F\{^1H\}$ NMR (377 MHz, $CDCl_3$) δ −60.15 (s). HRMS (ESI TOF) m/z for $C_{14}H_{17}F_3NaO_4$ $[M + Na]^+$ calcd. 329.0977, found 329.0972.

*5,5,5-Trifluoro-3-hydroxy-3-methylpentyl 4-Nitrobenzoate (**3u**).* The title compound **3u** was prepared according to the general procedure **C** starting from **1u** (0.2 mmol) and CF_3SO_2Na **2** (3 equiv). Colorless liquid (42 mg, 66% yield), R_f = 0.45 (petroleum ether/EtOAc 70:30). ^1H NMR (400 MHz, $CDCl_3$) δ 8.31−8.28 (m, 2H), 8.21−8.17 (m, 2H), 4.58 (t, J = 6.7 Hz, 2H), 2.44 (q, J = 11.3 Hz, 2H), 2.18−2.06 (m, 2H), 1.99 (s, 1H), 1.46 (s, 3H). $^{13}C\{^1H\}$ NMR (100 MHz, $CDCl_3$) δ 164.8 (s), 150.8 (s), 135.5 (s), 130.8 (s), 126.0 (q, J = 278.0 Hz), 123.8 (s), 69.6 (q, J = 1.9 Hz), 62.0 (s), 45.2 (q, J = 26.1 Hz), 40.3 (s), 27.5 (d, J = 1.5 Hz). $^{19}F\{^1H\}$ NMR (377 MHz, $CDCl_3$) δ −60.17 (s). HRMS (ESI TOF) m/z for $C_{13}H_{15}F_3NO_5$ $[M + H]$ calcd. 322.0902, found 322.0910.

*5,5,5-Trifluoro-3-hydroxy-3-methylpentyl Pivalate (**3v**).* The title compound **3v** was prepared according to the general procedure **C** starting from **1v** (0.2 mmol) and CF_3SO_2Na **2** (3 equiv). Colorless

https://doi.org/10.1021/acs.joc.4c00967
J. Org. Chem. 2024, 89, 14695−14709

liquid (29 mg, 56% yield), R_f = 0.31 (petroleum ether/EtOAc 80:20). ^{1}H NMR (400 MHz, $CDCl_3$) δ 4.25 (t, J = 6.4 Hz, 2H), 2.43−2.32 (m, 2H), 2.26 (s, 1H), 2.00−1.88 (m, 2H), 1.38 (s, 3H), 1.19 (s, 9H). $^{13}C\{^1H\}$ NMR (100 MHz, $CDCl_3$) δ 178.6 (s), 126.1 (q, J = 277.9 Hz), 69.7 (q, J = 3.9 Hz), 60.7 (s), 45.0 (q, J = 26.0 Hz), 40.4 (d, J = 1.3 Hz), 38.8 (s), 27.3 (s), 27.2 (s). $^{19}F\{^1H\}$ NMR (377 MHz, $CDCl_3$) δ −60.24 (s). HRMS (ESI TOF) for m/z $C_{11}H_{20}F_3O_3$ $[M + H]^+$ calcd. 257.1365, found 257.1363.

*3-Hydroxy-3-methyl-2-(trifluoromethyl)butyl Benzoate (**3w**).* The title compound **3w** was prepared according to the general procedure **C** starting from **1w** (0.2 mmol) and CF_3SO_2Na **2** (3 equiv). Colorless liquid (43 mg, 78% yield), R_f = 0.28 (petroleum ether/EtOAc 85:15). ^{1}H NMR (400 MHz, $CDCl_3$) δ 8.04−8.01 (m, 2H), 7.59−7.55 (m, 1H), 7.57−7.43 (m, 2H), 4.76 (ddd, J = 12.2, 3.6, 0.6 Hz, 1H), 4.59 (dd, J = 12.3, 6.1 Hz, 1H), 2.68 (qdd, J = 9.8, 6.1, 3.6 Hz, 1H), 2.10 (s, 1H), 1.48 (s, 3H), 1.42 (s, 3H). $^{13}C\{^1H\}$ NMR (100 MHz, $CDCl_3$) δ 166.4 (s), 133.4 (s), 129.8 (s), 129.7 (s), 128.6 (s), 126.8 (q, J = 282.2 Hz), 70.8 (s), 60.6 (q, J = 2.9 Hz), 52.9 (q, J = 23.4 Hz), 29.7 (q, J = 1.9 Hz), 27.9 (d, J = 1.9 Hz). $^{19}F\{^1H\}$ NMR (377 MHz, $CDCl_3$) δ −63.32 (s). HRMS (ESI TOF) m/z for $C_{13}H_{16}F_3O_3$ $[M + H]^+$ calcd. 277.1052, found 277.1056.

*5,5,5-Trifluoro-3-hydroxy-3-methylpentyl 4-Methylbenzenesulfonate (**3x**).* The title compound **3x** was prepared according to the general procedure **C** starting from **1x** (0.2 mmol) and CF_3SO_2Na **2** (3 equiv). Colorless liquid (50 mg, 76% yield), R_f = 0.45 (petroleum ether/EtOAc 85:15). ^{1}H NMR (400 MHz, $CDCl_3$) δ 7.78 (d, J = 8.3 Hz, 2H), 7.35 (d, J = 8.3 Hz, 2H), 4.07 (t, J = 6.3 Hz, 2H), 2.45 (s, 3H), 2.08−1.82 (m, 3H), 1.80−1.74 (m, 1H), 1.58−1.50 (m, 1H), 0.96 (d, J = 6.2 Hz, 3H). $^{13}C\{^1H\}$ NMR (100 MHz, $CDCl_3$) δ 145.1 (s), 133.0 (s), 130.1 (s), 128.0 (s), 126.9 (q, J = 277.4 Hz), 67.9 (s), 40.0 (q, J = 27.3 Hz), 35.4 (s), 24.6 (q, J = 2.4 Hz), 21.7 (s), 19.2 (s). $^{19}F\{^1H\}$ NMR (377 MHz, $CDCl_3$) δ −63.23 (s). HRMS (ESI TOF) m/z for $C_{13}H_{18}F_3O_4S$ $[M + H]^+$ calcd. 327.0878, found 327.0872.

*2-((6,6,6-Trifluoro-4-hydroxyhexyl)oxy)isoindoline-1,3-dione (**3y**).* The title compound **3y** was prepared according to the general procedure **C** starting from **1y** (0.2 mmol) and CF_3SO_2Na **2** (3 equiv). White solid (43 mg, 67% yield), R_f = 0.31 (petroleum ether/EtOAc 85:15), mp 73−75 °C. ^{1}H NMR (400 MHz, $CDCl_3$) δ 7.84 (dd, J = 5.5, 3.1 Hz, 2H), 7.75 (dd, J = 5.5, 3.1 Hz, 2H), 4.21 (t, J = 6.4 Hz, 2H), 2.18−2.06 (m, 2H), 1.81 (p, J = 6.6 Hz, 2H), 1.69−1.61 (m, 4H). $^{13}C\{^1H\}$ NMR (100 MHz, $CDCl_3$) δ 163.8 (s), 134.6 (s), 129.1 (s), 127.3 (q, J = 276.3 Hz), 123.7 (s), 78.2 (s), 33.8 (q, J = 28.4 Hz), 28.0 (s), 25.0 (s), 21.8 (q, J = 3.0 Hz). $^{19}F\{^1H\}$ NMR (377 MHz, $CDCl_3$) δ −66.39 (s). HRMS (ESI TOF) m/z for $C_{14}H_{15}F_3NO_4$ $[M + H]^+$ calcd. 318.0953, found 318.0947.

*1,1,1-Trifluoro-5-phenoxypentan-3-ol (**3z**).* The title compound **3z** was prepared according to the general procedure **C** starting from **1z** (0.2 mmol) and CF_3SO_2Na **2** (3 equiv). White solid (40 mg, 86% yield), R_f = 0.33 (petroleum ether/EtOAc 90:10), mp 61−63 °C. ^{1}H NMR (400 MHz, $CDCl_3$) δ 7.32−7.26 (m, 2H), 7.00−6.96 (m, 1H), 6.93−6.90 (m, 2H), 4.34 (tt, J = 8.0, 3.9 Hz, 1H), 4.21 (ddd, J = 9.6, 7.1, 4.6 Hz, 1H), 4.14 (ddd, J = 9.6, 6.3, 4.8 Hz, 1H), 2.59 (s, 1H), 2.42−2.30 (m, 2H), 2.05−1.98 (m, 2H). $^{13}C\{^1H\}$ NMR (100 MHz, $CDCl_3$) δ 158.5 (s), 129.7 (s), 126.4 (q, J = 277.1 Hz), 121.4 (s), 114.6 (s), 65.0 (s), 64.7 (q, J = 3.1 Hz), 41.4 (q, J = 26.7 Hz), 36.2 (s). $^{19}F\{^1H\}$ NMR (377 MHz, $CDCl_3$) δ −63.42 (s). HRMS (ESI TOF) m/z for $C_{11}H_{14}F_3O_2$ $[M + H]^+$ calcd. 235.0946, found 235.0940.

*1,1,1-Trifluoro-6-phenoxyhexan-3-ol (**3aa**).* The title compound **3aa** was prepared according to the general procedure **C** starting from **1aa** (0.2 mmol) and CF_3SO_2Na **2** (3 equiv). Colorless liquid (36 mg, 72% yield), R_f = 0.37 (petroleum ether/EtOAc 85:15). ^{1}H NMR (400 MHz, $CDCl_3$) δ 7.31−7.27 (m, 2H), 6.98−6.92 (m, 1H), 6.91−6.89 (m, 2H), 4.12−4.09 (m, 1H), 4.04−4.00 (m, 2H), 2.35−2.25 (m, 3H), 1.98−1.89 (m, 2H), 1.79−1.69 (m, 2H). $^{13}C\{^1H\}$ NMR (100 MHz, $CDCl_3$) δ 158.8 (s), 129.6 (s), 126.5 (q, J = 277.1 Hz), 121.0 (s), 114.6 (s), 67.6 (s), 66.0 (q, J = 3.0 Hz), 41.4 (q, J = 26.5 Hz), 34.2 (s), 25.3 (s). $^{19}F\{^1H\}$ NMR (377 MHz, $CDCl_3$) δ −63.46 (s). HRMS (ESI TOF) m/z for $C_{12}H_{16}F_3O_2$ $[M + H]^+$ calcd. 249.1102, found 249.1107.

*1,1,1-Trifluoro-8-phenoxyoctan-3-ol (**3ab**).* The title compound **3ab** was prepared according to the general procedure **C** starting from **1ab** (0.2 mmol) and CF_3SO_2Na **2** (3 equiv). Colorless liquid (36 mg, 65% yield), R_f = 0.41 (petroleum ether/EtOAc 85:15). ^{1}H NMR (400 MHz, $CDCl_3$) δ 7.30−7.25 (m, 2H), 6.95−6.91 (m, 1H), 6.90−6.87 (m, 2H), 4.03−3.99 (m, 1H), 3.98−3.94 (m, 2H), 2.35−2.17 (m, 2H), 1.88 (d, J = 4.0 Hz, 1H), 1.83−1.77 (m, 2H), 1.59−1.37 (m, 6H). $^{13}C\{^1H\}$ NMR (100 MHz, $CDCl_3$) δ 159.1 (s), 129.6 (s), 126.6 (q, J = 277.2 Hz), 120.7 (s), 114.6 (s), 67.7 (s), 66.2 (q, J = 2.9 Hz), 41.3 (q, J = 26.4 Hz), 37.2 (s), 29.3 (s), 26.0 (s), 25.1 (s). $^{19}F\{^1H\}$ NMR (377 MHz, $CDCl_3$) δ −63.49 (s). HRMS (ESI TOF) m/z for $C_{14}H_{20}F_3O_2$ $[M + H]^+$ calcd. 277.1415, found 277.1410.

*4,4-Difluoro-2-hydroxybutyl Benzoate (**3ac**).* The title compound **3ac** was prepared according to the general procedure **C** starting from allyl benzoate **1a** (0.2 mmol) and CF_3SO_2Na **2** (3 equiv). White solid (29 mg, 62% yield), R_f = 0.21 (petroleum ether/EtOAc 85:15), mp 48−50 °C. ^{1}H NMR (400 MHz, $CDCl_3$) δ 8.05 (dt, J = 8.5, 1.5 Hz, 2H), 7.62−7.57 (m, 1H), 7.48−7.44 (m, 2H), 6.25−5.94 (m, 1H), 4.45−4.40 (m, 1H), 4.33−4.25 (m, 2H), 2.52 (s, 1H), 2.19−2.06 (m, 2H). $^{13}C\{^1H\}$ NMR (100 MHz, $CDCl_3$) δ 166.8 (s), 133.6 (s), 129.8 (s), 128.7 (s), 128.7 (s), 115.9 (t, J = 238.3 Hz), 68.7 (s), 65.7 (dd, J = 8.2, 4.4 Hz), 38.1 (t, J = 21.5 Hz). $^{19}F\{^1H\}$ NMR (377 MHz, $CDCl_3$) δ −117.02 (q, J = 286.4 Hz). HRMS (ESI TOF) m/z for $C_{11}H_{13}F_2O_3$ $[M + H]^+$ calcd. 231.0833, found 231.0824.

*5,5,5-Trifluoro-3-hydroxy-3-methylpentyl thiophene-2-carboxylate (**3ad**).* The title compound **3ad** was prepared according to the general procedure **C** starting from **1ad** (0.2 mmol) and CF_3SO_2Na **2** (3 equiv). Colorless liquid (42 mg, 74% yield), R_f = 0.26 (petroleum ether/EtOAc 85:15). ^{1}H NMR (400 MHz, $CDCl_3$) δ 7.80 (dd, J = 3.8, 1.3 Hz, 1H), 7.57 (dd, J = 5.0, 1.2 Hz, 1H), 7.11 (dd, J = 5.0, 3.8 Hz, 1H), 4.50 (t, J = 6.5 Hz, 2H), 2.44 (qd, J = 11.4, 2.4 Hz, 2H), 2.17−2.01 (m, 3H), 1.44 (s, 3H). $^{13}C\{^1H\}$ NMR (100 MHz, $CDCl_3$) δ 162.2 (s), 133.8 (s), 133.5 (s), 132.8 (s), 128.0 (s), 126.1 (q, J = 277.9 Hz), 69.7 (q, J = 1.9 Hz), 61.3 (s), 45.1 (q, J = 26.0 Hz), 40.5 (d, J = 1.3 Hz), 27.4 (d, J = 1.5 Hz). $^{19}F\{^1H\}$ NMR (377 MHz, $CDCl_3$) δ −60.15 (s). HRMS (ESI TOF) m/z for $C_{11}H_{13}F_3NaO_3S$ $[M + Na]^+$ calcd. 305.0435, found 305.0427.

*5,5,5-Trifluoro-3-hydroxy-3-methylpentyl furan-2-carboxylate (**3ae**).* The title compound **3ae** was prepared according to the general procedure **C** starting from **1ae** (0.2 mmol) and CF_3SO_2Na **2** (3 equiv). Colorless liquid (28 mg, 52% yield), R_f = 0.48 (petroleum ether/EtOAc 85:15). ^{1}H NMR (400 MHz, $CDCl_3$) δ 7.57 (d, J = 0.8 Hz, 1H), 7.17 (d, J = 3.5 Hz, 1H), 6.51 (dd, J = 3.5, 1.7 Hz, 1H), 4.50 (t, J = 6.5 Hz, 2H), 2.43 (q, J = 11.4 Hz, 2H), 2.31 (s, 1H), 2.14−1.99 (m, 2H), 1.42 (s, 3H). $^{13}C\{^1H\}$ NMR (100 MHz, $CDCl_3$) δ 158.6 (s), 146.7 (s), 144.5 (s), 126.1 (q, J = 277.9 Hz), 118.4 (s), 112.1 (s), 69.7 (s), 61.1 (s), 45.0 (q, J = 26.1 Hz), 40.2 (d, J = 1.2 Hz), 27.3 (s). $^{19}F\{^1H\}$ NMR (377 MHz, $CDCl_3$) δ −60.21 (s). HRMS (ESI TOF) m/z for $C_{11}H_{14}F_3O_4$ $[M + H]^+$ calcd. 267.0844, found 267.0842.

*4,4,4-Trifluoro-2-hydroxybutyl benzo[b]thiophene-2-carboxylate (**3af**).* The title compound **3af** was prepared according to the general procedure **C** starting from **1af** (0.2 mmol) and CF_3SO_2Na **2** (3 equiv). White solid (40 mg, 65% yield), R_f = 0.23 (petroleum ether/EtOAc 85:15), mp 85−87 °C. ^{1}H NMR (400 MHz, $CDCl_3$) δ 8.11 (s, 1H), 7.88 (t, J = 8.7 Hz, 2H), 7.50−7.41 (m, 2H), 4.49−4.34 (m, 3H), 2.56−2.38 (m, 3H); $^{13}C\{^1H\}$ NMR (100 MHz, $CDCl_3$) δ 162.8 (s), 142.5 (s), 138.7 (s), 132.4 (s), 131.3 (s), 127.5 (s), 126.3 (q, J = 225.6 Hz), 125.9 (s), 125.3 (s), 122.9 (s), 68.21 (s), 64.9 (q, J = 3.1 Hz), 38.0 (q, J = 28.0 Hz). $^{19}F\{^1H\}$ NMR (377 MHz, $CDCl_3$) δ −63.47 (s). HRMS (ESI TOF) m/z for $C_{13}H_{12}F_3O_3S$ $[M + H]^+$ calcd 305.0459, found 305.0456.

*4,4,4-Trifluoro-2-hydroxybutyl 1-methyl-5-(trifluoromethyl)-1H-pyrrole-2-carboxylate (**3ag**).* The title compound **3ag** was prepared according to the general procedure **C** starting from **1ag** (0.2 mmol) and CF_3SO_2Na **2** (3 equiv). Colorless liquid (28 mg, 43% yield), R_f = 0.29 (petroleum ether/EtOAc 85:15). ^{1}H NMR (400 MHz, $CDCl_3$) δ 6.93 (d, J = 4.2 Hz, 1H), 6.55 (d, J = 4.2 Hz, 1H), 4.39−4.24 (m, 3H), 4.02 (s, 3H), 2.50 (d, J = 3.7 Hz, 1H), 2.46−2.35 (m, 2H). $^{13}C\{^1H\}$ NMR (150 MHz, $CDCl_3$) δ 160.6 (s), 128.1 (q, J = 38.0 Hz), 126.1 (q, J = 276.9 Hz), 125.6 (d, J = 1.8 Hz), 120.7 (q, J =

https://doi.org/10.1021/acs.joc.4c00967
J. Org. Chem. 2024, 89, 14695−14709

268.3 Hz), 116.7 (s), 110.7 (q, J = 3.5 Hz), 67.2 (s), 64.9 (q, J = 3.0 Hz), 38.0 (q, J = 28.0 Hz), 33.9 (d, J = 1.9 Hz). $^{19}F\{^1H\}$ NMR (377 MHz, $CDCl_3$) δ −59.79 (s), −63.53 (s). HRMS (ESI TOF) m/z for $C_{11}H_{12}F_6NO_3$ $[M + H]^+$ calcd. 320.0721, found 320.0720.

*5,5,5-Trifluoro-3-hydroxy-3-methylpentyl 1-Methyl-5-(trifluoromethyl)-1H-pyrrole-2-carboxylate (**3ah**).* The title compound **3ah** was prepared according to the general procedure **C** starting from **1ah** (0.2 mmol) and CF_3SO_2Na **2** (3 equiv). Colorless liquid (38 mg, 55% yield), R_f = 0.24 (petroleum ether/EtOAc 85:15). ^1H NMR (400 MHz, $CDCl_3$) δ 6.85 (d, J = 4.3 Hz, 1H), 6.53 (d, J = 4.2 Hz, 1H), 4.46 (t, J = 6.5 Hz, 2H), 4.02 (s, 3H), 2.42 (qd, J = 11.3, 1.6 Hz, 2H), 2.16−1.95 (m, 3H), 1.43 (s, 3H). $^{13}C\{^1H\}$ NMR (100 MHz, $CDCl_3$) δ 160.7 (s), 127.7 (d, J = 37.8 Hz), 126.2 (d, J = 1.9 Hz), 126.0 (q, J = 277.9 Hz), 120.7 (q, J = 268.0 Hz), 116.2 (s), 110.6 (dd, J = 7.1, 3.6 Hz), 69.7 (d, J = 2.0 Hz), 60.6 (s), 45.1 (q, J = 26.1 Hz), 40.4 (s), 33.8 (d, J = 2.0 Hz), 27.4 (d, J = 1.5 Hz). $^{19}F\{^1H\}$ NMR (377 MHz, $CDCl_3$) δ −59.76 (s), −60.22 (s). HRMS (ESI TOF) m/z for $C_{13}H_{16}F_6NO_3$ $[M + H]^+$ calcd. 348.1034, found 348.1031.

*(3S,5S,6R,8S,9S,10R,13S,14S,17S)-17-Acetyl-5-hydroxy-10,13-dimethyl-6-(trifluoromethyl)hexadecahydro-1H-cyclopenta[a]phenanthren-3-yl Benzoate (**3ai**).* The title compound **3ai** was prepared according to the general procedure **C** starting from **1ai** (0.2 mmol) and CF_3SO_2Na **2** (3 equiv). White solid (66 mg, 65% yield), R_f = 0.17 (petroleum ether/EtOAc 85:15), mp 192−194 °C. ^1H NMR (400 MHz, $CDCl_3$) δ 8.02 (d, J = 7.1 Hz, 2H), 7.55 (t, J = 7.4 Hz, 1H), 7.43 (t, J = 7.7 Hz, 2H), 5.41 (tt, J = 10.3, 5.0 Hz, 1H), 2.52 (t, J = 8.9 Hz, 1H), 2.45 (s, 1H), 2.28 (t, J = 12.5 Hz, 2H), 2.12 (s, 3H), 2.05 (dd, J = 7.7, 4.7 Hz, 2H), 2.03−1.95 (m, 2H), 1.86−1.73 (m, 3H), 1.68 (ddd, J = 13.3, 8.1, 3.7 Hz, 3H), 1.61−1.51 (m, 2H), 1.51−1.40 (m, 2H), 1.40−1.26 (m, 2H), 1.26−1.20 (m, 2H), 1.10 (s, 3H), 0.63 (s, 3H). $^{13}C\{^1H\}$ NMR (100 MHz, $CDCl_3$) δ 209.5 (s), 166.4 (s), 133.1 (s), 130.6 (s), 129.7 (s), 129.5 (dd, J = 463.4, 337.3 Hz), 128.5 (s), 76.4 (s), 71.3 (s), 63.8 (s), 56.3 (s), 50.8 (dd, J = 50.3, 25.2 Hz), 45.9 (s), 44.4 (s), 39.5 (s), 39.1 (s), 38.8 (s), 33.2 (s), 32.0 (s), 31.6 (s), 26.9 (s), 26.5 (s), 24.4 (s), 23.0 (s), 21.3 (s), 16.5 (dd, J = 7.5, 3.7 Hz), 13.7 (s). $^{19}F\{^1H\}$ NMR (377 MHz, $CDCl_3$) δ −60.38 (s). HRMS (ESI TOF) m/z for $C_{29}H_{37}F_3NaO_4$ $[M + Na]^+$ calcd. 529.2542, found 529.2542.

*(3S,5S,6R,8S,9S,10R,13R,14S,17R)-5-Hydroxy-10,13-dimethyl-17-((R)-6-methylheptan-2-yl)-6-(trifluoromethyl)hexadecahydro-1H-cyclopenta[a]phenanthren-3-yl Benzoate (**3aj**).* The title compound **3aj** was prepared according to the general procedure **C** starting from **1aj** (0.2 mmol) and CF_3SO_2Na **2** (3 equiv). White solid (62 mg, 54% yield), R_f = 0.59 (petroleum ether/EtOAc 85:15), mp 173−175 °C. ^1H NMR (600 MHz, $CDCl_3$) δ 8.03 (d, J = 7.8 Hz, 2H), 7.55 (t, J = 7.4 Hz, 1H), 7.43 (t, J = 7.7 Hz, 2H), 5.42 (td, J = 11.0, 5.3 Hz, 1H), 2.42 (s, 1H), 2.30−2.26 (m, 2H), 2.06−2.00 (m, 3H), 1.87−1.81 (m, 2H), 1.79−1.72 (m, 4H), 1.64−1.56 (m, 3H), 1.51 (td, J = 13.1, 6.5 Hz, 1H), 1.46−1.41 (m, 1H), 1.41−1.32 (m, 4H), 1.31−1.24 (m, 2H), 1.22−1.18 (m, 1H), 1.16−1.13 (m, 3H), 1.11 (s, 3H), 1.10−1.07 (m, 2H), 1.01−0.96 (m, 1H), 0.91 (d, J = 6.5 Hz, 4H), 0.87 (d, J = 2.6 Hz, 3H), 0.86 (d, J = 2.6 Hz, 2H), 0.68 (s, 3H). $^{13}C\{^1H\}$ NMR (150 MHz, $CDCl_3$) δ 166.5 (s), 133.1 (s), 130.7 (s), 129.7 (s), 128.4 (s), 127.2 (q, J = 280.9 Hz), 76.3 (s), 71.7 (s), 56.4 (s), 56.0 (s), 51.7 (q, J = 24.9 Hz), 46.0 (s), 42.9 (s), 40.0 (s), 39.6 (s), 39.4 (s), 38.7 (s), 36.3 (s), 36.0 (s), 33.2 (s), 31.9 (s), 28.4 (s), 28.2 (s), 27.0 (s), 26.5 (s), 24.2 (s), 24.1 (s), 23.0 (s), 22.7 (s), 21.3 (s), 18.8 (s), 16.5 (d, J = 3.5 Hz), 12.4 (s). $^{19}F\{^1H\}$ NMR (565 MHz, $CDCl_3$) δ −61.32 (s). HRMS (ESI TOF) m/z for $C_{35}H_{52}F_3O_3$ $[M + H]^+$ calcd. 577.3869, found 577.3863.

*Methyl 10-Hydroxy-9-(trifluoromethyl)octadecenoate (**3ak**).* The title compound **3ak** was prepared according to the general procedure **C** starting from **1ak** (0.2 mmol) and CF_3SO_2Na **2** (3 equiv). Colorless liquid (36 mg, 47% yield), R_f = 0.27 (petroleum ether/EtOAc 90:10). ^1H NMR (600 MHz, $CDCl_3$) δ 3.98−3.81 (m, 1H), 3.66 (s, 3H), 2.30 (t, J = 7.5 Hz, 2H), 2.24−2.02 (m, 1H), 1.70−1.34 (m, 11H), 1.35−1.21 (m, 16H), 0.87 (t, J = 7.0 Hz, 3H). $^{13}C\{^1H\}$ NMR (150 MHz, $CDCl_3$) δ 174.4 (s), 128.6 (q, J = 281.3 Hz), 128.0 (qd, J = 281.6, 3.2 Hz), 70.2 (s), 69.6 (d, J = 2.5 Hz), 51.6 (s), 48.5 (q, J = 22.6 Hz), 48.3 (dq, J = 45.4, 22.6 Hz), 48.1 (dd, J = 45.5, 22.8 Hz), 34.7 (d, J = 11.3 Hz), 34.2 (d, J = 2.1 Hz), 34.1 (s), 32.0 (d, J = 1.2 Hz), 31.9 (d, J = 0.9 Hz), 30.0 (d, J = 4.1 Hz), 29.8 (d, J = 2.7 Hz), 29.7 (d, J = 2.1 Hz), 29.6 (d, J = 3.1 Hz), 29.5 (d, J = 1.7 Hz), 29.4 (d, J = 4.5 Hz), 29.3 (s), 29.2 (s), 29.1 (d, J = 2.1 Hz), 29.0 (d, J = 3.5 Hz), 28.6 (d, J = 13.9 Hz), 27.8 (s), 27.7 (s), 26.4 (d, J = 4.2 Hz), 26.3 (s), 26.2 (s), 25.0 (s), 24.9 (d, J = 2.1 Hz), 24.8 (d, J = 2.0 Hz), 23.1 (d, J = 1.7 Hz), 22.8 (s), 22.7 (s), 14.2 (s). ^{19}F NMR (377 MHz, $CDCl_3$) δ −65.17 (d, J = 5.8 Hz), −67.47 (s). HRMS (ESI TOF) m/z for $C_{20}H_{38}F_3O_3$ $[M + H]^+$ calcd. 383.2773, found 383.2775.

*7-Hydroxy-3,7-dimethyl-6-(trifluoromethyl)octyl Benzoate (**3al**).* The title compound **3al** was prepared according to the general procedure **C** starting from **1al** (0.2 mmol) and CF_3SO_2Na **2** (3 equiv). Colorless liquid (32 mg, 46% yield), R_f = 0.27 (petroleum ether/EtOAc 90:10). ^1H NMR (600 MHz, $CDCl_3$) δ 8.03 (d, J = 7.6 Hz, 2H), 7.55 (t, J = 7.4 Hz, 1H), 7.44 (t, J = 7.7 Hz, 2H), 4.38−4.33 (m, 2H), 2.08−2.04 (m, 1H), 1.88−1.79 (m, 1H), 1.76−1.72 (m, 1H), 1.67−1.62 (m, 3H), 1.61−1.54 (m, 2H), 1.50−1.44 (m, 1H), 1.34 (s, 3H), 1.30 (s, 3H), 0.99 (dd, J = 6.4, 3.6 Hz, 3H). $^{13}C\{^1H\}$ NMR (150 MHz, $CDCl_3$) δ 166.8 (d, J = 1.8 Hz), 133.0 (s), 130.5 (s), 129.7 (s), 128.5 (s), 128.3 (q, J = 282.1 Hz), 71.6 (d, J = 2.3 Hz), 63.4 (d, J = 13.4 Hz), 54.0−53.5 (m), 37.3 (d, J = 16.2 Hz), 35.3 (dd, J = 62.7, 35.6 Hz), 30.3 (d, J = 12.7 Hz), 29.3−28.7 (m), 27.7 (s), 23.3 (dd, J = 35.7, 2.3 Hz), 19.5 (d, J = 30.1 Hz). $^{19}F\{^1H\}$ NMR (565 MHz, $CDCl_3$) δ −64.86 (d, J = 53.7 Hz). HRMS (ESI TOF) m/z for $C_{18}H_{25}F_3NaO_3$ $[M + Na]^+$ calcd. 369.1653, found 369.1655.

*4-Hydroxy-3-(trifluoromethyl)hexyl Benzoate (**3xx**).* The title compound **3xx** was prepared according to the general procedure **C** starting from benzoate **1am** or **1an** (0.2 mmol) and CF_3SO_2Na **2** (3 equiv). Colorless liquid, R_f = 0.30 (petroleum ether/EtOAc 85:15). ^1H NMR (400 MHz, Chloroform-*d*) δ 8.02 (d, J = 7.3 Hz, 2H), 7.59−7.54 (m, 1H), 7.44 (t, J = 7.8 Hz, 2H), 4.68−4.34 (m, 2H), 4.20−3.83 (m, 1H), 2.63−2.29 (m, 1H), 2.28−1.87 (m, 3H), 1.85−1.48 (m, 2H), 1.12−0.95 (m, 3H). $^{13}C\{^1H\}$ NMR (100 MHz, $CDCl_3$) δ 167.2, 167.0, 166.6, 133.4, 133.3, 133.2, 130.2, 130.1, 130.0, 129.8, 129.7, 129.6, 128.6, 128.5, 127.8 (q, J = 280 Hz), 127.5 (q, J = 280 Hz), 71.5 (q, J = 2.3 Hz), 70.6 (q, J = 2.7 Hz), 66.5 (q, J = 2.4 Hz), 66.2 (q, J = 3.1 Hz), 63.3, 62.9, 62.2, 62.1, 50.1 (q, J = 22.9 Hz), 45.4 (q, J = 23.6 Hz), 44.6 (q, J = 23.7 Hz), 34.1, 33.2 (d, J = 1.8 Hz), 28.1, 26.6 (d, J = 1.6 Hz), 24.2 (d, J = 2.7 Hz), 22.5 (d, J = 2.3 Hz), 17.7 (d, J = 2.5 Hz), 16.9 (d, J = 2.4 Hz), 13.0, 12.3, 10.7, 10.5. $^{19}F\{^1H\}$ NMR (377 MHz, $CDCl_3$) δ −65.21, −65.69, −66.87, −68.13. HRMS (ESI TOF) m/z for $C_{14}H_{18}F_3O_3$ $[M + H]^+$ calcd. 291.1208, found 291.1206.

*4,4,4-Trifluoro-2-hydroxybutyl 2′-methyl-[1,1′-biphenyl]-2-carboxylate (**5a**).* To a solution of **3n** (50 mg, 1.0 equiv) in toluene/H_2O (1 mL/0.3 mL) at room temperature was added *o*-tolylboronic acid **4a** (1.5 equiv), $Pd(PPh_3)_4$ (10 mol %) and K_3PO_4 (2.5 equiv) sequentially under nitrogen atmosphere. The reaction mixture was heated to 80 °C and maintained at this temperature for stirring 24 h. After which (monitored by TLC), the reaction mixture was cooled to room temperature and it was filtered through Celite bed and the solvent was evaporated under reduce pressure. The residue was purified by column chromatography over silica gel (100−200 mesh) using mixture of petroleum ether/EtOAc as an eluent to afford the desired compound **5a** (37 mg, 82% yield). Yellow liquid, R_f = 0.38 (petroleum ether/EtOAc 80:20). ^1H NMR (400 MHz, $CDCl_3$) δ 8.05 (ddd, J = 7.8, 4.2, 1.3 Hz, 1H), 7.61−7.56 (m, 1H), 7.47 (t, J = 7.6 Hz, 1H), 7.34−7.27 (m, 3H), 7.23 (dd, J = 7.7, 1.1 Hz, 1H), 7.15 (dd, J = 7.5, 2.6 Hz, 1H), 4.13 (ddd, J = 22.1, 11.4, 3.2 Hz, 1H), 3.91 (ddd, J = 22.7, 11.4, 6.2 Hz, 1H), 3.81−3.74 (m, 1H), 2.10 (d, J = 2.7 Hz, 3H), 2.06−1.87 (m, 2H). $^{13}C\{^1H\}$ NMR (100 MHz, $CDCl_3$) δ 167.9 (d, J = 7.6 Hz), 142.4 (d, J = 13.5 Hz), 142.2 (d, J = 7.2 Hz), 135.6 (d, J = 17.5 Hz), 132.3 (d, J = 11.9 Hz), 131.2 (d, J = 0.6 Hz), 131.1 (d, J = 1.0 Hz), 130.0 (d, J = 16.7 Hz), 129.7 (d, J = 6.2 Hz), 128.7 (d, J = 6.5 Hz), 127.9 (d, J = 1.6 Hz), 127.7 (d, J = 1.4 Hz), 125.8 (dd, J = 553.5, 276.8 Hz), 125.8 (d, J = 3.7 Hz), 68.5 (d, J = 6.7 Hz), 64.2 (d, J = 2.1 Hz), 37.3 (q, J = 28.1 Hz), 20.1 (d, J = 4.4 Hz). $^{19}F\{^1H\}$ NMR (377 MHz, $CDCl_3$) δ −63.65 (d, J = 8.0 Hz). HRMS

https://doi.org/10.1021/acs.joc.4c00967
J. Org. Chem. 2024, 89, 14695−14709

(ESI TOF) m/z for $C_{18}H_{17}F_3NaO_3$ $[M + Na]^+$ calcd. 361.1027, found 361.1021.

*4,4,4-Trifluoro-2-hydroxybutyl 2′-methoxy-[1,1′-biphenyl]-2-carboxylate (**5b**).* The title compound **5b** was prepared according to the above-mentioned procedure as that of **5a** stating with (2-methoxyphenyl)boronic acid **4b**. Yellow liquid (41 mg, 87% yield), R_f = 0.21 (petroleum ether/EtOAc 80:20). ^{1}H NMR (400 MHz, $CDCl_3$) δ 7.94 (dd, J = 7.8, 1.0 Hz, 1H), 7.58 (td, J = 7.6, 1.4 Hz, 1H), 7.44 (td, J = 7.6, 1.3 Hz, 1H), 7.38 (td, J = 8.2, 1.7 Hz, 1H), 7.32 (dd, J = 7.7, 0.9 Hz, 1H), 7.28 (dd, J = 7.4, 1.6 Hz, 1H), 7.08 (td, J = 7.4, 0.9 Hz, 1H), 6.96 (d, J = 8.2 Hz, 1H), 4.17 (d, J = 8.7 Hz, 1H), 3.93 (s, 1H), 3.87 (s, 1H), 3.73 (s, 3H), 2.04−1.87 (m, 2H), 1.59 (s, 1H). $^{13}C\{^1H\}$ NMR (100 MHz, $CDCl_3$) δ 168.3 (s), 156.1 (s), 138.5 (s), 132.2 (s), 131.6 (s), 131.0 (s), 130.2 (s), 130.1 (s), 129.3 (s), 127.6 (s), 125.9 (q, J = 276.8 Hz), 121.1 (s), 110.6 (s), 68.2 (s), 64.3 (s), 55.6 (s), 37.4 (q, J = 28.1 Hz). $^{19}F\{^1H\}$ NMR (377 MHz, $CDCl_3$) δ −63.70 (s). HRMS (ESI TOF) m/z for $C_{18}H_{17}F_3O_4$ $[M]^+$ calcd. 354.1079, found 354.1079.

*4,4,4-Trifluoro-2-((2-(4-isobutylphenyl)propanoyl)oxy)butyl Benzoate (**5c**).* To a stirred solution of **3a** (50 mg, 1 equiv), 2-(4-isobutylphenyl)propanoic acid **4c** (1.5 equiv) and dimethylaminopyridine, DMAP (10 mol %) in anhydrous CH_2Cl_2 (5 mL) was added *N*,*N*′-dicyclohexylcarbodiimide, DCC (1.5 equiv) at 0 °C, which is then stirred for 5 min at 0 °C and then at room temperature. The progress of the reaction was monitored by TLC. After completion of the reaction, precipitated urea is then filtered off in CH_2Cl_2. The CH_2Cl_2 solution is washed twice with ∼ HCl (0.5 N) and with saturated $NaHCO_3$ solution. The combined organic layers were washed with brine solution and dried over anhydrous Na_2SO_4. The crude product was purified by column chromatography over silica gel (100−200 mesh) using mixture of petroleum ether/EtOAc as an eluent to afford **5c**. Colorless liquid (71 mg, 81% yield), R_f = 0.38 (petroleum ether/EtOAc 90:10). ^{1}H NMR (400 MHz, $CDCl_3$) δ 7.98 (dd, J = 8.4, 1.3 Hz, 1H), 7.88 (dd, J = 8.4, 1.3 Hz, 1H), 7.62−7.55 (m, 1H), 7.47−7.39 (m, 2H), 7.16 (t, J = 8.1 Hz, 2H), 7.03 (d, J = 8.1 Hz, 1H), 6.97 (d, J = 8.1 Hz, 1H), 5.56−5.51 (m, 1H), 4.54−4.27 (m, 2H), 3.72 (p, J = 7.1 Hz, 1H), 2.62−2.41 (m, 2H), 2.40 (d, J = 7.2 Hz, 1H), 2.35 (d, J = 7.2 Hz, 1H), 1.85−1.73 (m, 1H), 1.49 (d, J = 7.2 Hz, 3H), 0.87 (d, J = 6.6 Hz, 3H), 0.84 (d, J = 6.6 Hz, 3H). $^{13}C\{^1H\}$ NMR (150 MHz, $CDCl_3$) δ 173.7 (s), 173.6 (s), 166.0 (s), 165.9 (s), 140.8 (s), 140.7 (s), 137.1 (s), 137.0 (s), 133.5 (s), 133.4 (s), 129.9 (s), 129.8 (s), 129.5 (s), 129.4 (s), 129.4 (s), 128.6 (s), 128.5 (s), 127.3 (s), 127.2 (s), 125.5 (q, J = 276.8 Hz), 125.3 (q, J = 277.0 Hz), 65.8 (q, J = 2.9 Hz), 65.6 (q, J = 2.8 Hz), 64.6 (s), 64.6 (s), 45.3 (s), 45.1 (s), 45.1 (s), 45.0 (s), 35.5 (q, J = 29.3 Hz), 35.4 (q, J = 29.4 Hz), 30.3 (s), 30.2 (s), 22.5 (s), 22.5 (s), 22.4 (s), 18.3 (s), 18.2 (s). $^{19}F\{^1H\}$ NMR (377 MHz, $CDCl_3$) δ −63.77 (s), −63.80 (s). HRMS (ESI TOF) m/z for $C_{24}H_{27}F_3NaO_4$ $[M + Na]^+$ calcd. 459.1759, found 459.1762.

*4,4,4-Trifluoro-2-oxobutyl Benzoate (**5d**).* To a stirred solution of **3a** (50 mg, 1 equiv), pyridinium chlorochromate (PCC) (1.5 equiv) was added in anhydrous CH_2Cl_2 (5 mL) then reflux for 14 h. The progress of the reaction was monitored by TLC. After completion of the reaction the solvent was evaporated under reduce pressure. The residue was purified by column chromatography over silica gel (100−200 mesh) using mixture of petroleum ether/EtOAc as an eluent to afford the desired compound **5d**. White solid (38 mg, 76% yield), R_f = 0.28 (petroleum ether/EtOAc 85:15), mp 98−100 °C. ^{1}H NMR (400 MHz, $CDCl_3$) δ 8.09 (dd, J = 8.3, 1.2 Hz, 2H), 7.64−7.60 (m, 1H), 7.50−7.46 (m, 2H), 4.96 (s, 2H), 3.38 (q, J = 10.2 Hz, 2H). $^{13}C\{^1H\}$ NMR (100 MHz, $CDCl_3$) δ 194.0 (q, J = 4.8 Hz), 165.8 (s), 133.9 (s), 133.6 (s), 130.1 (s), 128.8 (s), 123.4 (q, J = 276.9 Hz), 68.4 (q, J = 2.4 Hz), 43.5 (q, J = 29.3 Hz). $^{19}F\{^1H\}$ NMR (377 MHz, $CDCl_3$) δ −62.00 (s). HRMS (ESI TOF) m/z for $C_{11}H_{10}F_3O_3$ $[M + H]^+$ calcd. 247.0582, found 247.0577.

■ ASSOCIATED CONTENT

Data Availability Statement

The data underlying this study are available in the published article and its Supporting Information.

Supporting Information

The Supporting Information is available free of charge at https://pubs.acs.org/doi/10.1021/acs.joc.4c00967.

Reaction optimization tables, procedure for reaction under sunlight, series of control experiments, and gram-scale synthesis of **3a**, fluorescence quenching plot, cyclic voltammograms, SCXRD data of compound **3ai** (CCDC 2292952), characterization data for all new compounds and copies of ^{1}H, $^{13}C\{^1H\}$, and $^{19}F\{^1H\}$ NMR spectra (PDF)

Accession Codes

CCDC 2292952 contains the supplementary crystallographic data for this paper. These data can be obtained free of charge via www.ccdc.cam.ac.uk/data_request/cif, or by emailing data_request@ccdc.cam.ac.uk, or by contacting The Cambridge Crystallographic Data Centre, 12 Union Road, Cambridge CB2 1EZ, UK; fax: +44 1223 336033.

■ AUTHOR INFORMATION

Corresponding Author

Ramakrishna G. Bhat − *Department of Chemistry, Indian Institute of Science Education and Research (IISER)-Pune, 411008 Pune, Maharashtra, India;* orcid.org/0000-0002-7739-9553; Email: rgb@iiserpune.ac.in

Authors

Mousumi Behera − *Department of Chemistry, Indian Institute of Science Education and Research (IISER)-Pune, 411008 Pune, Maharashtra, India;* orcid.org/0000-0003-2609-5987

Pankaj D. Dharpure − *Department of Chemistry, Indian Institute of Science Education and Research (IISER)-Pune, 411008 Pune, Maharashtra, India*

Ajit K. Sahu − *Department of Chemistry, Indian Institute of Science Education and Research (IISER)-Pune, 411008 Pune, Maharashtra, India*

Complete contact information is available at: https://pubs.acs.org/10.1021/acs.joc.4c00967

Notes

The authors declare no competing financial interest.

■ ACKNOWLEDGMENTS

R.G.B. thanks Science and Engineering Research Board Department of Science and Technology (SERB-DST), New Delhi, Government of India (File no: CRG/2023/004226 and CRG/2019/005753) for the generous research grant. The authors also thank IISER Pune for financial assistance. M.B. thanks IISER Pune for the fellowship. The authors thank Dr. Utpal Das for providing ^{18}O labeled oxygen and Mr. Manish Kumar for assisting. We sincerely thank Dr. Nirmala Mohanta for helping in obtaining single crystal X-ray data.

■ REFERENCES

(1) (a) Kirsch, P. *Modern Fluoroorganic Chemistry*; Wiley-VCH, Weinheim, 2004. (b) Zhu, W.; Wang, J.; Wang, S.; Gu, Z.; Aceña, J. L.; Izawa, K.; Liu, H.; Soloshonok, V. A. Recent advances in the trifluoromethylation methodology and new CF_3-containing drugs. *J.*

Fluorine Chem. **2014**, *167*, 37−54. (c) Zhou, Y.; Wang, J.; Gu, Z.; Wang, S.; Zhu, W.; Aceña, J. L.; Soloshonok, V. A.; Izawa, K.; Liu, H. Next generation of fluorine containing pharmaceuticals, compounds currently in phase II−III clinical trials of major pharmaceutical companies: new structural trends and therapeutic areas. *Chem. Rev.* **2016**, *116*, 422−518. (d) Inoue, M.; Sumii, Y.; Shibata, N. Contribution of organofluorine compounds to pharmaceuticals. *ACS Omega* **2020**, *5*, 10633−10640. (e) Jeschke, P. The unique role of fluorine in the design of active ingredients for modern crop protection. *ChemBioChem* **2004**, *5*, 570−589. (f) Ogawa, Y.; Tokunaga, E.; Kobayashi, O.; Hirai, K.; Shibata, N. Current contributions of organofluorine compounds to the agrochemical industry. *iScience* **2020**, *23*, 101467−101489. (g) Hird, M. Fluorinated liquid crystals − properties and applications. *Chem. Soc. Rev.* **2007**, *36*, 2070−2095. (h) Ametamey, S. M.; Honer, M.; Schubiger, P. A. Molecular imaging with PET. *Chem. Rev.* **2008**, *108*, 1501−1516. (i) Francis, F.; Wuest, F. Advances in [^{18}F]trifluoromethylation chemistry for PET imaging. *Molecules* **2021**, *26*, 6478−6502.

(2) (a) Ma, J.-A.; Cahard, D. Strategies for nucleophilic, electrophilic, and radical trifluoromethylations. *J. Fluorine Chem.* **2007**, *128*, 975−996. (b) Studer, A. A "Renaissance" in radical trifluoromethylation. *Angew. Chem., Int. Ed.* **2012**, *51*, 8950−8958. (c) Barata-Vallejo, S.; Lantaño, B.; Postigo, A. Recent advances in trifluoromethylation reactions with electrophilic trifluoromethylating reagents. *Chem. - Eur. J.* **2014**, *20*, 16806−16829. (d) Xiao, H.; Zhang, Z.; Fang, Y.; Zhu, L.; Li, C. Radical trifluoromethylation. *Chem. Soc. Rev.* **2021**, *50*, 6308−6319. (e) Mandal, D.; Maji, S.; Pal, T.; Sinha, S. K.; Maiti, D. Recent advances in transition metal-mediated trifluoromethylation reactions. *Chem. Commun.* **2022**, *58*, 10442−10468.

(3) (a) Lan, X.-W.; Wang, N.-X.; Xing, Y. Recent advances in radical difunctionalization of simple alkenes. *Eur. J. Org. Chem.* **2017**, *2017*, 5821−5851. (b) Yao, H.; Hu, W.; Zhang, W. Difunctionalization of alkenes and alkynes via intermolecular radical and nucleophilic additions. *Molecules* **2021**, *26*, 105−135. For selective reviews on Trifluoromethylating difunctionalization of alkenes. (c) Egami, H.; Sodeoka, M. Trifluoromethylation of alkenes with concomitant introduction of additional functional groups. *Angew. Chem., Int. Ed.* **2014**, *53*, 8294−8308. (d) Merino, E. X. B.; Nevado, C. Addition of CF_3 across unsaturated moieties: a powerful functionalization tool. *Chem. Soc. Rev.* **2014**, *43*, 6598−6608. (e) Kawamura, S.; Barrio, P.; Fustero, S.; Escorihuela, J.; Han, J.; Soloshonok, V. A.; Sodeoka, M. Evolution and future of hetero- and hydro-trifluoromethylations of unsaturated C−C bonds. *Adv. Synth. Catal.* **2023**, *365*, 398−462.

(4) (a) Yang, X.; He, L.; Tsui, G. C Hydroxytrifluoromethylation of alkenes using fluoroform-derived $CuCF_3$. *Org. Lett.* **2017**, *19*, 2446−2449. (b) Yang, Y.; Liu, Y.; Jiang, Y.; Zhang, Y.; Vicic, D. A. Manganese-catalyzed aerobic oxytrifluoromethylation of styrene derivatives using CF_3SO_2Na as the trifluoromethyl source. *J. Org. Chem.* **2015**, *80*, 6639−6648. (c) Liu, C.; Lu, Q.; Huang, Z.; Zhang, J.; Liao, F.; Peng, P.; Lei, A. NMP and O_2 as radical initiator: trifluoromethylation of alkenes to tertiary β-trifluoromethyl alcohols at room temperature. *Org. Lett.* **2015**, *17*, 6034−6037. (d) Jud, W.; Kappe, C. O.; Cantillo, D. Catalyst-free oxytrifluoromethylation of alkenes through paired electrolysis in organic-aqueous media. *Chem. - Eur. J.* **2018**, *24*, 17234−17238. (e) Luo, H.-Q.; Zhang, Z.-P.; Dong, W.; Luo, X.-Z. A practical method for metal-free radical trifluoromethylation of styrenes with $NaSO_2CF_3$. *Synlett* **2014**, *25*, 1307−1311. (f) Yasu, Y.; Koike, T.; Akita, M. Three-component oxytrifluoromethylation of alkenes: highly efficient and regioselective difunctionalization of C−C bonds mediated by photoredox catalysts. *Angew. Chem., Int. Ed.* **2012**, *51*, 9567−9571.

(5) (a) Roth, H. G.; Romero, N. A.; Nicewicz, D. A. Experimental and calculated electrochemical potentials of common organic molecules for applications to single-electron redox chemistry. *Synlett* **2016**, *27*, 714−723. (b) Surprisingly, during the screening and optimization of our protocol, we observed the lower oxidation potential for some of the unactivated alkenes (< 2.0 V vs SCE, for details ESI, S16-S20, Figures S14-S21). (c) Li, Q.; Fan, W.; Peng, D.; Meng, B.; Wang, S.; Huang, R.; Liu, S.; Li, S. Cobalt−tertiary-amine-mediated hydroxytrifluoromethylation of alkenes with CF_3Br and atmospheric oxygen. *ACS Catal.* **2020**, *10*, 4012−4018. (d) Shen, W.-G.; Wu, Q.-Y.; Gong, X.-Y.; Aoa, G.-Z.; Liu, F. A facile method for hydroxytrifluoromethylation of alkenes with Langlois reagent and DMSO. *Green Chem.* **2019**, *21*, 2983−2987.

(6) (a) Narayanam, J. M. R.; Stephenson, C. R. J. Visible light photoredox catalysis: applications in organic synthesis. *Chem. Soc. Rev.* **2011**, *40*, 102−113. (b) Prier, C. K.; Rankic, D. A.; MacMillan, D. W. C. Visible light photoredox catalysis with transition metal complexes: applications in organic synthesis. *Chem. Rev.* **2013**, *113*, 5322−5363. (c) Staveness, D.; Bosque, I.; Stephenson, C. R. J. Free radical chemistry enabled by visible light-induced electron transfer. *Acc. Chem. Res.* **2016**, *49*, 2295−2306. (d) Shaw, M. H.; Twilton, J.; MacMillan, D. W. C. Photoredox catalysis in organic chemistry. *J. Org. Chem.* **2016**, *81*, 6898−6926. (e) Xi, Y.; Yi, H.; Lei, A. Synthetic applications of photoredox catalysis with visible light. *Org. Biomol. Chem.* **2013**, *11*, 2387−2403.

(7) Koike, T.; Akita, M. New horizons of photocatalytic fluoromethylative difunctionalization of alkenes. *Chem* **2018**, *4*, 409−437.

(8) Long, W.; Lian, P.; Li, J.; Wan, X. Mn-catalysed photoredox hydroxytrifluoromethylation of aliphatic alkenes using CF_3SO_2Na. *Org. Biomol. Chem.* **2020**, *18*, 6483−6486.

(9) Lee, Y.; Kwon, M. S. Emerging organic photoredox catalysts for organic transformations. *Eur. J. Org. Chem.* **2020**, *2020*, 6028−6043.

(10) (a) Dharpure, P. D.; Bhowmick, A.; Warghude, P. K.; Bhat, R. G. Visible-light mediated facile dithiane deprotection under metal free conditions. *Tetrahedron Lett.* **2020**, *61*, 151407−151415. (b) Bhowmick, A.; Warghude, P. K.; Dharpure, P. D.; Bhat, R. G. Direct access to α-acyloxycarbonyl compounds and esters via oxidative esterification of aldehydes under visible light. *Org. Chem. Front.* **2021**, *8*, 4777−4784. (c) Khade, V. V.; Thube, A. S.; Dharpure, P. D.; Bhat, R. G. Direct synthesis of 1,3-dithiolanes from terminal alkynes via visible light photoredox catalysis. *Org. Biomol. Chem.* **2022**, *20*, 1315−1319. (d) Bhowmick, A.; Warghude, P. K.; Bhat, R. G. Visible light promoted metal-free sustainable reduction of α-alkylidene oxindoles/succinimides. *Asian J. Org. Chem.* **2022**, *11*, No. e202200205. (e) Dharpure, P. D.; Behera, M.; Khade, V. V.; Thube, A. S.; Bhat, R. G. Direct access to thiocyano-thioesters from cyclic thioacetals via photoredox catalysis: an introduction of two functional groups in one pot. *Org. Lett.* **2022**, *24*, 6919−6924. (f) Dharpure, P. D.; Behera, M.; Thube, A. S.; Bhat, R. G. Base dependent rearrangement of dithiane and dithiolane under visible-light photoredoxcatalysis. *Chem. - Asian J.* **2023**, *18*, No. e202201128. (g) Behera, M.; Dharpure, P. D.; Sahu, A. K.; Bhat, R. G.Visible light induced organophotoredox catalyzed β-hydroxytrifluoromethylation of unactivated alkenes *ChemRxiv* 2024 DOI: 10.26434/chemrxiv-2024-sh4gw.

(11) CCDC 2292952 (compound **3ai**) contain the supplementary crystallographic data. These data can be obtained free of charge by The Cambridge Crystallographic Data Centre.

(12) (a) Fukuzumi, S.; Kotani, H.; Ohkubo, K.; Ogo, S.; Tkachenko, N. V.; Lemmetyinen, H. Electron-transfer state of 9-mesityl-10-methylacridinium ion with a much longer lifetime and higher energy than that of the natural photosynthetic reaction center. *J. Am. Chem. Soc.* **2004**, *126*, 1600−1601.

(13) Tommasino, J.-B.; Brondex, A.; M'edebielle, M.; Thomalla, M.; Langlois, B. R.; Billard, T. Trifluoromethylation reactions with potassium trifluoromethanesulfinate under electrochemical oxidation. *Synlett* **2002**, 1697−1699.

(14) White, H. S.; Bard, A. J. Electrogenerated chemiluminescence. 41. Electrogenerated chemiluminescence and chemiluminescence of the $Ru(2,2^1\text{-}bpy)_3^{2+}$-$S_2O_8^{2-}$ system in acetonitrile-water solutions. *J. Am. Chem. Soc.* **1982**, *104*, 6891−6895.

(15) Ren, X.; Liu, Q.; Wang, Z.; Chen, X. Visible-light-induced direct hydrodifluoromethylation of alkenes with difluoromethyltriphenylphosphonium iodide salt. *Chin. Chem. Lett.* **2023**, *34*, 107473−107476.

(16) Neises, B.; Steglich, W. Simple method for the esterification of carboxylic acids. *Angew. Chem., Int. Ed. Engl.* **1978**, *17*, 522−524.
(17) Wang, Q.; Lübcke, M.; Biosca, M.; Hedberg, M.; Eriksson, L.; Himo, F.; Szabó, K. J. Enantioselective construction of tertiary fluoride stereocenters by organocatalytic fluorocyclization. *J. Am. Chem. Soc.* **2020**, *142*, 20048−20057.

https://doi.org/10.1021/acs.joc.4c00967
J. Org. Chem. 2024, 89, 14695−14709

Publications not included in the thesis

Synlett M. Behera et al. Letter

Electrochemically Promoted Regioselective C3–H Trifluoro/Difluoromethylation of 2*H*-Indazoles at Room Temperature

Mousumi Behera◊
Ajit Kumar Sahu◊
Shubham Y. Shukla
Ramakrishna G. Bhat*

Department of Chemistry, Indian Institute of Science Education and Research (IISER) Pune, Dr. Homi Bhabha Road, Pashan, 411008, Maharashtra, India
rgb@iiserpune.ac.in
◊These authors contributed equally

Dedicated to Prof. B. C. Ranu on the occasion of his 75th Birthday

Published as part of the Special Issue
to Celebrate the 75th Birthday of Prof. B. C. Ranu

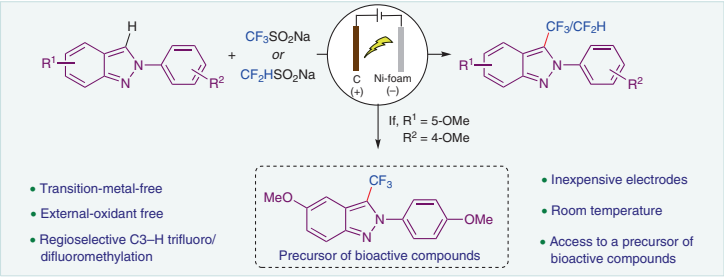

Received: 12.08.2024
Accepted after revision: 25.09.2024
Published online: 25.09.2024 (Accepted Manuscript), 31.10.2024 (Version of Record)
DOI: 10.1055/a-2422-1340; Art ID: ST-2024-08-0280-L

Abstract A green and sustainable electrochemical approach is developed for the regioselective C3–H trifluoro/difluoromethylation of 2*H*-indazoles at room temperature. Relatively less expensive C-soft (+)/Ni-foam (–) electrodes are utilized to selectively functionalize the 2*H*-indazoles effectively by avoiding the use of any external oxidant and transition-metal salt. Moreover, along with the C3–H trifluoromethylation, for the very first time, direct C3–H difluoromethylation of 2-phenyl-2*H*-indazoles is accomplished. Diverse C3–H trifluoro/difluoromethylated 2*H*-indazoles having an array of functionalities are successfully synthesized in moderate to very good yields. As an application, a precursor of both an estrogen receptor ligand and an acetyl Co-A carboxylase inhibitor is synthesized. A plausible reaction mechanism is proposed based on control experiments and cyclic voltammetry studies.

Key words trifluoromethylation, difluoromethylation, regioselective, 2*H*-indazole, transition-metal-free, external-oxidant-free

Heterocyclic scaffolds hold a distinctive position in both natural products as well as in synthetic organic chemistry, serving as precursors for accessing numerous biologically active compounds. Owing to their significance and importance, considerable efforts have been made to develop methods for their functionalization.[1] Indazole is one of the many heterocyclic scaffolds that is known to elicit significant biological activity, including antiviral, antimicrobial, antitumor, anticancer, anti-inflammatory, and anticonvulsant properties.[2] Interestingly, indazole can act as a bioisostere of other aromatic heterocycles such as benzimidazole, benzotriazole, and indole.[3] Indazole-containing compounds can interact with various biological targets, including enzymes, receptors, and ion channels. This versatility makes indazole scaffolds valuable in drug discovery and development.[4] For example, the C3-H substituted indazole **A** is utilized as a very specific ligand for estrogen receptor β (ERβ), while compound **B** shows acetyl-CoA carboxylase (ACC) inhibitory action making it useful as an agent for the prophylaxis or treatment of obesity and diabetes (Figure 1).[5] Consequently, numerous methods have been developed for the functionalization of indazoles.[6]

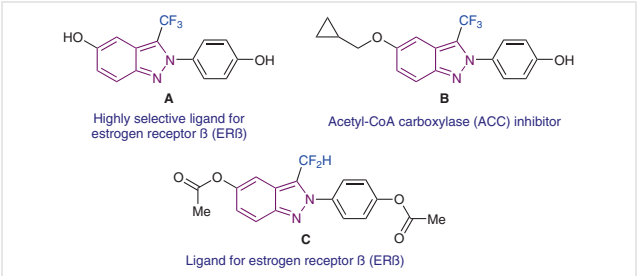

Figure 1 Representative drug candidates containing trifluoro/difluoromethylated indazole moieties

Likewise, organofluorine compounds find applications in numerous pharmaceuticals, agrochemicals, functional organic materials (e.g., liquid crystal displays), and have been used as effective tracers for positron emission tomography (PET) imaging.[7] Among various fluorine-containing groups, the trifluoromethyl group has been extensively explored in the literature. It shows very strong electron-withdrawing properties and its inclusion in target molecules can often improve physical, chemical and bioactive properties.[8] For instance, fluvoxamine, which acts as an antidepressant, and nirmatrelvir/ritonavir, which is sold under the brand name of Paxlovid, have proven to be pivotal for the antiviral treatment of COVID-19.[9] Undoubtedly, the trifluoromethylation of hetero(aromatic) compounds is of significant interest.[7a,10] In addition, the difluoromethyl (CF_2H) group is important for its lipophilic hydrogen bond donor ability. It is also considered as an isostere of thiol, hydroxy and amide groups.[11]

© 2024. Thieme. All rights reserved.

Downloaded by: Ind Inst of Science Edu & Res PUNE. Copyrighted material.

The difluoromethylated 2*H*-indazole C (Figure 1) is an estrogen receptor β ligand used for the prevention and treatment of multiple sclerosis and other demyelinating, inflammatory and neurodegenerative diseases.[11b]

Many of the earlier approaches relied on cross-coupling reactions between organohalides or boronic acids (or their esters) and trifluoromethylating reagents to access CF_3-containing heteroarenes.[12] Although facilitating the regioselective introduction of a CF_3 group to aromatic rings, these methods rely on multi-step syntheses of starting materials and subsequently generate metal as well as other by-product waste. To overcome some of these limitations, direct hetero(aromatic) C–H trifluoromethylation has gained greater attention. Hajra and co-workers have reported the regioselective C3–H trifluoromethylation of 2*H*-indazoles using the Langlois reagent (CF_3SO_2Na) as the trifluoromethyl source and *tert*-butyl hydroperoxide (TBHP) as an oxidant at an elevated temperature of 60 °C in dimethyl sulfoxide (DMSO) (Scheme 1a).[13] Later, Sharada and co-workers introduced a visible-light-promoted, regioselective C–H trifluoromethylation of 2*H*-indazoles using the Langlois reagent as the trifluoromethylating agent, phenyliodine(III) diacetate (PIDA) as the oxidant and methylene blue as a photocatalyst under irradiation with light (CFL 60 W, Scheme 1b-I).[14] However, these methods relied on the use of stoichiometric amounts of oxidants. Recently, in 2023, Chu and co-workers reported a visible-light-mediated approach for the trifluoromethylation of 2*H*-indazoles by using TT-$CF_3^+OTf^-$ as the trifluoromethylation reagent and eosin Y as the photocatalyst in an ionic liquid (Scheme 1b-II).[15]

Over the years electroorganic synthesis has grown rapidly as an alternative, sustainable and elegant strategy to construct useful compounds in organic synthesis, having several advantages over traditional methods. Owing to the importance of the 2*H*-indazole scaffold, the electrochemical sulfonylation, amination, selenylation, and halogenation of 2*H*-indazoles have been explored under milder reaction conditions.[16] However, electrochemical fluoroalkylation of 2*H*-indazoles has been rarely explored in the literature. Recently, Xie and co-workers reported an electrochemical regioselective C–H trifluoromethylation of 2*H*-indazoles using the Langlois reagent at an elevated temperature (50 °C). Also, the method employed an expensive platinum electrode as the cathode and carbon as the anode (Scheme 1c).[17] It is highly desirable to develop the electrochemical direct C3–H trifluoromethylation of 2*H*-indazoles at room temperature, and interestingly, there are no reports on the direct C3–H difluoromethylation of 2*H*-indazoles in the literature.[18] Herein we present a straightforward and direct regioselective method for the C3–H trifluoro/ difluoromethylation of 2*H*-indazoles using inexpensive and commercially available electrodes and the Langlois and Hu reagents (CF_3SO_2Na (**2**) and CF_2HSO_2Na (**2′**)) at room temperature (Scheme 1d).

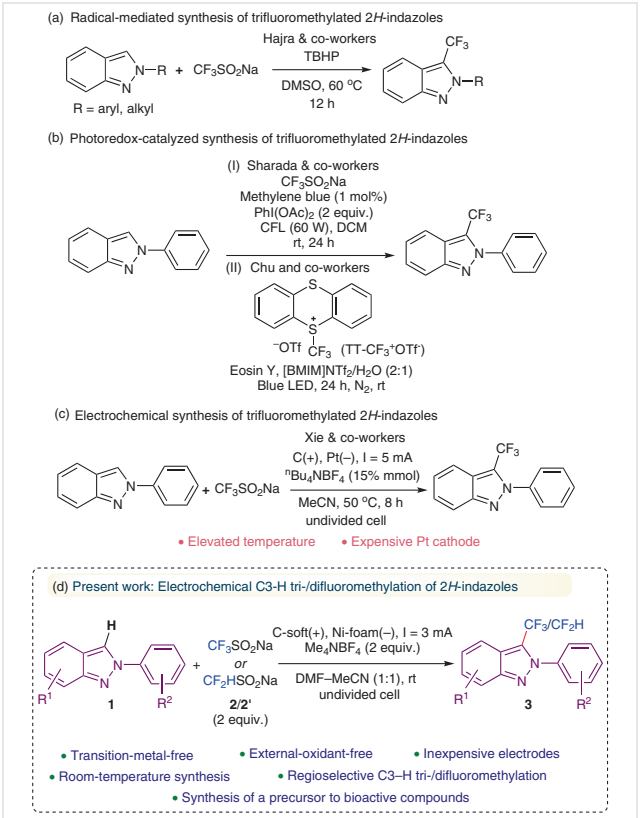

Scheme 1 Methods for the synthesis of trifluoromethylated 2*H*-indazoles

We commenced our studies with a model reaction by employing 2-(*p*-tolyl)-2*H*-indazole (**1a**), the Langlois reagent (CF_3SO_2Na) (**2**) as the trifluoromethyl source and Bu_4NPF_6 as the supporting electrolyte in an undivided cell setup (a nickel-foam cathode and a carbon-soft anode) in acetonitrile (MeCN) at room temperature under a constant supply of current (5 mA). Gratifyingly, the desired C3–H trifluoromethylated 2*H*-indazole **3a** was obtained in a modest 42% yield (Table 1, entry 1). To optimize the reaction further, we decided to explore the use of different electrodes. The reactions of **1a** and **2** using carbon rods (electrodes), both as the anode and cathode, or a carbon cathode and a nickel-foam anode, while maintaining the other initial reaction conditions, did not afford the desired product **3a** (Table 1, entries 2 and 3). Interestingly, when a carbon rod was employed as the anode and nickel or platinum as the cathode, the product **3a** was obtained in modest yields (Table 1, entries 4 and 5). Among all the electrodes screened, the combination of a nickel-foam cathode and a carbon-soft anode proved to be optimum for the desired transformation.

Downloaded by: Ind Inst of Science Edu & Res PUNE. Copyrighted material.

Table 1 Optimization of the Reaction Conditions[a]

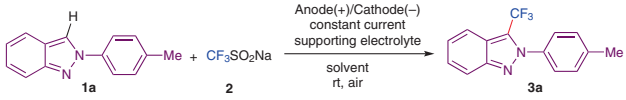

Entry	Electrodes (+)/(–)	Supporting electrolyte	Current (mA)	Solvent	Yield (%)[b]
1	C-soft (+)/Ni-foam (–)	Bu_4NPF_6	5	MeCN	42
2	C-rod (+)/C-rod (–)	Bu_4NPF_6	5	MeCN	ND
3	Ni-foam (+)/C-rod (–)	Bu_4NPF_6	5	MeCN	ND
4	C-rod (+)/Ni (–)	Bu_4NPF_6	5	MeCN	39
5	C-soft (+)/Pt (–)	Bu_4NPF_6	5	MeCN	34
6	C-soft (+)/Ni-foam (–)	Bu_4NBF_4	5	MeCN	34
7	C-soft (+)/Ni-foam (–)	Bu_4NI	5	MeCN	ND
8	C-soft (+)/Ni-foam (–)	Bu_4NBr	5	MeCN	ND
9	C-soft (+)/Ni-foam (–)	Bu_4NCl	5	MeCN	ND
10	C-soft (+)/Ni-foam (–)	Bu_4NClO_4	5	MeCN	37
11	C-soft (+)/Ni-foam (–)	$LiClO_4$	5	MeCN	27
12	C-soft (+)/Ni-foam (–)	Me_4NBF_4	5	MeCN	62
13	C-soft (+)/Ni-foam (–)	Me_4NBF_4	3	MeCN	66
14	C-soft (+)/Ni-foam (–)	Me_4NBF_4	10	MeCN	47
15	C-soft (+)/Ni-foam (–)	Me_4NBF_4	3	DMF	68
16	C-soft (+)/Ni-foam (–)	Me_4NBF_4	3	DMSO	65
17	C-soft (+)/Ni-foam (–)	Me_4NBF_4	3	$MeNO_2$	<5
18	C-soft (+)/Ni-foam (–)	Me_4NBF_4	3	DMF/MeCN (2:1)	60
19	C-soft (+)/Ni-foam (–)	Me_4NBF_4	3	DMF/MeCN (1:2)	55
20	**C-soft (+)/Ni-foam (–)**	**Me_4NBF_4**	**3**	**DMF/MeCN (1:1)**	**78 (72)[c]**
21[d]	C-soft (+)/Ni-foam (–)	Me_4NBF_4	3	DMF/MeCN (1:1)	67
22[e]	C-soft (+)/Ni-foam (–)	Me_4NBF_4	3	DMF/MeCN (1:1)	76
23[f]	C-soft (+)/Ni-foam (–)	Me_4NBF_4	3	DMF/MeCN (1:1)	54
24[g]	C-soft (+)/Ni-foam (–)	Me_4NBF_4	3	DMF/MeCN (1:1)	72

[a] *Reaction conditions*: 2-(*p*-tolyl)-2*H*-indazole (**1a**) (0.2 mmol), CF_3SO_2Na (**2**) (2 equiv.), supporting electrolyte (2 equiv.), solvent (3 mL), anode (+), cathode (–), constant current (I), room temperature (rt), air.
[b] Determined by ^1H NMR analysis using 1,3,5-trimethoxybenzene as an internal standard; ND = not detected.
[c] Isolated yield after column chromatography.
[d] CF_3SO_2Na (1.5 equiv.).
[e] CF_3SO_2Na (3 equiv.).
[f] Me_4NBF_4 (1 equiv.).
[g] Me_4NBF_4 (3 equiv.).

To enhance the yield, we screened different supporting electrolytes while using a nickel-foam cathode and carbon-soft anode as electrodes. The reaction of **1a** and **2** in the presence of tetrabutylammonium tetrafluoroborate (Bu_4NBF_4) afforded the desired product **3a** in a modest 34% yield (Table 1, entry 6). However, tetrabutylammonium iodide (Bu_4NI), tetrabutylammonium bromide (Bu_4NBr), and tetrabutylammonium chloride (Bu_4NCl) as supporting electrolytes did not afford the desired product **3a** (Table 1, entries 7–9). In contrast, Bu_4NClO_4 and $LiClO_4$ furnished product **3a**, albeit in low yields (Table 1, entry 10 and 11).

Gratifyingly, the reaction in the presence of tetramethylammonium tetrafluoroborate (Me_4NBF_4) at a constant current of 5 mA afforded **3a** in a good yield of 62% (Table 1, entry 12).

Encouraged by this result, we varied the constant current to investigate its influence on the reaction outcome. The reaction at a constant current of 3 mA resulted in an incremental improvement in the yield of **3a** to 66% (Table 1, entry 13). However, increasing the constant current value to 10 mA significantly reduced the yield of **3a** to 47% (Table 1, entry 14). Next, we screened different solvents to study their effect on the yield of **3a**. The reaction of **1a** and **2** in

© 2024. Thieme. All rights reserved.

Downloaded by: Ind Inst of Science Edu & Res PUNE. Copyrighted material.

solvents such as MeCN, DMF and DMSO afforded the desired product **3a** in similar yields, while that in $MeNO_2$ afforded product **3a** in a poor yield (Table 1, entries 15–17). Based on these results, we further screened different mixtures of DMF and MeCN as solvents (Table 1, entries 18–20). A 1:1 ratio of DMF and MeCN proved to be the most efficient, affording the desired product **3a** in the highest yield of 78% (Table 1, entry 20).

Subsequently, we carried out the reaction by varying the amount of CF_3SO_2Na (**2**) to study its effect on the outcome. We observed that a reduction in the loading of CF_3SO_2Na (**2**) (1.5 equiv.) reduced the yield of **3a**, while increasing the amount (3 equiv.) had no significant impact on the overall yield when compared to 2 equivalents of **2** (Table 1, entries 20–22). We observed a similar trend with respect to the yield of **3a** when the amount of Me_4NBF_4 was varied (Table 1, entries 23 and 24). Based on this systematic and detailed screening, the optimized reaction conditions to access trifluoromethylated product **3a** are as follows: a carbon-soft anode and a nickel-foam cathode dipped in a solution containing 2-(*p*-tolyl)-2*H*-indazole (**1a**) (1.0 equiv.), CF_3SO_2Na (**2**) (2.0 equiv.) and Me_4NBF_4 (2.0 equiv.) in DMF/MeCN (1:1) with a constant current supply (3 mA) in an undivided cell setup (Table 1, Entry 20).

Having established optimized reaction conditions, we proceeded to explore the broader substrate scope as well as the applicability of this protocol (Scheme 2). Initially, we synthesized different indazole derivatives **1a–l** by varying the substituents on the pyrazole ring (see Table S1 in the Supporting Information).[19]

The 2-phenyl 2*H*-indazole derivatives **1a–d** bearing electron-donating groups (Me, ^{i}Pr, OMe and SMe) on the *N*-phenyl ring afforded the desired trifluoromethylated products **3a–d** in very good yields (up to 78%) (Scheme 2). Electron-deactivating groups (F, Cl, Br) on the *N*-phenyl group of the 2*H*-indazole under the optimum reaction conditions furnished the desired products **3e–g** in moderate to good yields (up to 65%). Notably, substrates having an electron-withdrawing CN group at the *ortho* and *meta* positions of the *N*-phenyl ring tolerated the reaction conditions to afford the corresponding products **3h** and **3i**. Indazole substrates having a keto and an ester moiety on the *N*-phenyl ring gave the desired products **3j** and **3k** in yields of 68% and 67%, respectively. An indazole having an *N*-pyridin-2-yl moiety also reacted smoothly to furnish the corresponding trifluoromethylated product **3l**. Next, we synthesized various indazole derivatives having electron-deactivating and electron-donating substituents at the C5 and C6 positions (see Table S1 in the Supporting Information).[19] Different C5-substituted 2*H*-indazole derivatives **1m–p**, on treatment with CF_3SO_2Na under the optimized reaction conditions, provided the desired trifluoromethylated products

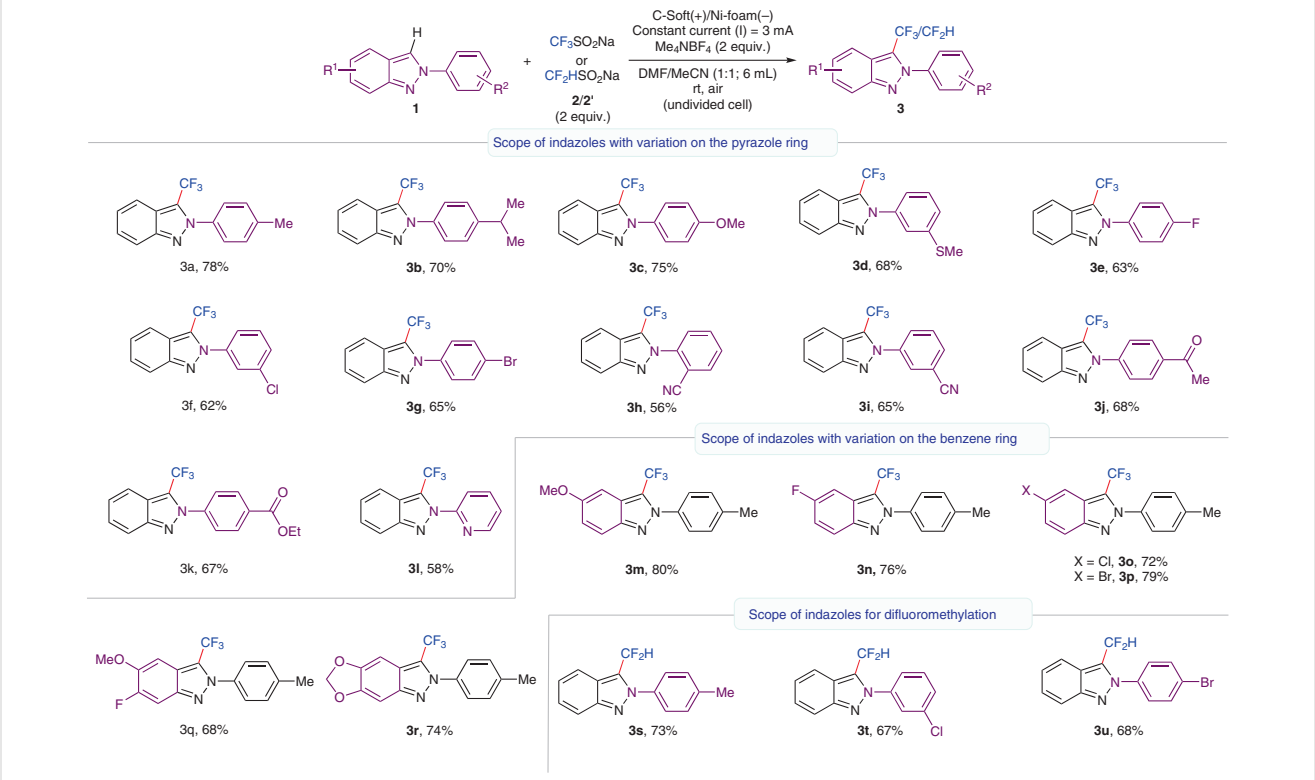

Scheme 2 Substrate scope of the trifluoromethylation/difluoromethylation of 2*H*-indazoles. Yields are those of isolated products after column chromatography.

Downloaded by: Ind Inst of Science Edu & Res PUNE. Copyrighted material.

3m–p in good yields (up to 80%). In addition, the C5- and C6-disubstituted 2*H*-indazole derivatives **1q** and **1r** afforded the corresponding products **3q** and **3r** in good yields (up to 74%).

Owing to the importance of difluoromethylated indazoles, we next turned our attention to explore the reactivity of 2*H*-indazoles towards C3–H difluoromethylation. Gratifyingly, the reactions of 2*H*-indazole derivatives with difluoromethane sulfinate (CF_2HSO_2Na, Hu's reagent) (**2'**) under the optimized reaction conditions afforded the corresponding difluoromethylated indazoles **3s–u** in good yields of up to 73% (Scheme 2). It is important to highlight that this is the first direct method to access difluoromethylated indazoles.[18]

To demonstrate the applicability of this protocol, we performed a scale-up reaction with **1b** (2.12 mmol, 0.5 g) and obtained the corresponding trifluoromethylated product **3b** in 67% yield (Scheme 3a). Furthermore, we synthesized the indazole derivative **3v** in 76% yield (Scheme 3b), which is an important precursor for a highly selective ligand for estrogen receptor β (Erβ) (**A**) and acetyl-CoA carboxylase inhibitor (ACC) **B** (see Figure 1).

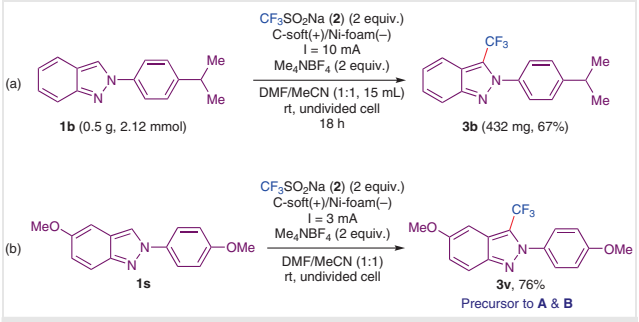

Scheme 3 (a) A scale-up reaction. (b) Synthesis of a precursor to bioactive molecules **A** and **B**.

To gain some mechanistic insights, we carried out control experiments (Scheme 4). To begin with, we performed the reactions of **1a** and CF_3SO_2Na (**2**) under the optimized conditions in the presence of the radical-trapping agents TEMPO and BHT. Under these radical-quenching conditions, we did not observe formation of the desired product **3a**, even in trace amount, and substrate **1a** was recovered quantitatively (Scheme 4a). These results clearly indicate that the reaction proceeds via a radical-mediated process.

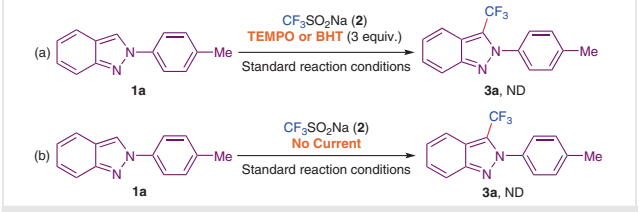

Scheme 4 Control experiments: (a) reaction with TEMPO and BHT; (b) reaction without applying a current.

We also performed the reaction without the constant current supply while maintaining the other optimized reaction conditions (Scheme 4b). Interestingly, we did not observe formation of the desired product **3a** and the starting material was recovered quantitatively. This observation indicates that the reaction proceeds via an electrochemical-mediated process.

In order to gain further insight into the mechanism, we carried out a series of EPR experiments (Figure 2) (for details, see the Supporting Information). The reaction mixture of **1a** in the presence of *N*-*tert*-α-phenyl-butylnitrone (PBN) but in the absence of CF_3SO_2Na (**2**) was found to be EPR silent (Figure 2a). This result indicated that 2*H*-indazole **1a** may not be undergoing oxidation at the anode. In contrast, the reaction mixture containing **2** and *N*-*tert*-α-phenyl-butylnitrone (PBN) while in the absence of **1a** showed a significant peak in the EPR spectrum (g = 2.004) after 20 minutes (Figure 2b). This result suggests that a trifluoromethyl radical ($CF_3^{\bullet}$) must be generated at the anode. Finally, the EPR spectrum of the reaction mixture containing **1a**, **2** and PBN matched with that of Figure 2b (see Figure 2c). Based on these experimental observations, we believe that a CF_3 radical might be adding to the neutral 2*H*-indazole **1a**, thus ruling out the radical–radical cross-coupling of an indazole radical and a CF_3 radical.

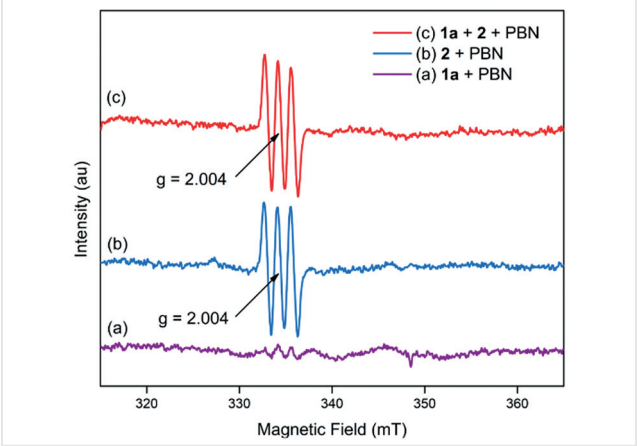

Figure 2 Stacked EPR spectra of electrochemically generated radical species

Cyclic voltammetry experiments were performed to obtain the redox potentials of 2-(*p*-tolyl)-2*H*-indazole (**1a**), CF_3SO_2Na (**2**) and that of the reaction mixture of **1a** and **2**. From the cyclic voltammograms (Figure 3), the oxidation potential of **1a** was found to be 1.81 V vs Ag/AgCl, and for CF_3SO_2Na (**2**) was 1.33 V vs Ag/AgCl. These data clearly suggest that CF_3SO_2Na (**2**) can be easily oxidized at the anode surface to generate $CF_3^{\bullet}$ (Scheme 5).

From the results obtained through control experiments, EPR spectra, cyclic voltammetry, and based on previous literature reports,[16b,20] a plausible reaction mechanism has

Downloaded by: Ind Inst of Science Edu & Res PUNE. Copyrighted material.

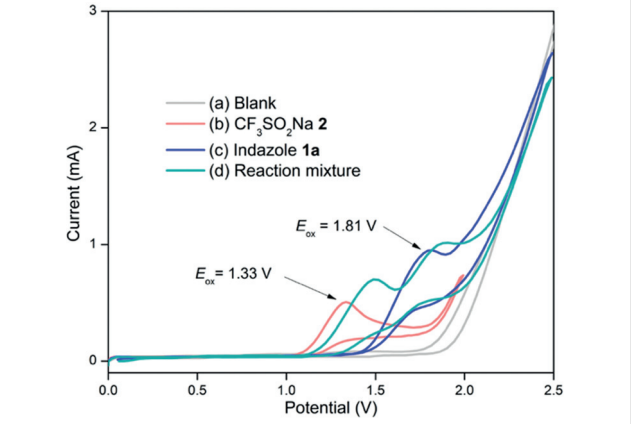

Figure 3 Cyclic voltammograms of (a) the blank, (b) CF_3SO_2Na (**2**), (c) 2*H*-indazole **1a**, and (d) the reaction mixture **1a** + **2**. Data were recorded using glassy carbon as the working electrode, a platinum-plated counter electrode and an Ag/AgCl reference electrode at a 100 mV/s scan rate. Samples were prepared in MeCN electrolyte solution with substrate concentrations of 10 mM and 100 mM Me_4NBF_4.

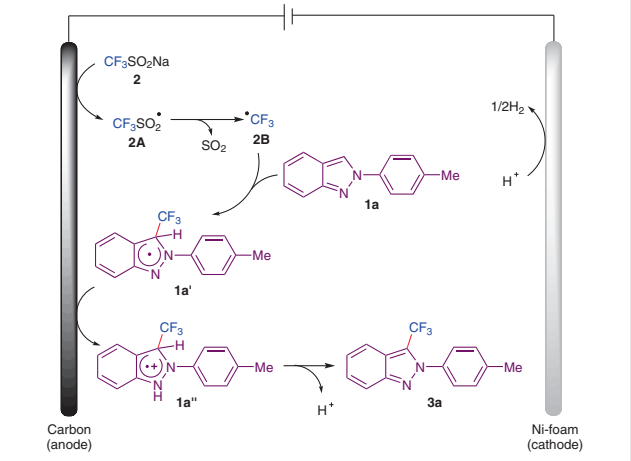

Scheme 5 A plausible reaction mechanism for the trifluoromethylation reaction

been proposed (Scheme 5). The reaction proceeds by the oxidation of CF_3SO_2Na (**2**) to the corresponding radical **2A** ($CF_3SO_2^{\bullet}$), and this generates the trifluoromethyl radical **2B** ($CF_3^{\bullet}$) by extrusion of SO_2. Further, the radical species **2B** reacts with the neutral 2*H*-indazole **1a** to form the corresponding intermediate **1a′**. This radical intermediate **1a′** undergoes oxidation at the surface of the carbon anode to give the radical cation intermediate **1a″**. This subsequently affords the desired product, (*p*-tolyl)-3-(trifluoromethyl)-2*H*-indazole (**3a**), via re-aromatization through loss of a proton. To maintain the electroneutrality, the released proton undergoes reduction at the cathode surface (Ni-foam) to generate dihydrogen (H_2).

In summary, we have reported a sustainable approach for the direct synthesis of trifluoromethylated 2*H*-indazole derivatives using CF_3SO_2Na as the trifluoromethyl source by applying a galvanostatic mode of operation. The synthetic utility of this protocol proved to be compatible with a wide range of 2*H*-indazole derivatives, containing electronically neutral, rich, and withdrawing substituents, to afford the corresponding trifluoromethylated 2*H*-indazole products in moderate to good yields. Gratifyingly, we have also developed the very first direct strategy to access the difluoromethylated indazoles. As an application of this protocol, an important precursor of biologically active compounds has been synthesized electrochemically. Control experiments, EPR studies and cyclic voltammetry investigations have been carried out to obtain mechanistic insights of the reaction pathway.

Conflict of Interest

The authors declare no conflict of interest.

Acknowlegment

R. G. B. thanks Science and Engineering Research Board Department of Science and Technology (SERB-DST), New Delhi, Government of India (File no: CRG/2019/005753 and CRG/2023/004226) for the generous research grant. Authors also thank DST-FIST Program, Govt. of India (Grant SR/FST/CS-II/2019/105) for providing the EPR facility at IISER Pune. The authors also thank IISER Pune for financial assistance. M. B. and S.Y. S. thank IISER Pune for the fellowship.

Supporting Information

Supporting information for this article is available online at https://doi.org/10.1055/a-2422-1340.

References and Notes

(1) (a) Kabir, E.; Uzzaman, M. *Results Chem.* **2022**, *4*, 100606. (b) Qadir, T.; Amin, A.; Sharma, P. K.; Jeelani, I.; Abe, H. *Open J. Med. Chem.* **2022**, *16*, e187410452202280.
(2) (a) Puri, S.; Sawant, S.; Juvale, K. *J. Mol. Struct.* **2023**, *1284*, 135327. (b) Zhang, S.-G.; Liang, C.-G.; Zhang, W.-H. *Molecules* **2018**, *23*, 2783.
(3) Fludzinski, P.; Evrard, D. A.; Bloomquist, W. E.; Lacefield, W. B.; Pfeifer, W.; Jones, N. D.; Deeter, J. B.; Cohen, M. L. *J. Med. Chem.* **1987**, *30*, 1535.
(4) (a) Mal, S.; Malik, U.; Mahapatra, M.; Mishra, A.; Pal, D.; Paidesetty, S. K. *Drug Dev. Res.* **2022**, *83*, 1469. (b) Gaikwad, D. D.; Chapolikar, A. D.; Devkate, C. G.; Warad, K. D.; Tayade, A. P.; Pawar, R. P.; Domb, A. J. *Eur. J. Med. Chem.* **2015**, *90*, 707.
(5) (a) Angelis, M. D.; Stossi, F.; Carlson, K. A.; Katzenellenbogen, B. S.; Katzenellenbogen, J. A. *J. Med. Chem.* **2005**, *48*, 1132. (b) Ikuo, F.; Takuya, F.; Hideki, H.; Zenichi, I.; Makoto, K.; Asato, K.; Ryo, M.; Masataka, M.; Tohru, Y.; Tsuneo, Y.; Kazuko, Y.

Downloaded by: Ind Inst of Science Edu & Res PUNE. Copyrighted material.

WO2012074126(A1), **2012**. (c) Ngo, T. N.; Ejaz, S. A.; Hung, T. Q.; Dang, T. T.; Iqbal, J.; Lecka, J.; Sévigny, J.; Langer, P. *Org. Biomol. Chem.* **2015**, *13*, 8277.

(6) (a) Yang, Z.; Yu, J.-T.; Pan, C. *Org. Biomol. Chem.* **2022**, *20*, 7746. (b) Giraud, F.; Anizon, F.; Moreau, P. *Targets in Heterocyclic Systems: Chemistry and Properties, Vol. 25*; Società Chimica Italiana: Roma, **2021**, 100–112.

(7) (a) Zhu, W.; Wang, J.; Wang, S.; Gu, Z.; Aceña, J. L.; Izawa, K.; Liu, H.; Soloshonok, V. A. *J. Fluorine Chem.* **2014**, *167*, 37. (b) Zhou, Y.; Wang, J.; Gu, Z.; Wang, S.; Zhu, W.; Aceña, J. L.; Soloshonok, V. A.; Izawa, K.; Liu, H. *Chem. Rev.* **2016**, *116*, 422. (c) Inoue, M.; Sumii, Y.; Shibata, N. *ACS Omega* **2020**, *5*, 10633. (d) Jeschke, P. *ChemBioChem* **2004**, *5*, 570. (e) Ogawa, Y.; Tokunaga, E.; Kobayashi, O.; Hirai, K.; Shibata, N. *iScience* **2020**, *23*, 101467. (f) Hird, M. *Chem. Soc. Rev.* **2007**, *36*, 2070. (g) Ametamey, S. M.; Honer, M.; Schubiger, P. A. *Chem. Rev.* **2008**, *108*, 1501. (h) Francis, F.; Wuest, F. *Molecules* **2021**, *26*, 6478.

(8) (a) Kiselyov, A. S.; Strekowski, L. *Org. Prep. Proced. Int.* **1996**, *28*, 289. (b) Kumadaki, I.; Ando, A.; Sato, K.; Tarui, A.; Omote, M. *Synthesis* **2010**, 1865.

(9) (a) Irons, J. *Neuropsychiatr. Dis. Treat.* **2005**, *1*, 289. (b) Akinosoglou, K.; Schinas, G.; Gogos, C. *Viruses* **2022**, *14*, 2540.

(10) (a) Barata-Vallejo, S.; Postigo, A. *Chem. Eur. J.* **2020**, *26*, 11065. (b) Kuninobu, Y. *Chem. Rec.* **2023**, *23*, e202300003.

(11) (a) Sessler, C. D.; Rahm, M.; Becker, S.; Goldberg, J. M.; Wang, F.; Lippard, S. J. *J. Am. Chem. Soc.* **2017**, *139*, 9325. (b) Katzenellenbogen, J. A.; Tiwari-Woodruif, S. K.; Kim, S. H.; Katzenellenbogen, B. WO2019226936 (A1), **2019**.

(12) (a) Roy, S.; Gregg, B. T.; Gribble, G. W.; Le, V.-D.; Roy, S. *Tetrahedron* **2011**, *67*, 2161. (b) Lundgren, R. J.; Stradiotto, M. *Angew. Chem. Int. Ed.* **2010**, *49*, 9322. (c) Lishchynskyi, A.; Novikov, M. A.; Martin, E.; Escudero-Adán, E. C.; Novák, P.; Grushin, V. V. *J. Org. Chem.* **2013**, *78*, 11126. (d) Chen, P.; Liu, G. *Synthesis* **2013**, *45*, 2919. (e) Tomashenko, O. A.; Grushin, V. V. *Chem. Rev.* **2011**, *111*, 4475.

(13) Ghosh, P.; Mondal, S.; Hajra, A. *J. Org. Chem.* **2018**, *83*, 13618.

(14) Murugan, A.; Babu, V. N.; Polu, A.; Sabarinathan, N.; Bakthadoss, M.; Sharada, D. S. *J. Org. Chem.* **2019**, *84*, 7796.

(15) He, X.; Chen, Z.; Zhu, X.; Liu, H.; Chen, Y.; Sun, Z.; Chu, W. *Org. Biomol. Chem.* **2023**, *21*, 1814.

(16) (a) Kim, W.; Kim, H. Y.; Oh, K. *Org. Lett.* **2020**, *22*, 6319. (b) Mahanty, K.; Maiti, D.; De Sarkar, S. *J. Org. Chem.* **2020**, *85*, 3699. (c) Sun, M.; Zhou, Y.; Li, L.; Wang, L.; Ma, Y.; Li, P. *Org. Chem. Front.* **2021**, *8*, 754. (d) Lin, S.; Cheng, X.; Hasimujiang, B.; Xu, Z.; Li, F.; Ruan, Z. *Org. Biomol. Chem.* **2022**, *20*, 117. (e) Wang, D.; Wang, J.; Ma, C.; Jiang, Y.; Yu, B. *Chin. J. Chem.* **2022**, *42*, 4024. (f) Liu, X.; Wu, Z.; Feng, C.; Liu, W.; Li, M.; Shen, Z. Eur. *J. Org. Chem.* **2022**, *2022*, e202200262.

(17) Wei, T.; Wang, K.; Yu, Z.; Hou, J.; Xie, Y. *Tetrahedron Lett.* **2021**, *86*, 153313.

(18) These methods required prefunctionalization of the starting material and multistep reactions to afford difluoromethylated 2*H*-indazoles, see (a) Bel Abed, H.; Weißing, N.; Schoene, J.; Paulus, J.; Sewald, N.; Nazaré, M. *Tetrahedron Lett.* **2018**, *59*, 1813. (b) Laru, S.; Bhattacharjee, S.; Hajra, A. *Chem. Commun.* **2022**, *58*, 13604.

(19) (a) Shi, A.; Xiang, P.; Wu, Y.; Ge, C.; Liu, Y.; Sun, K.; Yu, B. *Synlett* **2023**, *34*, 457. (b) Kumar, M. R.; Park, A.; Park, N.; Lee, S. *Org. Lett.* **2011**, *13*, 3542.

(20) Ghosh, D.; Ghosh, S.; Hajra, A. *Adv. Synth. Catal.* **2021**, *363*, 5047.

Downloaded by: Ind Inst of Science Edu & Res PUNE. Copyrighted material.

Check for updates

EurJOC
European Journal of Organic Chemistry

Research Article
doi.org/10.1002/ejoc.202400471

Chemistry Europe
European Chemical Societies Publishing

www.eurjoc.org

Stable and Reusable Pd/Cu Bimetallic Nanoparticle Catalysts for the Synthesis of Hydroxy Isoindolones by Domino C–H Activation and Annulation

Gollapalli Narasimha Rao,[a] Mousumi Behera,[a] Krishnamoorthy Kathirvel,[a] and Govindasamy Sekar*[a]

A domino C–H activation and annulation process catalyzed by stable and reusable bimetallic nanoparticles (Pd/Cu-binapthyl nanoparticles) was developed for the synthesis of 3-hydroxyisoindolin-1-ones/thiones. The scope of the reaction was examined utilizing a variety of *N*-alkoxy benzamide/benzothioamide derivatives and benzaldehydes, which yielded moderate to good yields of 3-hydroxyisoindolin-1-ones/thiones, one of which was used to synthesize a BRD4 inhibitor. A gram-scale synthesis is also reported. The Pd/Cu-binapthyl nanocatalyst has been recovered and reused up to four times without any major change in particle size and reactivity.

Introduction

3-Hydroxyisoindolin-1-ones are important structural motifs in numerous natural products, such as antihypertensive agent chlorthalidone,[1] isoindolobenzazepine chilenine,[2] isoquiniline fumadensine,[3] UCN-01(7-hydroxy staurosporine),[4] (−)-leuconolam[5] and eszopiclone[6] (Figure 1).

The traditional methods to synthesize hydroxy isoindolone derivatives are based on regioselective addition to phthalimide derivatives of organometallic reagents or nucleophilic agents.[7] However, these methodologies involve harsh reaction conditions and Grignard reagents (anhydrous reaction conditions). In 2010, Liu *et al.* described a regioselective tandem synthesis of 3-hydroxyisoindolin-1-ones without a transition-metal catalyst.[8] However, this approach had harsh reaction conditions, limited functional group tolerance, and required multistep prefunctionalization to acquire substrates. Transition-metal catalyzed *ortho* direct C–H activation has been described for the synthesis of bioactive heterocyclic compounds.[9] This approach involves a modular and concise synthesis, which is environmentally benign. To the best of our knowledge, Kim *et al.* reported the first rhodium-catalyzed synthesis of 3-hydroxyisoindolin-1-one on the basis of oxidative acylation of secondary benzamides with aldehydes through C–H activation/annulation (Scheme 1a),[10] and their methodology shows a novel solution for the synthesis of hydroxy isoindolonoes in the context of homogeneous transitionmetal-catalyzed reactions.

Subsequently, in 2013, Zhao *et al.* reported a Pd-catalyzed oxidative acylation of *N*-methoxybenzamide with aldehydes using tertiary butyl hydroperoxide as an oxidant (Scheme 1b).[11]

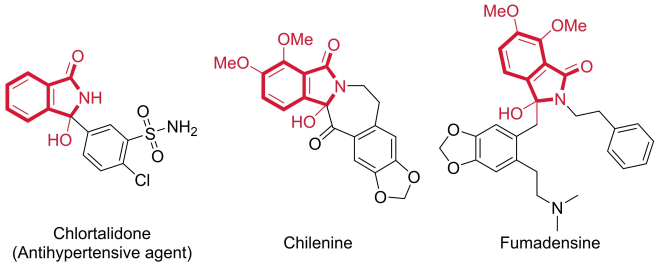

Figure 1. Selected examples of biologically active structures of 3-hydroxyisoindolin-1-ones.

Later Zhang *et al.* employed a Pd-mediated C–H bond *ortho* acylation followed by annulation with toluene derivatives.[12] In 2016, Walsh *et al.* reported a straightforward functionalization of isoindolinones with aryl bromides.[13] Subsequently, Shen *et al.* reported base-promoted cascade C–C coupling/N-α-sp^3 C–H hydroxylation for the synthesis of 3-hydroxyisoindolinone derivatives.[14] In 2017, Wang *et al.* reported Pd-catalyzed decarboxylative *ortho* acylation of benzamides with α oxo carboxylic acids.[15] Additionally, in 2018 Xiao *et al.* employed Eosin Y as a redox catalyst and photosensitizer for consecutive benzylic C–H amination and oxidation.[16]

Recently, in the presence of CuCl and cesium carbonate in dimethyl sulfoxide, an effective one-pot, two-step sequential reaction for the synthesis of biologically active 3-hydroxyisoindolin-1-one derivatives from 2-iodobenzamide and different substituted benzyl cyanides has also been reported.[17] However, these strategies have some drawbacks, such as the inefficiency of separating homogeneous transition-metal catalysts from the final product. Over the past two decades, transition-metal nanoparticles have been used in both academia and industry to overcome these difficulties, which has shown significant advantages over homogeneous catalysis. Without losing their size or catalytic activity, the metal nanoparticles are readily recovered and recycled for several catalytic cycles.[18–21] In 2013, Zhao *et al.* reported the homogeneous $Pd(OAc)_2$ catalyzed

[a] G. Narasimha Rao, M. Behera, K. Kathirvel, G. Sekar
Department of Chemistry, Indian Institute of Technology Madras, Chennai, Tamil Nadu 600036, India
E-mail: gsekar@iitm.ac.in

Supporting information for this article is available on the WWW under https://doi.org/10.1002/ejoc.202400471

© 2024 Wiley-VCH GmbH

Research Article
doi.org/10.1002/ejoc.202400471

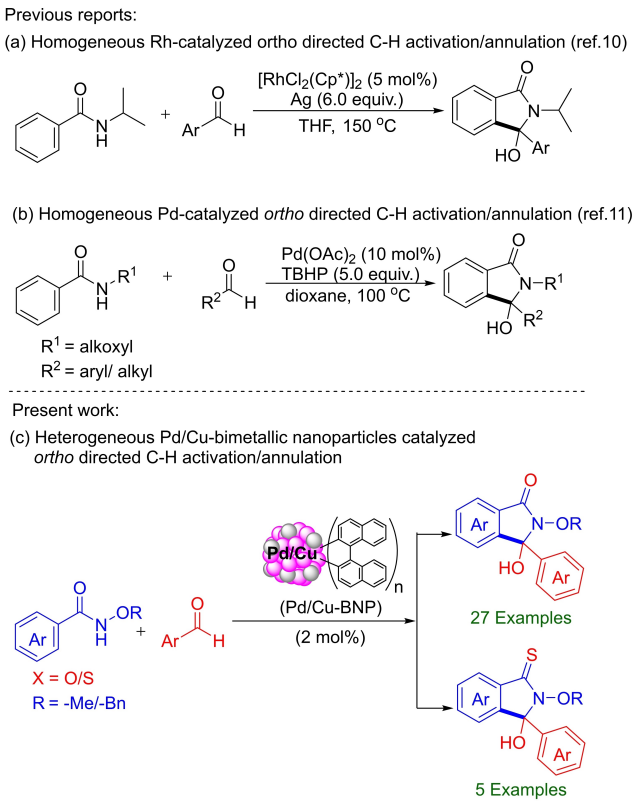

Scheme 1. Synthetic methods towards 3-hydroxyisoindolin-1-ones.

synthesis of imino/keto carboxylic acids by C–H activation.[22] Recently, the Pralay group reported polystyrene-supported palladium nanoparticles (NPs) catalyzed amino carbonylation of aryl halides with amines using oxalic acid as a CO source for the synthesis of amides.[23]

As part of our ongoing research interest towards the development of transition-metal nanoparticles catalyzed domino organic transformations,[24] herein we report binaphthyl backbone stabilized Pd/Cu-bimetallic nanoparticles as a catalyst for the synthesis of 3-hydroxyisoindolin-1-one by domino oxidative acylation of *N*-methoxy benzamide with an aldehyde followed by intramolecular cyclization (C–N bond formation) (Scheme 1c).

Results and Discussion

The initial study was carried out by using *N*-methoxy benzamide **1a** and benzaldehyde **2a** as model substrates in the presence of Pd- Binapthyl Nanoparticles (BNP) (2 mol %) as a catalyst along with various oxidizing agents (5.0 equiv.) and 1,4-dioxane as solvent at 100 °C under oxygen atmosphere. To our delight, the corresponding domino C–H activation/annulation product **3a** was detected in a 13% yield. Further, the reaction was carried out with various oxidizing agents such as H_2O_2, *meta*-chloroperoxybenzoic acid (m-CPBA), $K_2S_2O_8$, Benzoyl peroxide, etc. However, the reaction did not take place (entries 2–5). Interestingly, when we replaced the tertiary butyl hydrogen peroxide (TBHP) (decane) with tertiary butyl hydrogen peroxide (TBHP) (aqueous) the product formation was observed in 60% yield (entry 6). Furthermore, to improve the yield, various solvents, such as AcOH, ^{t}BuOH, THF, 1,4-dioxane/AcOH, and toluene were screened. However, none of them yielded a better yield than 1,4-dioxane (entries 7–11), and in the case of DCE as a solvent, the product formation was completely inhibited (entry 12).

Next, the reaction was carried out with other nanoparticles, such as surface-enriched bimetallic palladium-copper binapthyl nanoparticles (Pd/Cu-BNP), giving the desired product at 70% yield (entry 13). When the reaction was carried out by decreasing the oxidizing agent tertiary butyl hydrogen peroxide (TBHP) (aqueous) from 5.0 equiv. to 3.0 equiv. The yield slightly decreased to 46% (entry 14), while the oxidizing agent increased from 5.0 equiv. to 7.0 equiv. gave the desired product in 66% yield. Increasing the loading of Pd/Cu-BNP from 2 mol% to 4 mol% decreased the yield of **3a** to 52% (entry 16, Table 1). When the reaction temperature was reduced from 100 °C to 80 °C, the reaction failed to yield the product **3a** (entry 17). In the case of the Pd-Binapthyl Nanoparticles (BNP) catalyst, the reaction gives a huge difference in the yield between an oxidizing agent using TBHP (dec.) and TBHP (aq.) (entries 1 and 6).

To know more about the reaction, we added stoichiometric amounts of water to the reaction mixture along with 5.0 equivalents of TBHP (dec.) to determine whether water plays a role or not, but we got only a 21% yield of the desired product (entry 18). Next, the reaction was carried out with 5.0 equiv. of TBHP (dec.) and 10 equiv. of water under standard conditions. After 1 h, the desired product **3a** was formed in 66% yield. Without water, using only 5.0 equiv. of TBHP (dec.) under the same conditions, this reaction yielded only 36%. These results indicate that the presence of water increases the yield (entries 19–20). When the reaction was tested with copper nanoparticles (Cu-BNP), the reaction did not proceed well, and only a trace amount of product formation was observed (entry 21). This result indicates that in Pd/Cu-BNP only palladium is catalyzing the reaction. Further, a mixture of Pd-BNP and Cu-BNP (1:1) catalyst was used for this transformation, and after 1 h, the desired product formed in 41% yield (entry 22). When the reaction was carried out with commercially available heterogeneous palladium catalysts, such as (10%) Pd/C and (5%) Pd/Al_2O_3 with 5.0 equiv. of aq. TBHP, the desired products formed 38% and 15%, respectively (entries 23 and 24). For a better understanding, a comparative study for isoindolones formation was examined by using different Pd and Cu ratios of Pd/Cu-BNP nanoparticles, such as Pd/Cu-BNP (1:2) and Pd/Cu-BNP (2:1) under the standard reaction condition, which gave the desired products yielded in 63% and 68%, which indicates that Pd/Cu-BNP (1:1) is the most suitable for the formation of isoindolone (entries 25 and 26).

Having optimized reaction conditions in hand, the scope of this protocol was explored with various substituted benzamides with benzaldehydes, and the results are summarized in (Scheme 2). First, various substituted *N*-alkoxy benzamides **1** were reacted with benzaldehyde **2a**. It was observed that the

© 2024 Wiley-VCH GmbH

10990690, 2024, 36, Downloaded from https://chemistry-europe.onlinelibrary.wiley.com/doi/10.1002/ejoc.202400471 by Indian Institute Of Science Education And Research Pune, Wiley Online Library on [23/06/2025]. See the Terms and Conditions (https://onlinelibrary.wiley.com/terms-and-conditions) on Wiley Online Library for rules of use; OA articles are governed by the applicable Creative Commons License

Research Article
doi.org/10.1002/ejoc.202400471

Table 1. Optimization of the reaction conditions.[a]

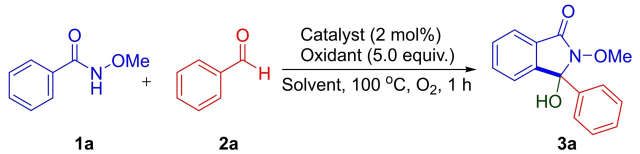

1a 2a 3a

Entry	Catalyst	Oxidant	Solvent	Yield[b] (%)
1	Pd-BNP	TBHP (dec.)	1,4-dioxane	13
2	Pd-BNP	H_2O_2	1,4-dioxane	0
3	Pd-BNP	m-CPBA	1,4-dioxane	0
4	Pd-BNP	$K_2S_2O_8$	1,4-dioxane	trace
5	Pd-BNP	Benzoyl peroxide	1,4-dioxane	0
6	Pd-BNP	TBHP (aq.)	1,4-dioxane	60
7	Pd-BNP	TBHP (aq.)	AcOH	48
8	Pd-BNP	TBHP (aq.)	^{t}BuOH	41
9	Pd-BNP	TBHP (aq.)	THF	40
10	Pd-BNP	TBHP (aq.)	1,4-dioxane/ AcOH	50
11	Pd-BNP	TBHP (aq.)	toluene	32
12	Pd-BNP	TBHP (aq.)	DCE	0
13[c]	**Pd/Cu-BNP**	**TBHP (aq.)**	**1,4-dioxane**	**70**
14[d]	Pd/Cu-BNP	TBHP (aq.)	1,4-dioxane	46
15[e]	Pd/Cu-BNP	TBHP (aq.)	1,4-dioxane	66
16[f]	Pd/Cu-BNP	TBHP (aq.)	1,4-dioxane	52
17[g]	Pd/Cu-BNP	TBHP (aq.)	1,4-dioxane	0
18	Pd-BNP	TBHP (dec.)	1,4-dioxane: H_2O	21
19[h]	Pd/Cu-BNP	TBHP (dec.)	1,4-dioxane	66
20	Pd/Cu-BNP	TBHP (dec.)	1,4-dioxane	36
21	Cu-BNP	TBHP (aq.)	1,4-dioxane	trace
22	Cu-BNP + Pd-BNP	TBHP (aq.)	1,4-dioxane	41
23	(10 %)Pd/C	TBHP (aq.)	1,4-dioxane	38
24	(5 %) Pd/Alumina	TBHP (aq.)	1,4-dioxane	15
25	Pd/Cu-BNP(1 : 2)	TBHP (aq.)	1,4-dioxane	63
26	Pd/Cu-BNP(2 : 1)	TBHP (aq.)	1,4-dioxane	68

[a] Reaction conditions: **1 a** (0.5 mmol), **2 a** (1.5 mmol) and 70 %aq.TBHP with 1 mL of solvent in 1 h [b] Yields were calculated by ^{1}H NMR spectroscopy using 1,3,5-trimethoxybenzene as an internal standard [c] Isolated yield [d] 3.0 equiv. of 70 % aq.TBHP was taken [e] 7.0 equiv. of 70 % aq.TBHP was taken [f] 4.0 mol % of Pd/Cu-BNP was used [g] Reaction conducted at 80 °C [h] 10 equiv. of water was added.

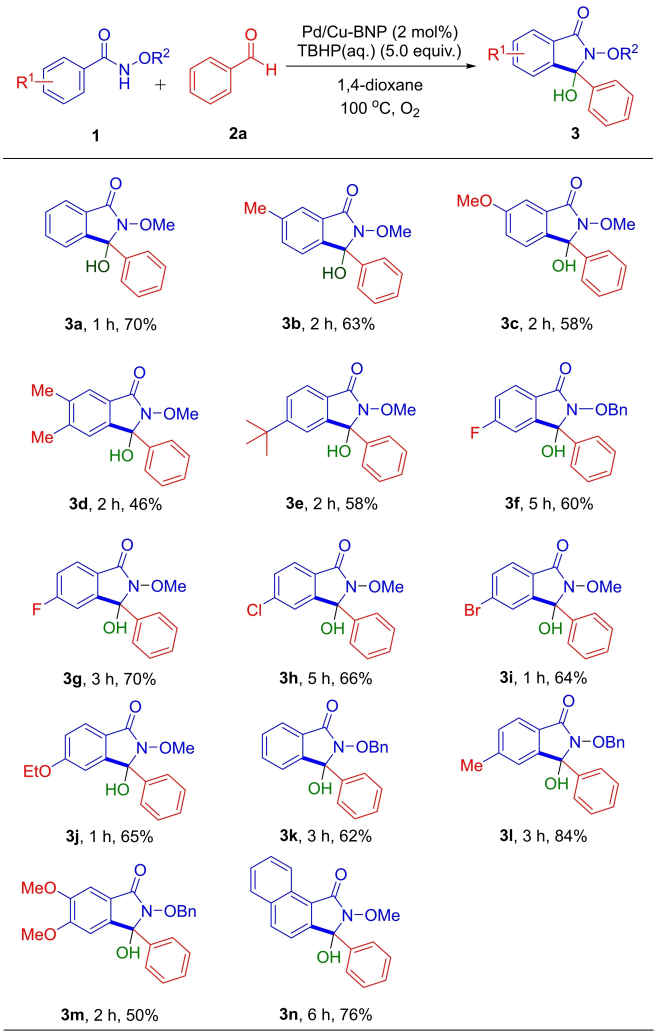

Scheme 2. Scope of various benzamides for the synthesis of 3-hydroxy isoindolones using bimetallic Pd/Cu-BNP catalyst. Reaction conditions: 1 (0.5 mmol), 2 (1.5 mmol) in 2 mL of 1,4-dioxane.

electron-donating substituents at *meta* and para position (−Me, -OMe) of benzamides gave the desired product, **3 b-3 d** with moderate to good yields. Sterically hindered para-tertiary butyl substituted benzamide also performed well and gave **3 e** in 58 % yield. When we screened the halogen-containing benzamides, **3 f, 3 g, 3 h**, and **3 i** formed 60–64 % yields of the desired cyclized products. An electron-donating ethoxy group substituted at the para-position of benzamide also gave the product **3 j** in 65 % yield.

N-benzyloxy-benzamide was tested under typical reaction conditions to determine the reactivity of the other *N*-alkoxy benzamides. The corresponding product, **3 k**, resulted in a 62 % yield. The substitution of the electron-donating group (−Me) at the para-position of *N*-benzyloxy benzamides functioned effectively, yielding the desired product **3 l** in 84 % of yield. The moderate yield of the product **3 m** was observed in the case of a disubstituted methoxy group at the *meta* and para position of *N*-benzyloxybenzamide. When the reaction was carried out with *N*-methoxy-1-naphthamide under the standard reaction condition, the reaction proceeded well and gave the cyclized product **3 n** in 76 % yield (Scheme 2).

In addition, the scope of various benzaldehydes containing both electron-releasing and withdrawing groups was examined, and the results are depicted in Scheme 3. The halogen-substituted benzaldehydes with various benzamides containing

© 2024 Wiley-VCH GmbH

10990690, 2024, 36, Downloaded from https://chemistry-europe.onlinelibrary.wiley.com/doi/10.1002/ejoc.202400471 by Indian Institute Of Science Education And Research Pune, Wiley Online Library on [23/06/2025]. See the Terms and Conditions (https://onlinelibrary.wiley.com/terms-and-conditions) on Wiley Online Library for rules of use; OA articles are governed by the applicable Creative Commons License

Research Article
doi.org/10.1002/ejoc.202400471

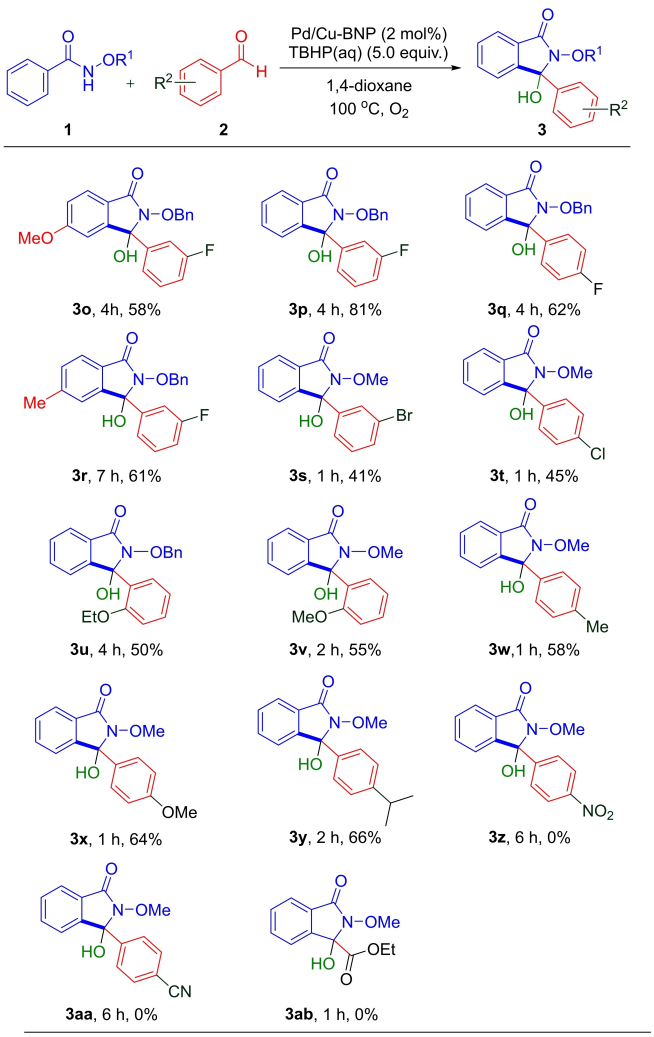

Scheme 3. Scope of various benzaldehydes for the synthesis of 3-hydroxy isoindolones using the bimetallic Pd/Cu-BNP catalyst. Reaction conditions: **1** (0.5 mmol), **2** (1.5 mmol) in 2 mL of 1,4-dioxane. [b] Isolated yield.

electron-donating groups formed **3o-3t** in 41 – 81% yields of the desired cyclized products, and one of the compounds (**3p**) was confirmed by single-crystal XRD (CCDC No. 2115665) (Figure 2).[25]

Electron donating (−Me, -^{i}Pr, -OMe, -OEt) groups at *ortho* and para-positions containing benzaldehydes performed well and gave the desired products **3u-3y** in 50–66% yields. Whereas electron-withdrawing groups such as -NO_2, -CN at the para position of benzaldehydes failed to give the desired products **3z-3aa** (Scheme 3).

Furthermore, we extended our methodology to develop 3-hydroxy-2-methoxy-3-phenylisoindoline-1-thione derivatives, which are a key component of the chemodosimeter's core.[26] Initially, *N*-methoxybenzothioamide **4** was treated with benzaldehyde under the optimized reaction conditions. The reaction went smoothly and provided the corresponding product **5a** in a 65% yield. The electron-donating groups, such as butoxy and ethoxy at para- the position of *N*-methoxybenzothioamide proceeded smoothly, yielding the desired products **5b-5c** in

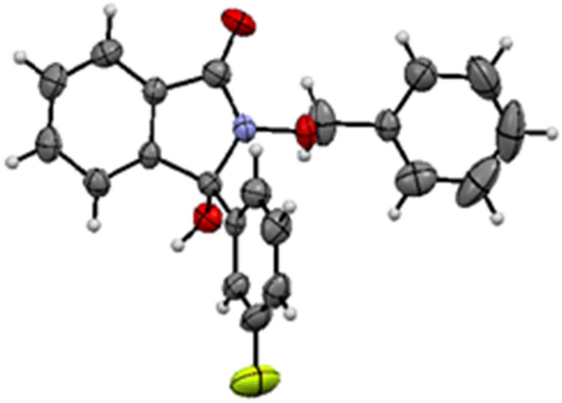

Figure 2. Single-crystal X-ray structure of compound 3p (CCDC No. 2115665). Ellipsoids represent a 50% probability level.

64% and 77% yields, respectively. Likewise, electron-donating groups (−Me, -OMe) at *ortho*-position also provided the desired products **5d-5e** in good yields (Scheme 4).

Additionally, we tested our methodology to develop hydroxy isoindolones using α-keto acid as an acyl source described in Scheme 5. Initially, *N*-methoxy benzamide with phenyl glyoxylic acid under the optimized reaction condition proceeded well and provided the corresponding product **3a** in 52% yield.

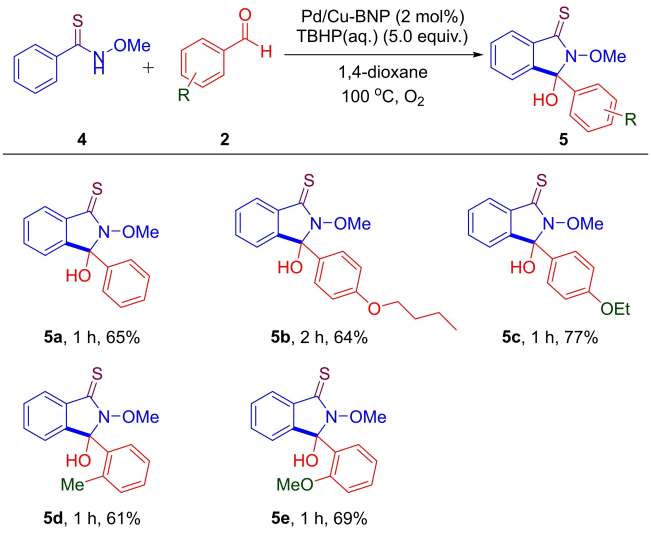

Scheme 4. Scope of various *N*-methoxybenzothioamides for the synthesis of 3-hydroxy-2-methoxy-3-phenylisoindoline-1-thiones using the bimetallic Pd/Cu-BNP catalyst. Reaction conditions: 1 (0.5 mmol), 2 (1.5 mmol) in 2 mL of 1,4-dioxane.

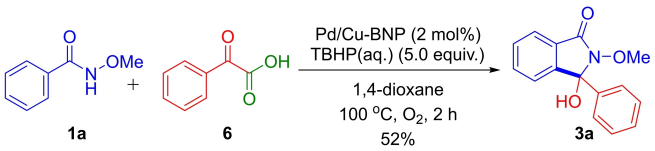

Scheme 5. Use of an α-keto acid.

© 2024 Wiley-VCH GmbH

10990690, 2024, 36, Downloaded from https://chemistry-europe.onlinelibrary.wiley.com/doi/10.1002/ejoc.202400471 by Indian Institute Of Science Education And Research Pune, Wiley Online Library on [23/06/2025]. See the Terms and Conditions (https://onlinelibrary.wiley.com/terms-and-conditions) on Wiley Online Library for rules of use; OA articles are governed by the applicable Creative Commons License

Research Article
doi.org/10.1002/ejoc.202400471

To check the scalability of our optimized reaction condition, a gram-scale reaction was carried out by using *N*-methoxy benzamide **1a** (8.0 mmol), benzaldehyde **2a** (24 mmol), Pd/Cu-BNP (Pd/Cu-Binapthyl Nanoparticles) (2 mol %) and 70% aq.TBHP (40 mmol) in a 1, 4-dioxane solvent at 100 °C for 1 h (Scheme 6). The reaction afforded 62% of the corresponding product **3a**.

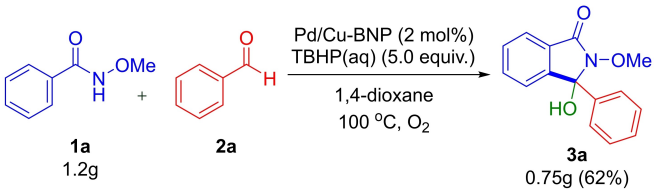

Scheme 6. Gram-scale reaction.

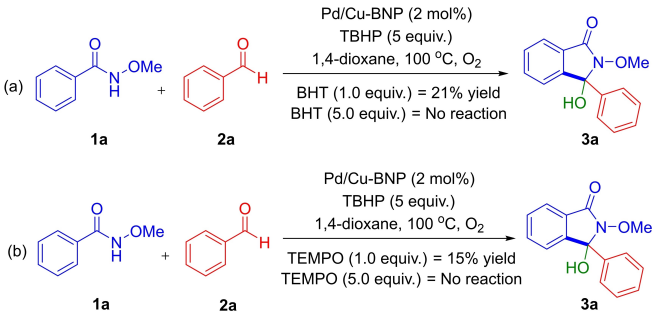

Scheme 7. Control experiments with radical inhibitors.

To gain a better understanding of the reaction mechanism, an experiment was carried out in the presence of radical inhibitor di-tert-butyl methyl phenol (BHT) (1.0 equiv.) under the optimized reaction condition (Scheme 7a) was observed only 21% yield of the desired product. When we increased the BHT, from 1.0 equiv. to 5.0 equiv., the reaction failed to yield the desired product. Furthermore, the reaction was carried out in the presence of 2,2,6,6-Tetramethylpiperidine-1-oxyl (TEMPO) (1.0 equiv.), and the formation of the desired product was observed in a 15% yield. Further increasing the equiv. of TEMPO from 1.0 equiv. to 5.0 equiv., it completely inhibited the reaction. Therefore, it was concluded that the reaction is proceeding *via* a radical mechanism (Scheme 7b).

To investigate the recovery and reusability of Pd/Cu-BNP catalyst, the reaction was carried out at a 1 mmol scale under optimal reaction conditions. The Pd/Cu-BNP catalyst was reused up to four times, resulting in 66%, 63%, 61%, and 58% yields of the desired product **3a** (Figure 3a).

Several experiments have been conducted to verify the heterogeneous nature of the Pd/Cu-BNP catalyst. These include the hot filtration test (Figure 3b) and the Hg-poisoning test (refer to supporting information for further details). Furthermore, the HRTEM analysis of the Pd/Cu-BNP catalyst post four catalytic cycles revealed no significant alteration in the size distribution and dispersion of the Pd/Cu-BNP nanoparticles in comparison to the initial catalyst (Figure 4). This confirms that the catalytic reaction is facilitated by heterogeneous palladium-copper bimetallic nanoparticles, rather than by leaching homogeneous palladium.

To explore the recovery and reusability of the Pd/Cu-BNP nanocatalyst, three parallel experiments were carried out under the optimal reaction conditions, and the yields were nearly comparable with a 5% error (Figure 5).

3-Hydroxy isoindolones are used as a key framework for the synthesis of biologically important molecules and pharmaceutical drugs. This encouraged us to use the current methodology for the synthesis of BDR4 inhibitor **9** (Scheme 8), using 5-bromo-3-hydroxy-2-methoxy-3-phenylisoindolin-1-one **3i**

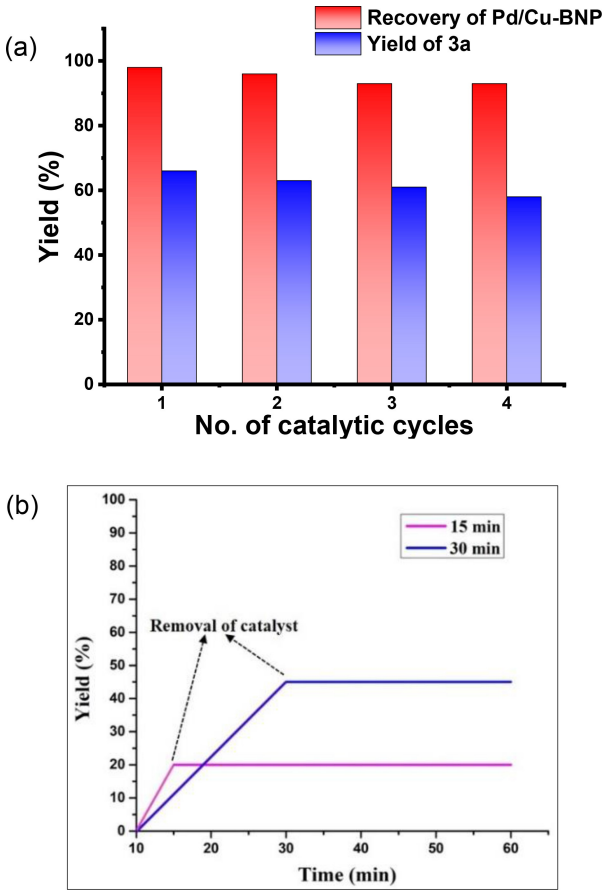

Figure 3. a) Recyclability of the Pd/Cu-BNP catalyst. b) Hot filtration test: Pink line: X = 15 min; blue line: X = 30 min.

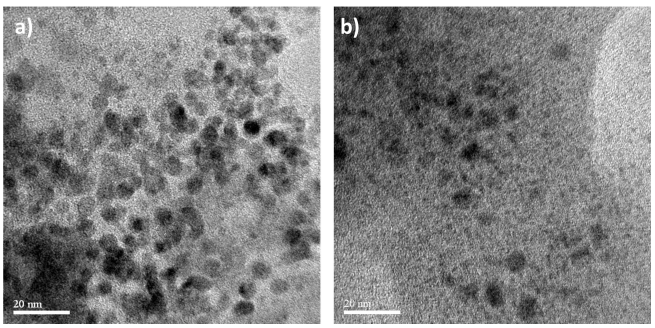

Figure 4. HRTEM images: a) freshly prepared Pd/Cu-BNP catalyst and b) after the fourth catalytic cycle.

© 2024 Wiley-VCH GmbH

10990690, 2024, 36, Downloaded from https://chemistry-europe.onlinelibrary.wiley.com/doi/10.1002/ejoc.202400471 by Indian Institute Of Science Education And Research Pune, Wiley Online Library on [23/06/2025]. See the Terms and Conditions (https://onlinelibrary.wiley.com/terms-and-conditions) on Wiley Online Library for rules of use; OA articles are governed by the applicable Creative Commons License

Research Article
doi.org/10.1002/ejoc.202400471

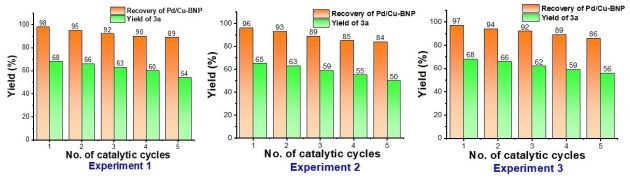

Figure 5. Error bar for three parallel experiments.

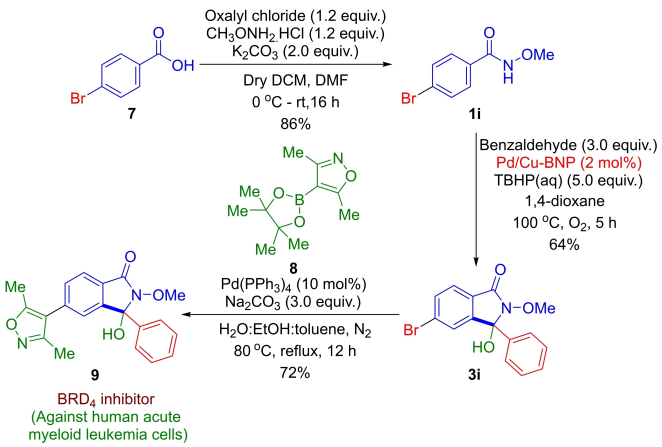

Scheme 8. Synthesis of a BDR4 inhibitor.

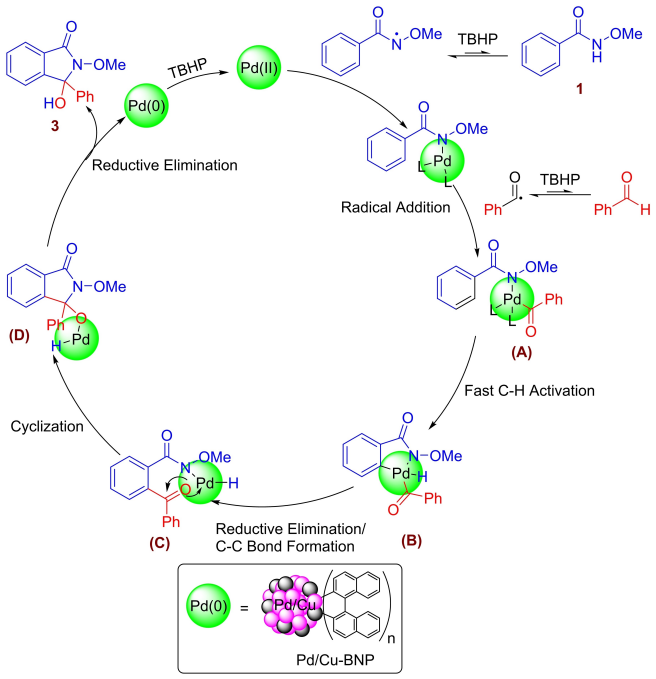

Scheme 10. Plausible catalytic cycle for the synthesis of 3-hydroxy isoindolones.

(0.5 mmol), boronic ester **8** (0.5 mmol), 10 mol% $Pd(PPh_3)_4$ and Na_2CO_3 (1.5 mmol) in H_2O/EtOH/toluene (2:1:2) solvent mixture at 80 °C reflux for 12 h to give the desired product BRD4 inhibitor (Against human acute myeloid leukemia cells)[27] **9** in 72% yield.

The synthetic application of 3-hydroxy isoindolone **3a** was further explored through derivatization to iminocarboxylic acid, which can be converted into various heterocyclic compounds.[28] 3-hydroxy isoindolone **3a** (0.5 mmol) was treated with 40 mol% BF_3•OEt_2 in DMSO/1,4-dioxane (4:1) solvent system at 130 °C to yield 85% of iminocarboxylic acid **10** in 8 h (Scheme 9).

Based on the previous literature reports[10,11] and experimental evidence, a plausible reaction mechanism for this transformation is proposed (Scheme 10). Benzamide and benzaldehyde in the presence of 70% aq.TBHP gives benzamide nitrogen radical and acyl radical respectively. Then, these radicals undergo radical addition with Pd(0) to form intermediate **A**, which undergoes fast C–H bond activation to form an intermediate **B**. That undergoes reductive elimination to form a new C–C bond, and Pd is attached to a benzamide nitrogen atom to form intermediate **C**. The intermediate **C**, upon intramolecular cyclization, forms intermediate **D** that readily undergoes reductive elimination to deliver the desired product **3a** with the generation of Pd(0), which will enter the next catalytic cycle.

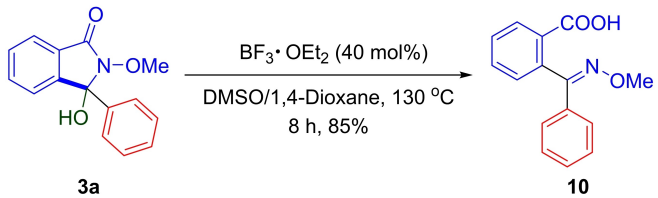

Scheme 9. Synthetic application of the product.

Conclusions

In conclusion, a method has been developed for the synthesis of hydroxy isoindolones using bimetallic Pd/Cu-BNP (Pd/Cu-Binapthyl Nanoparticles) catalysts for a domino C–H activation/annulation reaction. Hydroxy isoindolones were synthesized from N-methoxy benzamide using the environmentally friendly oxidant 70% aqueous TBHP. Benzamides/benzothioamides and aryl aldehydes containing various substituents containing provided moderate to good yields of the corresponding hydroxy isoindolones. Control experiments were undertaken to investigate the reaction mechanism, providing evidence for the radical pathway. Heterogeneity tests, including the mercury poisoning test and hot filtration test, demonstrated that the Pd/Cu-BNP heterogeneous catalyst facilitated the reaction rather than leached homogeneous palladium.

Experimental Section

Experimental Procedure for the Synthesis of Pd-Nanoparticles (Pd-BNP)[24]

Potassium tetrachloropalladate (326.5 mg, 1.0 mmol) in nanopore water (50 mL), 1,1′-binaphthyl,–2,2′-bis(diazonium tetrafluoroborate) (482.1 mg, 1.0 mmol) and toluene (50 ml) was added to a

© 2024 Wiley-VCH GmbH

10990690, 2024, 36, Downloaded from https://chemistry-europe.onlinelibrary.wiley.com/doi/10.1002/ejoc.202400471 by Indian Institute Of Science Education And Research Pune, Wiley Online Library on [23/06/2025]. See the Terms and Conditions (https://onlinelibrary.wiley.com/terms-and-conditions) on Wiley Online Library for rules of use; OA articles are governed by the applicable Creative Commons License

250 mL round-bottomed flask. The reaction mixture was stirred vigorously for 1 hour. After that, $NaBH_4$ (226.9 mg, 6.0 mmol) in water (2 mL) was added dropwise at room temperature to the solution and the immediate color change to dark greenish black signifies the Pd NPs formation. The reaction mixture was stirred at room temperature for 2 hours. The toluene layer was separated and washed with 0.5 M aq. H_2SO_4 (3×50 mL) and 0.5 M aq. $NaHCO_3$ (3×50 mL) to remove unreacted metal complex. The residual solvent was removed using a rotary evaporator. The solid particles were suspended in ethanol (2×10 mL) and sonicated for 30 min. The suspension was centrifuged (4500 rpm, approx. 30 min.). The ethanol was removed and the isolated mass was dried in vacuo to yield Pd-binaphthyl nanoparticles (Pd-BNP) as a black solid.

Experimental Procedure for the Synthesis of Pd/Cu-BNP Bimetallic Nanoparticles[24]

BINAM diazonium tetrafluoroborate (10 mmol) was added to a stirred solution of $Cu(OAc)_2$ (1.0 equiv.) and $Pd(OAc)_2$ (1.0 equiv.) (1:1) in acetonitrile (20 mL) in a 250 mL round bottom flask and vigorously stirred in a magnetic stirrer for 3 hours. Then $NaBH_4$ (2.26 gm, 60 mmol) in water (5 mL) was added dropwise at room temperature and the immediate color change to dark greenish black indicates the formation of palladium/copper nanoparticles. Then the reaction mixture was further stirred at room temperature for another 3 hours. After that, nano pure water (20 mL) was added to the reaction mixture, followed by sonication for 30 min. The Pd/Cu-BNP was separated from the reaction mixture and washed with 0.5 M aq. H_2SO_4 (2×20 mL) and 0.5 M aq. $NaHCO_3$ (2×20 mL) to remove the unreacted metal complexes. Finally, Pd/Cu-BNP was washed with nano pure water (10×2 mL) followed by ethanol (10×2 mL) and sonicated for 30 minutes at room temperature. Then further centrifugation (5000 rpm) of the suspension was done for 30 min. The ethanol was decanted and dried in a vacuum to obtain the Pd/Cu-binaphthyl NPs (Pd/Cu-BNP). This Pd/Cu-BNP catalyst is highly stable and can be stored in a vial at room temperature for several months.[24b]

Experimental Procedure for the Synthesis of Diazonium Salts[24]

The binaphthyl diazonium salt was synthesized by the diazotization of (1,1′-binaphthalene)-2,2′-diamine (BINAM). The stable binaphthyl diazonium salt was prepared by the slow addition of an aqueous solution of sodium nitrite ($NaNO_2$) to stirred solution of BINAM in HBF_4 at 0 °C for 30 minutes. The color change from pale brown to yellow indicates the formation of the diazonium salt. The resulting yellow solid was filtered and washed with cold HBF_4, H2O and EtOH. The diazonium salt was dried under a vacuum desiccator and stored at 0 °C.

Experimental Procedure for the Preparation of BRD4 Inhibitor

A mixture of 5-Bromo-3-hydroxy-2-methoxy-3-phenylisoindolin-1-one (0.5 mmol), 3,5-dimethyl-4-(4,4,5,5-tetramethyl-1,3,2-dioxaborolan-2-yl)isoxazole (0.5 mmol), sodium carbonate (1.5 mmol), Tetrakis (triphenylphosphine) palladium (10 mol%) in a mixed solvent of water (3 mL), ethanol (1 mL) and toluene (3 mL) was refluxed under N_2 for 12 h. After the reaction was completed, the mixture was diluted with water (20 mL) and filtered with diatomite. Then the filtrate was extracted with ethyl acetate (10 mL×3). The combined organic layers were dried over anhydrous Na_2SO_4 and concentrated under reduced pressure to give a brown oil. The resulting crude oil was purified by silica gel column chromatography (hexane/ethyl acetate, 3:1) to afford target product 5-(3,5-dimethylisoxazol-4-yl)-3-hydroxy-2-methoxy-3-phenylisoindolin-1-one (BRD4 inhibitor).

Experimental Procedure for the Synthesis of Imino Carboxylic Acid

A solution of 3-hydroxy-2-methoxy-3-phenylisoindolin-1-one (0.5 mmol) and $BF_3{\cdot}OEt_2$ (40 mol%) in DMSO/Dioxane (V:V = 4:1, 1.5 mL) was heated at 130 °C under air. The reaction was monitored by TLC. After the reaction was completed, the reaction mixture was allowed to cool down to room temperature, and EtOAc (20 mL) was added. The resulting mixture was washed with water (10 mL×3). The organic layer was dried over anhydrous Na_2SO_4, filtered and the solvent was removed under reduced pressure to provide the crude product. The purification was performed by flash column chromatography on silica gel.

Experimental Procedure for hot Filtration Test for Pd/Cu-BNP[24]

To confirm that the reaction was catalyzed by a heterogeneous Pd/Cu-BNP catalyst, not by the leached homogeneous Pd. A hot filtration test was executed under the optimized reaction condition. Two separate reactions were carried out by using 1a (0.5 mmol), 2a (1.5 mmol), and Pd/Cu-BNP (2 mol %), 70% aq.TBHP (2.5 mmol) in a 1,4-dioxane solvent was added to an oven-dried reaction tube equipped with a magnetic pellet and stirred at 100 °C. After 15 min, one set of the reaction was removed and cooled down to room temperature, and the solvent was removed. Then ethanol was added and the reaction mixture was centrifuged, and the Pd/Cu-BNP catalyst was removed from the reaction mixture by celite filtration. This process was repeated several times sequentially, and the mother liquid, which was completely free from the catalyst, and the solvent was evaporated under a vacuum followed by flash column chromatography, giving the desired product 3a in 20% yield. The remaining mother liquid, i.e., Pd/Cu-BNP catalyst free-reaction mixture, was allowed for a further 60 min under similar conditions. After 60 min the reaction was stopped and isolated the product was with no improvement in the yield was observed indicating no active catalyst was present to catalyze the further reaction. The same procedure was followed for another set of reactions.

Experimental Mercury Poisoning Experiment[24]

The Hg-poisoning test was performed to support our observation that the reaction was catalyzed by a heterogeneous Pd/Cu-BNP catalyst, not by the leached homogeneous Pd.

- In this experiment, Pd/Cu-BNP catalyst (2 mol %) and Hg (20.0 equiv.) in 1,4-dioxane stirred at room temperature for 1 h; after that, *N*-methoxy benzamide (0.5 mmol), benzaldehyde (3.0 equiv.) and 70% aq.TBHP (5.0 equiv.) was added and stirred at 100 °C. The formation of the desired product was not observed in the reaction.
- In the second set of reactions was tried with the addition of Hg (20.0 equiv.) at a time with all other reagents: 1a (0.5 mmol), 2a (1.5 mmol), and Pd/Cu-BNP (2 mol %), 70% aq.TBHP (2.5 mmol) was added and stirred at 100 °C complete inhibition of the product formation was observed. These experiments confirm that the Pd/Cu-BNP bimetallic nanoparticles catalyst is a heterogeneous catalyst.

© 2024 Wiley-VCH GmbH

10990690, 2024, 36, Downloaded from https://chemistry-europe.onlinelibrary.wiley.com/doi/10.1002/ejoc.202400471 by Indian Institute Of Science Education And Research Pune, Wiley Online Library on [23/06/2025]. See the Terms and Conditions (https://onlinelibrary.wiley.com/terms-and-conditions) on Wiley Online Library for rules of use; OA articles are governed by the applicable Creative Commons License

Experimental Procedure for Recoverability and Reusability of the Pd/Cu-BNP Catalyst [29]

To recover and reuse the Pd/Cu-BNP catalyst, the reaction was performed at a 1 mmol scale under the optimized reaction conditions using **1 a** (0.5 mmol), **2 a** (1.5 mmol), and Pd/Cu-BNP (2 mol %), 70% aq.TBHP (2.5 mmol) in 1,4-dioxane solvent at 100 °C. After completion of the reaction, the reaction mixture was allowed to cool to room temperature. EtOH (2 mL) was added to the reaction mixture and centrifuged. The liquid was decanted to a 50 mL conical flask. Again EtOH (5 mL) was added and centrifuged and decanted to the same conical flask. This procedure was repeated up to two to three times. After that, the catalyst was washed with nano pure water (5 mL) and ethanol (5 mL) two to three times. Finally, the resulting solid residue (Pd/Cu-BNP) was dried under a vacuum. The dried catalyst was reused for further catalytic cycle. The collected liquid was concentrated reducing pressure. The resulting reaction mixture was purified by column chromatography on silica gel (hexanes: ethyl acetate) to afford **3 a** at the desired product.

Experimental Procedure for Pd/Cu-BNP Catalyzed Amide Group Assisted Synthesis of Hydroxy Isoindolones *via* Domino C–H Activation/Annulation Reaction

N-alkoxy benzamide **1** (0.5 mmol), benzaldehyde **2** (3.0 equiv.), Pd/Cu-BNP (10.6 mg, 2 mol %) and tertiary butyl hydrogen peroxide (TBHP) (70% aq. solution) (5.0 equiv.) were successively added to the oven-dried reaction tube and 1, 4-Dioxane (2 mL) was added into the reaction tube. Then the reaction tube was immersed in a 100 °C preheated oil bath under an O_2 atmosphere. The reaction was heated with continuous stirring till the complete consumption of *N*-alkoxy benzamide occurred. The reaction mixture was first cooled down to room temperature. The solvent was then removed under reduced pressure. Then water was added to the reaction mixture and it was extracted with ethyl acetate (3×5 mL). Brine wash (1×10 mL) was given to the combined organic layer and dried over anhydrous Na_2SO_4 followed by drying of solvent under rotary evaporator. Then, the silica gel column separation of crude using a hexane and ethyl acetate mixture (70:30) afforded the corresponding hydroxy isoindolones.

Experimental Procedure for the Synthesis of *N*-alkoxy Benzamides [29]

To a solution of aromatic carboxylic acid (5 mmol) in dry dichloromethane (DCM) (10 mL) under nitrogen atmosphere, oxalyl chloride (6 mmol, 1.2 equiv.) was added dropwise at 0 °C, followed by the addition of a catalytic amount of dry DMF (2 drops). The reaction was continued to stir at room temperature until completion (approx. 3 h). After completion of the reaction, dichloromethane (DCM) was removed under reduced pressure to get crude acid chloride (Scheme 3). Then alkoxyamine hydrochloride salt (1.1 equiv.) was added to a mixture of K_2CO_3 (2 equiv.) in ethyl acetate and water (2:1; 30 mL) at room temperature. To this solution, crude acid chloride (1 equiv.) was added dropwise at 0 °C. The reaction was continued to be stirred at room temperature until completion. Then the reaction mixture was extracted with ethyl acetate (2×20 mL). The organic phase was purified by column chromatography on silica gel using a mixture of ethyl acetate and hexane to get *N*-alkoxy benzamide as the desired product.

Acknowledgements

G.S. thanks to IIT Madras for financial support. G.N.R. and K.V. thank IIT Madras for the fellowship.

Conflict of Interests

The authors declare the following competing financial interest(s): A patent is pending for the method described herein (Indian Patent Application 202441030383, April 15, 2024).

Data Availability Statement

The data that support the findings of this study are available in the supplementary material of this article.

Keywords: Pd nanoparticles · Heterogeneous catalysis · *N*-alkoxy benzamide/benzothioamides · 3-hydroxyisoindolin-1-ones/thiones · C–H activation

[1] a) J. G. Topliss, L. M. Konzelman, N. Sperber, F. E. Roth, *J. Med. Chem.* **1964**, *7*, 453–456; b) B. R. Davis, J. A. Cutler, C. D. Furberg, J. T. Wright, Jr., M. A. Farber, J. V. Felicetta, J. D. Stokes, *Ann. Intern. Med.* **2002**, *137*, 313–320.
[2] F. G. Fang, S. J. Danishefsky, *Tetrahedron Lett.* **1989**, *30*, 2747–2750.
[3] M. H. Abu Zarga, S. S. Sabri, S. Firdous, M. Shamma, *Phytochemistry* **1987**, *26*, 1233–1234.
[4] E. Fuse, T. Kuwabara, A. Sparreboom, E. A. Sausville, W. D. Figg, *J. Clin. Pharmacol.* **2005**, *45*, 394–403.
[5] a) E. C. Izgu, T. R. Hoye, *Chem. Sci.* **2013**, *4*, 2262–2266; b) S. H. Goh, C. Wei, A. R. M. Ali, *Tetrahedron Lett.* **1984**, *25*, 3483–3484.
[6] W. S. McKenzie, M. Rosenberg, *J. Mass. Dent. Soc.* **2007**, *56*, 44–45.
[7] a) P. Pigeon, B. Decroix, *Tetrahedron Lett.* **1996**, *37*, 7707–7710; b) D. Bootwicha, Panichakul, C. Kuhakarn, S. Prabpai, P. Kongsaeree, P. Tuchinda, V. Reutrakul, M. Pohmakotr, *J. Org. Chem.* **2009**, *74*, 3798–3805.
[8] Y. Zhou, Y. Zhai, J. Li, D. Ye, H. Jiang, H. Liu, *Green Chem.* **2010**, *12*, 1397–1404.
[9] a) M. Yi, X. Cui, C. Zhu, C. Pi, W. Zhu, Y. Wu, *Asian J. Org. Chem.* **2015**, *4*, 38–41; b) P. Fang, M. Li, H. Ge, *J. Am. Chem. Soc.* **2010**, *132*, 11898–11899.
[10] S. Sharma, E. Park, J. Park, I. S. Kim, *Org. Lett.* **2012**, *14*, 906–909.
[11] Q. Yu, N. Zhang, J. Huang, S. Lu, Y. Zhu, X. Yu, K. Zhao, *Chem. - Eur. J.* **2013**, *19*, 11184–11188.
[12] L. Yang, L. Han, B. Xu, L. Zhao, J. Zhou, H. Zhang, *Asian J. Org. Chem.* **2016**, *5*, 62–65.
[13] J. Jimenez, B.-S. Kim, P. J. Walsh, *Adv. Synth. Catal.* **2016**, *358*, 2829–2837.
[14] J. Shen, Q. You, Q. Fu, C. Kuai, H. Huang, L. Zhao, Z. Zhuang, *Org. Lett.* **2017**, *19*, 5170–5173.
[15] K. Jing, J.-P. Yao, Z.-Y. Li, Q.-L. Li, H.-S. Lin, G.-W. Wang, *J. Org. Chem.* **2017**, *82*, 12715–12725.
[16] D.-M. Yan, Q.-Q. Zhao, L. Rao, J.-R. Chen, W.-J. Xiao, *Chem. - Eur. J.* **2018**, *24*, 16895–16901.
[17] V. Kavala, C.-Y. Wang, C.-C. Wang, P. B. Patil, C.-C. Fang, C.-W. Kuo, C.-F. Yao, *Org. Biomol. Chem.* **2020**, *18*, 988–998.
[18] A. Balanta, C. Godard, C. Claver, *Chem. Soc. Rev.* **2011**, *40*, 4973–4985.
[19] G. Savitha, R. Saha, G. Sekar, *Tetrahedron Lett.* **2016**, *57*, 5168–5178.
[20] I. Favier, D. Madec, E. Teuma, M. Gomez, *Curr. Org. Chem.* **2011**, *15*, 3127–3174.
[21] M. Perez-Lorenzo, *J. Phys. Chem. Lett.* **2012**, *3*, 167–174.
[22] N. Zhang, Q. Yu, R. Chen, J. Huang, Y. Xia, K. Zhao, *Chem. Commun. (Cambridge, U. K.)* **2013**, *49*, 9464–9466.
[23] C. B. Reddy, S. Ram, A. Kumar, R. Bharti, P. Das, *Chem. Eur. J* **2019**, *25*(16), 4067–4071.

© 2024 Wiley-VCH GmbH

10990690, 2024, 36, Downloaded from https://chemistry-europe.onlinelibrary.wiley.com/doi/10.1002/ejoc.202400471 by Indian Institute Of Science Education And Research Pune, Wiley Online Library on [23/06/2025]. See the Terms and Conditions (https://onlinelibrary.wiley.com/terms-and-conditions) on Wiley Online Library for rules of use; OA articles are governed by the applicable Creative Commons License

[24] a) D. Ganapathy, G. Sekar, *Catal. Commun.* **2013**, *39*, 50–54; b) R. Saha, D. Arunprasath, G. Sekar, *J. Catal.* **2019**, *377*, 673–683.
[25] CCDC-2115665 (for 3p) contains the supplementary crystallographic data for this paper. These data can be obtained free of charge from The Cambridge Crystallographic Data Centre and Fachinformationszentrum Karlsruhe Access Structures service.
[26] H. Zali-Boeini, M. Zareh Jonaghani, N. Fadaei, H. A. Rudbari, *Spectrochim. Acta, Part A* **2017**, *178*, 198–202.
[27] P. Chen, Y. Yang, L. Yang, J. Tian, F. Zhang, J. Zhou, H. Zhang, *Bioorg. Chem.* **2019**, *86*, 119–125.
[28] N. N. Smolyar, Y. M. Yutilov, *Russ. J. Org. Chem.* **2008**, *44*, 274–28.
[29] N. Sharma, R. Saha, N. Parveen, G. Sekar, *Adv. Synth. Catal.* **2017**, *359*, 1947–1958.

Manuscript received: April 26, 2024
Revised manuscript received: June 15, 2024
Accepted manuscript online: July 12, 2024
Version of record online: September 3, 2024

© 2024 Wiley-VCH GmbH

10990690, 2024, 36, Downloaded from https://chemistry-europe.onlinelibrary.wiley.com/doi/10.1002/ejoc.202400471 by Indian Institute Of Science Education And Research Pune, Wiley Online Library on [23/06/2025]. See the Terms and Conditions (https://onlinelibrary.wiley.com/terms-and-conditions) on Wiley Online Library for rules of use; OA articles are governed by the applicable Creative Commons License

OL Organic Letters

pubs.acs.org/OrgLett Letter

Direct Access to Thiocyano-Thioesters from Cyclic Thioacetals via Photoredox Catalysis: An Introduction of Two Functional Groups in One Pot

Pankaj D. Dharpure, Mousumi Behera, Vikas V. Khade, Archana S. Thube, and Ramakrishna G. Bhat*

Cite This: *Org. Lett.* 2022, 24, 6919–6924 Read Online

ACCESS | Metrics & More | Article Recommendations | Supporting Information

ABSTRACT: The cyanation of organic compounds is an important synthetic transformation and mainly relies on a toxic CN source. Undeniably, thiocyanate salt has emerged as a very mild and environmentally benign CN source, yet its synthetic utility for cyanation is highly limited to very few types of organic compounds. Herein, we report the direct cyanation of cyclic thioacetals for accessing compounds with two different functional groups (thiocyano-thioesters) in one pot using sodium thiocyanate via photoredox catalysis. The protocol has been further extended for the direct cyanation of disulfides and diselenide to access aryl thiocyanates and aryl selenocyanate. A plausible mechanism has been proposed based on a series of control experiments, cyclic voltammetry and Stern–Volmer studies.

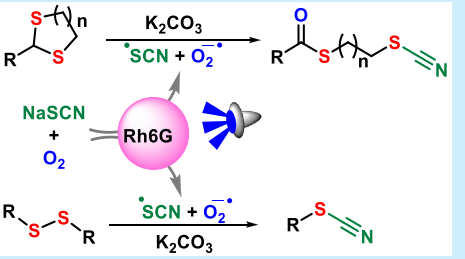

Downloaded via IISER PUNE on June 23, 2025 at 14:00:00 (UTC).
See https://pubs.acs.org/sharingguidelines for options on how to legitimately share published articles.

Organic thiocyanates are very useful intermediates for the synthesis of tetrazoles and different functionalities such as thiols, disulfides, thioethers, trifluoromethyl thioethers, thiocarbamates, thioesters and sulfonyl cyanides.[1−9] Likewise, thioesters are important intermediates in many biosynthetic pathways such as native chemical ligation, protein synthesis and nucleic acid synthesis.[10] In addition, thioesters have been utilized in the drug delivery applications and biomolecule labeling.[11] Thioesters have also been employed as important acyl radical equivalents in many acyl transfer reactions.[12] Traditionally, the cyanation of organic molecules has been achieved using cyanating agents or combined "CN source" comprising solvent (as a carbon source) and ammonium iodide/ammonium carbonate/ammonium bicarbonate/urea (as a nitrogen source) using palladium catalysis or a stoichiometric amount of copper at an elevated reaction temperature.[13] Most of these protocols rely on stoichiometric amount of oxidants, transition metals, ligands, costly reagents or more importantly the usage of extremely toxic CN sources (CuCN).

In order to overcome these limitations, different thiocyanate salts have been explored for cyanation as a "CN source" that are inexpensive, easily available, comparatively nontoxic and bench-stable.[14−17] The reaction of quinoxaline and tertiary amines with KSCN under oxidizing reaction condition (*t*-butyl hydroperoxide as an oxidant) is known to afford the corresponding nitriles (Scheme 1A and B).[15a,b] The cyanation of carbene generated *in situ* from the tosylhydrazone has been reported using KSCN and CuI at 80 °C under alkaline reaction condition (Scheme 1C).[16] Very recently for the first time, metal-free cyanation of thiophenol under visible light photoredox conditions has been achieved by generating electrophilic thiocyanate radical as a "CN source" to access a wide variety of aryl thiocyanates under oxygen atmosphere (Scheme 1D).[17]

Another light mediated photoinduced cyanation of *tert*-amines has been achieved by irradiating the donor–acceptor complex of *tert*-amines and benzoyl cyanide under purple LEDs (Scheme 1E).[18]

Nevertheless, such useful and straightforward protocols are known to introduce CN functionality only at activated positions of very few classes of compounds. To the best of our knowledge, the cyanation of thioethers has been rarely achieved till date.

Our continuous interest on photoredox catalysis led us to focus on developing a protocol for the direct cyanation of cyclic thioacetals under milder reaction conditions using inexpensive and environmentally friendly cyanating reagents. Based on our previous experience, C–S bond formation as well as cleavage in dithioacetals proceeds via thiyl radical under photoredox catalysis.[19a−c]

Recently, our research group developed a protocol for the synthesis of disulfide-linked-dithioesters starting from dithioacetals that has been proved to proceed via the cleavage of the C–S bond under basic conditions.[19c] Based on the same concept, we envisaged that the *in situ* generated electrophilic thiocyanate radical can be trapped with cyclic thioacetals to generate the molecules with dual functional groups (thiocyano-

Received: August 3, 2022
Published: September 19, 2022

ACS Publications © 2022 American Chemical Society

https://doi.org/10.1021/acs.orglett.2c02601
Org. Lett. 2022, 24, 6919–6924

Scheme 1. Application of Thiocyanates in Organic Transformations

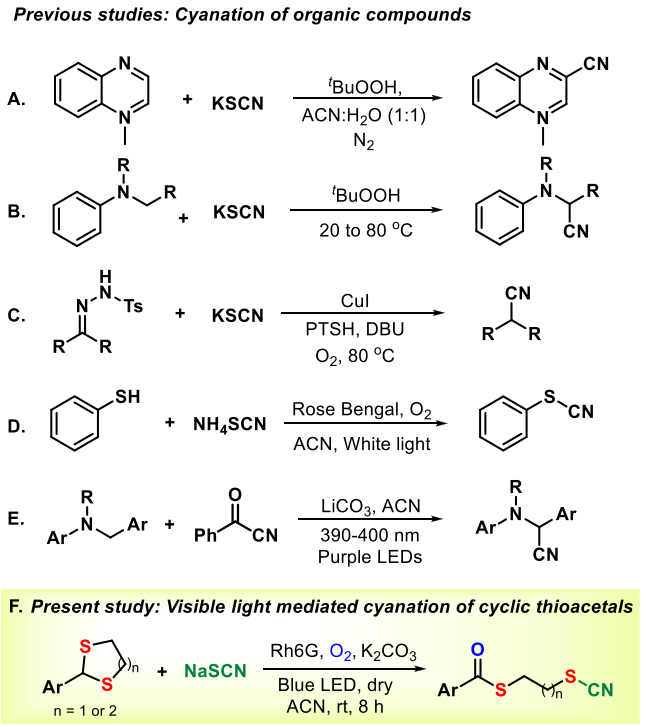

thioesters) in a single step. Herein, we report the direct one-pot generation of two functional groups in a molecule to access thiocyano-thioesters from cyclic thioacetals via photoredox catalysis.

In order to validate our hypothesis, we commenced with the model reaction of dithiolane **1a** and ammonium thiocyanate in the presence of K_2CO_3 as a base, Rh6G (2 mol %) as a photocatalyst in dry acetonitrile under oxygen atmosphere and irradiated the reaction mixture using blue LEDs for 8 h. The reaction afforded the corresponding desired product **2a** albeit in poor yield (15%, Table 1, Entry 1). Gratifyingly, the reaction of **1a** in the presence of sodium thiocyanate under the same reaction conditions afforded the desired product **2a** in very good yields (83%, Table 1, Entry 2). In order to further optimize the reaction conditions, we screened different photocatalysts such as; Eosin Y, Rhodamine 6G (Rh6G), $Ru(bpy)_3Cl_2$, $Ir(bpy)_3$, Acridinium-perchlorate, and Rose Bengal (Table 1, Entries 2 and 3−6). Among all the photocatalysts, Rh6G was found to be optimum for the desired transformation affording the desired product **2a** in very good yield (83%, Table 1, Entry 2). Further, among all the light sources screened, blue LEDs proved to be the most efficient in terms of yield and time (see SI 1.3B). Later, we screened different solvents and among all anhydrous acetonitrile proved to be advantageous for the smooth transformation of **1a** to thiocyano-thioester **2a** (Table 1, Entries 2 and 7−11). Among different bases screened, K_2CO_3 turned out to be the most suitable base to provide the desired product **2a** in very good yield (83%, Table 1, Entries 2 and 12−15). There was no significant difference in the reactivity of sodium thiocyanate and potassium thiocyanate in terms of the outcome of desired product **2a** formation (83% and 82% yields respectively, see SI 1.3A, Entries 5 and 6). Later, we screened variable stoichiometric amounts of sodium thiocyanate and we

Table 1. Reaction Optimization[a]

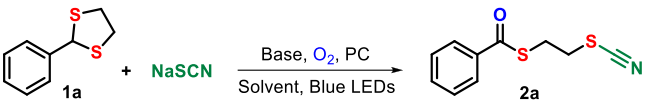

Entry	Catalyst	Solvent[g]	Base	Yield **2a** (%)
1[b]	Rh6G	MeCN	K_2CO_3	15
2	**Rh6G**	**MeCN**	**K_2CO_3**	**83**
3	Eosin Y	MeCN	K_2CO_3	67
4	Acr	MeCN	K_2CO_3	60
5	$Ru(bpy)_3Cl_2$	MeCN	K_2CO_3	49
6	Rose Bengal	MeCN	K_2CO_3	24
7	Rh6G	^{t}BuOH	K_2CO_3	61
8	Rh6G	DMSO	K_2CO_3	19
9	Rh6G	THF	K_2CO_3	43
10	Rh6G	Dioxane	K_2CO_3	51
11	Rh6G	$CHCl_3$	K_2CO_3	33
12	Rh6G	MeCN	DMAP	70
13	Rh6G	MeCN	TEA	41
14	Rh6G	MeCN	Na_2CO_3	62
15	Rh6G	MeCN	$NaHCO_3$	58
16[c]	--	MeCN	K_2CO_3	N.R.
17	Rh6G	MeCN	--	Trace
18[d]	Rh6G	MeCN	K_2CO_3	N.R.
19[e]	Rh6G	MeCN	K_2CO_3	N.R.
20[f]	Rh6G	MeCN	K_2CO_3	71

[a]0.1 mmol **1a**, 2 mol % catalyst, 0.2 mmol base, 0.5 mmol NaSCN, 2 mL solvent, O_2 balloon. [b]NH_4SCN [c]Without catalyst at 60 °C [d]Under argon. [e]Without light. [f]Open air atmosphere, Blue LED (15 W). [g]All solvents used were anhydrous.

observed that excess sodium thiocyanate (5 equiv) was essential for the smooth transformation to access the desired product **2a** in very good yield (see SI 1.3). The desired reaction did not work in the absence of light, photocatalyst and oxygen, indicating that these are very essential and necessary requirements for the smooth and facile transformation (Table 1, Entries 16, 18, and 19). The reaction in the absence of base offered a trace amount of desired product **2a** (Table 1, Entry 17). In order to validate the necessity of anhydrous solvent, we carried out the reaction in moist acetonitrile (undried) and we observed the reduction in the yield of desired product **2a** (71%, Table 1, Entry 20). Based on the exhaustive screening, dithiolane **1a** (1 equiv), NaSCN (5 equiv), K_2CO_3 (2 equiv), Rh6G (2 mol %) in dry acetonitrile under O_2 atmosphere and blue LEDs (15 W) proved to be optimum reaction conditions.

Having optimized the reaction condition, we planned to explore the diverse substrate scope of dithiolanes so as to generalize this protocol (Table 2). All the electronically neutral dithiolanes (**1a−c**) under the optimized reaction conditions offered the corresponding thiocyanao-thioesters (**2a−c**) in very good yields (up to 87%). Electron-rich substrates (**1d−f**) reacted smoothly to afford the corresponding desired products (**2d−f**) in very good yields (up to 89%). Substrates (**1g−m**) containing electron deactivating substituents at *o*/*m*/*p*-positions also worked well under optimized reaction conditions to furnish the desired products (**2g−m**) in very good yields (up to 82%, Table 2).

Naphthalene-1-dithiolane as well as naphthalene-2-dithiolane derivatives (**1n**, **1o**) also offered the corresponding desired products **2n** and **2o** in very good yields (up to 83%). Further, dithiolane derived from aromatic aldehyde having an electron withdrawing substituent (−CN) also afforded the

https://doi.org/10.1021/acs.orglett.2c02601
Org. Lett. 2022, 24, 6919−6924

Table 2. Substrate Scope[a]

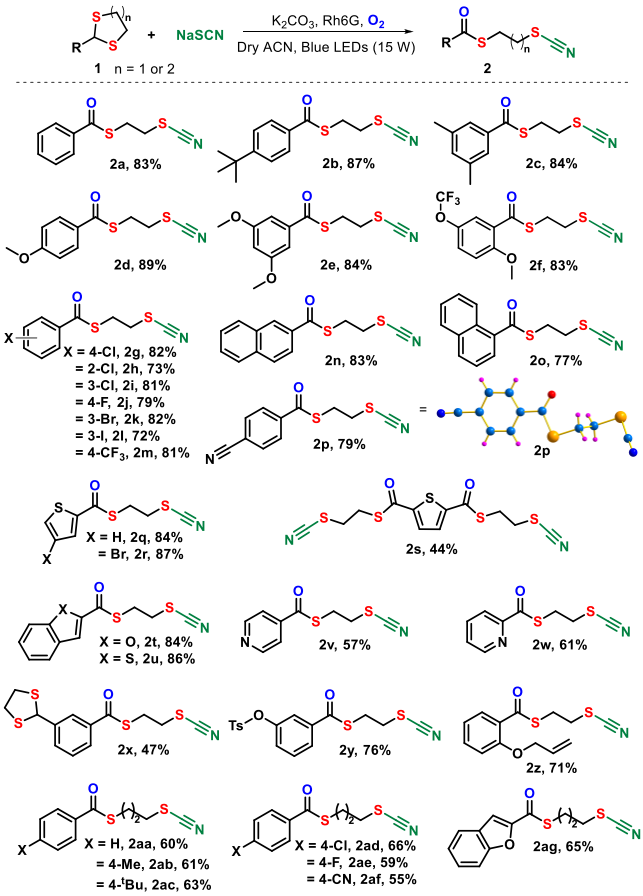

[a]0.1 mmol **1a**, 2 mol % Rh6G, 0.2 mmol K_2CO_3, 0.5 mmol NaSCN, 2 mL MeCN, O_2 balloon; 15 W Blue LEDs; isolated yields in after column chromatography.

desired product **2p** in good yield and the molecular structure of the **2p** was unambiguously confirmed by the single crystal X-ray analysis.[20] Even the dithiolanes derived from different thiophene carboxaldehydes **1q−s** worked smoothly under the optimized reaction conditions to furnish the corresponding products **2q−s** in moderate to good yields (up to 87%, Table 2). Other heterocyclic thioacetals derived from benzofuran, benzothiophene and pyridine carboxaldehydes **1t−w** worked well to give the desired products **2t−w** in moderate to good yields (up to 86%, Table 2). Dithiolane substrates containing protecting groups afforded the corresponding products **2x−z** in moderate to good yields (up to 76%), and interestingly, all protecting groups tolerated the reaction conditions. Later reactivity of dithianes (six-membered cyclic thioacetals) were explored to generalize this protocol. Gratifyingly, different dithianes **1aa−ag** derived from electron-rich as well as electron-deficient aromatic aldehydes and heteroaromatic aldehydes afforded the corresponding desired products **2aa−ag** in good yields (up to 66%, Table 2).

In order to have an insight into the reaction mechanism, we carried out a few control experiments systematically. The reaction of dithiolane **1a** in the presence of TEMPO did not work, thus confirming the radical nature of the transformation (Scheme 2a). The reaction in the absence of oxygen (under argon atmosphere) did not work indicating the necessary requirement of oxygen for this reaction (Scheme 2b). In order

Scheme 2. Control Experiments

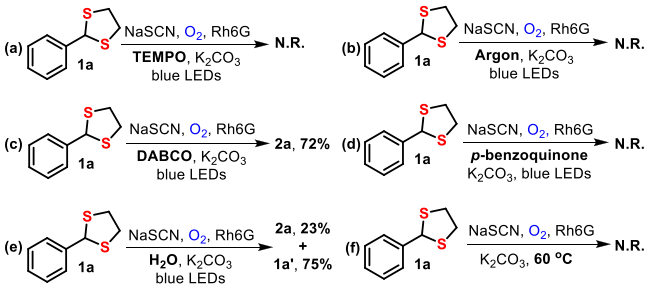

to investigate the involvement of singlet oxygen, if any, in the reaction pathway, reaction of **1a** was carried out in the presence of DABCO (singlet oxygen quencher). We observed that the reaction worked smoothly and DABCO did not have any impact on the yield of **2a** thus indicating that singlet oxygen has no significant role in the reaction pathway (Scheme 2c).[21] While, the reaction of **1a** in the presence of *p*-benzoquinone under standard optimized reaction conditions did not work; confirming the involvement of superoxide radical anion in the reaction mechanism (Scheme 2d).[22] The reaction in the presence of water led to significant reduction in the yield of desired product **2a** along with the corresponding benzaldehyde as a side-product **1a′** (Scheme 2e). The reaction in the presence of photocatalyst under dark conditions (absence of light) at an elevated reaction temperature (60 °C) did not work (Scheme 2f). This clearly indicated that both photocatalyst as well as light are absolutely essential for this transformation, and the temperature does not have any role for the desired product formation.

In order to confirm the possible single electron transfer (SET) event of excited photocatalyst (Rh6G*) with dithioacetal or NaSCN, we carried out the Stern−Volmer experiment. This study revealed that the efficiency of the SET of Rh6G* with NaSCN is much higher than that of **1a** (see Stern−Volmer graph, SI 1.5A, S4). The efficiency of SET of NaSCN with the Rh6G* was further supported by the oxidation potential of NaSCN (E^{ox} = +0.66 V vs SCE) which is less than the reduction potential of Rh6G* (E^{red} = +1.39 V vs SCE).[23,24]

Based on the control experiments, Stern−Volmer plot and preceding literature,[19b] we have depicted the plausible reaction mechanism (Figure 1). Upon irradiation with blue light, the photocatalyst Rh6G gets excited to Rh6G*. This excited species Rh6G* (E^{red} = +1.39 V vs SCE)[22] takes part in SET

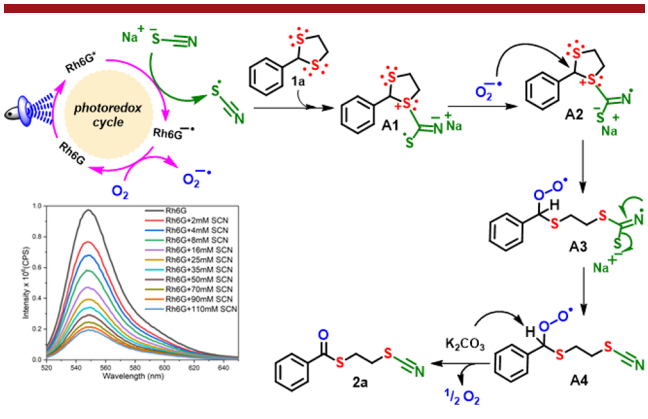

Figure 1. Plausible reaction mechanism.

https://doi.org/10.1021/acs.orglett.2c02601
Org. Lett. 2022, 24, 6919−6924

process with sodium thiocyanate (E^{ox} = +0.66 V vs SCE)[24] instead of **1a** (E^{ox} = +1.26 V vs SCE) by the reductive quenching pathway to generate the photocatalyst radical anion (Rh6G$^{\bullet-}$, reduced form) and thiocyanate radical (oxidized form $^{\bullet}$SCN). This SET event was confirmed by the Stern–Volmer experimental studies (SI 1.5). Further, Rh6G$^{\bullet-}$ takes part in another SET event with oxygen to generate a superoxide radical anion and the ground-state Rh6G, thus completing the photocatalytic cycle (Figure 1).

Simultaneously, the reactive thiocyanate radical species reacts with dithiolane **1a** to form an intermediate **A1**. This would further form the corresponding intermediate **A2** by shifting of an electron from nitrogen to sulfur. Next, the nucleophilic superoxide radical anion attacks the intermediate **A2** at the electrophilic carbon to generate intermediate **A3**. This intermediate would further collapse to form peroxide intermediate **A4**. This unstable intermediate ultimately breaks down to form the desired product **2a** in the presence of K_2CO_3 (Figure 1). Base (2 equiv of K_2CO_3) is essential to abstract acidic proton of **A4** and also to maintain the alkaline reaction medium to avoid any side product formation.

Based on the plausible reaction mechanism (Figure 1), it is evident that after the SET process the *in situ* generated thiocyanate radical is more likely to be electrophilic and has a high possibility to be attacked by the nucleophilic sulfur atom of dithioacetal followed by the cleavage of bond (with the neighboring carbon atom). In order to explore the reactivity of thiocyanate radical and to validate this hypothesis, we planned to trap this radical using suitable compounds such as diaryl disulfides to access the aryl thiocyanates which can be otherwise accessed by the reaction of TMSCN or nitromethane or CuCN with disulfide at elevated reaction temperature or from other starting materials.[25a−d]

In this regard, we commenced with a model reaction of diphenyl disulfide **3a**, sodium thiocyanate (5 equiv) under standard optimum reaction conditions used for obtaining thiocyano-thioesters. Gratifyingly, we obtained the corresponding desired phenyl thiocyanate **4a** in excellent yield (93%, Table 3). Encouraged by this initial success, we planned to generalize this protocol for wider applicability (Table 3). The reaction of different diaryl disulfides **3b−3f** reacted smoothly with sodium thiocyanate under the reaction conditions to afford the corresponding aryl thiocyanates **4b−4f** in excellent yields (up to 95%, Table 3). Even diphenyl diselenide **3g** reacted smoothly with sodium thiocyanate to afford the corresponding phenyl selenocyanate **4g** in very good yield (89%). This protocol also proved to be very efficient for one-pot synthesis of aryl thiocyanates from easily accessible diaryl disulfides.

Table 3. Substrate Scope

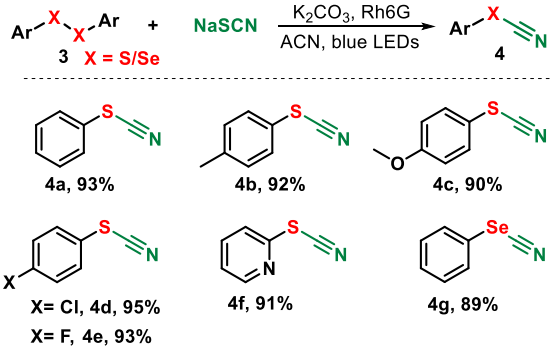

[a]**3** (0.1 mmol), Rh6G (2 mol %), K_2CO_3 (0.2 mmol), NaSCN (0.5 mmol), MeCN (2 mL), O_2 baloon, Blue LEDs (15W).

In summary, we have successfully developed a novel, safe and environmentally benign protocol for the cyanation of cyclic thioacetals and disulfides to access thiocyano-thioesters and aryl thiocyanates respectively, using commercially viable and nontoxic sodium thiocyanate as a cyanating source under photoredox catalysis using visible light. A wide range of thiocyano-thioesters have been synthesized in a single step starting from different dithiolanes under ambient reaction conditions. This protocol proved to be efficient and practical and worked well using a clean energy source such as visible light and the method did not rely on any external oxidizing reagent.

■ ASSOCIATED CONTENT

Supporting Information

The Supporting Information is available free of charge at https://pubs.acs.org/doi/10.1021/acs.orglett.2c02601.

Full experimental procedure, Stern–Volmer graph, SCXRD data of compound **2p**, characterization data for all new compounds and copies of ^{1}H and ^{13}C NMR spectra (PDF)

Accession Codes

CCDC 2175599 contains the supplementary crystallographic data for this paper. These data can be obtained free of charge via www.ccdc.cam.ac.uk/data_request/cif or by emailing data_request@ccdc.cam.ac.uk or by contacting The Cambridge Crystallographic Data Centre, 12 Union Road, Cambridge CB2 1EZ, UK; fax: +44 1223 336033.

■ AUTHOR INFORMATION

Corresponding Author

Ramakrishna G. Bhat − *Department of Chemistry, Indian Institute of Science Education and Research (IISER) Pune, 411008 Pune, Maharashtra, India;* orcid.org/0000-0002-7739-9553; Email: rgb@iiserpune.ac.in

Authors

Pankaj D. Dharpure − *Department of Chemistry, Indian Institute of Science Education and Research (IISER) Pune, 411008 Pune, Maharashtra, India*

Mousumi Behera − *Department of Chemistry, Indian Institute of Science Education and Research (IISER) Pune, 411008 Pune, Maharashtra, India;* orcid.org/0000-0003-2609-5987

Vikas V. Khade − *Department of Chemistry, Indian Institute of Science Education and Research (IISER) Pune, 411008 Pune, Maharashtra, India*

Archana S. Thube − *Department of Chemistry, Indian Institute of Science Education and Research (IISER) Pune, 411008 Pune, Maharashtra, India*

Complete contact information is available at: https://pubs.acs.org/10.1021/acs.orglett.2c02601

Notes

The authors declare no competing financial interest.

https://doi.org/10.1021/acs.orglett.2c02601
Org. Lett. 2022, 24, 6919−6924

■ ACKNOWLEDGMENTS

R. G. B. thanks Science and Engineering Research Board (SERB)-DST (CRG/2019/005753), Govt. of India for the generous research grant. Authors also thank IISER Pune for the financial assistance. P. D. D. thanks CSIR, New Delhi, V. V. K. thanks UGC, New Delhi, Govt. of India for providing fellowship. M. B. thank IISER Pune for the fellowship. A. S. T. thanks SERB-DST, New Delhi, Government of India for the project fellowship. We thank Mr. Ravinder Malothu of IISER Pune for helping in for obtaining the crystal data of 2p.

■ REFERENCES

(1) Pawliczek, M.; Garve, L. K. B.; Werz, D. B. Activation of Aryl Thiocyanates Followed by Aryne Insertion: Access to 1,2-Thiobenzonitriles. *Org. Lett.* **2015**, *17*, 1716−1719.

(2) (a) Zhang, T.; Deng, G.; Li, H.; Liu, B.; Tan, Q.; Xu, B. Cyclization of 2-Biphenylthiols to Dibenzothiophenes under $PdCl_2$/DMSO Catalysis. *Org. Lett.* **2018**, *20*, 5439−5443. (b) Hoggarth, E.; Sexton, W. A. New Reactions of Thiocyanic Esters. *J. Chem. Soc.* **1947**, 815−818.

(3) Danoun, G.; Bayarmagnai, B.; Gruenberg, M. F.; Goossen, L. J. Sandmeyer Trifluoromethylthiolation of Arenediazonium Salts with Sodium Thiocyanate and Ruppert−Prakash Reagent. *J. Chem. Sci.* **2014**, *5*, 1312−1316.

(4) Segalovich-Gerendash, G.; Rozenberg, I.; Alassad, N.; Nechmad, N. B.; Goldberg, I.; Kozuch, S.; Lemcoff, N. G. Imposing Latency in Ruthenium Sulfoxide-Chelated Benzylidenes: Expanding Opportunities for Thermal and Photoactivation in Olefin Metathesis. *ACS Catal.* **2020**, *10*, 4827−4834.

(5) Chen, J.; Wang, T.; Wang, T.; Lin, A.; Yao, H.; Xu, J. Copper Catalyzed C5-selective Thio/Selenocyanation of 8-aminoquinolines. *Org. Chem. Front.* **2017**, *4*, 130−134.

(6) Yang, L.; Tian, Z.-Y.; Zhang, C.-P. Transition-Metal-Free Selective Synthesis of (Z)-1,2-Diarylthio-1-arylalkenes, (2-Arylethene-1,1,2-triyl)tris(arylsulfane)s and Alkynyl Sulfides from Thiocyanates and Terminal Arylalkynes. *ChemistrySelect* **2019**, *4*, 311−315.

(7) Grieco, P. A.; Yokoyama, Y.; Williams, E. Aryl Selenocyanates and Aryl Thiocyanates: Reagents for the Preparation of Activated Esters. *J. Org. Chem.* **1978**, *43*, 1283−1285.

(8) Vaghasiya, B. K.; Satasia, S. P.; Thummar, R. P.; Kamani, R. D.; Avalani, J. R.; Sapariya, N. H.; Raval, D. K. Oxidative Cyanide-free Cyanation on Arylboronic Acid Derivatives using Aryl/Heteroaryl Thiocyanate using Novel IL-$PdCl_4$ Catalyst under Mild Condition. *J. Sulfur Chem.* **2018**, *39*, 507−515.

(9) Kelly, T. R.; Kim, M. H.; Curtis, A. D. M. Structure Correction and Synthesis of the Naturally Occurring Benzothiazinone BMY 40662. *J. Org. Chem.* **1993**, *58*, 5855−5857.

(10) (a) Echelman, D. J.; Lee, A. Q.; Fernández, J. M. Mechanical Forces Regulate the Reactivity of a Thioester Bond in a Bacterial Adhesion. *J. Biol. Chem.* **2017**, *292*, 8988−8997. (b) Folikumah, M. Y.; Behl, M.; Lendlein, A. Thiol−Thioester Exchange Reactions in Precursors Enable pH-Triggered Hydrogel Formation. *Biomacromolecules* **2021**, *22*, 1875−1884. (c) Xuan, W.; Collins, D.; Koh, M.; Shao, S.; Yao, A.; Xiao, H.; Garner, P. P.; Schultz, P. G. Site-specific Incorporation of a Thioester Containing Amino Acid into Proteins. *ACS Chem. Biol.* **2018**, *13*, 578−581. (d) Schuler, B.; Pannell, L. K. Specific Labeling of Polypeptides at Amino-Terminal Cysteine Residues Using Cy5-benzyl Thioester. *Bioconjugate Chem.* **2002**, *13*, 1039−1043. (e) Sletten, E. M.; Bertozzi, C. R. Bioorthogonal Chemistry: Fishing for Selectivity in a Sea of Functionality. *Angew. Chem., Int. Ed.* **2009**, *48*, 6974−6998. (f) Rinalducci, S.; Murgiano, L.; Zolla, L. Redox Proteomics: Basic Principles and Future Perspectives for the Detection of Protein Oxidation in Plants. *J. Exp. Bot.* **2008**, *59*, 3781−3801. (g) Le, N. T. T.; Nguyen, T. N. Q.; Cao, V. D.; Hoang, D. T.; Ngo, V. C.; Hoang Thi, T. T. Recent Progress and Advances of Multi-Stimuli-Responsive Dendrimers in Drug Delivery for Cancer Treatment. *Pharmaceutics* **2019**, *11*, 591.

(11) (a) Franke, J.; Hertweck, C. Biomimetic Thioesters as Probes for Enzymatic Assembly Lines: Synthesis, Applications, and Challenges. *Cell Chem. Bio* **2016**, *23*, 1179−1192. (b) Burke, H. M.; McSweeney, L.; Scanlan, E. M. Exploring Chemoselective S-to-N Acyl Transfer Reactions in Synthesis and Chemical Biology. *Nat. Commun.* **2017**, *8*, 15655. (c) Chen, B.; Sun, Y.; Niu, J.; Jarugumilli, G. K.; Wu, X. Protein Lipidation in Cell Signaling and Diseases: Function, Regulation, and Therapeutic Opportunities. *Cell Chem. Bio.* **2018**, *25*, 817−831. (d) Yang, W.; Xia, S.-H. Mechanisms of Regulation and Function of G-protein-coupled Receptor Kinases. *World J. Gastroenterol.* **2006**, *12*, 7753−7757.

(12) (a) Rossi, S.; Benaglia, M.; Cozzi, F.; Genoni, A.; Benincori, T. Organocatalytic Stereoselective Direct Aldol Reaction of Trifluoroethyl Thioesters. *Adv. Synth. Catal.* **2011**, *353*, 848−854. (b) Yang, H.; Li, H.; Wittenberg, R.; Egi, M.; Haung, W.; Liebeskind, L. S. Ambient Temperature Synthesis of High Enantiopurity *N*-Protected Peptidyl Ketones by Peptidyl Thiol Ester−Boronic Acid Cross-Coupling. *J. Am. Chem. Soc.* **2007**, *129*, 1132−1140. (c) Iida, A.; Osada, J.; Nagase, R.; Misaki, T.; Tanabe, Y. Mild and Efficient Pentafluorophenylammonium Triflate (PFPAT)-Catalyzed C-Acylations of Enol Silyl Ethers or Ketene Silyl (Thio)Acetals with Acid Chlorides. *Org. Lett.* **2007**, *9*, 1859−1862.

(13) (a) Kim, J.; Chang, S. A New Combined Source of "CN" from *N,N*-Dimethylformamide and Ammonia in the Palladium-catalyzed Cyanation of Aryl C-H bonds. *J. Am. Chem. Soc.* **2010**, *132*, 10272−10274. (b) Ren, X.; Chen, J.; Chen, F.; Cheng, J. The Palladium-Catalyzed Cyanation of Indole C−H Bonds with the Combination of NH_4HCO_3 and DMSO as a Safe Cyanide Source. *Chem. Commun.* **2011**, *47*, 6725−6727.

(14) Wang, C.; Geng, X.; Zhao, P.; Zhou, Y.; Wu, Y.-D.; Wu, A.-X. Employing Thiocyanate Salts as a Nitrogen Source via CN Bond Cleavage: Divergent Synthesis of α-Ketoamides and 2-Acyloxazoles. *Org. Chem. Front.* **2019**, *6*, 2534−2538.

(15) (a) Wang, J.; Sun, B.; Zhang, L.; Xu, T.; Xie, Y.; Jin, C. Transition-Metal-Free Direct C-3 Cyanation of Quinoxalin-2(1H)-ones with Ammonium Thiocyanate as the "CN" source. *Org. Chem. Front.* **2020**, *7*, 113−118. (b) Wagner, A.; Ofial, A. R. Potassium Thiocyanate as Source of Cyanide for the Oxidative α-Cyanation of Tertiary Amines. *J. Org. Chem.* **2015**, *80*, 2848−2854.

(16) Huang, Y.; Yu, Y.; Zhu, Z.; Zhu, C.; Cen, J.; Li, X.; Wu, W.; Jiang, H. Copper-Catalyzed Cyanation of *N*-Tosylhydrazones with Thiocyanate Salt as the "CN" Source. *J. Org. Chem.* **2017**, *82*, 7621−7627.

(17) Guo, W.; Tan, W.; Zhao, M.; Zheng, L.; Tao, K.; Chen, D.; Fan, X. Direct Photocatalytic S−H Bond Cyanation with Green "CN" Source. *J. Org. Chem.* **2018**, *83*, 6580−6588.

(18) Xia, Q.; Li, Y.; Cheng, L.; Liang, X.; Cao, C.; Dai, P.; Deng, H.; Zhang, W.; Wang, Q. Electron Donor−Acceptor Complex-Initiated Photochemical Cyanation for the Preparation of α-Amino Nitriles. *Org. Lett.* **2020**, *22* (24), 9638−9643.

(19) (a) Khade, V. V.; Thube, A. S.; Dharpure, P. D. Direct Synthesis of 1,3-dithiolanes from Terminal Alkynes via Visible Light Photoredox Catalysis. *Org. Biomol. Chem.* **2022**, *20*, 1315−1319. (b) Dharpure, P. D.; Bhowmick, A.; Warghude, P. K.; Bhat, R. G. Visible-light Mediated Facile Dithiane Deprotection under Metal Free Conditions. *Tetrahedron Lett.* **2020**, *61*, 151407−151415. (c) Dharpure, P.; Behera, M.; Thube, A.; Bhat, R. G. Base Dependent 1,3-dithioacetals Rearrangement over Sulfoxidation under Visible-Light Photocatalysis to Access Disulfide-Linked-Dithioesters. *ChemRXiv* **2021**, DOI: 10.26434/chemrxiv-2021-x9kht.

(20) CCDC 2175599 (compound **2p**) contain the supplementary crystallographic data. These data can be obtained free of charge by The Cambridge Crystallographic Data Centre.

(21) Guo, J.-T.; Yang, D.-C.; Guan, Z.; He, Y.-H. Chlorophyll-Catalyzed Visible-Light-Mediated Synthesis of Tetrahydroquinolines from *N,N*-Dimethylanilines and Maleimides. *J. Org. Chem.* **2017**, *82*, 1888−1894.

(22) Pelaez, M.; Falaras, P.; Likodimos, V.; O'shea, K.; De la Cruz, A.; Dunlop, P. S. M.; Byrne, J. A.; Dionysiou, D. D. Use of Selected

https://doi.org/10.1021/acs.orglett.2c02601
Org. Lett. 2022, 24, 6919−6924

Scavengers for the Determination of NF-TiO_2 Reactive Oxygen Species During the Degradation of Microcystin LR under Visible Light Irradiation. *J. Mol. Catal. A Chem.* **2016**, *425*, 183−189.
(23) (a) Dietrich, A.; Buschmann, V.; Müller, C.; Sauer, M. Fluorescence Resonance Energy Transfer (FRET) and Competing Processes in Donor−Acceptor Substituted DNA Strands: A Comparative Study of Ensemble and Single-Molecule Data. *Rev. Mol. Biotechno.* **2002**, *82*, 211−231. (b) Doose, S.; Neuweiler, H.; Sauer, M. Fluorescence Quenching by Photoinduced Electron Transfer: A Reporter for Conformational Dynamics of Macromolecules. *ChemPhysChem* **2009**, *10*, 1389−1398.
(24) Mitra, S.; Ghosh, M.; Mishra, S.; Hajra, A. Metal-Free Thiocyanation of Imidazoheterocycles through Visible Light Photoredox Catalysis. *J. Org. Chem.* **2015**, *80*, 8275−8281.
(25) (a) Zhou, P.; Chen, C.; Li, S. Selecfluor-Initiated Cyanation of Disulfides to Thiocyanates. *J. Chem. Res.* **2020**, *44*, 376−380. (b) Wang, Z.-H.; Ji, X.-M.; Hu, M.-L.; Tang, R.-Y. Nitromethane as a Cyanating Reagent for the Synthesis of Thiocyanates. *Tetrahedron Lett.* **2015**, *56*, 5067−5070. (c) Castanheiro, T.; Gulea, M.; Donnard, M.; Suffert, J. Practical Access to Aromatic Thiocyanates by CuCN-Mediated Direct Aerobic Oxidative Cyanation of Thiophenols and Diaryl Disulfides. *Eur. J. Org. Chem.* **2014**, *2014*, 7814−7817. (d) Todorovic, U.; Klose, I.; Maulide, N. Straightforward Access to Thiocyanates via Dealkylative Cyanation of Sulfoxides. *Org. Lett.* **2021**, *23*, 2510−2513. (e) Chen, Y.; Qi, H.; Chen, N.; Ren, D.; Xu, J.; Yang, Z. Fluorium-Initiated Dealkylative Cyanation of Thioethers to Thiocyanates. *J. Org. Chem.* **2019**, *84*, 9044−9050.

Recommended by ACS

Isothiouronium-Mediated Conversion of Carboxylic Acids to Cyanomethyl Thioesters
Irmgard Tiefenbrunner, Nuno Maulide, *et al.*
FEBRUARY 28, 2023
THE JOURNAL OF ORGANIC CHEMISTRY READ

Ring-Opening Cyclization (ROC) of Aziridines with Propargyl Alcohols: Synthesis of 3,4-Dihydro-2*H*-1,4-oxazines
Bharat Singh, Manas K. Ghorai, *et al.*
MARCH 27, 2023
THE JOURNAL OF ORGANIC CHEMISTRY READ

Diastereoselective Synthesis of *trans*-β-Amino Cyclohexyl Ketones and *trans*-3-Amino-4-acyl-tetrahydropyrans from Intramolecular C-Alkylation of ω-Halo-Substituted β-Sulf...
Kanniyappan Silambarasan, Kavirayani R. Prasad, *et al.*
FEBRUARY 08, 2023
THE JOURNAL OF ORGANIC CHEMISTRY READ

Carboazidation of Terminal Alkenes with Trimethylsilyl Azide and Cyclic Ethers Catalyzed by Copper Powder under Oxidative Conditions
Yuichi Ikemoto, Yasushi Nishihara, *et al.*
MARCH 22, 2023
THE JOURNAL OF ORGANIC CHEMISTRY READ

Get More Suggestions >

https://doi.org/10.1021/acs.orglett.2c02601
Org. Lett. 2022, 24, 6919−6924

Check for updates

ACES Asian Chemical Editorial Society

doi.org/10.1002/asia.202201128

CHEMISTRY AN ASIAN JOURNAL Research Article

www.chemasianj.org

Base Dependent Rearrangement of Dithiane and Dithiolane under Visible-light Photoredox catalysis

Pankaj D. Dharpure, Mousumi Behera, Archana S. Thube, and Ramakrishna G. Bhat*[a]

Abstract: The rearrangement of dithiolanes and dithianes to access disulfide-linked-dithioesters under visible-light photoredox catalysis via controlled C–S bond cleavage has been disclosed. Unlike, the usual deprotection of dithioacetals to corresponding aldehydes under the oxidative conditions, we observed unique regioselective oxidative reactivity of five and six membered cyclic dithioacetals to form disulfide-linked-dithioesters by exchanging DMAP and imidazole bases. The generality of the protocol has been demonstrated by exploring a wide range of substrates. As an application, *in situ* generated thiyl radical has been trapped with disulfides to prepare hetero-disulfides of potential utility. The protocol proved to be practical on gram scale quantity and relied on clean energy source for the transformation. Based on the series of control experiments, cyclic voltammetry and Stern-Volmer studies the plausible mechanism has been proposed.

Introduction

The rearrangement reactions in organic chemistry offer an unconventional one pot route to access a wide variety of molecular scaffolds. It is well known in literature that many of the sulfur compounds are known to undergo rearrangements under Lewis acid as well as Brønsted acid conditions.[1] The cyclic thioacetals are very useful intermediates in organic synthesis and have been well explored for the umpolung reactivity in a variety of transformations.[2] Interestingly, the ability of cyclic thioacetals to undergo rearrangement reactions for accessing thioesters has been rarely explored in the literature. Molecules containing the thioester moiety are found in important intermediates in biosynthetic pathways such as fatty acids, esters, polyketides as well as non-ribosomal peptide synthesis.[3] Also thioester moiety plays a vital role in the native chemical ligation by S–N shift, lipidation of G-protein coupled receptor for the signal regulation and acts as probe for enzymatic assembly lines.[4] These useful compounds have been utilized in the solid phase synthesis of phosphorodithioate-modified DNA that has a wide utility for the gene silencing technology.[5] Traditionally, thioesters are synthesized by the reaction of carboxylic acids, acid chlorides or acid anhydrides with thiols.[6] Thioesters have also been prepared using metal catalyst by thiocarbonylation.[7] However, some of the reported protocols are not clean and require the use of metal catalysts, toxic reagents and activating-promoting reagents.[8] Similarly disulfide-linkage plays an important role in maintaining the structure, function and stability of proteins and peptides because of its reversible-nature under biological conditions.[9] Undoubtedly owing to their reactivity, thioesters and disulfides have been widely utilized for labelling the biomolecules (proteins, nucleic acids, carbohydrates and lipids).[10] These have also been extensively utilized in the drug delivery applications as well as in the synthesis of biomaterials.[11]

Despite the enormous utility of both disulfides and thioesters, there are not many straightforward protocols to prepare the molecules containing both these functionalities.[12] Few available methods require multiple steps to synthesize the same.[5]

The photoredox catalysis is an emerging research area in organic synthesis that provides a milder and sustainable approach to carry out useful organic transformations using visible light.[13] Many molecules containing both disulfide and thioester functionalities are known to show interesting reactivity under photocatalytic conditions. The cleavage of C–S bond has been well studied in presence of oxidizing reagent under photocatalytic conditions.[14] However, to the best of our knowledge selective cleavage of single C–S bond of cyclic thioacetal under the oxidizing reaction condition has not been reported till date. This may be presumably due to the difficulty in controlling the selective cleavage of one of the two C–S bonds of thioacetal under oxidizing conditions.[15] Generally cleavage of first C–S bond of thioacetal would instantly lead to the cleavage of second C–S bond to furnish the corresponding deprotected compounds such as aldehydes and in some cases, thioacetals would undergo facile oxidation to afford the corresponding sulfoxides (Scheme 1A).[15,16] There are few examples of autoxidation reported in literature that describe *in situ* generation of lithiated-thioacetals to access unusual thioacetal derivatives (Scheme 1B, C).[17,18]

However, these protocols rely on low temperature and strong base such as *n*-butyl lithium. Schmink and coworkers have demonstrated palladium catalyzed synthesis of dithioether via the selective cleavage of single C–S bond of thioacetal in the absence of oxidizing reagent at an elevated temperature (Scheme 1D).[19] However, this protocol was limited to thioacetals containing benzylic β-hydrogen with respect to sulfur atom of thioacetals. Interestingly all the efforts towards the selective

[a] *P. D. Dharpure, M. Behera, A. S. Thube, Prof. Dr. R. G. Bhat*
Department of Chemistry, Indian Institute of Science Education and Research (IISER)-Pune, Dr. Homi Bhabha Road, Pashan, 411008, Pune, Maharashtra (India)
E-mail: rgb@iiserpune.ac.in

Supporting information for this article is available on the WWW under https://doi.org/10.1002/asia.202201128

© 2023 Wiley-VCH GmbH

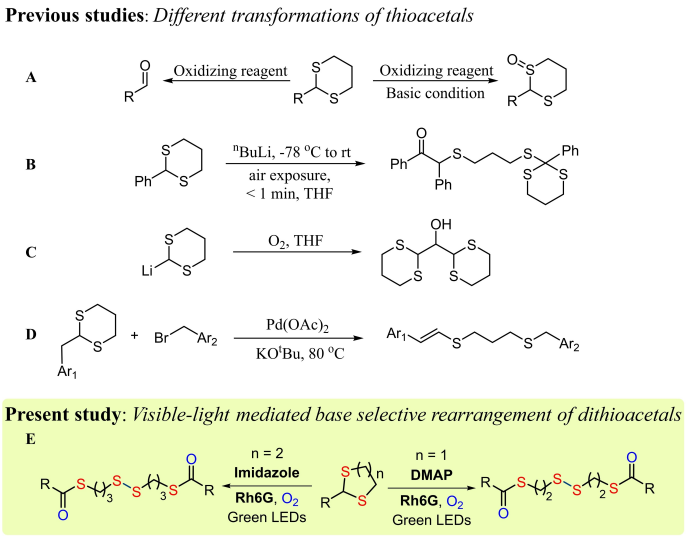

Scheme 1. Reactivity of Thioacetals in Organic Synthesis.

cleavage of single C–S bond of thioacetal have led to diverse products (Scheme 1B–D). It is highly challenging and demanding to explore the selective cleavage of single C–S bond of the thioacetal under oxidizing and metal-free reaction conditions to access thioesters. While our research group was exploring the deprotection of thioacetals to corresponding aldehydes under visible light photoredox catalysis,[15a] we presumed based on the literature report[15b] that deprotection may be going through few different reactive intermediates. We hypothesized that the use of suitable bases under appropriate photoredox conditions may lead to the formation of thioesters. Herein we present one pot selective synthesis of disulfide-linked-dithioester from 1,3-dithiolanes/1,3-dithianes by simply switching the bases using photoreodox catalysis under oxygen atmosphere at room temperature. The transformation involves rearrangement of cyclic thioacetals in presence of a mild base via single C–S bond cleavage under visible light irradiation (Scheme 1E).

Results and Discussion

In order to validate the hypothesis, we commenced with a model reaction of **1a** in presence of Eosin Y and K_2CO_3 under green LEDs (15 W) at room temperature in open-air condition to afford the unanticipated product disulfide-linked-dithioester **2a** along with deprotection of dithiolane to aldehyde **1a′** as a major product (Table 1, entry 1). From our previous protocol we know that the presence of water molecules facilitates the deprotection of dithioacetals to aldehydes hence we have carried out the reaction using dry acetonitrile.[15a] The reaction in presence of Rhodamine 6G (Rh6G) under the reaction conditions furnished similar results as observed in case of Eosin Y (Table 1, entry 2). Interestingly the reaction of **1a** in presence of Rh6G, K_2CO_3 under oxygen atmosphere and green LEDs (15 W) at room temperature afforded the corresponding disulfide-linked-dithioester **2a** in relatively higher yields (60%, Table 1, entry 3). In order to optimize the reaction further we screened different photocatalysts such as Eosin Y, Rh6G,

Table 1. Optimization of Reaction.[a]

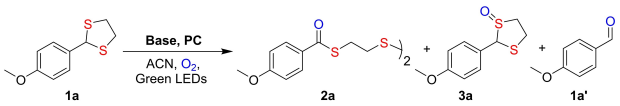

Entry	Cat.	Atm.	Base	2a	3a	1a′
1[a]	Eosin Y	Open Air	K_2CO_3	33	trace	50
2[a]	Rh6G	Open Air	K_2CO_3	33	trace	52
3[b]	Rh6G	O_2	K_2CO_3	60	22	0
4[b]	Rh6G	O_2	–	24	43	29
5[b]	Rh6G	Argon	K_2CO_3	0	0	0
6[b]	–	O_2	K_2CO_3	0	0	0
7[b,c]	Rh6G	O_2	K_2CO_3	0	0	0
8[d]	**Rh6G**	**O_2**	**DMAP**	**70**	**16**	**Trace**

[a] General reaction conditions: **1a** (0.2 mmol), K_2CO_3 (0.4 mmol), DMAP (0.4 mmol), Imd (1 mmol), ACN (2 mL), catalyst (2 mol%), Green LEDs (15 W), under O_2/Argon balloon 6 h. [b] dry reaction condition-dry ACN, [c] 60 °C without light source, [d] dry acetonitrile 1.8 mL, dry toluene 0.2 mL, Yields are in percentage.

© 2023 Wiley-VCH GmbH

1861471x, 2023, 4, Downloaded from https://aces.onlinelibrary.wiley.com/doi/10.1002/asia.202201128 by Indian Institute Of Science Education And Research Pune, Wiley Online Library on [23/06/2025]. See the Terms and Conditions (https://onlinelibrary.wiley.com/terms-and-conditions) on Wiley Online Library for rules of use; OA articles are governed by the applicable Creative Commons License

$Ru(bpy)_3Cl_2$, $Ir(bpy)_3$, Acridinium-perchlorate and Pyrylium tetrafluroborate. Among all we observed that Rh6G is more suitable for the desired transformation (ESI-2.1). Anhydrous acetonitrile proved to be more advantageous for the desired transformation based on the solvent screening (ESI-2.2). We also observed that for the desired transformation, base, oxygen atmosphere, catalyst (Rh6G) and green LEDs are absolutely essential (Table 1, entries 4–7). In absence of light even at elevated temperature (60 °C), the reaction did not work indicating the necessity of visible light (Table 1, entry 7). In order to optimize the reaction further we screened the reaction of **1a** in presence of DMAP as a base while maintaining other optimized reaction conditions. Interestingly we observed that desired product **2a** was formed in good yield (70%, Table 1, entry 8 and ESI 2.3) and the corresponding sulfoxide **3a** in trace amount. Our further attempts to improve the yield of reaction using other additives and the oxidizing reagents did not prove to be beneficial (ESI-2.4). Based on exhaustive screening, 2-(4-methoxyphenyl)-1,3-dithiolane **1a**, DMAP, Rh6G (2 mol%) in anhydrous solvent (ACN: toluene; 9:1, v/v) under oxygen atmosphere proved to be the optimized reaction condition to obtain rearrangement product disulfide-linked-dithioester **2a**.

Having obtained the optimized reaction conditions, we planned to explore the substrate scope for the rearrangement reactions for the practicality and generality of the protocols. In this regard, the reactions of different dithiolanes **1** were explored under two different optimized reaction conditions to obtain the corresponding disulfide-linked-dithioesters (**2a–2z, 2aa–2ac**) in good yields (Table 2). Further the molecular structure of the compound **2e** was unambiguously confirmed by single crystal X-ray analysis.[20] We also observed that dithiolanes derived from *m*-substituted aromatic aldehydes (**1h–1k**) afforded the corresponding products (**2h–2k**) in good yields (up to 71%, Table 2). Also, dithiolanes (**1a–1g**) derived from aromatic aldehydes containing electron donating as well as electron withdrawing substituents at *p*-position afforded the corresponding rearranged products (**2a–2g**) in moderate to very good yields. However, the reaction of dithiolanes containing free hydroxyl (**1j**) and chloro substituents at *o*-position (**1l**) of the aryl ring furnished corresponding products (**2j**, **2l**) in modest yields. While, the polyaromatic derivatives as well as dioxalane substituted dithiolanes under the optimized reaction conditions gave the corresponding products (**2n–2p**) in good yields (Table 2). The dithiolanes containing ester as well as ether moiety afforded the products (**2q**, **2m**, **2r**) in good yields (Table 2). Also, different heterocyclic and aliphatic dithiolanes worked smoothly under reaction conditions to furnish the rearranged products (**2s–2y**) in good yields. In order to explore wider application of the protocol, we investigated dithiolanes containing different protecting group substituted aryl rings such as propargyl, allyl, benzyl and tosyl moieties. In all the cases reactions worked smoothly to afford the corresponding products (**2z**, **2aa–2ac**) in good yields (Table 2).

Next, we switched our attention to explore other cyclic thioacetals such as 1,3-dithianes. We commenced with phenyl-1,3-dithiane **4a** as a substrate under optimized reaction conditions using DMAP as a base (Table 3).

Table 2. Substrate Scope for Rearrangement of Dithiolane.[a]

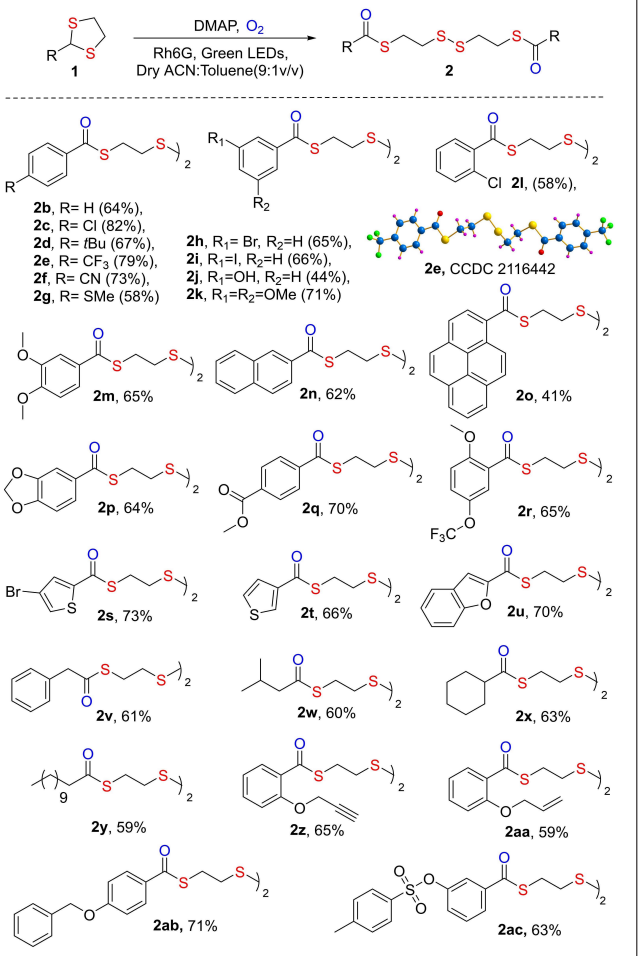

[a] General reaction conditions: **1** (0.2 mmol), Rh6G (2 mol%), DMAP (0.4 mmol), Imidazole (1 mmol), Solvent (2 mL), Green LEDs (15 W), under O_2, 6–12 h.

Table 3. Optimization of Reaction.[a]

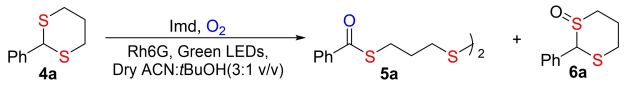

Entry	Solvent	Atm.	Base	5a	6a
1[a]	ACN	O_2	DMAP	00	90
2[a]	ACN	O_2	Imd	30	trace
3[a]	1,4-dioxane	O_2	Imd	17	trace
4[a]	Ethyl acetate	O_2	Imd	12	trace
5[a]	*t*-BuOH	O_2	Imd	28	trace
6[a]	ACN: *t*-BuOH	O_2	Imd	37	trace

[a] General reaction conditions: **4a** (0.2 mmol), Imidazole (1 mmol), Solvent (2 mL), Rh6G (2 mol%), light source, under O_2 balloon, 24 h.

However, we obtained the corresponding sulfoxide product **6a** instead of the anticipated rearrangement product **5a** (Table 3, Entry 1). Based on the literature we surmise that most probably due to an extra stability arising in the single electron oxidized 1,3-dithiane species (6-membered ring, σ-σ*-3e–2 centered interaction) sulfoxide **6a** was obtained. However, this

© 2023 Wiley-VCH GmbH

1861471x, 2023, 4, Downloaded from https://aces.onlinelibrary.wiley.com/doi/10.1002/asia.202201128 by Indian Institute Of Science Education And Research Pune, Wiley Online Library on [23/06/2025]. See the Terms and Conditions (https://onlinelibrary.wiley.com/terms-and-conditions) on Wiley Online Library for rules of use; OA articles are governed by the applicable Creative Commons License

phenomenon is believed to be absent in the corresponding single electron oxidized 1,3-dithiolane species (5-membered ring).[21] Hence, in order to obtain the rearrangement product disulfide-linked-dithioester from **4a**, we screened different bases, solvents, and catalysts systematically (see ESI 2.5, 2.6, 2.7 for details). Among all the solvents screened ACN and *t*-BuOH proved to be efficient for the desired transformation (See Table 3, Entries 2–6). Based on exhaustive screening, dithiane **4a**, Rh6G (2 mol%), imidazole, anhydrous ACN and *t*-BuOH (3:1, v/v) proved to be optimum reaction condition to obtain **5a** (Table 3, entry 6). Surprisingly, our attempts to increase the yield of **5a** by elevating the reaction temperature (50 °C) did not afford the desired product even in trace amount. Under the optimized reaction conditions different substrates **(4a, 4b, 4c, 4d, 4e, 4f)** afforded corresponding rearranged products disulfide-linked-dithioesters (**5a**, **5b**, **5c**, **5d**, **5e**, **5f**) in moderate yields (up to 47%, Table 4).

In order to have insight into the mechanism, we planned to carry out few control experiments systematically. We initiated the experiment with the reaction of **1a** under standard reaction condition with the addition of water (10 equiv.). This led to the deprotection of **1a** to afford the corresponding aldehyde **1a′** exclusively (Scheme 2a). However, the reaction of **1a** under inert atmosphere (absence of oxygen) did not work. This result indicated that molecular oxygen is essential for the desired transformation (Scheme 2b). In order to verify the role of singlet oxygen if any, we planned to perform the reaction using singlet oxygen quencher such as DABCO.[22] The reaction of **1a** in presence of DABCO (2 equiv.) under the optimized condition afforded the desired product **2a** in moderate yield (Scheme 2c).

This result indicated that probably the singlet oxygen may not be involved in the reaction pathway. To validate the involvement of superoxide radical anion ($O_2^{\bullet-}$) in the reaction pathway, we carried out the reaction of **1a** in presence of a superoxide radical anion quencher *p*-benzoquinone (Scheme 2d).

It is interesting to note that reaction did not proceed under the said conditions thus strongly supporting the formation and involvement of superoxide radical anion ($O_2^{\bullet-}$).[23] The reaction did not work in presence of TEMPO confirming the radical pathway during the course of the reaction (Scheme 2e). In order to understand the role of hydrogen bonding if any in obtaining the rearrangement product from **4a**, we carried out the reaction of **4a** in presence of *N*-methyl imidazole (instead of Imd) (Scheme 2f). It is very interesting to note that we obtained the sulfoxide product **6a** in 71% yield instead of rearrangement product **5a**. This result clearly supported the possible role of hydrogen bonding in the reaction mechanism (Scheme 2f). This is further supported by the observation that the reaction of **4a** at elevated reaction temperature (50 °C) in presence of Imd afforded **6a** albeit in low yield instead of desired product **5a** (Scheme 2g). We surmise that possibly the weak hydrogen bonding might have been disrupted under the higher reaction temperature thus further supporting the role of hydrogen bonding to drive the reaction. Based on several control experiments, Stern-Volmer plot, cyclic voltammetry studies and previous literature reports,[14] the plausible reaction pathways have been outlined (see Scheme 3 A/B). CV measurements indicated that (see ESI 4.2 A–E) all the substrates have redox potential [**1a** (+1.26 V), **4a** (+1.15 V), DMAP (+1.27 V), Imd (+1.12 V) vs Ag/AgCl] in the range of Rh6G* (+1.39 V).[24] Further Stern-Volmer plot revealed that SET is much more favorable for DMAP in comparison to **1a**/**4a** and more favorable for **1a**/**4a** with respect to imidazole (see ESI 4.1 A). Based on these experimental observations, we believe that the photocatalyst (Rh6G) upon irradiation gets excited (Rh6G*) (+1.39 V vs SCE)[24] and this would in turn take the single electron from DMAP (+1.27 V) to generate the corresponding oxidized species DMAP and Rh6G(see Scheme 3A). As the rate of single electron transfer of DMAP with the Rh6G* is much more pronounced, hence by relay of SET process further it oxidises the **1b** (+1.26 V) to afford **A1** efficiently thus regenerating DMAP. The unstable oxidized species **A1** collapses to generate the transient radical cation intermediate **A2**. This would further react with superoxide radical anion ($O_2^{\bullet-}$) to generate the intermediate **A3** that would eventually collapse to form the reactive radical intermediate **A4** by releasing $^1/_2O_2$ and proton. The presence of DMAP as a base (in excess) in the reaction medium traps the released proton during this step and maintains the reaction medium basic enough for the smooth progress of the reaction. This would further dimerize to afford the final product **2b** (see Scheme 3A). In presence of Imd, 6-membered cyclic thioacetal

Table 4. Substrate Scope for Rearrangement and Sulfoxidation of Dithiane.[a]

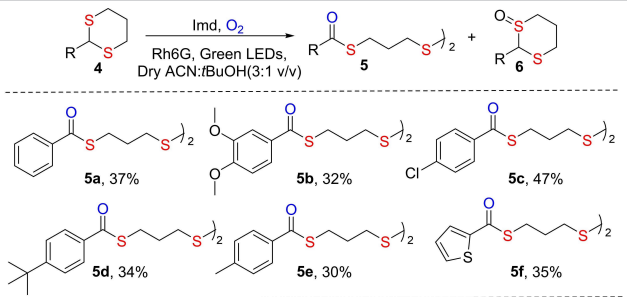

[a] General reaction conditions: **4** (0.2 mmol), Rh 6G (2 mol%), DMAP (0.4 mmol), Imidazole (1 mmol), Solvent (2 mL), Green LEDs (15 W), under O_2, 24 h. *reaction of **4a** at elevated temperature (50 °C) did not work to offer **5a**.

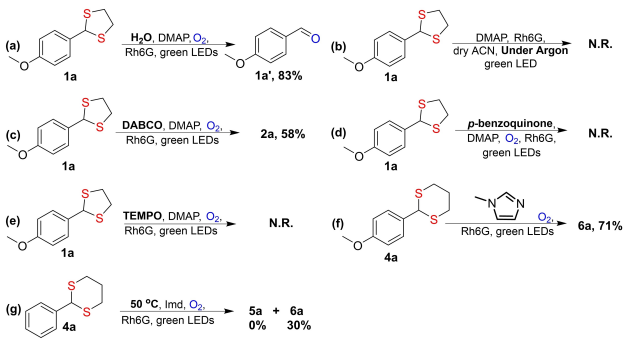

Scheme 2. Control Experiments.

© 2023 Wiley-VCH GmbH

1861471x, 2023, 4, Downloaded from https://aces.onlinelibrary.wiley.com/doi/10.1002/asia.202201128 by Indian Institute Of Science Education And Research Pune, Wiley Online Library on [23/06/2025]. See the Terms and Conditions (https://onlinelibrary.wiley.com/terms-and-conditions) on Wiley Online Library for rules of use; OA articles are governed by the applicable Creative Commons License

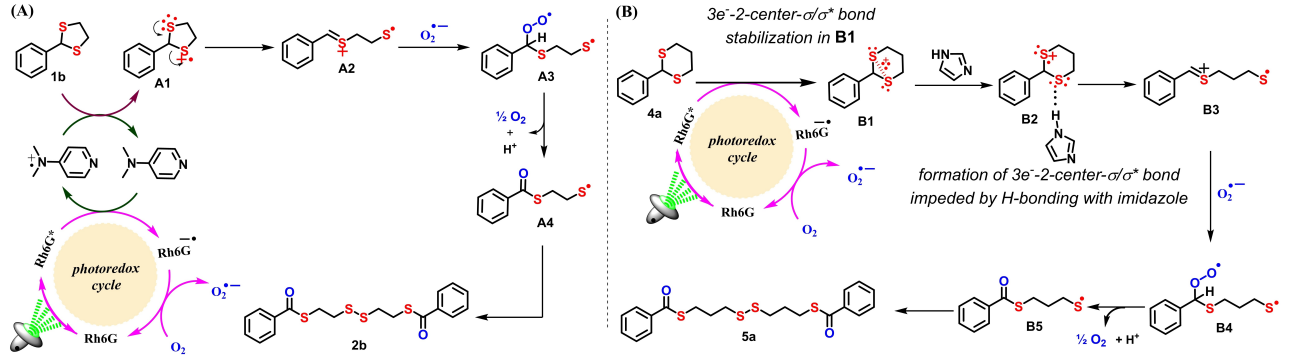

Scheme 3. Plausible Reaction Mechanism.

(dithiane, **4a**) generates intermediate **B1** after SET with Rh6G* because the quenching efficiency of **4a** is more than that of Imd (Scheme 3B). Intermediate **B1** is believed to be stabilized by the 3e–2-center σ-σ* bond formation between two sulfur atoms in a six membered cycle.[21] However, imidazole (Imd) having an intrinsic property of making hydrogen bonding may disturb this 3e-2-center σ-σ* interaction to form intermediate **B2** (see Scheme 3B). This would in turn destabilize the ring resulting in cleavage to generate a radical cation intermediate **B3**. Further **B3** would be trapped by superoxide radical anion ($O_2^{\bullet-}$) to form intermediate **B4**. This reactive and unstable intermediate would collapse to form a radical intermediate **B5** by releasing the proton and $^1/_2O_2$ under basic medium. Finally, this would undergo dimerization to furnish the desired product **5a** (Scheme 3B). However, in presence of other bases the stabilized intermediate **B1** (by the 3e–2-center σ-σ* interaction) will stay intact due to inability of other bases to form the hydrogen bonding because of electronic and steric crowding and some of the bases interfere in the photocatalytic cycle thus resisting to ring opening. The intermediate **B1** eventually reacts with superoxide radical anion ($O_2^{\bullet-}$) to furnish the desired sulfoxide product **6a** instead of **5a**.[25]

Based on plausible reaction mechanism (Scheme 3A), we predicted that *in situ* generated thiyl radical intermediate **A4** could be trapped with the suitable disulfide to synthesize the hetero-disulfide compounds. The synthesis of hetero-disulfide is quite challenging as homo-disulfide is also known to be formed in competition.[26]

In order to extend the utility of this protocol further, we planned to explore the synthesis of different hetero-disulfides (Table 5). We treated dithiolanes (**1**) with little excess of aromatic disulfides (**7a**–**7e**) under the optimized reaction conditions to afford the corresponding hetero-disulfides (**8aa**–**8ie**) in moderate to good yields (up to 73%, Table 5). We observed that disulfides (**7**) containing aryl rings substituted with electron-donating groups as well as free hydroxyl group worked smoothly under the optimized reaction conditions while the corresponding disulfide containing electron withdrawing groups did not work. We also observed that the aliphatic disulfides were ineffective under the reaction conditions to furnish the corresponding hetero-disulfide compounds. Finally, for the practicality of the standard protocol, we

Table 5. Substrate Scope for the Disulfide Trapping.

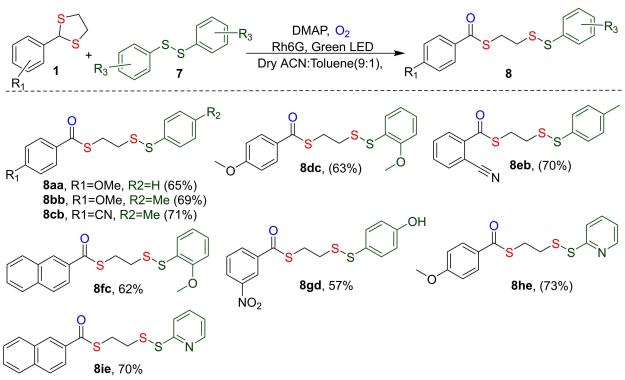

[a] General reaction conditions: **1** (0.2 mmol), **7** (0.6 mmol), Rh6G (2 mol%), DMAP (0.4 mmol), Solvent (3 mL), Green LEDs (15 W), under O_2.

demonstrated the gram scale reaction of **1a** under optimized reaction conditions to afford the desired product **2a** (62%, ESI, 3).

Conclusion

In conclusion we have developed a visible light mediated base dependent rearrangement reaction of dithiolane as well as dithiane to afford the disulfide-linked-dithioesters under photoredox catalysis. A wide range of dithiolanes and dithianes reacted smoothly to afford a variety of disulfide-linked-dithioesters. We have also demonstrated the practicality of the protocol by synthesizing the suitable hetero-disulfides by trapping the thiyl radical with aryldisulfides. We studied the unusual reactivity of dithiolanes and dithianes by manipulating bases with and without hydrogen bonding capability under photooredox conditions for the very first time. This one pot protocol does not rely on external oxidizing agents or metal reagents and works well under mild reaction conditions. The method gives an access to very useful molecules with two different functional groups in a single step starting from easily synthesizable dithiolanes and dithanes. The protocol has been proven to be scalable on gram quantity. The observed unique

© 2023 Wiley-VCH GmbH

1861471x, 2023, 4, Downloaded from https://aces.onlinelibrary.wiley.com/doi/10.1002/asia.202201128 by Indian Institute Of Science Education And Research Pune, Wiley Online Library on [23/06/2025]. See the Terms and Conditions (https://onlinelibrary.wiley.com/terms-and-conditions) on Wiley Online Library for rules of use; OA articles are governed by the applicable Creative Commons License

reactivity of thioacetals may open up the new horizon for synthesizing different useful molecules by exploring reactions with different nucleophiles and electrophiles.

Experimental Section

General Information: Reagent Information: All reactions were carried out with distilled and dried solvents using oven-dried glassware under dry Argon atmosphere, unless otherwise stated. All reagents were purchased from commercial sources and used as received, unless otherwise indicated. Thin layer chromatography (TLC) was performed using silica gel 60 GF_{254} pre-coated aluminum backed plates (2.5 mm) with detection by UV light. Visualization was accomplished by irradiation with a UV light at 254 nm and vanillin staining agent. Column chromatography was performed using silica gel (100–200 mesh) eluting with petroleum ether and ethyl acetate. Petroleum ether and ethyl acetate mixture was used as gradient elution for column chromatography. Analytical Information: All isolated compounds were characterized by Proton (^{1}H) and carbon (^{13}C) NMR spectra were recorded on a 400 MHz Jeol ECS-400 and Bruker Avance III HD Ascend 400 MHz spectrophotometers. All Nuclear Magnetic Resonance spectra were recorded in $CDCl_3$. The NMR spectra were recorded using tetramethyl silane (TMS) as the internal standard. ^{1}H NMR spectra were recorded at 400 MHz and ^{13}C NMR spectra were recorded at 100/150 MHz (Bruker and Jeol), unless otherwise noted. Chemical shifts (δ) are reported in ppm downfield from $CDCl_3$ (δ = 7.26 ppm) for ^{1}H NMR and relative to the central $CDCl_3$ resonance (δ = 77.16 ppm) for ^{13}C NMR spectroscopy. For 1H NMR, data are reported as follows: chemical shift, multiplicity (s = singlet, d = doublet, t = triplet, q = quartet, p = pentet, s = sextet, h = heptet, m = multiplet, br = broad), coupling constants (*J*) and integration. Coupling constants (*J*) are reported in Hertz (Hz). Carbon chemical shifts are reported in ppm from tetramethyl silane (TMS) with the solvent resonance as the internal standard ($CDCl_3$ δ 77.0 ppm). ^{13}C NMR spectra were recorded with complete proton decoupling. ^{19}F NMR spectra were recorded at 377 MHz. Mass samples were analyzed by high resolution mass spectrometer (HRMS) using ESI TOF. Melting points were measured using Büchi B-540 apparatus in an open glass capillary and values are uncorrected. Fluorescence emission spectra were obtained on a Fluoromax-4 spectrofluorometer from Horiba Jobin-Yvon, with xenon light source in a 3 mL, Hellma fluorescence cuvette (path length 1.0 cm). The light source used for the optimized reaction: Green LEDs, (IBRA Pure 15 W Green LED Flood Light, IP Rating: IP66; and reaction mixture was irradiated from 5 cm away from the green LEDs.

General procedure A for the synthesis of compounds 1 and 4: (1,3-dithiane and 1,3-dithiolane protection of aldehyde)[28]

To a round bottom flask containing SiO_2, PPA (6.5 w/w %) was added to DCM (10 mL) and stirred well for 15 min. After that DCM was evaporated to obtain a well mixed SiO_2-PPA mixture. To this mixture, DCM (15 mL), aldehyde (1 equiv.; 1.5 mmol) and 1, 2-dithiane (1.2 equiv.), or 1,3-dithiane (1.2 equiv.) were added and stirred for the 6 h at room temperature. After completion of the reaction (monitored by TLC) the solution was filtered through cotton. The filtrate was treated with saturated KOH solution (5 mL) and stirred for 30 min to quench excess dithiane. After which, solution was extracted with dichloromethane (3 x 20 mL). The combined extract was dried over anhydrous sodium sulfate, filtered and concentrated under reduced pressure. The crude product was further purified by column chromatography over silica gel to afford the corresponding compound **1** or **4**.

General procedure B for the synthesis of Disulfide-linked-dithioester 2

An oven-dried round bottom flask equipped with a stir bar and rubber septum is charged with dithiolane **1** (0.2 mmol, 1 equiv.), DMAP (0.4 mmol, 2 equiv.), Rhodamine 6G (2 mol%), dry CH_3CN (1.8 mL) and dry toluene (0.2 mL). The reaction mixture was initially purged with O_2 for 5 min and the oxygen atmosphere was maintained throughout the reaction (using an Oxygen balloon). The reaction mixture was stirred under the irradiation of Green LED (15 W) at room temperature for 6–12 h (Monitored by TLC). After completion of the reaction, the solvent was removed under reduced pressure and the crude residue was purified by column chromatography over silica gel using mixture of petroleum ether/EtOAc as an eluent to afford the corresponding **2** (Note-The presence of moisture and the impurity of 1, 2-ethanedithiol in dithiolane (**1**) greatly influences the yield of reaction. Dry solvent is must to avoid the deprotection to corresponding aldehyde.)

General procedure C for the synthesis of Disulfide-linked-dithioester 5

An oven-dried round bottom flask equipped with a stir bar and rubber septum is charged with dithiane **4** (0.2 mmol, 1 equiv.), imidazole (1 mmol, 5 equiv.), Rhodamine 6G (0.004 mmol, 2 mol%), dry CH_3CN (1.5 mL) and ^{t}BuOH (0.5 mL). The reaction mixture was initially purged with O_2 for 5 min and the oxygen atmosphere was maintained throughout the reaction (using a balloon). The reaction mixture was stirred under the irradiation of Green LED (15 W) at room temperature for 6–12 h (Monitored by TLC). After completion of the reaction, the solvent was removed under reduced pressure and the crude residue was purified by column chromatography over silica gel using mixture of petroleum ether/EtOAc as an eluent to afford the corresponding **5** (Note–The presence of moisture and the impurity of 1, 3-propanedithiol in dithiane (**4**) influence the yield of reaction. Dry solvent is must to avoid the deprotection to corresponding aldehyde).

General procedure D for the synthesis of Hetero disulfide 8

An oven-dried round bottom flask equipped with a stir bar and rubber septum is charged with dithiolane **1** (0.2 mmol, 1 equiv.), disulfide **7** (0.6 mmol, equiv.), DMAP (0.4 mmol, equiv.), Rhodamine 6G (0.004 mmol, mol%), dry CH_3CN (1.8 mL) and dry toluene (0.2 mL). The reaction mixture was initially purged with O_2 for 5 min and the oxygen atmosphere was maintained throughout the reaction (using a balloon). The reaction mixture was stirred under the irradiation of Green LED (15 W) at room temperature for 8–12 h (Monitored by TLC). After the completion of the reaction, the solvent was removed under reduced pressure and the crude residue was purified by column chromatography over silica gel using mixture of petroleum ether/EtOAc as an eluent to afford the corresponding hetero disulfide **8** (Note–The presence of moisture and the impurity of 1, 2-ethanedithiol in dithiolane (**1**) influence the yield of reaction. Dry solvent is must to avoid the deprotection to corresponding aldehyde).

Product Characterization Data

*S,S′-(disulfanediylbis(ethane-2,1-diyl)) bis(4-methoxybenzothioate) (**2a**)*[12a]: The compound **2a** was prepared following the General Procedure **B**. White solid (32 mg, 70% yield), Mp: 81.5–82.5 °C; R_f = 0.4 (1 : 15::EA : pet ether).^{1}H NMR (400 MHz, $CDCl_3$): δ 7.93 (d, *J* = 8.8 Hz, 4H), 6.91 (d, *J* = 8.8 Hz, 4H), 3.86 (s, 6H), 3.40 (m, 4H), 2.99 (m, 4H). ^{13}C{^{1}H} NMR (100 MHz, $CDCl_3$): δ (ppm) 189.4, 163.6, 129.8,

© 2023 Wiley-VCH GmbH

18614171x, 2023, 4, Downloaded from https://aces.onlinelibrary.wiley.com/doi/10.1002/asia.202201128 by Indian Institute Of Science Education And Research Pune, Wiley Online Library on [23/06/2025]. See the Terms and Conditions (https://onlinelibrary.wiley.com/terms-and-conditions) on Wiley Online Library for rules of use; OA articles are governed by the applicable Creative Commons License

129.6, 113.6, 55.3, 38.0, 28.2. HRMS (ESI-TOF) m/z calcd. For $C_{20}H_{23}O_4S_4$ $[M+H]^+$ 455.0479; found 455.0483.

*S,S′-(disulfanediylbis(ethane-2,1-diyl)) dibenzothioate (**2b**)*: The compound **2b** was prepared following the General Procedure **B**. Colorless liquid (25 mg, 64%), R_f=0.4 (1:39::EA:pet ether). ^{1}H NMR (400 MHz, $CDCl_3$) δ 7.96 (d, J=7.4 Hz, 4H), 7.58 (t, J=7.4 Hz, 2H), 7.45 (t, J=7.8 Hz, 4H), 3.43 (m, 4H), 3.00 (m, 4H). $^{13}C\{^1H\}$ NMR (100 MHz, $CDCl_3$): δ (ppm) 191.3, 136.9, 133.7, 128.7, 127.4, 38.1, 28.6. HRMS (ESI-TOF) m/z calcd. For $C_{18}H_{18}NaO_2S_4$ $[M+Na]^+$ 417.0087; found 417.0077.

*S,S′-(disulfanediylbis(ethane-2,1-diyl)) bis(4-chlorobenzothioate) (**2c**)*[12a]: The compound **2c** was prepared following the General Procedure **B**. Colorless liquid, R_f=0.4 (1:39::EA:pet ether) (38 mg, 82%). ^{1}H NMR (400 MHz, $CDCl_3$) δ 7.89 (d, J=8.5 Hz, 4H), 7.43 (d, J=8.5 Hz, 4H), 3.43 (m, 4H), 2.99 (m, 4H). $^{13}C\{^1H\}$ NMR (100 MHz, $CDCl_3$): δ (ppm) 190.2, 140.1, 135.2, 129.1, 128.7, 38.0, 28.7. HRMS (ESI-TOF) m/z calcd. For $C_{18}H_{16}Cl_2NaO_2S_4$ $[M+Na]^+$ 484.9308; found 484.9307.

*S,S′-(disulfanediylbis(ethane-2,1-diyl)) bis(4-(tert-butyl)benzothioate) (**2d**)*: The compound **2d** was prepared following the General Procedure **B**. White solid (Melting point- 64.6-65.3 °C), R_f=0.5 (1:39::EA:pet ether) (34 mg, 67%). ^{1}H NMR (400 MHz, $CDCl_3$) δ 7.9 (d, J=8.7 Hz, 4H), 7.46 (d, J=8.7 Hz, 4H), 3.47–3.33 (m, 4H), 3.04–2.92 (m, 4H), 1.33 (s, 18H). $^{13}C\{^1H\}$ NMR (100 MHz, $CDCl_3$): δ (ppm) 190.9, 157.5, 134.3, 127.3, 125.7, 38.3, 35.3, 31.2, 28.5. HRMS (ESI-TOF) m/z calcd. For $C_{26}H_{35}O_2S_4$ $[M+H]^+$ 507.1520; found 507.1529.

S,S′-(disulfanediylbis(ethane-2,1-diyl)) bis(4-(trifluoromethyl)benzothioate) (**2e**): The compound **2e** was prepared following the General Procedure **B**. White solid (Melting point- 92.7-94.0 °C), R_f=0.5 (1:9::EA:pet ether) (42 mg, 79%). ^{1}H NMR (400 MHz, $CDCl_3$) δ 8.06 (d, J=8.4 Hz, 4H), 7.72 (d, J=8.4 Hz, 4H), 3.49–3.45 (m, 4H), 3.03–3.00 (m, 4H); $^{13}C\{^1H\}$ NMR (100 MHz, $CDCl_3$): δ (ppm) 190.5, 139.6, 135.0 (d, 32 Hz), 134.8, 127.7, 125.9 (q, 4 Hz), 123.6 (q, 555 Hz), 37.9, 28.9. ^{19}F NMR (100 MHz, $CDCl_3$) δ 63.2. HRMS (ESI-TOF) m/z calcd. For $C_{20}H_{17}F_6O_2S_4$ $[M+H]^+$ 531.0016; found 531.0025.

S,S′-(disulfanediylbis(ethane-2,1-diyl)) bis(4-cyanobenzothioate) (**2f**): The compound **2f** was prepared following the General Procedure **B**. White solid (Melting point- 91.3- 94.7 °C), R_f=0.4 (1:9::EA:pet ether) (32 mg, 73%). ^{1}H NMR (400 MHz, $CDCl_3$) δ 8.04 (d, J=8.7 Hz, 4H), 7.76 (d, J=8.7 Hz, 4H), 3.46 (m, 4H), 3.05–2.81 (m, 4H). $^{13}C\{^1H\}$ NMR (100 MHz, $CDCl_3$): δ (ppm) 190.2, 139.9, 132.7, 127.8, 117.8, 117.0, 37.7, 29.0. HRMS (ESI-TOF) m/z calcd. For $C_{20}H_{17}N_2O_2S_4$ $[M+H]^+$ 445.0173; found 445.0171.

S,S′-(disulfanediylbis(ethane-2,1-diyl)) bis(4-(methylthio)benzothioate) (**2g**): The compound **2g** was prepared following the General Procedure **B**. White solid (Melting point- 85.1-86.9 °C), R_f=0.45 (1:14::EA:pet ether) (28 mg, 58%). ^{1}H NMR (400 MHz, $CDCl_3$) δ 7.86 (d, J=8.7 Hz, 4H), 7.24 (d, J=8.7 Hz, 4H), 3.45–3.35 (m, 4H), 3.03–2.94 (m, 4H), 2.52 (s, 6H). $^{13}C\{^1H\}$ NMR (100 MHz, $CDCl_3$): δ (ppm) 190.3, 146.7, 133.1, 127.7, 125.1, 38.2, 28.6, 14.9. HRMS (ESI-TOF) m/z calcd. For $C_{20}H_{23}O_2S_6$ $[M+H]^+$ 487.0022; found 487.0022.

*S,S′-(disulfanediylbis(ethane-2,1-diyl)) bis(3-bromobenzothioate) (**2h**)*: The compound **2h** was prepared following the General Procedure **B**. Yellow solid (Melting point- 71.3-72.5 °C), R_f=0.45 (1:39::EA:pet ether) (36 mg, 65%). ^{1}H NMR (400 MHz, $CDCl_3$) δ 8.08 (m, 2H), 7.88 (m, 2H), 7.70 (m, 2H), 7.33 (m, 2H), 3.51–3.39 (m, 4H), 3.03–2.94 (m, 4H). $^{13}C\{^1H\}$ NMR (100 MHz, $CDCl_3$): δ (ppm) 190.1, 138.6, 136.5, 130.3, 126.0, 123.1, 37.9, 28.8. HRMS (ESI-TOF) m/z calcd. For $C_{18}H_{17}Br_2O_2S_4$ $[M+H]^+$ 550.8478; found 550.8482.

*S,S′-(disulfanediylbis(ethane-2,1-diyl)) bis(3-iodobenzothioate) (**2i**)*: The compound **2i** was prepared following the General Procedure **B**. White solid (Melting point- 61.0-62.2 °C), R_f=0.4 (1:99::EA:pet ether) (43 mg, 66%) ^{1}H NMR (400 MHz, $CDCl_3$) δ 8.26 (m, 2H), 7.98–7.81 (m, 4H), 7.19 (m, 2H), 3.46–3.36 (m, 4H), 3.02–2.92 (m, 4H). $^{13}C\{^1H\}$ NMR (100 MHz, $CDCl_3$): δ (ppm) 189.8, 142.3, 138.4, 136.0, 130.3, 126.4, 94.2, 37.8, 28.7. HRMS (ESI-TOF) m/z calcd. For $C_{18}H_{17}I_2O_2S_4$ $[M+H]^+$ 646.8201; found 646.8209.

*S,S′-(disulfanediylbis(ethane-2,1-diyl)) bis(3-hydroxybenzothioate) (**2j**)*: The compound **2j** was prepared following the General Procedure **B**. White solid (Melting point- 96.7-97.9 °C), R_f=0.5 (3:7::EA:Pet ether) (18 mg, 44%). ^{1}H NMR (400 MHz, $CDCl_3$) δ 7.55–7.50 (m, 2H), 7.45–7.41 (m, 2H), 7.32 (m, 2H), 7.07 (m, 2H), 5.79 (s, 1H), 3.45–3.35 (m, 4H), 3.06–2.94 (m, 4H); $^{13}C\{^1H\}$ NMR (100 MHz, $CDCl_3$): δ (ppm) 191.4, 155.9, 138.2, 130.0, 120.8, 119.8, 113.7, 38.0, 28.6. HRMS (ESI-TOF) m/z calcd. For $C_{18}H_{19}O_4S_4$ $[M+H]^+$ 427.0166; found 427.0168.

*S,S′-(disulfanediylbis(ethane-2,1-diyl)) bis(3,5-dimethoxybenzothioate) (**2k**)*: The compound **2k** was prepared following the General Procedure **B**. White solid (Melting point- 85.9-86.7 °C), R_f=0.45 (1:9:: EA:pet ether) (37 mg, 71%). ^{1}H NMR (400 MHz, $CDCl_3$) δ 7.09 (t, J=2.7 Hz, 4H), 6.65 (t, J=2.3 Hz, 2H), 3.82 (s, 12H), 3.44–3.38 (m, 4H), 3.02–2.95 (m, 4H$^{13}C\{^1H\}$ NMR (100 MHz, $CDCl_3$): δ (ppm) 191.2, 160.9, 138.8, 106.1, 105.1, 55.7, 38.0, 28.8. HRMS (ESI-TOF) m/z calcd. For $C_{22}H_{27}O_6S_4$ $[M+H]^+$ 515.0690; found 515.0695.

*S,S′-(disulfanediylbis(ethane-2,1-diyl)) bis(2-chlorobenzothioate) (**2l**)*: The compound **2l** was prepared following the General Procedure **B**. Colorless liquid, R_f=0.4 (1:19::EA:pet ether) (27 mg, 58%). ^{1}H NMR (400 MHz, $CDCl_3$): δ 7.66 (m, 2H), 7.42 (m, 4H), 7.32 (m, 2H), 3.54–3.31 (m, 4H), 3.06–2.95 (m, 4H). $^{13}C\{^1H\}$ NMR (100 MHz, $CDCl_3$): δ (ppm) 191.4, 137.2, 132.5, 131.0, 131.0, 129.4, 126.8, 37.8, 29.6. HRMS (ESI-TOF) m/z calcd. For $C_{18}H_{16}Cl_2NaO_2S_4$ $[M+Na]^+$ 484.9307; found 484.9310.

*S,S′-(disulfanediylbis(ethane-2,1-diyl)) bis(3,4-dimethoxybenzothioate) (**2m**)*: The compound **2m** was prepared following the General Procedure **B**. White solid (Melting point- 122.8-124.2 °C), R_f=0.5 (2:8::EA:pet ether) (33 mg, 65%). ^{1}H NMR (400 MHz, $CDCl_3$) δ 7.66 (dd, J=8.4, 2.1 Hz, 2H), 7.47 (d, J=2.1 Hz, 2H), 6.89 (d, J=8.4 Hz, 2H), 3.95 (s, 6H), 3.94 (s, 6H), 3.47–3.39 (m, 4H), 3.06–2.98 (m, 4H). $^{13}C\{^1H\}$ NMR (100 MHz, $CDCl_3$): δ (ppm) 189.8, 153.6, 148.9, 129.7, 121.8, 110.2, 109.4, 56.1, 56.0, 38.1, 28.5. HRMS (ESI-TOF) m/z calcd. For $C_{22}H_{27}O_6S_4$ $[M+H]^+$ 515.0690; found 515.0695.

*S,S′-(disulfanediylbis(ethane-2,1-diyl)) bis(naphthalene-2-carbothioate) (**2n**)*: The compound **2n** was prepared following the General Procedure **B**. White solid (Melting point-94.7-96.2 °C), R_f=0.4 (1:29::EA:pet ether) (31 mg, 62%). ^{1}H NMR (400 MHz, $CDCl_3$): δ 8.52 (s, 2H), 7.96 (t, J=7.1 Hz, 4H), 7.87 (d, J=7.7 Hz, 4H), 7.57 (dd, J=12.9, 8.5 Hz, 4H), 3.56–3.43 (m, 4H), 3.06 (m, 4H). $^{13}C\{^1H\}$ NMR (100 MHz, $CDCl_3$): δ (ppm) 191.2, 135.8, 134.1, 132.4, 129.6, 128.8, 128.5, 128.5, 127.8, 126.9, 123.1, 38.1, 28.6. HRMS (ESI-TOF) m/z calcd. For $C_{26}H_{23}O_2S_4$ $[M+H]^+$ 495.0581; found 495.0580.

*S,S′-(disulfanediylbis(ethane-2,1-diyl)) bis(pyrene-1-carbothioate) (**2o**)*: The compound **2o** was prepared following the General Procedure **B**. Yellow viscus liquid, R_f=0.4 (1:9::EA:pet ether) (26 mg, 41%), ^{1}H NMR (400 MHz, $CDCl_3$): δ 8.84 (d, J=9.4 Hz, 2H), 8.50 (d, J=8.1 Hz, 2H), 8.23–8.18 (m, 2H), 8.17–8.06 (m, 8H), 8.01 (m, 4H), 3.64–3.59 (m, 4H), 3.24–3.18 (m, 4H). $^{13}C\{^1H\}$ NMR (100 MHz, $CDCl_3$): δ (ppm) 193.6, 134.2, 131.1, 131.0, 130.5, 129.9, 129.7, 128.5, 127.1, 126.5, 126.5, 126.2, 124.7, 124.3, 124.2, 124.1, 38.4, 29.8. HRMS (ESI-TOF) m/z calcd. For $C_{38}H_{27}O_2S_4$ $[M+H]^+$ 643.0894; found 643.0888.

*S,S′-(disulfanediylbis(ethane-2,1-diyl)) bis(benzo[d][1,3]dioxole-5-carbothioate) (**2p**)*: The compound **2p** was prepared following the General Procedure **B**. White solid (Melting point-93.1-94.6 °C), R_f= 0.5 (1:9::EA:pet ether) (31 mg, 64%), δ^{1}H NMR (400 MHz, $CDCl_3$) δ 7.59 (dd, J=8.2, 1.7 Hz, 2H), 7.40 (d, J=1.7 Hz, 2H), 6.83 (d, J= 8.2 Hz, 2H), 6.05 (s, 4H), 3.52–3.30 (m, 4H), 3.02–2.81 (m, 4H). ^{13}C NMR (100 MHz, $CDCl_3$) δ$^{13}C\{^1H\}$ NMR (100 MHz, $CDCl_3$): δ (ppm)

© 2023 Wiley-VCH GmbH

1861471x, 2023, 4, Downloaded from https://aces.onlinelibrary.wiley.com/doi/10.1002/asia.202201128 by Indian Institute Of Science Education And Research Pune, Wiley Online Library on [23/06/2025]. See the Terms and Conditions (https://onlinelibrary.wiley.com/terms-and-conditions) on Wiley Online Library for rules of use; OA articles are governed by the applicable Creative Commons License

189.4, 152.1, 148.0, 131.3, 123.4, 108.1, 107.2, 101.9, 38.1, 28.6. HRMS (ESI-TOF) m/z calcd. For $C_{20}H_{19}O_6S_4$ $[M+H]^+$ 483.0064; found 483.0067.

*dimethyl 4,4′-(((disulfanediylbis (ethane-2,1-diyl)) bis (sulfanediyl)) bis (carbonyl)) dibenzoate (**2q**)*: The compound **2q** was prepared following the General Procedure **B**. White solid (Melting point- 112.9–114.5 °C), R_f = 0.5 (2 : 8::EA : pet ether) (36 mg, 70%). ^{1}H NMR (400 MHz, $CDCl_3$) δ 8.10 (d, J = 8.7, 4H), 7.99 (d, J = 8.7, 4H), 3.95 (s, 6H), 3.50–3.41 (m, 4H), 3.06–2.95 (m, 4H). $^{13}C\{^1H\}$ NMR (100 MHz, $CDCl_3$): δ (ppm) 190.9, 166.2, 140.1, 134.4, 130.0, 127.3, 52.6, 37.9, 28.9. HRMS (ESI-TOF) m/z calcd. For $C_{22}H_{23}O_6S_4$ $[M+H]^+$ 511.0377; found 511.0373.

*S,S′-(disulfanediylbis(ethane-2,1-diyl)) bis(2-methoxy-5-(trifluoromethoxy)benzothioate) (**2r**)*: The compound **2r** was prepared following the General Procedure **B**. White solid (Melting point- 76.6–77.9 °C), R_f = 0.5 (2 : 18::EA : pet ether) (40 mg, 65%). ^{1}H NMR (400 MHz, $CDCl_3$) δ 7.67 (dd, J = 3.0, 0.6 Hz, 2H), 7.41–7.27 (m, 2H), 6.99 (d, J = 9.1 Hz, 2H), 3.94 (s, 6H), 3.43–3.30 (m, 4H), 2.98 (ddd, J = 8.1, 5.7, 3.5 Hz, 4H). $^{13}C\{^1H\}$ NMR (100 MHz, $CDCl_3$): δ (ppm) 189.1, 156.6, 142.2 (d, J = 2 Hz), 127.1, 126.5, 122.7, 120.5 (q, J = 256 Hz), 113.1, 56.3, 37.7, 29.2. HRMS (ESI-TOF) m/z calcd. For $C_{22}H_{21}$ $F_6O_6S_4$ $[M+H]^+$ 623.0125; found 623.0129.

*S,S′-(disulfanediylbis(ethane-2,1-diyl)) bis(4-bromothiophene-2-carbothioate) (**2s**)*: The compound **2s** was prepared following the General Procedure **B**. Yellow liquid, R_f = 0.5 (1 : 39::EA : pet ether) (42 mg, 73%). ^{1}H NMR (400 MHz, $CDCl_3$) δ 7.69 (d, J = 1.4 Hz, 2H), 7.52 (d, J = 1.4 Hz, 2H), 3.46–3.39 (m, 4H), 3.00–2.93 (m, 4H). $^{13}C\{^1H\}$ NMR (100 MHz, $CDCl_3$): δ (ppm) 182.4, 142.2, 133.3, 130.1, 110.8, 37.8, 28.8. HRMS (ESI-TOF) m/z calcd. For $C_{14}H_{13}Br_2O_2S_6$ $[M+H]^+$ 562.7607; found 562.7610.

*S,S′-(disulfanediylbis(ethane-2,1-diyl)) bis(thiophene-2-carbothioate) (**2t**)*: The compound **2t** was prepared following the General Procedure **B**. Yellow liquid, R_f = 0.4 (1 : 29::EA : pet ether) (27 mg, 66%). ^{1}H NMR (400 MHz, $CDCl_3$): δ 8.12 (s, 2H), 7.52 (d, 2H), 7.34 (d, 2H), 3.59–3.20 (m, 4H), 2.98 (m, 4H). $^{13}C\{^1H\}$ NMR (100 MHz, $CDCl_3$): δ (ppm) 184.7, 140.7, 130.8, 126.5, 125.9, 38.1, 28.4. HRMS (ESI-TOF) m/z calcd. For $C_{14}H_{15}$ O_2S_6 $[M+H]^+$ 406.9396; found 406.9398.

*S,S′-(disulfanediylbis(ethane-2,1-diyl)) bis(benzofuran-2-carbothioate) (**2u**)*: The compound **2u** was prepared following the General Procedure **B**. White solid (Melting point- 137.7–138.4 °C), R_f = 0.45 (1 : 18::EA : pet ether) (30 mg, 70%). ^{1}H NMR (400 MHz, $CDCl_3$) δ 7.74–7.68 (m, 2H), 7.60 (dd, J = 8.4, 0.8 Hz, 2H), 7.55 (d, J = 0.8 Hz, 2H), 7.49 (ddd, J = 8.4, 6.2, 1.3 Hz, 2H), 7.33 (ddd, J = 8.0, 7.2, 1.0 Hz, 2H), 3.49 (m, 4H), 3.17–2.88 (m, 4H). $^{13}C\{^1H\}$ NMR (100 MHz, $CDCl_3$): δ (ppm) 181.7, 155.7, 151.0, 128.4, 127.0, 124.2, 123.3, 112.6, 111.7, 38.0, 28.1. HRMS (ESI-TOF) m/z calcd. For $C_{22}H_{19}O_4S_4$ $[M+H]^+$ 475.0166; found 475.0167.

*S,S′-(disulfanediylbis(ethane-2,1-diyl)) bis(2-phenylethanethioate) (**2v**)*: The compound **2v** was prepared following the General Procedure **B**. Colorless liquid, R_f = 0.4 (1 : 49::EA : pet ether) (27 mg, 61%). ^{1}H NMR (400 MHz, $CDCl_3$) δ 7.42–7.21 (m, 10H), 3.82 (s, 4H), 3.25–3.10 (m, 4H), 2.87–2.73 (m, 4H); $^{13}C\{^1H\}$ NMR (100 MHz, $CDCl_3$): δ (ppm) 196.9, 133.4, 129.7, 128.8, 127.6, 50.6, 37.8, 28.9. HRMS (ESI-TOF) m/z calcd. For $C_{20}H_{22}NaO_2S_4$ $[M+Na]^+$ 445.0400; found 445.0408.

*S,S′-(disulfanediylbis(ethane-2,1-diyl)) bis(3-methylbutanethioate) (**2w**)*: The compound **2w** was prepared following the General Procedure **B**. Colorless liquid, R_f = 0.3 (1 : 99::EA : pet ether) (21 mg, 60%). ^{1}H NMR (400 MHz, $CDCl_3$) δ 3.31–3.08 (m, 4H), 2.95–2.67 (m, 4H), 2.44 (d, J = 7.1 Hz, 4H), 2.16 (dp, J = 7.1, 6.6 Hz, 2H), 0.95 (d, J = 6.6 Hz, 12H). $^{13}C\{^1H\}$ NMR (100 MHz, $CDCl_3$): δ (ppm) 198.5, 53.1, 38.2, 28.5, 26.6, 22.4. HRMS (ESI-TOF) m/z calcd. For $C_{14}H_{26}NaO_2S_4$ $[M+Na]^+$ 377.0713; found 377.0714.

*S,S′-(disulfanediylbis(ethane-2,1-diyl)) dicyclohexanecarbothioate (**2x**)*: The compound **2x** was prepared following the General Procedure **B**. Colorless liquid, R_f = 0.3 (1 : 99::EA : pet ether) (22 mg, 63%). ^{1}H NMR (400 MHz, $CDCl_3$) δ 3.17 (dd, J = 8.6, 6.5 Hz, 4H), 2.84 (dd, J = 8.6, 6.5 Hz, 4H), 2.48 (tt, J = 11.5, 9.6 Hz, 2H), 1.91 (dd, J = 11.5, 3.0 Hz, 4H), 1.78 (dd, J = 9.6, 3.0 Hz, 4H), 1.52–1.36 (m, 4H), 1.34–1.12 (m, 8H). $^{13}C\{^1H\}$ NMR (100 MHz, $CDCl_3$): δ (ppm) 202.5, 52.8, 38.2, 29.6, 28.1, 25.7, 25.6. HRMS (ESI-TOF) m/z calcd. For $C_{18}H_{31}$ O_2S_4 $[M+H]^+$ 407.1207; found 407.1207.

*S,S′-(disulfanediylbis(ethane-2,1-diyl)) didodecanethioate (**2y**)*: The compound **2y** was prepared following the General Procedure **B**. White solid (Melting point- 51.1-52.9 °C), R_f = 0.2 (1 : 199::EA : pet ether) (21 mg, 59%). ^{1}H NMR (400 MHz, $CDCl_3$) δ 3.23–3.15 (m, 4H), 2.89–2.80 (m, 4H), 2.54 (m, 4H), 1.65 (m, 4H), 1.36–1.19 (m, 32H), 0.88 (t, J = 6.9 Hz, 6H). $^{13}C\{^1H\}$ NMR (100 MHz, $CDCl_3$): δ (ppm) 199.1, 44.2, 38.0, 31.9, 29.6, 29.3, 29.2, 28.9, 28.3, 25.6, 22.7, 14.1. HRMS (ESI-TOF) m/z calcd. For $C_{28}H_{55}O_2S_4$ $[M+H]^+$ 551.3085; found 551.3088.

*S,S′-(disulfanediylbis(ethane-2,1-diyl)) bis(2-(prop-2-yn-1-yloxy)benzothioate) (**2z**)*: The compound **2z** was prepared following the General Procedure **B**. Colorless liquid, R_f = 0.5 (1 : 19::EA : pet ether) (33 mg, 65%). ^{1}H NMR (400 MHz, $CDCl_3$) δ 7.88–7.59 (m, 2H), 7.50–7.26 (m, 2H), 7.14–7.02 (m, 2H), 7.00 (m, 2H), 4.76 (s, 4H); 3.33 (m, 4H), 2.93 (m, 4H), 2.49 (s, 2H); $^{13}C\{^1H\}$ NMR (100 MHz, $CDCl_3$): δ (ppm) 190.1, 155.8, 133.6, 133.3, 129.9, 127.4, 121.5, 113.9, 77.9, 77.3, 77.0, 76.7, 76.4, 56.6, 37.9, 37.7, 29.7, 29.1, 28.9. HRMS (ESI-TOF) m/z calcd. For $C_{24}H_{22}NaO_4S_4$ $[M+Na]^+$ 525.0299; found 525.0299.

*S,S′-(disulfanediylbis(ethane-2,1-diyl)) bis(2-(allyloxy)benzothioate) (**2aa**)*: The compound **2aa** was prepared following the General Procedure **B**. Colorless liquid, R_f = 0.5 (1 : 19::EA : pet ether) (30 mg, 59%). ^{1}H NMR (400 MHz, $CDCl_3$) δ 7.91–7.59 (m, 2H), 7.44 (m, 2H), 7.04–6.81 (m, 2H), 6.10 (m, 2H), 5.48 (dd, J = 17.2, 1.3 Hz, 2H), 5.32 (dd, J = 10.5, 1.3 Hz, 2H), 4.67 (m, 4H), 3.47–3.20 (m, 4H), 3.12–2.85 (m, 4H). $^{13}C\{^1H\}$ NMR (100 MHz, $CDCl_3$): δ (ppm) 190.2, 157.1, 133.7, 132.5, 129.8, 126.9, 120.7, 118.1, 113.4, 69.8, 38.0, 29.1. HRMS (ESI-TOF) m/z calcd. For $C_{24}H_{26}Na$ O_4S_4 $[M+Na]^+$ 529.0612; found 529.0615.

*S,S′-(disulfanediylbis(ethane-2,1-diyl)) bis(4-(benzyloxy)benzothioate) (**2ab**)*: The compound **2ab** was prepared following the General Procedure **B**. White solid (Melting point- 115.8–117.2 °C), R_f = 0.5 (1 : 39::EA : pet ether) (43 mg, 71%). ^{1}H NMR (400 MHz, $CDCl_3$) δ 7.93 (d, J = 8.8 Hz, 4H), 7.51–7.29 (m, 10H), 6.99 (d, J = 8.8 Hz, 4H), 5.12 (s, 4H), 3.40 (m, 4H), 2.98 (m, 1H). $^{13}C\{^1H\}$ NMR (100 MHz, $CDCl_3$): δ (ppm) 189.83, 163.17, 136.2, 130.0, 129.6, 128.8, 128.4, 127.6, 114.8, 70.3, 38.3, 28.5. HRMS (ESI-TOF) m/z calcd. For $C_{32}H_{31}O_4S_4$ $[M+H]^+$ 607.1105; found 607.1109.

*S,S′-(disulfanediylbis(ethane-2,1-diyl)) bis(3-(tosyloxy)benzothioate) (**2ac**)*: The compound **2ac** was prepared following the General Procedure **B**. Colorless liquid, R_f = 0.5 (2 : 8::EA : pet ether) (41 mg, 63%). ^{1}H NMR (400 MHz, $CDCl_3$) δ 7.90–7.78 (m, 2H), 7.72 (d, J = 8.3 Hz, 4H), 7.55–7.48 (m, 2H), 7.40 (m, 2H), 7.33 (d, J = 8.3 Hz, 4H), 7.26–7.20 (m, 2H), 3.45–3.34 (m, 4H), 3.00–2.89 (m, 4H), 2.45 (s, 6H). $^{13}C\{^1H\}$ NMR (100 MHz, $CDCl_3$): δ (ppm) 190.0, 149.9, 145.9, 138.4, 132.1, 130.2, 130.1, 128.6, 127.6, 125.9, 121.3, 37.8, 28.8, 21.9. HRMS (ESI-TOF) m/z calcd. For $C_{32}H_{31}O_8S_6$ $[M+H]^+$ 735.0343; found 735.0350.

*2-(4-methoxyphenyl)-1,3-dithiolane 1-oxide (**3a**)*[29]: The compound **3a** was prepared following the General Procedure **B**. White solid (Melting point- 115.8-117.2 °C), R_f = 0.3 (1 : 1::EA : pet ether) (38 mg, 83%). ^{1}H NMR (400 MHz, $CDCl_3$) δ 7.40 (d, J = 8.7 Hz, 2H), 7.89 (d, J = 8.7 Hz, 2H), 3.84 (m, 4H), 3.59 (m, 1H), 3.34 (m, 1H), 2.90 (m, 1H); $^{13}C\{^1H\}$ NMR (100 MHz, $CDCl_3$): δ (ppm) 160.2, 129.9, 124.9, 114.5, 77.3,

© 2023 Wiley-VCH GmbH

1861471x, 2023, 4, Downloaded from https://aces.onlinelibrary.wiley.com/doi/10.1002/asia.202201128 by Indian Institute Of Science Education And Research Pune, Wiley Online Library on [23/06/2025]. See the Terms and Conditions (https://onlinelibrary.wiley.com/terms-and-conditions) on Wiley Online Library for rules of use; OA articles are governed by the applicable Creative Commons License

55.5, 53.1, 32.4. HRMS (ESI-TOF) m/z calcd. For $C_{10}H_{13}O_2S_2$ $[M+H]^+$ 229.0357; found 229.0358.

*S,S′-(disulfanediylbis(propane-3,1-diyl))dibenzothioate (**5a**)*: The compound **5a** was prepared following the General Procedure **C**. Colorless liquid, R_f = 0.5 (1 : 49::EA : pet ether) (15 mg, 37%); ^{1}H NMR (400 MHz, $CDCl_3$) δ 8.07–7.84 (m, 4H), 7.61–7.50 (m, 2H), 7.47–7.36 (m, 4H), 3.18 (t, *J* = 7.1 Hz, 4H), 2.81 (t, *J* = 7.1 Hz, 4H), 2.10 (p, *J* = 7.1 Hz, 4H). $^{13}C\{^1H\}$ NMR (100 MHz, $CDCl_3$): δ (ppm) 191.8, 137.1, 133.5, 128.7, 127.4, 37.6, 29.1, 27.7. HRMS (ESI-TOF) m/z calcd. For $C_{20}H_{22}NaO_2S_4$ $[M+Na]^+$ 445.0400; found 445.0412.

*S,S′-(disulfanediylbis(propane-3,1-diyl)) bis(3,4-dimethoxybenzothioate) (**5b**)*: The compound **5b** was prepared following the General Procedure **C**. White solid (Melting point- 62.3–63.4 °C), R_f = 0.5 (1 : 15::EA : pet ether) (18 mg, 32%); ^{1}H NMR (400 MHz, $CDCl_3$) δ 7.65 (dd, *J* = 8.4, 2.1 Hz, 2H), 7.46 (d, *J* = 2.1 Hz, 2H), 6.87 (d, *J* = 8.4 Hz, 2H), 3.93 (s, 6H), 3.93 (s, 6H), 3.16 (t, *J* = 7.1 Hz, 4H), 2.80 (t, *J* = 7.1 Hz, 4H), 2.09 (p, *J* = 7.1 Hz, 4H); $^{13}C\{^1H\}$ NMR (100 MHz, $CDCl_3$): δ (ppm) 190.5, 153.6, 153.6, 149.0, 130.1, 121.8, 110.3, 109.5, 56.2, 56.1, 37.6, 29.2, 27.6. HRMS (ESI-TOF) m/z calcd. For $C_{24}H_{30}NaO_6S_4$ $[M+Na]^+$ 565.0822; found 565.0820.

*S,S′-(disulfanediylbis(propane-3,1-diyl)) bis(4-chlorobenzothioate) (**5c**)*: The compound **5c** was prepared following the General Procedure **C**. White solid (Melting point- 40.4-41.2 °C), R_f = 0.45 (1 : 29::EA : pet ether) (23 mg, 47%). ^{1}H NMR (400 MHz, $CDCl_3$) δ 8.00–7.79 (m, 4H), 7.47–7.36 (m, 4H), 3.18 (t, *J* = 7.1 Hz, 1H), 2.80 (t, *J* = 7.1 Hz, 1H), 2.09 (p, *J* = 7.1 Hz, 1H); $^{13}C\{^1H\}$ NMR (100 MHz, $CDCl_3$): δ (ppm) 190.6, 139.9, 135.4, 129.1, 128.7, 37.6, 29.1, 27.8. HRMS (ESI-TOF) m/z calcd. For $C_{20}H_{21}Cl_2O_2S_4$ $[M+H]^+$ 490.9801; found 490.9803.

*S,S′-(disulfanediylbis(propane-3,1-diyl)) bis(4-(tert-butyl)benzothioate) (**5d**)*: The compound **5d** was prepared following the General Procedure **C**. White solid (Melting point- 57.3–57.8 °C), R_f = 0.4 (1 : 29::EA : pet ether) (18 mg, 34%). ^{1}H NMR (400 MHz, $CDCl_3$) δ 8.02–7.80 (m, 4H), 7.57–7.36 (m, 4H), 3.17 (t, *J* = 7.1 Hz, 4H), 2.80 (t, *J* = 7.1 Hz, 4H), 2.08 (p, *J* = 7.1 Hz, 4H), 1.33 (s, 18H). $^{13}C\{^1H\}$ NMR (100 MHz, $CDCl_3$): δ (ppm) 191.3, 157.3, 134.5, 127.3, 125.7, 37.6, 35.3, 31.2, 29.2, 27.6. HRMS (ESI-TOF) m/z calcd. For $C_{28}H_{39}O_2S_4$ $[M+H]^+$ 535.1833; found 535.1836.

*S,S′-(disulfanediylbis(propane-3,1-diyl)) bis(4-methylbenzothioate) (**5e**)*: The compound **5e** was prepared following the General Procedure **C**. Colorless liquid, R_f = 0.4 (1 : 39::EA : pet ether) (28 mg, 30%). ^{1}H NMR (400 MHz, $CDCl_3$) δ 7.97–7.75 (m, 4H), 7.32–7.13 (m, 4H), 3.16 (t, *J* = 7.1 Hz, 4H), 2.80 (t, *J* = 7.1 Hz, 4H), 2.40 (s, 6H), 2.08 (p, *J* = 7.1 Hz, 4H); $^{13}C\{^1H\}$ NMR (100 MHz, $CDCl_3$): δ (ppm) 191.4, 144.4, 134.6, 129.4, 127.4, 37.6, 29.2, 27.6, 21.8. HRMS (ESI-TOF) m/z calcd. For $C_{22}H_{27}O_2S_4$ $[M+H]^+$ 451.0894; found 451.0895.

*S,S′-(disulfanediylbis(propane-3,1-diyl)) bis(thiophene-3-carbothioate) (**5f**)*: The compound **5f** was prepared following the General Procedure **C**. Colouless liquid, R_f = 0.4 (1 : 39::EA : pet ether) (14 mg, 35%). ^{1}H NMR (400 MHz, $CDCl_3$) δ 8.11 (dd, *J* = 3.0, 1.3 Hz, 2H), 7.52 (dd, *J* = 5.1, 1.3 Hz, 2H), 7.33 (dd, *J* = 5.1, 3.0 Hz, 2H), 3.16 (t, *J* = 7.1 Hz, 4H), 2.78 (t, *J* = 7.1 Hz, 4H), 2.08 (p, *J* = 7.1 Hz, 4H). $^{13}C\{^1H\}$ NMR (100 MHz, $CDCl_3$): δ (ppm) 185.3, 141.0, 130.7, 126.6, 126.1, 37.5, 29.2, 27.5. HRMS (ESI-TOF) m/z calcd. For $C_{16}H_{19}O_2S_6$ $[M+H]^+$ 434.9709; found 434.9714.

*2-phenyl-1,3-dithiane 1-oxide (**6a**)*[30]: The compound **6a** was prepared following the General Procedure **C**. White solid (Melting point- 138.5–140.8 °C), R_f = 0.5 (9 : 1::EA : pet ether) (38 mg, 90%). ^{1}H NMR (400 MHz, $CDCl_3$) δ 7.43-7.35 (m, 5H), 4.55 (s, 1H), 3.58–3.54 (m, 1H), 2.92–2.84 (m, 1H), 2.79–2.65 (m, 2H), 2.56–2.47 (m, 1H), 2.42–2.31 (m, 1H). $^{13}C\{^1H\}$ NMR (100 MHz, $CDCl_3$): δ (ppm) 133.1, 129.1, 128.9, 128.5, 69.3, 54.5, 31.1, 29.3. HRMS (ESI-TOF) m/z calcd. For $C_{10}H_{12}OS_2$ $[M+H]^+$ 213.0408; found 213.0410.

*S-(2-(phenyldisulfanyl)ethyl) 4-methoxybenzothioate (**8aa**)*: The compound **8aa** was prepared following the General Procedure **D**. Colorless liquid, R_f = 0.35 (1 : 19::EA : pet ether) (44 mg, 65%). ^{1}H NMR (400 MHz, $CDCl_3$) δ 7.98–7.89 (m, 2H), 7.65–7.53 (m, 2H), 7.34 (m, 2H), 7.26–7.20 (m, 1H), 6.95–6.89 (m, 2H), 3.86 (s, 3H), 3.41–3.18 (m, 2H), 3.03–2.86 (m, 2H); $^{13}C\{^1H\}$ NMR (100 MHz, $CDCl_3$): δ (ppm) 189.8, 164.0, 137.2, 129.8, 129.6, 129.2, 128.1, 127.2, 113.9, 55.7, 38.5, 28.3. HRMS (ESI-TOF) m/z calcd. For $C_{16}H_{17}O_2S_3$ $[M+H]^+$ 337.0391; found 337.0399.

*S-(2-(p-tolyldisulfanyl)ethyl) 4-methoxybenzothioate (**8bb**)*: The compound **8bb** was prepared following the General Procedure **D**. Colorless liquid, R_f = 0.35 (1 : 19::EA : pet ether) (49 mg, 69%). ^{1}H NMR (400 MHz, $CDCl_3$) δ 8.04–7.85 (m, 2H), 7.55–7.43 (m, 2H), 7.14 (m, 2H), 6.95–6.85 (m, 2H), 3.86 (s, 2H), 3.43–3.25 (m, 1H), 3.02–2.88 (m, 1H), 2.33 (s, 2H). $^{13}C\{^1H\}$ NMR (100 MHz, $CDCl_3$): δ (ppm) 189.8, 164.0, 137.6, 133.8, 130.0, 129.8, 129.6, 129.1, 113.9, 55.6, 38.34, 28.3, 21.2. HRMS (ESI-TOF) m/z calcd. For $C_{17}H_{19}O_2S_3$ $[M+H]^+$ 351.0547; found 351.0554.

*S-(2-(p-tolyldisulfanyl)ethyl) 4-cyanobenzothioate (**8cb**)*: The compound **8cb** was prepared following the General Procedure **D**. Colorless liquid, R_f = 0.35 (1 : 9::EA : pet ether) (50 mg, 71%). ^{1}H NMR (400 MHz, $CDCl_3$) δ 8.06–7.99 (m, 2H), 7.78–7.72 (m, 2H), 7.50–7.45 (m, 2H), 7.18–7.11 (m, 2H), 3.45–3.40 (m, 2H), 3.00–2.95 (m, 2H), 2.34 (s, 3H). $^{13}C\{^1H\}$ NMR (100 MHz, $CDCl_3$): δ (ppm) 190.2, 140.0, 137.9, 133.5, 132.6, 130.1, 129.3, 127.8, 117.9, 116.9, 77.1, 37.8, 28.8, 21.2. HRMS (ESI-TOF) m/z calcd. For $C_{17}H_{16}NOS_3$ $[M+H]^+$ 346.0394; found 346.0393.

*S-(2-((2-methoxyphenyl)disulfanyl)ethyl) 4-methoxybenzothioate (**8dc**)*: The compound **8dc** was prepared following the General Procedure **D**. Colorless liquid, R_f = 0.4 (1 : 9::EA : pet ether) (46 mg, 63%). ^{1}H NMR (400 MHz, $CDCl_3$) δ 8.01–7.86 (m, 2H), 7.73 (dd, *J* = 7.7, 1.6 Hz, 1H), 7.26–7.20 (m, 1H), 7.26–7.15 (m, 1H), 6.99 (td, *J* = 7.7, 1.1 Hz, 1H), 6.94–6.89 (m, 2H), 6.87 (dd, *J* = 8.3, 1.1 Hz, 1H), 3.90 (s, 3H), 3.86 (s, 3H), 3.37 (m, 2H), 3.01–2.96 (m, 2H). $^{13}C\{^1H\}$ NMR (100 MHz, $CDCl_3$): δ (ppm) 189.9, 164.0, 157.1, 129.8, 129.6, 129.0, 128.5, 125.0, 121.4, 113.9, 110.9, 56.1, 55.6, 38.1, 28.4. HRMS (ESI-TOF) m/z calcd. For $C_{17}H_{19}O_3S_3$ $[M+H]^+$ 367.0496; found 367.0497.

*S-(2-(p-tolyldisulfanyl)ethyl) 2-cyanobenzothioate (**8eb**)*: The compound **8eb** was prepared following the General Procedure **D**. Colorless liquid, R_f = 0.45 (1 : 9::EA : pet ether) (49 mg, 70%). ^{1}H NMR (400 MHz, $CDCl_3$) δ 8.05–8.01 (m, 1H), 7.84–7.80 (m, 1H), 7.70–7.66 (m, 2H), 7.51–7.47 (d, 2H), 7.18–7.12 (d, 2H), 3.50–3.41 (m, 2H), 3.04–2.96 (m, 2H), 2.34 (s, 3H). $^{13}C\{^1H\}$ NMR (100 MHz, $CDCl_3$): δ (ppm) 189.5, 139.2, 137.8, 135.2, 133.5, 132.9, 132.7, 130.1, 129.4, 129.3, 117.4, 110.3, 37.6, 29.3, 21.2. HRMS (ESI-TOF) m/z calcd. For $C_{17}H_{15}NOS_3$ $[M]^+$ 345.0316; found 345.0315.

*S-(2-((2-methoxyphenyl)disulfanyl)ethyl) naphthalene-2-carbothioate (**8fc**)*: The compound **8fc** was prepared following the General Procedure **D**. Colorless liquid, R_f = 0.4 (1 : 9::EA : pet ether) (48 mg, 62%). ^{1}H NMR (400 MHz, $CDCl_3$) δ 8.51 (s, 1H), 7.97 (dd, *J* = 8.6, 1.7 Hz, 2H), 7.88 (dd, *J* = 8.3, 4.4 Hz, 2H), 7.75 (dd, *J* = 7.7, 1.6 Hz, 1H), 7.58 (m, 2H), 7.23 (dd, *J* = 7.7, 1.3 Hz, 1H), 7.01 (td, *J* = 7.6, 1.1 Hz, 1H), 6.88 (dd, *J* = 8.3, 1.0 Hz, 1H), 3.92 (s, 3H), 3.49–3.43 (m, 2H), 3.07–3.01 (m, 2H). $^{13}C\{^1H\}$ NMR (100 MHz, $CDCl_3$): δ (ppm) 191.4, 157.2, 135.9, 134.3, 132.5, 129.7, 129.1, 128.9, 128.7, 128.6, 128.5, 127.9, 127.1, 125.0, 123.2, 121.4, 110.9, 56.0, 38.0, 28.7. HRMS (ESI-TOF) m/z calcd. For $C_{20}H_{19}O_2S_3$ $[M+H]^+$ 387.0547; found 387.0544.

*S-(2-((4-hydroxyphenyl)disulfanyl)ethyl) 3-nitrobenzothioate (**8gd**)*: The compound **8gd** was prepared following the General Procedure **D**. Colorless liquid, R_f = 0.5 (3 : 7::EA : pet ether) (42 mg, 57%). ^{1}H NMR (400 MHz, $CDCl_3$) δ 8.77 (m, 1H), 8.42 (dd, *J* = 2.3, 1.1 Hz, 1H), 8.27 (dd, *J* = 1.6, 1.1 Hz, 1H), 7.68 (m, 1H), 7.50 (d, *J* = 8.7 Hz, 2H), 6.82 (d, *J* = 8.7 Hz, 2H), 5.20 (s, 1H), 3.69–3.24 (m, 3H), 3.01 (m, 3H);

© 2023 Wiley-VCH GmbH

1861471x, 2023, 4, Downloaded from https://aces.onlinelibrary.wiley.com/doi/10.1002/asia.202201128 by Indian Institute Of Science Education And Research Pune, Wiley Online Library on [23/06/2025]. See the Terms and Conditions (https://onlinelibrary.wiley.com/terms-and-conditions) on Wiley Online Library for rules of use; OA articles are governed by the applicable Creative Commons License

$^{13}C\{^1H\}$ NMR (100 MHz, $CDCl_3$): δ (ppm) 189.4, 156.8, 148.4, 138.1, 132.8, 132.7, 129.9, 127.9, 127.7, 122.3, 116.3, 37.5, 28.7. HRMS (ESI-TOF) m/z calcd. For $C_{15}H_{14}NO_4S_3$ $[M+H]^+$ 368.0085; found 368.0086.

*S-(2-(pyridin-2-yldisulfanyl)ethyl) 4-methoxybenzothioate (**8he**)*: The compound **8he** was prepared following the General Procedure **D**. White solid (Melting point- 59.3-59.9 °C), R_f = 0.5 (1 : 9::EA : pet ether) (49 mg, 73%). ^1H NMR (400 MHz, $CDCl_3$) δ 8.47 (ddd, *J* = 4.8, 1.8, 0.9 Hz, 1H), 8.02–7.82 (m, 2H), 7.72 (dt, *J* = 8.1, 1.0 Hz, 1H), 7.64 (ddd, *J* = 8.1, 7.4, 1.8 Hz, 1H), 7.09 (ddd, *J* = 7.4, 4.8, 1.1 Hz, 1H), 6.94–6.87 (m, 2H), 3.86 (s, 3H), 3.41–3.32 (m, 2H), 3.11–3.02 (m, 2H); $^{13}C\{^1H\}$ NMR (100 MHz, $CDCl_3$): δ (ppm) 189.8, 164.0, 160.0, 149.8, 137.2, 129.7, 129.6, 120.9, 120.0, 113.9, 55.6, 38.6, 28.4. HRMS (ESI-TOF) m/z calcd. For $C_{15}H_{16}NO_2S_3$ $[M+H]^+$ 338.0343; found 338.0347.

*S-(2-(pyridin-2-yldisulfanyl)ethyl) naphthalene-2-carbothioate (**8ie**)*: The compound **8ie** was prepared following the General Procedure **D**. Colorless liquid, R_f = 0.45 (2 : 8::EA : pet ether) (50 mg, 70%). ^1H NMR (400 MHz, $CDCl_3$) δ 8.53–8.46 (m, 2H), 7.96 (d, *J* = 8.5 Hz, 2H), 7.88 (dd, *J* = 8.1, 4.3 Hz, 2H), 7.74 (d, *J* = 8.1 Hz, 1H), 7.68–7.51 (m, 3H), 7.13–7.07 (m, 1H), 3.48-3.44 (m, 2H), 3.12-3.08 (m, 2H). $^{13}C\{^1H\}$ NMR (100 MHz, $CDCl_3$): δ (ppm) 191.3, 159.9, 149.8, 137.2, 135.9, 134.1, 132.5, 129.7, 128.9, 128.7, 128.7, 127.9, 127.1, 123.2, 121.0, 120.1, 38.5, 28.6. HRMS (ESI-TOF) m/z calcd. For $C_{18}H_{16}NOS_3$ $[M+H]^+$ 358.0394; found 358.0398.

*2-(4-(tert-butyl)phenyl)-1,3-dithiolane (**1d**)*: The compound **1d** was prepared following the General Procedure **A**. white solid (Melting point- 78.9–80.2 °C), R_f = 0.4 (1 : 9::EA : pet ether) (352 mg, 98%). ^1H NMR (400 MHz, $CDCl_3$) δ 7.48–7.43 (m, 2H), 7.36–7.31 (m, 2H), 5.64 (s, 1H), 3.55–3.46 (m, 2H), 3.39–3.30 (m, 2H), 1.31 (s, 9H). $^{13}C\{^1H\}$ NMR (100 MHz, $CDCl_3$): δ 151.2, 137.2, 127.7, 125.6, 56.2, 40.3, 34.7, 31.4. HRMS (ESI-TOF) m/z calcd. For $C_{13}H_{19}S_2$ $[M+H]^+$ 239.0923; found 239.0928.

*2-(3-iodophenyl)-1,3-dithiolane (**1i**)*: The compound **1i** was prepared following the General Procedure **A**. yellow solid (Melting point- 62.3–63.7 °C), R_f = 0.4 (1 : 9::EA : pet ether) (448 mg, 97%). ^1H NMR (400 MHz, $CDCl_3$) δ 8.10 (d, *J* = 2.2 Hz, 1H), 7.50 (d, *J* = 8.3 Hz, 1H), 7.25 (dd, *J* = 8.3, 2.2 Hz, 2H), 5.77 (s, 1H), 3.48–3.45 (m, 2H), 3.40–3.37 (m, 2H). $^{13}C\{^1H\}$ NMR (100 MHz, $CDCl_3$): δ 142.8, 137.9, 135.5, 135.2, 134.9, 96.8, 56.7, 37.0. HRMS (ESI-TOF) m/z calcd. For $C_9H_{10}IS_2$ $[M+H]^+$ 308.9263; found 308.9267.

*2-(pyren-1-yl)-1,3-dithiolane (**1o**)*: The compound **1o** was prepared following the General Procedure **A**. yellow solid (Melting point- 68.1–69.7 °C), R_f = 0.4 (1 : 19::EA : pet ether) (441 mg, 96%). ^1H NMR (400 MHz, $CDCl_3$) δ 8.57 (d, J = 8.1 Hz, 1H), 8.43 (d, J = 9.3 Hz, 1H), 8.21–8.13 (m, 4H), 8.08–7.98 (m, 3H), 6.79 (s, 1H), 3.69–3.60 (m, 2H), 3.56–3.48 (m, 2H). $^{13}C\{^1H\}$ NMR (100 MHz, $CDCl_3$): δ 132.8, 131.4, 131.1, 130.7, 128.6, 128.0, 127.6, 127.4, 126.0, 125.5, 125.3, 125.3, 125.1, 124.7, 124.8, 122.4, 53.1, 40.3. HRMS (ESI-TOF) m/z calcd. For $C_{19}H_{15}S_2$ $[M+H]^+$ 307.0610; found 307.0613.

2-(2-methoxy-5-(trifluoromethoxy)phenyl)-1,3-dithiolane (*1r*): The compound **1r** was prepared following the General Procedure **A**. colorless liquid, R_f = 0.4 (1 : 9::EA : pet ether) (422 mg, 95%). ^1H NMR (400 MHz, $CDCl_3$) δ 1H NMR (400 MHz, Chloroform-d) δ 7.63–7.58 (m, 1H), 7.09–7.05 (m, 1H), 6.81 (d, J = 8.9 Hz, 1H), 5.96 (s, 1H), 3.86 (s, 3H), 3.38–3.29 (m, 4H). $^{13}C\{^1H\}$ NMR (100 MHz, $CDCl_3$): δ 155.1, 142.5, 131.7, 124.5, 121.9, 121.4, 121.3, 119.39, 116.84, 111.12, 56.10, 48.62, 39.37. HRMS (ESI-TOF) m/z calcd. For $C_{11}H_{12}F_3O_2S_2$ $[M+H]^+$ 297.0225; found 297.0227.

*2-(1,3-dithiolan-2-yl)benzofuran (**1u**)*: The compound **1u** was prepared following the General Procedure **A**. white solid (Melting point- 85.3–86.9 °C), R_f = 0.4 (1 : 9::EA : pet ether) (313 mg, 94%). ^1H NMR (400 MHz, $CDCl_3$) δ 7.49 (ddd, *J* = 7.5, 1.5, 0.9 Hz, 1H), 7.44 (dq, *J* = 8.2, 0.9 Hz, 1H), 7.28–7.22 (m, 1H), 7.19 (td, *J* = 7.5, 1.1 Hz, 1H), 6.69 (s, 1H), 5.69 (s, 1H), 3.49–3.43 (m, 2H), 3.39–3.32 (m, 2H). $^{13}C\{^1H\}$ NMR (100 MHz, $CDCl_3$): δ 154.4, 152.4, 125.2, 121.5, 120.0, 118.1, 108.4, 101.0, 44.9, 36.3. HRMS (ESI-TOF) m/z calcd. For $C_{11}H_{11}OS_2$ $[M+H]^+$ 223.0246; found 223.0251.

*2-(2-(prop-2-yn-1-yloxy)phenyl)-1,3-dithiolane (**1z**)*: The compound **1z** was prepared following the General Procedure **A**. colourless liquid, R_f = 0.4 (1 : 9::EA : pet ether) (336 mg, 95%). ^1H NMR (400 MHz, $CDCl_3$) δ 7.75 (dd, *J* = 7.7, 1.8 Hz, 1H), 7.23 (ddd, *J* = 8.3, 7.5, 1.6 Hz, 1H), 7.03–6.89 (m, 2H), 6.07 (s, 1H), 4.75 (d, *J* = 2.3 Hz, 2H), 3.46–3.23 (m, 4H). $^{13}C\{^1H\}$ NMR (100 MHz, $CDCl_3$): δ 154.6, 130.1, 128.7, 128.5, 121.7, 112.2, 78.5, 75.8, 56.4, 49.0, 39.5. HRMS (ESI-TOF) m/z calcd. For $C_{12}H_{13}OS_2$ $[M+H]^+$ 237.0402; found 237.0407.

*2-(2-(allyloxy)phenyl)-1,3-dithiolane (**1aa**)*: The compound **1aa** was prepared following the General Procedure **A**. colourless liquid, R_f = 0.4 (1 : 9::EA : pet ether) (333 mg, 93%). ^1H NMR (400 MHz, $CDCl_3$) δ 7.74 (dd, *J* = 7.7, 1.8 Hz, 1H), 7.20 (ddd, *J* = 8.1, 7.4, 1.8 Hz, 1H), 6.95 (td, *J* = 7.5, 1.1 Hz, 1H), 6.83 (dd, *J* = 8.3, 1.1 Hz, 1H), 6.14–6.01 (m, 2H), 5.46 (dq, *J* = 17.3, 1.6 Hz, 1H), 5.30 (dq, *J* = 10.6, 1.5 Hz, 1H), 4.59 (dt, *J* = 5.0, 1.6 Hz, 2H), 3.46–3.10 (m, 4H). $^{13}C\{^1H\}$ NMR (100 MHz, $CDCl_3$): δ 152.6, 130.3, 126.9, 125.8, 125.2, 117.9, 114.5, 108.9, 66.2, 46.3, 36.5. HRMS (ESI-TOF) m/z calcd. For $C_{12}H_{15}OS_2$ $[M+H]^+$ 239.0559; found 239.0562.

*3-(1,3-dithiolan-2-yl)phenyl 4-methylbenzenesulfonate (**1ac**)*: The compound **1ac** was prepared following the General Procedure **A**. White solid (Melting point- 96.4–97.7 °C), R_f = 0.4 (15 : 85::EA : pet ether) (518 mg, 98%). ^1H NMR (400 MHz, $CDCl_3$) δ 7.70 (d, *J* = 7.4 Hz, 2H), 7.34 (m, 3H), 7.22 (td, *J* = 8.2, 1.8 Hz, 1H), 7.08 (d, *J* = 2.4 Hz, 1H), 6.91 (d, *J* = 8.2 Hz, 1H), 5.50 (s, 2H), 3.58–3.01 (m, 4H), 2.45 (s, 3H). $^{13}C\{^1H\}$ NMR (100 MHz, $CDCl_3$): δ (ppm) 149.7, 145.4, 143.2, 132.3, 129.8, 129.6, 128.7, 126.6, 122.1, 122.0, 55.3, 40.2, 21.8. HRMS (ESI-TOF) m/z calcd. For $C_{16}H_{17}O_3S_3$ $[M+H]^+$ 353.0334; found 353.0337.

Acknowledgements

R. G. B. thanks SERB-Department of Science and Technology (CRG/2019/005753), New Delhi, Govt. of India for the generous research grant. Authors also thank IISER Pune for the financial assistance. P. D. D. thanks CSIR, New Delhi, M. B. thanks IISER Pune for the fellowship and A. S. T. thanks DST-SERB New Delhi, Government of India for providing project assistant fellowship. We also thank Mr. Ashokkumar Basavarajappa of IISER Pune for helping in for obtaining the crystal data.

Conflict of Interest

The authors declare no conflict of interest

Data Availability Statement

The data that support the findings of this study are available in the supplementary material of this article.

Keywords: Dithioacetals · disulfide-linked-dithioesters · photoredox catalysis · rearrangement · thioester

© 2023 Wiley-VCH GmbH

1861471x, 2023, 4, Downloaded from https://aces.onlinelibrary.wiley.com/doi/10.1002/asia.202201128 by Indian Institute Of Science Education And Research Pune, Wiley Online Library on [23/06/2025]. See the Terms and Conditions (https://onlinelibrary.wiley.com/terms-and-conditions) on Wiley Online Library for rules of use; OA articles are governed by the applicable Creative Commons License

[1] D. Kaiser, I. Klose, R. Oost, J. Neuhaus, N. Maulide, *Chem. Rev.* **2019**, *119*, 8701–8780.
[2] a) E. J. Corey, D. Seebach, *Angew. Chem. Int. Ed. Engl.* **1965**, *4*, 1075–1077; b) E. J. Corey, D. Seebach, *J. Org. Chem.* **1975**, *40*, 231–237; c) D. Seebach, *Angew. Chem. Int. Ed. Engl.* **1979**, *18*, 239–258.
[3] D. A. Herbst, C. A. Townsend, T. Maier, *Nat. Prod. Rep.* **2018**, *35*, 1046–1069.
[4] a) J. Franke, C. Hertweck, *Cell Chem. Biol.* **2016**, *23*, 1179–1192; b) H. M. Burke, L. Sweeney, E. M. Scanlan, *Nat. Commun.* **2017**, *8*, 15655; c) B. Chen, Y. Sun, J. Niu, G. K. Jarugumilli, X. Wu, *Cell Chem. Biol.* **2018**, *25*, 817–831; d) W. Yang, S.-H. Xia, *World J. Gastroenterol.* **2006**, *12*, 7753–7757.
[5] a) K. Bleicher, J. Duschmale, M. Brigitte, D. Henrik, F. Hansen, T. Koch, M. Li, A. Schaeublin, Xi. Sue, Y. Wu, **2019**, PTC/EP2018/086457; b) X. Yang, M. Sierant, M. Janicka, L. Peczek, C. Martinez, T. Hassell, N. Li, X. Li, T. Wang, B. Nawrot, *ACS Chem. Biol.* **2012**, *7*, 1214–1220; c) W. T. Wiesler, M. H. Caruthers, *J. Org. Chem.* **1996**, *61*, *4272–4281*.
[6] a) M. Kazemia, L. Shiri, *J. Sulfur Chem.* **2015**, *36*, 613–623; b) T.-C. Zheng, M. Burkart, D. E. Richardson, *Tetrahedron Lett.* **1999**, *40*, 603–606.
[7] a) C. F. Li, W. J. Xiao, H. Alper, *J. Org. Chem.* **2009**, *74*, 888–890; b) H. Cao, L. McNamee, H. Alper, *J. Org. Chem.* **2008**, *73*, 3530–3534; c) M. N. Burhardt, A. Ahlburg, T. Skrydstrup, *J. Org. Chem.* **2014**, *79*, 11830–11840; d) B. Kang, S. K. Hong, *Chem. Sci.* **2017**, *8*, 6613–6618.
[8] a) C. Yi, Y. Huang, C. Lee, *Green Chem.* **2013**, *15*, 2476–2484; b) J. Chung, U. R. Seo, S. Chun, Y. K. Chung, *ChemCatChem.* **2016**, *8*, 318–321; c) S. Xie, L. Su, M. Mo, W. Zhou, Y. Zhou, J. Dong, *J. Org. Chem.* **2021**, *86*, 739–749; d) Y. Shi, X. Liu, H. Cao, F. Bie, Y. Han, P. Yan, R. Szostak, M. Szostak, C. Liu, *Org. Biomol. Chem.* **2021**, *19*, 2991–2996.
[9] a) J. M. Thorton, *J. Mol. Biol.* **1981**, *151*, 261–287; b) P. J. Hogg, *Trends Biochem. Sci.* **2003**, *28*, 210–214; c) A. J. Saunders, G. B. Young, G. J. Pielak, *Protein Sci.* **1993**, *2*, 1183–1184.
[10] a) D. J. Echelman, A. Q. Lee, J. M. Fernández, *J. Biol. Chem.* **2017**, *292*, 8988–8997; b) M. Y. Folikumah, M. Behl, A. Lendlein, *Biomacromolecules* **2021**, *22*, 1875–1884; c) W. Xuan, D. Collins, M. Koh, S. Shao, A. Yao, H. Xiao, P. P. Garner, P. G. Schultz, *ACS Chem. Biol.* **2018**, *13*, 578–581; d) B. Schuler, L. K. Pannell, *Bioconjugate Chem.* **2002**, *13*, 1039–1043; e) E. M. Sletten, C. R. Bertozzi, *Angew. Chem. Int. Ed.* **2009**, *48*, 6974–6998; *Angew. Chem.* **2009**, *121*, 7108–7133; f) S. Rinalducci, L. Murgiano, L. Zolla, *J. Exp. Bot.* **2008**, *59*, 3781–3801; g) N. T. Trang Le, T. N. Quynh Nguyen, V. D. Cao, D. T. Hoang, V. C. Ngo, T. T. Hoang Thi, *Pharmaceutica* **2019**, *11*, 591; h) I. Altinbasak, M. Arslan, R. Sanyal, A. Sanyal, *Polym. Chem.* **2020**, *11*, 7603–7624; i) J. R. Winther, C. Thorpe, *Biochim. Biophys. Acta.* **2014**, *1840*, 838–846; j) O. Konievab, A. Wagner, *Chem. Soc. Rev.* **2015**, *44*, 5495–5551; k) M. V. Trivedi, J. S. Laurence, T. J. Siahaan, *Curr. Protein Pept. Sci.* **2009**, *10*, 614–625; l) A. R. Stasińskaa, P. Putaj, M. K. Chmielewskia, *Bioorg. Chem.* **2020**, *95*, 103518–103534.
[11] D. De la Fuente-Herreruela, A. K. Monnappa, M. Muñoz-Úbeda, A. Morallón-Piña, E. Enciso, L. Sánchez, F. Giusti, P. Natale, I. López-Montero, *J. Nanobiotechnol.* **2019**, *17*, 77–91.
[12] a) K. Tanemura, H. Dohya, M. Imamura, T. Suzuki, T. Horaguchi, *Chemistry Lett.* **1994**, 965–968; b) K. Tanemura, H. Dohya, M. Imamura, T. Suzuki, T. Horaguchi, *J. Chem. Soc. Perkin Trans. 1* **1996**, 453–457; c) T. Ichige, A. Miyake, N. Kanoh, M. Nakata, *Synlett.* **2004**, *10*, 1686–1690; d) H. Firouzabadi, N. Iranpoor, *Sci. of Synth.* **2007**, *30*, 505–586.
[13] a) G. Crisenza, P. Melchiorre, *Nat. Commun.* **2020**, *11*, 803–806; b) R. C. McAtee, E. J. McClain, C. R. J. Stephenson, *Trends Chem.* **2019**, *1*, 111–125; c) M. H. Shaw, J. Twilton, D. W. C. MacMillan, *J. Org. Chem.* **2016**, *81*, 6898–6926; d) S. Reischauer, B. Pieber, *iScience* **2021**, *24*, 102209–102226; e) A. Wimmer, B. König, *Beilstein J. Org. Chem.* **2018**, *14*, 54–83; f) M. Teders, C. Henkel, L. Anhäuser, F. Strieth-Kalthoff, A. Gómez-Suárez, R. Kleinmans, A. Kahnt, A. Rentmeister, D. Guldi, F. Glorius, *Nat. Chem.* **2018**, *10*, 981–988.
[14] a) M. Lanzi, J. Merad, D. V. Boyarskaya, G. Maestri, C. Allain, G. Masson, *Org. Lett.* **2018**, *20*, 5247–5250; b) B. Hong, K. C. C. Aganda, A. Lee, *Org. Lett.* **2020**, *22*, 4395–4399; c) M. Krumb, T. Lucas, T. Opatz, *Eur. J. Org. Chem.* **2019**, *28*, 4517–4521.
[15] a) P. D. Dharpure, A. Bhowmic, P. K. Warghude, R. G. Bhat, *Tetrahedron Lett.* **2020**, *61*, 151407–151415; b) G. Oksdath-Mansilla, V. Hajj, D. M. Andrada, J. E. Argüello, J. Bonin, J. M. Robert, A. B. Peñeńory, *J. Org. Chem.* **2015**, *80*, 2733–2739; c) Matthias Krumb, Lisa Marie Kammer, Robert Forster, Caroline Grundke, Prof. Dr. Till Opatz. *ChemPhotoChem.* **2020**, *4*, 101–104.
[16] a) B. Pandey, S. Y. Bal, U. R. Khire, *Tetrahedron Lett.* **1989**, *30*, 4007–4008; b) B. Pandey, S. Y. Bal, U. R. Khire, A. T. Rao, *J. Chem. Soc.-Perkin Trans.* **1990**, *11*, 3217–3218; c) X. Gu, X. Li, Y. Chai, Q. Yang, P. Li, Y. Yao, *Green Chem.* **2013**, *15*, 357–361; d) S. Zhang, G. Li, L. Li, X. Deng, G. Zhao, X. Cui, Z. Tang, *ACS Catal.* **2020**, *10*, 245–252; e) E. L. Clennan, C. Liao, *Photochem. and Photobio.* **2014**, *90*, 344–357.
[17] R. A. Valiulin, R. Kottani, A. G. Kutateladze, *J. Org. Chem.* **2006**, *71*, 5047–5049.
[18] J. R. Vale, T. Rimpiläinen, E. Sievänen, K. Rissanen, C. A. M. Afonso, N. R. Candeias, *J. Org. Chem.* **2018**, *83*, 1948–1958.
[19] N. Abidi, J. R. Schmink, *J. Org. Chem.* **2015**, *80*, 4123–4131.
[20] CCDC number of compound **2e** is 2116442. The number contains all crystallographic details of this publication and is available free of charge at https://www.ccdc.cam.ac.uk/structures/.
[21] K. D. Asmus, *Acc. Chem. Res.* **1979**, *12*, 436–442.
[22] J.-T. Guo, D.-C. Yang, Z. Guan, Y.-H. He, *J. Org. Chem.* **2017**, *82*, 1888–1894.
[23] M. Pelaez, P. Falaras, V. Likodimos, K. O'shea, A. De la Cruz, P. S. M. Dunlop, J. A. Byrne, D. D. Dionysiou, *J. Mol. Catal. A* **2016**, *15*, 183–189.
[24] a) A. Dietrich, V. Buschmann, C. Müller, M. Sauer, *Rev. Mol. Biotechnol.* **2002**, *82*, 211–231; b) S. Sören Doose, H, Neuweiler, M. Sauer, *ChemPhysChem.* **2009**, *10*, 1389–1398.
[25] B. L. Miller, T. D. Williams, C. Schöneich, *J. Am. Chem. Soc.* **1996**, *118, 11014–11025*.
[26] a) R. Hunter, M. Caira, N. Stellenboom, *J. Org. Chem.* **2006**, *71*, 8268–8271; b) N. Spiliopoulou, C. G. Kokotos, *Green Chem.* **2021**, *23*, 546–551; c) D. H. Dethe, A. Srivastava, B. D. Dherange, B. V. Kumar, *Adv. Synth. Catal.* **2018**, *360*, 3020–3025.
[27] M. H. Ali, M. G. Gomes, *Synthesis* **2005**, *8*, 1326–1332.
[28] H. R. Shaterian, K. Azizi, N. Fahimi, *J. Sulfur Chem.* **2011**, *32*, 85–91.
[29] J. R. Cashman, L. D. Olsen, L. M. Bornheims, *J. Am. Chem. Soc.* **1990**, *112*, 3191–3195.
[30] Z.-M. Liu, H. Zhao, M.-Q. Li, Y.-B. Lan, Q.-B. Yao, J.-C. Tao, X.-W. Wang, *Adv. Synth. Catal.* **2012**, *354*, 1012–1022.

Manuscript received: November 8, 2022
Revised manuscript received: January 4, 2023
Accepted manuscript online: January 11, 2023
Version of record online: January 23, 2023

© 2023 Wiley-VCH GmbH

1861471x, 2023, 4, Downloaded from https://aces.onlinelibrary.wiley.com/doi/10.1002/asia.202201128 by Indian Institute Of Science Education And Research Pune, Wiley Online Library on [23/06/2025]. See the Terms and Conditions (https://onlinelibrary.wiley.com/terms-and-conditions) on Wiley Online Library for rules of use; OA articles are governed by the applicable Creative Commons License

C—H Bond Functionalization by the Confluence of Organocatalysis and/or Transition Metal Catalysis with Photoredox Catalysis

Diverse Strategies

Anindita Bhowmick, Mousumi Behera, Ramakrishna G. Bhat

First published: 29 November 2022
https://doi.org/10.1002/9783527834242.chf0086

Abstract

Over the years, the visible-light photoredox catalysis has gained a great interest and attention to achieve efficient and attractive strategies to construct useful organic scaffolds relatively more sustainable manner using a clean energy source. There has been a great focus on the C—H bond functionalization via photoredox catalysis over the last few years owing to its atom- and step-economical features. Recently, the merger of photoredox catalysis with transition metal catalysis or organocatalysis is emerging as a very powerful and promising tool to access useful molecules which otherwise were difficult via traditional approaches. This article highlights some of the recent advancements in the C—H bond functionalization by the merger of photoredox catalysis with organocatalysis and/or transition metal catalysis, and some of the miscellaneous reactions of photoredox catalysis. This article also highlights the protocols based on dual catalysis using organic photoredox catalysts to avoid the metal catalysts. The strategic merging of photoredox catalysis with complementary activation modes of catalysis has successfully allowed the interesting transformations to construct useful compounds.

References

1 (a) Alberico, D., Scott, M.E., and Lautens, M. (2007). *Chem. Rev.* **107**: 174.

CAS | PubMed | Web of Science® | Google Scholar

(b) Kakiuchi, F. and Kochi, T. (2008). *Synthesis* **19**: 3013.

CAS | Web of Science® | Google Scholar

(c) McGlacken, G.P. and Bateman, L. (2009). *Chem. Soc. Rev.* **38**: 2447.

CAS | PubMed | Web of Science® | Google Scholar

(d) Chen, X., Engle, K.M., Wang, D.-H., and Yu, J.-Q. (2009). *Angew. Chem. Int. Ed.* **48**: 5094.

CAS | PubMed | Web of Science® | Google Scholar

(e) Lyons, T.W. and Sanford, M.S. (2010). *Chem. Rev.* **110**: 1147.

CAS | PubMed | Web of Science® | Google Scholar